The Meteorological Magazine

January 1991

Temperature predictions for the UK winter
Thames Valley storms of 24 May 1989
The UK winter of 1989/90

HMSO

Met.O.998 Vol. 120 No. 1422

First published 1991

HMSO

HMSO publications are available from:

HMSO Publications Centre
(Mail and telephone only)
PO Box 276, London, SW8 5DT
Telephone orders 071-873 9090
General enquiries 071-873 0011
(queuing system in operation for both numbers)

HMSO Bookshops
49 High Holborn, London, WC1V 6HB 071-873 0011 (counter service only)
258 Broad Street, Birmingham, B1 2HE 021-643 3740
Southey House, 33 Wine Street, Bristol, BS1 2BQ (0272) 264306
9–21 Princess Street, Manchester, M60 8AS 061-834 7201
80 Chichester Street, Belfast, BT1 4JY (0232) 238451
71 Lothian Road, Edinburgh, EH3 9AZ 031-228 4181

HMSO's Accredited Agents
(see Yellow Pages)

and through good booksellers

3 8078 0010 2452 2

The Meteorological Magazine

January 1991
Vol. 120 No. 1422

551.509.331:551.524.36(410)

Temperature predictions for the UK winter

T.D. Hewson
Joint Centre for Mesoscale Meteorology, University of Reading

Summary

The suggestion that the shape of the late autumn circumpolar vortex can be used to forecast UK winter temperatures is discussed and a simple mathematical predictor proposed. This predictor is assessed using correlation tests on a 44-year data set; investigating also the predictability of individual months and the value of different predictor periods. A simulation of real-time forecasts suggests that useful skill could have been achieved.

1. Introduction

Several articles appearing in *Weather* over the last 10 years have dealt specifically with long-range temperature predictions for the winter period in the United Kingdom. The prediction method used was essentially statistical and was based on upper-air patterns occurring across the higher latitudes of the northern hemisphere during October and November. It was first described by Davies and Reeve (1980). In Davies *et al.* (1986) a simple verification of the technique against 17 winters, although not conclusive, did give reason to believe that useful skill could be achieved. A similar but more quantitative approach used in Davies (1989) and Ratcliffe (1990) produced equally encouraging results. Again, though, the databases analysed were rather small, being 10 and 12 winters respectively.

In this investigation a quantitative adaptation of the prediction method described in Davies *et al.* (1986) is tested out on a 44-year data set. This begins in section 3, and included is an attempt to identify the best 'predictor' periods and also the 'most predictable' parts of the winter. In section 6, real-time predictions are simulated for the last 19 winters, by creating for each winter new regression equations based only on previous years. Section 2 gives a comprehensive description of the physical mechanisms underlying the statistics.

To put this study into some sort of context it is worthwhile considering which, to date, have been the most accurate long-range UK temperature predictions. Excluding the aforementioned leaves those of Murray (1972 and 1977) as perhaps the best. In a five-category system he achieved about 7 correct forecasts out of 24.

A major incentive for this work was that the financial worth of accurate long-range forecasts would be very great indeed.

2. Physical background

2.1 Link between autumn upper-air patterns and winter temperatures

Hughes (1981) investigated 'Central England' temperatures in 357 winter months. Of the 52 he classified as 'very cold', 48 were of a north-easterly, easterly or south-easterly type. This is clear evidence that winter temperatures in the United Kingdom are very closely related to wind direction. It is of course the atmospheric flow patterns which dictate the wind direction; these can be divided into two simple categories:

(a) a mobile westerly type giving above average temperatures, due to anticyclones to the south of the British Isles, and

(b) a blocked easterly type giving below average temperatures, due to anticyclones to the north of the British Isles.

As far as the predictive method is concerned the main factor affecting the probability of either (a) or (b) occurring is considered to be the forcing effect of

'boundary conditions' occurring at the earth's surface during the winter. Boundary conditions likely to be important are sea surface temperatures, snow cover and sea-ice cover; it is principally the forcing effect of sea ice which is being considered here. This is the same mechanism alluded to in Davies *et al.* (1986), and in earlier work. (Davies (1989) proposes a different mechanism, in which the *high* pressure present at high latitudes in cold winters is explained by net poleward *mass* transport 1–3 months earlier.)

Observational studies indicate that the sea-ice pattern sets itself for the winter late in the autumn (Davies *et al.* 1986). The shape of this pattern should depend largely on the distribution of cold air around the North Pole in October and November; a distribution which will be evident from upper-air patterns. Thus there should be a connection between upper-air patterns around the North Pole late in the autumn, and winter temperatures across the United Kingdom.

A good guide to the distribution of cold air around the North Pole on a given date can be gained from circumpolar 1000–500 mb thickness charts. Contour height charts for the lower stratosphere (e.g. 100, 200 mb) also provide a good guide, as low contour heights at such levels usually reflect the presence of deep, cold tropospheric air below. Most patterns on these charts can be approximated by an ellipse, such that the lowest thickness values or lowest contour heights (and hence coldest air) are in alignment with its major axis. It then seems reasonable to expect the most pronounced sea-ice development to be in that direction too.

The original prediction method entailed analysing one chart per day for (say) a 30-day period and identifying the direction of orientation of the major axis on each. Then from these 30 directions a polar diagram was constructed to represent the frequency of each direction of orientation. This diagram was the basis for the winter prediction, whereby a large east–west component on it pointed to a high probability of the cold flow pattern (b) occurring, whilst if other orientations were dominant the chances of getting mild type (a) conditions were increased.

2.2 The importance of the east–west component

To understand the significance of the 'east–west component' the following 'thought experiment' should prove helpful.

> During winter the higher latitudes of the northern hemisphere have to accommodate a certain amount of deep, cold, tropospheric air. For convenience consider 'higher latitudes' to be north of 50° N. The 'certain amount' can be represented by a domain of any shape whose area is equal to that bounded by a latitude circle at 65° N. What then will dictate the possible configurations of this domain? In other words how easily can different locations support the presence of very cold air above (see Fig. 1)?

Sea water rapidly modifies very cold air, warming it up through vigorous convection. Sea ice, snow and land have a much smaller modifying effect; mainly because their heat capacities are lower, but also because only in sea water is it possible to redistribute heat rapidly by advection and mixing. So the main restriction on the configuration of the cold air domain is that it cannot be allowed to encroach very far into sea areas ('seas open all year' in Fig. 1). Given a homogeneous planet the most likely configuration would be a circular one centred on

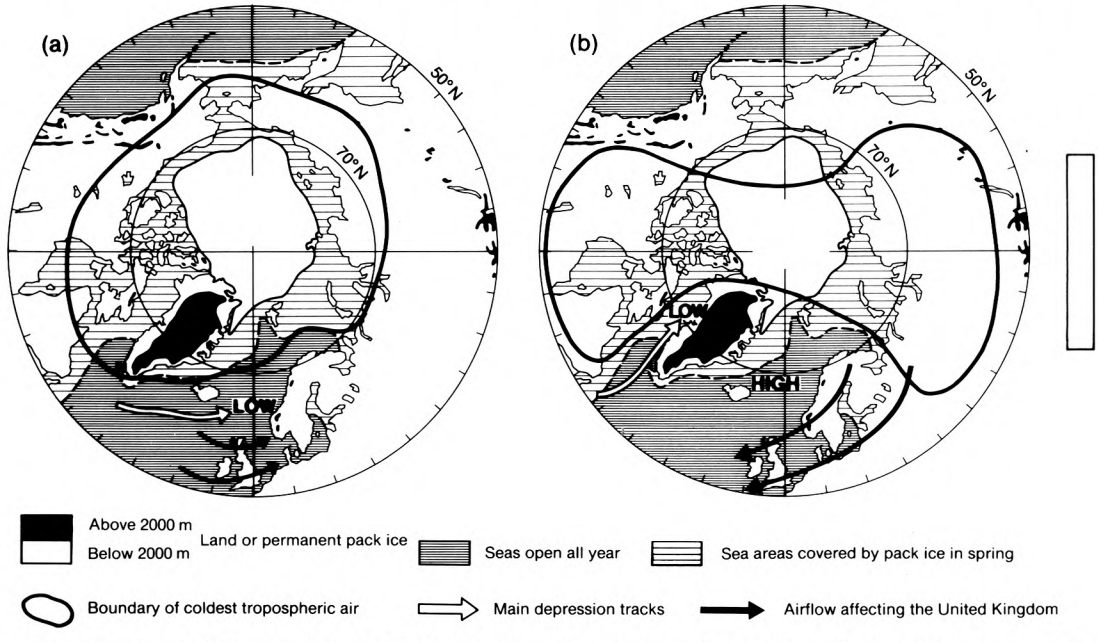

Figure 1. Circumpolar maps illustrating how the distribution of cold tropospheric air around the North Pole in winter can dictate which airstreams affect Britain: (a) mobile westerly, (b) blocked easterly. The block alongside represents $*1.6 \times 10^6$ km^2, a measure of the extreme interannual variability of winter sea-ice cover (see text).

the North Pole, but clearly this is disallowed here because of the presence of seas north-west of Norway.

Fig. 1(a) shows a configuration which is about as close to the circular type as it is possible to get. This type of pattern is quite common. It is best thought of as representing an average over several days (in reality short-wave troughs would be observed to run east around the vortex, at least across the Atlantic). Such a pattern would be accompanied by a strong baroclinic zone extending east or north-east across the Atlantic, with deepening depressions tracking between Iceland and Scotland. This results in mild south-west or westerly winds prevailing over the United Kingdom, but with some colder outbreaks of north or north-westerlies.

Fig. 1(b) illustrates another configuration in which the cold air has almost split up into two centres. The land–sea distribution dictates that if there are going to be two major centres then these must be located over the Soviet Union and North America. This type of pattern is also fairly common, though not nearly as common as (a). The southward displacement of cold polar air over Canada results in a backing of the jet stream south of Greenland and in turn this can often steer depressions up the Davis Strait west of Greenland. The resulting warm advection between Greenland and Iceland helps build high pressure to the east of Iceland, or perhaps reinforce a Scandinavian anticyclone. In this way the United Kingdom comes under the influence of east or north-easterly winds. If these are fuelled by the cold-air centre over the Soviet Union it can become very cold indeed (as happened for example in February 1956, January 1972 and January 1987).

Synoptic charts indicate that there are many possible configurations of the very cold air, but it is felt that most winter patterns can be roughly approximated by one of the above.

Fig. 2 gives some observational evidence for these ideas. It shows a frequency distribution, as a function of longitude, of atmospheric blocks occurring north of about 50°N during the seven northern hemisphere winters from 1980/81 to 1986/87 (taken from Fig. 1 in Tibaldi and Molteni (1990)). It is immediately clear that there is a strong link between block frequency at a given longitude and the extent of 'sea water' along that longitude, albeit with a small phase shift in the Atlantic/European sector. The two maxima — over the Pacific and the Atlantic — fit in well with the atmospheric pattern in Fig. 1(b). Whilst Fig. 2 partly represents a 'chicken and egg' scenario, it also seems to show that boundary conditions at the earth's surface do have a forcing effect on the atmospheric circulation, in which the main physical mechanisms are those outlined above.

To tackle the forecasting problem one must now consider how the chances of (b) occurring in winter might be influenced by atmospheric patterns occuring in autumn.

If a feedback mechanism which involves sea-ice

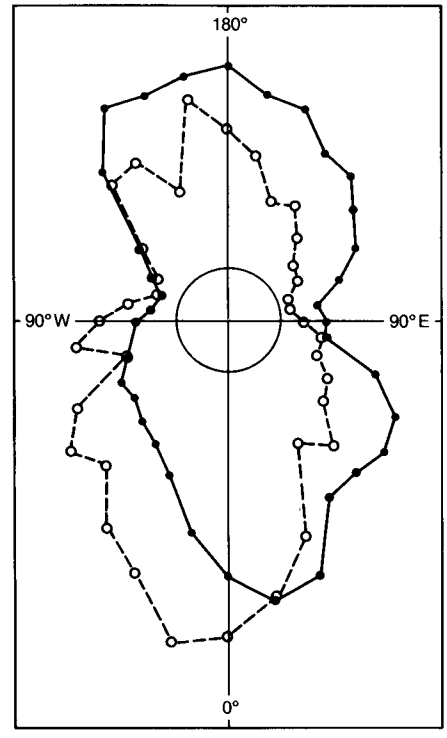

Figure 2. Polar diagram representing winter blocking frequency (solid line) and 'sea water extent' north of 50°N (dashed line) as a function of longitude. 'Sea water extent' was calculated from Fig. 1 to be the sum, along a longitude line, of the total distance occupied by 'seas open all year' and half the distance occupied by 'sea areas covered by pack ice in spring'. Scales are linear, the central circle being zero.

distribution does take place then it is probably worthwhile looking at the areas in which sea ice forms and melts each year. These correspond roughly with the sea areas 'covered by pack ice in spring' on Fig. 1 — subsequently referred to as 'key areas'.

To increase the chances of (b) occurring, and persisting for some time, it seems important that the key areas which fall within the domain have as great a cover of sea ice as possible during the winter because this would reduce the chances of the cold air being warmed out from below. Equally important, perhaps, is that the key areas which fall outside the domain in (b) have as little sea-ice cover as possible. Reducing the amount of sea ice in these areas which fall outside the domain in (b) would also seem to make (a) less likely.

Such an explanation would only be plausible if the interannual variability of winter sea-ice cover were reasonably large. The box drawn alongside Fig. 1(b) represents* the difference between the greatest and least 'mid-winter' areal extents of sea-ice (defined as where cover is greater than 10%) observed between 1973 and 1989 (data from NOAA, USA). Here the term 'mid-winter' means averaged over a 2-month period beginning

* The maps in Fig. 1 are on a zenithal equidistant projection, implying that the ratio between area on the page and area on the earth's surface is not quite fixed, but a slowly varying function of latitude. The area of the block alongside is normalized to 65°N. If normalized to 90°N, the area would be 3% smaller than shown, or to 50°N then 5% larger.

1 January. This area is considered large enough to support the above arguments (especially as energy considerations suggest the attendant anomalies in sea surface temperatures might be even more marked — the latent heat of fusion of ice is about 80 times greater than the specific heat capacity of water).

How then can sea-ice patterns which favour pattern (b) come about? The formation of sea ice must to some extent depend on the distribution of cold air around the North Pole during October and November, and naturally a distribution similar to that indicated by the domain in (b) is going to favour sea-ice development in the right areas. If this domain were approximated by an ellipse the orientation of the major axis would probably be 90° W — hence the importance of the 'east–west component'. The longer such a pattern persists during the autumn the greater will be the chances that the desired sea-ice patterns have developed.

It is also worthwhile outlining two of the limitations of these ideas. Where sea ice develops will partly be determined by the early autumn sea surface temperatures; no real account of this is taken here. Also an over-simplified view of sea ice has been taken. Rarely if ever does it have a well-defined edge — the distance in which the fractional cover of sea ice ranges from 10/10 (pack ice) to 1/10 can easily be over a hundred miles.

3. Method

In Davies *et al.* (1986) the retrospective temperature predictions were based on subjective analysis of the shapes of polar diagrams, whilst for the verification all winters were classified into just two categories, cold or mild. Here the intention was to improve upon this by adopting a quantitative approach. The polar diagram's shape would be represented by a single number, or 'winter index'; and actual temperature levels would be used in preference to categorized ones.

3.1 Data sources

Clearly two basic types of data were required: autumn upper-air charts to base the 'predictions' on, and winter temperature levels to verify against. The number of years it was possible to investigate was limited to 44 because of a lack of appropriate upper-air charts before 1946.

3.1.1. Upper-air charts

Davies concluded that November's charts would probably be a more useful guide to winter temperatures than those of October, perhaps because more sea ice forms in November than October. Thus this study concentrates on late in the autumn, using a 45-day period from 17 October to 30 November in every year.

The choice of which types of chart to use was determined by two factors, availability and suitability. The 100 mb level proved most suitable, indeed frequently the contours at this level are roughly elliptical (wave number 2), as the smaller more transient wavelengths rarely have much amplitude by the time they reach this height in the atmosphere. The 200 mb level was next best, followed by the thickness patterns. Consideration was given to using 50 mb charts, but at this level the patterns were too close to circles to be of any use. So 100 mb charts were used wherever possible (1960 onwards), thickness patterns for years when only they were available (1946–57), and 200 mb charts for 1958 and 1959. It was felt that the disadvantages of using different chart types were far outweighed by the advantages of having a long data set.

All charts were necessarily of the northern hemisphere circumpolar type, and there was one for each day, the analysis time usually being midnight. They came from three sources — the *European Meteorological Bulletin* for 1976 onwards, the Soviet SINOP bulletin for 1958–75, and the Meteorological Office (hand plotted) for 1946–57.

Scarcity of observations made it quite difficult using some of the 1946 and 1947 charts. There is, however, a fair degree of confidence in the orientations found for these years, particularly 1946.

3.1.2. Temperatures

The UK *Monthly Weather Review* provided the winter temperature data to verify against; as anomalies from 30-year climatological means for the England and Wales region. Scotland and Northern Ireland were excluded on the grounds that, with a relatively wide expanse of sea to the east, temperatures there would be less sensitive to a change in wind direction from west to east.

Anomalies were extracted for both the individual winter months and the winter as a whole; assuming for convenience that 'winter' is comprised of December, January and February.

3.2 Derivation of the winter index

In order to create a winter index, a simple weighting system was devised whereby each occurrence of a particular orientation of the circumpolar vortex on the upper-air charts scored a set number of points. The final winter index was then calculated by summing the points scored in a given period, such as 1–15 November; the idea being that the magnitude of this score was indicative of the likely severity of the forthcoming winter. Table I shows the weighting system used — the choice of 'scores' is explained below.

Table I. Weighting system for calculating winter indices

Point score	Orientation					
	60° W	70° W	80° W	90° W	80° E	Others
Axis ratio ≥ 2:	2	4	4	4	2	0
Axis ratio < 2:	1	2	2	2	1	0

From past studies it is apparent that the important 'east–west component' is made up principally of orientations 70° W, 80° W and 90° W; hence these directions are afforded the highest weights of all (subsequently referred to as 'COs', meaning 'cold orientations'). Physically there is only a small difference between two adjacent orientations, such as 60° W and 70° W, or 90° W and 80° E. So for consistency it was felt that some weight had also to be given to 60° W and 80° E; half the score allocated to the COs was chosen. This also meant that the relationship betweeen 'orientation' and 'score' was free from large discontinuities.

Davies *et al.* (1986) also defined 'mild orientations' as being those between 0° W and 50° W; saying that out of all possible orientations these were the ones most likely to precede mild winter weather. To take account of this, negative scores could have been added to Table I for all orientations between 0° W and 50° W. The reasons for leaving them scoring zero were twofold: Davis had generally put much more emphasis on the COs, and the COs were far more common — occurring more than twice as often as the mild orientations.

Within any subjective analysis of archived data, unfortunately there is always scope for the analyst to interpret the data in a way which will lead to results which are more interesting or more significant than would have been the case had an objective analysis been used. Here, for example, it was not always possible to approximate the atmospheric pattern with an elliptical shape. Sometimes the patterns were almost circular making a direction of orientation much harder to identify precisely. To reduce the impact of this problem two sets of scores were incorporated into the weighting system (one being simply a factor of two greater than the other). For the atmospheric pattern on a particular chart to realize the higher of the two scores the necessary condition was that the 'axis ratio' (meaning the ratio of the length of the major axis to the length of the minor axis of the ellipse judged to best fit the atmospheric pattern) was greater than or equal to two. This approach is also physically consistent with the ideas presented earlier, because the greater the axis ratio the more elongated will the cold polar air have become, and thus the greater will be the forcing of sea-ice development along that direction of elongation (i.e. the orientation).

Fig. 3 shows one of the 100 mb charts used. To approximate the contour pattern with an ellipse the analyst must concentrate on the area north of 50° N, as this is where most of the sea ice will be forming. With this guideline in mind it should be fairly easy to see why the orientation came out as 90° W and the axis ratio about 3; giving a score of 4. Most patterns were easier to approximate with an ellipse than this one.

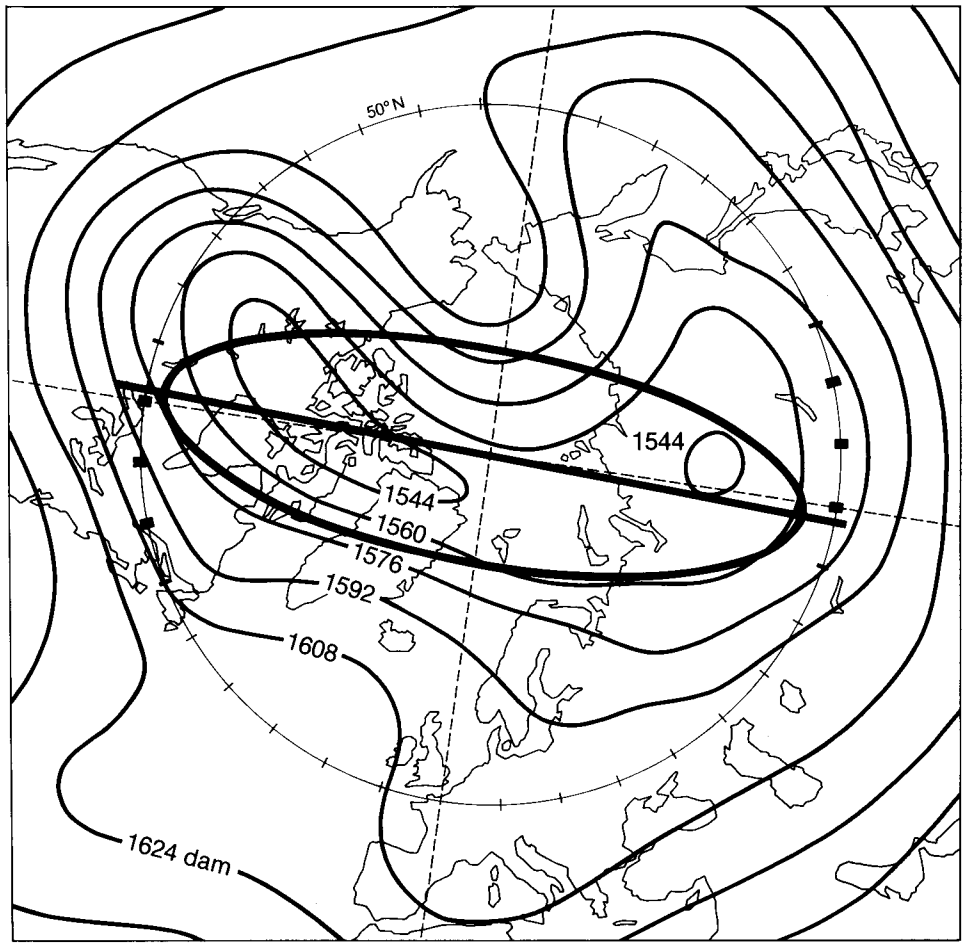

Figure 3. 100 mb analysis for 0000 UTC on 24 November 1985, with ellipse superimposed. Tickmarks are at 10° intervals.

So to calculate the winter indices the following procedure was adopted:

(a) On each chart the direction of orientation of the circumpolar vortex was identified (45 charts for each of the 44 years).

(b) On those charts where the orientation was 60° W, 70° W, 80° W, 90° W or 80° E the axis ratio was also calculated.

(c) According to the results of (a) and (b) a points score (0, 1, 2, 4) was assigned to each date.

(d) The points scored in a given period were summed. This sum was the winter index.

Initially four indices were calculated for each year; one for the 45-day period, and also one for each of the 15-day periods 17–31 October, 1–15 November and 16–30 November (see Table II). By dividing up in this way it would be seen whether or not the predictive value of an index depended on the part of the autumn on which it was based.

4. Results

As the winter index increases so should the temperature of the winter months, on average, decrease.

Table II. Winter indices and temperature anomalies for England and Wales, 1946–89

Year*	Winter index (WI)				Temperature anomalies (TA) — England and Wales (°C)				WI	TA
	17–31 Oct.	1–15 Nov.	16–30 Nov.	17 Oct.–30 Nov.	Dec.	Jan.	Feb.	Winter mean**	1–30 Nov.	Jan. and Feb. mean***
1946	18	20	50	88	−1.4	−2.1	−5.7	−3.0	70	−3.8
1947	0	9	17	26	0.7	1.1	0.4	0.7	26	0.8
1948	4	1	5	10	1.1	1.2	1.4	1.2	6	1.3
1949	4	10	5	19	1.2	0.2	1.3	0.9	15	0.7
1950	12	10	42	64	−3.1	−0.3	−0.5	−1.3	52	−0.4
1951	7	29	20	56	1.0	−1.3	−0.8	−0.4	49	−1.1
1952	36	33	12	81	−1.4	−0.6	0.1	−0.7	45	−0.3
1953	8	11	9	28	2.6	−1.1	−1.7	−0.0	20	−1.4
1954	15	41	17	73	2.1	−1.3	−2.7	−0.6	58	−2.0
1955	4	15	23	42	1.3	−0.3	−4.4	−1.0	38	−2.3
1956	12	19	11	42	1.3	1.4	1.1	1.3	30	1.3
1957	16	38	30	84	0.0	−0.5	0.7	0.0	68	0.1
1958	4	19	34	57	0.2	−2.1	0.2	−0.6	53	−1.0
1959	16	30	10	56	1.4	0.1	−0.2	0.5	40	0.0
1960	12	25	7	44	−0.5	−0.3	2.7	0.6	32	1.1
1961	17	8	7	32	−1.8	0.4	0.3	−0.4	15	0.4
1962	9	46	38	93	−2.3	−5.3	−4.5	−4.0	84	−4.9
1963	4	0	5	9	−2.0	−0.3	0.5	−0.6	5	0.1
1964	22	3	39	64	−1.2	−0.1	−0.7	−0.7	42	−0.4
1965	17	56	8	81	−0.2	−0.7	1.7	0.2	64	0.4
1966	2	47	28	77	0.5	0.7	1.6	0.9	75	1.1
1967	0	28	5	33	−0.5	0.7	−1.7	−0.5	33	−0.4
1968	0	21	32	53	−1.5	1.9	−2.8	−0.7	53	−0.3
1969	50	5	14	69	−1.4	0.1	−0.7	−0.7	19	−0.3
1970	5	5	49	59	−0.5	0.9	0.9	0.4	54	0.9
1971	10	14	1	25	1.7	0.2	0.5	0.8	15	0.3
1972	41	12	3	56	1.0	0.9	0.5	0.8	15	0.7
1973	3	13	0	16	0.1	2.5	1.9	1.5	13	2.2
1974	34	8	9	51	3.2	3.2	1.0	2.5	17	2.1
1975	5	3	35	43	0.5	2.2	0.8	1.2	38	1.5
1976	25	12	11	48	−2.3	−0.5	1.5	−0.5	23	0.5
1977	3	0	26	29	1.5	−0.1	−1.1	0.1	26	−0.6
1978	10	23	44	77	−0.3	−3.1	−2.3	−1.9	67	−2.7
1979	16	15	4	35	1.2	−0.9	2.1	0.8	19	0.5
1980	3	12	3	18	0.9	1.2	−0.5	0.6	15	0.4
1981	42	12	2	56	−3.7	−0.4	1.3	−1.0	14	0.4
1982	16	10	19	45	−0.2	3.0	−1.6	0.5	29	0.8
1983	0	5	0	5	1.2	0.2	0.0	0.5	5	0.1
1984	22	43	9	74	0.6	−2.7	−1.3	−1.1	52	−2.0
1985	6	11	41	58	1.6	0.1	−4.5	−0.8	52	−2.1
1986	20	50	19	89	1.2	−2.6	0.0	−0.5	69	−1.4
1987	11	10	23	44	1.0	1.8	1.1	1.3	33	1.5
1988	22	26	8	56	2.6	2.7	2.3	2.5	34	2.5
1989	11	41	9	61	0.3	3.1	3.7	2.3	50	3.4

* Year is the year containing October, November and December.

** Winter mean = (Dec. × 31 + Jan. × 31 + Feb. × 28.25)/90.25

*** Jan. and Feb. mean = (Jan. × 31 + Feb. × 28.25)/59.25

However there is nothing to suggest that any relationship between the two variables would necessarily be linear. Perhaps then the best statistical test to apply to the data sets in the first instance is one based purely on rank.

4.1 Rank correlations

Kendall's coefficient of rank correlation (described in Williams 1986) was calculated for all possible pairings of 'temperature anomaly' against 'winter index', yielding the results shown in Table III.

Table III. Kendall coefficients of rank correlation, calculated for winter indices against winter temperature anomalies; 44 ranks in each case

Winter index	England and Wales temperature anomaly			
	Dec.	Jan.	Feb.	Winter
17–31 Oct.	−0.093	−0.159	+0.081	−0.111
1–15 Nov.	−0.011	−0.273*	+0.007	−0.099
16–30 Nov.	−0.145	−0.172	−0.329**	−0.329**
17 Oct.–30 Nov.	−0.197	−0.327**	−0.158	−0.332**

* and ** indicate significance levels of 95% and 99.5% respectively. No coefficient was significant at the 99.95% level.

The following conclusions can be drawn from the coefficients:

(a) All but two of the coefficients are negative, strongly supporting the idea that higher winter indices point to lower winter temperatures.

(b) Considering December alone, no coefficient quite reaches the 95% level, suggesting little if any predictability. In turn this suggests that the correct prediction of the very cold December in 1981 (Reeve 1982) may have been fortuitous.

(c) Of the three winter months the results for January are perhaps most encouraging, suggesting that some accuracy in long-range forecasts could be achieved here.

(d) For February there are surprisingly large differences between the four coefficients; but there would seem to be some predictability if the late November index were used alone.

(e) November has more predictive value for the forthcoming winter than does late October.

In view of (b), (c) and (d) it would seem sensible not to try to use the winter index to forecast the temperature for the whole winter, but rather to concentrate on forecasting for just January and February.

4.2 A way of preparing future forecasts

Rank correlations help illustrate whether relationships between two sets of variables exist, but they don't really allow a forecast of one to be made knowing the other. Clearly if proper predictions for January and February are to be made then either a graph or an equation relating temperature to winter index will be required.

Least squares regression techniques were employed to achieve this; putting 'best-fit' polynomial curves through the data points. Brooks and Carruthers (1953) suggest using this approach when there is no theoretical guidance as to the nature of the correlation. They also state that rarely in meteorology would there be justification in using anything more complex than a second-order curve (i.e. quadratic). Hence that was what was used. The usual assumptions about data distribution applied.

Three cases were considered:

(a) January temperature compared with a 45-day index (17 Oct.–30 Nov.)

(b) February temperature compared with 15-day index (16–30 Nov.)

(c) January–February temperature compared with 30-day index (1–30 Nov.)

These pairings were chosen after careful examination of the coefficients in Table III; the intention being to match up a given predictand with it's most accurate predictor. Table II shows all data points used, Fig. 4 the fitted curves, and Table IV useful statistics derived from

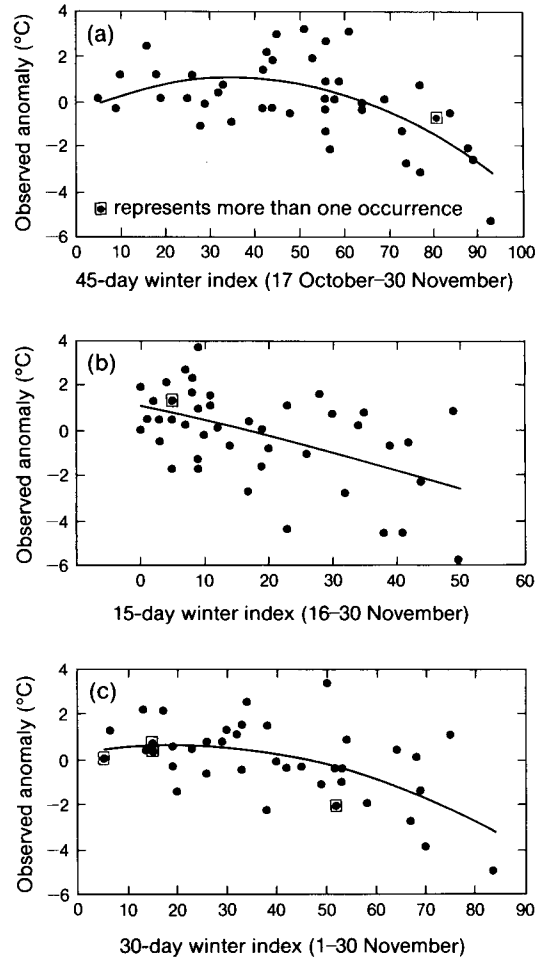

Figure 4. Plots of temperature anomaly against winter index, with best-fit quadratic curves added for (a) January, (b) February and (c) January and February combined.

Table IV. Statistics relating to the graphs in Fig. 4

	(a)	(b)	(c)
Equation (y=)	$-0.00125x^2 + 0.088x - 0.5$	$-0.00015x^2 - 0.066x + 1.1$	$-0.00090x^2 + 0.034x + 0.3$
Variance explained (%)	36	24	28
Significance level (%)	99.995	99.5	99.95
Standard error of estimate (°C)	1.4	1.8	1.4
Prediction accuracy for 75% confidence (°C)	1.8	2.2	1.8

the regressions. Use of both linear and quadratic coefficients was justified at the 95% level only in case (a), but to maintain consistency and facilitate inter-comparison all coefficients were retained in all three cases.

The reader may decide whether there is sufficient justification for making two separate forecasts (using (a) and (b)) rather than just a single forecast (using (c)). The author's view is that two separate forecasts could be made, because the differences between the coefficients for January and February in Table III are so large. However it is acknowledged that no physical explanation has been offered for these large differences.

5. Discussion

Perhaps the most illuminating of the figures in Table IV are those showing 'variance explained'. It would be interesting to see how these figures compared with those produced by other long-range forecasting techniques. Barnston and Livezey (1989) infer that the operational seasonal weather forecasts issued by the Climate Analysis Center in the USA achieve a skill level around 15%. Unfortunately these are categorical forecasts where the skill has been calculated in such a way that comparison with 'variance explained' is not valid. To overcome this problem the points on Fig. 4 were reanalysed as if forecasts in three equi-probable categories had been made. For the three cases (a), (b) and (c) this yielded respective skill levels of 14, 16 and 16% — clearly on a par with the above. This result is particularly encouraging in view of the long lead-time (1–3 months) between prediction and event.

Barnston and Livezey investigated complex analogue-based prediction methods for all four seasons for the USA using a 35-year database. The best skill level they could achieve was 16% for the winter season. There was also an indication that the latter months of the winter (i.e. January, and more especially February) were more predictable than December. This ties in well with conclusion (b) in section 4.1, and suggests that there could be a long-range predictability 'peak' in the latter part of the winter across much of the northern hemisphere.

Namias (personal communication from Davis) has found that November is a better predictor of conditions in January and February in the USA than is October. This is in agreement with conclusion (e) in section 4.1, and so must lend further weight to the results of this investigation.

It is important to consider what level of significance needs to be achieved to justify there being a physical relationship between winter index and winter temperatures. It is common for the 95% level to be used in 'a priori' type regressions — where there is a sound physical reason for expecting a relationship to exist between two variables. Nicholls (1980) states that a higher confidence level is appropriate when the relationship is 'a posteriori' — i.e. with no physical reasoning behind it. This investigation perhaps falls between these two extremes — a physical reason has been given but it is perhaps open to question. Either way the levels indicated in Table IV are too high to be dismissed lightly, even though there was an element of 'selectivity' involved in choosing the predictors. It is worth noting here that in some past papers in this field all sorts of predictors have been investigated, only to find that not much more than 5% of them reach a significance level of 95% (see for example Bergen and Harnack, 1982).

How 'useful' then might a prediction made using the above graphs be? This can be directly answered by quoting the values for 'variance explained'. Alternatively the '75% confidence limits' might be useful — an example will serve to illustrate their worth.

Assuming that having analysed the October and November charts, and calculated a 45-day index, a prediction for January was required. Say the index was 80. This reads off at about −1.5 °C, the most likely temperature anomaly. Then it could also be said that there was about a 75% chance that the temperature

anomaly for January would fall between +0.3 °C and −3.3 °C (i.e. −1.5 ±1.8 °C).

The significance levels in Table IV are rather higher than those in Table III. This is partly because the best-fit lines are curves — notably on graph (a). It is interesting to consider what might explain this phenomena. There appear to be two possibilities — one statistical, the other physical. It is probable that both play some part.

The statistical explanation is that the dominance of the squared term is a manifestation of the predictor's ability to foresee cold winters but not mild ones.

The physical explanation arises out of having results which seem to bear out the supposition that the cold-air distributions and main depression tracks on Figs 1(a) and 1(b) are respectively related to low and high winter indices. In this way 'mid-range' winter indices could well be linked to an average cold-air distribution which fell somewhere between Figs 1(a) and 1(b), and thus a main depression track often directed north-eastwards through the Denmark Strait (between Greenland and Iceland). This would result in the UK's weather being dominated by an anticyclone over France, giving mainly south or south-westerly winds, with little chance of getting colder north or north-westerlies. Such a synoptic pattern would usually lead to higher winter temperatures than that shown in Fig. 1(a). So this may be the reason why the mildest Januarys on graph (a) are clustered around a winter index score of 50, and hence why there is a turning point on the fitted curve. Why the graph for February fails to show a similar effect is not clear.

The above explanation gives also a good example of why long-range forecasting is so difficult; because the atmospheric states leading to 'very cold' and 'very mild' conditions can be so close together.

The southern Greenland area seems to be a crucial 'dividing line' between depression tracks which are associated with very different types of winter weather in Britain. One reason for this must be the height of the Greenland ice cap. Note that nowhere else on Fig. 1 is there such a large extent of ground above 2000 m (a fact often lost on topographical maps because permanent ice is usually coloured white). This high ground helps in 'trapping' depression tracks either to the east or to the west for long periods. If then the winter atmospheric circulation is influenced by sea ice it could well be that the distribution around Greenland is most important of all.

6. A real-time forecast simulation

In section 4 a method was developed for preparing forecasts in the future using correlations identified in data from the past. Section 5 gave a discussion of these correlations and in particular the levels of accuracy that one might expect to attain. Whilst this is all statistically sound, it is also slightly speculative in the sense that no real-time test of prediction accuracy was attempted. Thus it was felt necessary to try to simulate a situation in which the method described had been used to prepare forecasts on an operational basis over a period of many years. To do this it was necessary to derive correlation equations of the type shown in Table IV using smaller data sets. The first set of equations would be derived using 15 years of data from 1946/47 to 1960/61. This set would be used to predict the 1961/62 winter, the input x values being winter indices from October and November 1961. The second set would be derived for 1946/47 to 1961/62, to predict 1962/63; and so on up to the last year of the data set. In this way 29 'real-time' forecasts were created, each of which could clearly be verified.

Table V illustrates the accuracies achieved by forecasts in this simulation and how they compared with two control predictions; namely climatology (predicting a zero anomaly every year) and persistence (predicting that the one- or two-month period will have a temperature anomaly equal to that of the same period in the previous year). In all cases the forecasts perform better than both controls, particularly those for January.

Table V. Root-mean-square errors (°C) in the real-time prediction simulation, for the same cases as in Fig. 4

	(a)	(b)	(c)
Simulated forecasts	1.65	1.77	1.49
Climatology	1.96	1.90	1.65
Persistence	2.35	2.41	1.80

For (a), (b) and (c) the variances explained by the predictions were 29%, 13% and 18% respectively. These values are consistent with those shown in Table IV. The fact that they are somewhat lower is not surprising as one would generally expect prediction accuracy to increase as the length of the database increased. Fig. 5 shows how predictions for January fared in each of the 19 years. Whilst it can be dangerous highlighting individual years, it is nevertheless interesting that the −1.4 °C anomaly predicted for the January of the infamous winter of 1962/63, based on just 16 years data, would have come out as −2.5 °C had a 43-year database (excluding 1962/63 itself) been available.

7. Conclusions

A simple, manual, statistical long-range forecasting technique has been developed which appears able to explain an unusually large amount of the variance of winter temperatures across England and Wales — 36% for January, and 24% for February. The lead times for predictions would be 1 and 2 months respectively. The investigation was based on 44 years of data — the significance of the relationships identified being about 99.95%. No skill was achieved in predicting December temperatures. In a simulation of real-time operational predictions over a 19-year period the variance explained reduced to 29% for January and 14% for February. This reduction seems consistent with the reduced database size (averaging 29 years).

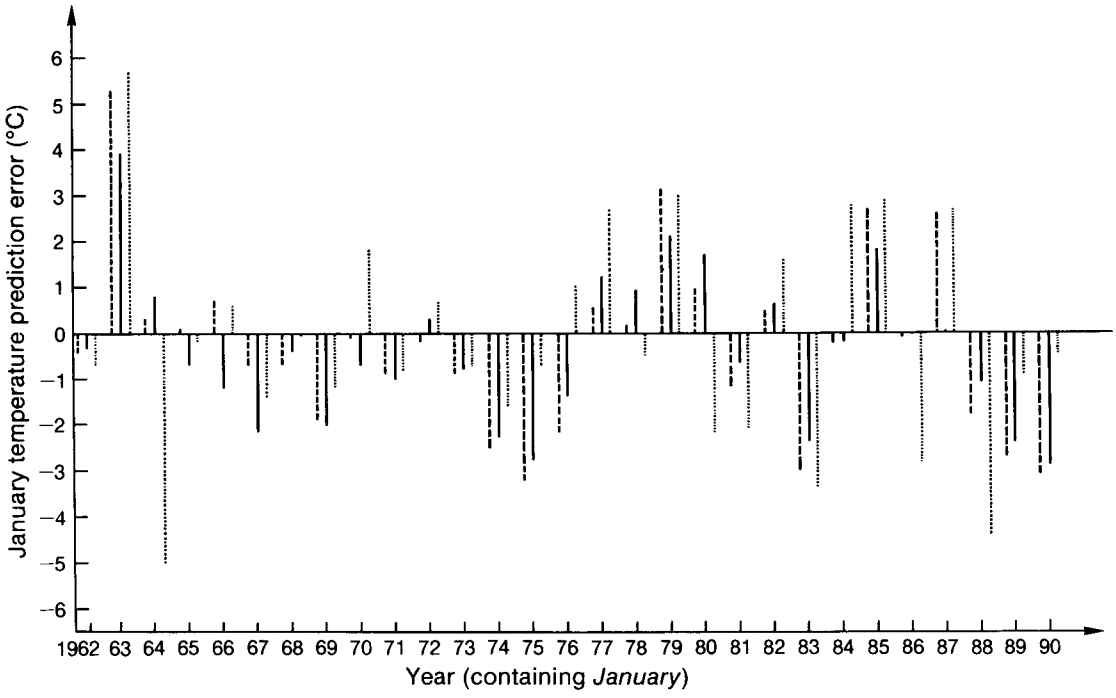

Figure 5. Errors in forecast January temperature anomalies during the real-time prediction simulation (central line of the trio for each year). The lines to the left and right in the trio represent errors in the control forecast — respectively climatology and persistence. (Note that labelling the year corresponding to *January* differs from earlier convention.)

The predictor comes from the distribution of cold air around the North Pole in late autumn. This distribution is thought to partly determine the areas where sea ice develops, which in turn, through feedback effects, partly determine the distribution of the coldest polar air through the winter. The position of the coldest polar air in winter is closely linked to the type of air masses simultaneously affecting Britain. There is some evidence to suggest that when there are anomalously small amounts of sea ice around Greenland, and also (perhaps to a lesser extent) between Alaska and Siberia, the probability of cold winter weather in the United Kingdom increases. Whilst the statistics are consistent with the physical explanation offered, it should be pointed out that they do not justify it. That would require a study based specifically on autumn/winter ice patterns. It is possible that the predictor is representing other physical mechanisms such as the poleward mass transport referred to in Davies (1989).

The lack of past successes has been in part attributable to a complete inability to foresee the development of atmospheric blocks, a problem which this study seems to have gone some small way towards overcoming. Too often in past work predictors have been sought on just local scales, whereas the physical mechanisms at work are probably operating on a hemispheric scale. Part of the problem is that so many of the routinely produced charts available to researcher and forecaster show only a relatively small section of the northern hemisphere — thus obscuring the way in which synoptic events on either side of that hemisphere are intimately linked. The beauty of the charts used in this investigation, aside from being circumpolar, was that the 100 mb level generally used was like a ready-made Fourier breakdown of the more complex atmospheric structure beneath, where only the very long-wavelength features were retained. This made calculating the 'winter indices' extremely easy — such that it would take only about 1 hour's work to come up with prediction(s) for the following winter.

It is likely that the winter indices described could also yield useful skill in forecasting winter temperatures for other countries in western Europe. France, Belgium and The Netherlands immediately spring to mind as the presence of warm sea to the west and a cold continent to the east make the peculiarities of their winter climates similar to those of the United Kingdom.

Future research could centre on the actual winter sea ice and sea surface temperature distributions, to see whether they genuinely do relate to both the winter and autumn circulation patterns. Lack of a well defined edge to most sea ice, and lack of sea-ice data in general, mean this task would not be easy though. The earlier assertion that sea surface temperature anomalies in early autumn in the 'key areas' could affect the winter sea-ice distribution also offers scope for improvements to the predictions. It would also be interesting to see whether the upper-air patterns in December had any predictive value for the rest of the winter. Indeed, to justify the 'isolated' correlation observed between atmospheric patterns in late November and February temperatures this is really a necessity.

The proof of the pudding, it is often said, is in the eating. It will be interesting to see whether or not future

predictions, based on the results of this paper, attain the quoted accuracy. In about 10 years time we should have some idea.

Acknowledgement

The author would like to thank M.N. Ward for his thorough appraisal of an earlier draft of this paper.

References

Barnston, A.G. and Livezey, R.E., 1989: An operational multifield analog/anti-analog prediction system for United States seasonal temperatures. Part II: spring, summer, fall and intermediate 3 month period experiments. *J Clim*, **2**, 513–541.

Bergen, R.E. and Harnack, R.P., 1982: Long-range temperature prediction using a simple analog approach. *Mon Weather Rev*, **110**, 1083–1099.

Brooks, C.E.P. and Carruthers, N., 1953: Handbook of statistical methods in meteorology. London, HMSO.

Davies, D.R., 1989: Winter prediction. *Weather*, **44**, 409–412.

Davies, D.R., Muir, D.J. and Linnard, D., 1986: On the feasibility of mid-winter predictions. *Weather*, **41**, 74–81.

Davies, D.R. and Reeve, C., 1980: Seasonal prediction: can it be done? *Weather*, **35**, 220–224.

Hughes, G.H., 1981: Very cold winters and winter months in central England. *Weather*, **36**, 268–274.

Murray, R., 1972: On predicting seasonal weather for England and Wales from anomalous atmospheric circulation over the northern hemisphere. *Weather*, **27**, 396–402.

—, 1977: The accuracy of seasonal forecasts based on pressure anomaly rules. *Weather*, **32**, 325–326.

Nicholls, N., 1980: Long-range weather forecasting: value, status and prospects. *Rev Geophys Space Phys*, **18**, 771–788.

Ratcliffe, R.A.S., 1990: Winter prediction. *Weather*, **45**, 271–272.

Reeve, C.E., 1982: Winter 1981/82. *Weather*, **37**, 29–29.

Tibaldi, S. and Molteni, F., 1990: On the operational predictability of blocking. *Tellus*, **42A**, 343–365.

Williams, R.B.G., 1986: Intermediate statistics for geographers and earth scientists. London, Macmillan.

551.577.2(410.11):551.577.51:551.515.42:551.501.45:551.501.81

The storms of 24 May 1989 — the rainfall in the Thames Valley area

R.A. Davis
Meteorological Office, Bracknell

Summary

Severe convective storms on 24 May 1989, following a spell of hot weather, led to some very intense point rainfalls at a number of places in southern England. This article examines the falls recorded by the rain-gauge network in an area within a 50 km radius of the Meteorological Office headquarters at Bracknell.

1. Introduction

The evolution of the severe convective storms of 24 May 1989, as shown by satellite and radar observation, is described in Waters (1991). This paper concentrates on the violent rainfall in the Thames Valley area, as recorded by the rain-gauge network.

2. The data

Initially, within a few days of the storm, only a limited amount of rain-gauge data was available, all from Meteorological Office manned sites. By a fortunate coincidence, two such sites, those at Easthampstead (Beaufort Park) and at South Farnborough, caught the full violence of the storms. By using readily available network radar data, it was possible to produce fairly quickly a sketch map showing the intensity of rainfall in the Bracknell, Farnborough and Woking area. This was incorporated into a short report, which was used by the then Advisory Services Branch of the Meteorological Office to answer the initial enquiries from those requesting information in regard to the flooding of premises. Most rainfall enquiries of this nature cannot normally be dealt with until quality-controlled rain-gauge data have been received from co-operating observers, which seldom happens less than 6 weeks after an event.

All the rain-gauge data having now been received and quality-controlled, a detailed map of daily rainfall over the main area of the storms has been prepared, and this is reproduced, in a reduced form, as Fig. 1. An earlier version of this map was included in an article on assessing and forecasting extreme rainfall by Collier (1990). Radar data from Chenies have been used to supplement the rain-gauge values to achieve a better definition of the shape of the isohyets. Within this area are six rain-gauges from which hourly data were available: Heathrow, Gatwick, Mickleham, South Farnborough, Beaufort Park and Odiham. Tilting-syphon rain recorder (TSR) records were available to the author from three sites: Mickleham, Beaufort Park and South Farnborough. The redrawn hyetogram from Mickleham is reproduced as Fig. 2, and the minute-by-minute record from the tipping-bucket rain-gauge (TBR) at South Farnborough appears as Fig. 3.

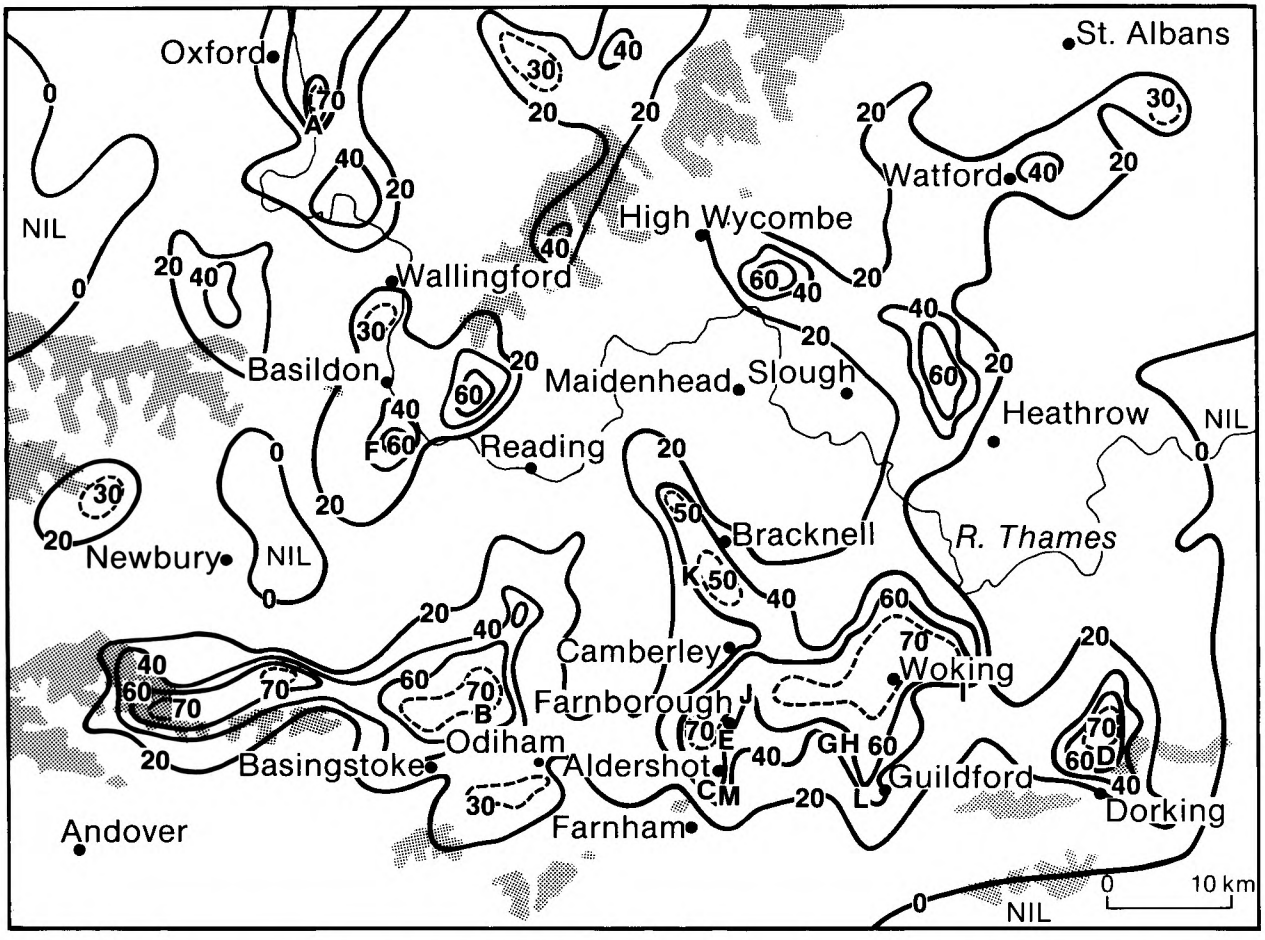

Figure 1. Contours of rainfall totals (mm) for the 24 hours from 0900 UTC on 24 May 1989, derived from rain-gauges in the Thames Valley area. Interpolation of isohyets was aided by the use of Chenies radar rainfall data integrated over the period 1100–1600 UTC. Ground above 600 ft is stippled and the letters refer to the stations included in Table I.

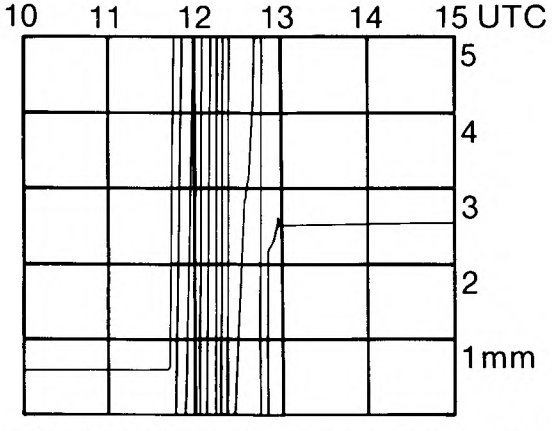

Figure 2. A reproduction of a section of the hyetogram from Mickleham tilting-syphon rain recorder for 24 May 1989.

3. Discussion

The records for 24 May show that by far the greater proportion of the rainfall took place in a very limited period, for example, 1215–1330 UTC at South Farnborough and 1145–1300 UTC at Mickleham. Very little rain fell outside the violent phase. It is therefore possible to say, with confidence, that Fig. 1 depicts fairly accurately the rainfall during the most intense 1¼ to 2 hours of the storms. The rain started earlier in the east than it did in the west; at Mickleham it began at 1140 UTC, but at Farnborough it did not start until about 1210 UTC.

Table I lists those rain-gauge sites in the area which recorded over 40 mm in the 24 hours starting at 0900 UTC on 24 May 1989; the table also shows the 1941–70 average monthly rainfall for May, where available.

A better impression of the size of these rainfalls is gained by the use of the return period, a statistical measure of the frequency with which an event is likely to recur (not a forecast of when it will occur again). For the 24-hour totals given in Table I it is possible to obtain a table of return periods, together with the modified Bilham (1935) classification as follows: 'noteworthy', having a return period of between 10 and 40 years, 'remarkable' between 40 and 160 years, and 'very rare' more than 160 years. These return periods are reproduced here as Table II.

However, as noted above, little rain fell outside a 2-hour period, and it is not unreasonable therefore to rework these return-period calculations as if the rainfalls were over only 2 instead of 24 hours. Table III shows the results.

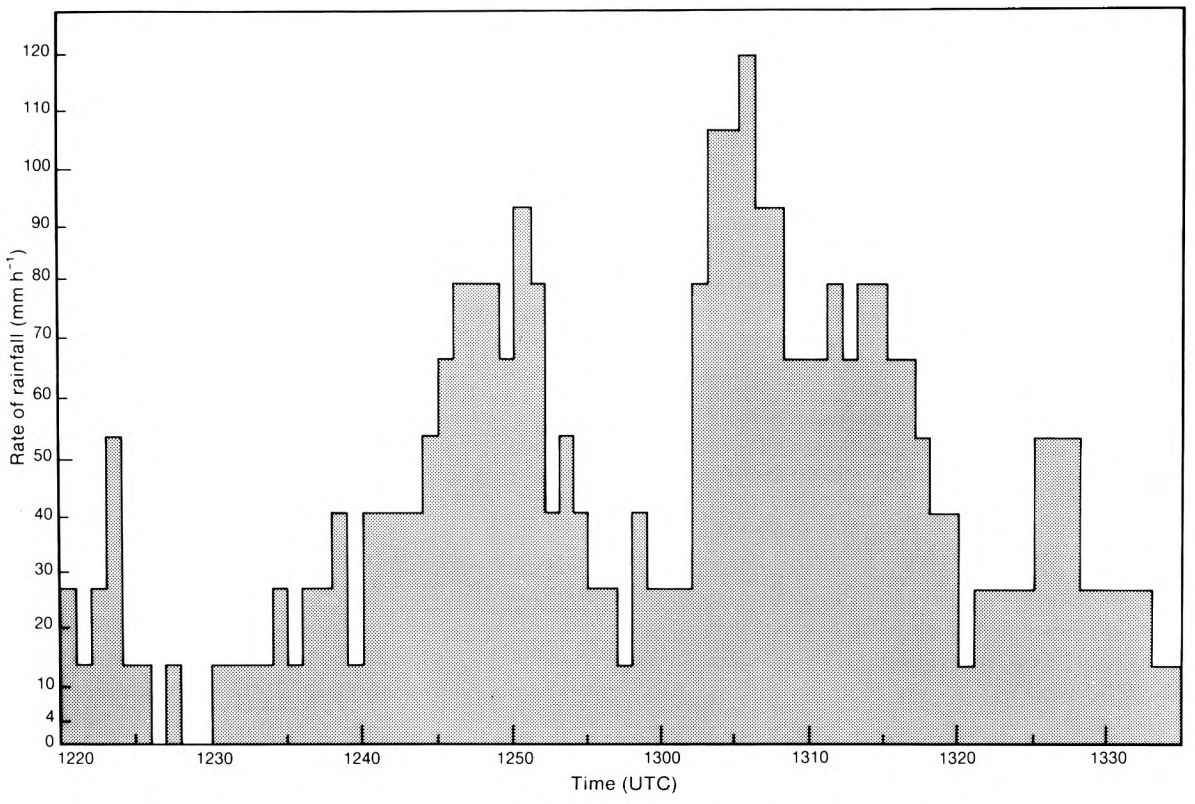

Figure 3. Minute-by-minute rates of rainfall at South Farnborough derived from tipping-bucket rain-gauge data for 24 May 1989.

Table I. Total 24-hour rainfalls from sites reporting over 40 mm at 0900 UTC on 24 May 1989, together with the average monthly figure where possible

Rain-gauge site	Total (mm)	Average monthly total (mm) for May (1941–70)
Sandford Sewage Works, Oxford (A)	68.5	
Chineham Sewage Works, Basingstoke, Hampshire (B)	68.5	
Aldershot Reservoir, Hampshire (C)	64.2	55
Juniper Hall, Mickleham, Surrey (D)	62.2	56
South Farnborough, Hampshire (E)	60.2	53
Upper Basildon, Berkshire (F)	57.0	
Pirbright Institute, Surrey (G)	56.5	50
Merrist Wood Agricultural College, Surrey (H)	53.5	
Royal Horticultural Society Gardens, Wisley, Surrey (I)	52.6	50
Frimley Pumping Station, Surrey (J)	51.6	54
Beaufort Park, Bracknell, Berkshire (K)	45.6	
Wodeland Avenue, Guildford, Surrey (L)	44.1	55
Aldershot Waterworks, Hampshire (M)	41.6	55

The letter in brackets after the site name identifies the location on the map at Fig. 1.

Some more-specific return periods have been determined from hyetograms and TBR data, particularly in relation to periods of less than 2 hours. The rarest falls were those lasting for about an hour; shorter falls of similar intensity are more common, as are similar totals achieved over longer durations. Tables IV and V respectively list return periods for a variety of amounts and durations at Mickleham (derived from Fig. 2) and at South Farnborough (from Fig. 3). No doubt similar figures could be obtained from the other sites listed, were suitable data available.

However, the pattern of rainfall in Fig. 1 makes it clear that these intense falls affected very restricted areas. On this occasion the intense cells were almost stationary throughout their lifetimes, and hence they show up on Fig. 1 as approximately circular areas of

Table II. Return periods and Bilham (1935) classification for the 24-hour rainfalls shown in Table I

Rain-gauge site	Return period (years)	Bilham classification
Sandford Sewage Works, Oxford	34.2	Noteworthy
Chineham Sewage Works, Basingstoke, Hampshire	34.2	Noteworthy
Aldershot Reservoir, Hampshire	28.5	Noteworthy
Juniper Hall, Mickleham, Surrey	19.3	Noteworthy
South Farnborough, Hampshire	21.3	Noteworthy
Upper Basildon, Berkshire	15.5	Noteworthy
Pirbright Institute, Surrey	13.9	Noteworthy
Merrist Wood Agricultural College, Surrey	10.2	Noteworthy
Royal Horticultural Society Gardens, Wisley, Surrey	11.5	Noteworthy
Frimley Pumping Station, Surrey	10.1	Noteworthy
Beaufort Park, Bracknell, Berkshire	6.3	Not significant
Wodeland Avenue, Guildford, Surrey	2.9	Not significant
Aldershot Waterworks, Hampshire	3.5	Not significant

Table III. Return periods and Bilham (1935) classification for the rainfalls shown in Table I, assuming that their duration was only 2 hours

Rain-gauge site	Return period (years)	Bilham classification
Sandford Sewage Works, Oxford	458	Very rare
Chineham Sewage Works, Basingstoke, Hampshire	458	Very rare
Aldershot Reservoir, Hampshire	400	Very rare
Juniper Hall, Mickleham, Surrey	292	Very rare *
South Farnborough, Hampshire	213	Very rare *
Upper Basildon, Berkshire	214	Very rare
Pirbright Institute, Surrey	193	Very rare
Merrist Wood Agricultural College, Surrey	147	Remarkable
Royal Horticultural Society Gardens, Wisley, Surrey	155	Remarkable
Frimley Pumping Station, Surrey	142	Remarkable
Beaufort Park, Bracknell, Berkshire	30	Noteworthy *
Wodeland Avenue, Guildford, Surrey	55	Remarkable
Aldershot Waterworks, Hampshire	60	Remarkable

* At Juniper Hall, South Farnborough and Beaufort Park, the 2-hour totals are known from hourly data, and these figures (instead of the 24-hour ones) have been used to calculate the return periods.

Table IV. Specific return periods and Bilham (1935) classification for the rainfall on 24 May 1989 at Juniper Hall

Start time (UTC)	Amount (mm)	Duration (h min.)	Return period (years)	Bilham classification
1200	41.2	0 54	135	Remarkable
1100	62.2	1 12	553	Very rare
1100	62.2	2 00	292	Very rare

Table V. Specific return periods and Bilham (1935) classification for the rainfall on 24 May 1989 at South Farnborough

Start time (UTC)	Amount (mm)	Duration (h min.)	Return period (years)	Bilham classification
1305	2.0	0 01	3	Not significant
1303	5.6	0 03	8	Noteworthy
1302	20.9	0 15	61	Remarkable
1240	41.3	0 30	374	Very rare
1233	50.1	1 00	307	Very rare
1200	56.2	2 00	213	Very rare
1200	60.2	6 00	93	Remarkable
1200	60.2	24 00	21	Noteworthy

diameters less than 10 km. Over most of the region in which rain fell, the totals mostly lie between 5 and 15 mm.

Another feature of Fig. 1 worth noting is the actual location of the heaviest centres of precipitation. All the cells with central rainfall totals over 50 mm were situated close to the line of the North Downs, and appear to have had some relationship with the river gaps, though the valley at Basingstoke is modest when compared with, say, the Mole gap at Mickleham. Maybe, the actual link is with the built-up areas associated with the river gaps, which might help to explain the location of the cell near Woking and that over south Bracknell, though the Upper Basildon cell is a little difficult to account for on this theory. Clearly, several factors were involved in triggering the intense convection responsible for these heavy falls, though the extra heat available over built-up areas is likely to have been one of them; another was probably the additional convergence associated with the North Downs themselves. Nonetheless, Fig. 1 is eloquent testimony to the considerable degree of topographic control that was operating.

4. Conclusions

Analysis of hourly and daily rain-gauge data for 24 May 1989, has shown how restricted were the areas of the Thames Valley affected by the most violent rain, and also how unusual the heaviest rainfalls were. Because the cells of precipitation remained almost stationary throughout their lifetimes, the distribution of rainfall shows a very strong degree of topographic control by the North Downs, even if it is somewhat difficult to explain the nature of that control.

Acknowledgements

The author wishes to thank his colleagues in the Production and Service Provision Branch of the Met. Office for their helpful comments and advice during the preparation of this article.

References

Bilham, E.G., 1935: Classification of heavy falls of rain in short periods. Revision of curves showing the lower limits of 'noteworthy', 'remarkable' and 'very rare' falls. *Br Rainfall*, **75**, 262–280.

Collier, C.G., 1990: Assessing and forecasting extreme rainfall in the United Kingdom. *Weather*, **45**, 103–112.

Waters, A.J., (1991): The role of satellite and radar imagery in short-period forecasting of mid-latitude mesoscale convective systems. (To be published in the *Meteorological Magazine*.)

551.506.1(41-4)

The winter of 1989/90 in the United Kingdom

G.P. Northcott
Meteorological Office, Bracknell

Summary

Generally the winter of 1989/90 in the United Kingdom was mild and wet, with seasonal sunshine values near average. A major feature of the season was the frequency of stormy weather from around the middle of December, and storms and severe gales in the last week of January, followed by a very stormy month in February.

1. The winter as a whole

Winter temperatures were above normal everywhere, ranging from 3.0 °C above normal in parts of the Home Counties to 0.3 °C above normal at Tiree, Strathclyde Region. Winter rainfall was above normal in most parts of the United Kingdom other than eastern Scotland and parts of north-east England, and ranged from 64% at Fyvie Castle, Grampian Region to 229% in the Cumbrian Mountains. Sunshine amounts were below average in Kent, east Sussex, south-west England, most of Wales, northern England and western Scotland, about average in Northern Ireland and above average elsewhere, ranging from less than half the normal around Loch Maree in north-west Scotland to 136% in the London area and the north-west of Grampian Region. The season was notable for the incidence of spells of stormy weather, the first of which affected the British Isles around the middle of December, followed by storms and severe gales in the last week of January, and a very stormy February.

Information about the temperature, rainfall and sunshine during the period from December 1989 to February 1990 is given in Fig. 1 and Table I.

2. The individual months

December. Mean monthly temperatures were above normal south of a line from South Wales to the Humber Estuary and below normal to the north, ranging from 3.1 °C below normal at Fort William, Highland Region to 1.6 °C above normal at Heathrow, Greater London. Mean monthly rainfall totals were above normal over most of England and Wales and below normal in Northern Ireland and most of Scotland, ranging from 232% at Brize Norton, Oxfordshire to 50% at Aberdeen Airport, Grampian Region. Hampstead, Greater London had no measurable rain from 10 November until 11 December, followed by 116.9 mm in the next 10 days. Parts of south-west Scotland were dry from 13 November to 12 December. In Northern Ireland it was the driest December since 1975. Monthly sunshine amounts were below normal in most parts of England and Wales, but above normal in Scotland, apart from the far north and east, ranging from 187% at Tiree, Strathclyde Region to 35% at Birmingham, West Midlands. Broom's Barn, Suffolk had the dullest December for 20 years. Sheffield, Weston Park, South Yorkshire, reported the lowest

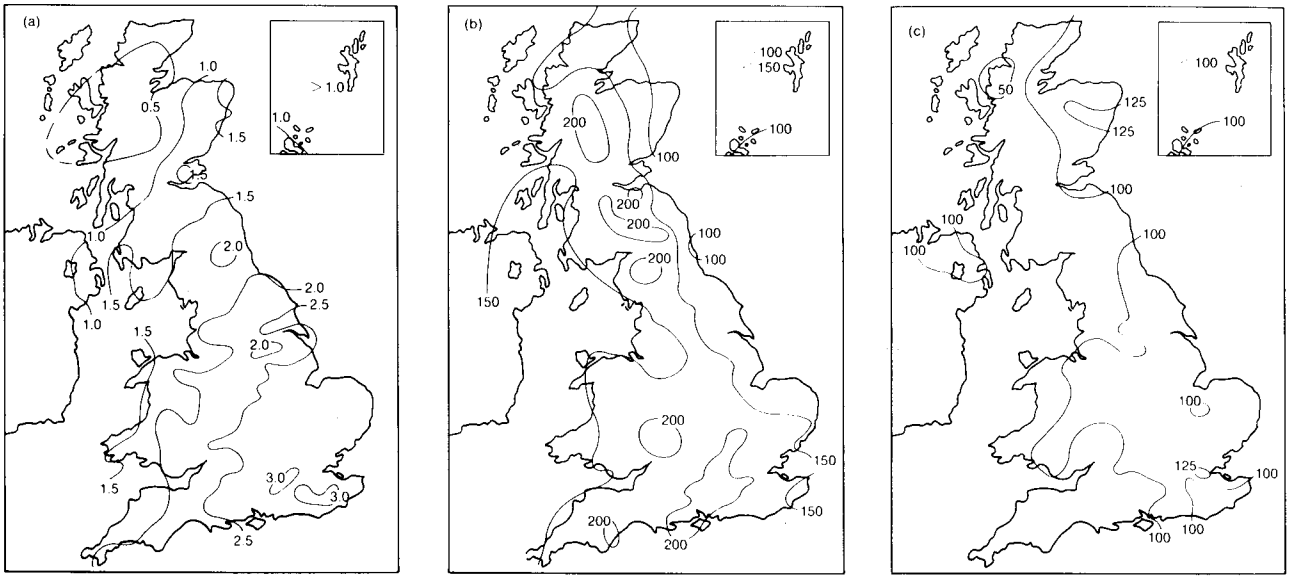

Figure 1. Values of (a) mean temperature difference (°C), (b) rainfall percentage and (c) sunshine percentage for winter, 1989/90 (December–February) relative to 1951–80 averages.

Table I. District values for the period December 1989–February 1990, relative to 1951–80 averages

District	Mean temperature (°C)	Rain-days	Rainfall	Sunshine
	Difference from average		Percentage of average	
Northern Scotland	+0.8	+2	181	97
Eastern Scotland	+1.2	+1	161	112
Eastern and north-east England	+2.3	+2	144	100
East Anglia	+2.7	+1	161	113
Midland counties	+2.5	+2	175	97
South-east and central southern England	+2.9	+3	196	97
Western Scotland	+1.8	+3	187	84
North-west England and North Wales	+1.8	+3	175	86
South-west England and South Wales	+2.2	+4	178	87
Northern Ireland	+0.9	+3	150	103
Scotland	+1.0	+2	180	98
England and Wales	+2.4	+3	171	97

Highest maximum: 18.0 °C in Midland counties in February.
Lowest minimum: −12.9 °C in eastern Scotland in December.

December sunshine total since 1933.

The month was mostly settled and dry with fog and frost at times until the 11th, after which followed a period of very wet and, between the 14th and 26th, windy weather, again becoming quiet for the last week. Strong winds from the south or south-west combined with an exceptionally high tide on the 14th to bring widespread flooding to many places on the south coast. A mini-tornado on the 14th at Long Stratton, Norfolk damaged more than 100 buildings. On the 16th gales and rain over south-west England caused severe flooding at Plymouth, Devon. On the 17th the observer at Falmouth, Cornwall, in an exposed coastal position, reported a gust of 104 kn while several anemographs in the area recorded gusts of more than 70 kn; these included 74 kn at Plymouth, Devon and 71 kn at Gwennap Head, Cornwall. However, the highest gust recorded by anemograph during the month was 78 kn at Fraserburgh, Grampian Region on the 18th. On the 13th snow fell as far south as the Midlands. Further snow fell in north Derbyshire on the 14th with up to 13 cm of level snow reported lying in the Buxton area. Moel-y-Crio, Clwyd measured 24 cm of snow lying at 09 UTC on the 15th. Further snow fell later on the 18th, over eastern Wales and the north-western Midlands. On the 21st a tornado struck the villages of West and East Stour in Dorset, uprooting trees and causing structural damage to buildings. A 500-gallon (2275-litre) oil drum was lifted and blown 200 metres and a 17-metre radio mast was toppled. A band of heavy rain with hail and thunder crossed southern areas of the United Kingdom on the 23rd. Over the Christmas period it was very mild, with strong south-westerly winds, followed by a quiet, dry end to the month over the United Kingdom.

January. Mean monthly temperatures were above normal everywhere ranging from 1.1 °C above normal at Cape Wrath, Highland Region to 3.8 °C above normal at Lyneham, Wiltshire. Monthly rainfall amounts were above normal everywhere except eastern coastal areas of England where they were slightly below normal and the east coast of Scotland where it was very dry. Wick, Highland Region had less than half the normal rainfall compared with over twice the normal over a large area of the western Highlands. Monthly sunshine amounts were below average in southern coastal counties and in Shetland and western Scotland, and above average elsewhere, reaching 156% in North Wales, but as little as 42% in southern Scotland.

The month was generally unsettled with periods of rain, heavy at times, or showers, occasionally wintry in northern areas. Much of England and Wales and north-west Scotland was dry on the 3rd and 4th, although there was heavy rain in the Glasgow area on the 3rd. Rain and strong winds affected all areas from time to time from the 9th. Thunder occurred in northern areas, mainly over Scotland and Northern Ireland between the 17th and 23rd. The night of the 16th/17th was very windy in northern areas, with gusts of 76 kn at Stornoway and 79 kn at Benbecula (both in Western Isles) late on the 16th and a record January gust of 109 kn with a mean speed of 72 kn at Fair Isle, Shetland early on the 17th. The 25th was an extremely windy day with severe gales over England and Wales with gusts to 93 kn at Aberporth, Dyfed and Gwennap Head, Cornwall. Gusts to more than 80 kn were widely reported on other exposed southern and western coasts and to more than 70 kn in many central and southern parts of England and Wales. A great deal of structural damage was done and a large number of trees brought down, the area affected was much more widespread than that during the storm of 16 October 1987. There were thunderstorms over both Scotland and southern England and Wales on the 26th, over north-west England and Wales on the 30th and over parts of the south on the 31st, frequently accompanied by hail.

February. Mean monthly temperatures were above normal everywhere and ranged from 0.4 °C above normal in the far north-west of Scotland to more than 4.3 °C in south-east England. Monthly rainfall totals were above normal everywhere in the United Kingdom and ranged from 111% at Aberdeen, Grampian Region to 438% in the western Highlands. At Fort Augustus, Highland Region it was the wettest February since records began in 1886, the previous wettest having been February 1989. At Paisley, Strathclyde Region it was the wettest February since 1894. Monthly sunshine amounts were generally above average in eastern areas and below average in western areas, ranging from 164% of average at Wyton, Cambridgeshire to 57% of average at Aspatria, Cumbria.

The month was generally unsettled and at times very wet with only about 7 dry days, mainly over England and Wales and eastern Scotland. It was generally very windy, with strong winds or gales on about 14 days and severe gales on the 1st, 19th, 27th and 28th. Gusts in excess of 60 kn were widely reported on the 12th and 26th, whilst gusts in excess of 70 kn were reported on the 1st, 7th and 11th in the south-west, including 81 kn at Burrington, Devon on the 11th. Early on the 3rd prolonged heavy rainfall occurred south-east of a line from the Bristol Channel to The Wash, resulting in flooding, and the rain turned to snow in many places before it cleared. On the 19th very heavy rainfall over north-west England and North Wales caused flooding, while central and eastern England stayed mainly dry. The coincidence on the 26th and 27th of strong winds, low atmospheric pressure and 'spring' tides led to severe flooding and wave damage along several British coasts: Towyn, Clwyd suffered a major disaster when sea defences were overwhelmed. On the 26th there were gusts of 85 kn at Leeds, West Yorkshire and 86 kn at Hemsby, Norfolk.

Notes and news

100 years ago.

SYMONS'S

MONTHLY

METEOROLOGICAL MAGAZINE.

CCC.] JANUARY, 1891. [PRICE FOURPENCE, *or 5s. per ann. post free.*

OUR THREE HUNDREDTH NUMBER.

To have been enabled to edit every one of three hundred consecutive monthly numbers is not given to many, and, looking back over the work of a quarter of a century, a feeling of thankfulness is naturally predominant.

We lay no claim to brilliancy or to financial success, or to a large circulation; but we are conscious of the friendliness of nearly all the leaders of Meteorological progress in both hemispheres. Perhaps because it is so small, but, be the reason what it may, we rejoice to know that the *Meteorological Magazine* has the highest honour which a book can have—that of being read. We know that this is so, because when we make a mistake (and of course the Editorial "we" is fallible), whether in dealing with Russia, America, or our Australian colonies, the very next mail is sure to tell us of it; and we rejoice that this is the case, for our whole aim has ever been to help forward the science which we love, and the best way to do that is to stamp out error wherever it can be found.

Comment: *Would it were ever thus!*

Review

Elementary fluid dynamics, by D.J. Acheson. 136 mm × 215 mm, pp. vi+397, *illus.* Oxford University Press, 1990. Price £15.00 (paperback), £45.00 (hardback). ISBN 0 19859 679 0.

Fluid dynamics is important in many branches of physics, engineering, chemistry and biology. Students and research workers in any of these areas require fluid dynamics textbooks tailored to their particular specialisms, but there is also a need for texts which give a broad view of the basic concepts. Dr Acheson's book comes into this wider category. It aims to give 'an introduction to fluid dynamics for students of applied mathematics, physics and engineering', and is part of the Oxford Applied Mathematics and Computing Science Series.

Topics covered include the equations of motion, vortex dynamics, waves, instability, aerofoil theory, boundary layers and viscous flow. As befits a text on elementary principles, a wide range of applications and contexts is indicated — from aeronautics and the flight of insects to Kelvin-Helmholtz billows and tornadoes. Each of the nine chapters is followed by several pages of exercises, some of which are demanding, and which extend the scope of the book considerably without adding much to its length. (The book, indeed, is physically compact — one could read it without difficulty or embarrassment on a bus or train.) Hints and answers to the exercises are given in a separate section. The reference list is comprehensive without being compendious. Text and figures are well presented and misprints are very few.

The chapters on waves, instability, vortex motion and boundary layers are those which are most relevant to meteorological concerns. Of these, the chapter on waves is particularly useful, having very clear discussions of dispersion, group velocity, sound waves, surface waves, internal gravity waves and various finite amplitude effects. The chapter on instability is also valuable; it gives a wide-ranging yet concise survey and is ambitious enough to treat some stability proofs in depth.

Although it does not hesitate to present the mathematical machinery and detail of the subject, the book maintains a refreshingly practical outlook. The first sentence of chapter 1 reads 'Take a shallow dish and pour in salty water to a depth of 1 cm', while on p. 342 the reader is enjoined to 'Take a pot of golden syrup, spoon out a generous helping, and let it drain slowly back into the pot'. The book also gives a welcome historical perspective to its subject, with extensive quotations from papers by Prandtl, Reynolds, Stokes, Taylor, Helmholtz and even Newton. In only one respect does the historical background seem insufficient: the text (on p. 265) leaves the impression that 19th century fluid dynamicists were somehow culpable because of their uncertainty about the applicability of the non-slip condition at rigid boundaries. The reader must consult referenced works by S. Goldstein (or G.K. Batchelor's *An introduction to fluid dynamics*) for clarification of this important issue.

This book can be highly recommended. It is written by an expert with wide experience of teaching and research in the field, who succeeds in communicating to the reader his enthusiasm for the subject. Some of the topics covered are highly relevant to meteorology, while others are clearly less so. However, the clarity and vigour of the presentation may encourage the specialist to venture beyond the purlieus of his usual interests, and there can be no harm in that!

A.A. White

Books received

The listing of books under this heading does not preclude a review in the Meteorological Magazine at a later date.

The telemetry of hydrological data by satellite, by I.C. Strangeways (Wallingford, Institute of Hydrology, 1990. £7.00) aims to bring together the basic information for a potential user of satellite telemetry. Although slanted hydrologically, much of the material can have a broader use.

Dynamics in atmospheric physics, by R.S. Lindzen (Cambridge University Press, 1990. £25.00, US$39.50) consists of 7 years of university lecture notes. An attempt is made towards general thinking about nature by including some history of the scientific inquiry into the subject. ISBN 0 521 36101 X.

Dynamics, transport and photochemistry in the middle atmosphere of the southern ocean, edited by A. O'Neill (Dordrecht, Boston, London, Kluwer, 1990. Dfl.145.00, US$89.00, £50.00) contains most of the papers included in the NATO Advanced Research Workshop held in San Francisco on 15–17 April 1989. The interdisciplinary nature of the study is accentuated. ISBN 0 7923 0977 4.

Global air pollution: Problems for the 1990s, by H.A. Bridgman (London, Belhaven Press, 1990. £30.00 (hardback), £12.95 (paperback)) aims to give students a firm grasp of the scientific principles of the subject in relation to the social and economic issues. The only equations used are chemical. ISBN 1 85293 094 2 (hardback), 1 85293 099 2 (paperback).

Satellite photographs — 3 September 1990 at 1521 UTC

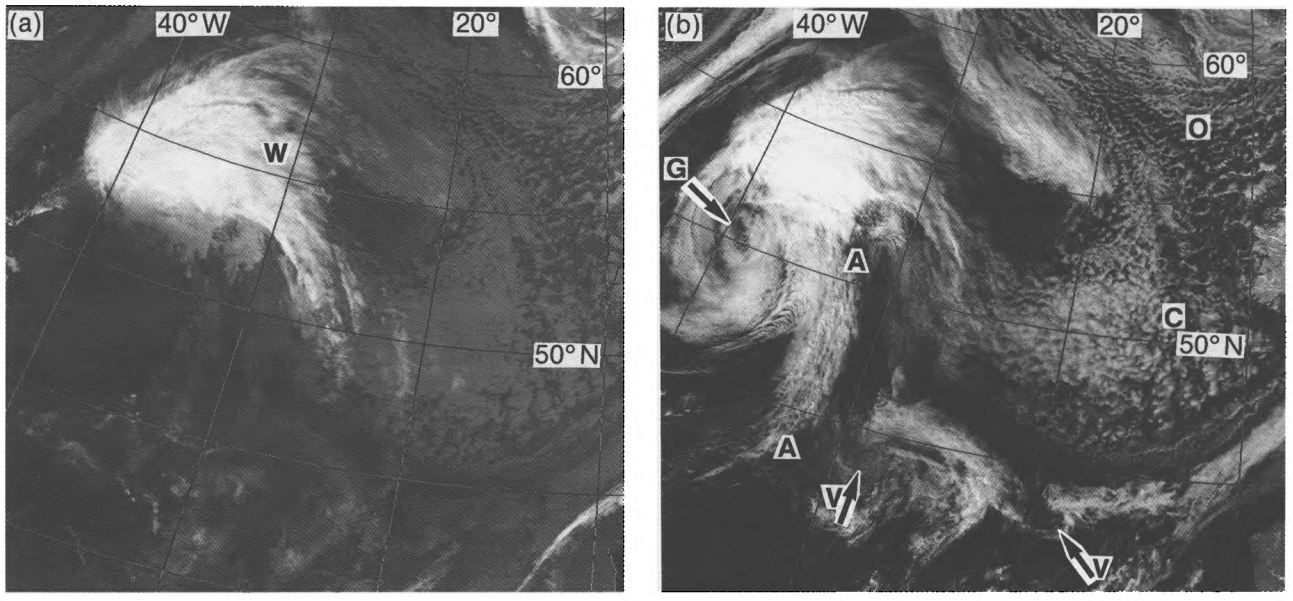

Photographs by courtesy of University of Dundee

Figure 1. NOAA-9 images for 1521 UTC on 3 September 1990, (a) infra-red, and (b) visual.

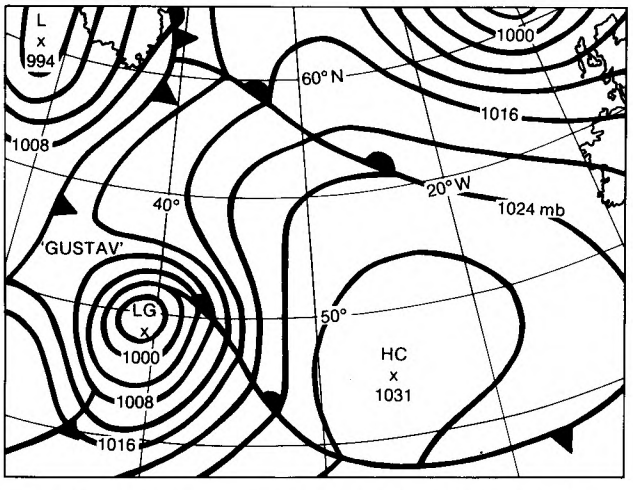

Figure 2. Surface analysis for 1200 UTC on 3 September 1990.

The satellite photographs in Fig. 1 were both taken from NOAA-9 at 1521 UTC on 3 September 1990. They show how particular cloud systems can appear very differently on visible and infra-red (IR) images, and highlight the complementary nature of data from these two channels. Key elements of cloud structure portrayed on visible images are cloud thickness and texture, and the response is not dependent on the cloud-top temperature. The response on IR channels, however, is very dependent on the temperature of the underlying surface and little detail in cloud structure can be detected in unenhanced images when the cloud-top temperature is similar to that of the background, i.e. land or sea surface.

The main feature towards centre-left on the IR image (Fig. 1(a)) is a wedge-shaped area of cloud tops (W), which is reminiscent of the signature associated with a wave depression before the occlusion process. It is very difficult to discern any significant circulation either at the surface or aloft. The visible image of the same system in Fig. 1(b) clearly shows, within the area of predominantly low cloud, that there is a marked circulation with a virtually cloud-free centre (G).

They are in fact images of ex-hurricane Gustav (see Fig. 2) which, although now degraded to a mere mid-latitude low, still had very strong winds in its circulation and 2 days later, on 5 September, still produced locally gale-force winds when it crossed close to northern Scotland. Coincident high spring tides resulted in local coastal flooding, e.g. near Towyn, North Wales, but the exceptionally high water levels were well predicted by the Meteorological Office Storm Tide Warning Service.

These images of Gustav are typical of hurricanes or tropical storms that have moved north, become engaged in the westerlies, but with no significant interaction with the polar front. The lack of any significant surface-based convection in the system — except possibly some remnants in the relatively shallow cloud band marked AA in Fig. 1(b) — is because the system has moved over progressively colder sea.

Other features of interest, highlighted on the visible image, include:

- Marked detail in the open (O) and closed (C) cell structure to the west of Ireland.
- Small vortices (V) along the weak cold front near 45° N.

A.J. Waters

GUIDE TO AUTHORS

Content

Articles on all aspects of meteorology are welcomed, particularly those which describe results of research in applied meteorology or the development of practical forecasting techniques.

Preparation and submission of articles

Articles, which must be in English, should be typed, double-spaced with wide margins, on one side only of A4-size paper. Tables, references and figure captions should be typed separately. Spelling should conform to the preferred spelling in the *Concise Oxford Dictionary* (latest edition). Articles prepared on floppy disk (Compucorp or IBM-compatible) can be labour-saving, but only a print-out should be submitted in the first instance.

References should be made using the Harvard system (author/date) and full details should be given at the end of the text. If a document is unpublished, details must be given of the library where it may be seen. Documents which are not available to enquirers must not be referred to, except by 'personal communication'.

Tables should be numbered consecutively using roman numerals and provided with headings.

Mathematical notation should be written with extreme care. Particular care should be taken to differentiate between Greek letters and Roman letters for which they could be mistaken. Double subscripts and superscripts should be avoided, as they are difficult to typeset and read. Notation should be kept as simple as possible. Guidance is given in BS 1991: Part 1: 1976, and *Quantities, Units and Symbols* published by the Royal Society. SI units, or units approved by the World Meteorological Organization, should be used.

Articles for publication and all other communications for the Editor should be addressed to: The Chief Executive, Meteorological Office, London Road, Bracknell, Berkshire RG12 2SZ and marked 'For Meteorological Magazine'.

Illustrations

Diagrams must be drawn clearly, preferably in ink, and should not contain any unnecessary or irrelevant details. Explanatory text should not appear on the diagram itself but in the caption. Captions should be typed on a separate sheet of paper and should, as far as possible, explain the meanings of the diagrams without the reader having to refer to the text. The sequential numbering should correspond with the sequential referrals in the text.

Sharp monochrome photographs on glossy paper are preferred; colour prints are acceptable but the use of colour is at the Editor's discretion.

Copyright

Authors should identify the holder of the copyright for their work when they first submit contributions.

Free copies

Three free copies of the magazine (one for a book review) are provided for authors of articles published in it. Separate offprints for each article are not provided.

Contributions: It is requested that all communications to the Editor and books for review be addressed to the Chief Executive, Meteorological Office, London Road, Bracknell, Berkshire RG12 2SZ, and marked 'For *Meteorological Magazine*'. Contributors are asked to comply with the guidelines given in the *Guide to authors* which appears on the inside back cover. The responsibility for facts and opinions expressed in the signed articles and letters published in *Meteorological Magazine* rests with their respective authors.

Subscriptions: Annual subscription £33.00 including postage; individual copies £3.00 including postage. Applications for postal subscriptions should be made to HMSO, PO Box 276, London SW8 5DT; subscription enquiries 071–873 8499.

Back numbers: Full-size reprints of Vols 1–75 (1866–1940) are available from Johnson Reprint Co. Ltd, 24–28 Oval Road, London NW1 7DX. Complete volumes of *Meteorological Magazine* commencing with volume 54 are available on microfilm from University Microfilms International, 18 Bedford Row, London WC1R 4EJ. Information on microfiche issues is available from Kraus Microfiche, Rte 100, Milwood, NY 10546, USA.

January 1991

Editor: F.E. Underdown
Editorial Board: R.J. Allam, R. Kershaw, W.H. Moores, P.R.S. Salter

Vol. 120
No. 1422

Contents

ISSN 0026–1149

ISBN 0-11-728852-7

9 780117 288522

Printed in the United Kingdom for HMSO
Dd 0291241 C13 1/91 503 12521

The Meteorological Magazine

February 1991

Rainfall frequency in south-west England
Verification of aerodrome forecasts
The spring of 1990

HMSO

Met.O.998 Vol. 120 No. 1423

First published 1991

HMSO publications are available from:

HMSO Publications Centre
(Mail and telephone only)
PO Box 276, London, SW8 5DT
Telephone orders 071-873 9090
General enquiries 071-873 0011
(queuing system in operation for both numbers

HMSO Bookshops
49 High Holborn, London, WC1V 6HB 071-
258 Broad Street, Birmingham, B1 2HE 021-
Southey House, 33 Wine Street, Bristol, BS1 2
9–21 Princess Street, Manchester, M60 8AS
80 Chichester Street, Belfast, BT1 4JY (0232)
71 Lothian Road, Edinburgh, EH3 9AZ 031

HMSO's Accredited Agents
(see Yellow Pages)

and through good booksellers

The Meteorological Magazine

February 1991
Vol. 120 No. 1423

551.577.36(423):551.501

A four-parameter model for the estimation of rainfall frequency in south-west England

C. Clark
Bruton, Somerset

Summary

A new method for the estimation of the frequency of heavy rainfall in south-west England has given results which indicate that big storms are more frequent than previous evidence suggests. The results are consistent with probability assessments of the expected return periods. The implications of the results are described.

1. Introduction

The two most well known methods that are used to estimate the return period (i.e. the number of years within which a particular extreme value is likely to be exceeded only once) of rainstorms, namely the Bilham method (Bilham 1935) and that used in Volume II of the *Flood Studies Report* (FSR-II) (Natural Environment Research Council 1975) produce different results according to the rarity of the storm and the average annual rainfall of the site (Kelway (1977) and Marshall (1977), respectively). In general the FSR method gives the higher return periods. This difference is of great practical importance for the design of culverts, flood alleviation schemes, and reservoir spillways. In the event of the capacity of an underdesigned spillway being exceeded, the possibility of dam failure, although slight, is too great to be dismissed in view of the damage and likely loss of life. FSR-II grew out of the acknowledged inadequacies of the now largely extinct Bilham method, especially with its uniform treatment of storms irrespective of their location. However, work by Bootman and Willis (1977, 1981) showed that for parts of Somerset the FSR-II method gave an under-estimation of the magnitude of 2-day rainfall. The difference between FSR-II and the local data, especially around Bridgwater, was considered important enough for the Institution of Civil Engineers to override the general advice that local rainfall data should not be used for the estimation of floods in relation to reservoir safety in Somerset (Institution of Civil Engineers 1978). This poses the question of whether or not this problem is confined to Somerset alone.

More recent work (Folland *et al.* 1981) revised the growth factors for estimates of rainfall frequency, and the problem of the station–year method was investigated by Reed and Dales (1988), Dales and Reed (1989) and Stewart (1989) in which the number of independent stations was assessed and regional growth curves introduced. The resulting 'FORGE' method was updated in December 1989 (Stewart and Reed 1989). These studies highlight the difficulty of rainfall frequency estimation but they also beg the question of an independent test in order to assess the validity of the results. A central problem of frequency analysis is that the data are often inadequate (Tabony 1983), but the chief problem of the FSR-II and FORGE methods is that they may be based upon dependent records. In addition they are both based upon 2-day rainfall which masks the true intensity characteristics; it is likely that this database will contain several different populations of rainstorm. For example, the largest daily rainfall at Martinstown occurred over a period of 18 hours (Twort *et al.* 1985). As time progresses more unprecedented

rainstorms are reported (Acreman 1989) and they suggest that values of probable maximum precipitation are too low.

This paper reports the results of an investigation into rainfall frequency over the Somerset Division of the Wessex Water Authority and the South West Water Authority areas. The area was chosen partly because it includes the area covered by Bootman and Willis (1977) who only considered 2-day rainfall, and also because south-west England is prone to heavy rainfall (Rodda 1970).

2. Study area and methods

A total of 44 autographic rain-gauge records were used in the study. Their distribution is shown in Fig. 1, and their location, elevation, duration of record and model parameter values given in Table I.

Much of the south-west peninsula is represented with the exception of a broad band between Exeter and Barnstaple. The records were of good quality with almost 100% coverage in the years analysed. Where one month or more was missing then that year of data was discarded. A careful check on daily rainfall was made in the event of an odd day's record being lost. The annual maxima of 1-, 2-, 4-, 8-, 12-, and 24-hour rainfalls were then subjected to an extreme frequency analysis wherein the return periods were calculated using the formula proposed by Clark (1983) which was based on a comparison of the theoretical return periods, and the return generated by a Monte Carlo analysis of a perfect 10 000-year record wherein the return periods were calculated using $N+1/M$. The resulting formula gives results which are very similar to the Gringorten formula as used in the FSR-II. The rainfall data were then plotted onto log Gumbel paper. This approach has been used by Perry and Howells (1982) and Dunne and Leopold (1978) when analysing rainfall frequency. The use of the logarithmic scale is preferred because it overcomes the problem encountered in data presented by Rodda (1970) and Tabony (1983), namely the apparent very high return periods for the highest events, herein called rank 1 events. In addition, if the data plotted on log Gumbel paper are then re-plotted onto linear Gumbel paper there are serious problems in the interpretation of the return period of the extreme events. The use of log Gumbel plotting paper gives rise to higher magnitudes of rare events which lie outside the range of the data.

The line of best fit was then fitted to the data using linear regression but omitting the largest event on account of its effect upon the result. The equation is of the form

$$\log Y = aX + b$$

where X (the reduced variate) is

$$-\ln_e\{-\ln_e(1-\frac{1}{T})\}$$

where T is the return period in years.

It was found that at certain sites the regression lines gave impossible values for a given duration of rainfall

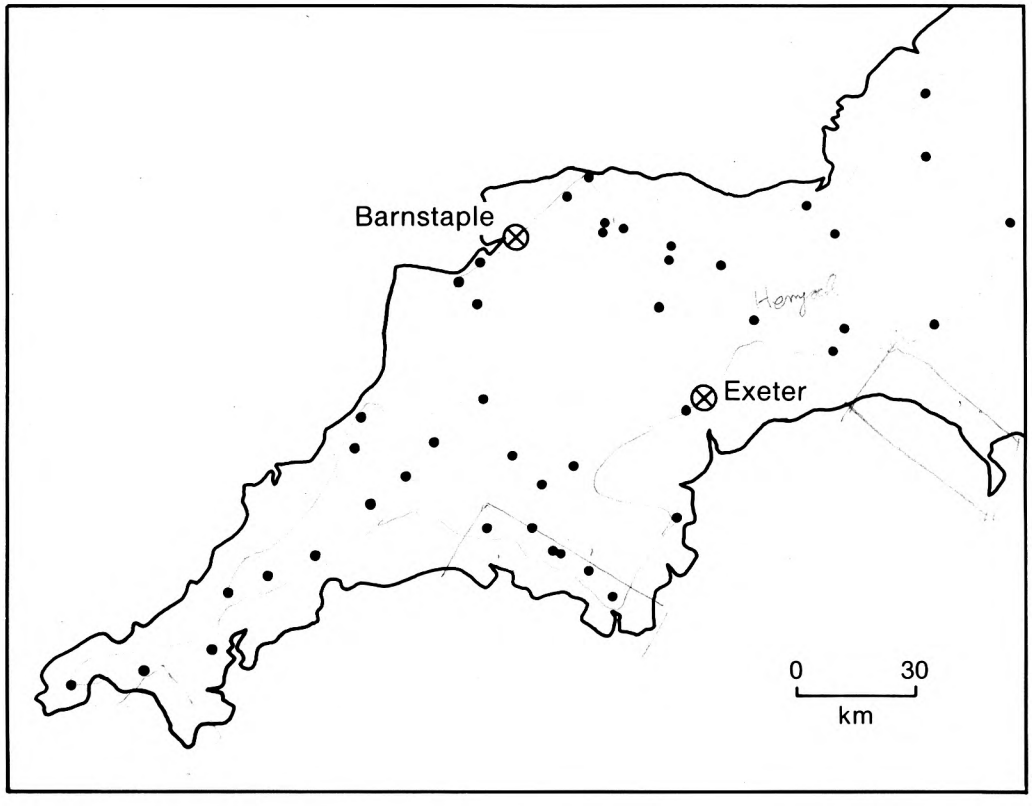

Figure 1. Distribution of autographic rain-gauge sites in south-west England used in this study.

because the value of a in the equation was not constant for all durations owing to the random nature of the data. To overcome this problem the average value of a was calculated to give, for all storm durations

$$\log Y = \bar{a}X + b.$$

This simplified the remainder of the analysis and acknowledges the fact that at higher return periods there cannot be more rain in one hour than in two. Fig. 2 shows the results of the method of analysis for two sites. From the results of the frequency analysis of 21 sites whose data were in excess of 15 years the four-parameter model was constructed.

3. The four-parameter model

For a method to predict the rainfall frequency at a site without any records it is essential that explanatory variables be identified which give realistic results. Considerable experiment revealed that four parameters

Table I. Site details and derived parameter values

Site name	National Grid Reference	Altitude (m)	Length of record (yrs)	AAR (mm)	Slope (deg.)	2-year, 24-hour rainfall (mm)	24−1 hour difference 2-year rainfall (mm)
Barrow Gurney	ST538672	91	7	883	36	44.3	32.4
Bastreet	SX244765	233	25	1706	28	59.5	45.3
Bideford	SS454271	4	11	912	35	45.4	33.4
Blackdown	SX522813	320	24	1650	28	59.1	44.9
Burrator	SX552685	221	23	1555	29	58.2	44.2
Cannington	ST245394	23	15	793	38	40.2	29.0
Carthew	SX002559	221	9	1400	30	56.4	42.7
Chard	ST319086	79	17	1060	33	50.1	35.7
Drift	SW437286	76	16	1191	32	53.1	39.9
Exeter	SX928917	27	8	820	37	41.5	30.1
Exton	SS961338	328	17	1500	29	57.6	43.7
Godolphin	SW602318	46	9	1080	33	50.6	37.8
Goosemoor	SS958354	369	6	1400	30	56.4	42.7
Hemyock	ST138129	165	24	1016	34	48.9	36.3
Higher Brockscombe	SX462950	186	11	1290	31	54.8	41.4
Hollamoor	SS443176	163	6	1137	32	51.9	38.9
Houndall	SX594592	188	9	1500	29	57.6	43.7
Kingsbridge	SX735441	34	7	1100	33	51.1	38.2
Ladock	SW892510	30	21	1115	32	51.5	38.5
Launceston	SX327839	128	24	1196	32	53.2	40.0
Lesnewth	SX130902	183	25	1400	30	56.4	42.7
Lowermoor	SX128831	267	9	1585	28	58.5	44.4
Lutton	SX588590	168	16	1500	29	57.6	43.7
Lynmouth	SS724495	12	7	1100	33	51.1	38.2
Maundown	ST065291	198	12	1100	33	51.1	38.2
Melbury	SS387202	143	11	1310	30	55.2	41.7
Modbury	SX667502	76	16	1200	32	53.3	40.0
North Brewham	ST722370	131	17	900	36	44.9	33.0
Northmoor P.S.	ST331330	8	39	695	40	34.5	24.3
Penryn Resr	SW778337	55	11	1159	32	52.4	39.3
Postbridge	SX653787	361	16	2032	26	61.6	46.9
Priddy	ST550505	268	13	1101	33	51.1	38.2
Princetown	SX586741	423	19	2136	26	62.1	47.3
Rumleigh	SX422680	23	11	1200	32	53.3	40.0
St. Neot	SX167707	223	24	1400	30	56.4	42.7
Simmonsbath	SS782394	381	6	1800	27	60.2	45.8
Stoodleigh	SS916185	245	8	1200	32	53.3	40.0
Sutton Bingham	ST556116	44	18	850	37	42.9	31.2
Thornmead	SS806382	387	5	1650	28	59.1	44.9
Threemilestone	SW780452	101	15	1100	33	51.1	38.2
Torquay	SX909637	8	15	898	36	44.9	32.9
Twist	ST290037	183	11	1050	33	49.8	37.1
Winstitchen	SS784389	369	11	1800	27	60.2	45.8
Woolhanger	SS698454	312	13	1800	27	60.2	45.8

of the frequency plots could be predicted using the average annual rainfall (AAR) for each site. The parameters are

(1) The 2-year, 24-hour rainfall.

(2) The 24 hour−1 hour difference in rainfall with a return period of 2 years.

(3) The slope of the frequency curve as measured in degrees.

(4) The percentage of the 24 hour−1 hour difference in rainfall for a given storm duration.

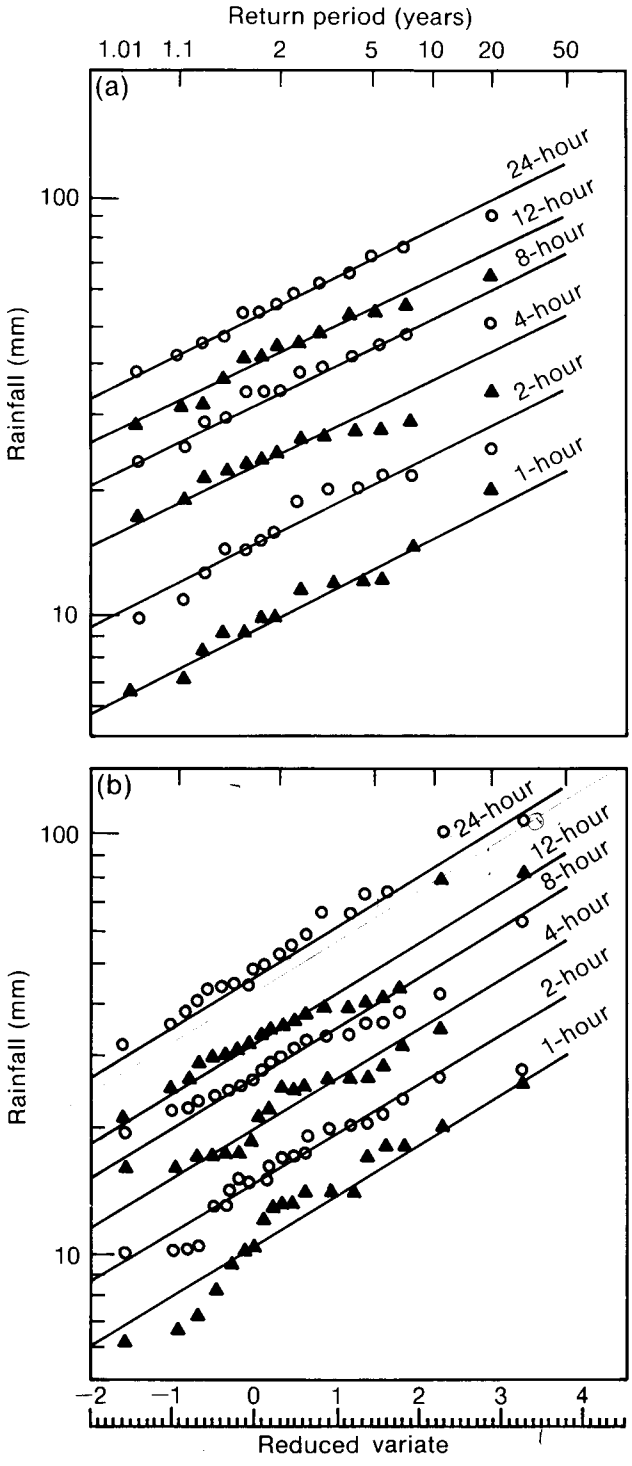

Figure 2. Rainfall frequency–duration relationships for (a) Woolhanger and (b) Hemyock.

Figs 3–6 show the results of these analyses. The AAR was extracted from rainfall records or by interpolation of the values given on the map produced by the Meteorological Office for the standard period 1941–70 for southern Britain.

The 2-year, 24-hour rainfall increases as the AAR increases, tending towards an upper limit for the wetter sites. The growth curves are very well related to the same parameter, probably on account of the drier sites being more subject to heavy downpours of convective rainfall whereas the wetter sites are more prone to relief rainfall and frontal rainfall. The 24 hour−1 hour difference in rainfall also increases with the AAR, probably because of similar reasons given above.

To predict the frequency of rainfall with other durations the stations were divided into four AAR groups, namely 690–899, 900–1099, 1100–1799 and 1800–2199 mm. The percentage of the 24 hour−1 hour difference in rainfall was calculated from the frequency plots for durations of 2, 4, 8, and 12 hours and an average percentage for each duration was obtained for each rainfall group. The results are plotted in Fig. 6 where there is a small but systematic variation between storm duration, AAR and the percentage of 24 hour−1 hour rainfall. Table II was then compiled from Fig. 6. From Fig. 5, Table III was constructed; this shows the slope of the frequency curve in relation to the growth factors for rainfall with return periods of 3–1000 years. It is not yet possible to give a reliable return period to storm events which are in excess of 100 years because of the relatively short lengths of the records. It should not be assumed that the magnitudes of a given duration of rainfall will increase indefinitely. Indeed from Jackson (1979) it appears that rainfall frequency may follow an EV2 distribution up to 10^4 years, but that beyond this an EV3 distribution is more appropriate. This means that rainfall increases at an increasing rate in relation to the return period in the range 100–10 000 years (EV2) and thereafter rainfall increases at a decreasing rate in relation to the return period (EV3). Together with the relationships in Figs 3–6, Tables II and III were used in order to predict the return periods of storms that occurred at all of the sites. The method is described in detail below.

(1) Obtain the AAR of the site from the standard-period rainfall map 1941–1970 for southern Britain, or from published records.

(2) Calculate the 2-year, 24-hour rainfall using the equation in Fig. 3.

(3) Calculate the 24 hour−1 hour difference in rainfall using the equation in Fig. 4.

(4) Calculate the 1-hour, 2-year rainfall (step (2)−step (3) above).

(5) Obtain the percentage of the 24 hour−1 hour difference in rainfall for a T-hour rainfall from Table II.

(6) Calculate the 2-year, T-hour rainfall ((percentage

of the 24 hour−1 hour rainfall difference (step (5)) × 24 hour−1 hour difference (step (3))) + 1-hour, 2-year rainfall (step (4))).

(7) Apply the equation in Fig. 5 to obtain the slope of the growth curve to the nearest whole degree.

(8) Calculate the growth factor as a ratio of storm rain in T-hour/2-year, T-hour rainfall.

(9) Interpolate from Table III the return period of the storm taking account of the non-linear progression of the return periods.

Example No. 1; Location — Launceston, AAR=1196 mm. Storm: 50 mm in 3 hours.

(1) AAR is 1196 mm.

(2) From Fig. 3 the 2-year, 24-hour rainfall is 53.2 mm.

(3) From Fig. 4 the 24 hour−1 hour difference in rainfall is 40 mm.

(4) Therefore the 1-hour, 2-year rainfall is $53.2 - 40 = 13.2$ mm.

(5) From Table II the percentage of the 24 hour−1 hour difference in rainfall for a 3-hour storm is 20.5%.

(6) Therefore the 2-year, 3-hour rainfall is $(0.205 \times 40) + 13.2 = 21.4$ mm.

(7) From Fig. 5 the slope of the rainfall growth curve is 32°.

(8) Growth factor is $50/21.4 = 2.34$.

(9) Interpolating from Table III gives a return period of 31 years.

Example No. 2; Location — North Brewham, AAR=900 mm. Storm: 40 mm in 2 hours.

(1) AAR is 900 mm.

(2) From Fig. 3 the 2-year, 24-hour rainfall is 44.9 mm.

(3) From Fig. 4 the 24 hour−1 hour difference in rainfall is 33 mm.

(4) Therefore the 1-hour, 2-year rainfall is $44.9 - 33 = 11.9$ mm.

(5) From Table II the percentage of the 24 hour−1 hour difference in rainfall for a 2-hour storm is 14.0%.

(6) Therefore the 2-year, 2-hour rainfall is $(0.14 \times 33) + 11.9 = 16.5$ mm.

(7) From Fig. 5 the slope of the rainfall growth curve is 36°.

(8) Growth factor is $40/16.5 = 2.42$.

(9) Interpolating from Table III gives a return period of 22 years.

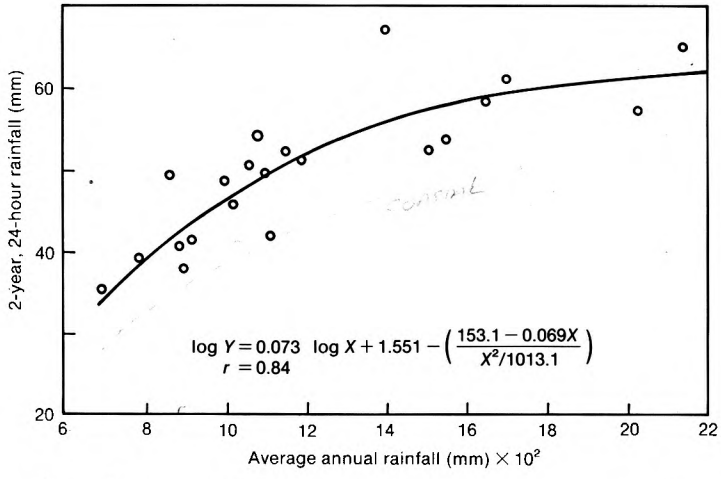

Figure 3. 2-year, 24-hour rainfall in relation to average annual rainfall.

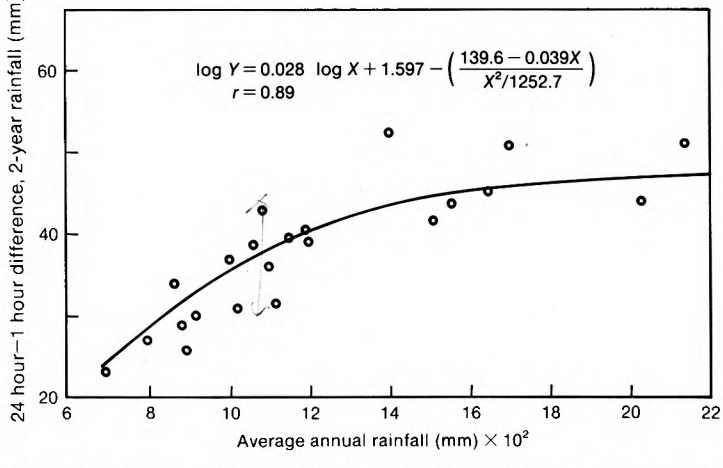

Figure 4. 24 hour−1 hour difference, 2-year rainfall in relation to average annual rainfall.

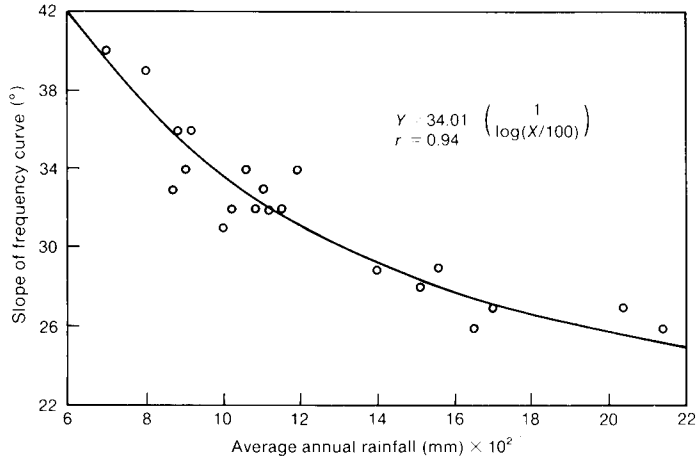

Figure 5. Relationship between the slope of the frequency curve and average annual rainfall.

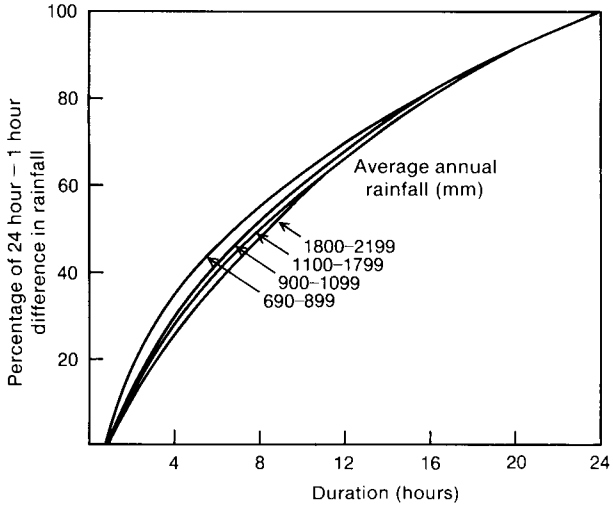

Figure 6. Relationship between storm duration, percentage of 24 hour—1 hour difference in rainfall and average annual rainfall (AAR).

4. Model testing and comparisons

To assess the validity of the results three methods of analysis were used:

Comparison with simulated return periods.

Comparison of return periods obtained using the FSR-II method.

Comparison of the return periods with those obtained from the data.

4.1 Comparison with simulated return periods

The number of sites whose return periods are in excess of the return periods which occur at the 50% and 5% probability levels was compared with the number of sites obtained by the Monte Carlo analysis described above. The largest return period was excluded from the analysis since a very rare event can occur in a short record, whereas two or more such events would be viewed as uncommon. When many more than 1 in 20 stations have storms which have return periods in excess of the return periods at the 5% probability level then there exists a prima facie case for overestimation of the return periods of the storms. Fig. 7 shows the nomogram which was used in order to assess whether the return periods are in excess of the 5% level. Table IV gives the results for the 44 sites in the study. Clearly for the FSR-II method the number of sites with return periods above the simulated periods is considerably greater than a 50–50 split; we would expect that half of the sites would have return periods above the median values and half would be below. But of even greater concern is the result that nearly half of the sites have return periods which are in excess of the 5% probability level as assessed by the FSR-II method. The distribution of these sites is shown in Fig. 8. The four-parameter model gives results which are more like what would be expected on the basis of the Monte Carlo analysis. Thus, when this evidence is considered it is difficult to give the return periods of the FSR-II very much credibility.

Table II. Percentage of 24 hour—1 hour difference, 2-year rainfall in relation to average annual rainfall (AAR) and storm duration

AAR	Storm duration											
	2	4	6	8	10	12	14	16	18	20	22	24
millimetres	*hours*											
690–899	18	34	45	54	62	69	75	81	85	90	95	100
900–1099	14	29	40	50	59	67	74	80	85	90	95	100
1100–1799	13	28	39	49	58	66	73	80	85	90	95	100
1800–2199	11	25	36	47	57	65	72	80	85	90	95	100

Table III. Growth factors for frequency curves with slopes 25–41° and return periods 3–1000 years

Slope	Return period									
	3	5	10	20	50	100	150	200	500	1000
degrees	*years*									
25	1.10	1.25	1.48	1.73	2.08	2.40	2.63	2.78	3.50	3.88
26	1.105	1.27	1.51	1.79	2.16	2.50	2.76	2.93	3.67	4.19
27	1.11	1.30	1.53	1.85	2.25	2.60	2.90	3.08	3.85	4.50
28	1.115	1.31	1.57	1.88	2.33	2.72	3.06	3.27	4.10	4.84
29	1.12	1.32	1.60	1.90	2.40	2.85	3.23	3.45	4.35	5.18
30	1.125	1.34	1.63	1.96	2.49	2.97	3.36	3.60	4.67	5.58
31	1.13	1.35	1.65	2.03	2.58	3.10	3.50	3.75	5.00	5.98
32	1.14	1.38	1.69	2.09	2.71	3.29	3.70	4.00	5.32	6.49
33	1.15	1.40	1.73	2.15	2.83	3.48	3.95	4.25	5.65	7.00
34	1.16	1.42	1.76	2.22	2.93	3.64	4.14	4.47	6.03	7.44
35	1.17	1.43	1.80	2.30	3.03	3.80	4.33	4.70	6.40	7.88
36	1.18	1.45	1.83	2.36	3.19	4.05	4.66	4.98	6.95	8.56
37	1.19	1.46	1.85	2.42	3.35	4.30	5.00	5.25	7.50	9.25
38	1.20	1.48	1.90	2.50	3.52	4.52	5.25	5.66	8.22	10.22
39	1.21	1.50	1.95	2.58	3.70	4.75	5.50	6.08	8.95	11.20
40	1.22	1.53	2.00	2.69	3.85	5.00	5.89	6.54	9.60	12.11
41	1.23	1.55	2.06	2.80	4.00	5.25	6.28	7.00	10.25	13.03

Table IV. Observed and expected frequencies of the 44 sites whose return periods are at a given probability level (p)

	FSR-II	Four-parameter model	Ideal
$p < 0.50$	30	20	22
$p \geqslant 0.50$	14	24	22
$p < 0.05$	19	2	2

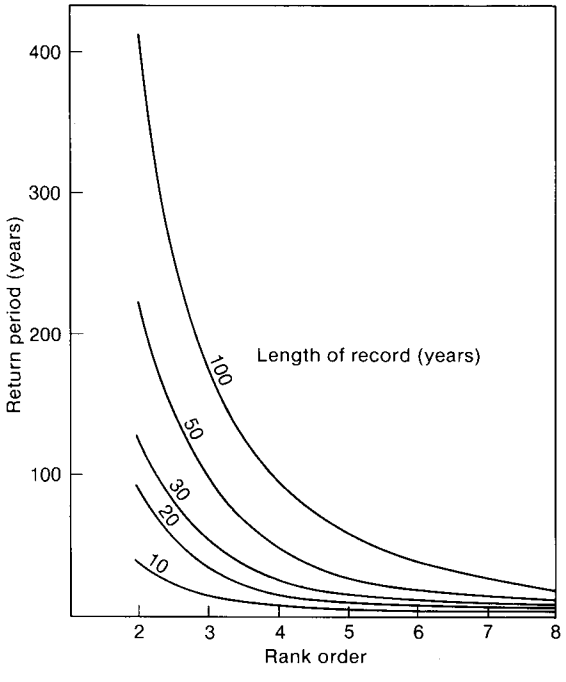

Figure 7. Relationship between rank order, return period and length of record at the $p = 0.05$ level.

4.2 Comparison of return periods obtained using the FSR-II method

The results of the two methods are compared in Fig. 9 wherein only independent storm events have been plotted. With the exception of four storm events, all remaining return periods as given by the FSR-II method are in excess of the current method. Of the remaining 29 events, 25 had return periods equal to or in excess of twice the return periods of the current method. Since FSR-II was published a revised set of growth factors has been published (Foliand *et al.* 1981), although the changes are only of minor consequence.

For Launceston the return periods of seven big storms as calculated using the present method, FSR-II, and the Bilham method are shown in Table V. For the rarer events there is a larger difference between the results than for the more common storms. The reason for these differences is unlikely to be the method of data analysis, namely the plotting of the logarithm of the rainfall against the reduced variate, since out of a total of 61 events there were only 10 return periods in excess of 40 years, which is within the normally accepted limit of twice the length of record from which estimates of the return period can be made. It is much more likely that since the FSR-II method was based on the station–year approach of combining records and assuming independence then the resulting return periods are inflated if the independence assumption is invalid. Thus if 10 stations each have 20 years of records then the return period of the largest event will be 286 years with an occurrence probability of 0.50. However, independence of the records was never assessed and given the areal coverage of many big storms many rain-gauges cannot be

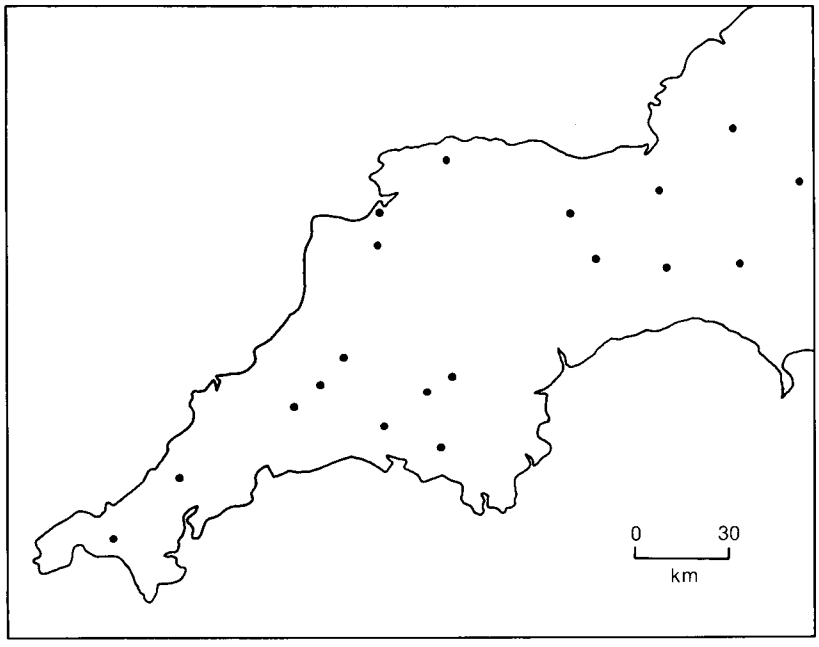

Figure 8. Distribution of sites whose return periods are in excess of the $p = 0.05$ level as assessed by the FSR-II method.

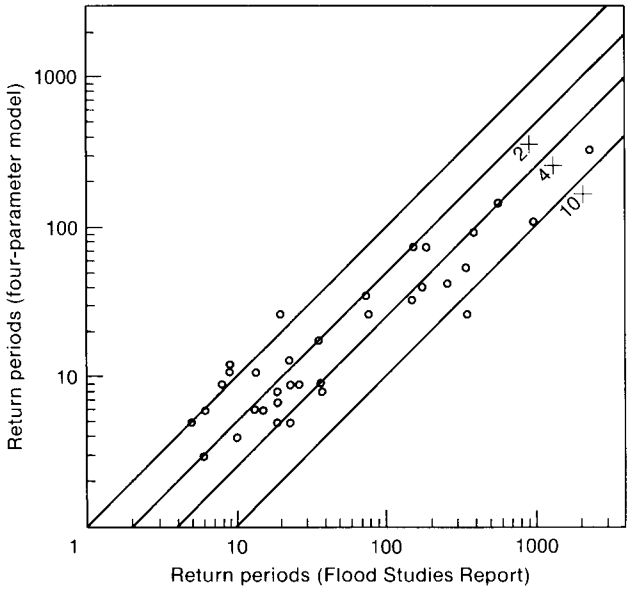

Figure 9. Comparison of the return periods using the FSR-II method and the four-parameter model.

independent of each other. The present method is based on a station by station analysis of the records, and the resulting model takes into account the variation of rainfall via the mean annual rainfall at each site. Recently May and Hitch (1989) have identified an 11-year cycle in the annual maximum 1-hour rainfall over the United Kingdom, and the possibility may exist that the records used in the present study have in some way been biased towards these periodic variations in heavy rainfall. When the dates of the records were compared with the dates of the rainfall peaks, no bias in this respect was found.

The problem of the station–year method was investigated by Dales and Reed (1989) and they described a method to calculate the number of independent sites within a given region. When this is applied to the 44 sites over south-west England only 13 were found to be independent, but some storm events can cover a big enough area to affect most if not all of these sites. An example of this is shown in Fig. 10 for 28 July 1969. Other storms have been known to cover very large areas so it is not yet possible to modify the station–year method to obtain truly independent rain-gauge sites. Furthermore, when the resulting FORGE method is applied to storm events the results which are obtained give cause for concern, see Table VI. Although some of the return periods are lower than those obtained using the FSR-II method there are some notable increases, which are for two extreme events. If the FSR-II results are at odds with both the Bilham and the present method, and a large proportion of the sites have return periods in excess of the expected return periods at the 5% level, then the results obtained using the FORGE method cannot give the user much confidence.

4.3 Comparison of the return periods with those obtained from the data

In order to investigate the reliability of the model further, the calculated return periods of storm events were compared with those derived from a direct analysis of the records. Fig. 11 shows the results wherein, with the exception of three events, all the calculated return periods are within twice the observed return periods. There is no clear evidence of a decrease in accuracy with increasing return period and only seven data points lie outside $\pm$ 1.5 times the observed values. It is impossible to state categorically if the differences are due to random variations within the data or are caused by a defect in the model.

Given the inherent uncertainty in any study of this nature the model appears to have given results which

Table V. Comparisons of the return periods, using four methods, for the seven most severe storms at Launceston

Date	Amount	Duration	Return period			
			FSR-II	Bilham	Four-parameter model	Log Gumbel plot
	millimetres	*hours*	*years*			
28 July 1969	96.5	8.9	335	113	56	42
26 Dec. 1979	95.0	18.4	150	52	19	15
15 Nov. 1963	50.8	2.8	150	38	37	42
7 July 1975	37.0	1.8	50	21	21	36
14 Oct. 1976	70.0	24.0	18	14	5	4
14 Oct. 1983	50.0	9.6	14	11	5	6
20 Sept. 1980	50.0	9.9	13	11	5	6

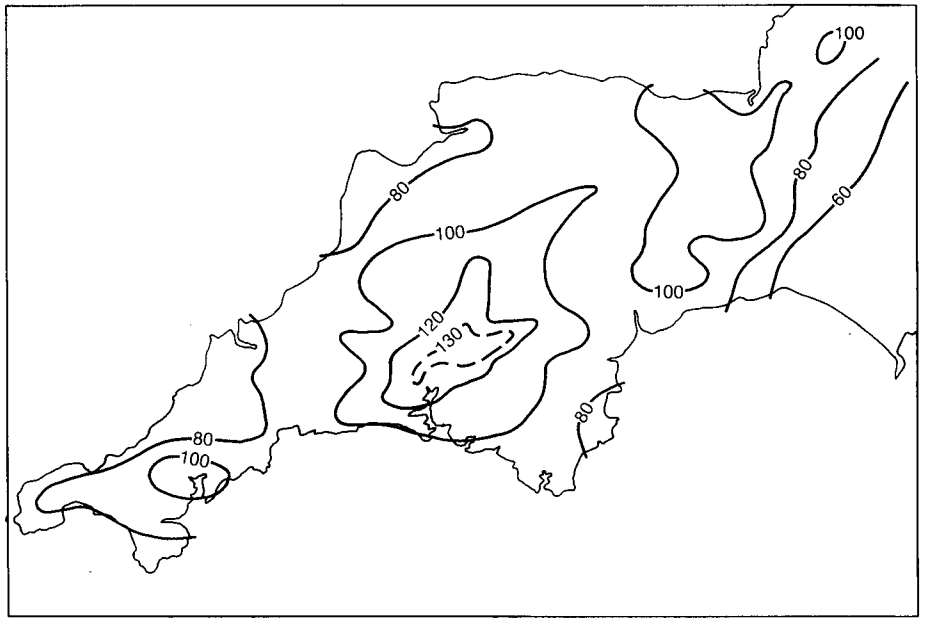

Figure 10. Distribution of 24-hour rainfall (mm), 28 July 1969.

match those from a Monte Carlo analysis of the return periods of a perfect 10 000-year record. Furthermore, an error of 50% on the return period for the 4-hour, 50-year storm for Exton gives an error in the depth of rainfall of + 4 mm or − 10 mm. The errors will be greater where the slope of the log Gumbel analysis is large. For example, for Cannington the corresponding errors are + 12 mm or − 15 mm and are equivalent to errors of + 15% and − 19% in the depth of rainfall.

5. Implications of the study

It would simplistic to extrapolate the results of the Gumbel analysis to high return periods (Reed and Stewart 1989), although Loukola *et al.* (1985) have followed this approach. But if extrapolations are made then the results are disquieting. For example, at Maundown in Somerset the 400-year, 24-hour storm is 254 mm, leaving scope for even bigger falls. Such an estimate of extreme rainfall is not unrealistic when the recorded falls during the August 1960 and June 1917 storms are considered. On this basis a fall in excess of 11 inches (279 mm) recorded at Martinstown would appear possible. Indeed Twort *et al.* (1985) quote an unofficial fall of 14 inches or 356 mm during the same event. Such falls make the estimate of the 10 000-year, 1-day fall for Wimbleball — 7 km to the west of Maundown — of 264 mm, seem modest. This estimate

Table VI. Return period of storm events using the FSR-II and FORGE methods

Date	Site	Return period	
		FSR-II	FORGE
		years	
24 Sept. 1976	St. Neot	398	240
11 July 1968	Northmoor P.S.	970	1590
12 July 1982	North Brewham	560	1000
5 Oct. 1977	Penryn Resr	266	120
28 July 1969	Launceston	335	290

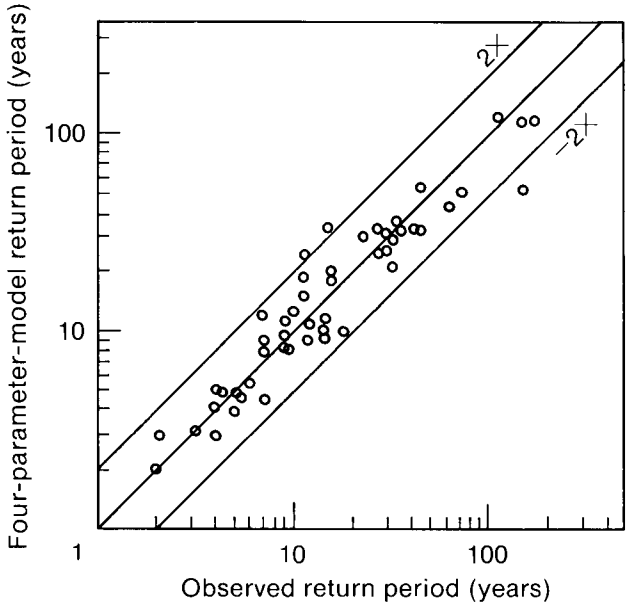

Figure 11. Comparison of the observed return periods and the calculated values using the four-parameter model.

was produced by the FORGE method (Stewart 1989). When the magnitude of a 4-hour duration storm with a return period of 2000 years is estimated using the present method, a figure around 200 mm is suggested. This is within the range of maximum recorded British rainfalls (Twort *et al.* 1985). For the Wimbleball dam site such a storm is likely to be in excess of the response time of the catchment area of 29 km^2, and assuming 100% run-off gives a peak flow of 403 $m^3 s^{-1}$, which is 100 $m^3 s^{-1}$ in excess of the design flood and the probable maximum flood quoted by Shaw (1989).

When the design of a reservoir spillway is considered, safety is of paramount importance. Records of rainfall intensity are important sources of data for design purposes. At present their biggest drawback is their very short duration. Therefore more work needs to be undertaken in order to extend the existing analysis by identifying stations which are completely independent of each other. It is likely that the widely spaced rain-gauges whose records Bilham analysed were far enough apart to be independent, so it is not surprising that the return periods which his method gives are often considerably below those given by the FSR-II method. Given that Bilham chose sites whose AAR was often below 800 mm and that there was only one gauge in south-west England, and considering that many of the sites were located near the coast, it is rather unlikely that this geographical coverage can represent the range of conditions which exist in the peninsula. In spite of this there is a closer agreement with the results using the present method and the Bilham method than with the FSR-II method.

6. Conclusions

A new method for estimating the frequency of heavy rainfall over south-west England has given results which suggest that heavy rainfall events are much more common than has been hitherto believed. By comparing the number of sites whose return periods are in excess of the 5% probability level of exceedance it is suggested that the large number of rare events as given by the FSR-II is too high. The main reason for the high return periods appears to be the pooling of rainfall data from stations that are not independent of each other. The associated FORGE method (Stewart 1989) also gives results which suggest that the problem of dependence between widely spaced rain-gauges has not yet been overcome.

A comparison of the calculated and observed return periods of storm events showed that the model was capable of giving realistic results and with an accuracy good enough to be used for design purposes.

The results which have been presented are only applicable to south-west England. It may be that the relationships here described will have to be modified for other areas. The study area covers part of the West Country and south-west England as defined by Reed and Stewart (1989); these have markedly different growth curves. Clearly for a catchment area which covers more than one region there will be problems assigning the return period of storm events. Furthermore, there can be marked intra-regional variation of the observed growth factors as this study has shown. The present method overcomes these problems by assigning a growth factor specific for the site in question in contrast to the uniform national growth-curve for the FSR-II and regional curves for the FORGE method. At present it is not possible to specify the magnitude and duration of storms in excess of the 100-year return period. This remains an important problem to be overcome.

Acknowledgements

The author would like to thank Celia Gibson and Andrew Gardiner of the Wessex Water Authority, and John Marks of the South West Water Authority for making available the autographic rainfall records.

References

Acreman, M., 1989: Extreme rainfall in Calderdale, 19 May 1989. *Weather*, **44**, 438–446.

Bilham, E.G., 1935: Classification of heavy falls in short periods. *In* British Rainfall 1935. London, HMSO.

Bootman, A.P. and Willis, A., 1977: Extreme two-day rainfall in Somerset. Bristol, Wessex Water Authority.

—, 1981: Discussion on papers 4–6. *In* Flood Studies report — five years on. London, Thomas Telford.

Clark, C., 1983: Discussion of Gumbel's extreme value I distribution: a new look. *Proc Amer Soc Civ Eng, J Hyd Eng*, **109**, 645–647.

Dales, M.Y. and Reed, D.W., 1989: Regional flood and storm hazard assessment. Wallingford, Institute of Hydrology, Report No. 102.

Dunne, T. and Leopold, L.B., 1978: Water in environmental planning. San Francisco, W.H. Freeman.

Folland, C.K., Kelway, P.S. and Warrilow, D.A., 1981: The application of meteorological information to flood design. *In* Flood studies report — five years on. London, Thomas Telford.

Institution of Civil Engineers, 1978: Floods and reservoir safety: an engineering guide. London, ICE.

Jackson, M.C., 1979: The largest fall of rain possible in a few hours in Great Britain. *Weather*, **34**, 168–175.
Kelway, P.S., 1977: Rare or not so rare? — the vital question. *Weather*, **32**, 358–363.
Loukola, E., Kuusista, E. and Reiter, P., 1985: The Finnish approach to dam safety. *Int Water Power and Dam Const*, **37**, 22–24.
Marshall, J.K., 1977: Use of Flood Studies Report for a drainage study at Hereford. *J Inst Water Eng and Sci*, **31**, 187–201.
May, B.R. and Hitch, T.J., 1989: Periodic variations in extreme hourly rainfalls in the United Kingdom. *Meteorol Mag*, **118**, 45–50.
Natural Environment Research Council, 1975: Flood Studies Report, Vol. II, Meteorological studies. London, NERC.
Perry, A.H. and Howells, K.A., 1982: Are large falls of rain in Wales becoming more frequent? *Weather*, **37**, 240–243.
Reed, D.W. and Dales, M.Y., 1988: Regional rainfall risk: a study of spatial dependence. IAHR Symposium of Stochastic Hydraulics, paper B2. University of Birmingham.
Reed, D.W. and Stewart, E.J., 1989: *In* Focus on rainfall growth estimation. Proceedings of 2nd National Hydrology Symposium, Sheffield.
Rodda, J.C., 1970: Rainfall excesses in the United Kingdom. *Trans Inst Br Geogr*, **49**, 49–60.
Shaw, E.M., 1989: Engineering hydrology techniques in practice. Chichester, Wiley.
Stewart, E.J., 1989: Regional rainfall frequency southwest England. Exeter, South West Water.
Stewart, L. and Reed, D., 1989: Rainfall frequency estimation in south west England: procedure for estimation of T-year, D-hour rainfall. Wallingford, Institute of hydrology.
Tabony, R.C., 1983: Extreme value analysis in meteorology. *Meteorol Mag*, **112**, 77–98.
Twort, A.C., Law, F.M. and Crowley, F.W., 1985: A textbook of water supply. London, Edward Arnold.

551.509.58:629.7

A verification method for aerodrome forecasts

N.G. Prezerakos and H.N. Prezerakos
Hellenic National Meteorological Service, Athens, Greece
S.C. Michaelides
Meteorological Service, Nicosia, Cyprus

Summary

A new method of verifying aerodrome forecasts, either manually or by means of a computer, is presented.

1. Introduction

By verification we mean the process of comparing the actual weather of a place at a certain time with the predicted weather for the same place and time. The result of this comparison is the forecast assessment expressed as a mark out of ten.

The basic aims of the verification are (Mason 1980):

(a) the everyday checking of weather forecasts,
(b) comparing improvements after the introduction of new means and methods of weather forecasting, and
(c) testing the ability of weather forecasters.

Everyday assessment of the quality of weather forecasts can result in: taking necessary measures for the forecasts' improvement when necessary, financial determination of the forecasts' value, and improving the weather forecaster's skill.

Published papers on aerodrome forecast (TAF) verification are very sparse. Wright (1971) describes a scheme which verifies a TAF or a set of TAFs at a particular moment of the TAF's time-period. The assessment is confined to visibility, surface wind, and low cloud. Thus, strictly, the accuracy of the whole forecast contained in the TAF is not tested; it is assessed in the way that it is often used by someone requiring a knowledge of the weather at specific times for planning purposes.

Von Bezold (1969) introduced a method of verifying all the details of a TAF for a continuous period including the qualifying statements TEMPO, INTER and PROB. Wright (1971) referred to another method introduced by Hoppestad which verifies TAFs in a similar manner to Von Bezold's method but deals with probability forecasts by testing the accuracy of TAFs over long time-periods, such as 3 months. Thus, the final scores cannot be attached to individual TAFs.

This paper introduces a method that can be applied manually or by means of a computer and does more than the above methods do. It deals individually with all weather elements contained in a TAF, tests them over the whole time period, and scores each separately.

To devise this method we considered various papers that dealt with local or regional forecast verifications (Bleeker 1946, Muller 1944, Dobryshman 1972, Johnson 1969, Zverev 1972, and Murphy 1985) and the Daan's (1985) technical memorandum that introduced an objective method, carried out by a computer, for the assessment of local weather forecasts.

2. Description of the method

2.1 General

TAF assessment can be carried in real or non-real time. If a system is designed to receive TAFs and

METARs (reports of actual weather) from the telecommunication network and can decode them using suitable programs, the TAFs can be assessed at the moment of each TAF's expiry. Thus, a quick evaluation of each TAF is provided quickly which can contribute to the improvement of the following TAF (this process requires computer time in the everyday operational routine which is not normally available at aerodrome forecasting offices).

2.2 Scoring method

TAFs serve aviation purposes (World Meteorological Organization 1988) and from this point of view the most important meteorological elements are visibility, low cloud (base $\leqq 5000$ ft), wind (direction and speed) and weather, so all these elements must be assessed separately; the weighted average of their derived scores being the final score for the TAF. The weight coefficients which, in the same time, show the order of the importance of each element are: visibility 6, height of low clouds 5, amount of low clouds 4, wind direction 3, wind speed 2, and weather 1.

It must be mentioned here that these processes may have to be repeated two, three or even more times for the same TAF since a TAF may contain many changes. For such a TAF the final score is the weighted average of the component element scores of the TAF, where the corresponding length of time is taken as the weight for every score. Marks for the separate and total scores are in the range 0 to 10.

2.2.1 Score assessment of the meteorological elements of specific time intervals

To assess the score of a meteorological element contained in a TAF we introduce the non-linear relationship:

$$S = 10^{(M-A)/M} \qquad (1)$$

where S is the forecast assessment, A the absolute error defined as $A = |X_{\text{forecast}} - \bar{X}_{\text{observed}}|$ where X is the element under consideration. The mean value of X is calculated from the corresponding METARs; M is the maximum tolerated absolute error which adopts a score, that is,

if $A \leqq M$ then $S = 10^{(M-A)/M}$, where S is in the range 1 to 10
if $A > M$ then $S = 0$
if $A = 0$ then $S = 10$.

M depends on the operational desirable accuracy of forecasts of each meteorological element contained in TAFs, so we defined the various maximum tolerated errors following the suggestions contained in the *Manual of aeronautical meteorological practice* (International Civil Aviation Organization 1985). These are:

Visibility: 200 m up to 700 m and $\pm 30\%$ between 700 m and 10 km,
low-cloud amount: 2 oktas,
low-cloud height: 100 ft up to 400 ft and $\pm 30\%$ between 400 ft and 5000 ft,
wind direction: 30°, and
wind speed: 5 kn up to 25 kn and $\pm 20\%$ above 25 kn.

To assess the score of the forecast weather we classified it into seven categories. Each category includes several similar weather kinds the number of which being the maximum tolerated error for the category. The indicated order within each category is considered as the value for each kind of weather, and is used for the assessment of A and hence the score S of the forecast weather. If the forecast and observed weather do not appear in the same category then $S = 0$, if they contain no weather then $S = 10$.

The various categories are:

Fog
1. fog
2. shallow fog
3. fog patches
4. freezing fog
5. mist
6 haze
7. smoke

Drizzle
1. drizzle
2. heavy drizzle
3. freezing drizzle
4. heavy freezing drizzle

Rain
1. rain
2. heavy rain
3. showers
4. heavy showers
5. rain and snow
6. thunderstorm
7. squall
8. snow
9. heavy snow

Snow
1. snow
2. heavy snow
3. rain and snow
4. rain
5. heavy rain
6. showers
7. heavy showers
8. thunderstorm
9. squall

Showers
1. showers
2. heavy showers
3. thunderstorm
4. squall
5. rain
6. heavy rain
7. snow and rain
8. snow
9. heavy rain

Thunderstorms
1. thunderstorm
2. squall
3. heavy shower
4. shower
5. heavy rain
6. rain
7. rain and snow
8. snow
9. heavy snow

Squalls
1. squall
2. thunderstorm
3. heavy shower
4. shower
5. heavy rain
6. rain
7. rain and snow
8. snow
9. heavy snow

2.2.2 Average values of the meteorological elements obtained from METARs

During each TAF validity period there is always a number of METARs, the number fluctuating according to the specific station. From here on all the METARs that fall into the duration of a TAF are called METARs of interest (MOI).

The average of all the values of an element from the MOI is the observed value of the element that is compared with that predicted in the TAF. The score for the particular element is found via equation (1). There are differences in the calculation of the average according to the method followed (manually or by computer) and according to the type of element (scalar or vector).

(a) Wind direction. The wind direction in a particular period is calculated by vector addition. Manually, addition is done graphically (e.g. by the use of a hodograph); using this process the mean vector speed and direction are both calculated. By computer the vector representing the wind is resolved into two components u and v (Brooks and Carruthers 1953) with the help of the relations

$$u = FF\sin(DD + 180)$$
$$v = FF\cos(DD + 180)$$

where u has a direction west–east adopting a negative value when it is easterly, v has a direction south–north adopting a negative value when it is northerly; DD is the wind direction in degrees and FF wind speed in knots. $\overline{\Sigma u}$ and $\overline{\Sigma v}$ are calculated from which the mean vector wind speed $\{(\overline{\Sigma u})^2 + (\overline{\Sigma v})^2\}^{1/2}$ derives. From the relation $w = \arctan|\Sigma u/\Sigma v|$ an angle $w < 90°$ is found, and by examining the signs of Σu and Σv the direction of the resultant wind is determined.

(b) Wind speed. To calculate the mean wind speed, the speed of the winds with certain directions and the speed of the variable winds are added and the total is divided by the number of METARs that include a wind observation. The ratio of the mean vector speed to the mean speed, multiplied by 100, is said to be the 'wind constancy' (Brooks and Carruthers 1953). Note that when in the TAF the term VRB (variable) has been given as the predicted wind direction, the score for the direction will be 10 if the mean wind speed derived from the corresponding METARs is less than 10 kn — otherwise the direction scores zero. The score for wind speed is calculated no matter what the predicted or observed direction was.

(c) Visibility. The mean visibility value is calculated by a weighted average of the visibility values in the MOI. Where the term CAVOK is used the visibility is taken as 9999 m.

(d) Weather. The kinds of weather that usually appear in a TAF have already been classified into seven numbered categories. To obtain the prevailing weather in a certain period of time from the METARs the following method is used. When in a particular period only one kind of the weather stated above was observed and in only one METAR, then the average weather for the complete period will be that kind of weather. When there is none of the aforementioned weather in any METAR then the weather characterization will be no weather.

(e) Amount of low cloud. To calculate the mean cloudiness that corresponds to a certain period of time, the amount of low cloud corresponding to each MOI is first determined. This amount is equal to the total of all reported low cloud in the METAR, 8/8 being taken when the total exceeds it. The mean cloudiness is then taken as the average of the MOI.

Example: METAR cloud reports for a 2-hour period from 10 to 12 UTC

Time	Cloud		
1020	2CU030	4SC035	5AC090
1050	2CB025	4CU025	4SC030
1120	2ST010	4CU030	4SC035
1150	3CU030	6AC090	

The amounts of the low cloud corresponding to the above METARs are 6/8, 8/8, 8/8 and 3/8, respectively. The mean cloudiness for the 2 hours is

$$\frac{6+8+8+3}{4} \approx 6 \text{ oktas.}$$

(f) Height of the base of low cloud. To calculate the mean height of the low cloud that corresponds to a certain period of time, weighted mean values are used. For each MOI the mean height is determined by adding the products of the height of every group of low cloud by the corresponding amount and dividing this sum of products by the total of the amount of low cloud. Then, using a similar method, the mean height of the low cloud is found.

Example: From the cloud information contained in the previous example the mean height of the low cloud for the first METAR is

$$\frac{(2\times3000)+(4\times3500)}{6} \approx 3300 \text{ ft}$$

where 2 and 4 are the amounts of low cloud (oktas) in the METAR with heights 3000 ft and 3500 ft respectively. In the same way we find that in the second METAR the mean is

$$\frac{(2\times2500)+(4\times2500)+(4\times3000)}{10} = 2700 \text{ ft.}$$

Likewise, the mean height of low cloud for the 3rd and 4th METARs is found to be 2800 and 3000 ft, respectively. The mean height, which approximately corresponds to the period of 2 hours, is found to be

$$\frac{(6\times3300)+(8\times2700)+(8\times2800)+(3\times3000)}{25} \approx 2900 \text{ ft}$$

where the divisor is the total of the four amounts of mean cloudiness.

2.2.3 TAFs with change groups (GRADU, TEMPO, INTER, PROB)

If there are change groups in the TAF then it is divided by the duration in hours of each section into time periods, and a score is found for each section, the products of the score by the duration in hours of each section being added and the total divided by 9 (for 9-hour TAFs) to find the final score.

(a) GRADU alteration. When GRADU is used, the TAF is divided into sections and the time corresponding to the half of the duration period that follows the GRADU term is taken as a separation point of every section.

Example: TAF LGAT 0110 35010 CAVOK GRADU 0204 VRB03 5000 10BR GRADU 0608 36020 9999 2CU030.

This TAF is divided into the following three sections
LGAT 0103 35010 CAVOK
LGAT 0307 VRB03 5000 10BR
LGAT 0710 36020 9999 2CU030
with corresponding durations of 2, 4 and 3 hours.

(b) TEMPO or INTER alterations. In this case the part score of the TAF corresponding to the period covered by this alteration is found separately. If, additionally, there is a GRADU group within the TAF, then the TAF is divided as described above and the score for each section found.

(c) PROB alterations. Since the prediction is given with probability the score is reckoned normally and then reduced by a percentage equal to the probability.

2.2.4 Final assessment

The final assessment is calculated from the scores of the separate sections 'weighted' for the corresponding period of time in which they are referred to, that is, every score is multiplied by the corresponding duration and all the products are added. The total divided by 9 (for a 9-hour TAF) gives the final score.

We must underline here that the final score of each section of the TAF is the weighted average score (S) obtained via equation (1) of each meteorological element described in section 2.2.

3. Worked examples

Consider the following TAF

TAF LGAT 1019 25010 9999 3CU035 5AC090 TEMPO 1113 5000 95TS 2CB020 5CU035 GRADU 1618 36012 9999 3CU035.

This TAF is first divided into two time periods (10–17 and 17–19) to take account of the GRADU group. For the period 10–17 the TEMPO section is accounted for by a further subdivision into sections of 2 hours (11–13) and the remaining 5 hours. This leads to:

first section (duration 5 hours) — LGAT 25010 9999 3CU035 5AC090,
second section (duration 2 hours) — LGAT 25010 5000 95TS 2CB020 5CU035,
third section (duration 3 hours) — LGAT 36012 9999 3CU035.

To assess this TAF we find the average values of the elements (visibility, cloud amount, wind and weather) from the MOI. Supposing that for each of the above sections of the TAF the mean values of the elements concerned have been assessed and the mean actual weather conditions are:

for the first section — LGAT 18015 9999 2CU035,
for the second section — LGAT 22015 5000 62RA 5CU030 8AS080, and
for the third section — LGAT 28015 9999 3CU035 6AC100.

One by one the elements of the TAF and the mean observed weather are compared as described in section 2.2.1; the scores of these separate elements are found in Table I. The mean general weighted score for the first section is 6.41, for the second section 5.80 and for the third section 7.86. The final score is found by reckoning weighted mean value (the weights will be the durations of the sections). Thus the final score is

$$\frac{(5\times6.41)+(2\times5.80)+(2\times7.86)}{9} = 6.59$$

giving the TAF characterization 'good' from Table II.

Table I. Scores of separate elements found in the various sections of the TAF worked example

Element weight	Elements	1st	2nd	3rd
6	Visibility	10	10	10
5	Height of low cloud	10	10	10
4	Amount of low cloud	3.16	1	10
3	Wind direction	0	1	0
2	Wind speed	1	1	2.51
1	Weather	10	2.78	10

4. Concluding remarks

The method of scoring the accuracy of the aerodrome weather predictions explained above can be a measure of their evaluation. The method may be applied for all TAFs but especially for those with a 9-hour duration, the scoring being made separately for each period, and for each meteorological element of a TAF which

Table II. Characterization of the TAF example from the final score

Scale 0–10	Specific	General
9–10	Excellent	Successful
7–8.9	Very good	
4.6–6.9	Good	
3–4.5	Bad	Unsuccessful
1–2.9	Very bad	
0–0.9	Worst	

includes change groups. All the calculations may be made manually or by using a computer.

The application of the method in the everyday work of a forecasting office will show the advantages, as well as the disadvantages of the method. The disadvantages of the method that will appear during its application will be overcome by some meteorologists who will try to improve on it.

An improvement which would make the method applicable operationally is the creation of a new computer program to enable the method to be used directly from TAFs and METARs; the scoring then being done automatically at the time the TAF expires.

References

Bleeker, W., 1946: The verification of weather forecasts. Mededelingen en Verhandelingen, Serie B, Deel 1, No. 2. De Bilt, KNMI.

Brooks, C.E.P. and Carruthers, N, 1953: Handbook of statistical methods in meteorology. London, HMSO.

Daan, H, 1985: A standardised verification scheme for local weather forecasts. Reading, ECMWF, Technical Memorandum No. 116.

Dobryshman, E.M., 1972: Review of forecast verification techniques. Geneva, WMO, No. 303, Tech. Note No. 120.

International Civil Aviation Organization, 1985: Manual of aeronautical meteorological practice. ICAO Doc. 8896-AN/893/3.

Johnson, D.H., 1969: Forecast verification: a critical survey of the literature. London, *Meteorol Res Pap*, No. 1056.

Mason, J., 1980: Weather forecasting as a problem in fluid dynamics. *Meteorol Mag*, **109**, 29–46.

Muller, R.H., 1944: Verification of short-range weather forecasts (a survey of the literature), I–III. *Bull Am Meteorol Soc*, **25**, 18–27, 47–53 and 88–95.

Murphy, A.H., 1985: Proposed standard procedures for verification of local weather forecasts. Geneva, WMO, PSMP Report No. 15.

Von Bezold, W., 1969: Eine methode, die güte von flugplatzwettervorhersagen (TAF) zu ermitteln. *Meteorol Rundsch*, **22**, 43–46.

World Meteorological Organization, 1988: Technical regulations. Volume II, Services for international air navigation. Geneva, WMO No. 49.

Wright, P.B., 1971: An assessment scheme for aerodrome forecasts. *Meteorol Mag*, **100**, 285–293.

Zverev, A.S., 1972: Practical work in synoptic meteorology, synoptic chart sequences for training purposes. Leningrad, Gidrometeoizdat.

551.506.1(41-4)

The spring of 1990 in the United Kingdom

G.P. Northcott

Meteorological Office, Bracknell

Summary

Spring 1990 was warm, sunny, and very dry in southern areas but wet in western Scotland. Although May was dry over Scotland, March was the wettest in the Scottish rainfall series beginning in 1869, giving a generally wet spring with more than one and a half times the normal rainfall in all but some eastern areas. Over England and Wales all three months were drier than normal resulting in the driest spring this century. However, there were thundery outbreaks during May with heavy thunderstorms moving across Wales, northern and western England and southern Scotland. It was the sunniest spring over England and Wales since 1948, but dull wet weather over north-western areas in March brought Scotland's sunshine closer to the average.

1. The spring as a whole

Mean temperatures over the spring of 1990 were above average everywhere in the United Kingdom, ranging from 0.5 °C above average in some parts of north-west Scotland to 2 °C above average in the Solent area, the coast of East Anglia, and at places in western Wales and the south-west Midlands. The Central England Temperature of 9.95 °C was the highest spring temperature since 1945 and the second highest this century in the register of Central England Temperatures dating back to 1659. Rainfall amounts over the three months were above average over western and northern parts of Scotland and below average elsewhere, reaching 243% in the area of Fort Augustus, Highland Region, with a contrasting 24% in the south Midlands. Although May was dry over Scotland, March was the wettest in the Scottish rainfall series beginning in 1869, giving a generally wet spring with more than one and a half times the normal rainfall in all but some eastern areas. Over England and Wales all three months were drier than normal resulting in the driest spring since 1893. Spring sunshine amounts were about the average in the Western Isles and above average elsewhere ranging from

97% at Benbecula, Western Isles to 154% at Watnall, Nottinghamshire. With above average sunshine in most places, particularly in south-eastern parts of the United Kingdom, England and Wales had the sunniest spring since 1948; however, a spell of dull wet weather over north-western areas in March brought Scotland's sunshine closer to the average.

Information about the temperature, rainfall and sunshine during the period from March to May 1990 is given in Fig. 1 and Table I.

2. The individual months

March. Mean monthly temperatures were above normal everywhere in the United Kingdom, ranging from just over 1 °C above normal in Shetland to 3.5 °C above normal at Leeming, North Yorkshire. Sheffield (Weston Park), South Yorkshire had the highest mean temperature for March since 1961. Coventry School (Bablake), Warwickshire reported the warmest March this century. Provisional values in the register of Central England Temperatures suggest that it was the warmest March since 1957. Monthly rainfall totals were below normal everywhere except western and northern Scotland and ranged from more than four times the normal at Fort William, Highland Region to as little as 7% of normal at Worthing, West Sussex. At Fort Augustus, March 1990 was the wettest month in the 100-year record; in contrast, provisional figures suggest that over England and Wales as a whole it was the driest March since 1961. Sheffield (Weston Park) had the lowest March rainfall total since 1973. Monthly sunshine amounts were above average in central and eastern areas but below average in western coastal areas from Scilly to Orkney, ranging from more than 150% of average in the east Midlands to less than half the average at Benbecula, Western Isles. Sheffield (Weston Park) had the highest March sunshine total since 1978. Coventry School (Bablake) reported the sunniest March since 1967.

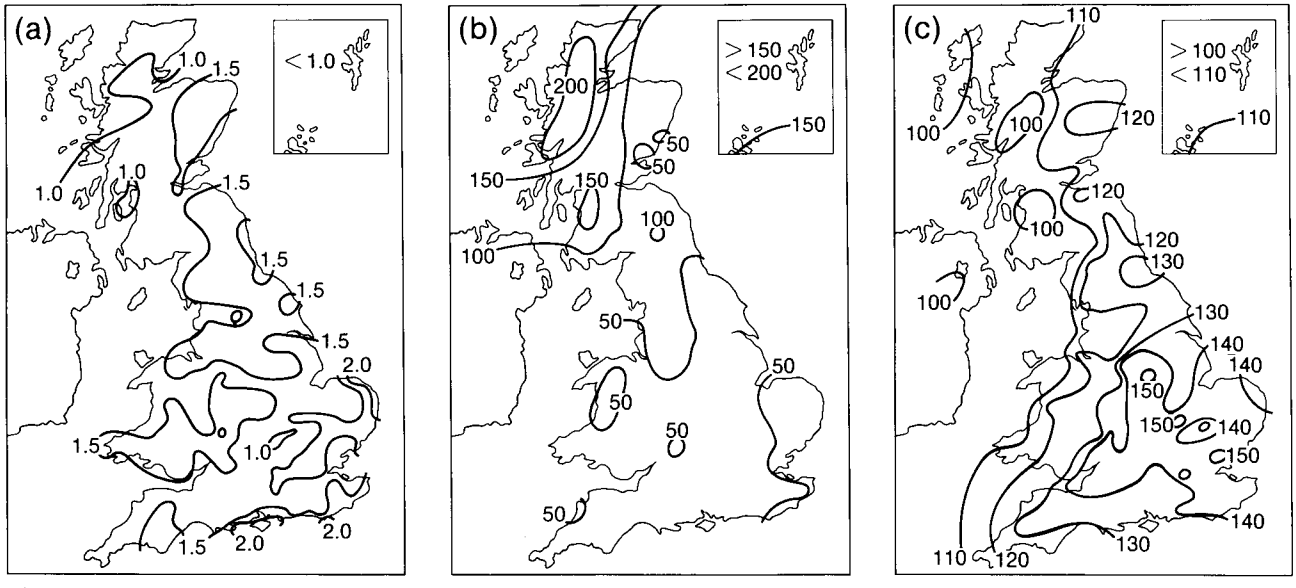

Figure 1. Values of (a) mean temperature difference (°C), (b) rainfall percentage and (c) sunshine percentage for spring, 1990 (March–May) relative to 1951–80 averages.

Table I. District values for the period March–May 1990, relative to 1951–80 averages

District	Mean temperature (°C)	Rain-days	Rainfall	Sunshine
	Difference from average		Percentage of average	
Northern Scotland	+1.0	+11	166	100
Eastern Scotland	+1.5	−2	81	115
Eastern and north-east England	+1.7	−4	50	132
East Anglia	+1.5	−6	55	143
Midland counties	+1.4	−6	40	136
South-east and central southern England	+1.6	−6	42	141
Western Scotland	+1.1	+2	131	99
North-west England and North Wales	+1.5	−3	60	110
South-west England and South Wales	+1.5	−4	42	120
Northern Ireland	+1.4	0	89	100
Scotland	+1.2	0	139	105
England and Wales	+1.6	−5	48	131

Highest maximum: 28.3 °C in Midland counties in May.
Lowest minimum: −6.8 °C in Northern Ireland in April.

The month was generally wet in western Scotland, but dry and mild in the south and east. Between the 7th and 21st it continued unsettled in Scotland. It was very wet at times in the western Highlands but on most days only small amounts of rain reached coastal fringes to the east of the Grampians and Southern Uplands. England and Wales continued to have a good deal of dry weather, but with short unsettled interludes. Thunderstorms, often accompanied by hail, occurred over north-east England and East Anglia on the 1st, locally in the north-west on the 19th and at Fair Isle, Shetland on the 22nd. On the 25th heavy showers with hail and thunder occurred in south-east England. Scattered hail showers fell in western Scotland on the 2nd, over Scotland and Northern Ireland on the 9th and there were widespread hail showers on the 24th. There were reports of deposits of coloured dust on the 19th at Llanymawddy, North Wales, Northwood, Greater London and Woodley, Berkshire.

April. Mean monthly temperatures were slightly above normal in most areas, although there were a few places with temperatures slightly below normal, ranging from 1.2 °C above normal at Lowestoft, Suffolk to 0.9 °C below normal at Lowtown, Co. Antrim. Severe frosts on the 4th and 5th damaged many plants that were further advanced than normal for early April. On the 30th, Sheffield, (Weston Park) reported the highest April maximum temperature since 1949. Monthly rainfall totals were below normal everywhere except for northern and western Scotland, south-east England and East Anglia, and ranged from 206% at Fort Augustus, Highland Region to as little as 17% at both Hartburn Grange, Cleveland and Leeming, North Yorkshire. The monthly total of 7 mm at Tynemouth, Tyne and Wear is the lowest for April at the station since 1912, when only 3 mm was measured. Monthly sunshine amounts were above average nearly everywhere, apart from a few locations in western Scotland and Northern Ireland, ranging from 179% at Writtle, Essex to 87% at Onich, Highland Region. Aberdeen Airport's sunshine total of 209 hours was the highest there in April since records began in 1946, and Leuchars had 217 hours, the sunniest April since the record began in 1922.

Most places had a dry month, although it was wet over western Scotland and east Kent. Much of the southern and eastern parts of England and Wales and eastern Scotland had one of the sunniest Aprils this century. After a warm start to the month the first week was generally cold, the coldest spell in the first four months of the year. It became warmer, but less settled during the second week. After rain on the 13th the following week was unsettled, cold and windy although with sunny periods. From the 27th it became sunny and warm once more. Thunderstorms were frequent during the second and third weeks, especially between the 13th and 24th, often with heavy showers and sometimes accompanied by hail. Hail showers were frequent during the month, occurring somewhere almost daily during the first three weeks.

May. Mean monthly temperatures were above normal everywhere and ranged from less than 0.5 °C above normal in north-west Scotland to 3 °C above normal in parts of the Midlands. Temperatures exceeded 26 °C somewhere in Great Britain on each of the first five days, giving the hottest start to May this century. Monthly rainfall totals were below normal everywhere except for a narrow band from about Prestwick to Newcastle, where totals were above normal. Much of England and Wales had less than half the normal rainfall and parts of the south Midlands and central and southern England had below 10%. Totals ranged from 146% at Newcastle upon Tyne to 6% at Benson, Oxfordshire and Easthampstead, Berkshire. Monthly sunshine amounts were above or near average everywhere, ranging from 100% at Dyce, Grampian Region to 157% at Rhoose, Mid Glamorgan.

After a hot, dry start a spell of much cooler, showery weather, lasting several days, moved slowly across the United Kingdom from north-west to south-east, though a few places escaped the showers. It became dry again in most places after the 15th, although there was further unsettled weather in many areas towards the end of the month. Isolated thunderstorms developed over western Scotland on the 4th and over southern England and East Anglia on the 6th. Showery outbreaks affected most northern areas on the 8th, sometimes accompanied by thunder; during the evening, thundery showers crossed the English Channel to the Kent coast. Thundery outbreaks occurred on the 9th over northern areas and on the 10th over southern England, spreading later into East Anglia and becoming more widespread during the afternoon, with further thunderstorms developing along the south coast. There were reports of isolated thunderstorms on the 14th and 15th. Hail showers fell over the far north of Scotland on the 24th and a thunderstorm was accompanied by hail over Humberside on the 27th. On the 27th a 20-metre high whirlwind was observed at Towy Castle, South Wales.

Notes and news

European Geophysical Society

This year sees the European Geophysical Society (EGS) celebrate its Twentieth Anniversary. To mark the occasion a special scientific programme of 95 sessions covering solid earth geophysics and marine, atmospheric, planetary and space sciences has been compiled for the 16th General Assembly to be held in Wiesbaden, Germany, 22–26 April 1991. About 2000 scientists from more than 40 different nations are expected to participate.

The 17th General Assembly will be held in Edinburgh, 6–10 April 1992. The meeting is open to all scientists of all nations. Deadline for receipt of abstracts is 15 January 1992. Further details can be obtained from the local organizer:

Prof. K.M. Creer
Dept of Geophysics
James Clerk Maxwell Building
Mayfield Road
Edinburgh EH9 3JZ

Further details on the EGS appeared under Notes and news in the February 1989 edition of *Meteorological Magazine*.

Review

The earth's climate and variability of the sun over recent millennia, edited by J-C. Pecker and S.K. Runcorn. 214 mm × 302 mm, pp. ix+289, *illus.* London, The Royal Society, 1990. Price £40.00. ISBN 0 85403 406 4.

This well-produced volume contains the 28 papers, and associated discussion, presented to the joint Royal Society and Académie des Sciences meeting held in February 1989. This was organized by Jean-Claude Pecker of the College de France and Stanley Keith Runcorn of the University of Newcastle upon Tyne, who have also edited the publication.

The 'trigger' for the meeting was the discovery, as a by-product of using tree rings to improve the calibration of carbon-14 dating, of an approximate 200-year period in the carbon-14 generation rate in the high atmosphere. This is almost certainly attributable to variations in cosmic rays, in their turn influenced by changes in the magnetic activity of the sun. Measurements of beryllium-10 in ice cores have provided additional evidence for this variation in solar activity.

The authors of the papers come from a variety of disciplines (geology, archaeology, astronomy and the environmental sciences) and from as far afield as the USA, China and Australia, as well as Europe. Most of the papers are concerned with carbon-14 and beryllium-10 investigations, but astronomical and observational aspects of solar variation, the possible relationships between climate and solar activity, and the study of the sun itself, are also covered. The papers appear to be 'state of the art' and are accompanied by copious up-to-date references. There is, however, no index.

The 11-year sunspot cycle is, of course, well documented, but attempts to find corresponding variations in the earth's climate have so far proved inconclusive. However, the 11-year variation has itself shown cyclic behaviour with a period of about 200 years. For example, the era of weak sunspot activity from about AD 1645–1715 (the so-called Maunder Minimum), at around the time of the Little Ice Age, was preceded by other minima at approximately 200-year intervals back to the end of the first millennium AD. H.H. Lamb's discovery that these minima correlated with cold winters in western Europe aroused much interest but, of course, evidence extending over less than 1000 years is insufficient to establish a 200-year cycle. Support for the existence of the 200-year cycle for possibly the last 2000 years is, however, found in the Chinese sunspot record.

The significance of the findings presented in this volume is that the examination of tree rings and ice cores enables the period over which solar variation can be studied, albeit by proxy, to be measured in thousands rather than hundreds of years.

Does this work have any relevance for meteorologists? To quote from S.K. Runcorn's closing remarks: 'The greenhouse effect points to the need for a better understanding of the atmosphere and of climatic change. By studying the effect of the changes of solar output with periods of 11 and 200 years on the atmosphere from the historic and archaeological records, we may hope to come to a better understanding of the earth's atmosphere and how it responds to changing energy input. In geophysics we have to wait for nature to do the experiment. But in assessing the influence of the greenhouse effect from observations over the past 150 years, the possibility that some of the change may be due to the 200-year cycle in the sun must be considered. We showed in the introductory remarks that the global increase in temperature over the second half of the last century and the first half of this correlates with the sun's activity, as determined by geomagnetic disturbances. This implies that at least some part of the observed increase in temperature is due to increased solar energy output'. Conversely, if the 200-year cycle places us in a solar minimum in the first half of the next century, might this not mitigate the greenhouse warming, at least to some extent.

In the preface to their book, the editors express the 'hope that this important interdisciplinary subject will attract young and enthusiastic workers'. Its publication should go a long way towards fulfilling that hope.

P.M. Stephenson

Satellite photographs — 24 October 1990 at 1242 UTC

The main feature on the AVHRR infra-red (IR) image of the central Mediterranean (Fig. 1) is the spectacular plume of cold cloud-tops extending over 500 km eastwards from an apparent generation point just south-west of Malta (M). The plume is associated with thunderstorms whose anvils have merged, and is a prime example of the distinctive patterns Mesoscale Convective Systems (MCSs) can display on IR images. Although little detail can be made out within the body of the plume, there are marked variations in cloud-top temperature gradient around the periphery. Note the very steep gradient at A and B compared with the much more gradual changes at C and D. Juying and Scofield* have shown that within an MCS cloud-shield, regions of steep cloud-top temperature gradient correlate closely with the heaviest precipitation.

The corresponding visible image in Fig. 2 provides additional detail on cloud structure within this system. Notice in particular the bright lumpy texture to the cloud tops — implying active convection — in the western portion (W) where a marked shadow (S) is being cast on much lower cloud, also in the more central portion of the cloud shield and along the spine. Much of the eastern portion is relatively thin cirrus.

The water vapour image from Meteosat (Fig. 3) shows that the MCS developed where dry mid-tropospheric air with relatively low wet-bulb potential temperature (θ_w) began to overrun a tongue of moist higher θ_w air at low levels (Fig. 3). A weak surface trough extended from Libya to Sicily and dew-points as high as 21 °C were reported in the Malta area. The plume formed in the region of marked vertical wind-shear with anvil cirrus carried eastwards in the strong westerly upper flow — 70 kn at 300 mb over Sicily (Fig. 4).

Other features of interest on both images include areas of deep convection over southern Italy (I on Fig. 1) and marked waves in the upper cloud over the Adriatic (E on Fig. 1). These may be gravity waves resulting from deep convection being 'damped' at the tropopause.

A.J. Waters and D. Ratcliff

* Juying, X. and Scofield, R.A.; Satellite-derived rainfall estimates and propagation characteristics associated with mesoscale convective systems (MCSs). Washington DC, NOAA, Technical Memorandum NESDIS 25, 1989.

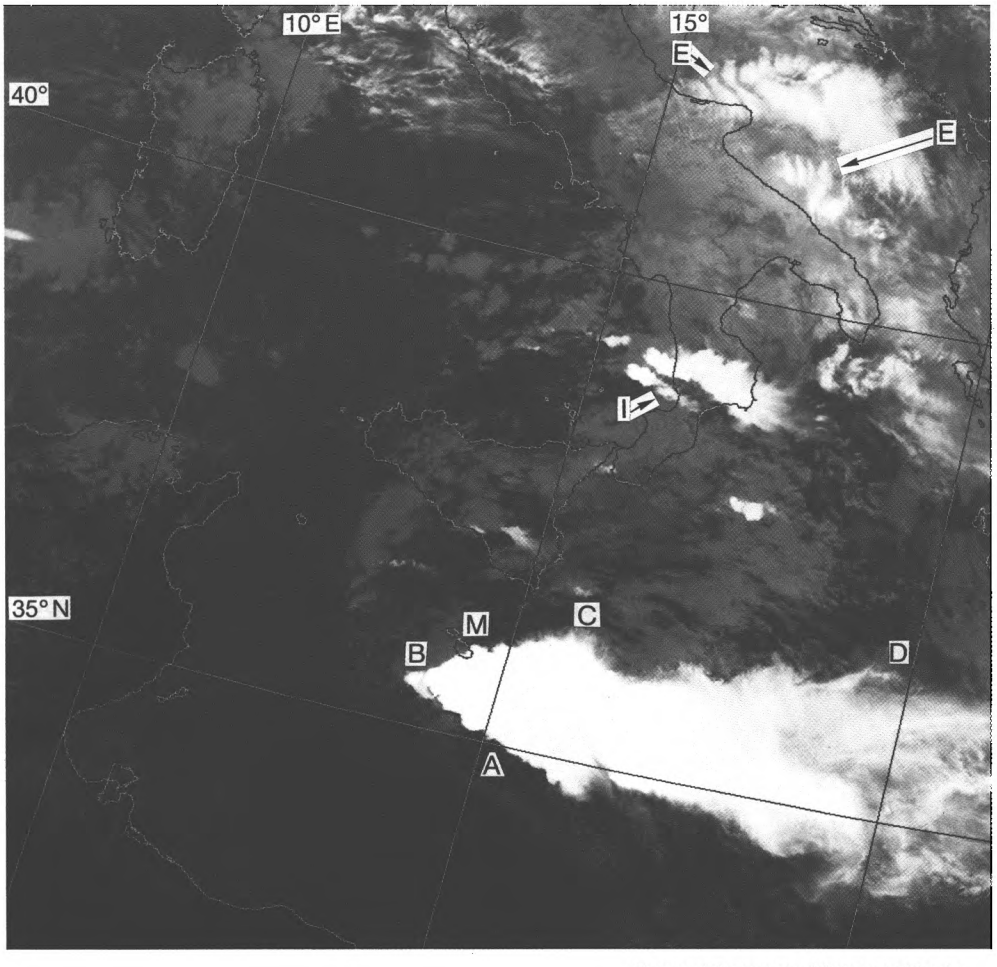

Photograph by courtesy of University of Dundee

Figure 1. NOAA-11 AVHRR infra-red image at 1242 UTC on 24 October 1990. The labels refer to features mentioned in the text.

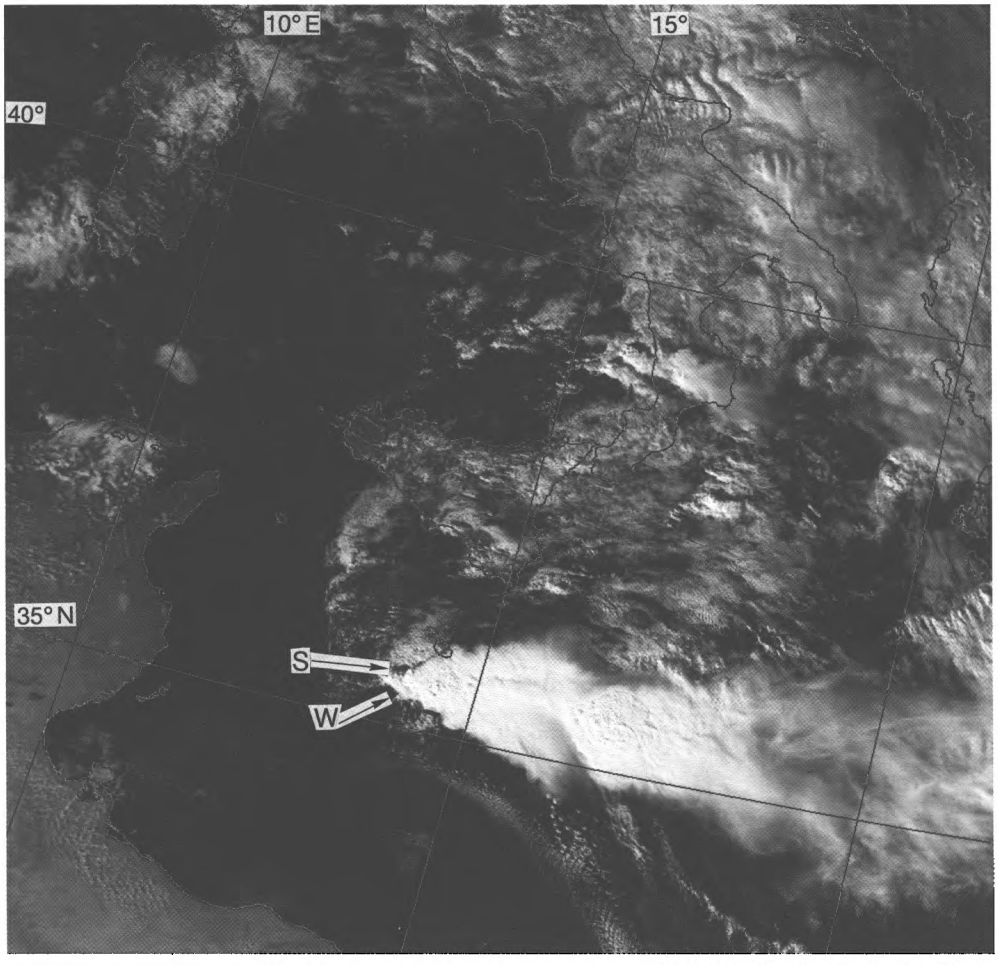

Photograph by courtesy of University of Dundee

Figure 2. As Fig. 1 but visible image.

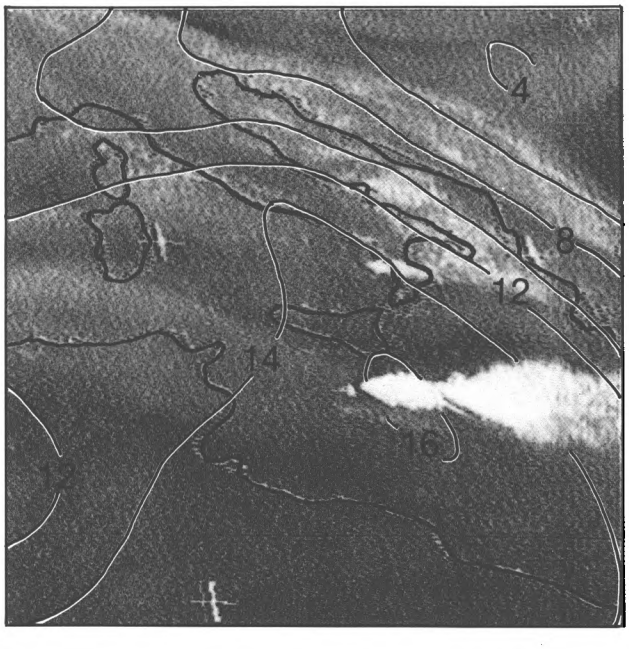

Figure 3. Meteosat water-vapour image at 1130 UTC on 24 October 1990. Black indicates dry mid-tropospheric air, higher moisture content being shown by progressively lighter shades of grey and the continuous lines indicate wet-bulb potential temperature (°C).

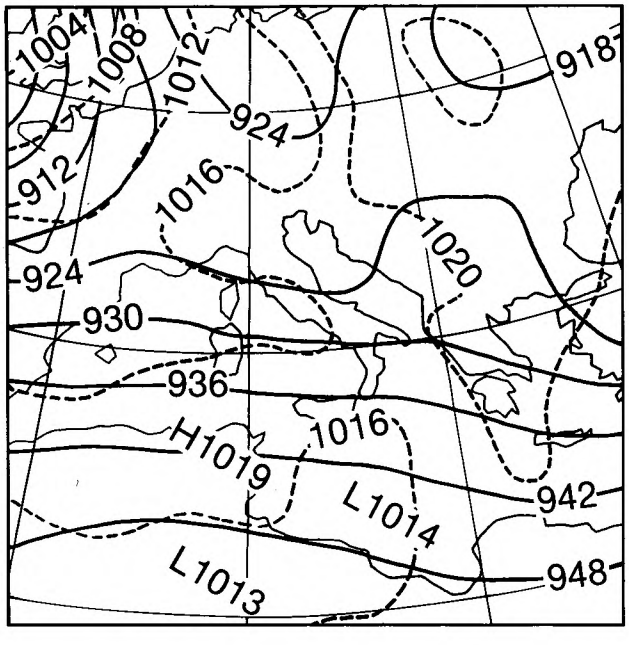

Figure 4. Contours of the 300 mb surface (dam) (continuous lines) at 1200 UTC on 24 October 1990 with mean-sea-level isobars (mb) superimposed as dashed lines.

GUIDE TO AUTHORS

Content

Articles on all aspects of meteorology are welcomed, particularly those which describe results of research in applied meteorology or the development of practical forecasting techniques.

Preparation and submission of articles

Articles, which must be in English, should be typed, double-spaced with wide margins, on one side only of A4-size paper. Tables, references and figure captions should be typed separately. Spelling should conform to the preferred spelling in the *Concise Oxford Dictionary* (latest edition). Articles prepared on floppy disk (Compucorp or IBM-compatible) can be labour-saving, but only a print-out should be submitted in the first instance.

References should be made using the Harvard system (author/date) and full details should be given at the end of the text. If a document is unpublished, details must be given of the library where it may be seen. Documents which are not available to enquirers must not be referred to, except by 'personal communication'.

Tables should be numbered consecutively using roman numerals and provided with headings.

Mathematical notation should be written with extreme care. Particular care should be taken to differentiate between Greek letters and Roman letters for which they could be mistaken. Double subscripts and superscripts should be avoided, as they are difficult to typeset and read. Notation should be kept as simple as possible. Guidance is given in BS 1991: Part 1: 1976, and *Quantities, Units and Symbols* published by the Royal Society. SI units, or units approved by the World Meteorological Organization, should be used.

Articles for publication and all other communications for the Editor should be addressed to: The Chief Executive, Meteorological Office, London Road, Bracknell, Berkshire RG12 2SZ and marked 'For Meteorological Magazine'.

Illustrations

Diagrams must be drawn clearly, preferably in ink, and should not contain any unnecessary or irrelevant details. Explanatory text should not appear on the diagram itself but in the caption. Captions should be typed on a separate sheet of paper and should, as far as possible, explain the meanings of the diagrams without the reader having to refer to the text. The sequential numbering should correspond with the sequential referrals in the text.

Sharp monochrome photographs on glossy paper are preferred; colour prints are acceptable but the use of colour is at the Editor's discretion.

Copyright

Authors should identify the holder of the copyright for their work when they first submit contributions.

Free copies

Three free copies of the magazine (one for a book review) are provided for authors of articles published in it. Separate offprints for each article are not provided.

Contributions: It is requested that all communications to the Editor and books for review be addressed to the Chief Executive, Meteorological Office, London Road, Bracknell, Berkshire RG12 2SZ, and marked 'For *Meteorological Magazine*'. Contributors are asked to comply with the guidelines given in the *Guide to authors* which appears on the inside back cover. The responsibility for facts and opinions expressed in the signed articles and letters published in *Meteorological Magazine* rests with their respective authors.

Subscriptions: Annual subscription £33.00 including postage; individual copies £3.00 including postage. Applications for postal subscriptions should be made to HMSO, PO Box 276, London SW8 5DT; subscription enquiries 071–873 8499.

Back numbers: Full-size reprints of Vols 1–75 (1866–1940) are available from Johnson Reprint Co. Ltd, 24–28 Oval Road, London NW1 7DX. Complete volumes of *Meteorological Magazine* commencing with volume 54 are available on microfilm from University Microfilms International, 18 Bedford Row, London WC1R 4EJ. Information on microfiche issues is available from Kraus Microfiche, Rte 100, Milwood, NY 10546, USA.

February 1991

Editor: F.E. Underdown
Editorial Board: R.J. Allam, R. Kershaw, W.H. Moores, P.R.S. Salter

Vol. 120
No. 1423

Contents

ISSN 0026–1149

Printed in the United Kingdom for HMSO
Dd 0291241 2/91 C130 0503 12521

The Meteorological Magazine

March 1991

Rainfall distribution around Athens
Comparison of UK road ice models

HMSO

Met.O.998 Vol. 120 No. 1424

First published 1991

HMSO publications are available from:

HMSO Publications Centre
(Mail and telephone only)
PO Box 276, London, SW8 5DT
Telephone orders 071-873 9090
General enquiries 071-873 0011
(queuing system in operation for both numbers)

HMSO Bookshops
49 High Holborn, London, WC1V 6HB 071-873 0011 (counter service only)
258 Broad Street, Birmingham, B1 2HE 021-643 3740
Southey House, 33 Wine Street, Bristol, BS1 2BQ (0272) 264306
9–21 Princess Street, Manchester, M60 8AS 061-834 7201
80 Chichester Street, Belfast, BT1 4JY (0232) 238451
71 Lothian Road, Edinburgh, EH3 9AZ 031-228 4181

HMSO's Accredited Agents
(see Yellow Pages)

and through good booksellers

3 8078 0010 2479 5

The Meteorological Magazine

March 1991
Vol. 120 No. 1424

551.577.21(495)

Spatial distribution of rainfall in the Greater Athens Area

G.T. Amanatidis, C. Housiadas and J.G. Bartzis
National Center for Scientific Research Demokritos, Institute of Nuclear Technology and Radiation Protection, 15310 Ag. Paraskevi Attikis, Greece

Summary

The annual and seasonal spatial distribution of rainfall in the Greater Athens Area in Greece is studied using the rainfall data from 24 rain-gauges for 1985–89. Both these rainfall distributions and the temporal variations of rainfall during the 5-year period present strong discrepancies among the different parts of the examined area. The influence of the complex topography and the atmospheric circulation on the rainfall distribution pattern for different seasons is examined. Finally, the relation of rainfall amounts to the station height above mean sea level is also investigated.

1. Introduction

The knowledge of the spatial distribution of rainfall is of interest not only from a meteorological viewpoint, but also for its importance in different fields such as agriculture, hydrology, water resources, atmospheric pollution or even in flood control. The estimation of the spatial distribution of rainfall is a complex task, especially in cases where detailed information concerning the impact of local topography on the dominant atmospheric circulation is not available. The problem becomes even more complicated by the varying pattern and intensity of near-surface atmospheric circulations.

In the case of the Greater Athens Area (GAA) (see Fig. 1) the knowledge of the spatial distribution of rainfall is rather limited though rainfall measurements have been carried out in the city of Athens for well over 130 years. One of the longest series of rainfall measurements in south-eastern Europe is that collected by the Meteorological Institute of the National Observatory of Athens (MINOA). This has been extensively analysed in the last 15 years (Katsoulis *et al.* 1976, Zerefos *et al.* 1977, Repapis 1986, Katsoulis and Kambezidis 1989), but since the knowledge is based on rainfall data obtained from only one rain-gauge, nothing can be said about the spatial distribution of rainfall in the GAA. Extrapolation of the results obtained at MINOA could create serious errors caused by the complex topography effects, especially during the cold period of the year when frontal rainfall is more common. During the warm period of the year, rainfall is predominantly convective and frequently has high intensity over small areas. Such local thunderstorm activity makes data extrapolation from one station even more unreliable.

In this study, the rainfall measured by 24 rain-gauges in the GAA for the 5-year period 1985–89 are analysed, in order to study the spatial distribution of rainfall in this area. The network used consists of all the reliable rain-gauges in operation for the examined period and covers the area in a mesoscale range. Although the results do not have an adequate climatological signific-

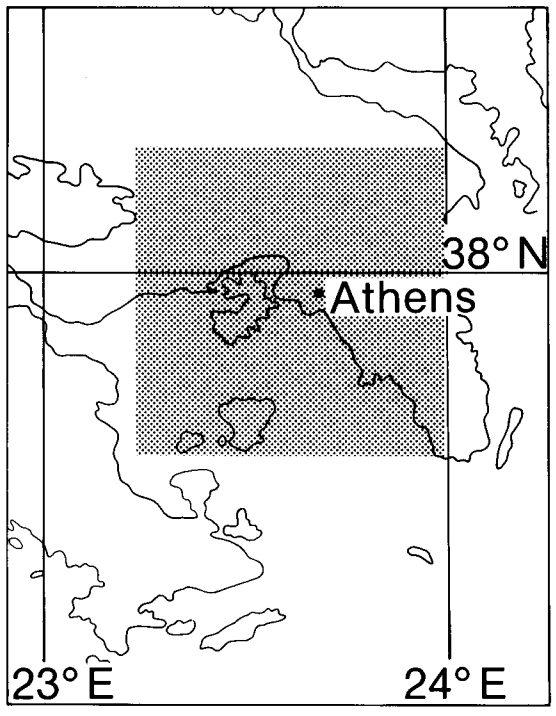

Figure 1. Map of the Attika peninsula. The Greater Athens Area is indicated by the shaded domain.

ance, because of the relatively short examined period, they confirm the expected strong irregularity of rainfall distribution in the GAA.

The results of this study may be useful in the assessment of numerical models that aim at predicting the rainfall pattern in the GAA. One such model is currently under development at the National Centre for Scientific Research (NCSR) 'Demokritos' for simulating rainfall distribution in complex topography (Housiadas *et al.* 1991). This model constitutes a further improvement of the three-dimensional atmospheric transport code, ADREA-I, developed in the context of environmental impact assessments for wind field and dispersion calculations (Bartzis *et al.* 1990, 1991).

2. Topography

The area studied in this paper is located at the south-eastern part of the Attika peninsula. The presence of mountains and sea in the GAA divide it into different regions; namely, the Athens Basin, the Thriassio Field, the Mesogia Plain, the Marathon Area and the islands of Salamina and Egina (Fig. 2).

The Athens Basin, where the city of Athens is located, is surrounded by mountains on three sides, while to the south there is sea (Saronikos Gulf). As shown in Fig. 2,

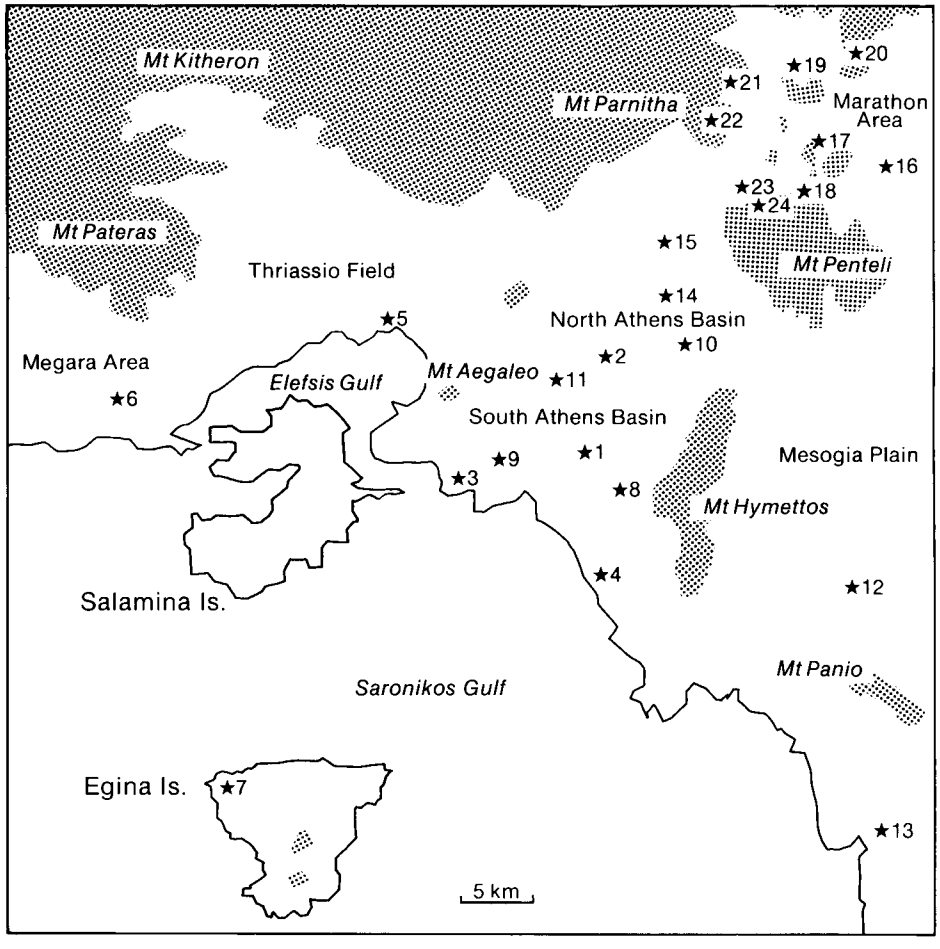

Figure 2. Map of the Greater Athens Area. Land above 400 m is indicated by shading, while the rain-gauge stations (see Table I) are indicated by numbered stars.

Mt Aegaleo (468 m) is situated to the west, Mt Parnitha (1413 m) and Penteli (1107 m) to the north and Mt Hymettos (1026 m) to the east. The Athens Basin is 30 km long and 12 km wide with a south-west to north-east major axis, and is interspersed by a series of small hills.

The Thriassio Field, located at the west side of the Athens Basin, is also surrounded by mountains. Mt Aegaleo is situated to the east, Mt Parnitha to the north, Mt Kitheron (1409 m) and Mt Pateras (1131 m) to the west, while to the south is the Elefsis Gulf coastline. Inside this area most of the Greek industry is concentrated, mainly along the coast, while inland, agricultural activities are dominant. To the east of the Thriassio Field and south of Mt Pateras extends the Megara Area, part of which is also included in the GAA.

The Mesogia Plain is located at the east of the Athens Basin and is separated from it by Mt Hymettos. Mt Penteli is situated to the north, Mt Panio (636 m) to the south, while to the east there is the Aegean Sea. Inside the plain there are some sparse industries, but agricultural activities predominate.

The Marathon Area is located to the north of Mt Penteli and east of Mt Parnitha and is washed to the north and east by the Evoikos Gulf. In the centre of the area there are the Marathon dam and the artificial homonymous lake. The lake is 250 m above mean sea level and is surrounded by forested hills.

Finally, the islands of Salamina and Egina are situated at the south-eastern part of the GAA in the Elefsis and Saronikos Gulfs respectively.

3. Climate

The climate of the GAA is Mediterranean with hot, dry summers and wet, mild winters. The summer dry period lasts for about 6 months. It begins at the end of April and continues until the beginning of October. The average daily winter temperature is 9.9 °C and the summer one is 25.8 °C. The total solar radiation is rather strong with average daily values of about 22 MJ m^{-2} in the summer and 8 MJ m^{-2} in the winter.

Most of the annual rainfall occurs in the months from October to March. This is due to the synoptic circulation which is related to extensive disturbances within the zonal westerlies (Repapis 1986). More precisely, during the summer the Atlantic anticyclone with its more northerly position dominates the Mediterranean region and therefore deflects the tracks of the storm systems. Consequently, summer is an inactive season and only infrequent local thunderstorms occur, especially in the afternoon. During the cold period of the year, this high moves to more south-westerly positions allowing depressions to enter the Mediterranean or to develop within the region. These rain-bearing depressions move from west to east (Conrad 1943, Meteorological Office 1962) and are responsible for great rainfall amounts over Greece. Contributions to the rainfall over Greece are also provided by the extension of the Siberian anticyclone over the Balkans. This creates a cold northerly airstream which, combined with possible warm and wet air masses over the central Mediterranean, produces considerable amounts of rainfall.

The upper-air flow over Greece is characterized by prevailing wind directions from the west/south-westerly sector during winter and spring, and of the northerly sector during summer and autumn (Pissimanis *et al.* 1989). Over the Athens Basin the winds tend to blow along the axis of the basin (Andreakos *et al.* 1984). The most frequent wind is that blowing from the northerly sector. The second most frequent wind blows from the south sector, while those from the east and the west sectors have a very low frequency. Except for the synoptically driven north or south winds, there are two permanent weather systems of regional character that substantially contribute to this high frequency of northerly and southerly winds. Firstly, the combination of high barometric pressure over the Balkans with low pressure over the eastern Mediterranean causes the north winds, known as the 'Etesians', in the summer months (Meteorological Office 1965). Secondly, the local sea- and land-breeze mechanism is responsible for winds from the southern sector during the warm hours of the day in late spring and in summer (Prezerakos 1986). Another sea-breeze cell is established in the Mesogia Plain and gives rise to an airflow through the pass between the Hymettos and Penteli mountains. At that point, because of the vertical motion created by the opposing sea-breeze currents (south-west and north-east), some convective clouds appear that are occasionally significant (Clement 1989).

4. Rainfall data in the Greater Athens Area

The 24 rain-gauges selected for the present investigation belong to different Greek institutions: the previously mentioned MINOA station, ten stations of the Water and Sewage Corporation (WSC), six stations of the National Meteorological Service (NMS), five stations of the Ministry of Environment, Planning and Public Works (MEPPW), one station of the Vineyard Institute of the Ministry of Agriculture (VIMA) and one private station. The list of the stations used, together with their geographical coordinates and their elevations above mean sea level, is given in Table I, and their network distribution is shown in Fig. 2.

Since the objective of the present study was to determine the spatial distribution of rainfall the GAA, a major effort was made to take into account data from the maximum number of stations with continuous records for the period 1985–89. On the other hand, special care was given to avoid effects arising from improper exposure, change of exposure, instrumental failures or change of station site during the examined period. The representativeness of the 5-year period was also examined by comparing it with the climatological

Table I. Rainfall stations in the Greater Athens Area used in this study. See Fig. 2 for locations, and text for explanation of acronyms.

No.	Station	Institution	Longitude	Latitude	Height (m)
1	MINOA	MINOA	23° 43′E	37° 58′N	107
2	Filadelfia	NMS	23° 44′E	38° 02′N	136
3	Peireas	NMS	23° 38′E	37° 56′N	3
4	Helliniko	NMS	23° 44′E	37° 54′N	10
5	Eleysina	NMS	23° 33′E	38° 03′N	30
6	Megara	NMS	23° 21′E	38° 00′N	36
7	Egina	NMS	23° 26′E	37° 45′N	3
8	Vyronas	MEPPW	23° 45′E	37° 57′N	120
9	Nikaia	MEPPW	23° 39′E	37° 58′N	20
10	Halandri	MEPPW	23° 48′E	38° 02′N	180
11	Peristeri	MEPPW	23° 42′E	38° 01′N	60
12	Markopoulo	MEPPW	23° 56′E	37° 53′N	85
13	Anavyssos	Private	23° 57′E	37° 42′N	80
14	Lykovrysi	VIMA	23° 47′E	38° 04′N	220
15	Tatoi	WSC	23° 47′E	38° 06′N	237
16	Horio	WSC	23° 58′E	38° 09′N	60
17	Fragma	WSC	23° 54′E	38° 10′N	240
18	Stamata	WSC	23° 53′E	38° 08′N	370
19	Kapandriti	WSC	23° 53′E	38° 13′N	340
20	Varnavas	WSC	23° 55′E	38° 14′N	480
21	Kiourka	WSC	23° 50′E	38° 12′N	400
22	Katsimidi	WSC	23° 49′E	38° 11′N	570
23	Hani	WSC	23° 51′E	38° 08′N	260
24	Bogiati	WSC	23° 51′E	38° 08′N	350

data obtained from the longest rainfall time-series of MINOA.

In order to study the rainfall amounts in the different regions in the GAA (as defined in section 2), the rainfall data from the 24 stations were grouped into six categories for further analysis; the criterion for this grouping was mainly geographical. Because of the length of the Athens Basin, it was subdivided into the South and North Athens Basins. The height of each station above mean sea level was also taken into consideration in this division, as a relationship between station height and rainfall amount exists (Smith 1979).

The categories into which the GAA was divided were the following:

South Athens Basin (SAB) which includes six stations (MINOA, Peireas, Helliniko, Nikaia, Vyronas and Peristeri).

North Athens Basin (NAB) which includes four stations (Filadelfia, Halandri, Lykovrysi and Tatoi).

Thriassio Field which includes two stations (Eleysina and Megara).

Egina Island with its homonymous station.

Mesogia Plain with two stations (Markopoulo and Anavyssos).

Marathon Area which includes nine stations (Horio, Fragma, Stamata, Kapandriti, Varnavas, Kiourka, Katsimidi, Hani and Bogiati).

5. Results and discussion

5.1 Temporal variations of rainfall

The monthly values of rainfall in the six regions of the GAA for the period 1985–89 are shown in Fig. 3 and the corresponding monthly mean values for the same period are shown in Fig. 4. It is obvious, that the rainfall in the GAA presents a strong seasonal variation with wet winters and dry summers, as in the typical Mediterranean climate, which is a result mainly caused by the synoptic circulation explained before. The monthly values of rainfall vary greatly from month to month. Calculations from the long-term rainfall series of MINOA have shown that the correlation between pairs of months is very low, which has been attributed to the relative independence among the synoptic conditions characterizing the rainfall in each season (Katsoulis and Kambezidis 1989). It is important to note that 1989 was relatively dry, especially for the southern part of the GAA. In that year rainfall (150.6 mm) was the lowest measured at the MINOA station for this century. This effect is related to the general drought problem experienced recently (continuing during 1990) all over Greece, which has in particular created severe problems for the water resources of the city of Athens.

The correlation among the records from the different parts of the GAA is relatively high, and the corresponding

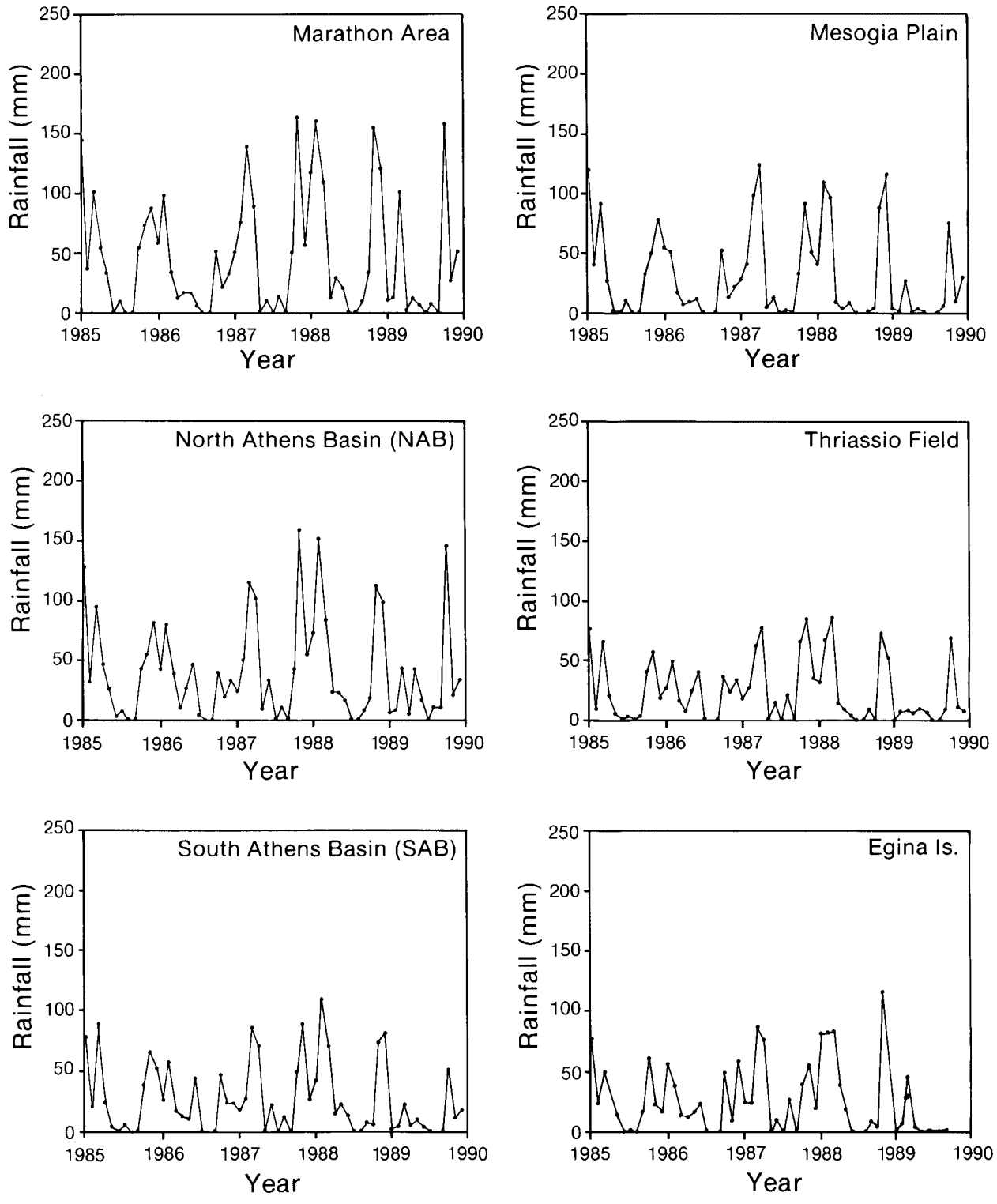

Figure 3. The monthly values of rainfall in the six regions of the Greater Athens Area for the period 1985–89.

coefficients are presented in Table II. The higher correlation coefficients are observed between the pairs of the SAB, NAB and Marathon Areas. This fact is explained by the coincidence of the geographically consecutive areas with the south-west to north-east alignment of the atmospheric circulation. The smaller correlation coefficient is observed when the area of Egina Island is considered. This may be attributed to the different behaviour of rainfall due to the airflow's divergence–convergence mechanism commonly observed in island regions.

The monthly mean variation of rainfall for the period 1985–89 in the six parts of the GAA, presented in Fig. 4, is characterized by a persistent and unexpected maximum in March for all groups of stations. At the end of the year the maximum rainfall appears in November. Consequently, the 5-year period presents a secondary minimum during winter. Katsoulis and Kambezidis (1989) have also

Table II. Correlation coefficients among the rainfall records in the Greater Athens Area. See Fig. 2 for locations of areas.

South Athens Basin (SAB)	1					
North Athens Basin (NAB)	0.949	1				
Mesogia	0.921	0.926	1			
Thriassio	0.934	0.888	0.884	1		
Marathon	0.904	0.949	0.914	0.841	1	
Egina	0.830	0.820	0.827	0.843	0.859	1
	SAB	NAB	Mesogia	Thriassio	Marathon	Egina

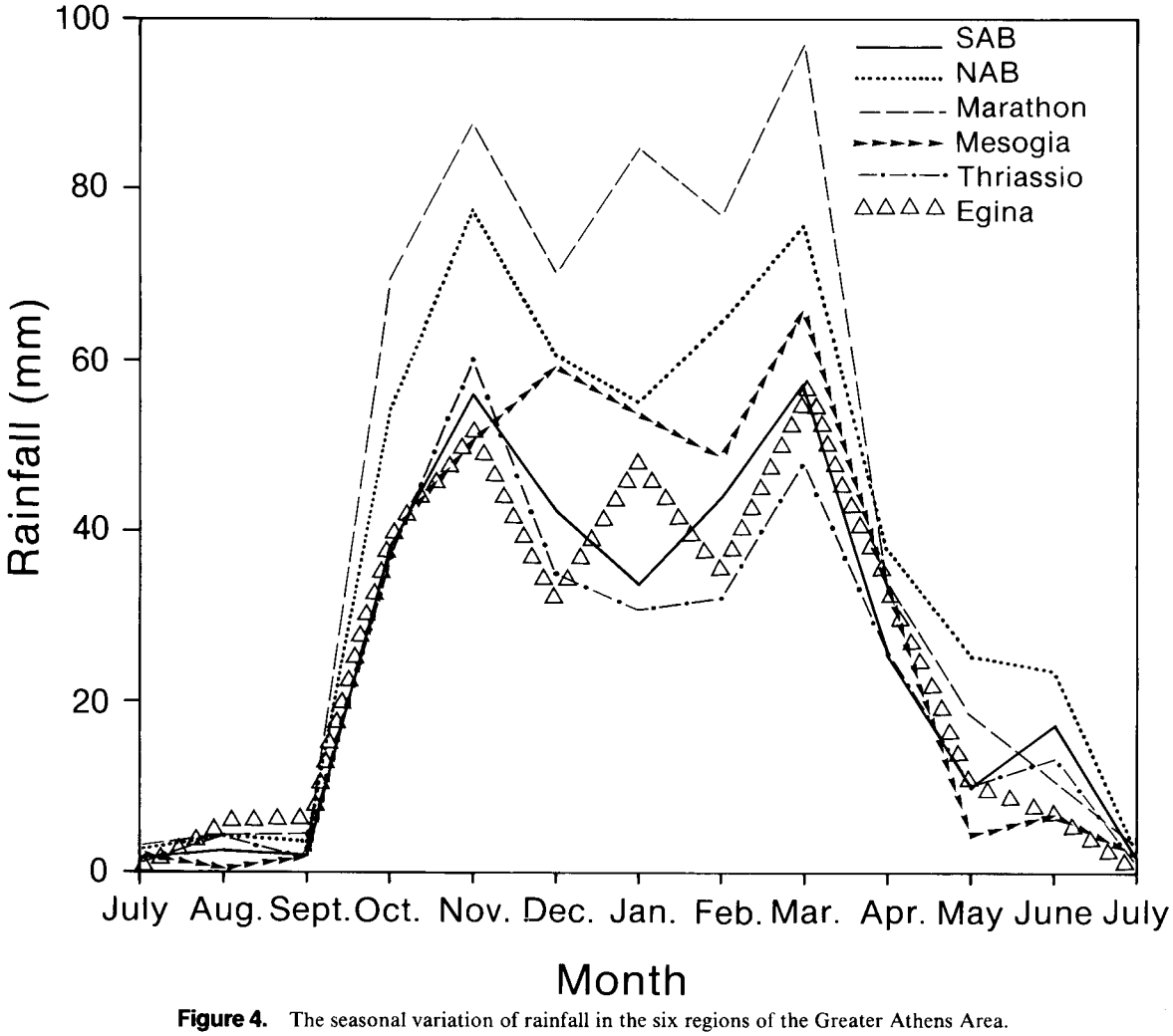

Figure 4. The seasonal variation of rainfall in the six regions of the Greater Athens Area.

observed during the most recent period (1951–85) at the MINOA station an increasing tendency of rainfall amount in the transitional seasons (which are the unstable part of the year), although at the same time a noteworthy significantly negative trend was found to characterize the annual rainfall amounts. They qualified this phenomenon as indicative of an urban effect (Changnon 1968, Goldreich and Manes 1979). The slightly increasing tendencies of rainfall amount are attributed to the urban heat-island effect and the surface roughness in the city, which both increase the turbulence and the atmospheric instability. A similar conclusion was also drawn by Goldreich and Manes (1979) for the Tel-Aviv urban area. In this respect, it is interesting to note that in the GAA the less pronounced decreases appear at the Marathon and Egina Areas which are the less urbanized.

In order to get more insight into the shift of the rainfall maximum towards March, the climatological data at the MINOA station for the periods 1891–1985, 1951–80 and 1980–89 along with the period of interest 1985–89 are plotted together in Fig. 5. The comparison shows that the March particularity appears also in the monthly mean variation of the last decade (1980–89). This result is likely to be of climatological interest.

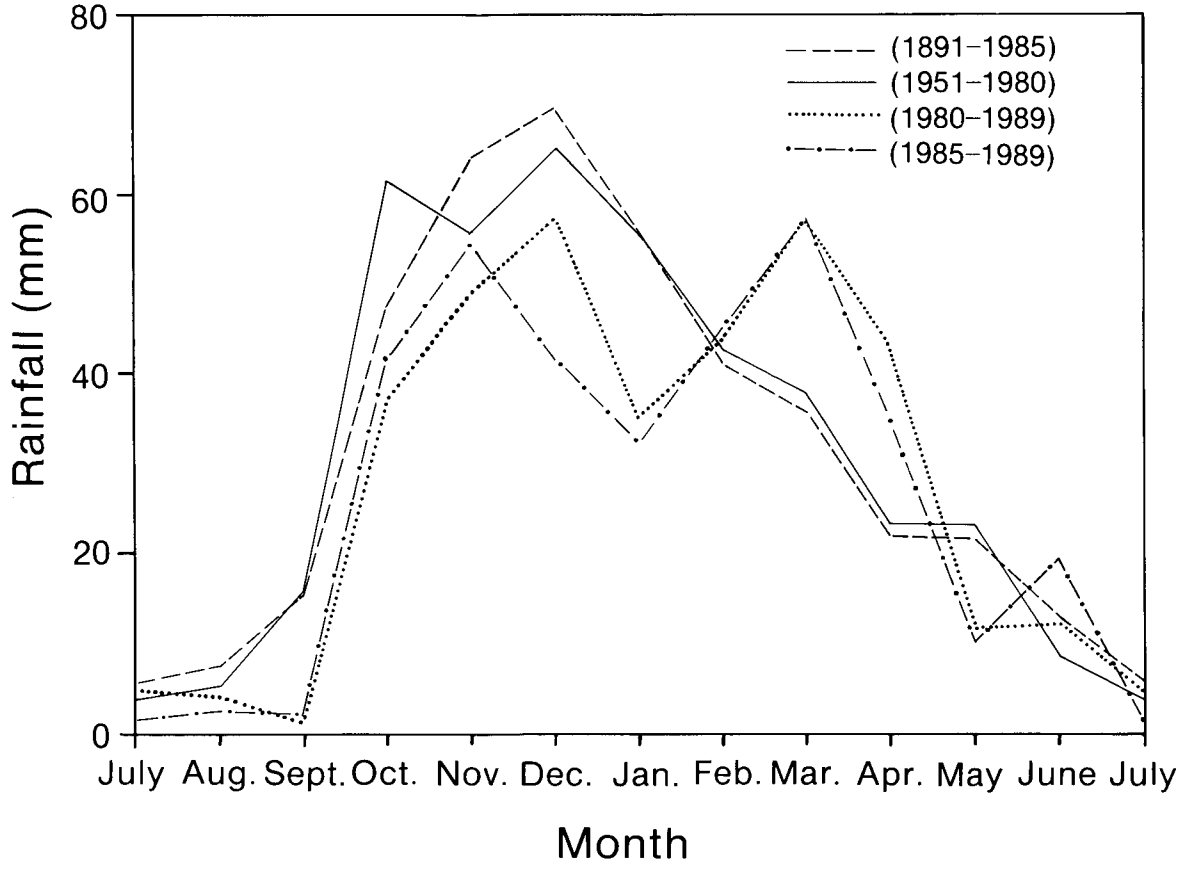

Figure 5. The seasonal variations of rainfall at the MINOA station (see Table I) for the periods 1891–1985, 1951–80, 1980–89 and 1985–89.

5.2 Rainfall variation with station height

As is well known, rainfall tends to increase with height and decreases with depth down in an isolated valley (Smith 1979). On very high mountains the rainfall increases up to a certain height (up to 2 km) and then decreases, because above this height the ascending air masses lose their water vapour content. The relationship between the average annual rainfall and the height of the station above mean sea level is in most cases linear. The scattering in the linear-regression representation is caused by the failure of the relationship to describe the upslope-rain to rain-shadow contrast, which is important for broad mountains. If the region under consideration has a consistent prevailing wind, this latter effect is well represented by the spatial distribution of annual rainfall.

In Table III, the average annual rainfall and the mean height of the stations for the six different areas in the GAA are presented. It is ascertained that rainfall increases with height. The maximum rainfall occurs in the hilly area around the Marathon lake. On the other hand, the minimum rainfall occurs in the south-west part of the GAA at the Thriassio Field and the Egina Island where the stations are very close to sea level.

In Fig. 6, the average annual rainfalls for the period 1985–89 at the 24 stations in the GAA have been plotted against the station heights. Although the station height used is not obtained by any averaging process considering the surrounding area (Goh and Lockwood 1974, Hill *et al.* 1981) the correlation is relatively high ($r = 0.826$), which indicates that variations of annual rainfall amounts account for 68% of the variance of the station height. The 32% uncorrelated variance of rainfall is attributed to the upslope-rain to rain-shadow contrast, as mentioned before. The linear-regression equation, obtained in Fig. 6, $R = 306.8 + 0.685H$ is valid for the GAA, where the rainfall R is measured in millimetres and the station height H in metres. The slope of the linear best fit suggests that annual rainfall amounts increase by 68.5 mm for each 100 m increase of the station height. The intercept of the linear best fit indicates that there is an annual rainfall of about 300 mm in the GAA for any stations with zero height.

The correlation between the monthly rainfall amounts and the station height presents a seasonal variation. The

Table III. Rainfall amounts at different regions of the Greater Athens Area. The areas are the same as in Table II.

Area	Number of stations	Average height (m)	Average annual rainfall (mm)
SAB	6	53	320.9
NAB	4	193	465.8
Mesogia	2	83	366.4
Thriassio	2	33	275.5
Egina	1	3	288.4
Marathon	9	341	557.2

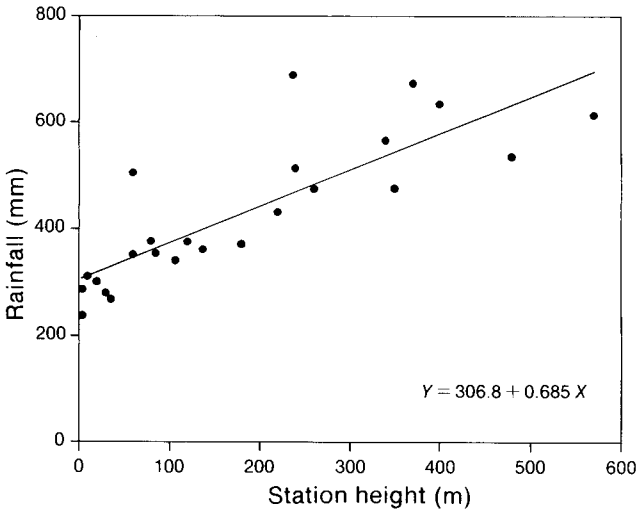

Figure 6. The average annual rainfall for the period 1985–89 versus station heights above mean sea level.

correlation coefficients are high for January (0.696) and October (0.789), but are low for April (0.271) and July (0.155). These results confirm that the frontal rainfall during the cold period of the year is strongly affected by the presence of mountains, while the thunderstorm activity during the warm period of the year is less affected by the local topography. The October maximum correlation coefficient calculated for the GAA is in accordance with Bergeron (1968, 1973). During the fall months, he found in Uppsala, Sweden, a remarkably strong dependence of rainfall on height — primarily caused by rain from stratified clouds.

5.3 Spatial variations of rainfall

The great spatial variability characterizing the rainfall in the GAA is not only attributed to the synoptic disturbances. Geographical and topographical factors, such as mountains, hills, plains, sea and islands in the GAA, produce microclimatic effects on the mesoscale circulations and significantly disturb the distribution of rainfall in the GAA. As a result, there will be as many different spatial rainfall distributions as there are days considered. Some degree of generalization is therefore essential, and consequently the spatial distribution of rainfall in the GAA is analysed on a monthly basis.

The average annual distribution of rainfall in the GAA for the 5-year period 1985–89 is shown in Fig. 7. The maximum rainfall occurs in the Marathon Area and more precisely on the south-east side of Mt Parnitha, while the minimum rainfall occurs in the south-west part of the GAA over the Salamina and Egina islands. A gradient is observed between inland and coastal areas along the south-west to north-east direction. The annual rainfall amounts double in the Marathon Area in comparison to the coastal areas. Repapis (personal communication) has also observed a similar gradient using earlier data from stations at SAB, NAB, Mesogia and Thriassio Areas. The rainfall gradient in the GAA is mainly attributed to the rain-bearing depressions

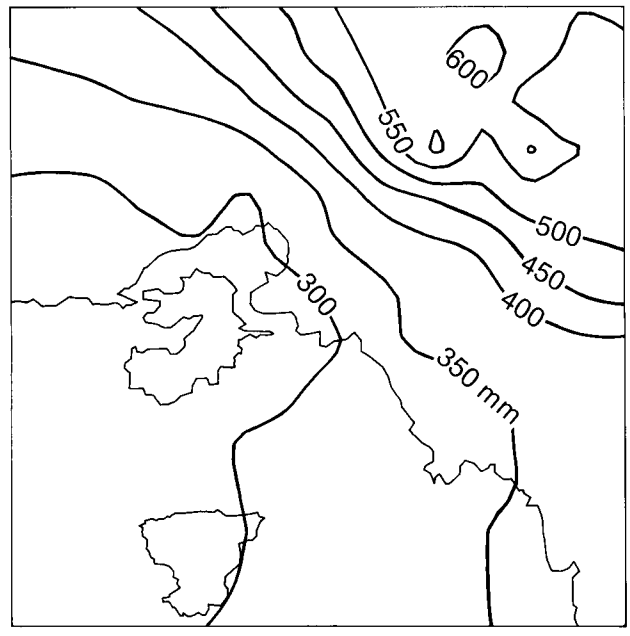

Figure 7. The average annual spatial distribution of rainfall in the Greater Athens Area for the period 1985–89.

moving from south-west to north-east over the Attika peninsula. The air masses are influenced by the presence of the surrounding sea which is warmer than the adjoining land during the cold period of the year. The passage from the sea to the land, together with the forced ascent due to topographic effects, are thought to be responsible for the gradient observed. Furthermore, superimposed on the above mechanisms, an additional effect seems to occur over the Marathon Area which explains the enhancement of the rainfall amounts measured in this area. Indeed, the hills and the small-scale mountains around the Marathon lake enhance rainfall by the so-called 'seeder-feeder' mechanism advanced by Bergeron (1965), in which raindrops from pre-existing (seeder) clouds aloft wash out small cloud droplets within low-level (feeder) clouds over the hills. According to field observations and theoretical studies (Bergeron 1968, 1973, Hill *et al.* 1981, Carruthers and Choularton 1983, Grabowski 1989), hills receive 40–100% more rain than the surrounding areas, while for convective-type rainfall, they appear to have negligible influence on the spatial rain distribution.

In order to analyse the seasonal aerial distribution of rainfall in the GAA, four months (January, April, July and October) considered as representative for the respective seasons are used. The spatial distribution for each month is shown in Fig. 8. The mean rainfall distribution for January and October present the same patterns as the annual one. But, in the January case, the gradient increases and the difference between the coastal area and the Marathon Area becomes more than three times bigger. During April, the rainfall pattern changes and the observed gradient becomes much less pronounced. Maximum amounts of rain fall on the

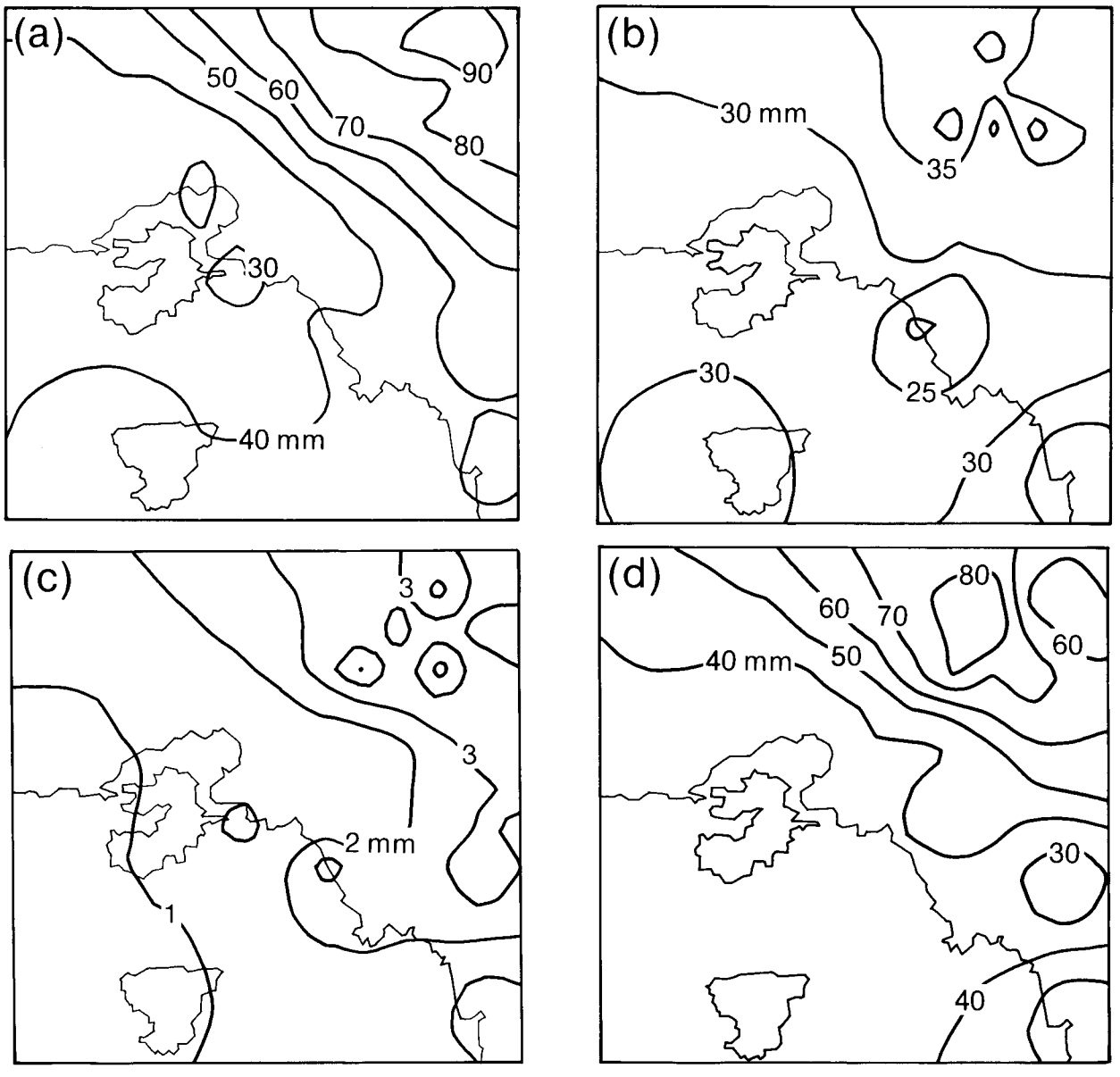

Figure 8. The spatial distribution of mean rainfall for the period 1985–89 in the Greater Athens Area for (a) January, (b) April, (c) July, and (d) October.

foot of Mt Parnitha and minimum at the south side of Mt Hymettos.

The July spatial distribution of rainfall is characterized by very low values (dry period of year). The influence of topography on rainfall distribution decreases, since for this season rainfall is only due to the local thunderstorm activity. High values of rainfall are observed in the Marathon Area and at Helliniko. The latter is in accordance with the work by Prezerakos (1989), who observed a greater number of thunderstorm days at Helliniko. He claimed that the thunderstorms start over the continental parts of Athens Basin and then develop towards the coasts of Saronikos Gulf.

6. Conclusions

The spatial distribution of rainfall in the GAA in Greece was examined in relation to the complex topography and the atmospheric circulation of this area. For this purpose, rainfall data from 24 stations for the 5-year period 1985–89 was analysed. This analysis revealed the following features:

(a) Although the rainfall in the GAA presents in general a seasonal variation with the maximum during the cold period of the year and a minimum during the warm period of the year, a secondary minimum is observed during winter in the examined period (appeared also in the last decade) intensified by the higher rainfall amounts measured in March.

(b) The annual rainfall amounts increase with height in the GAA by 68.5 mm for each 100 m increase of the station height above the mean sea level. A background annual rainfall of about 300 mm is considered as independent from the relief in the GAA. The correlation coefficient between the monthly mean

rainfall and the station height presents a seasonal variation with high values during the cold period of the year and low values during the warm period.

(c) The annual spatial distribution of rainfall presents a gradient between inland and coastal areas. As a result, rainfall at Marathon Area doubles in comparison with the coastal areas. The same distribution pattern is observed for January and October, while for April and July the gradient is much less pronounced due to the thunderstorm activity, which is less influenced by the local topography.

Acknowledgements

The authors are indebted to Pr. S.D. Papagiannakis for providing the rainfall data from his station at Anavyssos. Rainfall data for the GAA have been kindly provided by MINOA, NMS, WSC, MEPPW and VIMA.

References

Andreakos, C., Prezerakos, N.G. and Xirakis, P., 1984: Analysis of the air field in Athens. Final report of B6612/9. Athens, Ministry of Physical Planning, Housing and Environment.

Bartzis, J.G., Varvayanni, M., Catsaros, N., Konte, K. and Amanatidis, G.T., 1990: Wind field and dispersion modelling in complex terrain. Proceedings of the CEC seminar on methods and codes for assessing the off-site consequences of nuclear accidents. Athens, CEC Publications.

Bartzis, J.G., Venetsanos, A.G., Varvayanni, M., Catsaros, N. and Megaritou, A., 1991: ADREA-I, a transient three dimensional transport code for complex terrain and other applications. To be published in *Nuclear Technology*.

Bergeron, T., 1965: On the low level redistribution of atmospheric water caused by the orography. *In* Supplementary Proceedings of an International Conference on Cloud Physics. Tokyo.

—, 1968: Studies of orogenic effects on the areal fine structure of rainfall distribution. Uppsala Meteorological Institute, Report No. 6.

—, 1973: Mesometeorological studies of precipitation. Part V: Monthly rainfall in Uppsala field. Uppsala Meteorological Institute, Report No. 38.

Carruthers, D.J. and Choularton, T.W., 1983: A model of the seeder-feeder mechanism of orographic rain including stratification and wind-drift effects. *Q J R Meteorol Soc*, **109**, 575–588.

Changnon, S.A. (Jun.), 1968: The La Porte weather anomaly — fact or fiction? *Bull Am Meteorol Soc*, **49**, 4–11.

Clement, F., 1989: Air quality in the Greater Athens Area. II: Numerical simulations of the wind field. EUR 12245 EN, Joint Research Centre, Ispra, Italy, Commission of the European Communities.

Conrad, V., 1943: The climate of the Mediterranean Region. *Bull Am Meteorol Soc*, **24**, 4.

Goh, K.C. and Lockwood, J.G., 1974: An assessment of topographical controls on the distribution of rainfall in the central Pennines. *Meteorol Mag*, **103**, 275–287.

Goldreich, Y. and Manes, A., 1979: Urban effects on precipitation patterns in the greater Tel-Aviv area. *Arch Meteorol Geophys Bioklimatol*, **27b**, 213–224.

Grabowski, W.W., 1989: On the influence of small-scale topography on precipitation. *Q J R Meteorol Soc*, **115**, 633–650.

Hill, F.F., Browning, K.A. and Bader, M.J., 1981: Radar and raingauge observations of orographic rain over south Wales. *Q J R Meteorol Soc*, **107**, 643–670.

Housiadas, C., Amanatidis, G.T. and Bartzis, J.G., (1991): Prediction of orographically induced rainfall using Cartesian coordinates and a single prognostic equation for the water substance. To be printed in *Boundary-Layer Meteorology*.

Katsoulis, B.D. and Kambezidis, H.D., 1989: Analysis of the long-term precipitation series in Athens, Greece. *Clim Change*, **14**, 263–290.

Katsoulis, B.D., Tselepidaki, H. and Theoharatos, G., 1976: Characteristics of precipitation in Athens. *Bull Hell Meteorol Soc*, **VI, 2**, 1–19. (In Greek.)

Meteorological Office, 1962: Weather in the Mediterranean, Vols 1 and 2. London, HMSO.

—, 1965: Weather in the Mediterranean. London, HMSO.

Pissimanis, D., Karras, G., Notaridou, V. and Bartzis, J.G., 1989: Preliminary study on the flow field over Greece. *In* DEMO 89/1. Athens, NCSR Demokritos.

Prezerakos, N.G., 1986: Characteristics of the sea breeze in Attica, Greece. *Boundary-Layer Meteorol*, **36**, 245–266.

—, 1989: An investigation into the conditions in which air-mass thunderstorms occur in Athens. *Meteorol Mag*, **118**, 31–36.

Repapis, C.C., 1986: Temporal fluctuations of precipitation in Greece. *Riv Meteorol Aeronaut*, N 1–2, 19–25.

Smith, R.D., 1979: The influence of mountains on the atmosphere. *Adv Geophys*, **21**, 87–230.

Zerefos, C.S., Kosmas, G.B., Repapis, C.C. and Zampakas, J.D., 1977: Time series analysis of rain at Athens National Observatory during the century 1871–1970. Greece, University of Athens, Climatology Laboratory. (In Greek.)

551.509.543:625.7(410)

A comparison of UK road ice prediction models

J.E. Thornes and J. Shao
University of Birmingham

Summary

The performance of three models are compared and analyzed using a variety of statistical techniques.

1. Introduction

The climate of the British Isles in winter is usually characterized by the fluctuation of road surface temperatures around 0 °C together with a high humidity, which can induce the formation of ice or frost on road surfaces. This is obviously a serious potential hazard to all road users. There is a need for an accurate prediction of road surface conditions, to allow time for winter maintenance engineers to spread de-icing chemicals to prevent the formation of ice or frost or the accumulation of snow. Such phenomena also occur in many other countries with a cold and wet winter climate, such as northern and western Europe, Japan and North America. Three numerical road ice prediction models have been developed in the United Kingdom (Thornes 1984, Parmenter and Thornes 1986; Rayer 1987, Thompson 1988; Shao 1990) specifically for this purpose. Some others have also been developed outside the United Kingdom, such as the Swedish (Kempe 1990), French (Isaka *et al.* 1990), American SSI model (Stephenson 1988) and Finnish (Nysten 1980) models. Partly for commercial reasons, these other models are not available for comparison.

There have been few comparisons between the road ice prediction models using observed road surface temperature data (Thornes 1989), the COST-309 (1991) study merely comments on the availability of such models. This paper presents the results of a detailed comparison between the three UK road ice prediction models and also suggests a standard set of statistical parameters for such comparisons using:

(a) bias, standard deviation (SD) and r.m.s. error for overall, maximum and minimum temperatures,
(b) freezing time and duration, and
(c) forecast versus frost/no frost analysis.

Table I shows, for a matrix of values of forecast minus actual road surface temperature, the different measures of bias, r.m.s. error and SD that can be calculated for hourly and daily values.

For comparison, Chapman's Hill road weather outstation on the M5 motorway, West Midlands was chosen as the test site, due to the availability of roadside data and weather data from the University of Birmingham some 7 miles to the north-east. The three available models, i.e. the Thornes model (Thornes 1984), the Met. Office model (Rayer 1987, Thompson 1988) and the Icebreak model (Shao 1990) — developed on a 1987/88 winter database — are compared using a standard set of input data for the site taken from the winter of 1988/89. A comparison of the similarities and differences of the three models is given in Table II. The models also use different methods for the computation of the radiative and turbulent fluxes.

Table I. The derivation of hourly (H), daily (D) and overall (O), bias (B), r.m.s. error (R) and standard deviation (SD) for a matrix of values of forecast minus actual road surface temperatures.

	Hour of the day from noon (i)						
	1	2	.	.	.	I	
Day (n)							
1	X_{11}	X_{12}	.	.	.	X_{1I}	$B_D\ R_D\ SD_D$, e.g. $B_D = 1/I \sum_{i=1}^{I} X_{ni}$
2	X_{21}	X_{22}	.	.	.	X_{2I}	
.							
.							
.							
N	X_{N1}	X_{N2}	.	.	.	X_{NI}	
	$B_H\ R_H\ SD_H$, e.g. $B_H = 1/N \sum_{n=1}^{N} X_{ni}$						$B_O\ R_O\ SD_O$, e.g. $B_O = 1/N \sum_{n=1}^{N} B_{Dn}$

Table II. Brief description of similarities and differences between the Icebreak, Thornes and Met. Office models

	Icebreak	Thornes	Met. Office
1. Basic equation	Heat conduction	Energy balance	Heat conduction
2. Road temperature profile	Yes	No	Yes
3. Energy balance	Yes	Yes	Yes
4. Longitude	Yes	Yes	No
5. Sky view factor	Yes	No	No
6. Influence of traffic	Yes	No	No
7. Inputs*	T_a, T_d, W, C_a, C_t, R	T_a, T_d, W, C_a, C_t, R	T_a, T_d, W, C_a, C_t, C_l, R, P_r
8. Outputs**	T_s and wetness	T_s and wetness	T_s and wetness
9. Method of discreterization	Control volume	—	Finite difference
10. Derivation of forecast	Solving basic equation by fully implicit scheme	Searching for root of basic equation by iteration	Solving basic equation by explicit scheme

* T_a = air temperature; R_d = dew-point; W = wind speed; C_a = total cloud amount; C_t = dominant cloud type; C_l = low cloud amount; R = rain period; P_r = previous day's road temperature profile.
** T_s = road surface temperature.

2. Description of input data

All three models are run on a 24-hour cycle, projecting forward the measured noon road surface temperature. The model inputs are similar for all three models and are composed of six elementary meteorological variables: air temperature, dew-point, wind speed, total cloud amount, cloud type and precipitation. Cloud type is assigned 1 for low, 2 for medium and 3 for high cloud. Precipitation is represented with 0 for no rain, 1 for light rain and 2 for moderate or heavy continuous rain. For the Met. Office model, low-cloud amount is also needed. For comparison purposes the mean values over a 3-hourly interval are used. Besides the meteorological variables, road surface and depth (0.30–0.45 m) temperatures at noon are required by all three models.

To give an objective comparison, the models are run against each other in two different ways. Firstly, actual data measured at the roadside are used for the input data to produce a retrospective prognosis (RSP) — sometimes called a perfect prognosis. This enables the internal errors of the model schemes (physical and mathematical approximations) to be compared, eliminating errors related to forecast input. The input for the RSP consists of 95 days of data from the winter of 1988/89. Air temperature, dew-point and wind speed are taken from the measurements of the instruments mounted in and on roadside screens at a non-standard height of 2.0 m (for temperatures) and 3.0 m (for wind speed). Cloud data and rainfall intensity and duration are derived from the observations of the nearby weather station at the University of Birmingham.

Secondly, to assess the size of errors due to model interior shortcomings plus forecast input errors, the models are compared using real-time input data — i.e. real-time prediction (RTP). The real-time input was produced by Birmingham Weather Centre at Elmdon for Hereford and Worcester County Council as part of an 'Open Road' commercial contract. For the purpose of this comparison the days selected are those when the forecast input was issued around noon and not updated later, which gives a data set of 65 days.

Each model is run at an initial time of 1200 UTC and compared with hourly measurements of road surface temperature obtained from a road surface sensor in the fast lane of the motorway. The accuracy of this sensor is approximately ± 0.5 °C, and the calibration was checked twice during the winter period considered.

3. Comparative results for RSP

3.1 Diurnal and overall analysis of RSP

The hourly differences of predicted and measured road surface temperatures are first calculated for the Thornes, Met. Office and Icebreak models with the actual observed inputs. The biases and SDs for each hour are shown in Figs 1–3. The results can be expressed as follows:

(a) The Met. Office model has a consistent cool bias that is more than −0.9 °C for every hour except 1300 UTC and is as low as −1.5 °C in the evening and morning. The Thornes predictions are less cool, its bias reduces in the late evening and early morning (2100–0700 UTC), but increases notably in the late morning. The Icebreak model has a relatively small bias that is the closest of the three to zero.

(b) For hourly SDs, all three models have smaller values at night. This can be explained by a simpler parametrization procedure at night as the main external forcing term — solar radiation (which is difficult to model due to the unknown shadowing effect of broken cloud) — is excluded, and the models can cope with the surface energy balance better. The

Thornes model has the largest SD, more than 1 °C during the day and night, whilst the Met. Office model and the Icebreak model have less than 1 °C SDs (as low as 0.7 °C for the Met. Office model and 0.6 °C for the Icebreak model) at night.

The overall bias, SD and r.m.s. error of model predictions were calculated by averaging the hourly errors and are shown in Table III. For the purpose of comparison, it should be noted that a bias expresses the mean status of prediction errors, such that a negative bias means that the model predictions are too cold. The SD indicates the range of variance of the errors and the r.m.s. error is referred to as a measure of the total errors. A good model is expected to have a small absolute bias and a small SD or small r.m.s. From Table III and Figs 1–3 it can be seen that, in the prediction of overall temperatures, the Icebreak model is of the highest accuracy. The Thornes model has a larger standard deviation and thus differs more from actual values. The Met. Office model tends to be much cooler than reality and has the largest r.m.s. value. For winter maintenance applications a small negative bias is preferable — erring on the side of caution, i.e. some de-icing chemicals wasted but fewer potential accidents (Thornes 1989). Obviously, small values of SD and r.m.s. error are also required.

3.2 Minima and time of freezing of RSP

One of the important aspects of model comparison is also to look at the minimum temperature prediction and the time of start and duration of freezing. The daily predicted minimum road surface temperature for each model has been compared with the observed minima to yield the mean of the difference of minimum temperature, r.m.s., SD and frequency distribution of the difference. When both predicted and measured temperatures fall to, or below, 0 °C ($T_s \leqslant 0$ °C), the time and duration are compared and their differences calculated. Table IV gives a comparison for the three models in the differences of the minima, start time and duration of freezing.

From Table IV it is interesting to note that in the prediction of minimum surface temperature, the Thornes model has a small bias with a large SD and the Met. Office model has a smaller SD with a much larger bias. The Icebreak model has both the smallest bias and SD. In comparing freezing time and duration, the prediction of the Thornes model is 37 minutes later than the actual freezing time and 19 minutes ahead of actual surface temperature rising above 0 °C. The Met. Office model tends to issue an icing warning almost an hour early, and the warning lasts 2 hours longer than the actual period of freezing. Compared with the Thornes and Met. Office models, the Icebreak model has the smallest errors in predicting freezing time (30 minutes early).

The frequency distributions of the difference between actual and predicted minimum temperatures for the

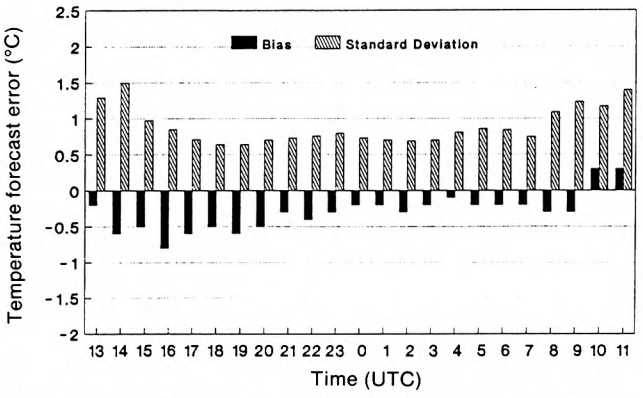

Figure 1. Hourly error analysis of retrospective prognosis for the Icebreak model (Chapman's Hill, winter 1988/89, 95 days).

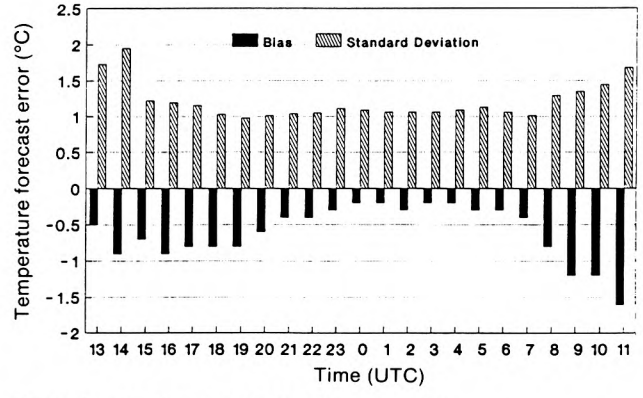

Figure 2. As Fig. 1 but for the Thornes model.

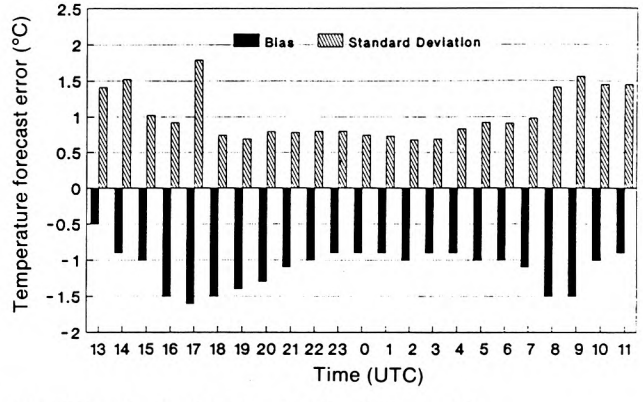

Figure 3. As Fig. 1 but for the Met. Office model.

Table III. Overall errors of retrospective predictions for model comparison (Chapman's Hill, winter 1988/89, 95 days) calculated from the average hourly errors

	Icebreak	Thornes	Met. Office
No. of hours*	2164	2164	2164
Bias	−0.29	−0.61	−1.14
SD	0.956	1.284	1.048
r.m.s.	1.000	1.418	1.543

* Note that 2164 hours of data were available for analysis out of 2280 (94.9%) owing to data loss from road sensor.

Table IV. Differences of predicted and measured road surface temperature minima (°C), freezing start time and duration (min.) for model comparison (Chapman's Hill, winter 1988/89, 95 days)

	Icebreak	Thornes	Met. Office
Minima:			
Number	95	95	95
Bias	−0.11	−0.17	−0.92
SD	0.757	1.022	0.786
Freezing:			
Number	19	16	19
Start time*	30	−37	57
Duration**	37	−19	123

* A positive number indicates that the road surface temperature was predicted to fall to 0 °C before it actually did.

** A positive number indicates that the duration of time at or below 0 °C was predicted to be too long.

models are shown in Figs 4–6. For an accuracy in absolute error in the prediction of minimum road surface temperature of ± 0.5 °C, 57.9% of the Icebreak model, 42.1% of the Thornes model and only 25.3% of the Met. Office model are found. Most of the absolute prediction errors of the Icebreak model (87.3%) and Thornes model (76.3%) are less than 1.0 °C;for the Met. Office model predictions 55.5% are of this accuracy.

An analysis of 'frost' (defined simply as road surface temperature falling to 0 °C or below) or 'no frost' forecasts against 'frost' or 'no frost' occurring (forecast/actual) has also been made and the results are given in Table V. As classified by Thornes (1989), the potential consequences of an erroneous forecast are:

Type 1 error (T1): Forecast 'no frost', actual 'frost' — potential for accidents,

Type 2 error (T2): Forecast 'frost', actual 'no frost' — potential for wasting de-icing chemicals.

Table V shows that for the 95 nights (with 21 frosts), T1 is the highest for the Thornes model, while T2 is the highest for the Met. Office model.

3.3 Maximum temperature of RSP

An accurate prediction of maximum road surface temperature (usually afternoon temperatures) is another important aspect of a successful model. It acts as to convince highway engineers of the model accuracy, for the engineers compare model prediction with sensor measurements in the afternoon, and may believe that an incorrect prediction of maxima will lead to a wrong prediction of minima in the night-time.

The analysis of model retrospective prognoses for the maximum temperature is given in Table VI. Both the Thornes model and the Met. Office model give much cooler bias than the Icebreak model, and the Thornes model has the largest SD. It is seen from the table that the Icebreak model has significantly improved the prediction of maximum temperature.

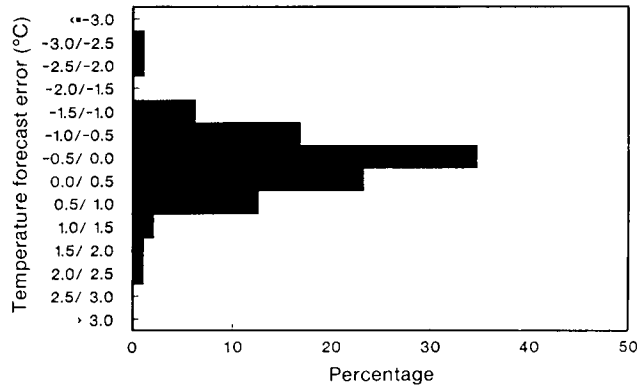

Figure 4. Distribution of the difference of forecast minus actual minimum temperature in retrospective use of the Icebreak model (Chapman's Hill, winter 1988/89, 95 days).

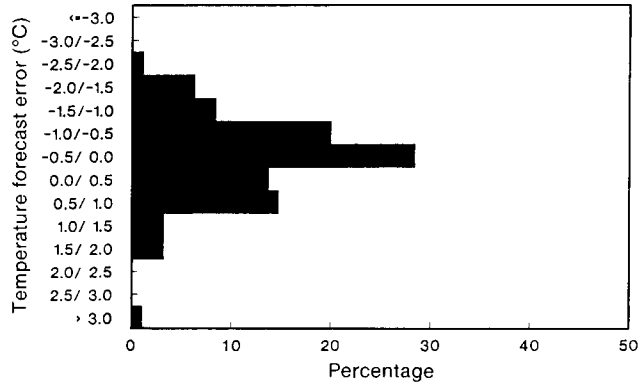

Figure 5. As Fig. 4 but for the Thornes model.

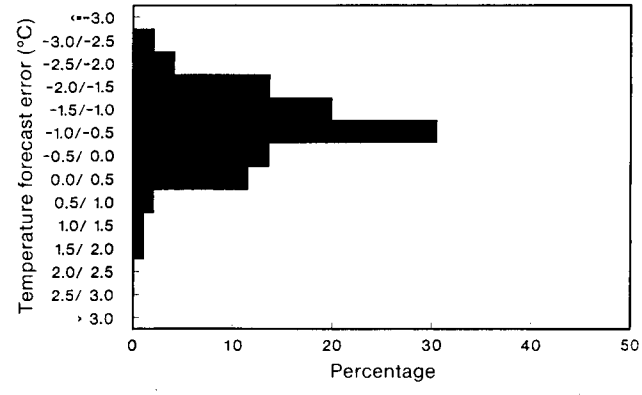

Figure 6. As Fig. 4 but for the Met. Office model.

4. Comparative results using 'realistic' Open Road input data

To see what the potential accuracy of model prediction is in view of the fact that perfect predicted data are never available, the three models were run using the 'realistic' input data used by the Birmingham Weather Centre for the nights concerned. This gives an estimate of the scale of model prediction errors in routine operation. Note that although only 65 days were

Table V. Model comparison of frost forecast accuracy with actual roadside input (Chapman's Hill, winter 1988/89, 95 days). (See text for explanation of T1 and T2)

Forecast/actual	Icebreak		Thornes		Met. Office	
	No.	%	No.	%	No.	%
No frost/no frost	73/74	98.6	74/74	100.0	69/74	93.2
Frost/no frost T2	1/74	1.4	0/74	0.0	5/74	6.8
Frost/frost	19/21	90.5	16/21	76.2	19/21	90.5
No frost/frost T1	2/21	9.5	5/21	23.8	2/21	9.5
Overall	92/95	96.8	90/95	94.7	88/95	92.6

Table VI. Model comparison for road surface temperature maxima prediction (Chapman's Hill, winter 1988/89, 95 days)

	Icebreak	Thornes	Met. Office
Number	95	95	95
Bias	−0.56	−1.22	−1.24
SD	1.597	1.972	1.571

selected for this analysis, the results for the retrospective model runs given in Table VII are very similar to those discussed in section 3.

4.1 Errors in predicted input

There is a need to investigate how accurate was the forecast input data used in the real-time prediction. The mean and maximum differences, SD and r.m.s. of the differences between real-time input (forecast) and retrospective input (actual) for screen air temperature and dew-point, wind speed, cloud amount, cloud type and rainfall for the 65 days are given in Table VIII. The differences are calculated from the values pertaining at 3-hourly intervals. It should be noted that there are height differences between actual (2.0 m) and forecast (1.2 m) air temperatures and dew-points, and actual (3.0 m) and forecast (10.0 m) wind speeds.

It is seen from the table that the most reliable variables predicted in real-time input seem to be air temperature and cloud type. All the others have a large difference. The difference in wind speed may be partly explained by the difference in the height where wind speed was derived, but this can only be surmised.

4.2 Comparison of model potential accuracy

The purpose of this exercise is to compare the size of errors due to model interior shortcomings (as discussed in section 3 for perfect predictions) with those due to forecast input errors. The comparison of retrospective prognoses and real-time predictions (of the same 65

Table VII. Model comparison of retrospective (RSP) and 'real-time' (RTP) runs (Chapman's Hill, winter 1988/89, 95 days)

	Icebreak		Thornes		Met. Office	
	RSP	RTP	RSP	RTP	RSP	RTP
No. of hours*	1480	1480	1480	1480	1480	1480
Overall:						
Bias (°C)	−0.33	−0.10	−0.61	−0.17	−1.15	−0.42
SD (°C)	0.75	1.14	0.97	1.12	0.81	1.02
r.m.s. (°C)	0.93	1.43	1.31	1.42	1.45	1.28
Maximum:						
Bias (°C)	−0.56	−0.16	−1.10	−0.73	−1.13	−0.78
SD (°C)	1.58	1.63	1.96	1.87	1.60	1.52
Minimum:						
Bias (°C)	−0.17	−0.38	−0.19	−0.11	−0.94	−0.26
SD (°C)	0.69	1.64	1.10	1.48	0.85	1.32
Time of freezing:						
Freezing (nights)	17	17	15	15	17	16
Start (minutes)	37	64	−28	52	46	−49
Duration (minutes)	52	56	−12	68	103	0

* 1480 hours out of 1560 possible (95% availability)

Table VIII. Comparison of meteorological variables between real-time input and actual roadside input (Chapman's Hill, winter 1988/89, 65 days)

	Realistic with actual		
	Mean error	SD	Maximum error
Air temperature (°C)	0.07	1.534	5.50
Dew-point (°C)	0.44	1.710	5.90
Wind speed (knots)	2.75	3.860	17.00
Cloud amount* (oktas)	−0.43	2.236	8.00
Cloud type* (1–3)**	−0.19	0.748	2.00
Rainfall* (0–2)**	−0.53	0.794	1.00

* Although these are discrete rather than continuous variables, the analysis has still been done for comparison.
** See text for explanation.

days) for the three models is shown in Table VII. Note that the days chosen for this analysis were the 65 occasions when no update was issued, and hence the original noon forecast was considered good, and weather conditions did not change significantly from the forecast.

In terms of overall RTP errors, all three models have a negative bias and the Met. Office model is the coldest. Their SDs and r.m.s. errors are not much different. For maximum temperature, the Icebreak model is marginally colder than actual maximum (−0.16 °C) with SD of 1.63 °C. The Thornes model and Met. Office model are cooler. In the real-time prediction of minimum temperature, the Icebreak model and Thornes model tend to issue a freezing warning nearly an hour earlier than actual freezing, while the Met. Office model has a lag of 49 minutes in predicting the start of freezing. The Met. Office model has an error of zero in the prediction of duration of freezing conditions.

The results of forecast/actual frost analysis for the realistic prediction is listed in Table IX. It can be seen from the table that the overall accuracy of the three model is similar.

Comparing the ten left columns with the ten right columns in Table VII for each model, the Icebreak (7/10) and Thornes (6/10) models show an improvement with retrospective actual inputs, while the Met. Office (3/10) model shows little improvement. This suggests that the forecasters at Birmingham Weather Centre were varying the inputs to produce better results, as discussed further below. For the Icebreak model, the overall mean bias and maximum temperature bias of RSP are a little cooler than those of RTP; significant improvements of RSP are seen in the reduction of r.m.s. and SD values of overall and minimum temperatures. It is clear that with actual input, the model has improved its overall and minimum predictions, and freezing time. But it shows no improvement in the prediction of maximum temperature and freezing time over real-time running.

Compared with real-time predictions, the Thornes model shows an improvement in the prediction of overall and minimum temperature and freezing time with actual roadside input, while the Met. Office model has cooler predictions using perfect prognosis.

Looking at the overall errors, it can be seen that the SD of the Icebreak model is reduced from 1.14 to 0.75 using the perfect prognosis, a reduction of 34%. For the Thornes model the percentage reduction is about 13%, and the Met. Office model about 21%. The Met. Office model shows little potential for improvement using accurate or actual input in terms of both bias and r.m.s. error however. It is notable that the input from the weather forecasters significantly improved the output of the Met. Office model.

5. Discussion and conclusion

Although it is indicated in the previous section that the Icebreak model and Thornes model achieve improvements with actual roadside input, perfect prognosis for the Met. Office model is not superior to realistic prediction — this requires further investigation.

The first question is whether the difference of temperature and wind speed height between actual (2.0 and 3.0 m) and forecast (1.2 and 10.0 m) input can be considered as a significant contributing factor to the abnormal results of the Met. Office model. The difference of temperature height is about 0.8 m. It is reasonable to believe that this difference of temperature height can be ignored because the near-ground layer over the road is such a well-mixed layer that no big difference of vertical temperature should exist within so small a vertical distance, except on exceptional nights.

The difference in wind speed height is relatively large. Because of the inaccuracy of interpolation for a wind speed profile, roadside wind speed was not extrapolated to 10 m height in retrospective prognoses. By the same consideration of a well-mixed layer, however, the difference of wind speed due to the difference in height is not expected to be significant to the results, as sensitivity analysis shows that wind speed has a small influence on model output (Shao 1990). Therefore it can be concluded that the results in the model comparison are reliable.

A probable explanation for the abnormal results of the Met. Office model is that the model has been used operationally for 2 years and the local forecasters at Birmingham Weather Centre have become familiar with optimizing model output by varying model input.

Farmer and Tonkinson (1989) have undertaken a verification of the Met. Office model by comparing the results of perfect prognoses against actual road surface sensor (fast lane Chapman's Hill) measurements in the winter of 1988/89. Their perfect prognoses were made using actual roadside observations and airfield observation from Birmingham Airport. Their results are compatible with those derived here. The results all show a cool bias of the Met. Office model predictions.

Table IX. Model comparison of frost forecast accuracy with realistic Open Road input (Chapman's Hill, winter 1988/89, 65 days). (See text for explanation of T1 and T2)

Forecast/actual	Icebreak		Thornes		Met. Office	
	No.	%	No.	%	No.	%
No frost/no frost	45/47	95.7	47/47	100.0	45/47	95.7
Frost/no frost T2	2/47	4.3	0/47	0.0	2/47	4.3
Frost/frost	17/18	94.4	15/18	83.3	16/18	88.9
No frost/frost T1	1/18	5.6	3/18	16.7	2/18	11.1
Overall	62/65	95.4	62/65	95.4	61/65	93.8

By comparing bias, SD and r.m.s. error in a retrospective analysis, we believe that we have shown that the Icebreak model provides improved accuracy in predictions of maximum and minimum road surface temperature prediction, such as in the prediction of maximum, and frost frequency. The predictions of the Thornes model have a larger variance, and the predictions of the Met. Office model are too cold.

The predictions of the Icebreak model can be further improved with more accurate input, such as for wind speed and cloud. The Thornes model is of smaller potential to improve its predictions, and the Met. Office model has no such potential unless the negative bias is removed and the forecasters do not subjectively alter the inputs.

The results presented here are restricted by the use of a single test site, and research is now continuing for a selection of sites across the United Kingdom.

Acknowledgements

The authors wish to thank the following for assistance with this work: P. Buchanan and S. Manstone of the Met. Office, and J. Kings, J. Hales and R. Johnson of the University of Birmingham Weather Service for their generosity in providing all the data required. This work was made possible by grants from Vaisala TMI, the British Council and the Strategic Highway Research Program.

References

COST-309, 1991: Final report (In press).

Farmer, S.F. and Tonkinson, P.J., 1989: Road surface temperature model verification using input data from airfields, roadside sites and the mesoscale model. (Unpublished, copy available in the National Meteorological Library, Bracknell.)

Isaka, H. *et al.*, 1990: Prediction of road surface temperature. *In* Proceedings of the 5th International Road Weather Conference, Tromsø, 13 March 1990. Standing International Road Weather Commission.

Kempe, C., 1990: An estimation of the value of special weather forecasts in a pilot project for road authorities in Sweden. *In* Proceedings of the Technical Conference on Economic and Social Benefits of Meteorological and Hydrological Services, Geneva, 26–30 March 1990. World Meteorological Organization.

Nysten, E., 1980: Determination and forecasting of road surface temperature in the COST-30 automatic road station (CARS). (Unpublished, copy available in the National Meteorological Library, Bracknell.)

Parmenter, B. and Thornes, J.E., 1986: The use of a computer model to predict the formation of ice on road surfaces. Research Report RR71. Crowthorne, Transport and Road Research Laboratory.

Rayer, P.J., 1987: The Meteorological Office forecast road surface temperature model. *Meteorol Mag*, **116**, 180–191.

Shao, J., 1990: A winter road surface temperature prediction model with comparison to others. (Ph.D. thesis, University of Birmingham.)

Stephenson, T.E., 1988: Wisconsin's winter weather system. *In* Proceedings of the 4th International Conference on Weather and Road Safety, Florence, 8–10 November 1988. Standing International Road Weather Commission.

Thompson, N., 1988: The Meteorological Office road surface temperature prediction model. *In* Proceedings of the 4th International Conference on Weather and Road Safety, Florence, 8–10 November 1988. Standing International Road Weather Commission.

Thornes, J.E., 1984: The prediction of ice formation on motorways. (Ph.D. thesis, University of Birmingham.)

—, 1989: A preliminary performance and benefit analysis of the UK national road ice prediction system. *Meteorol Mag*, **118**, 93–99.

Satellite and radar photographs — 11 January 1991 at 0300 and 0316 UTC

On 11 January 1991 a frontal band of cloud (F–F–F in Fig. 1) was slow-moving, lying across northern France and the south-east coast of England. The eastern Atlantic was awash with vortices. In particular, cold air comma clouds (labelled A, B, C, D in Fig. 1), revealing enhanced convection, were running north-east just north of the frontal band. These brought thunderstorms with hail to southern counties of England and Wales during the day.

Comma A had induced a shallow wave on the front, at 0300 UTC near Luxembourg (see Fig. 1 inset). Comma B had a well-developed head of cirrus outflow and the

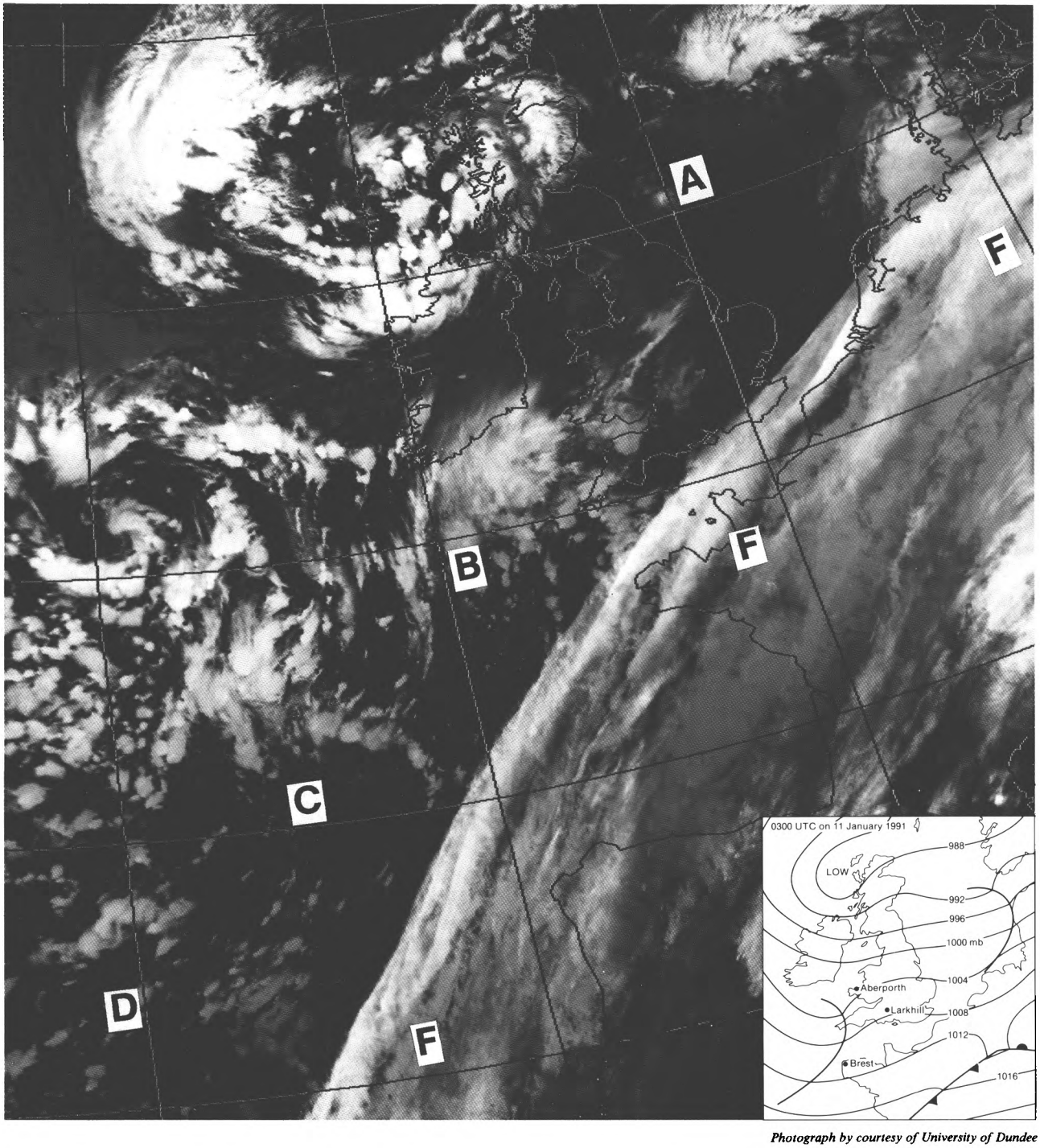

Photograph by courtesy of University of Dundee

Figure 1. NOAA-11 Channel 4 (infra-red) satellite picture at 0316 UTC on 11 January 1991. F–F–F is a slow-moving frontal band of cloud. A, B, C, D are four of the many vortices covering the Atlantic. The surface analysis for 0300 UTC is inset.

convection in the tail of the comma can be clearly seen beneath the frontal cloud to the west of Brest in Fig. 2.

The COST-73 satellite/radar composite for 0300 UTC (Fig. 3) shows the line of convective precipitation in the tail of the comma. Unfortunately the picture is complicated by previous storms to the north of Brittany. At 0600 UTC (Fig. 4) the radar picture is clearer, with the line of showers and thunderstorms extending well south over Brittany beneath the frontal cloud.

Radiosonde ascents show the air over England and Wales was unstable to around 400 mb — Larkhill (03743) is typical of this air (Fig. 5). Convective tops over Brittany were limited to 600 mb.

The orientation of certain cloud patterns is determined by the windflow relative to a moving system, rather than the actual winds reported, so it is useful to examine the relative flow to clarify the dynamical interpretation of the imagery. The relative wind is found by vectorially subtracting the system velocity (for comma B this was 245° 35 kn) from the actual winds. Plotted winds in Fig. 2 show the relative winds at 400 mb from radiosonde stations, plotted at appropriate positions relative to the

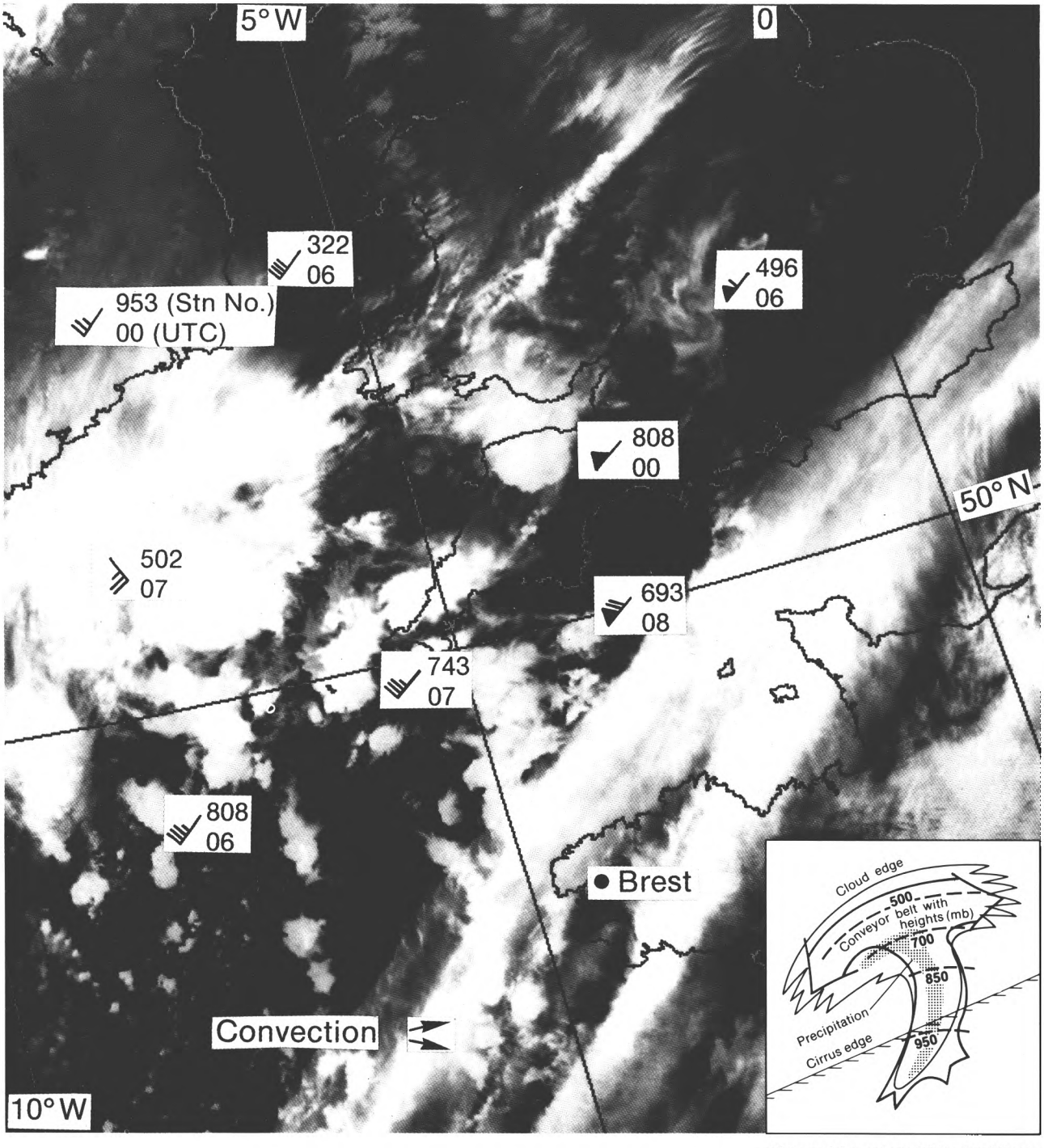

Photograph by courtesy of University of Dundee

Figure 2. As Fig. 1 but Channel 3. For explanation of wind plots and insert see text.

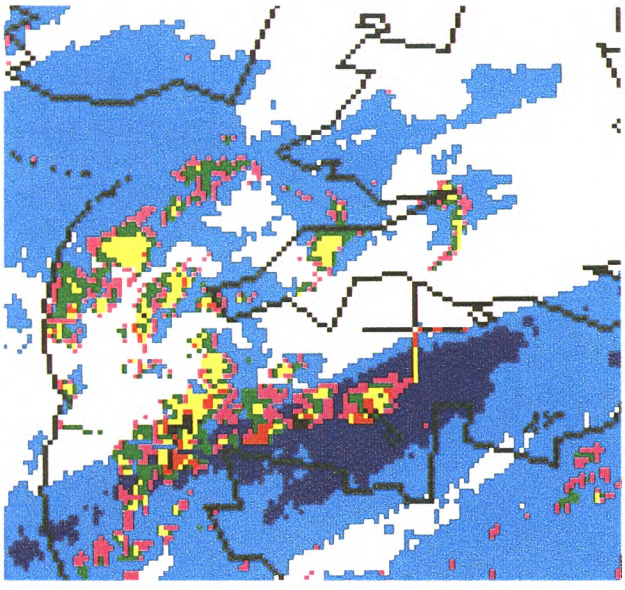

Figure 3. COST-73 satellite and radar image for 0300 UTC on 11 January 1991. Light blue represents cloud tops with temperatures between −15 and −45 °C and dark blue < −45 °C. Rainfall intensities (mm h^{-1}) are shown as follows: pink < 1, green 1–3, yellow 3–10, red 10–30. Coastlines, national boundaries and the limits of radar coverage are shown in black.

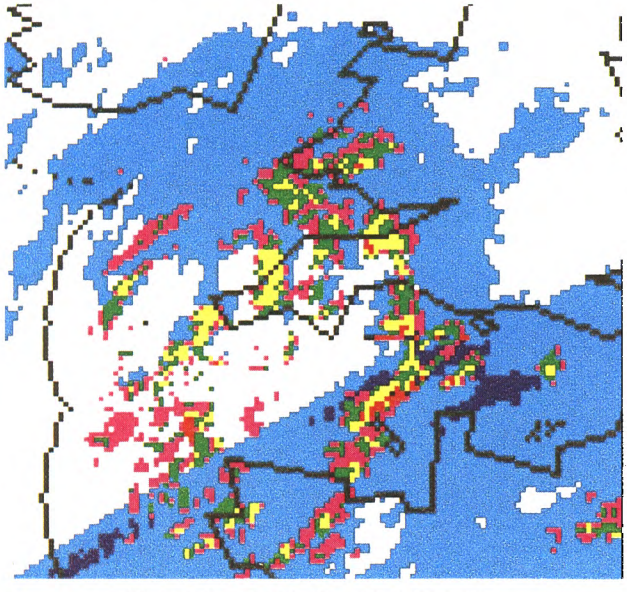

Figure 4. As Fig. 3 but for 0600 UTC.

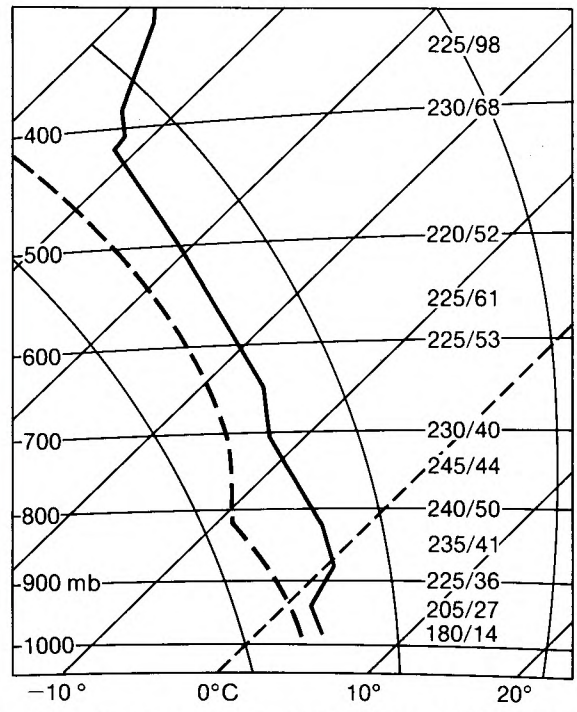

Figure 5. Tephigram for Larkhill (03743) at 0700 UTC on 11 January 1991.

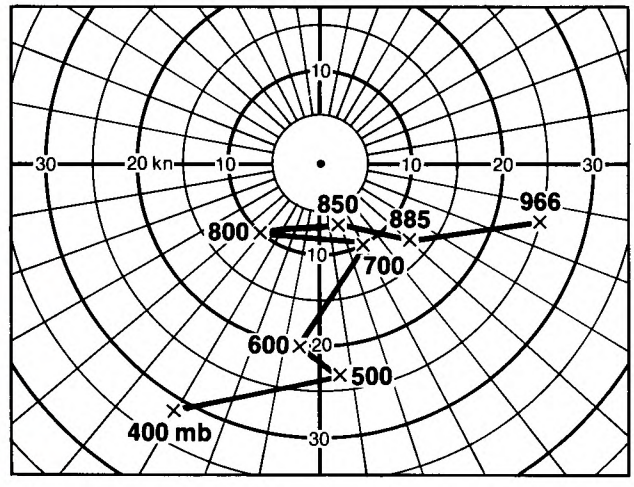

Figure 6. Hodograph for Larkhill (03743) at 0700 UTC on 11 January 1991. Winds shown are relative to the storm motion.

comma head at 0300 UTC. In general these show the cirrus outflow being carried to the north-east. However, Aberporth (which was near the centre of the comma head at 0700 UTC) has a relative wind of 135° 24 kn. This agrees well with the anticyclonically curved striations in the cirrus outflow. Although layered cloud is also present due to mass ascent within it, the comma head as seen by the satellite is mostly cirrus outflow from cumulonimbus clouds feeding into its southern flank. This is confirmed by the precipitation shown in the radar pictures.

Another notable feature was that individual storms in the Channel could be tracked for over 5 hours. To achieve this life-span, new cells were building into each storm, and this requires directional shear in the winds (see Bennetts *et al.**). Fig. 6 shows the Larkhill winds relative to a storm moving from 245° at 40 kn. With sea temperatures of 10 or 11 °C, convection would be from the surface. The low-level inflow is from the south-east quadrant, the cells lean to the north, and outflow is to the north-east. This can be inferred in some of the individual storms near the Larkhill plot in Fig. 2.

Using isentropic analysis and relative winds, a tentative conceptual model of the comma cloud is given in Fig. 2 (inset) showing the ascending conveyor belt.

J.R. Grant

* Bennetts, D.A., McCallum, E. and Grant, J.R.; Cumulonimbus clouds: an introductory review. *Meteorol Mag*, **115**, 1986, 242–256.

GUIDE TO AUTHORS

Content

Articles on all aspects of meteorology are welcomed, particularly those which describe results of research in applied meteorology or the development of practical forecasting techniques.

Preparation and submission of articles

Articles, which must be in English, should be typed, double-spaced with wide margins, on one side only of A4-size paper. Tables, references and figure captions should be typed separately. Spelling should conform to the preferred spelling in the *Concise Oxford Dictionary* (latest edition). Articles prepared on floppy disk (Compucorp or IBM-compatible) can be labour-saving, but only a print-out should be submitted in the first instance.

References should be made using the Harvard system (author/date) and full details should be given at the end of the text. If a document is unpublished, details must be given of the library where it may be seen. Documents which are not available to enquirers must not be referred to, except by 'personal communication'.

Tables should be numbered consecutively using roman numerals and provided with headings.

Mathematical notation should be written with extreme care. Particular care should be taken to differentiate between Greek letters and Roman letters for which they could be mistaken. Double subscripts and superscripts should be avoided, as they are difficult to typeset and read. Notation should be kept as simple as possible. Guidance is given in BS 1991: Part 1: 1976, and *Quantities, Units and Symbols* published by the Royal Society. SI units, or units approved by the World Meteorological Organization, should be used.

Articles for publication and all other communications for the Editor should be addressed to: The Chief Executive, Meteorological Office, London Road, Bracknell, Berkshire RG12 2SZ and marked 'For Meteorological Magazine'.

Illustrations

Diagrams must be drawn clearly, preferably in ink, and should not contain any unnecessary or irrelevant details. Explanatory text should not appear on the diagram itself but in the caption. Captions should be typed on a separate sheet of paper and should, as far as possible, explain the meanings of the diagrams without the reader having to refer to the text. The sequential numbering should correspond with the sequential referrals in the text.

Sharp monochrome photographs on glossy paper are preferred; colour prints are acceptable but the use of colour is at the Editor's discretion.

Copyright

Authors should identify the holder of the copyright for their work when they first submit contributions.

Free copies

Three free copies of the magazine (one for a book review) are provided for authors of articles published in it. Separate offprints for each article are not provided.

Contributions: It is requested that all communications to the Editor and books for review be addressed to the Chief Executive, Meteorological Office, London Road, Bracknell, Berkshire RG12 2SZ, and marked 'For *Meteorological Magazine*'. Contributors are asked to comply with the guidelines given in the *Guide to authors* which appears on the inside back cover. The responsibility for facts and opinions expressed in the signed articles and letters published in *Meteorological Magazine* rests with their respective authors.

Subscriptions: Annual subscription £33.00 including postage; individual copies £3.00 including postage. Applications for postal subscriptions should be made to HMSO, PO Box 276, London SW8 5DT; subscription enquiries 071–873 8499.

Back numbers: Full-size reprints of Vols 1–75 (1866–1940) are available from Johnson Reprint Co. Ltd, 24–28 Oval Road, London NW1 7DX. Complete volumes of *Meteorological Magazine* commencing with volume 54 are available on microfilm from University Microfilms International, 18 Bedford Row, London WC1R 4EJ. Information on microfiche issues is available from Kraus Microfiche, Rte 100, Milwood, NY 10546, USA.

March 1991

Editor: F.E. Underdown
Editorial Board: R.J. Allam, R. Kershaw, W.H. Moores, P.R.S. Salter

Vol. 120
No. 1424

Contents

ISSN 0026–1149

Printed in the United Kingdom for HMSO
Dd 0291241 C13 03/91 0503 12521

The Meteorological Magazine

April 1991

Variability of global surface temperature
Noctilucent clouds during 1989

HMSO

Met.O.998 Vol. 120 No. 1425

First published 1991

HMSO publications are available from:

HMSO Publications Centre
(Mail and telephone only)
PO Box 276, London, SW8 5DT
Telephone orders 071-873 9090
General enquiries 071-873 0011
(queuing system in operation for both

HMSO Bookshops
49 High Holborn, London, WC1V 6
258 Broad Street, Birmingham, B1 2
Southey House, 33 Wine Street, Bris
9–21 Princess Street, Manchester, M
80 Chichester Street, Belfast, BT1 4J
71 Lothian Road, Edinburgh, EH3 9

HMSO's Accredited Agents
(see Yellow Pages)

and through good booksellers

The Meteorological Magazine

April 1991
Vol. 120 No. 1425

551.524.32(4/9)

The normal distribution and the interannual variability of the global surface temperature record

A.H. Gordon
Flinders Institute for Atmospheric and Marine Sciences, Flinders University of South Australia, Bedford Park, South Australia

Summary

If the hypothesis is put that the frequency distributions of the year-to-year changes in the hemispheric surface-temperature anomalies, constituting the available climatic record, fit the normal density function curve, then the distributions may be assumed to have been randomly drawn from a normally distributed population. If there are significant differences between the observed and expected distributions, such differences could suggest fingerprints of some outside forcing. Chi-square tests between the frequencies of the actual values and the expected frequencies computed from the normal density function for the Meteorological Office series and for the Climatic Research Unit series of hemispheric surface-temperature anomalies indicate that there is no significant difference between them in the northern hemisphere. In the southern hemisphere the Meteorological Office series shows no significant difference whereas the Climatic Research Unit series indicates a significant difference at the 1% level. The latter significance arises partly from the two values at each of the two tails of the distribution, the arithmetical sums of which almost cancel one another. When these values are removed there remains a difference at the 5% level caused by insufficient negative values in the −0.05 °C to −0.25 °C class intervals.

1. Introduction

Karoly (1990) has stated that there are two parts to the detection of climate change: (a) the identification of a pattern of climate change or fingerprint which is specific to an enhanced greenhouse-effect and could not be due to any other climatic process, and (b) the observation of a significant trend or change in amplitude of such a fingerprint. The *Scientific assessment of climate change* (IPCC 1990) states that the global temperature has increased by 0.3 °C to 0.6 °C during the last century, and that this warming is consistent with climate model predictions, but also of the same magnitude as natural climate variability.

One suggested avenue of search and closer identification of the predicted global warming is to investigate to what extent and in what respects frequency distributions of the interannual variability of the hemispheric temperature series for the period covered by past climatic records differ from those to be expected from the normal distribution. It is recognized that the frequency distributions of many kinds of observational and experimental data closely approximate the normal curve. Among these are time series of surface temperature anomalies from some reference mean value. An example might be a series of mean temperatures for a

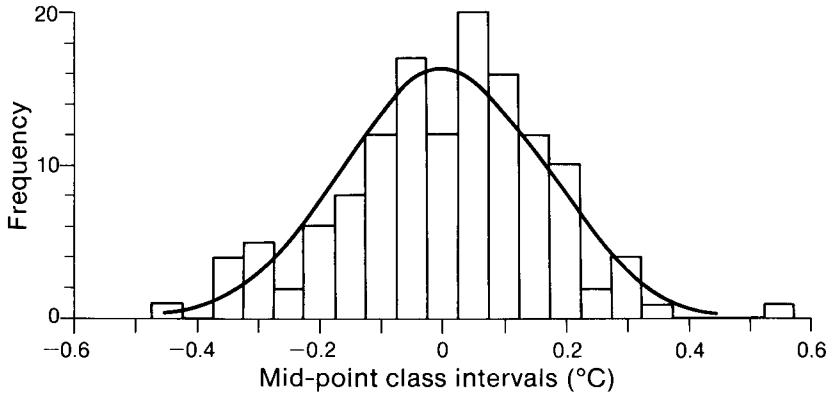

Figure 1. Histogram of the frequency distribution of the year-to-year changes of mean surface temperatures for the northern hemisphere for the Meteorological Office data set, superimposed by the normal curves corresponding to the expected values for the hypothetical normal distribution of the series. The expected frequencies are computed to two decimal places for a normal distribution of mean zero and a standard deviation 0.164 °C.

given day of the year for a given station covering a period of 100 years, compared with the mean value for that day for the whole period. There is no obvious artificial constraint at either end of the extremes of the distribution of anomalies. It might be reasonable to suppose therefore that, barring some imposed forcing or trend, such anomalies would be likely to be normally distributed within acceptable levels of significance. In such a case the cumulative sum of the anomalies would tend to approach zero.

Two sets of combined land- and marine-surface temperature anomalies for the two hemispheres have been tabulated in the form of anomalies from a 30-year reference mean. The first set, assembled by the Meteorological Office, henceforth called the MO set, covers the period 1856–1989. The second set, assembled by the Climate Research Unit of the University of East Anglia, henceforth called the CRU set, covers the period 1861–1989 (Jones 1988). If each value of a given series is subtracted from the value for the preceding year the individual series may be converted into ones expressing the changes in temperature from one year to the next, that is, the interannual variability. We will assume that the various series of interannual changes possess a normal distribution of mean zero and standard deviation computed from the real data. In effect, the true means for the two data sets and the two hemispheres are displaced from zero by from 0.003 °C to 0.006 °C, giving rise to positive trends which account for the observed global warming. These displaced mean values are approximately one half of the smallest magnitude to which the accuracy of the series is calculated (0.01 °C). We want to find out in more detail the reasons why the long-term means of the changes in temperature from one month to the next are displaced from zero. The difference between the two means and zero are not statistically significant.

2. Discussion

Figs 1 and 2 show histograms of the actual frequency distributions of the interannual variability of the surface

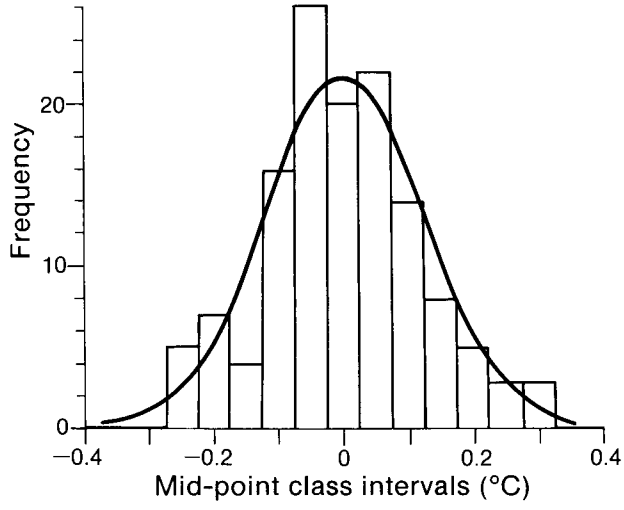

Figure 2. As Fig. 1 but for the southern hemisphere. The standard deviation is 0.121 °C.

temperature anomalies for the two hemispheres for the MO data set. The value 0.05 °C has been chosen as a reasonable class-interval, allowing mid-points at multiple integrals of 0.05 °C. The histograms have been superimposed by the normal curves corresponding to the expected values for the hypothetical normal distributions of the series, computed from the normal density function tables. The sum of the expected values is very close to the total frequency of 133 cases. In the northern hemisphere there are a few class intervals at the extremes of the distribution for which these expected frequencies are less than unity. These have been excluded in calculating chi-square test sums. The tests conducted over the remaining range of values are shown in Table I. The differences are not significant at the 10% level for either the MO or CRU data sets. Tests for symmetry show that both sets of data are symmetrical, that is, chi-square sums testing for asymmetry do not reach the 10% level of significance.

The class intervals were divided into four categories:

(a) positive values contributing to warming,
(b) lack of positive values contributing to cooling,
(c) negative values contributing to cooling, and
(d) lack of negative values contributing to warming,

where the description contributing to warming or cooling means whether the actual frequencies are greater or less than the expected frequencies on the two halves of the x-axis of the normal distribution. Chi-square tests do not show significance at the 10% level for any of the four categories. Table II shows the actual amount of warming or cooling contributed by each of the four categories for the two data sets. The values are obtained by multiplying the differences between the actual and expected frequencies in each class interval by the value at the centre-point of that class interval. The warming is divided fairly evenly between the positive and negative class intervals in the MO series, but is contributed entirely by the negative values in the CRU series. The total warming is almost the same for both data sets.

The chi-square test for the whole MO series is not significantly different from a normal distribution at the 10% level. Neither is the distribution of values within any of the four categories significant at that level. However, the CRU series gives significance at the 1% level for the whole series. This is mainly due to the contributions made by the outer two extreme class-intervals on both the positive and negative sides of the y-axis, i.e. |0.20|°C and |0.25|°C. The arithmetical sum of these class intervals almost cancels out. Nevertheless, categories (a) and (c) both reach the 1% level, suggesting that these two categories are not normally distributed. Category (d) is significant to the 5% level. The contributions made by category (d) are caused by a lack of negative values in the band widths covering the class intervals from −0.05 °C to −0.25 °C with maximum warming centred at about −0.17 °C or about 1.23 standard deviations. A chi-square test for asymmetry shows that both data sets are symmetric. The sums do not reach the 10% level. Table II shows the individual contributions made by each set within each category.

3. Results

It will be useful to classify results of the analyses according to whether they are common to both data sets or differ between the two sets, bearing in mind the fact that some sampling errors may arise in using the mid-points of the class intervals to compute the contributions to warming and cooling.

Table I. Values of chi-square test sums applied to the differences between observed and theoretical normal distribution values for the different class-intervals. In the northern hemisphere values have been excluded where the expected frequency is less than unity; in the southern hemisphere there are no class intervals where this occurs. Figures in brackets are significance levels (n.s. denotes not significant). $K-3$ degrees of freedom where K is the number of class intervals (Bendat and Piersol 1986).

	Data set	
	Climate Research Unit	Meteorological Office
Northern hemisphere	13.65 (n.s.)	13.38 (n.s.)
Southern hemisphere	31.69 (1%)	13.68 (n.s.)

Table II. Contributions to warming and cooling (°C) made by the total number of above- and below-expected frequencies for the four categories (a)–(d) described in the text.

Data set	Category				Total
	(a)	(b)	(c)	(d)	
Northern hemisphere					
Meteorological Office	1.88	−1.58	−1.77	2.17	0.70
Climate Research Unit	1.18	−1.24	−1.23	1.88	0.59
Southern hemisphere					
Meteorological Office	0.78	−0.73	−1.24	1.39	0.20
Climate Research Unit	1.45	−0.83	−1.46	2.05	1.21

Results common to both sets include:

1. A warming in each hemisphere.
2. In the northern hemisphere the values at the extremes of the distribution where the expected frequencies are less than unity contribute to slight cooling.
3. The northern hemisphere temperature changes are normally distributed to an acceptable level of significance according to chi-square tests.
4. Both hemispheres are symmetrical to an acceptable level of significance.
5. The greatest contribution to warming is made by a lack of negative values centred at about −0.17 °C.
6. The total warming for the northern hemisphere is in good agreement.
7. If one includes all the observations in both hemispheres the negative values contribute a greater share of the warming than the positive values.
8. If we call the contributions (a) and (c) real values and the contributions (b) and (d) ghost values we find that the real values contribute to cooling while the ghost values contribute to warming when the average of these values is found for the two hemispheres.

Results which show differences between the two data sets are:

1. In the southern hemisphere the chi-square test for the CRU set shows high levels of significance that the distribution of year-to-year changes is not normally distributed.
2. The average trend for the CRU set for the two hemispheres is nearly 1.5 times greater than for the MO set.
3. The warming shown in Table II for the southern hemisphere is six times greater for the CRU than for the MO set.
4. In the northern hemisphere the individual contributions to each of the four categories are numerically greater for the MO set.
5. In the southern hemisphere the individual contributions to each of the four categories are greater for the CRU set.
6. The mean warming for the two hemispheres as given in Table II for the CRU set is just double that given by the MO set.

4. Conclusions

The search for some fingerprint to detect an enhanced greenhouse-effect global warming requires a kind of Sherlock Holmes approach. The chief finding in the analysis presented is that although there is no statistical evidence of a forced warming, on the basis of comparisons with assumed normal distributions of the year-to-year changes, at least in the MO data set, if such a warming does exist it could be accounted for by a lack of negative values of the interannual variability, particularly centred about the −0.17 °C class interval bandwidth. This could result from an imposed interannual forcing, the amplitude of which is in phase with the cooling bandwidth of about −0.17 °C. Alternatively, the atmosphere is unable to lose heat efficiently by longwave radiation within this bandwidth. Both mechanisms could be due to the enhanced greenhouse-effect.

The second main conclusion arises from a comparison of the two data sets. It seems that the MO series is more stable and subject to less erratic behaviour than the CRU series in so far as the southern hemisphere series is concerned. Comparison of the southern hemisphere results would indicate that those given by the MO set are more reasonable than those obtained from the CRU set. In particular the CRU series might give a false impression that the southern hemisphere was warming faster than the northern hemisphere, or even that the warming was in some way being forced by the southern hemisphere. The MO series gives rise to a much more cautious approach to global warming.

Acknowledgements

I would like to express my thanks for the helpful advice of Jonathan Tawn of the Department of Statistics and Probability of the University of Sheffield and also to the Editor of the *Meteorological Magazine* for comments and suggestions.

References

Bendat, J.S. and Piersol, A.G., 1986: Random data. New York, Wiley.

IPCC, 1990: Scientific assessment of climate change. Geneva, WMO/UNEP, Intergovernmental Panel on Climate Change.

Jones, P.D., 1988: The influence of ENSO on global temperatures. *Clim Mon*, **17**, 80–89.

Karoly, D., 1990: Greenhouse climate change fingerprint detection. Canberra, IGBP Workshop No. 13, Mathematical and statistical modelling of climate change processes.

551.593.653(4):551.605.1

Noctilucent clouds over western Europe during 1989

D.M. Gavine
29 Coillesdene Crescent, Edinburgh EH15 2JJ

Summary

Noctilucent cloud reports by voluntary and professional observers in the British Isles, Denmark, The Netherlands and Belgium suggest that a high incidence of the phenomenon is maintained.

Table I summarizes the noctilucent cloud (NLC) reported to the Aurora Section of the British Astronomical Association (BAA) during 1989. The times (UT) are of the reported sightings, not necessarily the duration of a display. 'Negative' nights (Table II) are based on the judgement of two or more experienced observers north of 54° N with clear or nearly clear sky conditions over the period of the night when NLC is likely to occur. There were 39 positive and 7 suspected NLC sightings. For brevity, the Finnish–Estonian NLC observations are not now mentioned here. Full details of these are published annually in the periodical *Ursa Minor* of the URSA Astronomical Association (Laivanvarustajankatu 3, SF-00140 Helsinki 14). Contributions were received from 41 individual observers and 8 meteorological stations in the United Kingdom, 11 stations of the Royal Netherlands Meteorological Institute, four observers in Denmark, one in Belgium and one in Eire. Superb photographs by Mr Olesen and Mr Andersen of Denmark have again enhanced BAA exhibitions and conferences.

As before, the intention of the Aurora Section is to provide a data bank for professional workers. Details of individual nights are available from the author, but all NLC data up to 1987 are held in the Balfour Stewart Archive at the University of Aberdeen.

Our thanks to all observers, amateur and professional, and to Mr Ron Livesey, Director of the BAA Aurora Section, Mr Tom McEwan, Director of the Junior Astronomical Society Aurora Section, Mr V. Mäkelä (Finland), Dr B. Zwart (The Netherlands), Mr J.Ø. Olesen (Denmark), Dr M. Gadsden (University of Aberdeen) and Mr M. Zalcik (USA–Canada NLC Network).

Table I. Displays of noctilucent clouds over western Europe during 1989

Date — night of	Times UT	Notes
5/6 May	2240	Faint NLC suspected at Fortrose.
7/8	2108–2125	Very faint bands, possible billows, visible up to 42° in binoculars at Morpeth.
9/10	2235–2320	Very faint bands below 10° at Fortrose.
14/15	2050	Orange tinted bands suspected at Gilze Rijen, The Netherlands.
20/21	2110–2300	Suspect faint bands very low, Fortrose.
21/22	2130–2215	Veil, faint bands and patches at Morpeth.
26/27	2150–2215	Bands up to 30°, Fortrose. Faint NLC at Appingedam, The Netherlands. Suspected aurora at Clwyd, 2330.
30/31	2230	Ronaldsway reports possible small NLC 'wisp'.
4/5 June	2303	Very faint veil and a few bands E and W at Milngavie by Glasgow.
5/6	2233–2247	Faint bands suspected at Genk, Belgium.
9/10	2215–2300	Possible faint bands in haze, Morpeth.
10/11 June	2215–0200	Moderate to faint bands and patches observed from Moray Firth to N. Wales. Billows developed from 0030.
13/14	0008–0100	Thin bands at 11°, St Andrews.
14/15	2230–0115	Faint bands and billows observed from Moray Firth to N. Wales.
15/16	0030–0215	Bands and patches seen at Witham, Essex; photographed in I. of Man.
16/17	2345	Fairly bright bands and billows photographed by Dr Soper in I. of Man. No NLC in Scotland.
17/18	0015–0035	Positive NLC sightings at Dundee and I. of Man, no details.
18/19	2230–0113	Faint bands observed in NW Highlands, Moray Firth and Teesside; detected by Mr Bone at Cambridge 2230–2300.
20/21	2330–0215	Moderate to faint bands and veil, max. altitude 20° at Kilbirnie by Ayr; faint bands at Dundee.

Date — night of	Times UT	Notes
21/22 June	2255–0200	Faint bands and patches at Dundee and Co. Clare. At Kilbirnie Mr McEwan observed NLC becoming bright and extensive with radiating band structure up to 45° from 0045.
22/23	2240–0215	Faint bands and billows observed from Edinburgh to Newport Pagnell, and at Vildbjerg, Denmark.
23/24	2230–2345	Faint veil, bands and billows in trop. cloud gaps in Co. Clare; moderately bright bands up to 20° at Rønne, Bornholm.
25/26	2200	Bands in haze at Rønne.
26/27	2300–2355	Faint bands to 10° at Kilbirnie, faint NLC in Co. Clare.
27/28	2253–0255	Bright display, all forms, observed from W. of Scotland to RAF Benson near Oxford and Witham, Essex. Complex structures developed from 0015.
29/30	2300–2310	Suspect faint band at Alness.
30/1 July	2300–0200	Bright bands, billows and whirls up to 20° at Copenhagen; faint bands at Cambridge 0200.
1/2	2300–0215	Bright blue bands and whirls, some patches of billows, observed throughout Scotland and at Teesside.
2/3	2230–0215	Rather faint veil, bands and billows seen from Moray Firth to Northampton, faint forms in zenith at Alness. Bright and extensive display at Vildbjerg 2230–0155, all forms, into S. sky at alt. 148° at 0155, photographed by Mr Andersen. Reported by 6 stations in The Netherlands.
3/4	2200–0215	Moderately bright bands and extensive veil, patches of billows, observed in central Scotland, I. of Man and as far S. as Northampton. Bright bands and billows photographed at Vildbjerg. Reported by 5 stations in The Netherlands.
4/5	2300–0030	Faint bands and patches from central Scotland to I. of Man.
6/7 July	2230–0105	Bright bands seen from Moray to Edinburgh.
7/8	2130–0015	Bright NLC visible in haze and trop. cloud at Kilbirnie, bands at Rønne and Kølvrå, Denmark.
9/10	2248–0048	Faint bands at Orkney.
10/11	2220–2245	'Bands and whirls' photographed at South Shields, probably cirrus.
12/13	0045–0215	Faint bands and billows at Morpeth.
13/14	2020–0150	Moderately bright bands and billows up to zenith at Sumburgh and Kirkwall. Bright NLC at Rhoon, Deventer and Valkenburg.
14/15	2220–0300	Fairly bright, all forms, observed from Moray to Essex, up to 80° at Morpeth at 0230. Billows and whirls developed later.
15/16	2130–0247	Bright, all forms, observed from Shetland to I. of Man, also Esbjerg and Bornholm.
16/17	0045–0247	Moderately bright bands and billows seen from Moray to Ayrshire, and Genk, Belgium.
17/18	0052–0215	Horizontal bands at Kilbirnie, no NLC before 0045.
19/20	0105–0300	NLC in haze at Kinloss; bright billows observed throughout The Netherlands.
20/21	2305–2345	Moderately bright bands at 10°, billows and whirls developing later, at Alrø, Denmark.
25/26	2040–0230	Faint bands observed at Aberdeen, Ayrshire, I. of Man, Vildbjerg and Funen.
31/1 Aug.	0108–0330	Faint bands appearing late, bright billows and whirls developing after 0200. Observed from S. Scotland to Swansea.
2/3	0050–0300	Bright NLC in patches at Wick, Orkney and Kinloss.

Table II. Negative nights (British Isles) north of latitude 54° N

May 25/26, 27/28, 29/30, 31/June 1; June 6/7, 19/20, 28/29; July 5/6, 18/19, 30/31; Aug. 6/7.

Correspondence

551.578.45(430.1):551.578.46:551.515

Contribution to the discussion on 'A heavy mesoscale snowfall event in northern Germany'

Among the interesting points in this discussion (*Meteorol Mag*, **119**, 271) are the techniques of snowfall measurement, radar observation of snowfall and the amounts of precipitation over land and sea.

1. Snowfall measurements

Difficulties associated with radar measurements of snow are well known. Perhaps the shortcomings of conventional measurements of snowfall, i.e. collecting the snow in vessels or measuring the depth of snow cover, are not so familiar. With high winds, as in this event, the snow is drifting and piles up at certain areas while other areas may be nearly free from snow. Open areas on the coast may get a very thin snow cover, not at all representative of the precipitation. Since snow cover measurements are point ones their representativeness must be questioned. Measurements with ordinary vessels suffer of course from drifting snow, but there are no means of knowing how much of the drifting snow is caught by the vessel, besides which a gauge suffers from wind losses. As an example I refer to Fig. 9 in the paper by Andersson and Nilsson (1990). During 9–13 January 1987 the station at the southern tip of Gotland recorded an accumulated precipitation of 183 mm (water equivalent). At the routine check by the Division of Climatology this amount was questioned. According to the observer snow had piled up at the observation point — the accumulation was then corrected to 57 mm! As a consequence, charts of snow depth after snowfall combined with high wind speeds may not be representative of the precipitation distribution. At least the radar does not suffer from these wind effects! Another consequence is that 'water-equivalent to snow depth ratios' do not say much about the density of snow cover in these weather events.

2. Radar observations

The radar observations from Hamburg and the 'continued snow shower generation' over the Lübeck Bight are seemingly contradictory to the satellite pictures (Figs 2 and 5 in Pike (1990)), and show that the cloud band extends much further north-east, well beyond Bornholm Island. Probably the detection range of the Hamburg radar in this case was something between 100 and 150 km (the distance from Hamburg to the south-west Lübeck Bight is about 70 km). The precipitation was probably shallow, and overshoots the radar beam beyond these ranges. An observer looking at the radar screen then gets the impression that cells form where they are actually advected into the area. An image from the Norrköping weather radar from the same event (see Fig. 1) shows another precipitation band that, according to satellite images, extended into the Gulf of Finland, but is visible only out to a range of about 120 km. This radar, the Ericsson prototype weather radar, probably had somewhat better sensitivity than the Hamburg radar (I assume the Hamburg radar was the EEC C-band with 8 ft antenna (described by Attmanspacher (1984)). This range effect is also illustrated in Fig. 2 showing the precipitation distribution according to the weather radar for a similar weather situation. Also in this case the precipitation band extended into the Gulf of Finland.

3. Snowfall over land and sea

Some mesoscale simulations with the HIRLAM forecasting system (horizontal grid spacing 22 km with 16 vertical levels) recently performed by Nils Gustafsson (who kindly put them at our disposal), show amazing similarities with the satellite pictures (Fig. 2 in Pike's paper). As an example Fig. 3 shows the computed precipitation accumulation from 0600 to 1800 UTC on 12 January 1987, from initial data at 0000 UTC (note that this was the day after Pike's picture but the weather situation was persistent, for instance Lübeck had 7 mm precipitation in the form of snow from 0600 UTC on 12 January to 0600 UTC on 13 January). Even the V-shape of the clouds just north of the German coast is reproduced on the computed precipitation distribution! The maximum precipitation is found north of Rügen, that is over the sea as in Figs 1 and 2.

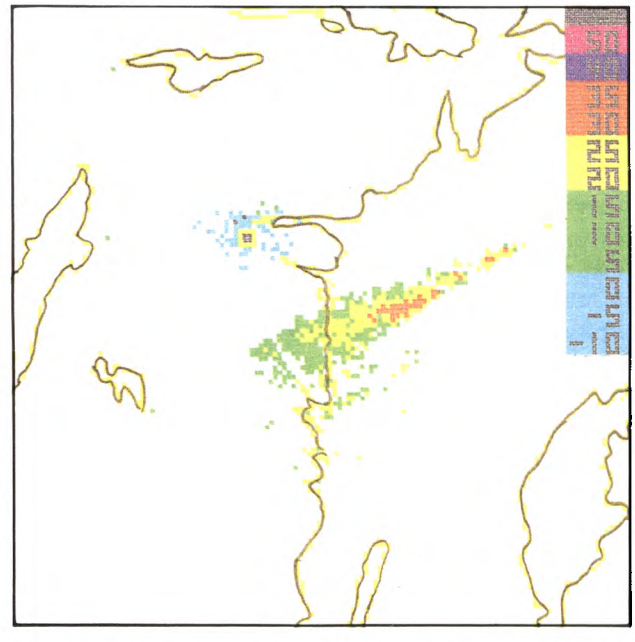

Figure 1. Map of reflectivity at 500 m height from the Norrköping radar, range 240 km, at 1000 UTC on 12 January 1987. The scale on the right gives reflectivity in dBz. The band of precipitation actually extended towards the east-north-east into the Gulf of Finland. Owing to range effects the radar can only detect precipitation out to about 120 km. The radar is at the centre of the picture surrounded by weak (blue) ground echoes.

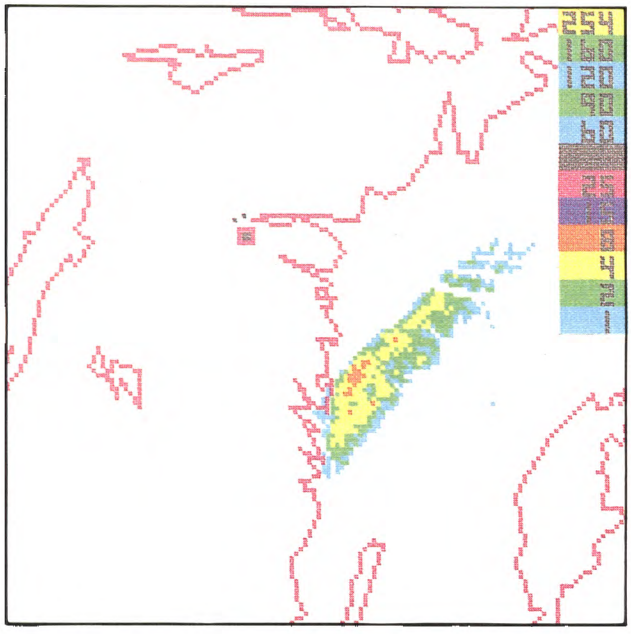

Figure 2. Radar map of accumulated precipitation from 0615–1200 UTC on 28 January 1987 from the Norrköping radar, range 240 km. The scale on the right gives precipitation in millimetres. The precipitation rate–reflectivity relation used is $Z = 200 \times R^{1.6}$, where Z is the reflectivity ($mm^6\ m^{-3}$) and R the precipitation rate ($mm\ h^{-1}$). Note that most of the precipitation lies at about the same distance from the radar. Though the amounts given at these ranges from a shallow precipitation system are uncertain, the maximum no doubt occurs over the sea.

References

Andersson, T. and Nilsson, S., 1990: Topographically induced convective snowbands over the Baltic Sea and their precipitation distribution. *Weather and Forecasting*, **5**, 299–312.

Attmannspacher, W., 1984: Radar network in Germany. *In* Seminar on radar meteorology, Erice, 4–14 October 1982. Geneva, WMO, No. 626.

Lumb, F.E. and Pike, W.S., 1990: Correspondence. *Meteorol Mag*, **119**, 271.

Pike, W.S., 1990: A heavy mesoscale snowfall event in northern Germany. *Meteorol Mag*, **119**, 187–195.

T. Andersson

Swedish Meteorological and Hydrological Institute
S-60176 Norrköping
Sweden

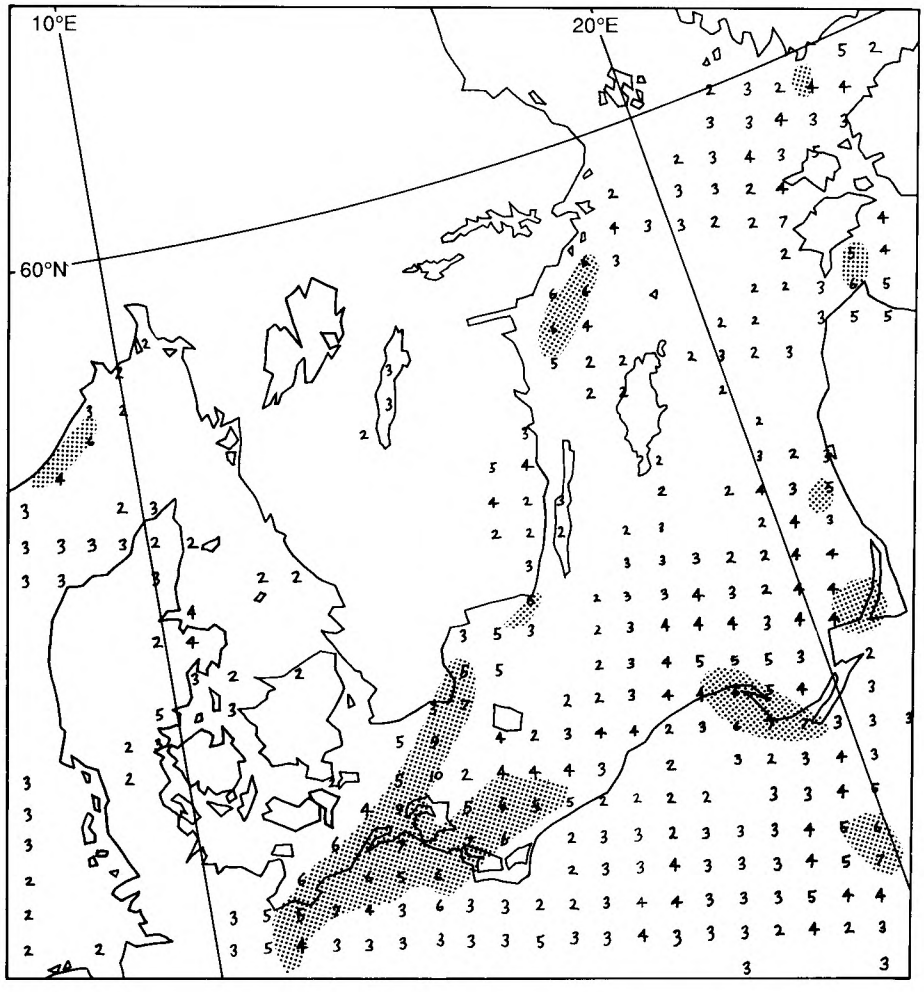

Figure 3. Accumulated precipitation (mm) from 0600 to 1800 UTC on 12 January 1987, according to the HIRLAM. Areas > 5 mm are stippled. The maximum precipitation, 10 mm, occurs just north of Rügen Island.

Reply by W.S. Pike

I will try to confront the majority of points raised and answer them as best as I am able.

1. Snowfall measurements

All available observations indicate that the heavy snowfall near Hamburg occurred with relatively light surface winds of only 5–15 kn. Hence, it appears that the fresh snow reports of 40–60 cm over the 24-hour period ending 0600 UTC on 12 January 1987 were very good estimates of the representative level depth. Presumably Andersson accepts them because he does not refer at all to this remarkable 'inland' maximum!

Throughout history confusion has arisen through the use of unstandardized methods and unsynchronized times of measurement. In the United Kingdom, to obtain average and representative figures for both snow depth and water equivalent, a mean of at least three snow samples is required (Meteorological Office (1982), chapter 9).

In 1942/43 Bergeron wisely instructed his observers in south-east Sweden 'to measure the snow depth, if possible, in forest glades, or in similar places, where it had not drifted' (Bergeron 1949). Had this been achieved at Hoburg (the south-west tip of Gotland, see Fig. 1) a more representative water equivalent for the long and non-standard period (9–13 January 1987) might have been made in the first place.

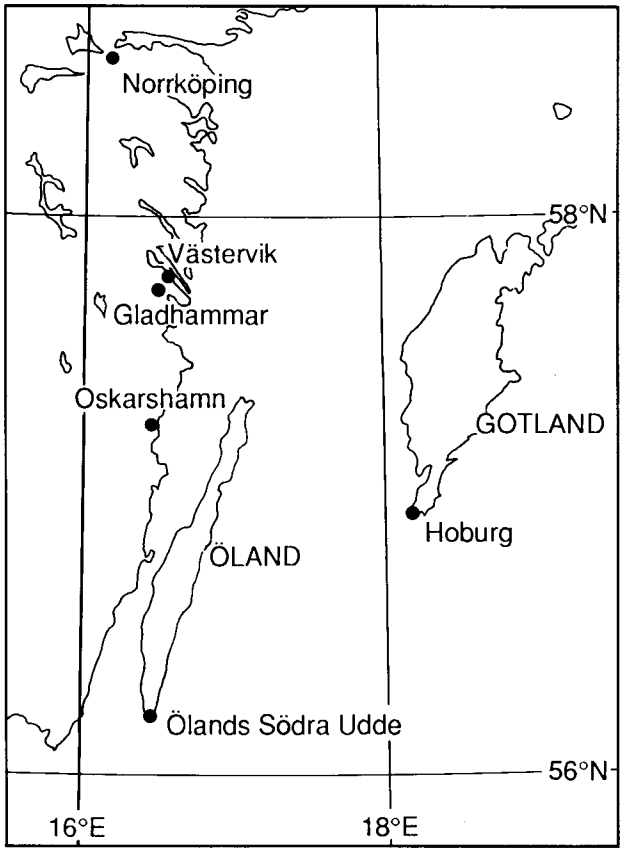

Figure 1. Locations of places mentioned in text.

Perhaps water equivalents have traditionally been more important in lowland United Kingdom than in Sweden where rivers are generally more youthful and fast-flowing. Water equivalents give engineers a useful idea of how much water would be additionally released, in a catchment area, by a sudden thaw. Such a problem has resulted in serious flooding of the Thames and Severn Rivers in England (e.g. in March 1947 when 14 000 hectares of the East Anglian Fens disappeared under water).

2. Radar observations

It is true that the cloud band extends beyond Bornholm, but Fig. 3 of Pike (1990) shows that the convection intensified in the Mecklenburg Bight. Is this not consistent with the Hamburg radar observations?

The radar interpreters at both Hamburg Airport and Maritime Weather Offices described a 50 km wide band of precipitation stretching from beyond radar range in the north-east, then passing away to the south-west. This broad quasi-stationary band was aligned over the Lübeck Bight, near the coast, and new shower cells were observed to be continually developing within the band over the water.

This seems acceptable for several reasons: (1) sea-surface temperatures were slightly higher in the Mecklenburg/Lübeck Bights, i.e. 3–3.5 °C, compared with 2.5 °C or less further north-east in the Baltic Sea, (2) land-breeze components from over northern Germany were adding strength to the convergence line convection near the Bight coast, and (3) two convergence lines themselves converge in the vicinity of Warnemünde (as illustrated in Pike (1990) Figs 1 and 7).

Bennetts *et al.* (1986) have shown that, in conditions of uni-directional wind shear, convective clouds are usually relatively short-lived (½–¾ hour). Ascents from Greifswald (not shown) indicate that east to north-east winds were increasing with height and time during Sunday evening (11 January) when the shower cells were seen to be continually developing over the Mecklenberg Bight. With cells taking perhaps 20–30 minutes to form and produce snow showers and tops to 12 000 ft it seems quite reasonable to assume that the Hamburg radar observations were genuine.

Figs 1 and 2 of Pike (1990) also show two convergence lines and the associated convective snow bands merging into a V-shape (at SGK) just off the Swedish coast near Gladhammar (G), which is precisely where radar observations of 'precipitation maxima' have occurred on several occasions (including 12 and 28 January 1987). We should remember, however, that these observations relate to snow in the clouds, which has yet to precipitate at quite a shallow angle in strong winds.

Fig. 6 of Andersson and Nilsson (1990) confirms that aligned precipitation cells sometimes meet in a V-shape; in the case of 3 January 1985 the merger took place some 100 km out to sea from the Norrköping radar. Such

precipitation cells perhaps take 20 minutes to develop over a short 'fetch' of Baltic Sea, aided here by the strength and involvement of a north to north-north-easterly land-breeze component from over the Stockholm peninsula. Other dependent factors would include instability, friction and cyclonic curvature of the isobars. No two cases are exactly alike.

F.E. Lumb (personal correspondence) now points out that Figs 2 and 4 of Pike (1990) show, at least over 11–12 January 1987, 'the topography (as modified by ice) favoured an east-north-east to west-south-west convergence zone extending from the Gulf of Finland to the vicinity of Västervik. It was able to maintain itself as a well-marked band all the way because the wind direction throughout the unstable layer (not just at 950 mb) was between east and north-east'.

3. Snowfall over land and sea

It is unfortunate that Fig. 3 in Andersson's letter does not cover the same period as the heavy snowfall near Hamburg (i.e. 24 hours up to 0600 UTC on 12 January 1987). Does the interesting 'HIRLAM' computer program take land-breeze convergence into account?

Referring to Fig. 5 of Pike (1990), this was based on some 140 observations from 'climatological and rain-gauge stations' of the Deutscher Wetterdienst, and 45 similar stations from the East German (as it then was) equivalent. At that time both German meteorological services seemed more willing to send the author this snowfall data than they were to exchange it between themselves! This situation has now changed and Herr Kresling has been joined by Dr Tiesel (from East Germany) in Hamburg, where they are currently (January and February 1991) working together investigating any further mesoscale snowfall events which might affect the southern Baltic area. Perhaps they will find that another snowfall maximum occurs over the sea to the north of Rügen Island? If not, verification is the responsibility of Andersson with respect to the case of 12 January 1987.

Concerning the snowfall over south-east Sweden, every situation is going to vary slightly from a similar one. The case of 3 January 1985 was quite similar to that of 28 January 1987 in that the snowfall was not prolonged and occurred with cyclonically curved isobars after passage of a depression. However, the depressions had very different tracks, the former passing southwards and the latter south-eastwards into the southern Baltic — these events lasting no more than 24–48 hours.

The situation over 9–13 January 1987 was very difficult again in that a prolonged east to north-easterly airflow was involved. F.E. Lumb (personal correspondence) makes the comment ... as regards Fig. 9 of Andersson and Nilsson (1990), 'the very rapid decrease in snowfall north of 58°N on the coast of Sweden is interesting. It can be explained by Fig. 1 of Pike (1990) which shows that, taking the ice areas into account, the open sea track of the surface wind (the key factor in initiating convection) shortened rapidly north of 58°N'.

The theoretical nocturnal maximum of coastal snowfall associated with convergence cloud bands due to slackening of the land to sea-surface thermal contrast by day is illustrated by the water equivalent and snowfall observations from Västervik over 10–14 January 1987 (Table I). Confirmation comes from the precipitation observer at Oskarshamn who reported dry spells between 0800 and 1600 UTC on the 11th, and 0900 and 1600 UTC on the 12th. A nocturnal maximum is, presumably, less of a feature further north, where there is little or no solar heating at this time of year.

Table I. Snowfall observations at Västervik, 10–14 January 1987

Date	Precipitation		Snow depth at 06 UTC	
	18–06 UTC (mm)	06–18 UTC (mm)	Fresh (past 24 hrs) (cm)	Total (cm)
10	0.2	nil	nil	43
11	0.6	8.7	2	45
12	11.5	3.2	23	68
13	6.5	4.1	10	78
14	2.6	1.9	12	90

4. Conclusion

The northerly land-breeze component from over the Stockholm peninsula, when added to the low-level north-easterly synoptic-scale airflow, is probably the single most significant factor in: (1) maintaining the convergence line and associated convective snow band over the sea, and (2) generating heavier shower cells within this snow band towards the Swedish coast (as shown in Figs 1 and 2 of Andersson (1990)). Careful study of the cloud-street alignment on satellite photographs is likely to help confirm this (e.g. Fig. 2 of Pike (1990) clearly points to such an effect of land-breeze involvement on 11 January 1987).

References

Andersson, T. and Nilsson, S.,1990: Topographically induced convective snowbands over the Baltic Sea and their precipitation distribution. *Weather and Forecasting*, **5**, 299–312.

Bennetts, D.A., McCallum, E. and Grant, J.R., 1986: Cumulonimbus clouds: an introductory review. *Meteorol Mag*, **115**, 242–256.

Bergeron, T., 1949: The problem of artificial control of rainfall on the globe. 2. The coastal orographic maxima of precipitation in autumn and winter. *Tellus*, **1**, 15–32.

Meteorological Office, 1982: Observer's handbook. London, HMSO.

Pike, W.S., 1990: A heavy mesoscale snowfall event in northern Germany. *Meteorol Mag*, **119**, 187–195.

W.S. Pike

19 Inholmes Common
Woodlands St. Mary
Newbury
Berkshire RG16 7SX

Notes and news

The warmest year ever globally

Global mean-surface-temperatures based on land and marine measurements during 1990 were the highest since comparable records began in the middle of the 19th century. The 1990 global mean-surface-temperature was 0.39 °C above the average level during the period 1951–80. This value exceeds that of the previous warmest year, 1988, by at least 0.05 °C. Six of the seven of the previous warmest years of the near 140-year-long record have all occurred since 1980. In descending order the years are 1990, 1988, 1983, 1987, 1944, 1989 and 1981. The 1990 value follows the warmest decade (1980–89) ever recorded when temperatures were 0.20 °C above the 1951–80 average.

The warmth of 1990 was particularly evident over Europe and western Siberia, the Far East and most of the United States and southern Canada. Some regions, nevertheless, remained cooler than the 1951–80 reference period, notably north-eastern Canada, Greenland and the central Arctic. The southern hemisphere was relatively less warm than the northern. For the globe, March 1990 was, relative to average, easily the warmest month of this or any other year.

There was also exceptional warmth in the 1.5–10 km layer of the lower atmosphere, where 1990 was the warmest year in records that begin in 1958. These data also reveal the 1980s as the warmest decade. Recent satellite-based observations have confirmed the reliability of the surface data and especially the upper-air data, but satellite results are not yet available for the whole of 1990.

Although it is still too early to confirm whether the recent exceptional warmth is related to the greenhouse effect, international scientific opinion strongly supports the reality of an enhanced greenhouse effect, and it is likely that it has played some role in contributing to the recent warmth.

Reviews

Weather radar networking, edited by C.G. Collier and M. Chapuis. 165 mm × 235 mm, pp. xvi+580, *illus.* Dordrecht, Boston, London, Kluwer Academic Publishers, 1990. Price Dfl.240.00, US $139.00, £89.00. ISBN 0 79230 672 4.

This book is an unedited version of the proceedings of a seminar, held in Brussels in September 1989, which marked the 'half-way stage' of the COST-73 project. The COST (European Co-operation in Science and Technology)-73 project 'associates 16 countries in western Europe with the aim of setting up a weather radar network providing real-time measurements of rain, snow and hail'.

From the outset, I found myself asking the question: why have these conference proceedings been made into a high quality text costing £89 rather than the usual relatively cheaply produced volume? Perhaps the key is found on page 444 when, after surveying the present use of weather radar data in a number of European countries, Newsome summarizes 'There is a danger, however, that the momentum of the international co-operative work that has been successfully carried out so far under COST-73 will be lost, unless it continues to be energetically pursued under the aegis of an international organisation'. I suspect this publication is an attempt to present the state of the art of weather radar networking to the appropriate organizations.

The 580 pages of the book take the reader through over 60 separate papers divided into six sessions which survey (exhaustively) the state of radar networking in nearly 20 different countries, current and new techniques in weather radar networking and the combining with other forms of data through to meteorological, hydrological and other applications of weather radar. The text is 'camera ready', reduced in size from the original. There are a variety of typefaces, some texts are closely spaced or painfully small to read. Unexplained jargon, acronyms and spelling mistakes abound, particularly in the first half of the book. There is also much repetition, for example the difficulty of measuring rainfall from radar using the radar rainfall 'Z R relationship' is discussed by countless authors. Sadly, there has been no editing, even of papers by contributors whose first language is not English.

These criticisms apart, within the maze of material, there are a number of very interesting papers, although some have been published in similar form elsewhere. Certainly for the country or organization just embarking on setting up a weather radar network, there is a wealth of material covering the meteorology, and current computer hardware and software technology, together with a very extensive list of references. However, the would-be user will find much of it hard going. A far more attractive and slimmer text could have been produced by thorough editing, particularly of the first section where a small number of tables and brief summaries could easily have replaced the bulk of pages 1–190.

G.A. Monk

Earth's rotation from eons to days, edited by P. Brosche and J. Sündermann. 168 mm × 247 mm, pp. xv+255, *illus.* Berlin, Heidelberg, New York, London, Paris, Tokyo, Hong Kong, Springer-Verlag, 1990. Price DM 128.00. ISBN 3 540 52409 6.

Fluctuations in both the magnitude and direction of the rotation vector of the 'solid' Earth (mantle, crust and cryosphere) occur over time-scales ranging from days to billions of years. They are caused by dynamical

processes occurring within the solid Earth; by interactions of the solid Earth with the underlying liquid metallic core and the overlying hydrosphere and atmosphere; and by the gravitational action of the Moon, Sun and other astronomical bodies. The accurate determination of these fluctuations and their reconciliation with models of the composition, structure, dynamics and evolution of all regions of the Earth present challenging problems in astronomy and many branches of the Earth sciences, including meteorology and oceanography.

The book under review reports the proceedings of a workshop that took place in Bielefeld in 1988, bringing together leading workers from several countries. The reports include summaries of recent work on: the radio-astronomical technique of very long baseline interferometry for making any accurate determinations of the orientation of the solid Earth in space and special and general relativistic corrections needed when making such determinations; Earth rotation changes in historical and geological times as revealed by observations of lunar occultations and eclipses and by various geological records; the dynamics of the Earth–Moon–Sun system; and long-term changes in the structure of the Earth associated with the gradual lengthening of the day over geological time. Of particular interest to meteorologists and oceanographers are the chapters on variations of the angular momentum budget for tides of the present oceans, the pole tide and the damping of the Earth's free nutation, the seasonal angular momentum of the thermohaline ocean circulation, and atmospheric effects on the Earth's rotation.

The book, which is aimed at research workers, contains much useful information, including many references, but it lacks a subject index. Most of the chapters are well-written, but some contain obscurities which seem to have escaped the scrutiny of the editors.

R. Hide

Weather Watch, by R.F. File. 158 mm × 240 mm, pp. xii+299, *illus.* London, Fourth Estate Ltd, 1990. Price £14.99. ISBN 1 872180 12 4.

The Guardian has always had good 'back page' coverage of weather details from around the British Isles and further afield. In the last few years an innovative column known as 'Weather Watch' has appeared as a very readable supplement to the daily maps, text and data. Dick File's name must very quickly have registered in the readers' minds as being identified with the provision of snappy and most often topical accounts designed to inform and educate. He has continued with this unique task and the measure of its success is presumably expressed in the appearance of this volume published by a *Guardian*-owned company.

The book is thus in essence a natural development of the kind of short column presentation and aims to be the 'complete guide to our weather, the perfect companion for both the professional and armchair weather watcher'. The 299 pages of text are wide ranging as is indicated by the chapter headings of Evidence of past climates, Understanding weather, World weather, British weather, Local weather, Signs in the sky, Observing the weather, Forecasting, Holiday weather, Weather for business, and Climate change. The book also contains a Glossary of some five dozen common terms, and six appendices ranging from temperature and pressure conversion tables to British and world climate data. Finally, 26 black and white plates are bound in the centre of the book in addition to a good range of figures scattered through the text.

The great strength of this book lies in Dick File's readable style in combination with his varied experience at the 'sharp end' of operational meteorology. Nowhere is the text 'dry' and his good humour is used to effect throughout the text — the feel of his genuine personal interest in weather and its links with other aspects of nature appear at regular intervals and make the book that bit more engaging.

So much for the style, how about the content? With any wide-ranging popular text there are almost inevitably going to be some errors. Overall this book treats its topics well and in an up-to-date fashion — even including the official record maximum temperature for the United Kingdom measured at Cheltenham last summer. Each topic is allotted about three to four hundred words in snappy sections which generally are linked in a logical succession in each chapter. The only bones I think should be picked relate to:

1. The perpetuation of the archaic notion that the Asian monsoon is a very large-scale sea-breeze feature — it would be much more interesting to engage the reader in a modern discussion of the sub-planetary nature of the phenomenon.
2. The inaccurate passage relating to storm surges sloshing into the Thames Estuary after being 'deflected' from the Dutch Coast — this is a topic which needs more accurate explanation, and
3. the idea that westerly jets occur because the Earth is rotating in that direction — this doesn't help much in explaining seasonal easterly jets in the tropical area for example.

It is a shame that the selection of black and white plates are not referred to in the text and that some of them could have been better quality — particularly the satellite images. The cloud pictures could, for example, have illuminated the discussion on static stability which is always a thorny topic — especially for the armchair reader.

These comments are meant to illustrate that, although there are a few things I feel could be improved, the vast majority of the text achieves its stated aims — and for

Correction

Meteorological Magazine, April 1991, p. 73, Review of *Global Air Pollution.*

The specific reference to Professor Scorer's book was accidentally transposed to the second paragraph, but should have been included at the end of the first paragraph, as an alternative book to the one under review. Apologies are offered for any implied misrepresentation.

the price of £14.99 is an excellent buy not only for professionals and armchair readers but also for school-teachers and upper-school students.

The author's humour and operational experience can no better be summarized than to quote his adaptation of Harold Wilson's famous adage — 'A week is a long time in meteorology'!

R. Reynolds

Global air pollution: Problems for the 1990s, by H.A. Bridgman. 155 mm × 235 mm, pp. xiv+261, *illus.* London, Belhaven Press, 1990. Price £12.95 (paperback), £30.00 (hardback). ISBN 1 85293 009 3 (paperback), 1 85293 094 2 (hardback).

Gone are the days when any informed person would suppose the atmosphere could take anything and everything we are prepared to throw into it, without the potential for adverse, and perhaps disastrous, consequences. Of course many many specialist and popular books have been written in the last decade or so discussing one or other of the important environmental issues related to air pollution. Howard Bridgman has attempted to bring many of these major issues together in one book. Topics include acid rain, the ozone hole, tropospheric oxidants and aerosols, climate warming, major radioactive releases, nuclear winter and urban air quality. The contents are fairly up-to-date (with a few exceptions) and are broadly based on the contents of a third-year course Dr Bridgman gives at the University of Newcastle in Australia. Although the approach is non-mathematical it goes into the issues seriously and to sufficient depth to be a potentially useful text. The nearest contenders on my own bookshelf are a 1988 WMO Conference Proceedings (No. 710) called *'The Changing Atmosphere'* (which incidentally is not referenced in Bridgman's book).

However, I regret having to report that Dr Bridgman's book, and Professor Scorer's excellent book *Meteorology of air pollution: implications for the environment and its future* which has recently appeared, deserve, and should quickly receive, more effort by both publisher and author. Glancing quickly through the book, I began to share the disappointment the author must have felt on seeing his first copy. In addition to some spelling mistakes and the irritating mix of English and American spellings, there are problems that are more serious. At least three tables have a most usual 'error': the final line is repeated and repeated up to 40 times! Why wasn't this picked up and removed? Furthermore the print is very small and rather feint. I can imagine anyone with weak eyesight finding it very tiresome to read. Some figures have background maps which are so feint that boundaries are almost invisible. It all gives a very poor impression.

The author could also be well advised to consult other experts in the various areas he covers for their comments. I will restrict my contenders for change to just four:

(a) Acid rain studies in Europe: this is an inadequate section, consisting largely of results from the rather dubious monthly data collected in the European Atmospheric Chemistry Network Programme. He should consult some recent European Monitoring and Evaluation Programme and EUROTRAC Reports (for example) which have thrown a lot more light on the subject.

(b) The section on dry deposition also lacks authority. He should consult the numerous papers by Hicks, Garland and Fowler. Nicholson's excellent review in *Atmos Environ,* **22**, p. 2653 (1988) should also be drawn from.

(c) Dr Bridgman quotes values of Cs-137 deposition in the United Kingdom resulting from the Chernobyl accident. Unfortunately most of his numbers in the text are a thousand too small!

(d) I found many of the definitions he gives in his Glossary unsatisfactory. To take the first entry as an example, he defines 'advection' simply as the horizontal movement of air.

To summarize then, Dr Bridgman has contributed a potentially very useful book. The first edition is marred by very low publishing standards and by inadequate scientific consultation. I would strongly urge him to put these right as quickly as he can and move into a second edition. The effort could be very worthwhile.

F.B. Smith

Television weathercasting: A history, by R. Henson. 155 mm × 234 mm, pp. xii+193, *illus.* Jefferson, North Carolina, McFarland, 1990. Price £26.25. ISBN 0 89950 492 2.

The first thing I did on receipt of the book was to flick through to see what had been said about the BBC presentations. No BBC. How can a book be written without considering the best and most sophisticated presentation in the world! Maybe ITN is considered, after all it is new and different! No ITN. What about the rest of Europe — nothing. I know that Americans are often accused of being insular but surely one cannot write a history of TV weathercasting without considering where it all started way back in 1936. After all, we see American broadcasts all the time at the BBC. The book itself looks as if it was printed in 1936, no colour and certainly not worth the cover price of £26.25.

Having said all that the book is unique. I do not know of another on a similar subject — the author himself saying that he was appalled to find that shelves were full of books on newscasts and sportscasts but not weathercasts, despite the fact that weather affects more people than the latest summit or football match.

The book deals in detail with all aspects of American TV weather forecasts with chapters covering the range from 'Technical Matters' to 'From Silly to Serious'. The author starts by saying that 'over the decades the weatherman has become a trusted yet sometimes scorned symbol' — I agree. He goes on 'despite the attention heaped on newscasters it is weather that consistently ranks top in the ratings' (as it does here with more people actually switching on for the 9.28 p.m. weather than watch the preceding news or the following light entertainment programme). He further makes the salient point that in the flashy world of TV, dry facts alone are not enough to attract audiences, weathercasters have to present their information with liveliness and friendliness. Some have gone to absurd lengths such as giving the forecast submerged in a tank of water or dressed as Carmen Miranda, whereas others stay on duty for 24 hours giving warnings and updates on either tornadoes or hurricanes.

The first chapter deals with the history of TV and radio forecasts and the way styles have changed. How flippant weathercasts waned during the Vietnam war and did not reappear to the same extent. It also mentions the concern of the American Meteorological Society whose seal of approval has done a lot to maintain professionalism.

It was also nice to read in chapter 2 that the American audience is as intolerant as ours, and does not take kindly to any alteration, or worse, elimination, of the regular reports. Equally nice was the fact that Bob Ryan of WRE (Washington), one of the biggest stations, has a working schedule and environment very similar to ours at the BBC (he also works in a cupboard with a camera and VDUs for company, although he does have an assistant).

Thankfully we have not resorted to the same antics here as described in chapter 3. Rather the reverse as, instead of using puppets, there is a puppet of Ian McCaskill used in Spitting Image. We do not use animals either, although we do have a fish! It is satisfying to read that the moans of the presenters are the same the world over; Rebecca Rehers of Salt Lake City says in this chapter 'I get 3½ mins. There's not a lot you can do. Plus, we cover five states' — we have to cover the whole of Europe in 1½ minutes! I read also that one certain way of improving the ratings is to deliver the forecast standing on one's head!

Chapter 4 notes that in the USA it was years before the National Weather Service employees were allowed to appear and even now it is a rare event, subject to many restrictions. Here in Britain we pioneered TV forecasts with few problems from unions, Parliament or the business community. No such restrictions appear to exist in the USA on the radio side as the chapter goes on to describe the NOAA 24-hour weather radio which, apart from a continuous flow of information, even provides a tone alert to radios that are switched off when a severe weather warning is issued.

The chapter on technical matters makes fascinating reading, at least it does for me, and again it is nice to read that throughout the decades the BBC has often been in the forefront as far as innovation is concerned, except for the introduction of radar where we lagged some 25 years behind (even now many USA stations are heavily into Doppler radar).

One the major criticisms of the book is that it is highly repetitive and could well have been fitted into half its 193 pages. By the time one gets to chapter 6 the repetitions become tedious, especially as they start virtually right from page 1.

There is one final item of interest, and that is the section on the Weather Channel; the channel, only available via cable, has become profitable in only 3 years. The book states that the Weather Channel 'talent' has a vast workload and spends about 75 minutes a day before the cameras with a team of 40 meteorologists and 10 graphic artists working behind the scenes. I feel that the productivity at the BBC is greater as we often spend 20 minutes on camera with no-one behind the scenes!

A final quote 'On 21 September 1938 a powerful hurricane approaching the Carolines veered north. Weather Bureau officials in Washington gave the all clear for the entire east coast. Morning forecasts in New England called for rain and breeziness; by evening gusts at Blue Hill, Mass. reached 186 mph' — sounds familiar!

In the States mass-produced weather is called McWeather — so what, we have McCaskill and MacFish (the older ones amongst you will remember the firm across the road from the Met. Office in Bracknell).

Of little or no interest to the British reader is the vast appendix listing biographies, awards and a large bibliography. This, with the index, takes up the last 60 pages.

M.J. Fish

Books received

The listing of books under this heading does not preclude a review in the Meteorological Magazine at a later date.

The mathematical theory of non-uniform gases, by S. Chapman and T.G. Cowling (Cambridge University Press, 1991, £19.50, US$32.50) presents a detailed account of viscosity, thermal conduction and diffusion based on the solution of the Maxwell–Boltzman equations. Also, the theory of Chapman and Enskog is extended in this paperback edition which is part of a series. ISBN 0 521 40844 X.

Sunsets, twilights, and evening skies, by A. and M. Meinel (Cambridge University Press, 1991, £13.95, US$19.95) contains many illustrations and explanations of the varied phenomena associated with the subject. It is a paperback version of an earlier edition. ISBN 0 521 40647 1

Radar photographs — 9 January 1991 from 1400 to 1515 UTC

Fig. 1 shows an example of a radar 'bright-band' which is exceptional in the way it conforms to the textbook structure of the phenomenon. Bright-bands are associated with melting snowflakes beneath the 0 °C wet-bulb level. At the wavelengths used by weather radars, ice has a reflectivity about one fifth that of water. Large, dry snowflakes are even less reflective than a solid ice particle of the same size would be because of the pockets of air between the crystals. Once a snowflake acquires a coating of water due to melting, it reflects like a giant raindrop. Such hydrometeors dominate the radar return because the radar reflectivity varies as the sixth power of the drop diameter. The consequence is that a radar scanning in a vertical plane sees a band of anomalously intense precipitation at a height near the 0 °C isotherm. On the black and white analogue displays used originally, this appeared as a brighter region, hence the name 'bright-band'. A radar scanning with its beam at constant elevation will see the bright band enhancement at a range which depends on the beam elevation as well as the height of the band. In steady cold rain this might be expected to produce an annulus of apparently heavier rain centred on the radar; in practice this is almost never observed for five reasons:

(1) The annulus can only be seen if there is precipitation at the appropriate range.

(2) The rainfall intensity is often so variable and patchy that the ring is disguised.

(3) With the quantized display system used by the UK radar network, the same colour is used for rates of 1–4 mm h^{-1}, 4–8 mm h^{-1}, 8–16 mm h^{-1}, etc. It follows that a brightening by a factor of ×3.5 will not be seen if the base rainfall rate is 1 mm h^{-1}. The brightening is often less than ×4 but in extreme cases it seems to reach ×16 (usually at ranges in excess of 100 km).

(4) Case studies suggest that the effect becomes more pronounced as rainfall rates approach 4 mm h^{-1} — but widespread rain of this intensity is uncommon over the British Isles unless the atmosphere is strongly baroclinic. The variation in height of the melting level through a well marked front will cause the annulus to be distorted.

(5) When the radar data is composited, part of the area occupied by the annulus may not be used, that replacing it will not, in general, be at the correct range from its radar to show bright-band effects.

Fig. 1 shows the development of an almost perfect bright band annulus about the Dyfed radar in south-west Wales during the afternoon of the 9 January 1991 as a warm front approached from the south-west (Fig. 2). The data is displayed in a slightly different way from the usual radar network one: the lower limit is $^{1}/_{32}$ mm h^{-1} instead of $^{3}/_{32}$; and an additional level has been inserted so that there is a colour change from yellow to red at 2 mm h^{-1}. Observe how an annulus of high intensity develops around the radar with outliers to east and west, also due to bright-band.

Because ground clutter is an inevitable consequence of a very low elevation beam, UK radars use a higher elevation beam (1.5° at Dyfed), called 'beam 1', for data

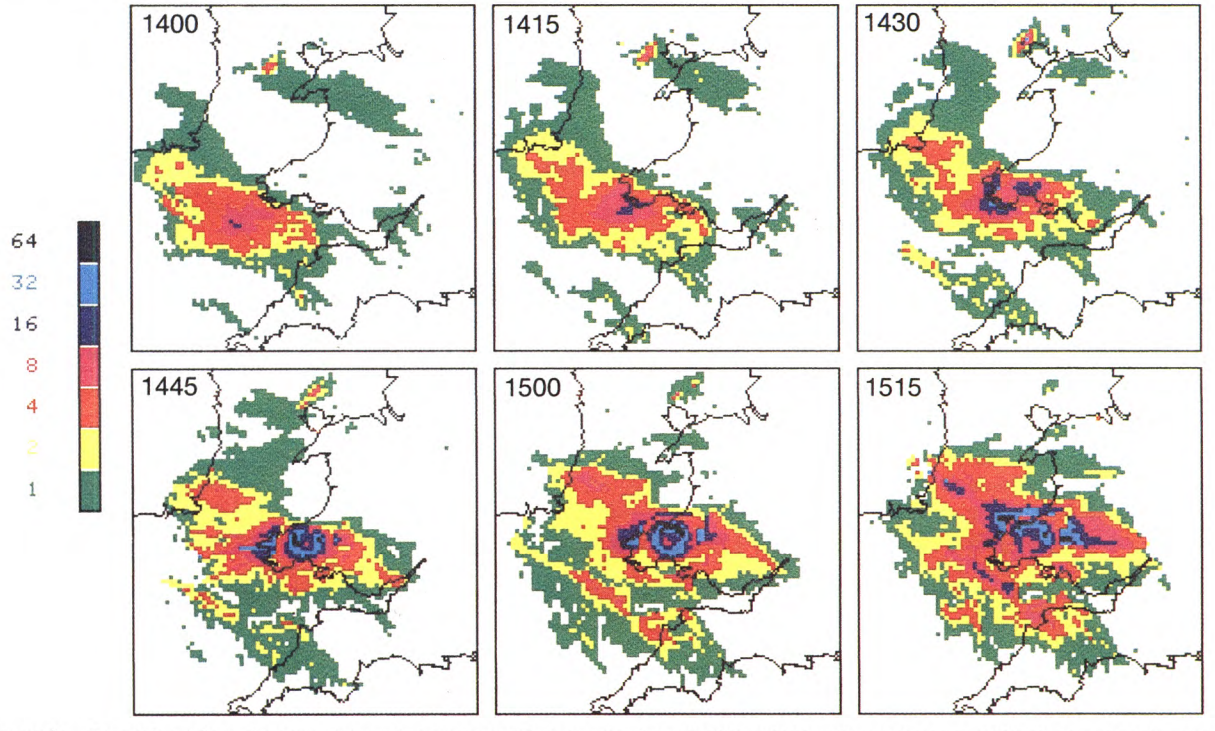

Figure 1. Evolution of a 'bright-band' annulus about the Dyfed radar from 1400 to 1515 UTC on 9 January 1991. Radar rainfall rates are indicated by the adjacent key, the number giving the rate (mm h^{-1}) at the top of the band.

gathering close to the radar (within about 35 km at Dyfed). The lowest elevation beam, 'beam 0', is used for greater ranges. Fig. 3 shows how this arrangement can lead to a double bright-band effect, as in this example. If the melting level is lower than L_1 the effect will only show on beam 1; if above L_2, only on beam 0: in this event the bright-band was at 440 m above the radar. The curve I shows schematically the cross-section of the intensity map assuming a uniform rainfall rate and making no allowances for the different reflectivities of rain and dry snow. Note that for a bright-band of uniform depth, the intensity will be higher nearer the radar where it occupies a greater fraction of the beam depth.

The overestimation of the rainfall rate caused by the bright band is clearly apparent from Fig. 4, the hyetogram from Brawdy, 48 km west of the radar. For the period of Fig. 1 (1400–1515 UTC) the ground truth is an almost constant 4 mm h^{-1} (red/magenta) as compared with cyan (16–32 mm h^{-1}) and possibly black (32–64 mm h^{-1}) pixels in the radar picture. The maximum rainfall rate at Brawdy was 10 mm h^{-1} at 1536 UTC on the line of strong echoes running north-west to south-east near the south-west boundary of the system, on the surface warm front in Fig. 2.

R.M. Blackall

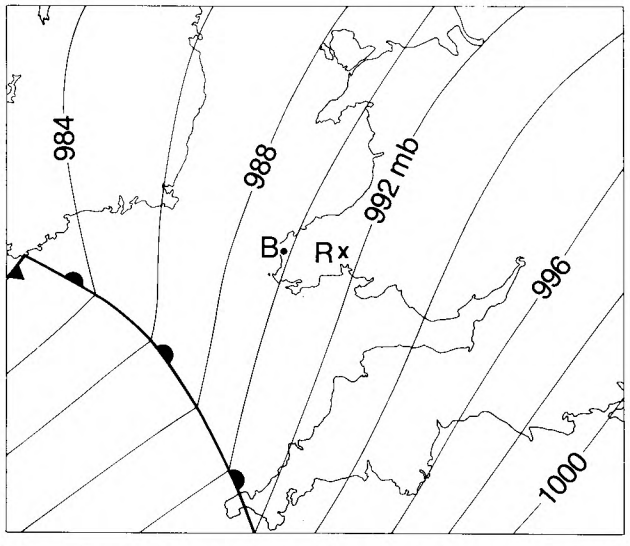

Figure 2. Surface synoptic chart for 1500 UTC on 9 January 1991. Isobars are at 2 mb intervals. R marks the location of the Dyfed radar and B the location of Brawdy.

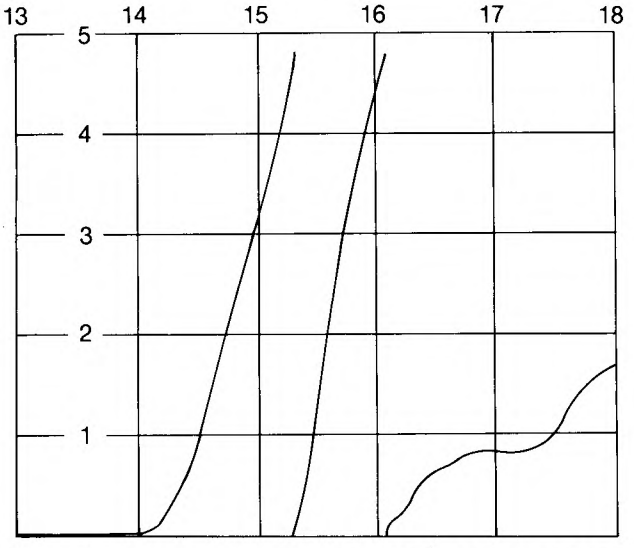

Figure 4. Hyetogram from RAF Brawdy from 1300 to 1800 UTC on 9 January 1991. The rainfall rate is 4 mm h^{-1} for the period shown in Fig. 1. The peak intensity is about 10 mm h^{-1} at 1536 at the passage of the warm front shown in Fig. 2.

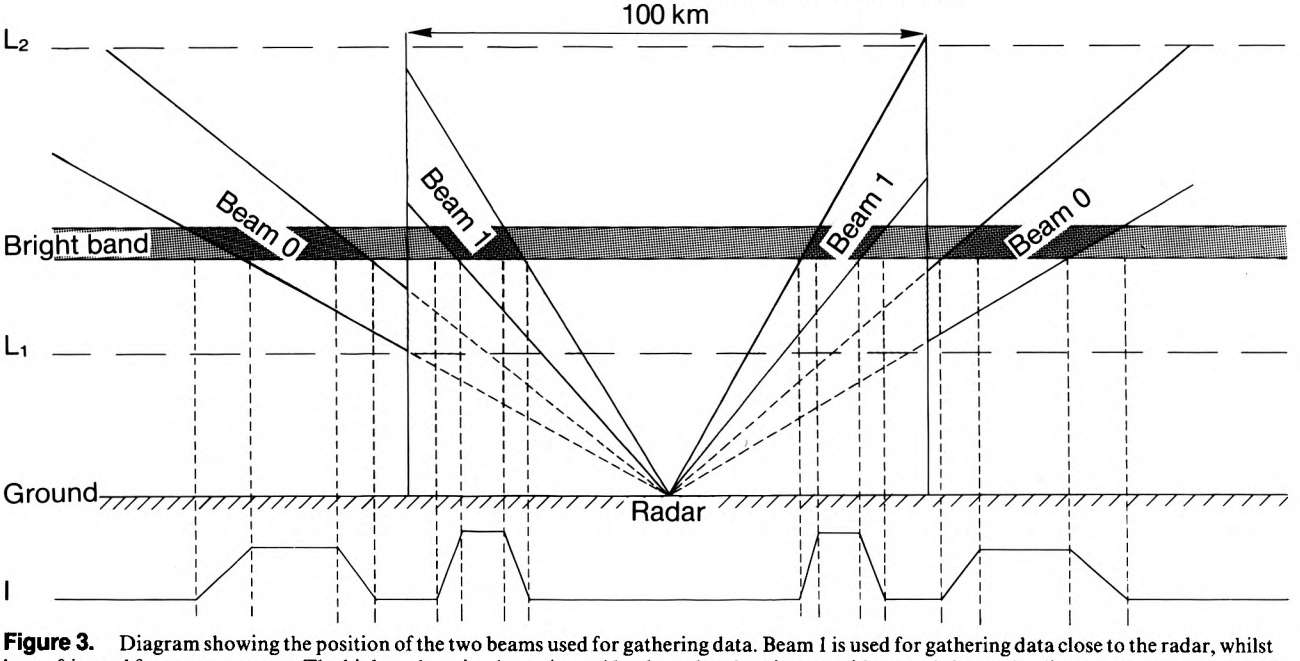

Figure 3. Diagram showing the position of the two beams used for gathering data. Beam 1 is used for gathering data close to the radar, whilst beam 0 is used for greater ranges. The higher-elevation beam is used by the radar close in to avoid ground clutter, leading to a double annulus if the bright band lies between levels L_1 and L_2 (vertical scale greatly exaggerated). The curve 'I' shows the level of enhancement of the radar return above the true value.

GUIDE TO AUTHORS

Content

Articles on all aspects of meteorology are welcomed, particularly those which describe results of research in applied meteorology or the development of practical forecasting techniques.

Preparation and submission of articles

Articles, which must be in English, should be typed, double-spaced with wide margins, on one side only of A4-size paper. Tables, references and figure captions should be typed separately. Spelling should conform to the preferred spelling in the *Concise Oxford Dictionary* (latest edition). Articles prepared on floppy disk (Compucorp or IBM-compatible) can be labour-saving, but only a print-out should be submitted in the first instance.

References should be made using the Harvard system (author/date) and full details should be given at the end of the text. If a document is unpublished, details must be given of the library where it may be seen. Documents which are not available to enquirers must not be referred to, except by 'personal communication'.

Tables should be numbered consecutively using roman numerals and provided with headings.

Mathematical notation should be written with extreme care. Particular care should be taken to differentiate between Greek letters and Roman letters for which they could be mistaken. Double subscripts and superscripts should be avoided, as they are difficult to typeset and read. Notation should be kept as simple as possible. Guidance is given in BS 1991: Part I: 1976, and *Quantities, Units and Symbols* published by the Royal Society. SI units, or units approved by the World Meteorological Organization, should be used.

Articles for publication and all other communications for the Editor should be addressed to: The Chief Executive, Meteorological Office, London Road, Bracknell, Berkshire RG12 2SZ and marked 'For Meteorological Magazine'.

Illustrations

Diagrams must be drawn clearly, preferably in ink, and should not contain any unnecessary or irrelevant details. Explanatory text should not appear on the diagram itself but in the caption. Captions should be typed on a separate sheet of paper and should, as far as possible, explain the meanings of the diagrams without the reader having to refer to the text. The sequential numbering should correspond with the sequential referrals in the text.

Sharp monochrome photographs on glossy paper are preferred; colour prints are acceptable but the use of colour is at the Editor's discretion.

Copyright

Authors should identify the holder of the copyright for their work when they first submit contributions.

Free copies

Three free copies of the magazine (one for a book review) are provided for authors of articles published in it. Separate offprints for each article are not provided.

Contributions: It is requested that all communications to the Editor and books for review be addressed to the Chief Executive, Meteorological Office, London Road, Bracknell, Berkshire RG12 2SZ, and marked 'For *Meteorological Magazine*'. Contributors are asked to comply with the guidelines given in the *Guide to authors* which appears on the inside back cover. The responsibility for facts and opinions expressed in the signed articles and letters published in *Meteorological Magazine* rests with their respective authors.

Subscriptions: Annual subscription £33.00 including postage; individual copies £3.00 including postage. Applications for postal subscriptions should be made to HMSO, PO Box 276, London SW8 5DT; subscription enquiries 071–873 8499.

Back numbers: Full-size reprints of Vols 1–75 (1866–1940) are available from Johnson Reprint Co. Ltd, 24–28 Oval Road, London NW1 7DX. Complete volumes of *Meteorological Magazine* commencing with volume 54 are available on microfilm from University Microfilms International, 18 Bedford Row, London WC1R 4EJ. Information on microfiche issues is available from Kraus Microfiche, Rte 100, Milwood, NY 10546, USA.

April 1991

Editor:
Editorial Board: R.J. Allam, R. Kershaw, W.H. Moores, P.R.S. Salter

Vol. 120
No. 1425

Contents

ISSN 0026–1149

ISBN 0-11-728855-1

9 780117 288553

Printed in the United Kingdom for HMSO
Dd 0291241 4/91 C13 503 12521

The Meteorological Magazine

May 1991

Overview of acid rain
The summer of 1990

HMSO

Met.O.998 Vol. 120 No. 1426

First published 1991

HMSO publications are available from:

HMSO Publications Centre
(Mail and telephone only)
PO Box 276, London, SW8 5DT
Telephone orders 071-873 9090
General enquiries 071-873 0011
(queuing system in operation for both numbers)

HMSO Bookshops
49 High Holborn, London, WC1V 6HB 071-873 0011 (counter service only)
258 Broad Street, Birmingham, B1 2HE 021-643 3740
Southey House, 33 Wine Street, Bristol, BS1 2BQ (0272) 264306
9–21 Princess Street, Manchester, M60 8AS 061-834 7201
80 Chichester Street, Belfast, BT1 4JY (0232) 238451
71 Lothian Road, Edinburgh, EH3 9AZ 031-228 4181

HMSO's Accredited Agents
(see Yellow Pages)

and through good booksellers

3 8078 0010 2475 3

The Meteorological Magazine

May 1991
Vol. 120 No. 1426

551.578.8

An overview of the acid rain problem

F.B. Smith
Meteorological Office, Bracknell

Summary

The formation, transport and deposition of acid-rain species, as well as their effect on the environment, is described. Ways of mitigating the effects are briefly presented.

1. Acid rain

Acid rain is a very general term which has grown in popular usage to include the deposition of all atmospheric pollutants which are acidic, or have the potential for being naturally transformed into acidic species, whether they be deposited in rain or snow or by dry-deposition processes. The major species contributing to acid rain are, or have been derived from, the so-called emitted primary pollutants, namely sulphur dioxide (SO_2), the nitrogen oxides (NO_x), ammonia (NH_3) and the various volatile organic compounds (VOCs). All these species are subject to chemical transformation within the air, sometimes involving oxidation which is often most rapid within cloud, or in the presence of sunlight, to form secondary more acidic species like sulphuric and nitric acids.

The pH of rainwater is a measure of its acidity and is directly related to the logarithm of the hydrogen ion concentration by:

$$pH = -\log_{10}(H^+).$$

Because the scale is logarithmic a change of one pH unit represents a tenfold change in real acidity. Table I shows typical values.

In 1987, at European stations that monitor daily average values of pH in rain and snow, the overall median value was 4.73. However the lowest daily values during the year ranged from pH 5.6 at a Romanian station down to one extreme value of pH 1.96 at a northern Italian station (a reading which may be suspect since a pH just below 3 is more usual). The median value of these minima was close to pH 3.8, nearly a whole unit below the median of the means.

Table I. Typical values of pH

Condition	pH
Extremely alkaline	14
Pure water	7
Pure water in presence of carbon dioxide gas	5.6
Rain in remote temperate areas of the world	4.5–5.6
Coffee	5
Annual average rain over Europe and the USA	4.1–5.1
Annual average rain over the United Kingdom	4.4–5.1
Average mountain-cloud water in north-east USA	3.5
Wine	3.5
Urban fogs	2.2–3.3
Lemon juice	2.0
Battery acid	1.0

2. The effect of acid rain on the environment

Considerable uncertainty still persists on the extent to which acid rain damages the environment. The reasons for this are twofold. Firstly, whilst damage is often evident, it is not always certain how important acid rain

is in creating this damage relative to damage from other possible causes like drought and disease. Secondly, once the rain reaches the surface the acidity and character of the rainwater is frequently modified, sometimes to an extreme degree. Soils, and in particular the near-surface humus layer, have the ability to modify dramatically the pH of water seeping through them. Almost all soils are in a state of long-term acidification by natural means, and this process can be accelerated or retarded not only by acid rain, but also often more importantly by ploughing, liming, the application of fertilizers, by soil erosion, by afforestation and deforestation, as well as by changes in climate. However, whenever the soil has reached a critically acidic state and the resident ecosystem is in a stressed state, the input of acidic rain can have a relatively rapid effect. Thus there are many parts of Scandinavia and upland Great Britain with underlying rocks which have a slow release rate of buffering minerals by weathering where the input of acidic pollution in rain, and in particular sulphate, is the main cause of acidification of their lakes and rivers and the elimination of fish and other organisms which once inhabited them.

2.1 The effect on fish

The strong acids not only affect the fish directly but have two other effects. The first is to release toxic aluminium from its 'locked-in' state within the soil. Secondly, acid rain has, over many years, depleted the soil of much of its available calcium so that water entering the rivers is deficient in it, and this has an adverse effect on the fish. As a result the fish suffer from one or more of the following afflictions:

(a) mucus clogging of the gills inhibiting effective oxygen uptake,
(b) difficulty in ridding the body of waste salts,
(c) a breakdown in the normal mechanism by which young fry can develop and escape from their egg sacs,
(d) a significant depletion of the food supply, the abundance of which may also be adversely affected by acidity, and
(e) an increased likelihood of being affected by disease.

2.2 The effect on trees

The situation appears to be more complicated still with regard to trees. Trees collect not only acidic species in rain but also enhance dry deposition by scouring the air of aerosols and particles some 20 times faster than over barren land. Jaenicke (1989) explains this enhancement, not through increased impaction (since wind velocities are generally too small), but through coagulation and settling of the particles and the typically long residence time within the forest allowing these processes to be of importance. In consequence the pH of rainwater may be significantly lowered as it passes through the canopy. A forest is a complex ecosystem which can be extremely sensitive to the stresses imposed upon it. These stresses include:

(a) Strong winds — damage to branches and roots which can lead to the onset of wet rot and fungal diseases.
(b) Drought — the 1975/76 drought severely affected trees, especially those on chalklands (e.g. beech and yew) and on sandy soils (e.g. pine). Weakened trees are subsequently prone to attack by disease and pests. Many such trees are still very evident in parts of southern Great Britain.
(c) Cold — extreme cold in winter or unseasonable cold after the sap has begun rising in springtime can cause cell damage and death of foliage.
(d) Disease, fungi, insect infestation, etc. — can seriously damage trees.
(e) Atmospheric ozone — ozone is a very reactive gas and can damage leaves causing visible markings. It can also damage the stomata by which the leaves 'breathe'.
(f) Acid rain — various hypotheses exist as to how acid rain affects trees, and each may have some validity in different conditions. Five of these are: (i) Ulrich's hypothesis in which acid rain acidifies the soil and releases toxic aluminium ions. These may damage the fine roots of the trees and result in insufficient or unbalanced uptake of nutrients, (ii) acidification of the soil may result in the fine-root system being confined to the upper layers of the soil, making the trees much more susceptible to periods of water-stress (Eichhorn 1989), (iii) acid rain leaches essential nutrients from the leaves; an effect which is increasingly probable if the stomata have been damaged by ozone and cannot open and close as efficiently as they should, (iv) very acidic fogs can cause damage to the coating leaf-waxes and this may result in a lower water-holding capacity of the trees; a result particularly serious in times of drought (Hogrebe and Mengel 1989), and (v) nitrates and ammonium in the rain can promote excessive and early growth which can make the tree more susceptible to damage from other stresses.

The problem with interpreting symptoms of stress is that different causes create very similar symptoms. Similarly, trends in damage over time have been difficult to ascertain since detailed surveys were not generally carried out until fairly recently, and an understanding of how to classify damage has developed only gradually since then.

Turning to trees in Britain, some are not in particularly good health at present and in some respects their state is comparable to the state in Germany, where so much public concern has been expressed. It is possible that the causes of the problem may be completely different and proper comparisons are difficult, if not impossible, because of the different environments and average tree-ages. Beeches appear to be most affected in the United Kingdom, but decline

seems to be restricted to certain areas only. Generally, beech stands, as distinct from more isolated specimens, are in better health than many stands in southern Germany. Where there is visible deterioration, this may be linked in some way to the fact that England is on the tree's northern geographical limit and also to the slow recovery many of the trees are making, or trying to make, from the damage caused by the prolonged 1975/76 drought.

Spruce also show some pockets of damage, but not always in areas of significant pollution. The reasons may again lie with climatic variations and other 'natural' causes.

Generally then, little evidence is available of serious damage to British woodlands which can be clearly attributed to acid rain. The situation in some parts of the continent is rather different. For example, some pine woods in the The Netherlands are being seriously affected and the damage appears to be linked to the large emissions of ammonia associated with intensive livestock production in that country (Table II). Ammonia tends to neutralize sulphuric acid in cloud droplets and can lead to increased sulphate formation (see later). Rain falling from such clouds is therefore high in ammonium sulphate. The ground then experiences an enhanced sulphate intake and the effective acidity is markedly increased as some of the ammonia is released back into the atmosphere, increasing the stress on the trees.

Fig. 1 shows the increasing damage to silver fir in east Bavaria from 1978 to 1986. Other conifers have suffered in a similar but usually less dramatic manner. Such decline is not always monotonic however and some evidence suggests individual trees can show partial recovery.

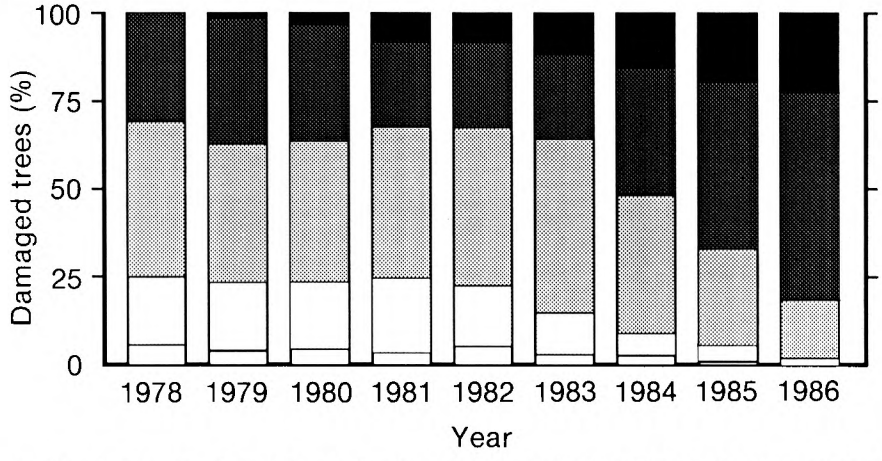

Figure 1. The decline in silver fir in eastern Bavaria (from Hoerteis and Schmidt (1986)). The stippling from white to black represents the percentage of trees from undamaged to dead.

Table II. Forest damage assessment in four European countries 1984–86 (from Innes 1987). The table gives needle or leaf loss as a percentage.

	0–10%			11–25%			26–60%			61–100%		
	84	85	86	84	85	86	84	85	86	84	85	86
United Kingdom												
Sitka spruce	65	83	45	28	12	39	6	5	15	1	0	1
Norway spruce	71	84	32	26	15	36	3	1	31	1	0	1
Scots pine	49	74	25	29	18	41	16	7	32	5	1	3
Germany												
Norway spruce	49	48	46	31	28	32	19	21	20	2	3	2
Scots pine	41	43	46	38	41	40	20	15	13	1	2	1
Silver fir	13	13	18	29	21	22	45	50	49	13	16	11
Beech	50	46	40	39	40	41	11	13	18	1	1	1
Switzerland												
Norway spruce	65	63	50	28	29	36	6	6	12	1	2	2
Scots pine	50	35	34	31	47	43	16	13	19	1	5	4
Silver fir	62	60	47	27	28	36	9	8	13	2	4	4
Beech	74	69	52	23	27	40	3	3	7	0	1	1
The Netherlands												
Norway spruce	62	48	49	28	41	34	7	9	12	3	2	4
Scots pine	34	48	50	51	36	33	12	14	13	2	2	3
Corsican pine	57	40	19	34	42	29	8	15	40	1	3	12
Beech	71	72	68	24	21	26	4	6	5	1	1	2

2.3 Damage to buildings

Air pollution, and principally sulphur dioxide, accelerates an otherwise natural process of degradation of building materials. In spite of a marked decline in the levels of urban smoke and sulphur dioxide in the United Kingdom over the last 30 years since the introduction of the Clean Air Acts, damage still continues at a high rate and this may be because the initial crucial damage occurred when levels of sulphur dioxide were still relatively high. Against this, however, damage to coverings made of zinc, which has a comparatively short 'memory' also continues unabated. This suggests that nitrogen oxides whose concentrations have remained much more static, because of the increase in vehicular emissions balancing reductions elsewhere, may play an important role, either on their own or synergistically with the sulphur dioxide.

Additionally, salt blown on the wind from the sea or applied to the roads in freezing weather together with surface cracking of the stonework by frost may also play an important role in the United Kingdom in causing damage, which is especially costly when it happens to historic architectural gems.

Even modern buildings do not escape. Many of the earlier reinforced concrete structures have shown considerable problems of corrosion in recent years. This is largely due to the inadequate understanding of the devastation acid rain could have on the form of concrete used at that time.

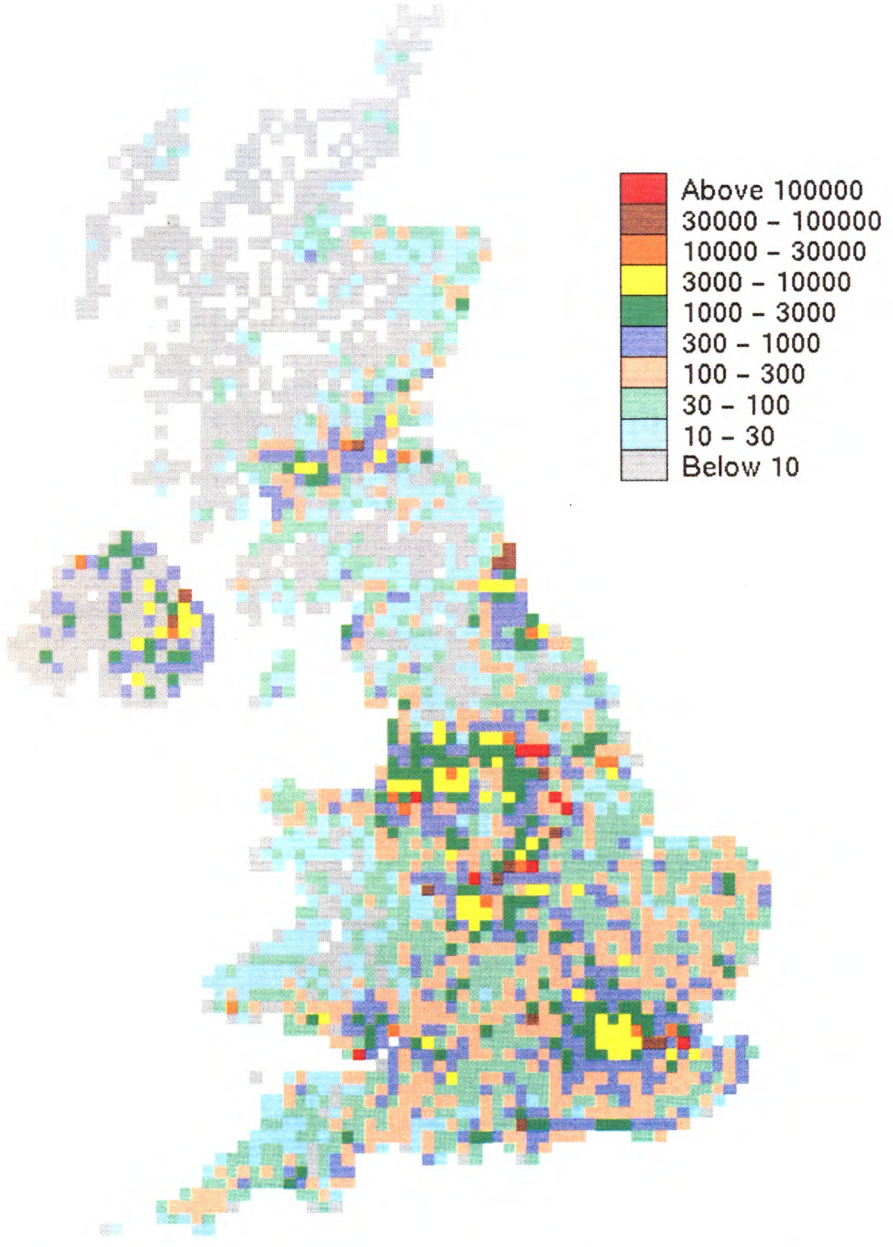

Figure 2. Total sulphur dioxide emissions (metric tonnes) within the United Kingdom for 1987. (Warren Spring Laboratory, 1989, personal communication.)

3. Emissions

Most countries in western Europe make an analysis of the emissions of the common air-pollutants, like sulphur dioxide and the nitrogen oxides, from a wide range of sources within their own country. In the United Kingdom, Warren Spring Laboratory in Stevenage derive annual maps of the emissions of SO_2 and NO_x in 10 km × 10 km Ordnance Survey grid squares. An example is shown in Fig. 2 for 1987. The national total was 3.867 million tonnes of SO_2, showing that after a substantial decrease from the 1970s values the UK emissions are creeping upwards again.

In Europe at least three series of emission maps are prepared on a much coarser grid. One is made by the European Monitoring and Evaluation Programme (EMEP) Western Centre at the Norwegian Meteorological Institute, Oslo, and these maps cover all of Europe on a 150 km × 150 km grid. The second series have been produced in the PHOXA photochemical oxidant project (Klug *et al.*, 1988). Their maps cover a more limited area of western and central Europe. The third series is from the OECD (1989) which covers only those countries in the OECD itself. On a national basis the emissions generally agree to within a few per cent but, on a grid-square basis, differences can be up to 50% or more, especially in east European countries where much less detailed source data are readily available. Note however that since some of the basic input data are common to all these maps, the magnitude of these differences may underestimate the real uncertainties. Figs 3–5 show a section of the latest EMEP maps for SO_2, NO_x and NH_3 for 1985. The largest grid-values tend to lie in a belt extending from central England across Germany into southern Poland and Czechoslovakia,

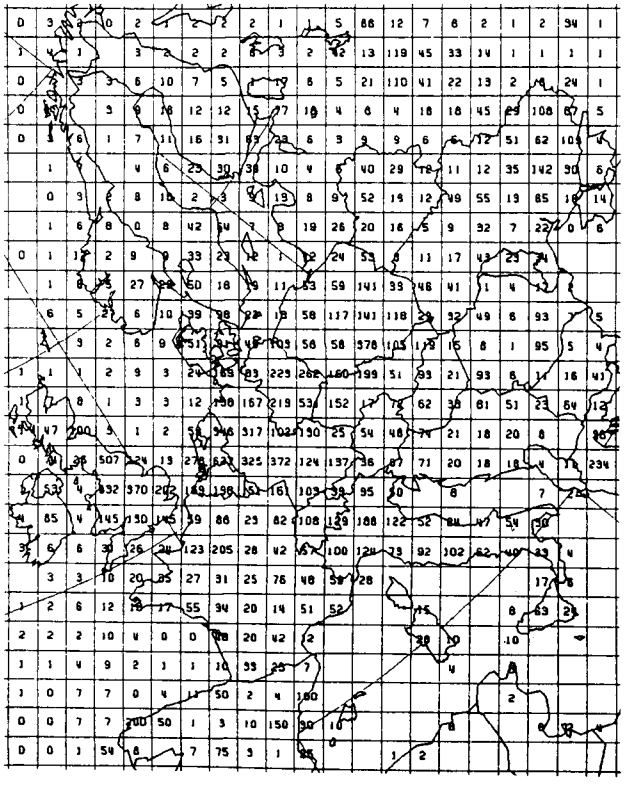

Figure 4. EMEP 1988 emission values (kt a^{-1}) for nitrogen dioxide expressed as equivalent nitrogen (EMEP MSC-W, 1990).

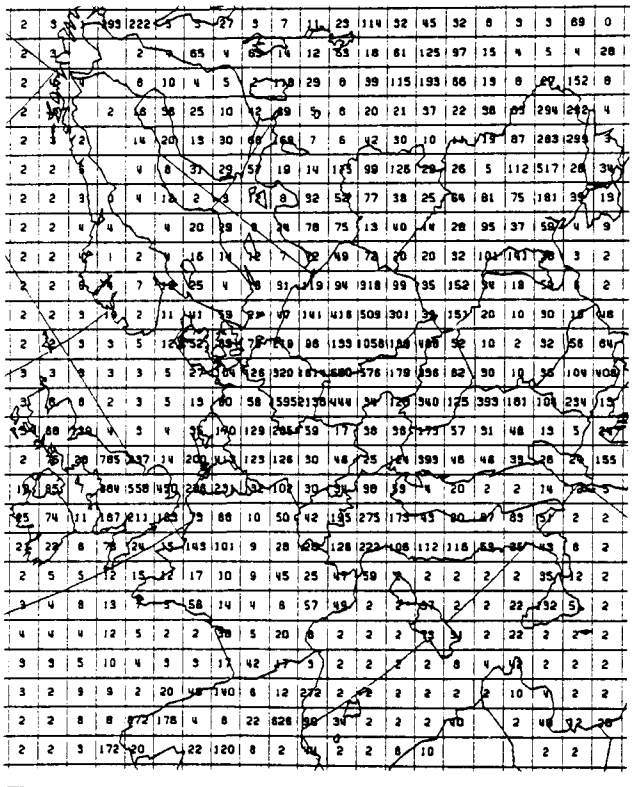

Figure 3. EMEP 1988 emission values (kt a^{-1}) for sulphur dioxide expressed as equivalent sulphur (EMEP MSC-W, 1990).

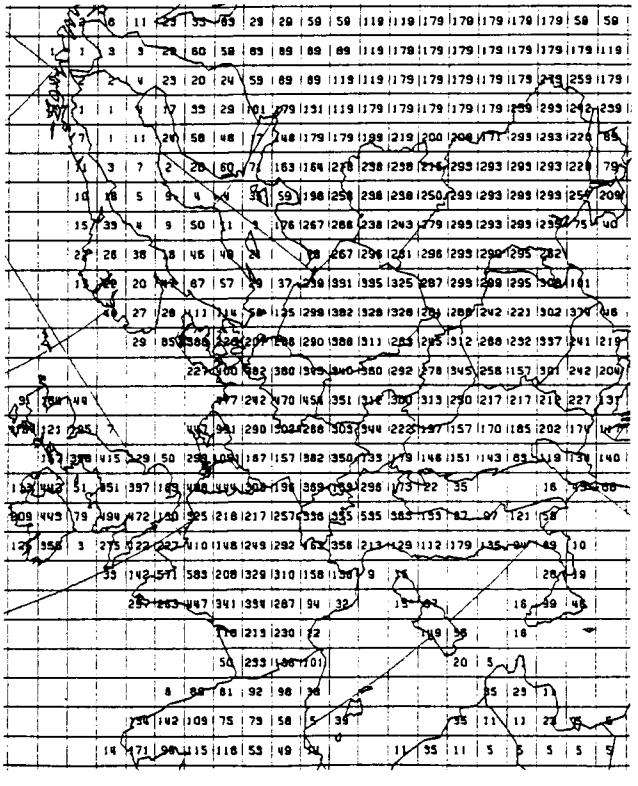

Figure 5. EMEP 1988 emission values (100 t a^{-1}) for ammonia (EMEP MSC-W, 1990).

with other pockets around Rostov in the USSR, northern Spain and in northern Italy.

National emissions of SO_2, NO_x, NH_3, and VOC (volatile organic compounds, which are important in the generation of ozone) are given in Table III in units of kt a^{-1}. In the United Kingdom, roughly 70% of the sulphur emissions are from fossil-fuel power stations. The remainder are from industrial and domestic sources. In the region as a whole, anthropogenic sources dominate, but in late spring and early summer significant amounts of dimethyl sulphide (DMS), and other related sulphur-containing species, are emitted by plankton in the sea, and these are readily oxidized to sulphate. During this period these natural emissions are believed to represent about 30% of the total sulphur depositions in Scandinavia, and are therefore quite significant. Not shown in Table III is that sulphur dioxide emissions peaked in about 1980 and have fallen since then at least in western Europe.

Nitrogen oxide emissions arise mainly from vehicles (typically about 40% of the total in western Europe) and from fossil-fuel power stations. Emissions have risen over the last decade very slowly due to the increase in the number of vehicles.

Ammonia emissions have increased by over 50% since 1950 due to more intensive livestock farming and fertilizer application to crops which then release ammonia in significant amounts during the growing season.

4. Chemical transformations in the atmosphere

Many of the primary pollutants associated with acid rain are subject to chemical transformations in the atmosphere, forming secondary pollutants. Sulphuric acid and nitric acid are formed by oxidants such as ozone, hydroxyl radicals and hydrogen peroxide.

4.1 Formation of oxidants

Ozone occurs naturally, being formed in the stratosphere by ultraviolet light and transported downwards by complex vertical circulations. However, ozone can also be produced within the lower, polluted layers of the atmosphere. Two reactions are principally involved:

Table III. Total national emissions of SO_2 as S, NO_x as N, NH_3 as N and VOC in units of kt a^{-1}, in 1985 (except for the VOC which refer to 1980), taken from Eliassen *et al.* (1988). The last three columns are as follows: emissions of SO_2 in kt a^{-1} per head of population, the position in a table when these emissions per head are ordered in magnitude, and the percentage change in emissions of SO_2 between 1980 and 1985.

Country 1985	SO_2	NO_x	NH_3	VOC	S/hd	Pos.	%
Albania (AL)	25	3	20	—	9	25	0
Austria (AT)	85	66	70	391	11	23	−52
Belgium (BE)	234	117	78	374	24	11	−41
Bulgaria (BG)	570	46	121	—	63	4	+11
Czechoslovakia (CS)	1575	373	165	—	102	2	+2
Denmark (DK)	163	72	109	197	32	8	−26
Finland (FI)	185	73	42	685	39	7	−36
France (FR)	923	515	693	2971	17	18	−48
Germany (East) (DD)	2500	291	200	—	148	1	+25
Germany (West) (DE)	1200	882	361	2724	19	16	−27
Greece (GR)	180	46	93	260	18	17	−10
Hungary (HU)	710	91	125	—	66	3	+2
Iceland (IS)	3	4	2	—	12	22	0
Ireland (IR)	69	21	114	94	20	14	−35
Italy (IT)	1252	485	351	2116	22	12	−35
Luxembourg (LU)	7	7	5	17	19	15	−39
The Netherlands (NL)	138	163	140	534	10	24	−41
Norway (NO)	50	68	34	319	12	21	−29
Poland (PL)	2150	457	394	—	59	5	+4
Portugal (PT)	134	58	45	436	13	20	0
Romania (RO)	100	119	288	—	4	27	0
Spain (ES)	1603	289	224	1786	42	6	−2
Sweden (SE)	135	92	51	1201	16	19	−45
Switzerland (CH)	48	65	51	361	7	26	−30
Turkey (TR)	161	53	575	—	3	28	0
USSR (SU)	5550	892	2619	—	21	13	−13
United Kingdom (GB)	1780	560	394	1746	32	9	−24
Yugoslavia (YU)	588	58	194	—	26	10	0

$$NO + O_3 = NO_2 + O_2.$$

This reaction takes place in sunlight. An equilibrium is established between the two sides of the reaction equation. The second reaction involves reactive hydrocarbons (RH) and forms further NO_2 which disturbs the equilibrium formed in the first reaction and results in a net production of ozone. The second reaction (which strictly is a multi-stage reaction) is as follows:

$$RH + 2NO + 2O_2 \rightarrow \text{carbonyl} + 2NO_2 + H_2O.$$

The carbonyl compounds formed then tend to break down in the presence of sunlight to form hydroperoxyl HO_2 radicals and carbon monoxide.

In the generation of hydroxyl radicals (OHs), two pathways dominate. The first involves ozone and water

$$O_3 + H_2O \rightarrow O_2 + 2OH$$

and requires sunlight; the second involves the HO_2 formed by the reaction described above and NO:

$$HO_2 + NO \rightarrow NO_2 + OH.$$

For the generation of hydrogen peroxide (H_2O_2), some of the hydroperoxyl radicals can recombine to form hydrogen peroxide and oxygen:

$$HO_2 + HO_2 \rightarrow H_2O_2 + O_2.$$

4.2 Oxidation of SO_2 and NO_2

4.2.1 Outside clouds

$$SO_2 + OH \rightarrow HSO_3$$

$$HSO_3 + O_2 \rightarrow HO_2 + SO_3 \rightarrow H_2SO_4.$$

Typically this converts SO_2 to sulphate at an average rate of about 1% per hour.

During the day

$$NO_2 + OH \rightarrow HNO_3$$

converting NO_2 at about 9% per hour.

At night or during the day, conversion is via a multi-stage reaction:

$$2NO_2 + O_3 + H_2O \rightarrow 2HNO_3 + O_2.$$

These two processes dominate nitric acid formation.

4.2.2 In clouds

SO_2 and hydrogen peroxide are both very soluble and form sulphuric acid at a rapid rate independent of the pH:

$$SO_2 + H_2O \rightarrow HSO_3^- + H^+$$

$$HSO_3^- + H_2O_2 \rightarrow SO_4^{2-} + H^+ + H_2O.$$

Two other routes exist which may be important if and when the available hydrogen peroxide has been depleted or is otherwise scarce. The first is through a reaction with less-soluble ozone at a rate which decreases rapidly with decreasing pH, and hence on the presence of other acidic species, like hydrochloric acid, or on alkaline species like ammonia dissolved within the cloud droplets.

The second route is by oxygen (O_2) which may become a significant process due to catalytic iron and manganese ions present after passing sources in major industrial areas.

5. Deposition processes

5.1 Dry deposition

The direct take-up of airborne gaseous or particulate material present in the lowest layers of the atmosphere to the surface or to vegetation by processes of absorption, impaction or sedimentation is called dry deposition, to distinguish it from deposition by precipitation, even though at times dew, cloud droplets or surface water may be involved.

Dry deposition on natural surfaces is very difficult to measure directly, certainly in any routine operational manner. The supposition is usually made that the rate of deposition, or flux (F), is proportional to the concentration in the air just below the surface of height z:

$$F = -v_d C(z).$$

The coefficient v_d has the dimensions of a velocity and is therefore called the deposition velocity. v_d is a slowly varying function of height z, and depends rather critically on the stability of the air. Normally we may assume that v_d is independent of the magnitude of $C(z)$ although the deposition rate of an acidic species on to a damp surface decreases as more of the species (and other acidic species) accumulate in the film.

The deposition velocity for sulphur dioxide has an overall average value of about 0.4 cm s^{-1} whereas that for sulphate aerosol is much smaller at about 0.05 cm s^{-1}.

5.2 Removal by rain and snow

Precipitation tends to be very efficient at removing most acidic species. Moderate rain will often remove more in one hour than dry deposition will over two or more days. Of course rain is a very sporadic event. In the lowlands of England it rains only about 3–4% of the time, and even in wet areas like north-west Scotland it rains only some 8–10% of the time. However wet deposition is usually comparable in importance to dry deposition and in the United Kingdom is typically

responsible for 70–80% of the total deposition of sulphate, for example.

Aerosols and particles can get into precipitation elements either:

(a) by being swept out as the element falls through the air, or

(b) by becoming cloud condensation nuclei for developing cloud droplets which subsequently turn into precipitation elements by coalescence, or

(c) by so-called phoretic effects in which various forces, like electrical forces, act on the particles pushing them towards the droplet.

Finally, particles can enter droplets by

(d) Brownian capture — when the particles are sufficiently small ($<< 0.1\ \mu$m) that they are moved by molecular bombardment and can collide with, and be captured by, larger cloud droplets.

Chemical changes may also be important. For example SO_2, which whilst it is to some extent absorbed directly into raindrops and reaches the ground as SO_2, can undergo oxidation to sulphate (which is a fine aerosol) either before or after being incorporated into rain, as just described. This increases the efficiency of the removal process. The oxidation rate depends not only on the availability of suitable oxidants (like ozone) but also on the relative humidity (or the amount of cloud).

Removal in-cloud is generally called 'rain-out' (even though the precipitation may be in the form of snow), whereas below-cloud removal is usually called 'wash-out'. Rain-out is more efficient than wash-out if the concentration is the same in and below cloud.

If the removal process affects the concentration uniformly over the plume volume, then the concentration decreases according to

$$C_a(t) = C_a(0)\exp(-\Lambda_w t).$$

The resulting concentration in the rain may be expressed in terms of a coefficient ω:

$$C_r = \omega C_a$$

where C_r is the resulting concentration in the rain. If C_a and C_r are expressed in g m^{-3} then ω is usually of the order of 10^5 for wash-out and 5×10^5 for rain-out. If, however, C_r is expressed in g l^{-1} then ω is three orders of magnitude less. Note that ω for wash-out depends on the total depth of the polluted column through which the rain falls. The values quoted refer to a depth of the order of 1000 metres.

5.3 Wet deposition

The resulting wet deposition, D_w, in g m^{-2} is obtained by multiplying the concentration in the rain, in terms of g l^{-1}, by the rainfall R in millimetres.

$$D_w = C_r \times R = \omega C_a R.$$

The wash-out ratio can also be used to define a wet deposition velocity by analogy to the dry deposition velocity (see later).

$$v_w = \frac{\mathrm{d}D_w}{\mathrm{d}t} / C_a = \omega \frac{\mathrm{d}R}{\mathrm{d}t}$$

where t is here time, and the units of v_w are here in m s^{-1}. With light rain falling at a rate of 1 mm h^{-1} and a value of ω of 100, v_w is about 3 cm s^{-1}, which is of the order of a 1000 times greater than the corresponding dry deposition velocity.

Wash-out ratios for snow tend to be severalfold higher than for rain although R for snow is usually less than for rain due to the lower temperatures involved.

Λ is related to ω through the relations:

$$\Lambda = \frac{\omega}{h} \frac{\mathrm{d}R}{\mathrm{d}t}$$

where h is the depth of the polluted layer through which the rain is falling, R is in mm, and t, the time, is in seconds. Assuming $\omega = 100$, $h = 1000$ m, then Λ is approximately $3 \times 10^{-5} R'$ for wash-out and $1.5 \times 10^{-4} R'$ for rain-out, where R' is the rainfall rate in mm h^{-1}. A value of Λ between 3×10^{-5} and 3×10^{-4} has been suggested, consistent with our estimate when both wash-out and rain-out are included and when we allow for heavier rainfall rates.

Note than we have assumed a linear relation between Λ and R. However, some theories and experimental evidence have pointed to a dependence:

$$\Lambda = aR'^{b}$$

where b is not 1 but lies in the range 0.7 to 0.9.

6. Topography

In many maritime regions, the tops of hills are immersed in a capping cloud for a high percentage of the time. This cloud is formed as boundary-layer air is forced up over the hill and the moisture it carries condenses. The cloud usually evaporates again on the downwind side of the hill, so the cloud appears to be stationary although in reality it is in a constant state of regeneration. The concentrations of the major acidifying ions in the cloud droplets are frequently much higher than are typical in normal rain. These droplets, blown by the wind, are rather readily deposited on any trees or vegetation in their path and can contribute significantly to the overall deposition of ions to the ground. This form of deposition is commonly called 'occult' deposition.

Rain also tends to increase with ground elevation so that the rainfall map for the United Kingdom is qualitatively very similar to the physical map showing contours of height above mean sea level, when viewed

Typical concentrations (μ eq. l^{-1})

	Cap cloud	Rain 200 m	Rain 800 m
SO_4^{2-}	100–2000	42	60
NO_3^-	30–2000	45	65
H^+	10–1000	25	40

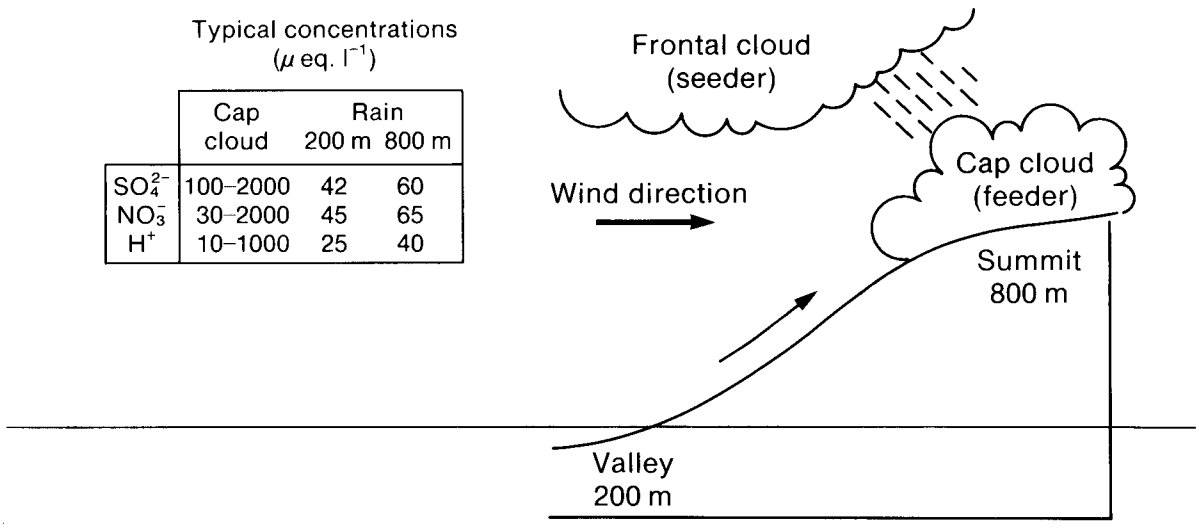

Feeder-seeder mechanism for enhanced rainfall concentrations of major ions in rain.

Figure 6. The influence of hills on the concentration in rain of three of the common ions. Results from the Great Dun Fell study in Cumbria carried out on behalf of the UK Dept of the Environment.

on a large scale. When rain falls from upper cloud (often called the seeder cloud in this context) through the capping cloud beneath (then called the feeder cloud), the rainfall rate is not only increased but the concentration of the acidifying ions also increases. At Great Dun Fell in Cumbria, this effect is being actively studied by several research teams under contract from the UK Department of the Environment. Fig. 6 summarizes some of their earlier findings.

At higher elevations more of the precipitation is in the form of snow. This has an effect on the average pH. Grosch and Georgii (1989) have studied the enrichment of trace elements in snow relative to rain. Anions, like sulphate, are typically increased by some 10–80%, with an observable increase with ground elevation. The enrichment is thought to be due to more efficient below-cloud scavenging by snow resulting from a slower descent rate and a longer residence time, and the filigree structure of snowflakes permitting better scavenging.

7. Concentrations in the air and depositions to the surface

7.1 Monitoring

For Europe, the most complete picture of concentrations and depositions on a day-to-day basis comes from the monitoring station network of the 'Cooperative programme for monitoring and evaluation of the long-range transmission of air pollutants in Europe' — the full title of the EMEP programme described earlier. The programme started in 1977 and is still active today. It replaced an earlier smaller programme covering much of western Europe under the auspices of the OECD. In 1987, 97 stations were participating across 24 countries at which some or all of the species summarized in Table IV were measured (see Schaug *et al.* 1989).

The samples are analysed within the station's own country, but are checked and collated at the Norwegian Institute for Air Research (NILU).

7.2 Modelling studies

Acid rain is concerned with the transport of material typically over distances out to a few thousand kilometres at average speeds of about a thousand kilometres per day. These large time- and space-scales complicate the description of transport considerably. However, models of various levels of complexity can be used to simulate the transport, dispersion, transformation and deposition processes involved. Unlike the monitored data, such models can provide information on the contribution one area of sources makes to the deposition in another country or region.

Determination of the transport of pollution requires a knowledge of wind fields. Most pollution is injected into the boundary layer, the layer of the atmosphere which is closest to the ground and is under its direct influence. The layer is typically several hundred metres deep, but varies considerably from place to place and from one time to another, usually being deepest during the day, especially on a hot sunny day, and being least at night when the air is nearly calm. Many of the earlier models, and many of the simplest models, assume the pollution remains within this well-mixed boundary layer and so can be carried by a single wind which varies only from

Table IV. EMEP's measurement programme in 1987

Gas	SO_2, NO_2, O_3
Particles	SO_4^{2-}
Precipitation	SO_4^{2-}, pH/H^+, NO_3, NH^+_4, Ca^{2+}, K^+, Cl^-, Na^+, Mg^{2+}, conductivity

one location to another, and with time. In reality some of the pollution escapes from the boundary layer into the so-called free troposphere where it may be carried with winds that differ substantially from those in the boundary layer. The most complete models have to take into account the 3-dimensional nature of the wind and do so by using the output of numerical weather prediction models, whether from the analysed fields or from the forecast fields.

Models can use various techniques to follow the pollution. These have been described in, for example, Pasquill and Smith (1983). Eulerian, Lagrangian, spectral and multi-particle stochastic methods have all been employed and details should be sought from the above reference. A further division can be made; models can be statistical, operational on a day-by-day basis, or complex, designed to study special events. Statistical models use statistics of wind, boundary-layer depth and precipitation. They are very simple and their results only have validity over long times — a year or longer. Best results are obtained when the sporadic nature of rain is incorporated using simple statistical techniques. Operational models, like that operated within the EMEP programme, use winds at a single level and interpolated data on precipitation and boundary-layer depths. Usually other properties like the rate of dry deposition are parametrized. Their results compare reasonably well with measured data when averaged over several weeks. Complex models are essentially mesoscale models working with quite fine grids which supplement the actual observed data by generating physically plausible data through the 3-dimensional equations of motion and heat and moisture, taking into account the effects of the known local topography. These complex models require a large computing facility and are intended to gain a greater understanding of the nature and importance of some of the difficult processes involved.

One of very simplest of the statistical models which can yield estimates of the deposition one country makes to another is as follows (the form given is specifically for sulphur species, but can be modified for other species):

(1) The average deposition within a country due to its own emissions is:

$$\text{total deposition} = 25E/\sqrt{A}\ \text{gS m}^{-2}\ \text{a}^{-1}$$

where roughly 56% comes from dry deposition and 44% from wet deposition. E is the annual emission of SO_2 in Mt a^{-1} and A is the area of the country in thousands of square kilometres.

(2) The total average deposition in country 1 due to emissions E_2 in country 2 is given by:

Table V. Sulphur budget (kt a^{-1}) for Europe for 1986 from the EMEP model (Eliassen *et al.* 1989). See Table III for explanation of lettering. 'IND' is explained in the text, and 'RE' means residual and 'SUM' is total.

Emitter countries

Receiver countries	AL	AT	BE	BG	CS	DK	FI	FR	DD	DE	GR	HU	IS	IE	IT	LU	NL	NO	PL	PT	RO	ES	SE	CH	TR	SU	GB	YU	RE	IND	SUM
AL	6	0	0	4	0	0	0	0	0	0	2	0	0	0	3	0	0	0	0	0	0	0	0	0	0	0	0	1	0	7	27
AT	0	21	1	2	27	0	0	3	15	10	0	22	0	0	18	0	0	0	17	0	0	0	0	1	0	1	3	15	0	24	185
BE	0	0	49	0	3	0	0	16	5	12	0	0	0	0	0	0	3	0	1	0	0	0	0	0	0	0	11	0	0	9	115
BG	0	0	0	153	2	0	0	0	1	0	1	2	0	0	1	0	0	0	3	0	3	0	0	0	1	12	0	4	0	18	206
CS	0	5	2	2	394	0	0	5	90	18	0	47	0	0	6	0	1	0	89	0	1	0	0	0	0	3	6	11	0	29	713
DK	0	0	1	0	2	31	0	1	11	7	0	0	0	0	0	0	1	0	4	0	0	0	0	0	0	1	9	0	0	9	81
FI	0	0	0	0	6	1	52	1	13	3	0	2	0	0	0	0	0	0	12	0	0	0	4	0	0	55	5	0	0	67	227
FR	0	2	19	1	22	0	0	330	36	42	0	7	0	1	38	0	4	0	14	1	0	47	0	4	0	1	40	7	1	150	768
DD	0	0	5	0	79	3	0	8	678	51	0	3	0	0	2	0	3	0	35	0	0	0	0	0	0	2	15	2	0	25	915
DE	0	4	22	1	62	3	0	46	137	331	0	10	0	0	14	1	12	0	36	0	0	2	0	2	0	2	47	5	0	71	813
GR	0	0	0	19	0	0	0	0	0	0	45	0	0	0	3	0	0	0	0	0	0	0	0	0	3	4	0	1	0	25	106
HU	0	3	0	5	21	0	0	0	7	2	0	190	0	0	7	0	0	0	14	0	2	0	0	0	0	3	1	28	0	16	303
IS	0	0	0	0	0	0	0	0	0	0	0	0	0	0	0	0	0	0	0	0	0	0	0	0	0	0	0	0	0	15	16
IE	0	0	0	0	1	0	0	1	2	1	0	0	0	16	0	0	0	0	1	0	0	0	0	0	0	0	10	0	0	25	62
IT	0	3	0	4	8	0	0	11	8	5	2	9	0	0	394	0	0	0	5	0	0	5	0	2	0	1	3	19	1	83	569
LU	0	0	0	0	0	0	0	2	0	1	0	0	0	0	0	1	0	0	0	0	0	0	0	0	0	0	0	0	0	1	7
NL	0	0	11	0	3	0	0	8	9	30	0	0	0	0	0	0	29	0	1	0	0	0	0	0	0	0	20	0	0	10	127
NO	0	0	2	0	5	4	1	3	14	10	0	0	0	0	0	0	1	9	7	0	0	0	2	0	0	9	22	0	0	100	193
PL	0	3	4	2	142	4	0	8	235	35	0	30	0	0	6	0	2	0	743	0	1	1	1	0	0	20	15	10	0	50	1317
PT	0	0	0	0	0	0	0	0	0	0	0	0	0	0	0	0	0	0	0	32	0	18	0	0	0	0	1	0	0	20	75
RO	0	0	0	21	17	0	0	1	11	2	0	31	0	0	5	0	0	0	23	0	35	0	0	0	1	32	1	26	0	41	250
ES	0	0	1	0	3	0	0	19	5	4	0	1	0	0	6	0	0	0	2	7	0	510	0	0	0	0	5	0	2	85	655
SE	0	0	2	0	18	13	6	3	50	16	0	2	0	0	1	0	2	3	30	0	0	0	40	0	0	17	20	1	0	103	331
CH	0	0	1	0	4	0	0	7	4	5	0	2	0	0	17	0	0	0	3	0	0	1	0	8	0	0	2	2	0	15	77
TR	0	0	0	10	1	0	0	1	1	0	4	1	0	0	3	0	0	0	1	0	0	0	0	0	53	14	0	1	0	83	178
SU	0	3	4	14	103	8	22	7	155	34	1	57	0	0	8	0	3	1	265	0	11	1	8	0	22143	29	22	0	412	3319	
GB	0	0	5	0	6	1	0	11	14	11	0	1	0	5	1	0	3	0	6	0	0	2	0	0	0	1	517	1	0	66	655
YU	1	2	0	54	11	0	0	2	6	2	3	30	0	0	32	0	0	0	11	0	3	1	0	0	1	6	1	200	0	71	445
RE	4	4	34	40	86	36	18	112	222	122	24	25	0	15	221	0	26	5	145	10	4	203	19	2	21	184	431	32	9	932	2991
SUM	14	54	166	338	1029	109	101	613	1734	763	86	478	0	45	794	5	95	20	1474	51	65	801	78	22	8625	1412	18	392	16256	415728	
	AL	AT	BE	BG	CS	DK	FI	FR	DD	DE	GR	HU	IS	IE	IT	LU	NL	NO	PL	PT	RO	ES	SE	CH	TR	SU	GB	YU	RE	IND	SUM

deposition over the whole country =
$$= 125 A_1 E_2 \exp(-x/1000)/x$$

in units of thousands of tonnes of sulphur per annum. The distance in kilometres between the centres of the two countries is given by x.

The results of these simple relationships can be compared with the results of the EMEP model. Table V gives a sulphur budget for countries in Europe from the EMEP model only for the year 1986. If the comparison is made then agreement is generally within a factor of 2, which is surprisingly good. Presumably the EMEP results are better than those of the simple model, but even so are still not in perfect agreement with the monitored data when averaged over a year. Fig. 7 shows the measure of the scatter for 1985. Some of this scatter must arise from the inadequacies of the model, but errors in measurement and analysis cannot be ruled out either.

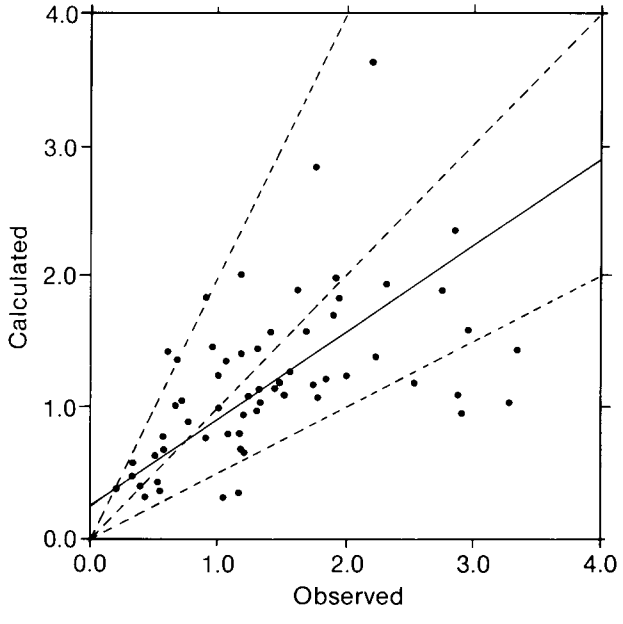

Figure 7. A comparison between observed and calculated sulphate concentrations in precipitation at EMEP monitoring stations for 1985. The pecked lines correspond to a line of perfect fit and 'within a factor of 2' agreement. The continuous line is the best-fit linear regression line.

8. The background or indeterminate contribution

The penultimate column in Table V is labelled 'IND' for indeterminate. This is the contribution from an imposed additional small background concentration of sulphate in rain that has to be added in all rain events in order to get a broad agreement over all of Europe between annual model and observed depositions. It is argued that the origins of this component are threefold:

(a) Sulphur is only tracked for 96 hours in the model and is then lost.

(b) Sulphur that is transported outside the model area is lost but in reality some of it may return and be deposited within the area. Studies of arctic haze have confirmed that this consists in part of acidic species that have reached this remote area along a favoured route that has passed over Europe and has then been advected northwards over Novaya Zemlya in northern USSR with one return path out of the Arctic again near Greenland and back towards Europe. Because of the extreme stability of the air and the low precipitation rates in the Arctic, relatively little of the sulphate load is lost on this long journey.

(c) Sources outside Europe will include natural emissions of dimethyl sulphide, and other sulphur compounds, emitted from plankton in the sea. These emissions are subsequently oxidized to sulphate.

Other sources are man's activities in North America. However it has been estimated in a preliminary study (Iversen *et al.* 1989) that approximately 10% or less of the indeterminate contribution in north-west Europe is of North American origin.

9. Sector analysis

It is to be expected that the highest mean concentrations of the acidic species will often be found at a receptor when the air trajectories have earlier crossed major sources of the corresponding primary pollutants. This is verified by so-called sector analyses in which concentrations at the receptor are related to the direction of the track the air has taken in reaching the receptor. Fig. 8 gives two examples of these averaged concentrations as a 'rose' (akin to a wind-rose). One is for Birknes in southern Norway, the other is for Eskdalemuir in

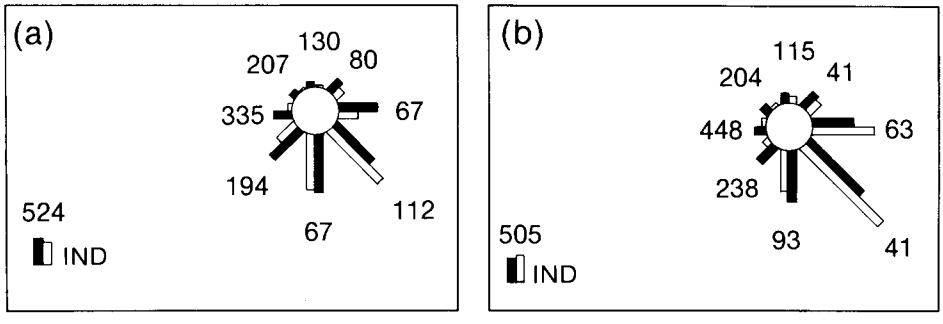

Figure 8. Concentration roses for sulphate in air at (a) Birknes in southern Norway and (b) Eskdalemuir in southern Scotland, showing how air travelling from major European source areas is likely to have the highest concentrations.

southern Scotland. At Birknes the highest concentrations of airborne sulphate are in flows coming from within 45° southerly and south-easterly sectors, that is from continental European areas. Similarly Eskdalemuir experiences its highest concentrations in the south-easterly sector. Annual deposition roses on the other hand show peak contributions in westerly and south-westerly sectors, implying that by far most of the rain comes in these directions and that even though the concentration of sulphate may be small the overall contribution to the deposition is dominant.

10. Episodes

Fish are an example of one part of the environment which can respond dramatically to episodes of acid rain, or more exactly, to acidic flushes of water into their habitat. These flushes usually reflect acid rain although conditions have to be right for this to occur. Three causes are common:

(a) when acidic rain is not modified by soil ion-exchange processes but runs straight off into the streams and lakes because of rocky slopes or frozen ground,

(b) in northern regions when winter snow begins to melt in springtime the first melt-water often carries off most of the acidic species trapped in the snow and runs directly into the streams since the ground is still frozen, and

(c) after a long dry spell rain takes up the accumulation of dry deposited acidic material on the vegetation and soil surface, and produces a highly acidic surge.

Furthermore even the most cursory examination of daily average concentrations or depositions at any monitoring site reveals the large variability in the magnitudes. Indeed, taking wet-deposition data as an example, if the values over a specified period like a year are listed in order of magnitude then the first few values have great importance to the year's total deposition. Smith and Hunt (1979) defined these days with the highest wet depositions which, when summed, account for 30% of the total annual wet deposition as episode-days, and 'episodicity' at that site as the ratio of the number of episode-days to the total number of rainfall days, expressed as a percentage. Fig. 9 gives an example of the definition for a site in eastern England.

The episodicity in Europe usually varies from about 3% to 15%. Confusingly the smaller the episodicity defined this way the more episodic is the character of the depositions. Smith and Hunt define sites as being 'highly episodic' if the episodicity is less than 5% and 'weakly episodic' if it is greater than 10%.

The episodicity shows some continuity between neighbouring sites so that maps can be drawn showing regions of high, medium and weak episodicity. The reasons for this continuity are obviously related to the location of the sites in relation to major source areas and

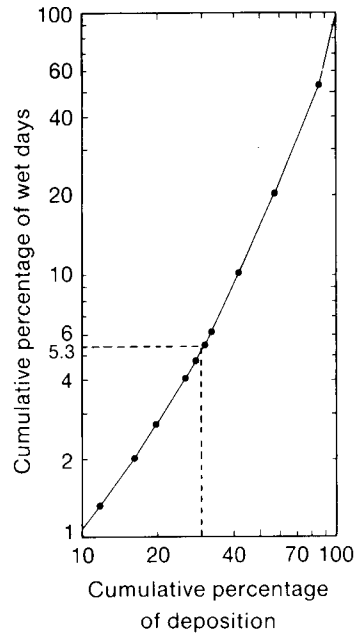

Figure 9. The cumulative percentage of deposition plotted against cumulative percentage of wet days, plotted on logarithmic scales, for Cottered in the eastern Midlands of the United Kingdom for 1974.

the main directions of rain-bearing winds. The episodicity regions do appear to change slowly however in time due to normal fluctuations in climate on a time-scale of several years or decades.

Episodes in concentration at any one site are often associated with similar synoptic situations. Examples are given in Fig. 10 for two of the EMEP monitoring stations. The synoptic situations shown are representative of conditions in approximately half the episodes experienced.

11. Remedial strategies

11.1 Sulphur dioxide

Probably marked changes in emissions can only come about through political legislation resulting from national and international accord, although hand-in-hand with such legislation have to go consideration of the economics, technological advances and perhaps the availability of alternative energy sources. A description of the progress on the political side up to the present time, and possible progress in the future, is beyond the scope of this paper, but an excellent summary is to be found in the Report of the Watt Committee on Energy (1988).

Two main options are available. One is to burn 'sulphur-free' natural gas (mainly methane) instead of coal in new power stations, and perhaps even in some existing stations after conversion. This appears to be the current intent of the Government. The obvious advantage of this policy is that it reduces SO_2 emissions more or less pro rata, the disadvantages are that it both consumes a valuable limited resource which might be

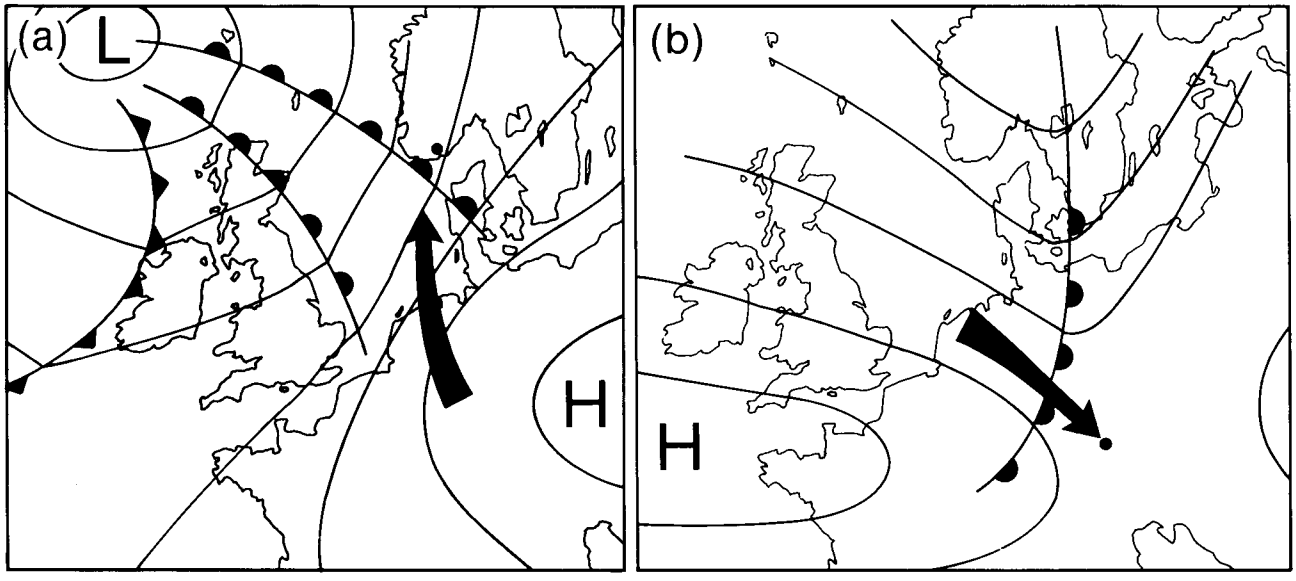

Figure 10. The commonest synoptic situations giving rise to episodes of concentration of sulphate in precipitation in (a) southern Norway and (b) Germany (Smith 1983).

better used, and that it gives a more uncertain future to the coal industry. The second option is to stay with coal as the main fuel and reduce emissions by fitting flue-gas desulphurization (FGD) systems, especially to all new power stations and to some existing large modern stations like Drax in South Yorkshire.

Two FGD systems are under consideration. The first uses lime or limestone and produces gypsum as a byproduct which can be used in the construction industry in the manufacture of cement and wall-board. The second method uses the British Wellman-Lord system which produces sulphur or sulphuric acid which also can be used by industry. This system has the added attraction of being able to reduce emissions of nitrogen oxides as well. The gases are absorbed by activated carbon which can subsequently be made to release the sulphur and nitrogen compounds and be used again.

11.2 Neutralizing additives

A novel suggestion by Dr Byron Lees, a fuel technology consultant, has yet to find full favour in the power-generation industry, although it seems to offer a relatively cheap alternative to FGD if thorny political 'side-effects' could be overcome. His suggestion involves the release of fine magnesium hydroxide powder (about 3 μm average diameter) into the flue gases whenever the airstream is expected to travel towards ecologically sensitive areas, and especially if rainfall is anticipated in those areas on arrival. The Meteorological Office believes, on the basis of preliminary tests, that it could successfully forecast such conditions on an acceptably high fraction of occasions. The magnesium hydroxide can be, and indeed is, produced commercially in the United Kingdom from seawater at a competitive cost of some £240 per tonne. It is very reactive, convenient to handle and non-hygroscopic. Being such a fine powder, little is lost by dry deposition from the atmosphere but it is effectively washed out when precipitation occurs where it can react with its companion sulphuric and nitric acids on the ground. The annual cost for a large power station is estimated to be in the range £10M to £30M, very significantly less than for other systems. It also has the advantage that it could help to correct the depleted levels of natural magnesium often found in many soils in areas badly affected by acid rain, thereby improving the balance of nutrients available to the vegetation.

11.3 Nitrogen oxides

Emissions from large combustion plants can be reduced in one or more of four ways:

(a) burn less fuel through economies,
(b) use less-polluting fuels,
(c) prevent NO_x being formed during combustion.

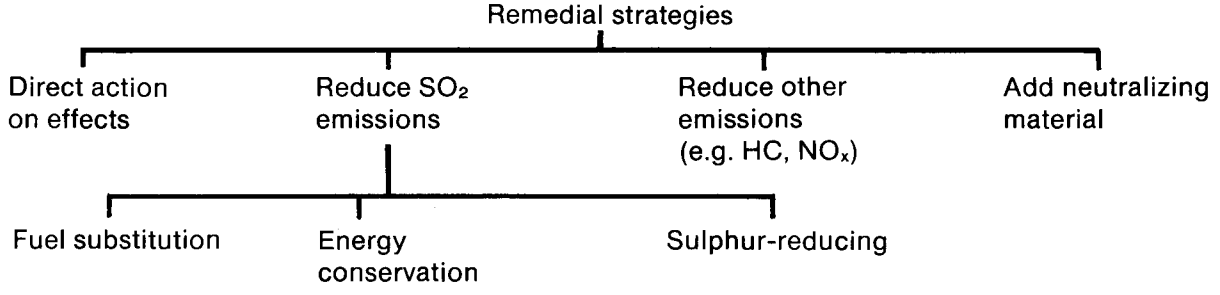

The source of the nitrogen which goes into the NO_x may be partially from within the fuel and partially of atmospheric origin. Keeping combustion temperatures down can reduce the formation of the NO_x, and

(d) remove any nitrogen oxides before the waste gases are released into the atmosphere. In-furnace control technologies can also have a very important impact and much productive research has gone on in this area.

Nitric oxide is also emitted from spark-ignition engined vehicles, along with carbon monoxide, carbon dioxide and unburnt hydrocarbons. In the United Kingdom vehicles contribute roughly 40% of the NO_x emissions and 35% of the volatile organic compounds (the hydrocarbons), some of which are released by evaporation from the fuel tanks, or during refuelling at petrol stations. Solvents and gas leakages are responsible for most of the remaining VOC emissions. Reduction of vehicular emissions is possible by either or both of two approaches:

(a) Catalytic converters which oxidize the combustion products to 'harmless' substances. New EEC regulations will require converters to be fitted to 2-litre engines and above.

(b) Reduced-temperature combustion (RTC) systems. Generally these result in a loss of efficiency.

Lean-burn engines endeavour to reduce emissions through burning weak mixtures of fuel in air in which good mixing has taken place and this leads to a reduction of NO_x formation without a loss in efficiency. However there appear to be limitations to these methods and attempts to overcome them have led to active research into stratified charge engines. One disadvantage of the RTC system is that in reducing NO_x emissions, hydrocarbon emissions are increased and this may tend to enhance the production of ozone in the atmosphere. The addition of a catalytic converter can substantially correct this defect however.

Emissions of nitrogen oxides and hydrocarbons from large diesel engines can be reduced by retarding the injection timing which reduces the combustion temperature at the expense of some loss in efficiency. A second approach involves exhaust-gas recirculation which reduces temperature by increasing the specific heat of the fuel mix.

11.4 Liming

Liming badly affected lakes to correct acidification has been successfully practised in Scandinavia for some years. However many lakes are very inaccessible for application using land-vehicles, especially in the high mountains, and this demands spraying from helicopters — a more costly process. Many have objected, saying the concept runs contrary to the principle of 'polluter pays' taken in its most general sense, and that it is the responsibility of the polluting nations to remove the nuisance. Such views in part reflect the feeling that liming is a possible substitute for emission-reduction. In fact, as Dr Peter Chester (National Power) has argued, liming is not a substitute; both are necessary to restore freshwater vitality. This claim has been supported not only by logical argument but also by a 5-year study at Loch Fleet in Galloway in south-west Scotland carried out by the (as was) Central Electricity Generating Board, the South of Scotland Electricity Board, the North of Scotland Hydro Electric Board and British Coal, with the scientific support of various university and research organizations.

The loch underwent acute acidification in the early 1970s and became fishless, it is believed, in 1975. The study set out amongst other things to discover the response of the lake and its catchment area to various forms of lime treatment. As mentioned earlier in section 2.1, acidity and calcium content of the water are of paramount importance to fish health. If concentrations are expressed in micro-equivalents per litre, then if

$$K = Ca^{2+} - 3H^{+}$$

(an approximate relation) is positive then brown trout will thrive; if negative they may disappear (see Fig. 11).If initially a lake has negative K but the acidifying emissions are substantially reduced, H^{+} concentrations will fall but so will the leaching of Ca^{2+} and the lake may remain with negative K and unable to support fish for many years. If however, sufficient calcium is also added to the catchment area then K will become positive and reintroduced fish have a reasonable chance of persistent survival.

First liming around Loch Fleet was carried out in April 1986 with further liming in other parts of the catchment in 1987. As Fig. 12 shows, the pH and the calcium and inorganic aluminium concentrations all responded beneficially in a very short time and these improvements have persisted. Fish were reintroduced in May 1987. These thrived and spread throughout the

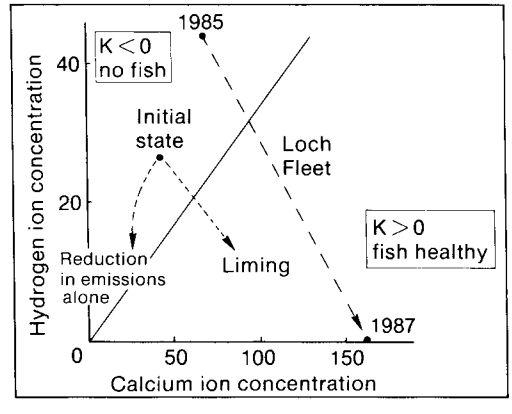

Figure 11. Fish health depends on the hydrogen ion and calcium ion concentrations in the water. Above the diagonal line fish stocks are threatened, below the line they are likely to remain healthy. The arrows show the response of the ions to three scenarios: to a reduction in emissions, to liming, and at Loch Fleet following liming in 1986.

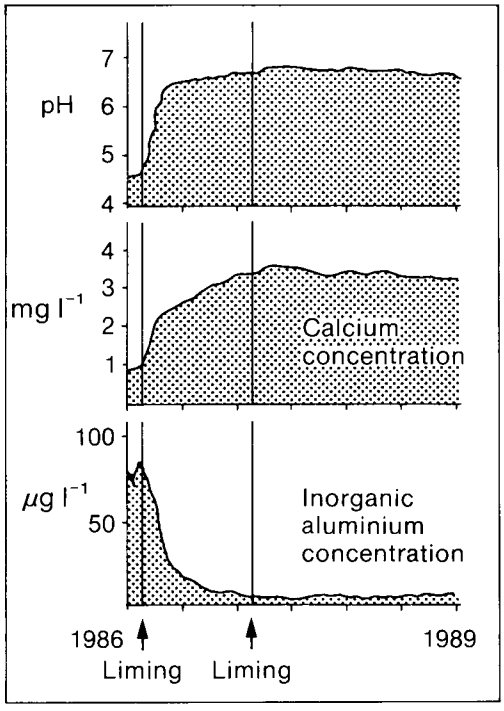

Figure 12. Time response of the concentration of major ions in tributary water at Loch Fleet following liming of the surrounding catchment area (CEGB *et al.* 1989).

lake and downstream. Subsequently trial catches were made in September 1988 and the fish were in excellent condition.

Experience from the project indicates that liming should be applied, preferably at a rate in excess of five tonnes per hectare, and that emphasis should be placed on liming areas that are boggy or have springs, and ensuring that a significant proportion of the dominant run-off water is intercepted. Best results are obtained with fine powder or pelleted limestone or chalk. The cost of liming is not cheap, varying in terms of overall cost between £20 and £70 per tonne, or at least £100–£350 per hectare, for lasting effects. The catchment area of Loch Fleet is some 110 hectares although not all of it need be limed to get excellent results. Assuming that some 200 other lochs in Scotland could also benefit from liming, some with much larger catchment areas, one can see that several million pounds are involved, but this is only a very small addition indeed to the money likely to be needed for desulphurization of emissions in the next 10 years in the United Kingdom.

References and bibliography

Barrett, C.F. and the UK Review Group on Acid Rain, 1983: Acid deposition in the United Kingdom. Stevenage, Warren Spring Laboratory.

Cresser, M. and Edwards, A, 1987: Acidification of freshwaters. Cambridge Environmental Chemistry Series. Cambridge University Press.

CEGB *et al.*, 1989: New life for acid waters; the Loch Fleet project. London, CEGB.

Davies, T.D., Farmer, G. and Barthelmie, R.J., 1988: The contribution of atmospheric circulation variability to the changing pattern of 'acidic deposition' in Europe. Norwich, University of East Anglia.

Eichhorn, J.M., 1989: Interactions between root and crown in 90-year-old spruce under documented conditions of deposition. *In* H.-W. Georgii, (ed.); Mechanics and effects of pollutant-transfer into forests. Dordrecht, Kluwer Academic Publishers.

Eliassen, A., Hov, O., Iversen, T., Saltbones, J. and Simpson, D., 1988: Estimates of airborne transboundary transport of sulphur and nitrogen over Europe. EMEP/MSC-W Report 1/88. Oslo, Norwegian Met Institute.

EMEP MSC-W., 1987: Sulphur budgets for Europe for 1979, 1980, 1981, 1982, 1983, 1984 and 1985. Oslo, Norwegian Meteorological Institute.

—, 1990: Calculated budgets for airborne sulphur and nitrogen in Europe. Oslo, Norwegian Meteorological Institute.

Forestry Commission Research and Development Papers. (Unpublished, copy available from Forestry Commission, 231 Corstorphine Rd, Edinburgh.)

Grosch, S. and Georgii, H.-W., 1989: Deposition by rain and snow — dry deposition on snow. *In* H.-W. Georgii (ed.); Mechanics and effects of pollutant-transfer into forests. Dordecht, Kluwer Academic Publishers.

Hogrebe, A.M.R. and Mengel, K., 1989: Effect of acidic fog on epicutular wax layer and water status of *Picea abies Karst. In* H.-W. Georgii, (ed.); Mechanics and effects of pollutant-transfer into forests. Dordrecht, Kluwer Academic Publishers.

HMSO, 1986: Acidity in United Kingdom freshwaters. Interim Report of the UK Acid Waters Review Group.

—, 1988: The effects of acid deposition on the terrestrial environment in the United Kingdom. First Report of the UK Terrestrial Effects Review Group.

Hoerteis, J. and Schmidt, A., 1986: Die Entwicklung des Gesundheitszustandes der Weisstanne auf 10 Beobachtungsflachen in Ostbayern. *Der Forst- und Holzwirt,* **41**, 580–82.

Iversen, T., Tarrason, L. and Eliassen, A., 1989: Transatlantic sulphur transport. Preliminary estimates from a three-dimensional Eulerian model. EMEP/MSC-W Note 1/89. Oslo, Norwegian Met. Institute.

Iversen, T., Saltbones, J., Sandnes, H., Eliassen, A. and Hov, O., 1989: Airborne transboundary transport of sulphur and nitrogen over Europe — model descriptions and calculations. EMEP/MSC-W Report 2/89. Oslo, Norwegian Met. Institute.

Jaenicke, R., 1989: The deposition of aerosol particles in a forest using an atmospheric residence time model. *In* H.-W. Georgii, (ed.); Mechanics and effects of pollutant-transfer into forests. Dordrecht, Kluwer Academic Publishers.

Klug, W., Goemer, D., and Wortmann, B., 1988: The application of several interregional Air Pollution Models for the simulation of acid deposition in the PHOXA-Programme. Report from the Inst. fur Met., Techn.Hochschule, Darmstadt.

Lubkert, B. and de Tilly, S., 1989: The OECD–MAP emission inventory for SO_2, NO_x and VOC in western Europe. *Atmos Environ,* **23**, 3–15.

OECD, 1979: Programme on the Long Range Transport of Air Pollutants: measurements and findings. Paris, OECD.

—, 1989: Emission inventory for OECD Europe. Report ENV/AIR 87.8 (Third revision). Paris. OECD.

Pasquill, F. and Smith, F.B., 1983: Atmospheric diffusion. Chichester, Ellis Horwood Ltd.

Schaug, J., Hanssen, J.E., Nodop, K., Ottar, B., and Pacyna, J.M., 1987: Summary Report from the Chemical Coordinating Centre for the Third Phase of EMEP. EMEP/CCC Report 3/87. Lillestrom, Norway, NILU.

Schaug, J., Skjelmoen, J.E., Walker, S.E., Harstad, A., and Pedersen, U., 1989: Data Report for 1987, Part 1: Annual Summaries. Lillestrom, Norway, NILU.

Smith, F.B. and Hunt, R.D., 1979: The dispersion of sulphur pollutants over western Europe. *Philo Trans R Soc London.* **A.290.** 523–542.

Smith, F.B., 1983: Conditions pertaining to high acid concentrations in rain. Proc. of V.D.I. Conference on 'Acid Precipitation — Origin and Effects', FRG, Lindau.

Stonehouse, B. (ed.), 1986: Arctic air pollution. Cambridge University Press.

Watt Committee on Energy Ltd., 1988: Air pollution, acid rain and the environment. ed. K.Mellanby. Amsterdam, Elsevier.

551.506.1(41-4)

The summer of 1990 in the United Kingdom

G.P. Northcott
Meteorological Office, Bracknell

Summary

Despite a somewhat cool, dull and wet period during June and the first half of July, the summer as a whole turned out to be warmer and drier than normal over England and Wales and eastern Scotland, although wetter than usual in the rest of Scotland.

1. The summer as a whole

The summer was warmer than average over the whole United Kingdom, with temperatures ranging from near average in parts of the north-west to 1.5 °C above average in the Midlands. Summer rainfall amounts were below average nearly everywhere in England and Wales, parts of the Border Region, eastern Scotland and the central Highlands, but above average elsewhere in Scotland and in Northern Ireland, ranging from 143% of average at Cape Wrath, Highland Region to less than half the average in some central and south-eastern areas of England. Despite the dull June the summer as a whole was sunnier than average nearly everywhere, and sunshine totals ranged from 83% of average in Shetland

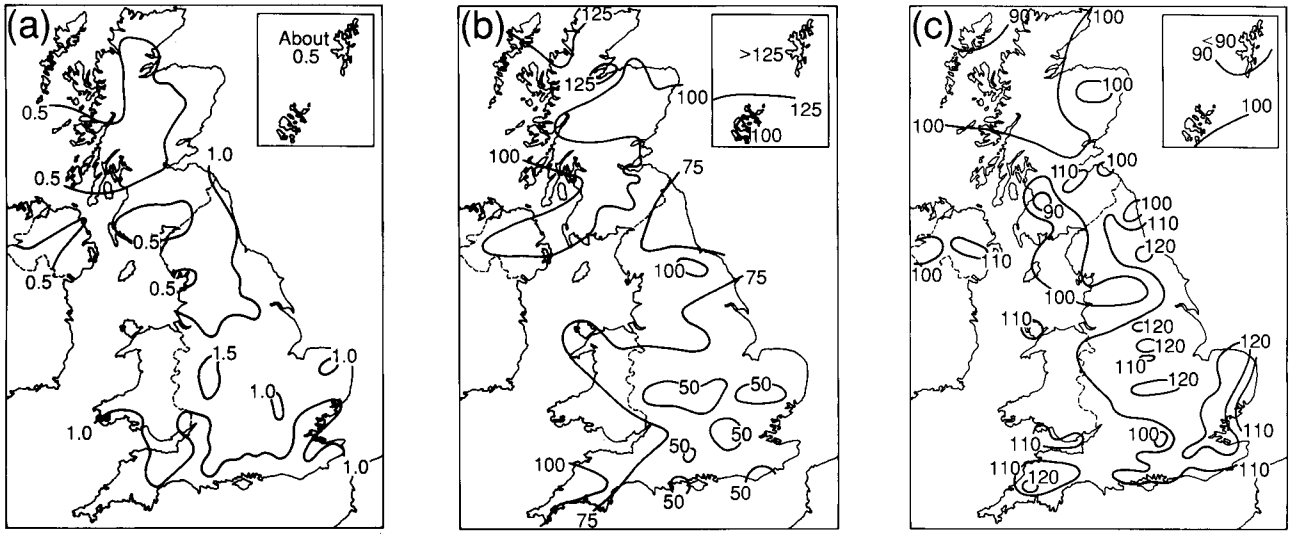

Figure 1. Values of (a) mean temperature difference (°C), (b) rainfall percentage and (c) sunshine percentage for summer, 1990 (June–August) relative to 1951–80 averages.

Table I. District values for the period June–August 1990, relative to 1951–80 averages

District	Mean temperature (°C)	Rain-days	Rainfall	Sunshine
	Difference from average		Percentage of average	
Northern Scotland	+0.6	+1	106	101
Eastern Scotland	+0.6	−1	96	102
Eastern and north-east England	+1.0	−1	78	115
East Anglia	+1.1	−3	58	118
Midland counties	+1.2	−3	64	111
South-east and central southern England	+1.2	−3	59	114
Western Scotland	+0.4	−3	106	100
North-west England and North Wales	+0.9	−1	78	105
South-west England and South Wales	+1.0	0	87	110
Northern Ireland	+0.7	+2	113	108
Scotland	+0.5	+1	104	101
England and Wales	+1.1	−2	72	112

Highest maximum: 37.1 °C in Midland counties in August.
Lowest minimum: 0.3 °C in northern and eastern Scotland in June.

to more than 120% of average in some, mainly eastern, areas of England.

Information about the temperature, rainfall and sunshine during the period from June 1990 to August 1990 is given in Fig. 1 and Table I.

2. The individual months

June. Mean monthly temperatures were below normal nearly everywhere, apart from the far north of Scotland, the Western Isles, Orkney, Shetland, the Channel Islands, and one or two places on the east coast, where temperatures were just above normal. Temperatures ranged from 0.6 °C above normal at Whitby, North Yorkshire to 1.3 °C below normal at Alice Holt and Martyr Worthy both in mid Hampshire. Monthly rainfall totals were above normal nearly everywhere, except in parts of western Scotland, East Anglia, north Devon and east Kent where amounts were below normal, and ranged from more than 280% at Edinburgh to 56% at Cambridge. At the Royal Observatory, Edinburgh, where records go back to 1896, the total of 127 mm was the highest since 1928 and the second highest on record. Monthly sunshine amounts were below average everywhere, except at Tiree, Strathclyde Region where it was just average, and ranged from 100% at Tiree to as little as 51% at Reading, Berkshire.

The month was generally unsettled, with rain at times followed by showers, and thundery outbreaks in most areas, but with a more settled spell from the 11th to 17th, after which unsettled weather returned, although rain fell mainly in northern areas. On the 6th parts of Scotland had the first substantial amount of rainfall for some time. During the night of the 6th/7th rain was very heavy in the Inverness area: at Carrbridge part of the railway embankment was washed away by a swollen burn and the Inverness to London morning express narrowly avoided derailment when it crossed the gaps. Later, on the 21st, there were thundery outbreaks over the Moray Firth, the Firth of Forth and Tynemouth, and on the 22nd over East Anglia, Kent, the south Midlands and the Firth of Forth. On the 23rd a group of thunderstorms in the unstable westerly airstream crossed from Merseyside to East Anglia, but amounts of rainfall were small everywhere. Late on the 27th thundery outbreaks came to much of northern England and the north Midlands; a severe thunderstorm occurred 3 km to the north of Keyworth, Nottinghamshire and there were reports of large hailstones, structural damage caused by lightning, and flooding. On the 30th severe thunderstorms caused cuts in power supplies in a wide area of north-west England, including the Lake District, and the National Garden Festival at Gateshead was hit by a freak thunderstorm.

July. Mean monthly temperatures were above normal everywhere except for one or two locations in the south-east, and ranged from 1.7 °C above normal at places in western Wales to 0.1 °C below normal at Folkestone, Kent. Monthly rainfall amounts were below normal in all areas except the far north-west of Scotland and the Isle of Man, with as little as 8% of normal at Eastbourne, East Sussex, compared with a rainfall amount more than 150% of normal at Stornoway, Western Isles. Southern parts of England and Wales had no significant rain from the 7th for the rest of the month, including Odiham and Farnborough, Hampshire, Easthampstead, Berkshire and Charing, Kent. Monthly sunshine amounts were above average everywhere and ranged from 168% at Aldergrove, Co. Antrim to 107% at Lerwick, Shetland.

The month began with a period of somewhat unsettled weather in northern areas, but more settled weather in southern areas. Early on the 5th an unstable north-westerly airstream covered all areas, with strong winds and some rain in most areas during the day, although amounts were mainly light. Rain fell in many places from the Midlands northwards on the 15th, but it became warm and sunny on the 16th, and southern areas remained so for the rest of the month. However, western and northern areas of Scotland had very small amounts of rain on the 18th, and on the 19th there was a little light rain or showers in western areas. On the 27th it became unsettled in most areas although remaining warm. The month was remarkable for the infrequency of thunder, although some outbreaks did occur, sometimes with hail in places.

August. Mean monthly temperatures were above normal nearly everywhere in the United Kingdom, ranging from 0.1 °C below normal at Dall, Tayside Region to 3.4 °C above normal in Cambridgeshire. The mean minimum temperature at Valley, Gwynedd was the highest there since records began in 1941 and equals the highest minimum values measured at nearby Holyhead in 1911 and 1933. Temperatures reached 32 °C in parts of the Home Counties on the 1st, and on the 3rd a temperature of 37.1 °C was measured at Cheltenham, Gloucestershire, the highest temperature recorded at an officially accredited station since records began. On the night of the 3rd/4th a minimum temperature of 24 °C was recorded at Brighton, East Sussex and in central London. Monthly rainfall totals were below normal everywhere except for parts of Northern Ireland and western and northern areas of Scotland, where they were above normal, and ranged from 153% at Lerwick, Shetland to as little as 20% at Guernsey, Channel Islands. During the late afternoon of the 6th a moderate shower gave 16.5 mm of rain at Wilsden, West Yorkshire. Most places had some rain on the 14th: for some places in southern England this rain ended a period of 38 days with no significant rainfall, the last having been recorded on 6 July. Monthly sunshine amounts were generally above average over most of England and Wales, but below average over most of Scotland and Northern Ireland, ranging from 154% at Monks's Wood, Cambridgeshire to 65% at Fort

Augustus, Highland Region. Brooms Barn, Suffolk reported the sunniest August at the station for over 40 years.

After four very hot days at the beginning of the month it became cooler with patchy rain from time to time in northern areas, but remained very warm in parts of East Anglia and south-east England until the 14th, when it became generally cooler and unsettled, with rain at times and a good deal of thundery activity. Thunderstorms occurred at Wick, Highland Region on the 14th, over the Midlands and East Anglia on the 15th, over much of central and south-eastern England and East Anglia on the 16th, and over East Anglia on the 19th. Further thunderstorms developed over North Wales and northern England on the 24th, with isolated thundery showers over central and southern England, and over the Channel Islands and parts of eastern Wales and Somerset later. Thundery outbreaks occurred in parts of south-east England and East Anglia on the 25th and 26th, and more extensively in eastern areas of England on the 29th.

Satellite and radar photographs — 8 March 1991

During 7 March 1991, cyclogenesis occurred over Iberia, resulting in a deep low which gradually moved northwards towards the British Isles. Fig. 1(a) shows this low pressure system as seen on the AVHRR visible image taken at 0749 UTC on 8 March, when a distinctive spiral cloud pattern was centred just north of Brittany. The surface analysis for 0600 UTC (inset) confirms the position of the low centre. The low sun angle reveals a great deal of detail in the image through shadow and highlight effects. For example, the high cirrus cloud at W can be seen to have a wispy texture, contrasting with the lumpy texture of the cloud at B to the north and east, which is more convective in nature. Near the centre of the system, where the air is most unstable, the edges of cumulonimbus clouds can be seen lit

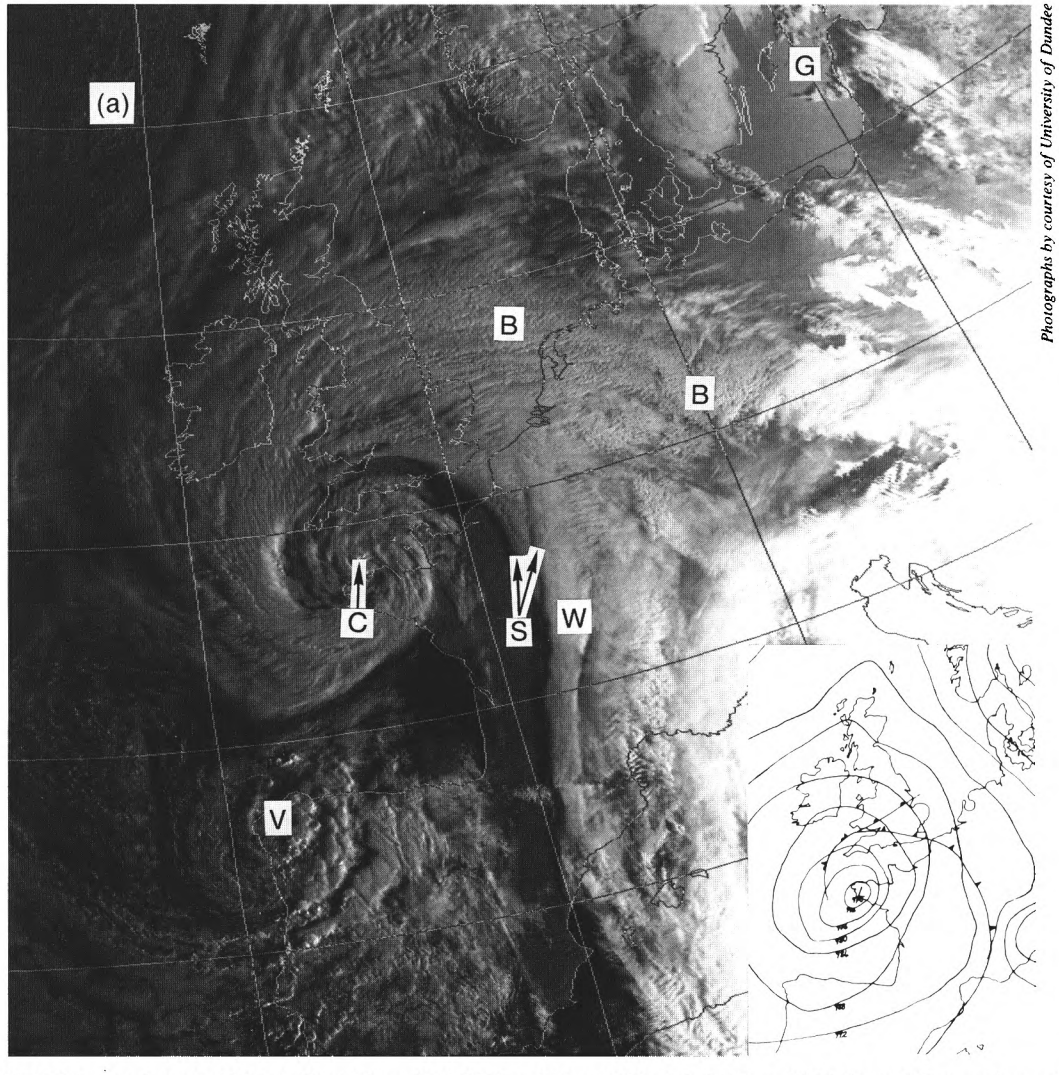

Figure 1. AVHRR images from the NOAA-10 satellite at 0749 UTC on 8 March 1991, (a) visible, and (b) infra-red. See text for explanation of lettering. The surface analysis for 0600 UTC is inset.

Figure 1. Continued.

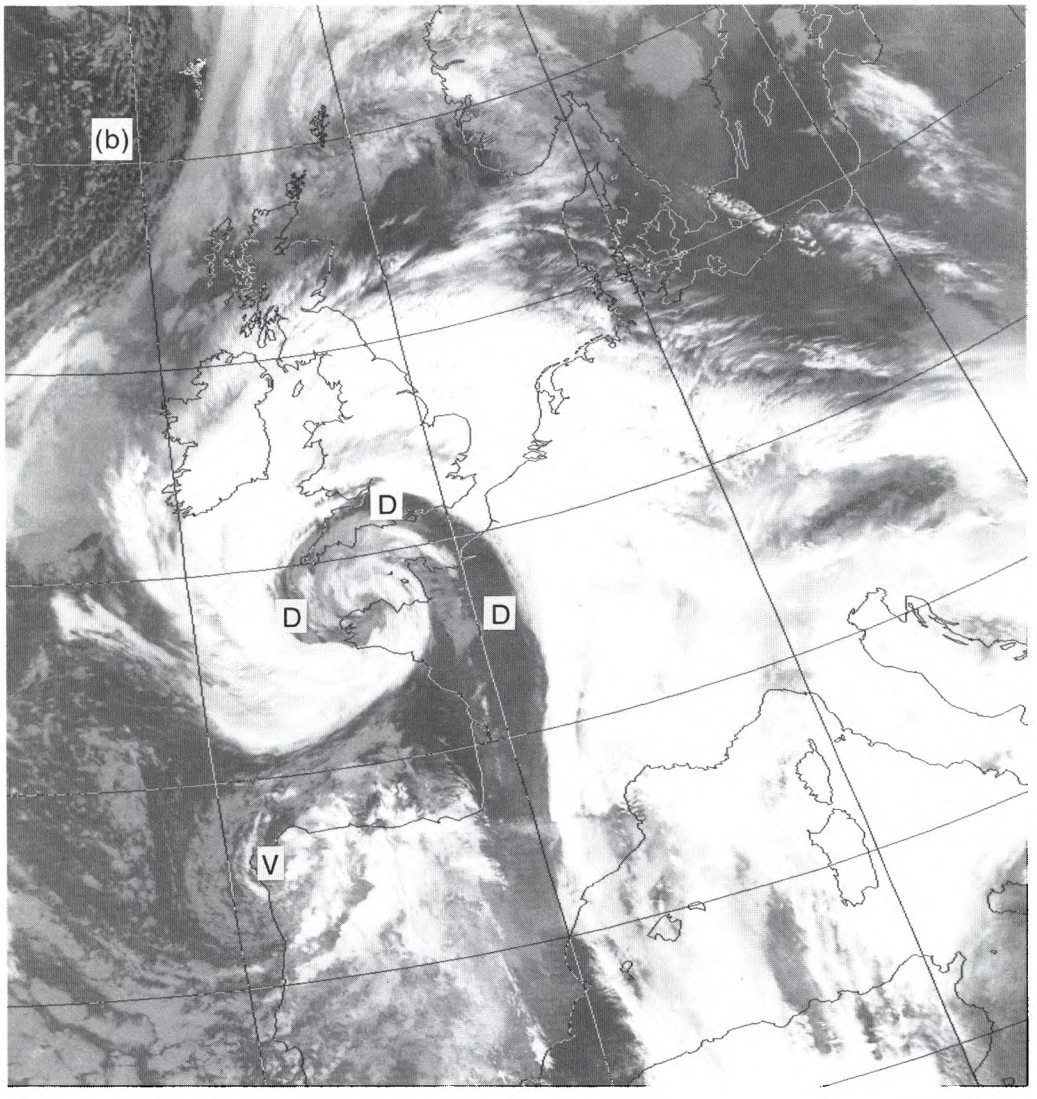

up at C. Note the two lines of shadow at S, both where the high cloud casts a shadow on lower mid-level cloud and again where the mid-level cloud casts a shadow on the ground. The sharpness of the cloud edge near these shadows can be seen better on the infra-red image for the same time, Fig. 1(b); west of the cloud edge is a mostly cloud-free slot D–D–D which spirals right in to the centre of the system.

The COST-73 European radar rainfall composite picture for 0600 UTC is shown in Fig. 2. The rainfall pattern shows the same spiral shape as the satellite pictures, and the shape of the rainband mirrors the shape of the high cloud just outside the dry slot, although the rainband is further forward that the high cloud edge. Note the high gradient of rainfall rate of the inner edge of the rainband, especially near A where rainfall rates above 10 mm h^{-1} are recorded.

Other features of interest on the images shown here include the loosely-ordered vortex of convective cloud V centred over Cape Finisterre at 0749 UTC (Fig. 1) which has moved to north-eastern Spain by 1428 UTC (Fig. 3). Notice also the area of diffuse sun glint at G on Fig. 1(a), where light from the low sun reflects brightly off the relatively calm waters of the Baltic Sea.

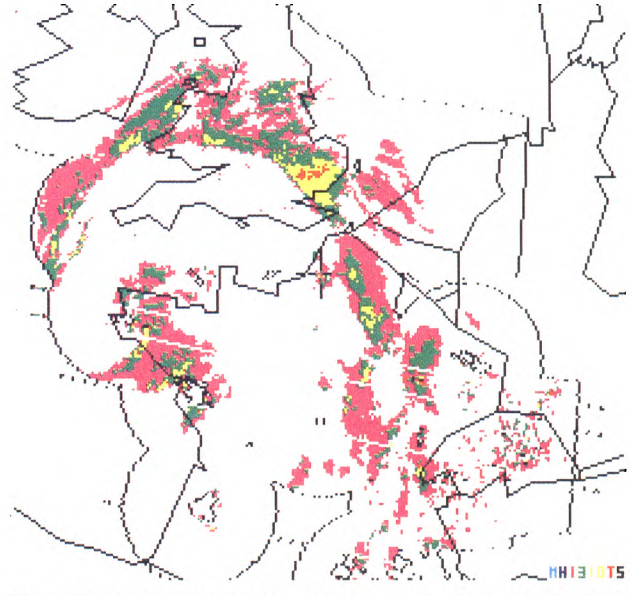

Figure 2. COST-73 European radar composite picture for 0600 UTC on 8 March 1991. Rainfall rates (mm h^{-1}) shown are: pink 0.3–1, green 1–3, yellow 3–10, red 10–30, black > 30. See text for explanation of lettering.

Photograph by courtesy of University of Dundee

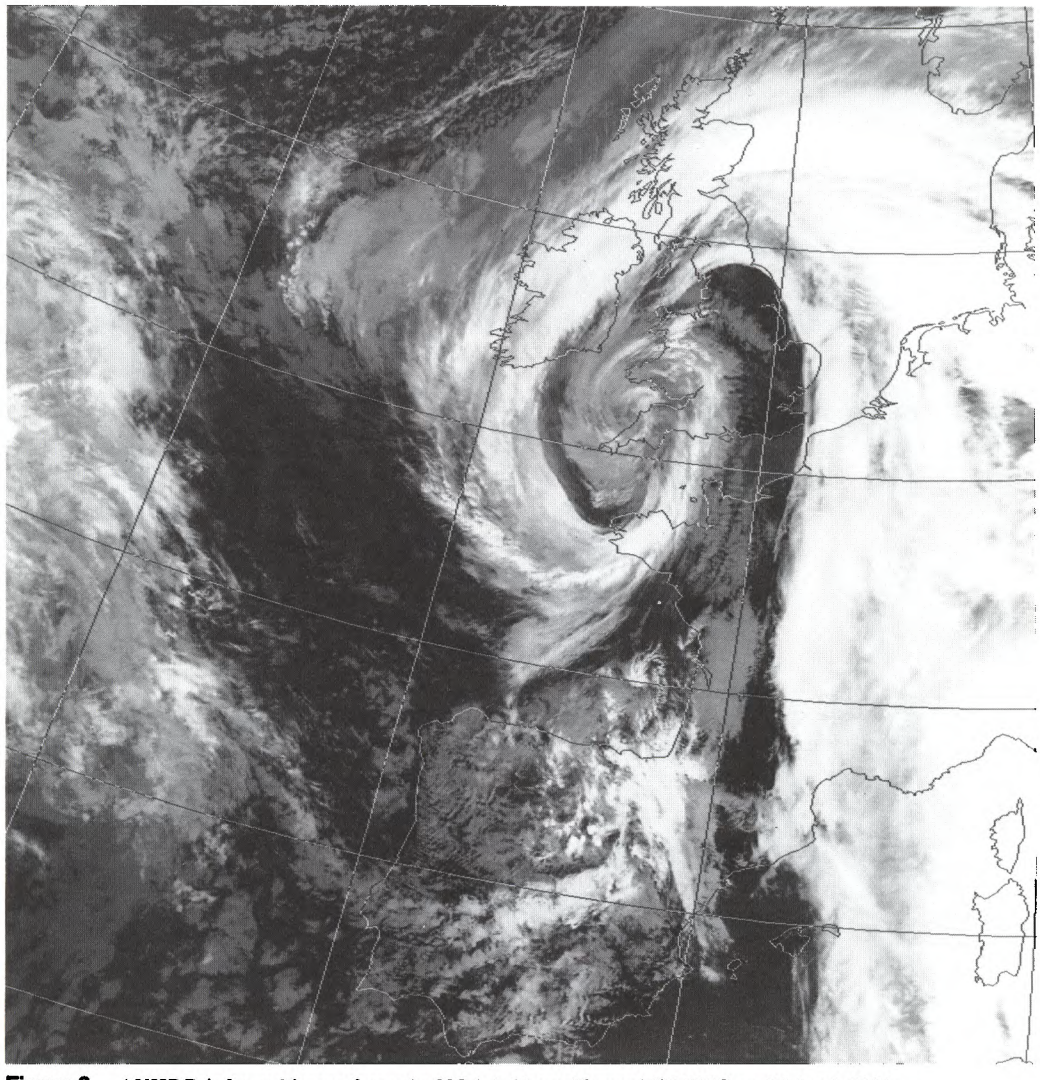

Figure 3. AVHRR infra-red image from the NOAA-11 satellite at 1428 UTC on 8 March 1991.

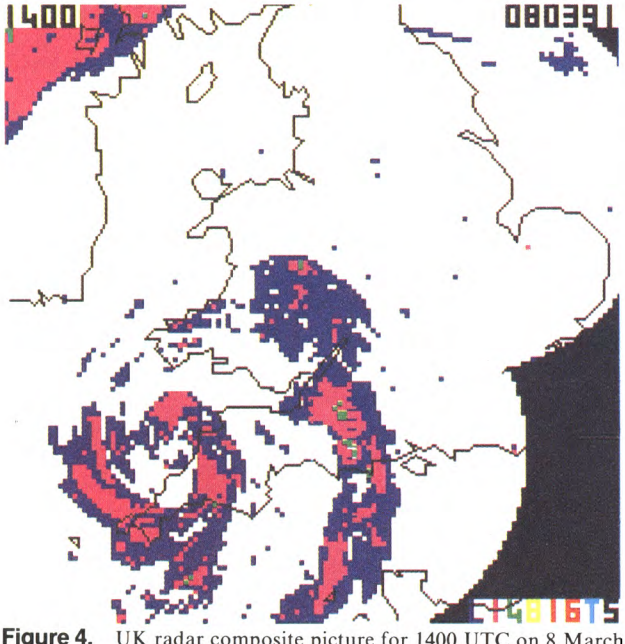

Figure 4. UK radar composite picture for 1400 UTC on 8 March 1991. Rainfall rates (mm h^{-1}) shown are: dark blue 0.1–1, pink 1–4, green 4–8.

The system continued to move northwards during 8 March, tracking across Cornwall and gradually filling. Fig. 3 shows the AVHRR infra-red image for 1428 UTC, by which time the low is centred in the Bristol Channel to the north of the Cornish coast. Surface observations for 1500 UTC suggest that the low has started to fill, but there is still a clear spiral shape to the cloud around the centre of the system. The UK radar rainfall composite picture for 1400 UTC, Fig. 4, shows the rainband also spiralling around the low centre, although the rain is somewhat lighter (mostly below 4 mm h^{-1}). At about this time, severe gales on the south-eastern flank of the system affected parts of south-west England; mean winds of 55 kn were recorded at Torquay at 1200 UTC, with 40 kn still being recorded at 1500 UTC.

R.B.E. Lilley

GUIDE TO AUTHORS

Content

Articles on all aspects of meteorology are welcomed, particularly those which describe results of research in applied meteorology or the development of practical forecasting techniques.

Preparation and submission of articles

Articles, which must be in English, should be typed, double-spaced with wide margins, on one side only of A4-size paper. Tables, references and figure captions should be typed separately. Spelling should conform to the preferred spelling in the *Concise Oxford Dictionary* (latest edition). Articles prepared on floppy disk (Compucorp or IBM-compatible) can be labour-saving, but only a print-out should be submitted in the first instance.

References should be made using the Harvard system (author/date) and full details should be given at the end of the text. If a document is unpublished, details must be given of the library where it may be seen. Documents which are not available to enquirers must not be referred to, except by 'personal communication'.

Tables should be numbered consecutively using roman numerals and provided with headings.

Mathematical notation should be written with extreme care. Particular care should be taken to differentiate between Greek letters and Roman letters for which they could be mistaken. Double subscripts and superscripts should be avoided, as they are difficult to typeset and read. Notation should be kept as simple as possible. Guidance is given in BS 1991: Part 1: 1976, and *Quantities, Units and Symbols* published by the Royal Society. SI units, or units approved by the World Meteorological Organization, should be used.

Articles for publication and all other communications for the Editor should be addressed to: The Chief Executive, Meteorological Office, London Road, Bracknell, Berkshire RG12 2SZ and marked 'For Meteorological Magazine'.

Illustrations

Diagrams must be drawn clearly, preferably in ink, and should not contain any unnecessary or irrelevant details. Explanatory text should not appear on the diagram itself but in the caption. Captions should be typed on a separate sheet of paper and should, as far as possible, explain the meanings of the diagrams without the reader having to refer to the text. The sequential numbering should correspond with the sequential referrals in the text.

Sharp monochrome photographs on glossy paper are preferred; colour prints are acceptable but the use of colour is at the Editor's discretion.

Copyright

Authors should identify the holder of the copyright for their work when they first submit contributions.

Free copies

Three free copies of the magazine (one for a book review) are provided for authors of articles published in it. Separate offprints for each article are not provided.

Contributions: It is requested that all communications to the Editor and books for review be addressed to the Chief Executive, Meteorological Office, London Road, Bracknell, Berkshire RG12 2SZ, and marked 'For *Meteorological Magazine*'. Contributors are asked to comply with the guidelines given in the *Guide to authors* which appears on the inside back cover. The responsibility for facts and opinions expressed in the signed articles and letters published in *Meteorological Magazine* rests with their respective authors.

Subscriptions: Annual subscription £33.00 including postage; individual copies £3.00 including postage. Applications for postal subscriptions should be made to HMSO, PO Box 276, London SW8 5DT; subscription enquiries 071–873 8499.

Back numbers: Full-size reprints of Vols 1–75 (1866–1940) are available from Johnson Reprint Co. Ltd, 24–28 Oval Road, London NW1 7DX. Complete volumes of *Meteorological Magazine* commencing with volume 54 are available on microfilm from University Microfilms International, 18 Bedford Row, London WC1R 4EJ. Information on microfiche issues is available from Kraus Microfiche, Rte 100, Milwood, NY 10546, USA.

May 1991

Edited by Corporate Communications
Editorial Board: R.J. Allam, R. Kershaw, W.H. Moores, P.R.S. Salter

Vol. 120
No. 1426

Contents

ISSN 0026–1149

ISBN 0-11-728856-X

9 780117 288560

Printed in the United Kingdom for HMSO
Dd 0291241 5.91 C13 503 12521

The Meteorological Magazine

June 1991

'Wet' stack plume analysis
Observations in climate study
L.G. Groves Awards

HMSO

Met.O.998 Vol. 120 No. 1427

First published 1991

HMSO publications are available from:

HMSO Publications Centre
(Mail and telephone only)
PO Box 276, London, SW8 5DT
Telephone orders 071-873 9090
General enquiries 071-873 0011
(queuing system in operation for both numbers)

HMSO Bookshops
49 High Holborn, London, WC1V 6HB 071-873 0011 (counter service only)
258 Broad Street, Birmingham, B1 2HE 021-643 3740
Southey House, 33 Wine Street, Bristol, BS1 2BQ (0272) 264306
9–21 Princess Street, Manchester, M60 8AS 061-834 7201
80 Chichester Street, Belfast, BT1 4JY (0232) 238451
71 Lothian Road, Edinburgh, EH3 9AZ 031-228 4181

HMSO's Accredited Agents
(see Yellow Pages)

and through good booksellers

3 8078 0010 2471 2

The Meteorological Magazine

June 1991
Vol. 120 No. 1427

551.551.8:628.53

An analysis of a 'wet' stack plume

F.B. Smith
Meteorological Office, Bracknell

Summary

How to calculate the visible length and ground-level concentrations resulting from a wet polluted plume emanating from an elevated stack is illustrated. In this example the stack is assumed to be on the outskirts of a fictitious town called Midville. It operates only during daytime, on a small slope within a housing area — typical of many such installations.

1. Introduction

It is assumed that an authority in Midville (somewhere in the Midlands of England) is proposing to build a new municipal incinerator with a stack for waste gases. The gases will contain sufficient water vapour to form a visible condensed plume which will be of potential concern to the local inhabitants.

The aims of the analysis in this paper can be summarized as:

(a) To determine the visible length of the plume in different weather conditions. The higher the humidity of the ambient air and the lower its temperature, the more slowly do the fine drops in the stack plume evaporate. Wind speed is also important since the stronger the wind the sooner, in terms of downwind distance, does the plume evaporate.

(b) To determine the maximum ground-level concentration of each significant pollutant contained in the plume, as measured over several minutes — say 10 minutes, wherever it may occur, as a function of stack height and weather conditions.

(c) To determine where these maximum concenations occur.

(d) To determine whether or not any surrounding houses are at risk from the effluent gases and what remedial action needs to be taken.

2. A list of the basic parameters

Values of the key parameters will be given the following values by way of illustration:

The temperature of the effluent gases at the stack top = 140 °C.

The efflux velocity (determined by a fan) = 15 m s^{-1}.

Maximum gas flow rate = 600 N m h^{-1}.

Internal stack diameter = 370 mm.

Water mixing ratio at the stack top = 0.3.

The stack height can be chosen to give least nuisance, remembering that local inhabitants will tend to object to a tall unsightly stack even more than to the occasional odour. Calculations are made for 16 m, 20 m and 23 m. Extreme values of 10 m and 30 m are also considered.

The effluent gas will contain a mixture of substances including hydrochloric acid (HCl), sulphur dioxide (SO_2), nitrogen oxides (NO_x) and carbon monoxide (CO). The assumed emission rates are: HCl 300 g h^{-1}, $SO_2/NO_x/CO$ 600 g h^{-1}.

3. The visible length of the plume

The gases rising up the stack contain a considerable amount of water which rapidly condenses on leaving the stack, giving a visible plume. As the plume broadens by turbulent mixing with the environmental air, drier and

colder air is mixed with the moist, stack air. This cools the plume, tending to retard its evaporation, but also dries it. How long the plume remains visible before this drying-out process results in total evaporation depends on the temperature and humidity of the environmental air. It also depends on the amount of natural turbulence in the air, which in turn depends on the stability of the lower atmosphere. The more stably stratified the air becomes, the lower is the level of turbulence and the slower the drying out of the plume.

The equations governing this process are now set out:

Let a = the emission of air = $1.67 \times 0.00127 \times 10^6$ g s^{-1} = 2.12×10^3 g s^{-1}, and

b = the emission of water = $0.3 \times 2.12 \times 10^3 = 0.64 \times 10^3$ g s^{-1}.

Define s = moisture content of the environmental air as a mixing ratio in g g^{-1}.

The total water emission is thus $(b + as)$ g s^{-1}, and the total dry air emission is $(1-s)a$ g s^{-1}.

The specific heat of air at constant pressure = 0.24, and that of water vapour = 0.48.

If, at a distance x downwind of the stack, the mass of entrained environmental air = m g, if T_f = the exit gas temperature = 140 °C, T_a = the temperature of the environmental air, T = the temperature of the plume at x, and S = the mixing ratio of the plume at x, then:

H_f = heat content of the flue gases = $(0.24(1-s)a + 0.48(b + sa))T_f$, where $a = 2120$, $b = 640$, and $T_f = 140$.

W_f = the water content of the flue gases = $(b + sa)$.

H_e = the heat content of the entrained air = $(0.24(1-s)m + 0.48\,sm)T_a$.

W_e = the water content of the entrained air = sm (which is a function of s and x).

H_p = the heat content of the plume = $T(0.24(1-s)(a+m) + 0.48(b + sa + sm))$.

W_p = the water content of the plume = $(a + b + m)S$.

Now $H_p = H_f + H_e$, so that $((1+s)a + 2b)(T_f - T) = (1+s)m(T - T_a)$.

Similarly $W_p = W_f + W_e$, so that $(a+b)(S_f - S) = m(S - s)$, where S_f is the water content of the flue gas = 0.3.

If we eliminate m from these two equations we arrive at the 'Mixing Curve' equation:

$$\frac{(1+s)a + 2b}{a+b}\left(\frac{T_f - T}{S_f - S}\right) = (1+s)\left(\frac{T - T_a}{S - s}\right).$$

Now after some mixing has occurred, certain simplifications can be made to this equation. We may assume that $T_f \gg T$, $S_f \gg S$ and $s \ll 1$. The Mixing Curve equation then simplifies to:

$$S - s = A(T - T_a)$$

where $A = (a+b)S_f/(a+2b)T_f = 0.00174$ if the values previously given are inserted. Strictly this value of A applies when $T = 0$. At $T = 10$ a more accurate value of A is 0.00187, and at $T = 20$ A is 0.00203. Now s is the mixing ratio of the environmental air and may be expressed as $rs_e(T_a)$, where s_e is the saturated mixing ratio at temperature T_a. If T_a is expressed in degrees Celsius then a good fit to $s_e(T_a)$ is given by:

$$s_e(T) = 10^{-3}(3.839 + 0.3008T + (0.00556T^2 + 0.0003587T^3)$$

r is the relative humidity (expressed as a fraction, not as a percentage).

The value of the plume temperature when the plume is on the point of evaporation is found by an iterative process. To begin, assume $T = T_a$. Insert this into the equation for s_e and find s_e. Insert this into the simplified mixing curve equation and find a new T. Repeat again and again until the solution converges to a constant value of T, and a corresponding value of S.

To find at what distance this occurs we must define how rapidly the plume broadens with distance. During the daytime, the plume will only persist a significant distance downwind in very humid conditions (when r is only a little less than 1). Such conditions occur in neutral stability conditions when the instantaneous plume width grows like:

$$R(x) = R(0) + 0.176x$$

where $R(x)$ is the radius (in metres) and x is the downwind distance, also in metres. The formula is consistent with the plume acting as a cone with a half-angle of about 10°. To find $R(0)$, we equate the volume flux emerging from the stack with the effective volume flux assuming the plume reaches its effective source height very rapidly and thereafter behaves like a horizontal plume being carried by the wind:

$$U\pi R^2(0) = \frac{a+b}{\rho}$$

where ρ = the air density = 1270 g m^{-3}.

Remembering that m is the mass of entrained air, an earlier equation gives

$$m = \frac{(a+b)(S_f - S)}{S - s} = \frac{0.3(a+b)}{0.0019(T - T_a)}$$

approximately. The total mass of the plume $M = m + (a+b) = 1270\pi R^2 U$. These equations relate the plume temperature T to distance x, and hence tells us the distance when the plume evaporates. These distances are given in Table I.

The figures summarize the results. Fig. 1 shows the saturation curve as a function of air temperature and its mixing ratio. The graph also shows a sample of 'mixing curve' lines which are virtually straight over the range of temperatures shown. Thus a plume from the stack emerging into an airstream whose temperature is 10 °C and relative humidity is 0.5 (as a fraction), evaporates when its temperature has fallen to 13 °C.

Table I. A table of the distances x, in metres, at which the plume from the stack evaporates, as a function of ambient temperature T_a, relative humidity r, and wind speed U (m s^{-1}) measured at 10 metres above ground

T_a	r	T_{evap}	$U=1$	$U=3$	$U=5$	$U=7$	$U=10$
0	0.4	1.45	44.9	25.9	20.1	17.0	14.2
	0.6	0.96	56.0	32.3	25.0	21.2	17.7
	0.8	0.48	81.1	46.8	36.3	30.6	25.6
	0.9	0.24	116.6	67.3	52.1	44.1	36.9
	0.95	0.12	166.8	96.3	74.6	63.0	52.7
	0.98	0.05	266.4	153.8	119.1	100.7	84.2
5	0.4	7.22	35.4	20.4	15.8	13.4	11.2
	0.6	6.47	44.4	25.7	19.9	16.8	14.1
	0.8	5.73	64.8	37.4	29.0	24.5	20.5
	0.9	5.36	93.7	54.1	41.9	35.4	29.6
	0.95	5.20	134.4	77.6	60.1	50.8	42.5
	0.98	5.07	215.3	124.3	96.3	81.4	68.1
10	0.4	13.53	27.2	15.7	12.2	10.3	8.6
	0.6	12.31	34.6	20.0	15.5	13.1	10.9
	0.8	11.14	51.1	29.5	22.9	19.3	16.2
	0.9	10.57	74.4	42.9	33.3	28.1	23.5
	0.95	10.28	107.2	61.9	48.0	40.5	33.9
	0.98	10.11	172.4	99.5	77.1	65.2	54.5
15	0.4	21.22	19.5	11.3	8.7	7.4	6.2
	0.6	18.93	25.6	14.8	11.4	9.7	8.1
	0.8	16.88	38.8	22.4	17.4	14.7	12.3
	0.9	15.92	57.3	33.1	25.6	21.6	18.1
	0.95	15.46	83.2	48.0	37.2	31.4	26.3
	0.98	15.18	134.5	77.7	60.2	50.8	42.5
20	0.8	23.52	27.3	15.7	12.2	10.3	8.6
	0.9	21.66	41.7	24.1	18.6	15.7	13.2
	0.95	20.81	61.7	35.6	27.6	23.3	19.5
	0.98	20.32	100.6	58.1	45.0	38.0	31.8
25	0.9	28.90	25.8	14.9	11.6	9.8	8.2
	0.95	26.70	41.3	23.8	18.5	15.6	13.1
	0.98	25.65	69.1	39.9	30.9	26.1	18.5

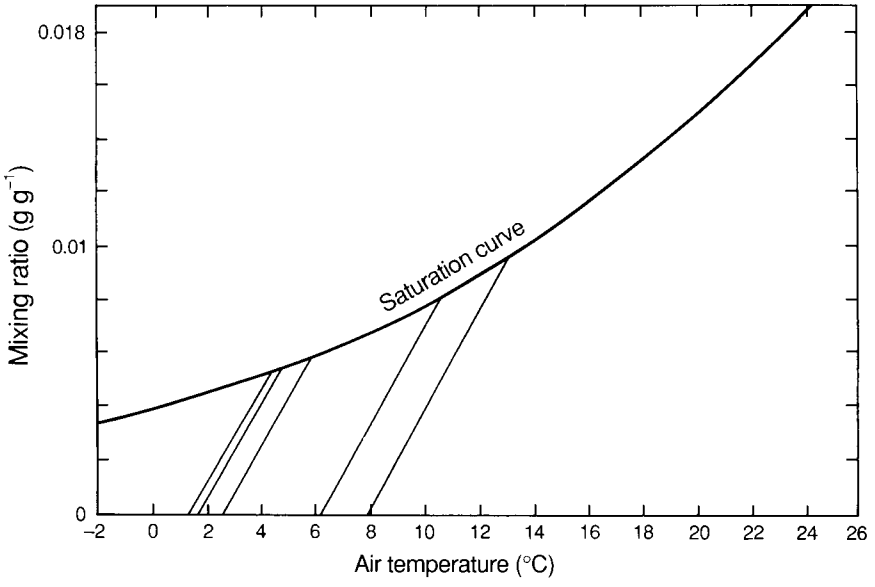

Figure 1. The saturation mixing ratio is a function of air temperature. Below the curve, the air is unsaturated. The nearly-straight lines running up to the saturation curve are the mixing curves for different ambient air conditions, but the same emerging plume conditions.

Fig. 2 shows how the maximum downwind extent of the visible plume varies with ambient air temperature, relative humidity and wind speed. It assumes near neutral stability conditions, which typically occur about 70% of the time in the United Kingdom. In unstable convective conditions, the plume would evaporate earlier whereas in stable conditions it would take longer. However, stable conditions are likely to occur during the daytime mainly at the very beginning and the very end of the working day when the stack is not operative. If stable conditions occur at other times (perhaps when milder air replaces bitterly cold air in winter) then the plume could be a temporary nuisance, and a case could be made for suspending incineration during such a period. During these times the plume length could be increased fivefold above the values given, although this is somewhat speculative.

As will be seen from the data, the visible length of the plume in neutral conditions exceeds 100 m in length only in very high humidity conditions and at low wind speeds and temperatures.

4. Maximum ground-level concentrations

Since concentrations are directly proportional to emissions, the calculations will be made using an emission rate $Q = 1\ g\ s^{-1}$. The ground-level concentrations are, however, not only dependent on source strength but on the effective height of the source, the wind speed and the stability of the air. The effective source height is defined as that height which, if the influences of gas temperature and efflux velocity were to be ignored, would give the same ground-level concentration pattern. The efflux gases are emitted within a vertical jet

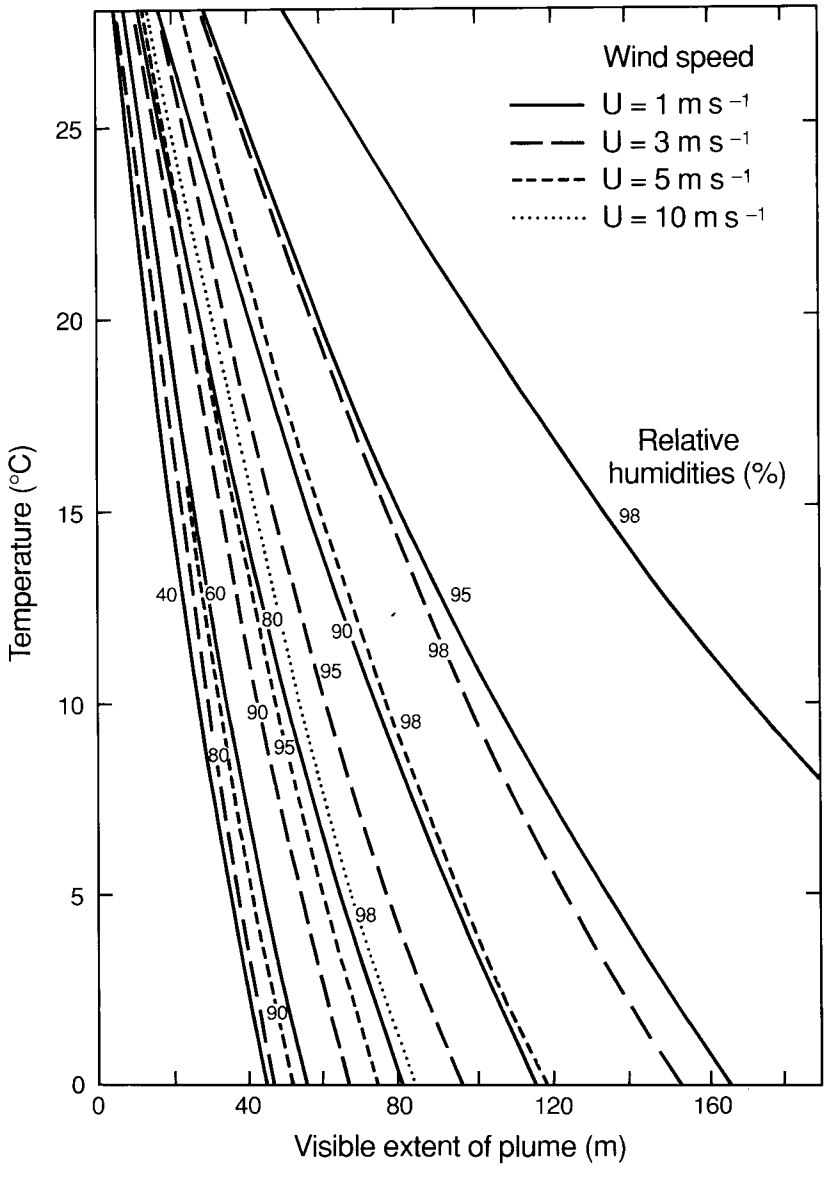

Figure 2. The maximum downwind extent of the visible plume from the stack, with different wind speeds and different ambient relative humidities and temperatures.

travelling upwards at 15 m s^{-1} and at a temperature of about 140 °C. Both these factors make the plume rise to some effective height h_e significantly greater than the stack height h_s.

The plume rise $\Delta h = h_e - h_e$ can be calculated using formulae given by Briggs (1984). Briggs states that the plume rise is given by:

$$\Delta h = \left(\frac{3F_m x}{\beta^2 U^2} + \frac{3F_b x^2}{2\beta^2 U^3}\right)^{1/3}$$

where U = wind speed in m s^{-1}, W = 15 m s^{-1}, the efflux velocity, x = the downwind distance in metres, F_m is the momentum flux, F_b is the buoyancy flux, and β is given by (0.4+ 1.2U/ W.

However, Briggs suggests replacing β in the second term (the buoyancy term) on the right-hand side by 0.6 to be consistent with the asymptotic behaviour of buoyant plumes.

The first term in the brackets on the right-hand side of the equation is given by

$$\left(\frac{3}{4}\right)^{1/3}\left(\frac{r_o R}{(0.2+0.6/R)}\right)^{2/3} x^{1/3}$$

where $R = W/U$ and W = 15 m s^{-1}.

The second term is given by putting

$$F_b = g\frac{T_{stack}}{T_{air}} W r_o^2$$

where W = 15, r_o is the stack internal radius = 0.185 m, T_{stack} = 140 + 273, T_{air} = 15 + 273, g = 9.81.

If h_s = 23 m, then h_e is given in Fig. 3 as a function of wind speed U. The effective height h_e increases rapidly as U falls below about 3 m s^{-1}. Increasing or decreasing the stack height simply raises or lowers the effective height by the same amount.

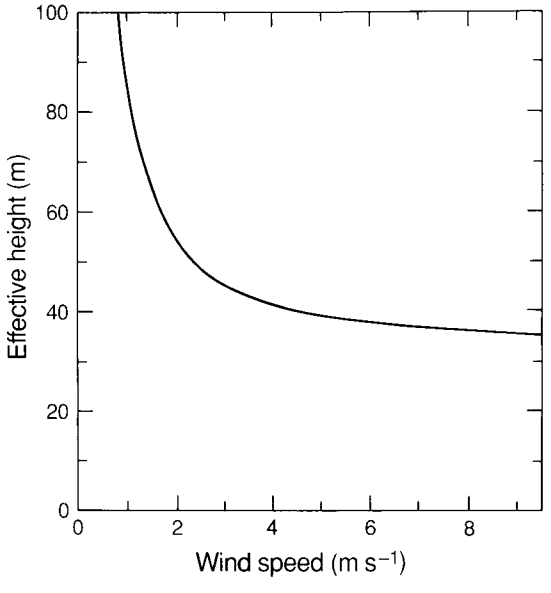

Figure 3. The effective height of the plume for a 23 m stack when the combined effects of the high temperature and the efflux velocity of the emerging plume are taken into account. Otherwise, effective height is principally a function of wind speed.

The plume rise may be ultimately halted by an elevated stable layer through which the plume cannot penetrate. However, before that, the plume may effectively level out and diffuse very much like a passive plume. It is assumed that, for modest emission rates, this occurs at 100 m downwind from the source. Since this is likely to provide an underestimate of the true plume rise, it will overestimate the ground-level concentrations to some extent.

Having so defined h_e, the plume is then assumed to act like a neutrally buoyant plume emanating from h_e. The approach of Weil (1988) is used. It is a very simple and effective method for neutral and unstable conditions. Essentially it calculates the concentration by assuming the plume elements travel along straight lines radiating out from the effective source according to the probability distribution of the turbulent velocities at the effective source. Elements are assumed to reflect off the ground or any elevated capping inversion above the source rather like light rays would off reflecting mirrors. Although this is not a perfect representation of what happens in the atmosphere, field trials indicate that the model gives reasonably satisfactory estimates of measured concentrations. Normally, out to the distance where the maximum concentration occurs, the effect of any capping inversion is not felt at ground level (except indirectly in its subtle effect on the structure of the turbulence).

The plume spreads not only vertically, of course, but horizontally as well. The acrosswind spread is particularly important in lowering the average concentration of pollutants in the plume with downwind distance. Following Briggs (1985) we assume the acrosswind distribution has a Gaussian shape:

$$C(y) = \frac{A}{\sqrt{2\pi}\sigma_y}\exp\left(-\frac{y^2}{2\sigma_y^2}\right)$$

where σ_y (the so-called 'standard deviation') is a measure of the width of the plume and is approximately given by:

$$\frac{\sigma_y}{h} = \frac{0.6X}{(1+2X)^{1/2}}$$

where $X = w_* x/(Uh)$, w_* is the convective velocity = $(gHh/\rho c_p T)^{1/3}$, and H is the surface sensible heat flux in W m^{-2}, h is the depth of the mixing layer.

Typical values of h, H and w_* can be ascribed to pairs of wind speed U and stability category P (see Table II). The mixing depth h strictly depends on a number of factors which are difficult to assess in any given situation without detailed meteorological data both at the time of interest and back in time along the trajectory of the air mass. Since such information is unknown in the present analysis, a rather simple approach which may introduce small errors into the results has to be used. It is believed that these errors do not significantly alter the conclusion. This belief is based on a sensitivity study by which changes in the results are obtained by changing the

Table II. A table of parameters governing the ground-level concentrations downwind of the stack. H is the heat flux in W m^{-2}, w_* is the convective velocity in m s^{-1}, h is the estimated mixing depth in metres and u_* is the friction velocity in m s^{-1}. The plume rise is given in metres as is the effective height of the source (= plume rise + stack height (23 m)).

Wind speed (average)		1–3 kn 1 m s^{-1}	4–6 kn 2.5 m s^{-1}	7–10 kn 4.25 m s^{-1}	11–16 kn 6.75 m s^{-1}	⩾17 kn ⩾9 m s^{-1}
Plume rise (m)		62	26	18	14	13
Effective h (m)		85	49	41	37	36
P	Param.					
A	H	150	300			
	w_*	1.86	2.63			
	h	1634	2368			
	u_*	0.1476	0.2928			
B	H	20	100	250		
	w_*	0.680	1.52	2.40		
	h	651	1459	2316		
	u_*	0.1176	0.2647	0.4272		
C	H	10	40	110	260	
	w_*	0.481	0.961	1.594	2.451	
	h	495	1028	1699	2618	
	u_*	0.110	0.2471	0.4056	0.6275	
D	H	0	0	0	0	0
	w_*	0	0	0	0	0
	h	217	543	923	1466	1955
	u_*	0.0869	0.2172	0.3692	0.5863	0.7821

values of h within sensible limits around the values given by our simple method.

The simple method uses the formula for the development in time of the depth of the convective mixing layer by Carson (1973):

$$\frac{dh^2}{dt} = \frac{2(1+2A)H(0,t)}{\rho c_p \gamma(t)}$$

where $H(0, t)$ is the surface sensible heat flux at $z = 0$ at time t, A is a factor to allow for the entrainment of heat from above the mixing layer and is usually given a value of 0.25, $\gamma(t)$ is the potential temperature gradient in the air above the capping inversion, and is given a default value of 0.003 °C m^{-1}. The equation can be solved for h if an analytic form for $H(0, t)$ is given. In steady meteorological conditions $H(0, t) = H_m \sin\omega t$ where H_m is the peak midday value of the heat flux, and ω is the inverse time-scale of the diurnal cycle. The maximum value of h is obtained in the afternoon, and it is this value that is used. It turns out that h depends almost entirely on H_m in a very simple way: $h = 130 H_m$. In the morning the depth of the mixing layer is likely to be less which leads to weaker turbulence and lower ground-level concentrations until the physical limits to vertical spreading imposed by the lower depth push up the concentrations to some degree at distances beyond which we are concerned.

So as to obtain the optimum estimate of h, and also to blend in with alternative estimates of h in neutral conditions, the value of $h = h_C$ given by Carson's equation is combined with $h = (u_*/4f)$ commonly used in neutral conditions:

$$h^2 = h_C^2 + (u_*/4f)^2.$$

The values of H are obtained from Smith's version of the Pasquill scheme for estimating stability. Fig. 4 shows Smith's curves which relate P, U and H. The table of parameters (Table II) also gives the convective velocity w_* and the friction velocity u_*. The convective velocity has already been defined and is used in the non-dimensional form of the downwind distance. The friction velocity, which is used in the mixing layer depth in neutral conditions, can be inferred from the 10 m wind speed and the heat flux by the following equations (which are standard equations used in micrometeorology and won't be explained properly here):

$$u_* = 0.4U / \left\{ \ln\left(\frac{(y-1)(y_o+1)}{(y+1)(y_o-1)}\right) + \right.$$

$$\left. + 0.0349(\tan^{-1} y - \tan^{-1} y_o) \right\}$$

where $y = (1 + 160/L)^{1/4}$, $y_o = (1 + 1.6/L)^{1/4}$, L is the

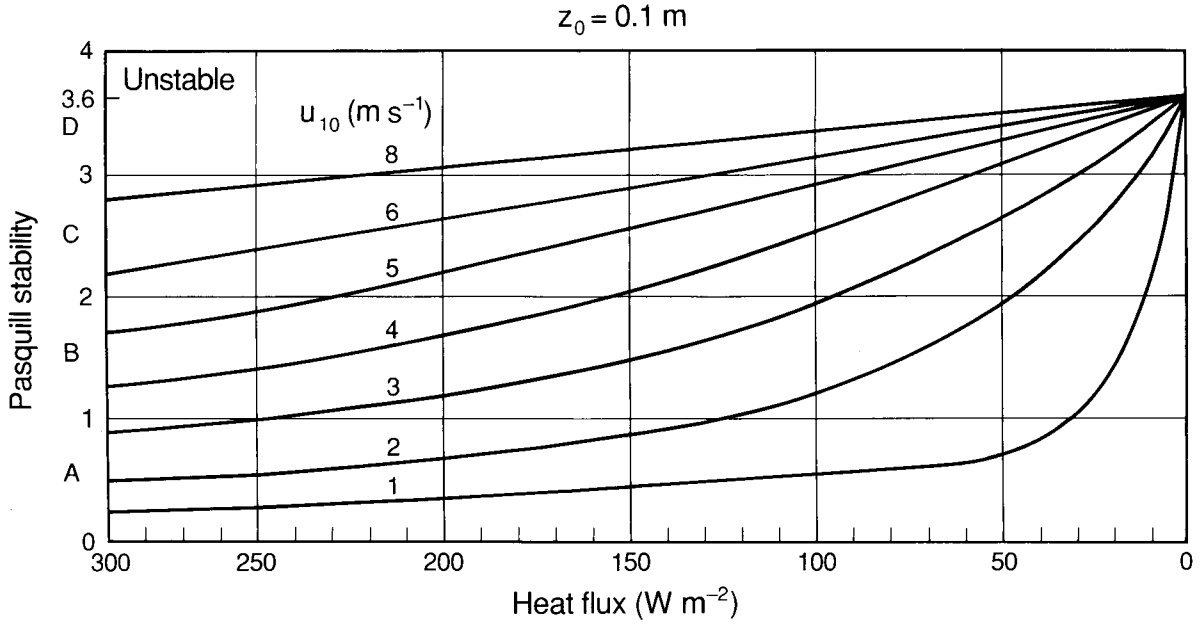

Figure 4. The revised scheme for Pasquill Stability based on heat flux and wind speed.

Monin–Obukhov length-scale $= 94\,700u_*^3/H$, and the surface roughness has implicitly been assumed to be 0.1 m. In neutral conditions $u_* = 0.087U$. To solve for u_* in convective conditions the neutral value of U_* is found, this is inserted into the expression for L to find L (for given heat flux H), y and y_o are found and inserted into the convective expression for u_*. This new value of u_* is then reinserted into the L expression and so on until a converged value of u_* is reached. To determine the ground-level concentrations, the formula provided by Weil (1988) will be used. The concentration below the plume centreline is given by:

$$C(X) = \frac{Q}{Uh^2}\frac{a(X)}{X}\,1.841\left\{\exp\left(-\frac{(\alpha/X-0.35)^2}{0.135}\right) + \right.$$

$$\left. + \; 0.361\exp\left(-\frac{(\alpha/X+0.4)^2}{0.461}\right)\right\}$$

where $a(X) = 0.665\,((1+2X)^{1/2}/X)$.

Q is the emission rate in g s^{-1}, $\alpha = h_s/h$, and $X = (w_* x/Uh)$.

5. Results

The equation for $C(X)$ above has been solved for $Q = 1$ g s^{-1} and for all the combinations of U and P in Table II, and for five stack heights: 10 m, 16 m, 20 m, 23 m and 30 m.

In each case the concentration distribution has the following characteristics: on the ground the concentration is zero close to the base of the stack but after some distance downwind it suddenly rises quite rapidly to its peak value, after which there is a gradually decreasing tail which persists for a long distance downwind. As an example, the results for stability $P = B$ and a wind speed of 2.5 m s^{-1} are given:

$X = 0.01 : C = 0$; $X = 0.02 : C = 0$; $X = 0.03 : C = 3.9$; $X = 0.04 : C = 27.2$; $X = 0.05 : C = 47.7$; $X = 0.06 : C = 52.1$; $X = 0.07 : C = 47.6$; $X = 0.08 : C = 40.5$, etc.

Two important conclusions can be drawn from the calculations:

(i) $C(X)$ is at a maximum with wind speeds around 2.5 m s^{-1}. For example with $P = C$ the maximum concentration varies with wind speed as follows: $U = 1 : C = 52.0$; $U = 2.5 : C = 53.1$; $U = 42.9 : C = 42.9$; $U = 6.75 : C = 29.3$;

(ii) $C(X)$ varies only very gradually with stability. C_{max} is the overall maximum concentration, regardless of where it occurs. It is given in Fig. 5 as a function of the most important parameter, h_s, the stack height. Note that decreasing h_s from 23 m to 16 m increases C_{max} from 59 to 79 μg m^{-3} with $Q = 1$ g s^{-1}. (With the proposed stack, having an emission rate of only 0.166 g s^{-1} for sulphur dioxide, the concentration increases from 10 to 13 μg m^{-2}.)

Fig. 6 shows the downwind distance x_m in metres where the maximum concentration is expected. x_m is virtually independent of wind speed U, but depends very much on stability P and h_s.

6. Maximum concentrations around the stack

Ignoring the sloping terrain in the vicinity of the stack, the concentrations of some of the pollutants emitted from the stack can be estimated.

6.1 HCl

The emission rate of HCl is given as 300 g h^{-1} or

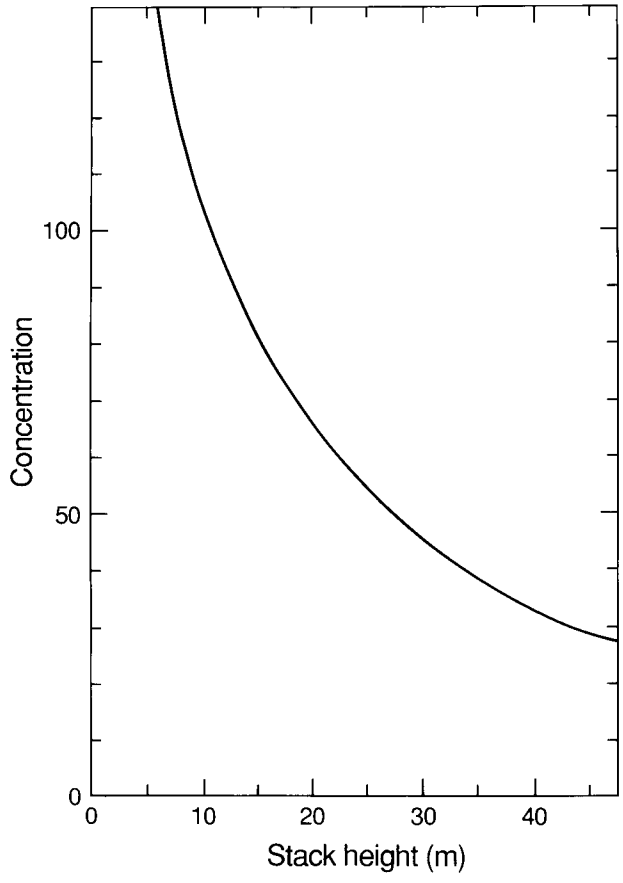

Figure 5. The 10-minute-mean peak concentration at ground level as a function of stack height for the resulting plume, but with an emission rate standardized to 1 g s^{-1}. The units of concentration are $\mu g\ m^{-3}$.

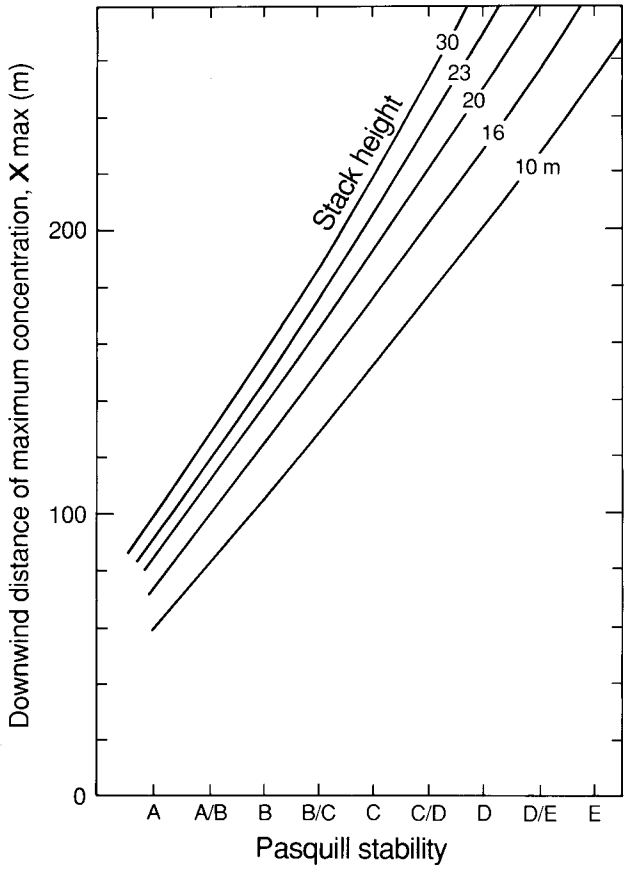

Figure 6. The distance downwind on flat terrain where the 10-minute-mean maximum concentration occurs, as a function of stack height and Pasquill Stability.

0.083 g s^{-1}. The 10-minute-average maximum concentration, as a function of h_s, in $\mu g\ m^{-3}$ is:

h_s(m) 10.0 16.0 20.0 23.0 30.0.

C_{max}: 8.7 6.6 5.5 4.9 3.8.

6.2 SO_2, NO_x, CO

The emission rate for each of these pollutants is estimated to be 600 g h^{-1} or 0.166 g s^{-1}. The concentrations are:

h_s(m) 10.0 16.0 20.0 23.0 30.0.

C_{max}: 17.4 13.2 11.0 9.8 7.6.

6.3 The effect of the slope

It is assumed that the ground rises some 5 metres to the north-east, say; and further that a tall house exists on the highest ground and is some 8–10 metres tall, so that its upper rooms may be some 14 metres above the base of the stack.

The slope of the ground will only be important in the relatively few cases of daytime stable conditions when, due to the increase of air temperature with height, air motions tend to be much more horizontal than in neutral or unstable conditions when the air readily follows the contours of the underlying terrain.

Although stable conditions can and do occur at any time of the day if the meteorological conditions are right, they most frequently occur soon after dawn and in the late afternoon an hour or so before sunset. They tend to develop whenever the winds are light and the skies are cloud-free. To avoid the great majority of these cases, it would be prudent to recommend, in this assumed scenario, that the stack should not be operated with very light winds after, or before, a cold night, with a south-westerly drift moving the air up the slope towards the tall house to the north-east, until at the earliest 9 a.m., or until the latest 4 p.m. Under these stable conditions the upper rooms of the house would otherwise be subject to emissions from a stack that is effectively 14 metres lower. Calculations show that for a 23-metre stack this apparent reduction doubles the maximum concentration likely to be experienced, even though the centreline of the plume will still easily clear the top of the house. In reality the proposed restriction will impose very little extra constraint on the stack's operation since firing would not normally take place at either end of the working day.

More precise criteria could be proposed, and a simple warning scheme arranged with the Meteorological Office at the nearest forecasting office.

7. Frequency data of the meteorological parameters

No meteorological observing station exists in Midville itself, and the nearest fully operational station is at Elmdon. Although some distance away, it is considered that the statistics of the relevant parameters are likely to be very similar. Between 08 and 18 UTC the Pasquill Stability Categories occur with the percentage frequencies given in Tables III and IV. All the stable cases (E, F and G) occur either at 08, 16, 17 or 18 UTC. The highest percentage frequency is seen to be in the neutral D category, and over 92% of hours at Elmdon lie within C–D, i.e. in neutral or slightly unstable conditions. The more unstable conditions tend to occur around midday when the incoming solar radiation is at its highest.

Fig. 7 shows the wind rose for Elmdon, which is less than 20 km to the north-west, as well as for Brize Norton (further to the south) and Wyton (more than 100 km to the east). A very similar wind rose to that for Elmdon should apply to the stack. South-west winds are seen to be considerably more frequent than other winds. The sector from south to west contains 75% more winds than the average in the north-east.

Between 08 and 18 UTC, the wind speed classes have the percentage frequencies as set out in Table V. As can be seen, very light winds below 2 m s^{-1} occur in about 5–6% of all hours, but many of these would be at night when the incinerator would not be operating.

Table III. Percentage frequencies of Pasquill stability categories at Birmingham Airport (Elmdon), Brize Norton and Wyton during daytime (08–17 UTC)

P	A	B	C	D	E	F	G
Elmdon	0.38	4.13	24.72	67.39	2.52	0.57	0.28
Brize Norton	0.32	3.96	22.76	69.73	2.17	0.67	0.28
Wyton	0.30	3.81	22.33	67.43	2.49	0.50	0.14

Table IV. Pasquill Stability Category frequencies by hour at Elmdon 1980–89

Hour (UTC)	Pasquill Stability Category A	B	C	D (day)	D (night)	E	F	G	Total
0	0	0	0	0	1068	1523	639	422	3652
1	0	0	0	0	1051	1518	637	446	3652
2	0	0	0	0	1066	1490	619	477	3652
3	0	0	0	0	1078	1492	583	499	3652
4	0	0	0	400	1003	1329	530	390	3652
5	0	0	0	1160	837	1045	354	256	3652
6	0	0	21	1739	720	781	229	162	3652
7	0	2	297	2050	510	549	151	93	3652
8	0	53	603	2373	261	259	51	52	3652
9	4	147	927	2574	0	0	0	0	3652
10	20	211	1227	2194	0	0	0	0	3652
11	33	258	1348	2012	0	0	0	0	3651
12	36	268	1315	2033	0	0	0	0	3652
13	29	233	1207	2183	0	0	0	0	3652
14	14	189	975	2473	0	0	0	0	3651
15	3	111	726	2812	0	0	0	0	3652
16	0	37	490	2732	187	165	31	10	3652
17	0	2	209	2287	489	496	126	42	3651
18	0	0	16	1883	689	754	222	87	3651
19	0	0	0	1300	865	1012	325	150	3652
20	0	0	0	620	1007	1325	493	207	3652
21	0	0	0	0	1124	1630	634	263	3651
22	0	0	0	0	1093	1613	638	307	3651
23	0	0	0	0	1081	1564	637	369	3651
Total	139	1511	9361	32825	14129	18545	6899	4232	87641

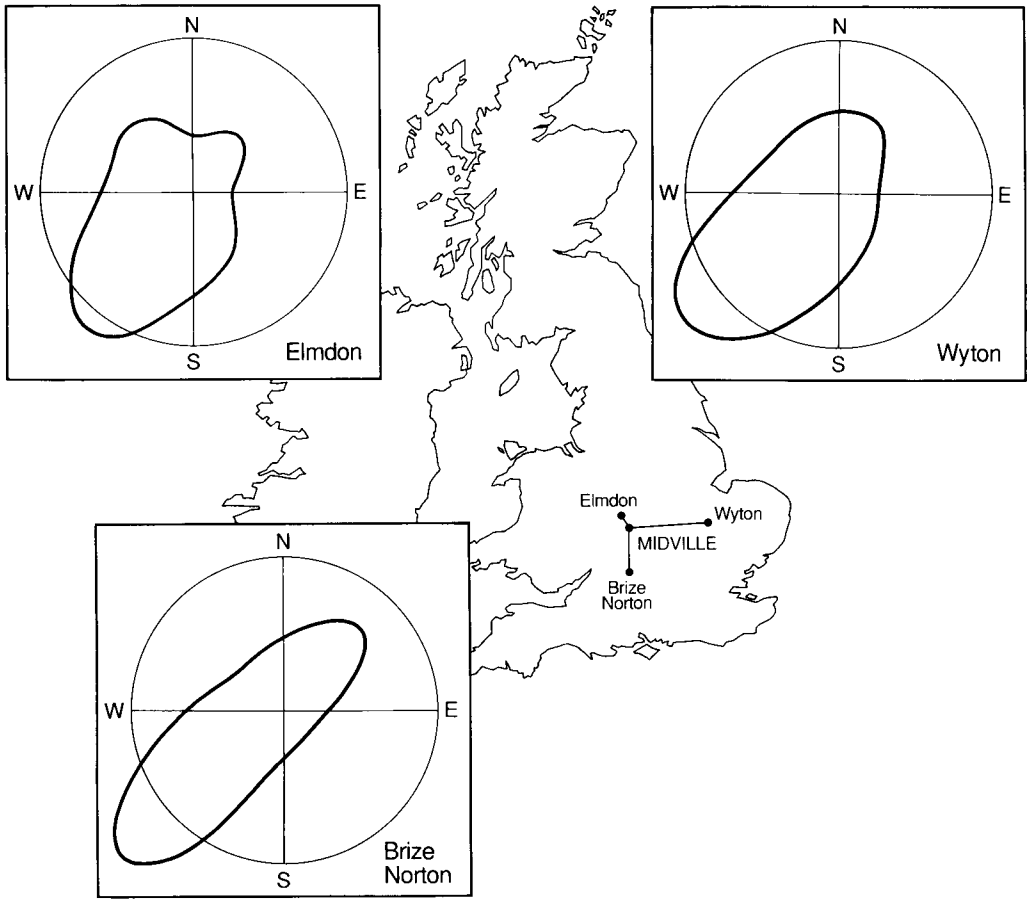

Figure 7. The wind rose at Elmdon (Birmingham Airport) shows the predominance of south-westerly winds, the circle delineating the 14% frequencies. The wind roses at Wyton and at Brize Norton have the same characteristic.

Table V. Wind speed percentage frequencies at Elmdon, Brize Norton and Wyton between 08 and 18 UTC. The U values are average values in the wind speed ranges. The frequencies are similar at the three stations.

Wind speed (kn)	U ($m\ s^{-1}$)	Percentage frequencies Elmdon	Brize Norton	Wyton
Calm	0	5	3	2
1–3	1	14	20	11
4–6	2.5	25	21	20
7–10	4.25	32	29	33
11–16	6.75	20	22	27
17–98	9	4	5	7

Conditions of high humidity (leading to long, visible plumes extending 100 metres or so) are very unusual during summer daylight hours; a relative humidity greater than 95% during the day occurs less than 4% of the time between May and the end of August.

In winter, however, this increases to around 30% at 9 a.m. between November and February, and 10% at 3 p.m. The required cold temperatures would also be experienced only in winter for such long plumes.

References

Briggs, G.A., 1984: Plume rise and buoyancy effects. *In* Randerson, D. (ed.); Atmospheric science and power. DOE/TIC 27601, US Department of Energy.

—, 1985: Analytical parametrizations of diffusion: the convective boundary layer. *J Clim Appl Meteorol*, **24**, 1167–1186.

Carson, D.J., 1973: The development of a dry inversion-capped convectively unstable boundary layer. *Q J R Meteorol Soc*, **99**, 450–467.

Weil, J.C., 1988: Dispersion in the convective boundary layer. *In* Venkatram, A. and Wyngaard, J.C. (eds); Lectures on air pollution modeling. Boston, American Meteorological Society.

551.583.1

The role of observations in climate prediction and research*

D.J. Carson
Meteorological Office, Bracknell

Summary

The main uses of climate data are listed. Some comments are made on the data requirements for climate modelling, detection and diagnostic studies. The discussion concentrates mainly on the data needed to provide boundary conditions, initialization and validation for climate models.

1. Introduction

Many uncertainties surround our understanding of, and ability to model, the climate system. These, and other technical limitations, make prediction of the nature, magnitude and timing of climate change, particularly at scales smaller than global, unreliable at present. Increasing concern over the need to detect, understand and predict global and regional environmental changes has highlighted the need to establish high-quality observational data sets relating to the earth's atmosphere, oceans, cryosphere and land-surface. The basic climate record needs to be better established from geological times up to the present and decisions must be taken now to ensure more comprehensive global data coverage of the climate system in future.

A prerequisite to designing and implementing a Global Climate Observing System (GCOS) is to identify the principal uses and users of the data to be collected in order to justify such a costly, long-term, internationally collaborative operation.

The major requirements for data in support of climate prediction and research, the latter to be interpreted in its widest sense, are for:

(a) monitoring the climate and its variability at global and regional scales, thereby enabling quantification of natural climatic fluctuations on a range of temporal and spatial scales and the detection of climate change,

(b) attribution of climate change to particular causes, as in the search for a fingerprint which will enable detection and attribution of climate change due to an enhanced greenhouse effect resulting from man-made emissions of greenhouse gases,

(c) detection (and attribution) of the environmental impacts of climate change,

(d) diagnostic studies to elucidate the behaviour of the climate system and its component parts, namely, atmosphere, oceans, land surface, cryosphere, etc. including studies of the mechanisms of natural climatic variability,

(e) development and testing of hypotheses relating to local and global climate variations and to the degree of predictability of climatic phenomena,

(f) process studies. Special data are needed in support of detailed research studies of a wide variety of complex dynamical, physical, chemical and biological processes which help govern the state and evolution of the climate system. Such specialized data sets are likely to need to be highly resolved in time and space and therefore gathered for a limited period over a restricted area of the globe. High-priority process studies include cloud–climate and air–sea interactions,

(g) providing boundary conditions for climate models. These include surface properties such as albedo, roughness length, vegetation index, soil physical parameters, etc. Some such data are also needed to identify changes in relevant surface properties, e.g. due to deforestation (see also (c) above),

(h) initialization of climate model integrations, especially of the oceanic and cryospheric components, and also some of the land-surface hydrological characteristics such as the 'soil moisture content',

(i) validation of climate models. A very wide range of data, including palaeoclimatic data, are needed to assess the performance of the models being used for climate simulation and prediction. Model behaviour is compared with that of the 'observed' climate, often leading to further development and improvement of the models, and

(j) data-assimilation techniques for climate model development. Aspects of the climate models can be improved through the use of climate observations in sophisticated four-dimensional data-assimilation schemes, such as those used with state-of-the-art operational weather forecasting models.

Although model and observational studies are becoming increasingly interdependent, it is convenient for the points to be focused on primarily in this article to consider the requirements (a)–(f) above as being, in the

* Background paper prepared for the World Climate Research Programme *ad hoc* Workshop on the Planning of the Global Climate Observing System, 14–15 January 1991, Winchester, England.

main, model-independent, whereas (g)–(j) are directly related to the development and use of climate-simulation and prediction models. A few comments on the data requirements for climate monitoring and diagnostic studies are given in section 2. Section 3 concentrates on the observational needs of climate-simulation and climate-prediction models, i.e. items (g)–(j) above.

It is worth stressing that the above needs and uses encompass a variety of types of data, for example :

'Stand-alone' instrumental data, including data from both *in situ* and remote-sensing (in particular satellite-borne) instruments. Examples of the former are surface and upper-air temperatures, rainfall, etc. The latter category also includes surface and upper-air temperatures, and cloud cover, etc.

'Blended' data, i.e. a data set produced from more than one data source; e.g. sea surface temperatures derived from both satellite- and ship-borne sensors.

(Climate studies are by their very nature global in character and this necessitates extensive use of space observations to provide the necessary coverage and continuity. Space observations are, however, in many respects difficult to interpret and special blending techniques are required in order for them to provide reliable information for climate research. In particular, they need to be combined with *in situ* observations to resolve ambiguities in their interpretation, to provide higher precision, and to enable estimates of fields of derived quantities, such as surface heat and moisture fluxes.)

Data assimilated by operational weather forecasting models. This is a powerful technique for the optimal combination of space-based and *in situ* observations. It provides 'complete' global data sets which are internally, dynamically and physically consistent, e.g. 3-dimensional, global wind fields. However, biases may be introduced by changes to the models used.

'Derived' data, i.e. data calculated from other directly measured or assimilated data, e.g. derived surface fluxes of heat, moisture and momentum. Information on land-surface characteristics, such as albedo and surface roughness, are usually 'derived' from a 'blend' of a variety of data types.

2. Data requirements for monitoring, detection and diagnostic studies

Studies of climatic processes often require short-lived specialized regional-scale data sets and associated field programmes. Studies of climate variability, change and predictability demand long-time-scale (decades to centuries or more) data sets which are homogeneous in time, i.e. without bias or with a constant bias. Studies of global environmental change (including climate change) clearly require global data sets, and regional variability, change and predictability are being studied increasingly in the context of the corresponding global-scale characteristics. The climate data sets to be assembled must reflect these diverse needs.

The 'operational' and research needs will also often lead to a hierarchy of data sets for a given variable, e.g. a real-time data set (used for operational weather forecasting, and for monthly and seasonal predictions), a delayed-mode data set (containing more data than the real-time one, and useful for preliminary monitoring and research studies), and a slow-mode data set (containing all available data with instrumental corrections, e.g. historical *in situ* sea surface temperature data sets).

Beside the routine production of analyses for climate research using data-assimilation techniques, it is essential to continue to process selected *in situ* and remotely sensed observations independently from the integrated data-assimilation systems. This is because information is needed on the atmosphere and oceans (for example, ocean and land surface temperature analyses) which are free from the biases that arise from the inclusion of (changing) modelling assumptions. For selected variables, long time-series of observations need to continue to be carefully processed to produce analyses which are as free as possible from the influence of changes to the observing or processing techniques introduced over the period. 'Pure-data' archives are necessary for this purpose. A particularly important example for validating climate models is the need for a reliable, homogeneous archive of atmospheric data from radiosondes.

For monitoring climate, quantifying climate variability and detecting climate change, a long historical perspective is needed, in contrast to the normal data requirements in operational weather forecasting. In this context, it is important to realize that many historic data are not yet in a form for use on computers. Indeed many of the data needed for climate purposes are not expected to be processed through data-assimilation schemes in the medium-term future. Criteria for the collection and assembly of data sets for climate monitoring include :

Data are required for different parts of the climate system, particularly for atmosphere and oceans.

There is a need to establish reliable homogeneous quasi-global historic 'base-line' data sets.

Current data need to be homogeneous with historic data; this is a difficult task and specialized techniques need to be developed to achieve the necessary high levels of homogeneity.

Satellite data need to be blended with more-conventional data.

Near real-time data are required to monitor short-period weather variability on time-scales ranging from a day to a month. Few daily data are available on the global scale and this prevents worldwide monitoring of extreme events such as frosts.

In the context of short-period weather variability it is worth noting the additional data needs for long-range (monthly–seasonal) forecasting. This activity requires daily, real-time global data sets with special requirements for particular regions (e.g. high-resolution climate data for the United Kingdom are needed for the long-range forecasting activities within the Meteorological Office). Also, long-range forecasting based on statistical methods needs long, homogeneous historical data sets.

Some suggested data sets for climate monitoring are listed in Table I. Many of the qualifying column entries in this table are somewhat tentative.

Diagnostic studies of data to explore climate mechanisms and processes, especially studies of low-frequency weather variability, have some additional and different requirements. The overriding need is for 3-dimensional, high-resolution, physically and dynamically self-consistent global data sets. This is generally only feasible by use of data assimilation allied to a global model. Data are needed at least twice daily (preferably 6-hourly) to avoid biases that can be introduced by diurnal effects. Homogeneity is another important requirement, but cannot always be achieved. Many of the data sets to be analysed are of derived physical and dynamical properties of the atmosphere and, where possible, the oceans, e.g. diabatic heating rates, eddy fluxes, ageostrophic quantities, etc.

3. Data needs for climate modelling and prediction

Some comments are offered on the following aspects of the data requirements in connection with the development and use of global numerical models for studying and predicting climate and climate change:

Boundary conditions.
Initialization.
Validation.
Data-assimilation techniques for model development.

3.1 Data for model boundary conditions

This encompasses a wide range of data which are prescribed in order to run climate models in various configurations (namely, atmosphere-only, ocean-only, coupled atmosphere–ocean). They may be held constant or updated prescriptively throughout a model integration, but they are not determined prognostically or diagnostically within the model itself. A range of boundary conditions is needed for application at the land-surface or air–sea interface, in the upper reaches of the atmosphere, throughout the atmosphere, oceans and soils, and at the lower ocean boundary.

The need to prescribe such boundary conditions depends to a very large extent on the state of development of the model being used, the configuration it is being used in, and what it is being used for. As models of the full climate system develop, and as they are used increasingly for making predictions of transient global and regional climate change, then correspondingly more degrees of freedom will be given to such models and the requirements for boundary conditions will evolve in response. Some quantities acknowledged at present as boundary conditions will become full prognostic variables in the models, whilst new boundary conditions will be needed for new and more complex representations of the sub-grid-scale processes (i.e. new parametrizations will require new boundary conditions).

Examples of important boundary conditions requiring better global data sets are :

Atmosphere-only models:
Sea surface temperatures (SSTs).
Sea ice extent, concentration, thickness.
Ozone distribution.
Land-surface characteristics (albedo, surface roughness length, vegetation type, etc.).
Land ice extent and thickness.
Orographic height (and sub-grid-scale variance).

Ocean-only models:

Aside from ocean bottom topography, the prime requirement here is for data to provide the surface forcing needed for ocean model integrations, namely:

Surface stress fields.
Wind mixing.
Heat fluxes (incoming solar and long-wave radiation, sensible and latent heat fluxes) and freshwater (precipitation less evaporation) fluxes.
River runoff.

Two basic approaches may be made to provide the appropriate forcing for the model, though in practice a combination of the two is frequently used.

The fluxes may be specified directly, in which case it is necessary to use a 'flux-correction' technique whereby the net heat flux (Q_o) is modified by a feedback term which helps to constrain the predicted sea surface temperature (T_p) in the model to the observed field (T_o) depending on the size of the feedback parameter (k), i.e. the applied heat flux (Q) is given by:

$$Q = Q_o + k(T_o - T_p).$$

A similar approach may be used for the freshwater flux, which is then constrained to the observed salinity field.

Alternatively, the basic meteorological parameters necessary to drive the turbulent fluxes can be specified and the fluxes derived via appropriate bulk formulae as the integration proceeds and with reference to the modelled SST (or ice surface temperature) where appropriate. In this case the data sets required are:

Surface wind field.
Wind mixing.
Surface air temperature.
Surface air humidity.
Surface pressure.

Table I. Data for climate monitoring (tentative)

Parameter	Data sources		Data types		Priority	Accuracy or precision	Desirable accuracy of long-term changes	Spatial resolution		Time resolution
	In situ	Remote	Pure	Assimil-ated	XXX suggests highest			Horizontal	Vertical	
SST	✓	✓	✓	✓	XXX	0.2 °C local or region 0.1 °C global	≤0.1 °C	100 km		2 weeks
Sub-surface ocean temperature	✓		✓	?	XX	0.1 °C	0.05 °C	500 km?	20 m above thermocline, 0.2 km below	Monthly
Marine surface air temperature	✓		✓	✓	XX	0.2 °C local and region 0.1 °C global	≤0.1 °C	500 km?		Monthly
Land surface air temperature	✓		✓	✓	XXX	0.2 °C local and region 0.1 °C global	≤0.1 °C	500 km		Monthly and daily
Atmospheric temperature	✓	✓	✓	✓	XXX	0.5 °C local 0.1 °C global	≤0.2 °C	500 km	1–2 km	Monthly
Humidity	✓	✓	✓	✓	XX	5–7% specific humidity	1% specific humidity	500 km	2–3 km	Monthly
Surface wind	✓	✓	✓	✓	XXX	1 m s^{-1}	≤1 m s^{-1}	500 km		Monthly
Winds aloft	✓	✓	✓	✓	XX	1 m s^{-1}	≤1 m s^{-1}	500 km	1–2 km	Monthly
Surface pressure	✓		✓	✓	XXX	1 mb	≤1 mb	500 km		Daily
Atmospheric geopotential heights	✓	✓	✓	✓	XXX	10 m	≤10 m	500 km	1 km	Daily
Precipitation over land	✓	✓	✓	?	XXX	10% daily 5% monthly	≤2%	Variable		Monthly and daily
Precipitation over ocean	If possible	✓	✓	?	XX	20%	≤5%	500 km		5 days?

Cloudiness variables	✓	✓	✓		XXX	Complex (10% of total amount)	Complex (≤ 5% of total amount)	250 km	1 km	Monthly or less
Sea ice extent	✓	✓	✓	?	XXX	5% open water	1% open water	100 km?		Monthly
Sea ice thickness	✓	?	✓	?	XXX	10% or 0.5 m?	2% or 0.1 m?	100 km		Monthly
Snow extent	✓	✓	✓	?	XXX	3%	1%	100 km?		3 days
Snow depth	✓	?	✓	?	X	20%?	< 5%?	100 km?		3 days
Salinity	✓	?	✓	?	XX	2%	1%	250 km	0.2 km	Monthly
Near surface ocean currents	✓	✓	✓	✓	XXX	2 cm s^{-1}	5%	20 km in major currents	0.2 km	Monthly
Sea surface height	✓	✓	✓	✓	XXX	5 cm	2 cm	200 km?		Monthly or less
Soil moisture	Few	?	?	?	XXX	10% of field capacity	2% of field capacity	100 km?	10 cm	Monthly and 5-daily
Vegetation		✓	✓		XX	10% of total biomass	5%? of total biomass	100 km		Monthly
Planetary radiation budget components		✓	✓	?	XXX	10 W m^{-2}	≤ 0.5 W m^{-2}	250 km?		Monthly
Solar 'constant'		✓	✓		XXX	0.05%	0.01% (≈ 0.1 W m^{-2})			Monthly
Atmospheric CO_2 concentration	✓		✓		XXX	0.5 ppm	0.5 ppm	Global		1 year
Atmospheric diagnostics	✓	✓		✓	XXX	5%	1%	500 km	1–2 km	Daily and 6-hourly

Incoming solar and long-wave radiation/cloudiness.

Coupled atmosphere–ocean general circulation models (AOGCMs):

Particular boundary data sets required here are:
Ozone distributions.
Land-surface characteristics, including land ice extent and thickness.
Topographic data for both land and oceans.

3.2 Data for model initialization

These are data needed to set the initial values of variables which will then be updated, usually prognostically, within the model itself. It is often not understood that climate modelling and climate prediction are not initial-value problems in the same way that short- to long-range forecasting are initial-value problems — at least as far as initializing the atmosphere is concerned. Initialization of the atmosphere is not a critical factor in climate modelling or prediction; it is quite acceptable to use model-compatible data from a single time from a previous climate model run or a numerical weather prediction analysis, and quite unnecessary and of no additional value to demand real-time global analyses.

In the current state of development of climate models, it may be more critical to initialize aspects of the land-surface prognostic variables, if not starting from a previously derived model data set. In particular, there is modelling evidence of long-lasting effects of the initial values used for some of the land-surface hydrological characteristics. Snow cover, soil moisture content and soil temperatures are examples of variables which may need to be initialized by 'spinning up' the model through at least a seasonal cycle.

The main current (and probably future) requirements for initializing climate models concern the oceans, whether in ocean-only models or coupled AOGCMs. Global fields of profiles of temperature, salinity and currents are required to provide a realistic initialization of ocean models. Currently the Levitus global temperature and salinity data set is used and the currents generated as the model runs. Repeated insertion of Levitus data may be useful and valid for high-resolution ocean models in this context (such as that used in NERC's FRAM project). Long (centuries or more), costly, computer integrations are necessary for the models to come into equilibrium with any specified forcing. Note that the final state may depart significantly from the 'observed' state.

Aspects of the cryosphere also require careful initialization in climate models. In particular, as a minimum, sea ice extent needs to be initialized. There is also need for sea ice concentrations and thicknesses, although the latter are particularly difficult to achieve.

In coupled AOGCMs a major problem is to bring the component systems into mutual adjustment with one another. The length of model integration necessary to achieve sufficient adjustment (and estimate flux corrections) for a given purpose may vary from decades to millenia. The initial data requirements for AOGCMs are as above. There is no doubt that initialization of the ocean component of the climate system presents by far the greatest challenge in this area of climate modelling and prediction. Note that careful specification of the 'observed' state is particularly necessary for TOGA-related predictions and hindcasts (e.g. the prediction of ENSO events).

3.3 Data for model validation

The IPCC WG1 Report identifies three categories of data needed for climate model validation:

(a) variables important for description of the atmospheric and oceanic circulation,
e.g. atmosphere: mean-sea-level pressure; wind and temperature profiles; variability as indicated by eddy kinetic energy, and
ocean: surface dynamic height (not often calculated in models); temperature, salinity and current structure; distribution of tracers; eddy statistics,
(b) variables critical in defining climate change,
e.g. atmosphere: surface air temperature; precipitation; soil moisture; monthly means plus interannual and daily variability, and
ocean: SST; ocean mixed-layer depth, and
(c) variables important for climate feedbacks,
e.g. snow cover; sea ice; clouds and their radiative effects.

Note that the above categories (a)–(c) are not mutually exclusive and many types of observations fit equally well into more than one.

Validation of selected regional aspects is also of relevance, e.g. occurrence of ENSO events in coupled models, and monsoon phenomena.

There are again particular considerations when verifying ocean models. On the seasonal time-scale, data are needed to validate simulations of the upper ocean mixed layer. Data on the spread of transient tracers provide valuable verification of decadal time-scale changes in the ocean. On the time-scale of a century or more data on deep ocean temperature and salinity structures, as well as of other tracers, will be of value.

Particular requirements for validating results from coupled AOGCMs include data on surface fluxes, SST and sea ice (extent, concentration and thickness).

3.4 Additional comments on the needs for boundary conditions, initialization and validation of climate models

Table II lists some of the recognized data requirements for initializing, validating and providing boundary conditions for climate models.

Data are needed with a range of temporal resolutions: monthly means and variances, both on a climatological basis and for individual months; daily data are explicitly required in some cases as are data on the diurnal cycle of some quantities.

Table II. Data required to provide initialization, validation and boundary conditions for climate models (tentative)

	Boundary	Initialization	Validation
Atmosphere			
T, q, V (surf & u/a)	★ (surf)		•
Cloudiness	★		•
Radiative fluxes (surface, vertical profiles & TOA)	★		•
Precipitation	★		•
Surface fluxes	★		•
Ozone	•		•
Land surface			
Albedo	•		•
Snow depth		•	•
Vegetation	•	(•)	•
Runoff	•		•
Soil moisture		•	•
Surface temperature		•	•
Topography	•		
Roughness	•		
Sea ice			
Extent/concentration	•	•	•
Thickness	•	•	•
Roughness	•		
Ocean			
Dynamic height		(•)	•
Surface *T, S, V*	• (SST)	•	•
T, S, V structure		•	•
Mixed-layer depth		•	•
Wave characteristics (height etc.)			•
Tracers		•	•
Water type (plankton, CO_2, etc.)	•		

Size of dots signifies probable importance.
★ signifies over ocean only.

Future model assessments would benefit particularly from improved data sets on:

Precipitation and evaporation rates over the oceans.

Evapotranspiration, soil moisture and snow depth over land.

Clouds.

Ocean properties (temperature, salinity, currents, etc.).

Sea ice.

With regard to the potential of climate data sets produced by means of sophisticated data-assimilation techniques there is a need for climate modellers to explore more thoroughly how 'operational' archives can be utilized more comprehensively for model validation. There is still considerable capital to be extracted from existing data sets and scope for carefully considered reanalyses of data from the recent past, using a fixed model.

There is increasing need to ensure that data are made available in machinable form, compatible with what models require. In that context, more-uniform practices need to be adopted in the retention of the model data which are needed increasingly for model intercomparison studies, e.g. snow-cover frequency and depth, extremes and means of daily near-surface temperature.

3.5 Data for assimilation techniques for development of climate models

There are insufficient observations at any one time to determine the state of the atmosphere (even less for the oceans). Therefore we need to invoke any additional information we have, and this is available indirectly as the knowledge of the behaviour and structure of the atmosphere and, to a lesser extent, of the oceans, which we have encapsulated in the formulations of our operational weather forecasting and climate models. In particular, knowledge of evolution with time is embodied in operational forecasting systems and this enables the use of data distributed in time. Such models also provide a dynamically and physically consistent means of representing the atmosphere and oceans, and of deriving fluxes and other diagnostic quantities.

Assimilation is the process of finding the model representation which is most consistent with the available observations. Given observations distributed in time and space, and a forecast model, we can perform a 4-dimensional data assimilation. This is normally done by adding observations as the model is integrated forward in time. The current model-state summarizes in an organized way the information from earlier observations and, given new observations, the model state is modified to be consistent with these and the earlier information.

It should be emphasized that at any given time the model state usually contains more information than can be extracted solely from the currently available observations. However, only variables which are well represented in the weather forecasting model can be assimilated sensibly in this way. There is considerable need and scope therefore for developing data assimilation techniques to process new types of observations within the framework of model assimilation in order to calculate the misfit between observed (or subsequently derived) properties and those produced (or diagnosed) from climate model integrations. Such observational and model comparisons can be used to validate and improve the representation of the physical processes in models and, conceivably, when such parametrizations have been demonstrated to represent an observed property adequately, then the model can be developed into a full assimilation using inverse methodology.

Acknowledgements

The above notes on the role of observations in climate prediction and research were compiled following discussions with several colleagues in the Meteorological Office. I am indebted in particular to H. Cattle, C.K. Folland, A.C. Lorenc, J.F.B. Mitchell, D.E. Parker and P.R. Rowntree.

Awards

L.G. Groves Memorial Prizes and Awards for 1989

At a joint ceremony at RAF Odiham on 10 December 1990 The Chief of Air Staff, Air Chief Marshal Sir Peter Harding, GCB, ADC, D.Sc., F.R.Ae.S., CBIM, presented the Wilkinson Battle of Britain Memorial Sword to the Support Helicopter Force and the L.G. Groves Prizes and Awards to the prize-winners. Air Vice-Marshal D.O. Crwys-Williams, RAF, Director General of Personnel Services, Air Officer Commanding No.1 Group, read the citations and announced the prize-winners.

Meteorology Prize — A.C. Lorenc

The citation for this award was:

'Mr Lorenc is one of the world's leading experts on research into effective methods of processing meteorological observations automatically to provide initial conditions for numerical weather forecasts. A hallmark of his work is its sound theoretical basis and its clear practical applicability.

Recently he showed that quality-control procedures could be built upon well-found statistical principles, and he demonstrated that automatic techniques can supplant time-consuming human scrutiny of data for errors.

Another of his innovations is the scheme currently used to provide operational analyses. One of its features is the ability to assimilate asynoptic observations (such as aircraft data) at the actual time that the measurements were made rather than (as was previously done) at the nearest 6-hour time slot; such a procedure makes better use of the data especially in rapidly developing synoptic situations. Its operational implementation in late 1988 has lead to improvements in the accuracy of wind forecasts for aviation.

More recently his attention has turned to the effective use of remotely sensed data. He is Principal Investigator for the American Earth Observation Satellite and for the European ERS-1 satellite. His advocacy of the use of numerical model forecasts, rather than climatology, as a first guess for satellite-derived temperatures has led to improved forecasts, and has strongly influenced US meteorologists to adopt a similar approach.'

Meteorological Observation Award — W.D.N. Jackson

The citation for this award was:

'Mr Jackson has been at the Meteorological Research Flight for 3½ years. During this time he has been in charge of the team of about 20 people responsible for the aircraft instrumentation and the airborne and ground-based computer systems used to analyse the resulting data. He has caused significant improvements and advancements in all these areas and during 1990 a new display and analysis system was completed. Large parts of these systems were designed and implemented by Mr Jackson himself. The end result is much better aircraft utilization due to both the new real-time displays of data on the aircraft and the ability to analyse flight data in detail overnight so as to identify problems and issues prior to subsequent flights. In addition to these technical advances Mr Jackson has created an atmosphere in which the staff recognize the importance of aircraft availability and have a framework within which to strive to maximize it. He has made a most significant contribution to the observing programme of the Meteorological Research Flight.'

Other prizewinners

The Air Safety Prize was presented to Flt. Lt. R.L. Foulkes B.Sc., RAF, but the Ground Safety Award was not presented as the prize-winner, Sqn. Ldr. M.A. Calame, RAF, was unable to attend.

Correction

Meteorological Magazine, April 1991, p. 73, Review of *Global Air Pollution.*

The specific reference to Professor Scorer's book was accidentally transposed to the second paragraph, but should have been included at the end of the first paragraph, as an alternative book to the one under review. Apologies are offered for any implied misrepresentation.

Satellite photographs — 2 February 1991 at 1533 UTC

The NOAA-11 pictures exhibit features which have come to be recognized as hallmarks of the onset of explosive cyclogenesis.

The images display several prominent features as highlighted on the schematic diagram in Fig. 1:

(a) Cloudy band, F, which is symptomatic of a warm conveyor belt flow associated with a well-established cold front.

(b) The 'cloud head' or 'baroclinic leaf', C, which is particularly striking. It is interpreted as a region of strong slantwise ascent occurring rearwards of a newly developing front RR. The corresponding infra-red image reveals a transition from warm cloud tops at the eastern edge of this cloud shield to coldest cloud tops near its sharply defined western boundary — a feature typical of slantwise ascending motion.

(c) A narrow cloud-free region separates cloud masses C and F — this is particularly prominent on infra-red imagery. Such 'dry intrusions' or 'dry wedges' (see Monk and Bader*) are often a feature of rapidly deepening depressions.

Further to the west, streets of convective cloud, P, stream eastwards around an upper trough, the accompanying cold advection reinforcing the thermal gradient along the new frontal zone. Lines of convective cloud can be seen undercutting the overhang of cirrostratus.

The southern, cyclonically curved, tail of the cloud head consists only of low cloud, at the leading edge of which is a well-marked narrow 'rope cloud' (RR). This probably represents line convection at the surface cold front which has been overridden by the intrusion of dry air aloft.

The transverse striations in the cloud head have been observed previously, notably in the Great Storm of October 1987 (see Shutts†), but are not fully understood. The latitudinal banding became less pronounced in later satellite passes, obscured by thickening cirrus layers generated by continued slantwise ascent.

The developing low, L, was estimated to have been centred near the northern end of the rope cloud, with a central pressure of about 990 mb. The midday operational analysis of the fine-mesh model had identified only an open wave of about 1000 mb, but 24 hours later the low had deepened to below 935 mb as it crossed Iceland, causing extensive structural damage. Many Icelandic stations observed hurricane force winds: Vestmannaeyjar on the south coast reported a mean wind of 103 kn at 1200 UTC on 3 February.

Although the numerical weather prediction guidance based on data at 1200 UTC on 2 February failed to capture the intense degree of cyclogenesis, the imagery was used as a basis for adjusting later model analyses to

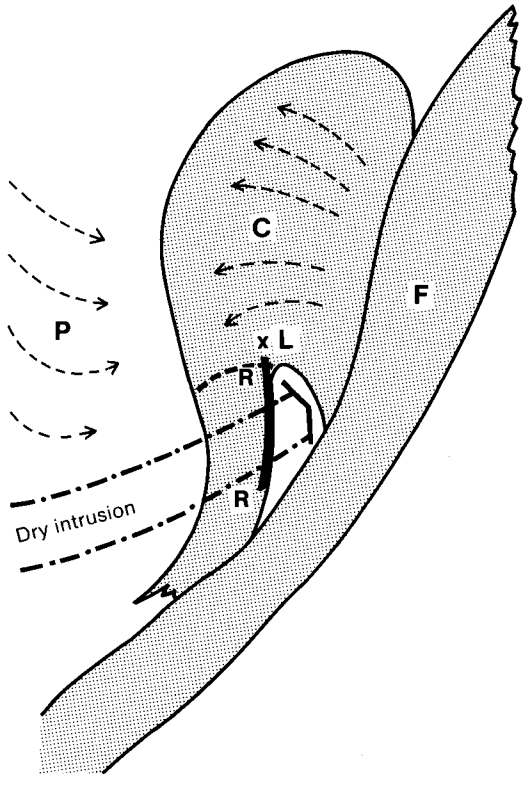

Figure 1. Schematic diagram of the features described in the text.

* Monk, G.A. and Bader, M.J.; Satellite images showing the development of the storm of 15–16 October 1987. *Weather*, **43**, 1988, 130–135.

† Shutts, G.J.; Dynamical aspects of the October storm 1987: A study of a successful fine-mesh simulation. *Q J R Meteorol Soc*, **116**, 1990, 1315–1347.

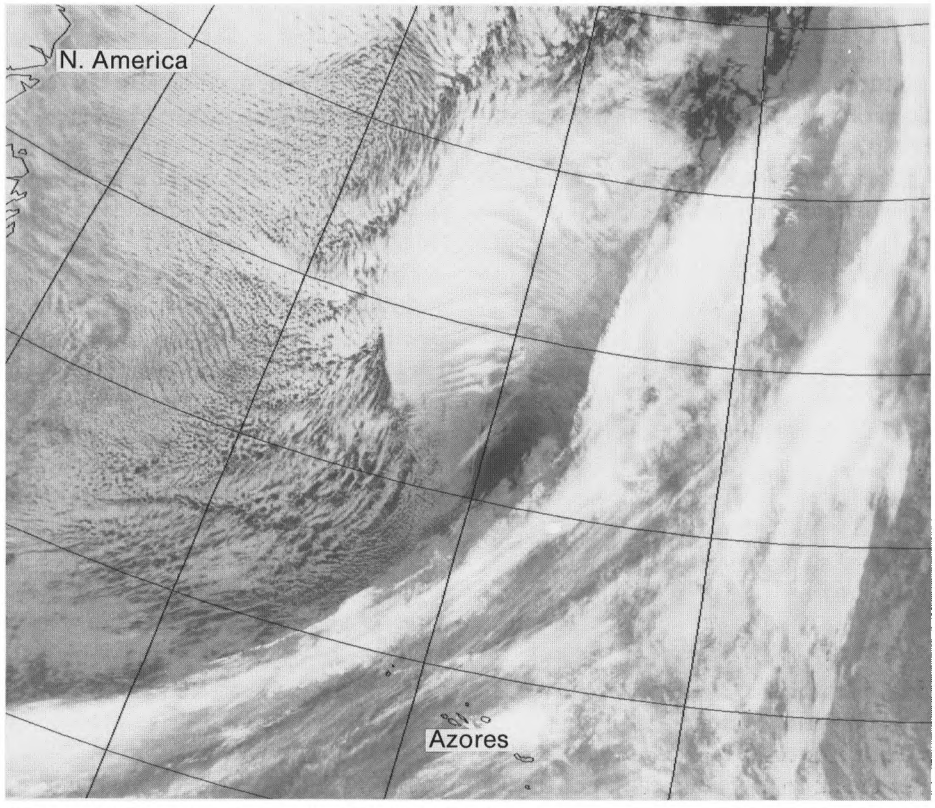

Figure 2. Infra-red image of the situation shown schematically in Fig. 1. *Photograph by courtesy of University of Dundee*

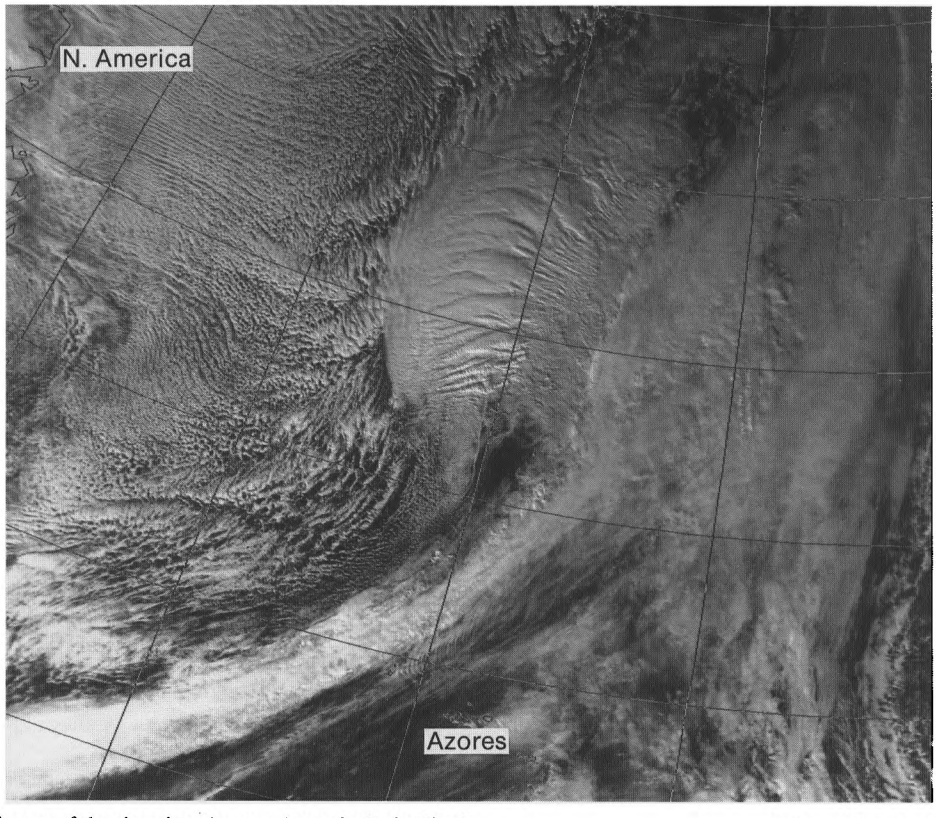

Figure 3. Visual image of the situation shown schematically in Fig. 1. *Photograph by courtesy of University of Dundee*

cater for the suspected existence of a much deeper depression. This successfully culminated in a much improved analysis, and a subsequent operational run of the model subsequently deepened the depression to 946 mb accompanied by an extremely vigorous circulation.

J. Norris and M.V.Young

GUIDE TO AUTHORS

Content

Articles on all aspects of meteorology are welcomed, particularly those which describe results of research in applied meteorology or the development of practical forecasting techniques.

Preparation and submission of articles

Articles, which must be in English, should be typed, double-spaced with wide margins, on one side only of A4-size paper. Tables, references and figure captions should be typed separately. Spelling should conform to the preferred spelling in the *Concise Oxford Dictionary* (latest edition). Articles prepared on floppy disk (Compucorp or IBM-compatible) can be labour-saving, but only a print-out should be submitted in the first instance.

References should be made using the Harvard system (author/date) and full details should be given at the end of the text. If a document is unpublished, details must be given of the library where it may be seen. Documents which are not available to enquirers must not be referred to, except by 'personal communication'.

Tables should be numbered consecutively using roman numerals and provided with headings.

Mathematical notation should be written with extreme care. Particular care should be taken to differentiate between Greek letters and Roman letters for which they could be mistaken. Double subscripts and superscripts should be avoided, as they are difficult to typeset and read. Notation should be kept as simple as possible. Guidance is given in BS 1991: Part 1: 1976, and *Quantities, Units and Symbols* published by the Royal Society. SI units, or units approved by the World Meteorological Organization, should be used.

Articles for publication and all other communications for the Editor should be addressed to: The Chief Executive, Meteorological Office, London Road, Brackneli, Berkshire RG12 2SZ and marked 'For Meteorological Magazine'.

Illustrations

Diagrams must be drawn clearly, preferably in ink, and should not contain any unnecessary or irrelevant details. Explanatory text should not appear on the diagram itself but in the caption. Captions should be typed on a separate sheet of paper and should, as far as possible, explain the meanings of the diagrams without the reader having to refer to the text. The sequential numbering should correspond with the sequential referrals in the text.

Sharp monochrome photographs on glossy paper are preferred; colour prints are acceptable but the use of colour is at the Editor's discretion.

Copyright

Authors should identify the holder of the copyright for their work when they first submit contributions.

Free copies

Three free copies of the magazine (one for a book review) are provided for authors of articles published in it. Separate offprints for each article are not provided.

Contributions: It is requested that all communications to the Editor and books for review be addressed to the Chief Executive, Meteorological Office, London Road, Bracknell, Berkshire RG12 2SZ, and marked 'For *Meteorological Magazine*'. Contributors are asked to comply with the guidelines given in the *Guide to authors* which appears on the inside back cover. The responsibility for facts and opinions expressed in the signed articles and letters published in *Meteorological Magazine* rests with their respective authors.

Subscriptions: Annual subscription £33.00 including postage; individual copies £3.00 including postage. Applications for postal subscriptions should be made to HMSO, PO Box 276, London SW8 5DT; subscription enquiries 071–873 8499.

Back numbers: Full-size reprints of Vols 1–75 (1866–1940) are available from Johnson Reprint Co. Ltd, 24–28 Oval Road, London NW1 7DX. Complete volumes of *Meteorological Magazine* commencing with volume 54 are available on microfilm from University Microfilms International, 18 Bedford Row, London WC1R 4EJ. Information on microfiche issues is available from Kraus Microfiche, Rte 100, Milwood, NY 10546, USA.

June 1991

Edited by Corporate Communications
Editorial Board: R.J. Allam, R. Kershaw, W.H. Moores, P.R.S. Salter

Vol. 120
No. 1427

Contents

ISSN 0026–1149

ISBN 0-11-728857-8

9 780117 288577

Printed in the United Kingdom for HMSO
Dd 0291241 6.91 C13 503 12521

The Meteorological Magazine

July 1991

Sensitivity tests for road surface temperature prediction
Estimating fluctuations in pollutant concentration

HMSO

Met.O.998 Vol. 120 No. 1428

First published 1991

HMSO publications are available from:

HMSO Publications Centre
(Mail and telephone only)
PO Box 276, London, SW8 5DT
Telephone orders 071-873 9090
General enquiries 071-873 0011
(queuing system in operation for both numbers)

HMSO Bookshops
49 High Holborn, London, WC1V 6HB 071-873 0011 (counter service only)
258 Broad Street, Birmingham, B1 2HE 021-643 3740
Southey House, 33 Wine Street, Bristol, BS1 2BQ (0272) 264306
9–21 Princess Street, Manchester, M60 8AS 061-834 7201
80 Chichester Street, Belfast, BT1 4JY (0232) 238451
71 Lothian Road, Edinburgh, EH3 9AZ 031-228 4181

HMSO's Accredited Agents
(see Yellow Pages)

and through good booksellers

3 8078 0010 2467 0

The Meteorological Magazine

July 1991
Vol. 120 No. 1428

551.525.2:551.509.314:625.7

Spectral analysis and sensitivity tests for a numerical road surface temperature prediction model

J.E. Thornes and J. Shao
University of Birmingham

Summary

Spectral analysis and sensitivity analysis are used to discover which meteorological input parameters and road thermal properties are most important to a road surface temperature prediction model. The results show that the model is most sensitive to air temperature and cloud cover, and not very sensitive to road thermal properties.

1. Introduction

Numerical road ice prediction models have successfully reproduced the major features of road surface conditions (Thornes 1984, 1989, Rayer 1987, Shao 1990). However, few studies, if any, have looked at the interrelationships between road surface temperature and the geographical, road construction and meteorological inputs to the models, for instance as shown in Table I. How does the output of a numerical model respond to the model parameters and model input, whose values usually cover a considerable range? Spectral analysis and sensitivity analysis are used in this paper in order to answer some of these questions.

Some general research has been carried out relating road surface temperatures to topography and certain weather parameters, such as the influence of topography and wind on the variation of minimum air temperatures and road surface temperatures (Tabony 1985, Bogren and Gustavsson 1988, Gustavsson 1990). Weather conditions have been classified for convenience into damped, intermediate and extreme days by Thornes (1989). Farmer and Tonkinson (1989) have looked at the sensitivity of the Meteorological Office model (Rayer 1987) to road thermal properties and road surface albedo. These researches have shown the value of

Table I. Parameters that control road surface temperature

Geographical	Road construction	Meteorological
Latitude	Depth of construction	Solar radiation
Altitude	Thermal conductivity	Terrestrial radiation
Topography	Thermal diffusivity	Air temperature
Sky view	Emissivity	Cloud cover
Land use	Albedo	Wind velocity
Pollution	Traffic	Humidity
Roughness length		Precipitation
De-icing chemical		

investigating the interaction and sensitivity of road surface temperatures to their environment, but they lack sufficient systematic and quantitative information for model users, and especially for modellers who wish to improve their model predictions. This paper aims to examine the importance of the meteorological inputs and road thermal properties in order to further our understanding of the problems involved.

A method of cross-spectral analysis is used to explore the cross-correlations between road surface temperatures and several meteorological parameters. Then a variety of sensitivity tests are carried out using the Icebreak model (Shao 1990) to examine the response of the model output to changes in both meteorological and road thermal properties, illustrating each with results from two control runs with typical values. Such results reflect model variability and provide suggestions to give better operational results, e.g. via a cautious selection of meteorological, road construction and geographical input data.

2. Cross-correlation analysis

As mentioned by Thornes and Shao (1991), model prediction error originates largely from meteorological input parameters, which include air temperature, dew-point, wind speed, cloud amount and type, and rainfall. All of these parameters are considered as random parameters or part of a time series. To examine correlations between road surface temperature and the meteorological parameters over different time-scales, spectral analysis is used. Details of the method are given in the Appendix.

The results of the spectral analysis are listed in Tables II and III. There are 456 sets of hourly observations from Chapman's Hill on the M5 motorway including road and air temperatures, relative humidity and wind speed. The maximum lag considered in Table II is 24 hours. The number of cloud observations is 129, and the maximum lag considered in Table III is also 24 hours. In these tables, T is the periodicity in hours; $C^2(T)$ is the coherence squared for each time-period (coherence measures the degree of correlation between two time-series) and $L(T)$ is the time difference of two time-series on the cycle of Tth periodicity in hours. The asterisk (*) in these tables indicates that the coherence passes the significance test at either a significance level of 0.01 (Table II) or 0.05 (Table III).

The results show that road surface temperature (T_s) has a close relationship with all the meteorological parameters except cloud cover on a half-day (12-hour) cycle. The small values in $L(T)$ indicate that the variation of T_s responds to that of meteorological parameters very quickly. A significant correlation also exists on some other cycles such as daily and 6-hour cycles. The results show that the air temperature is the most important factor to which road surface temperature responds. When there is a negative phase-difference the air temperature changes are driving the road surface temperatures (e.g. 6- and 16-hour lag), whereas with a positive value of phase difference the road surface temperature is driving air temperature changes (e.g. 8- and 24-hour lag). The lags are not simple to interpret in physical terms due to the effect of traffic, but basically one would expect that the lags should be positive during the day when the road is likely to be warmer than the air, and the opposite at night.

3. Sensitivity tests for meteorological inputs

The most reliable information about the physical nature of the variation of road surface temperature is obtained by actual measurement. Such an experimental investigation is expensive on time and resources and, in most cases, impossible. For instance one would have to wait a long time to measure all cloud combinations at a given wind speed. Sensitivity analysis, by using a mathematical and physical model, is a valuable way to quickly gain an insight into the controlling aspects of the variation of road surface temperature and to develop confidence in model predictions. The Icebreak model is run with standard meteorological observations (for the so-called control runs) for 4 December 1987 and 24 February 1988, representing a 'damped' day and an

Table II. Results of cross-power spectrum analysis between road surface temperature ($X_j(t)$) and meteorological parameters ($X_k(t)$) for Chapman's Hill, winter 1987/88, 456 samples

T hour	Air temperature $C^2(T)$	Air temperature $L(T)$	Humidity $C^2(T)$	Humidity $L(T)$	Wind speed $C^2(T)$	Wind speed $L(T)$
24.0	0.669*	0.44	0.163	−2.39	0.067	1.73
16.0	0.619*	−0.79	0.096	2.19	0.005	2.47
12.0	0.744*	0.08	0.386*	0.35	0.277*	0.38
8.0	0.569*	0.72	0.199	0.99	0.021	−1.16
6.0	0.588*	−0.70	0.267*	−0.76	0.183	−0.50
4.0	0.115	−0.24	0.020	−0.22	0.129	−0.23
3.0	0.147	−0.30	0.296*	−0.24	0.043	−0.33
2.0	0.375*	0.02	0.161	0.24	0.129	−0.05

* see text for further explanation

Table III. Results of cross-power spectrum analysis between road surface temperature ($X_j(t)$) and cloud cover ($X_k(t)$) for Chapman's Hill, winter 1987/88, 129 samples

T hour	Cloud amount $C^2(T)$	Cloud amount $L(T)$	Cloud type $C^2(T)$	Cloud type $L(T)$
24.0	0.249*	−0.22	0.197	0.49
20.0	0.106	0.23	0.048	0.35
15.0	0.210	0.83	0.013	−1.04
12.0	0.156	−0.34	0.057	−0.02
10.0	0.310*	0.57	0.048	−0.18
8.0	0.095	0.26	0.132	0.62
6.0	0.554*	0.22	0.071	−0.06

* see text for further explanation

'extreme' day. Figs. 1 and 2 show the results of model prediction with standard input.

In the tests, each of the input parameters (air temperature, dew-point, wind speed, cloud amount and cloud type) is varied through a range of values and all other parameters are held constant. The range of values shown here for each parameter are added or subtracted for each 3-hour input. The model is run from noon to noon and input values are supplied for 1500, 1800, 2100, 0000, 0300, 0600, 0900 and 1200 hrs:

(a) Air temperature: ± 1 °C: the results are shown in Figs 3 and 4.

(b) Dew-point: ± 1 °C (Figs 5 and 6).

(c) Wind speed is the most variable atmospheric parameter considered. In the test, it undergoes a ± 3 kn change which is in accordance with typical forecast input errors (see Thornes and Shao (1991)). Figs 7 and 8 show the results.

(d) Cloud amount: ± 1 okta when the amount is less than 8 oktas (Figs 9 and 10).

(e) Cloud type: ± 1 cloud type (1 = low cloud to 3 = high cloud) where appropriate (Figs 11 and 12).

The results of the test runs are displayed in Tables IV and V, and compared with the control runs. The bias, standard deviation (SD) and difference of minimum surface temperatures (DT(min)) are given in the tables. The running difference shown in the tables is given by:

$$\text{running difference} = V_m - V_c$$

where V_m is the bias, or SD, or DT(min) with modified input, and V_c is that of control run.

It is seen from the tables that of all of these meteorological parameters, air temperature is the most important. A change of ± 1 °C in air temperature results in an extra error of about ± 0.8 °C in the road surface temperature bias and minimum road surface temperature. This result accords with that of the spectral analysis discussed above. Cloud cover is the second most important factor. Its impact on the model predictions, especially on the prediction of minimum surface temperature, is as expected. The impact of wind speed is small and it is greater on an 'extreme' day than on a 'damped' day. Dew-point seems to only have a minor influence on model output.

4. Sensitivity tests for road thermal properties

It is very difficult to obtain accurate values for the thermal properties of a road construction. Firstly, if sample cores are taken from a road to be analysed in the laboratory, inevitably water is needed to cool the diamond cutter. Water contamination in the sample is impossible to correct for, and significantly affects the thermal properties of the sample. Secondly, the depth of the sub-layers below the surface is often unknown, and therefore one has to make assumptions about the overall thermal properties of a road structure including the sub-base. Hence one has to take published data from the literature and select sensible values for the particular road being dealt with. Model runs are then used to test the sensitivity of road surface temperature to the thermal properties of the road construction.

Table VI shows the typical values of road thermal properties used by several authors. The thermal properties of asphalt, concrete and soil are also unlikely to be the same at different sites, but inevitably the same values have to be used. It can be seen that in general the

Table IV. Results of sensitivity tests for meteorological parameters and comparison to standard results for Chapman's Hill, 4 December 1987

Tests	Output of tests			Running difference		
	Bias	SD	DT(min)	A	B	C
Standard	0.15	0.289	0.00	—	—	—
T_a (+1)	0.86	0.287	0.74	0.71	0.00	0.74
T_a (−1)	−0.64	0.266	−0.81	−0.79	−0.02	−0.81
DP (+1)	0.15	0.288	0.03	0.00	0.00	0.03
DP (−1)	0.05	0.246	−0.16	−0.10	−0.04	−0.16
WS (+3)	0.07	0.278	0.01	−0.08	−0.01	0.01
WS (−3)	0.24	0.313	0.04	0.09	0.02	0.04
CA (+1)	—	—	—	—	—	—
CA (−1)	0.04	0.466	−0.27	−0.11	0.18	−0.27
CT (+1)	−0-14	0.432	−0.48	−0.29	0.14	−0.48
CT (−1)	—	—	—	—	—	—

Key: T_a — air temperature (°C)
DP — dew-point (°C)
WS — wind speed (kn)
CA — cloud amount in oktas
CT — cloud type (0 = no cloud, 1 = low cloud, 2 = medium cloud and 3 = high cloud
A — difference of mean errors
B — difference of standard deviations
C — difference of minimum surface temperature errors

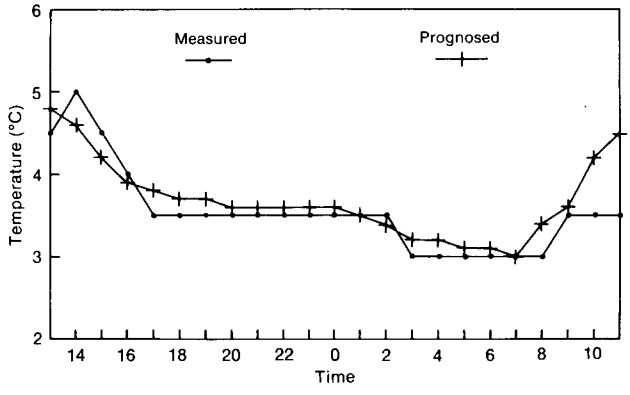

Figure 1. Output with standard input for Chapman's Hill 4 December 1987.

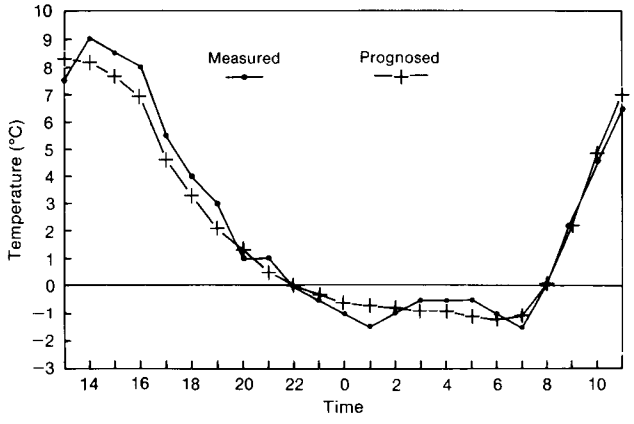

Figure 2. Output with standard input for Chapman's Hill 24 February 1988.

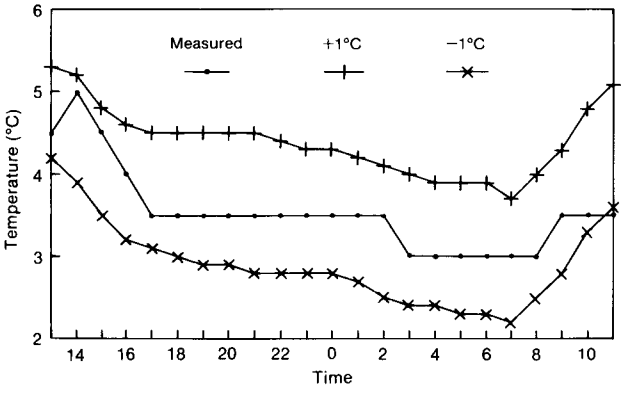

Figure 3. Output with changes in air temperature for Chapman's Hill 4 December 1987.

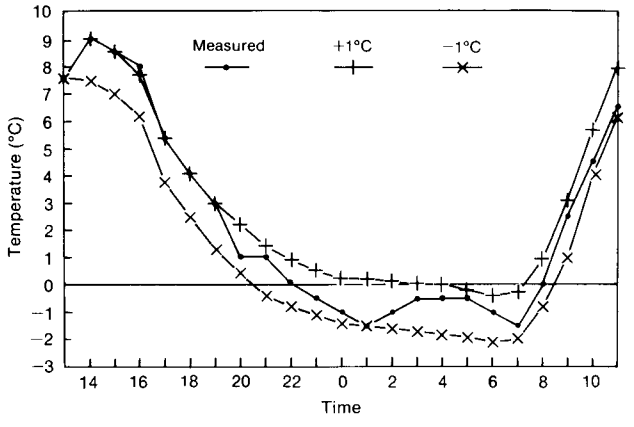

Figure 4. Output with changes in air temperature for Chapman's Hill 24 February 1988.

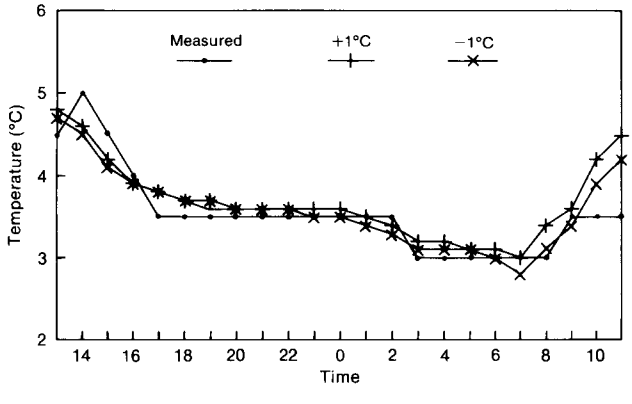

Figure 5. Output with changes in dew-point for Chapman's Hill 4 December 1987.

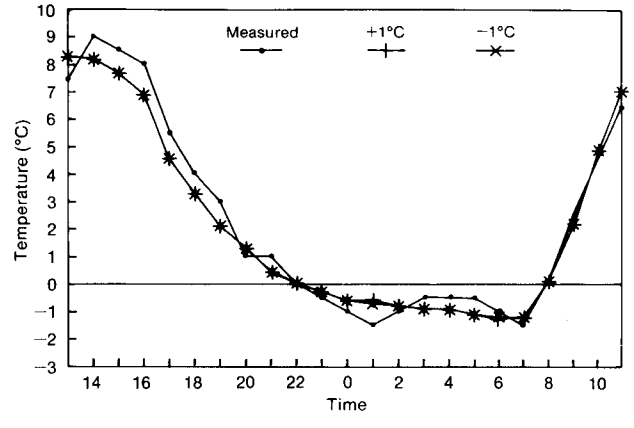

Figure 6. Output with changes in dew-point for Chapman's Hill 24 February 1988.

conductivity of asphalt is lower than that of concrete, and that heat capacity varies less than conductivity.

For this sensitivity analysis the Icebreak model is run with a range of ± 20% of the thermal parameters. The road construction is assumed to be: the top sub-layer (0–10 cm asphalt), the middle sub-layer (10–40 cm concrete) and the bottom sub-layer (40–100 cm soil or granite). Table VII shows the values of conductivity and capacity of asphalt, concrete and soil (or granite) used in the sensitivity tests.

In Table VII, tests (a)–(b) and tests (c)–(d) are for a change of conductivity and capacity of asphalt and concrete, test (e) is for sandy soil and test (f) is for granite. The results of the tests are compared with those of the standard input in Tables VIII and IX. Comparing the model predictions of the control runs to those of the

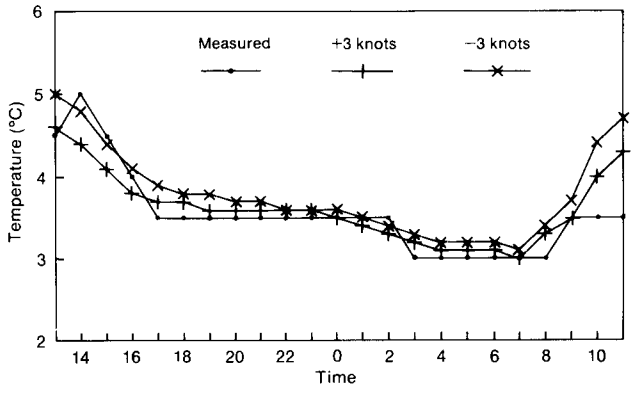

Figure 7. Output with changes in wind speed for Chapman's Hill 4 December 1987.

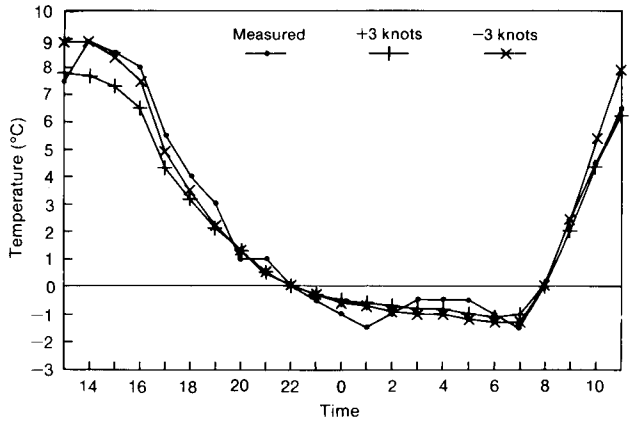

Figure 8. Output with changes in wind speed for Chapman's Hill 24 February 1988.

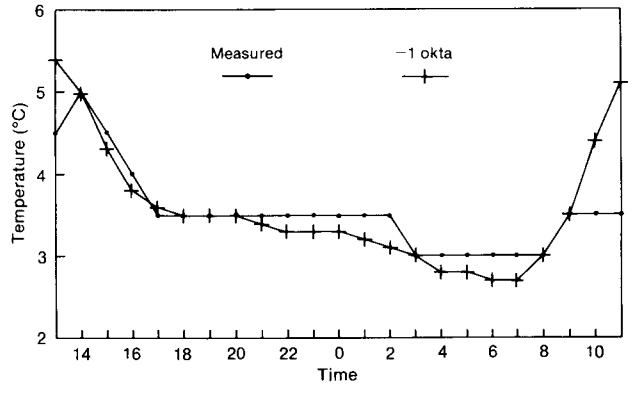

Figure 9. Output with changes in cloud amount for Chapman's Hill 4 December 1987.

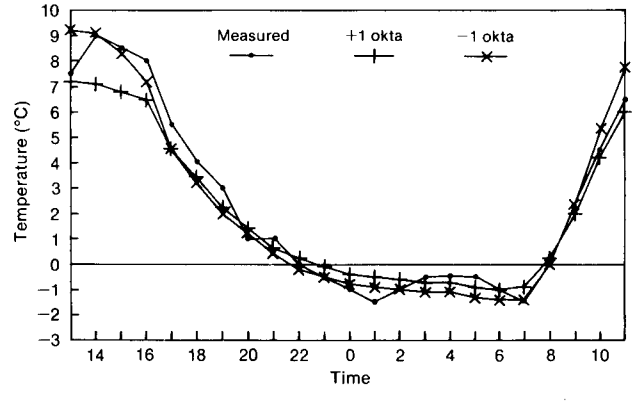

Figure 10. Output with changes in cloud amount for Chapman's Hill 24 February 1988.

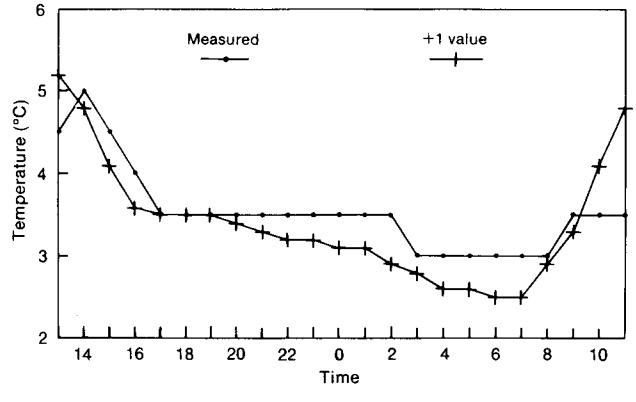

Figure 11. Output with changes in cloud type for Chapman's Hill 4 December 1987.

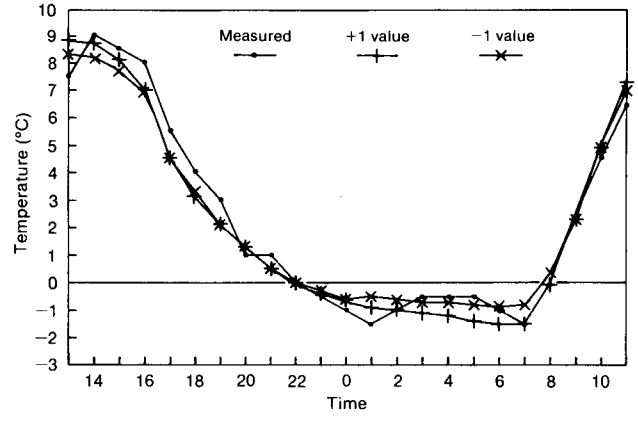

Figure 12. Output with changes in cloud type for Chapman's Hill 24 February 1988.

modified runs, it can be seen that a 20% change of conductivity or capacity of the road sub-layers does not significantly influence model output.

5. Conclusions

Of the many factors that influence the variation of road surface temperature, air temperature is the most important. In routine operation of an ice prediction model when forecast meteorological input is provided, any error in the forecast of air temperature will result in a similar error in model road surface temperature prediction.

Cloud cover (i.e. cloud amount and cloud type) is another key factor governing the variation in road surface temperatures. On an 'extreme' day, the road surface temperature responds quickly to a change of

Table V. Results of sensitivity tests for meteorological parameters and comparison to standard results for Chapman's Hill, 24 February 1988

Tests	Output of tests			Running difference		
	Bias	SD	DT(min)	A	B	C
Standard	−0.16	0.573	0.30	—	—	—
T_a (+1)	0.68	0.571	1.14	0.84	0.00	0.84
T_a (−1)	−0.99	0.568	−0.57	−0.83	−0.01	−0.87
DP (+1)	−0.16	0.571	0.23	0.00	0.00	0.07
DP (−1)	−0.17	0.567	0.26	−0.01	−0.01	−0.04
WS (+3)	−0.28	0.638	0.37	−0.12	0.07	0.07
WS (−3)	0.02	0.615	0.17	0.18	0.04	−0.13
CA (+1)	−0.28	0.738	0.48	−0.12	0.17	0.18
CA (−1)	−0.09	0.687	0.08	0.07	0.11	−0.22
CT (+1)	−0.18	0.620	−0.04	−0.02	0.05	−0.34
CT (−1)*	−0.06	0.600	0.55	0.10	0.03	0.25

* Only the values of cloud type at 0000, 0300 and 0600 UTC are changed.
Key — see Table IV.

Table VI. Typical values of thermal properties of road materials

Source	Substance		Conductivity W m^{-1} K^{-1}	Heat capacity 10^6 J m^{-3} K^{-1}
Farmer and Tonkinson (1989)	Asphalt:	wearing	1.40	2.1
		basecourse	1.00	2.1
		roadbase	1.00	2.0
		sub-base	1.25	1.9
		subsoil	1.30	2.5
	Concrete:	roadbed	2.60	2.4
		sub-base	1.25	1.9
		subsoil	1.30	2.5
Thornes (1984)	Asphalt		1.30	1.855
	Concrete		2.01	1.675
Oke (1987)	Asphalt		0.75	1.940
	Concrete:	dense	1.51	2.11
McCabe and Thompson (1989)	Individual B-road:			
		laboratory	1.40	1.73–2.49
		field	0.97–1.48	1.59–2.40
	Multi-layer road:			
		unfrozen	0.88–1.09	1.77–2.10
		dry ground	0.63–0.95	—
		wet ground	0.98–1.26	—
Weng *et al.* (1981)	Loam soil 70% saturated		1.58	3.10

Table VII. Conductivity (k) (W m^{-1} K^{-1}) and capacity (C_m) (10^6 J m^{-3} K^{-1}) of road sub-layers for sensitivity tests

Test	Asphalt		Concrete		Soil (granite)	
	k	C_m	k	C_m	k	C_m
Standard	1.25	1.90	1.30	1.90	1.58	3.10
Test (a)	1.50	1.90	1.56	1.90	1.58	3.10
Test (b)	1.00	1.90	1.04	1.90	1.58	3.10
Test (c)	1.25	2.28	1.30	2.28	1.58	3.10
Test (d)	1.25	1.52	1.30	1.52	1.58	3.10
Test (e)	1.25	1.90	1.30	1.90	0.30	1.28
Test (f)	1.25	1.90	1.30	1.90	2.50	1.89

Table VIII. Results of sensitivity test for road thermal properties for Chapman's Hill, 4 December 1987

Tests	Output of tests			Running difference		
	Bias	SD	DT(min)	A	B	C
Standard input	0.15	0.289	0.00	—	—	—
Test (a)	0.17	0.269	0.10	0.02	−0.02	0.10
Test (b)	0.10	0.307	0.00	−0.05	0.02	0.00
Test (c)	0.18	0.278	0.07	0.03	−0.01	0.07
Test (d)	0.10	0.302	−0.01	−0.05	0.01	−0.01
Test (e)	0.15	0.289	0.04	0.00	0.00	0.04
Test (f)	0.14	0.286	0.02	−0.01	0.00	0.02

Table IX. Results of sensitivity test for road thermal properties for Chapman's Hill, 24 February 1988

Tests	Output of tests			Running difference		
	Bias	SD	DT(min)	A	B	C
Standard input	−0.16	0.573	0.30	—	—	—
Test (a)	−0.10	0.559	0.40	0.06	−0.01	0.10
Test (b)	−0.20	0.590	0.20	−0.04	0.02	−0.10
Test (c)	−0.08	0.560	0.41	0.08	−0.01	0.11
Test (d)	−0.22	0.595	0.14	−0.06	0.02	−0.16
Test (e)	−0.14	0.572	0.30	0.02	0.00	0.00
Test (f)	−0.16	0.567	0.28	0.00	−0.01	−0.02

cloud amount and cloud type. Some error in the forecast and observation of cloud cover is usually unavoidable and is thus one of the major sources of model prediction error.

The influence of dew-point temperature and wind speed are normally small. The impact of wind speed on model output is greater on 'extreme' days than on 'damped' days. A 20% variation in the thermal conductivity and capacity of the layers of road construction and soil has a small impact on model predictions.

Acknowledgements

This research was supported in part by Vaisala TMI, the Strategic Highway Research Program and the British Council. The authors are grateful to Bill Fairmaner of Vaisala TMI, and J. Kings, J. Hales and R.J. Johnson of the Birmingham University Weather Service (BUWS) for their assistance in data collection.

References

Båth, M., 1974: Spectral analysis in geophysics. Amsterdam, Elsevier.

Bogren, J. and Gustavsson, T., 1988: A brief survey of the project — applied climatology, road maintenance and increased traffic safety. SERWEC, Highways Meteorology (newsletter) No. 3.

Farmer, S.F.G. and Tonkinson, P.J., 1989: Road surface temperature model verification using input data from airfields, roadside sites and the mesoscale model. Bracknell, Meteorological Office, Special Investigations Technical Note No. 60. (Unpublished, copy available from National Meteorological Library, Bracknell.)

Gustavsson, T., 1990: Variation in road surface temperature due to topography and wind. *Theor Appl Climatol*, **41**, 227–236.

Koopmans, L.H., 1974: The spectral analysis of time series. New York, Academic Press.

McCabe, E.Y. and Thompson, D.S., 1989: Thermal properties of multi-layered road structures. Grampian Regional Council, Department of Roads, Report No. C201.

Oke, T.R., 1987: Boundary layer climates, 2nd edition. London, Methuen.

Rayer, P.J., 1987: The Meteorological Office forecast road surface temperature model. *Meteorol Mag*, **116**, 180–191.

Shao, J., 1990: A winter road surface temperature prediction model with comparison to others. (Unpublished PhD thesis, University of Birmingham.)

Tabony, R.C., 1985: Relations between minimum temperature and topography in Great Britain. *J Climatol*, **5**, 503–520.

Thornes, J.E., 1984: The prediction of ice formation on motorways. (Unpublished PhD thesis, University of London.)

—, 1989: A preliminary performance and benefit analysis of the UK national road ice prediction system. *Meteorol Mag*, **118**, 93–99.

Thornes, J.E. and Shao, J., 1991: A comparison of UK road ice prediction models. *Meteorol Mag*, **120**, 51–57.

Wèng, D.M., Chen, J.C., Shen, J.C. and Gao, J.B., 1981: Microclimate and micro-agroclimate. Peking, Agriculture Press.

Appendix

In spectral analysis, phase ($P_{j,k}(l)$) and coherence ($C_{j,k}(l)$) are the most useful parameters for measuring the relationship between two time-series $x_j(t)$ and $x_k(t)$. Here l stands for frequency which is the reciprocal of the length of time (period) for $x(t)$ to go through one complete cycle. The phase and coherence are calculated from the power spectral densities ($f_{j,j}(l), f_{k,k}(l)$), cospectrum ($c_{j,k}(l)$) and quadrature spectrum ($q_{j,k}(l)$) by means of the relations

$$c^2_{j,k}(l) = \frac{c^2_{j,k}(l) + q^2_{j,k}(l)}{f_{j,j}(l)\, f_{k,k}(l)} \qquad \text{(A1)}$$

and

$$P_{j,k}(l) = -\arctan(q_{j,k}(l)/c_{j,k}(l)). \qquad \text{(A2)}$$

The spectral densities, cospectrum and quadrature spectrum in equations (A1) and (A2) are estimated from cross-correlation functions (Koopmans 1974, Båth 1974).

The phase function is simply the difference of phase of the two time-series at frequency l or, more precisely, the phase lead of $x_j(t)$ over $x_k(t)$. In practice it is expressed by a time difference in the form

$$L(l) = \frac{mP(l)}{\pi l} .$$

The coherence (coefficient of coherence) has the properties of the absolute value of a correlation at frequency l. In some sense it measures the degree of linear association between the time series $x_j(t)$ and $x_k(t)$.

The significance of coherence is assessed by the statistical variable (Koopmans 1974)

$$F' = \frac{(v-1)C_c^2}{1-C_c^2}$$

where v is calculated from

$$v = \frac{2n - m/2}{m} .$$

Here n is a sample number or size, m the maximum lag and C_c a critical value. F' follows the F-distribution with 2 and $2(v-1)$ degrees of freedom. If

$$C_{j,k}^2 > C_c^2$$

the coherence is considered to be significant.

551.510.42:551.511.61:628.53

A scheme for estimating fluctuations in concentration of an emitted airborne pollutant

F.B. Smith
Meteorological Office, Bracknell

Summary

A simple practical scheme is presented for estimating the probability of exceeding a prescribed concentration, when averaged over a given time-interval, of a passive pollutant emitted from a finite-sized continuous source. A brief summary of the background theory and typical examples are given, with the option of obtaining the required answers simply using the diagrams presented or, somewhat more accurately, the analytical equations. The method has widespread applications in risk analyses wherever the danger of accidental release of hazardous materials to the atmosphere exists.

1. Introduction

Fig. 1 shows an example of a time-record of concentration in a plume at a point some distance downwind of a continuous point source. It shows that, as expected, the plume must be meandering under the action of eddies that are bigger than the width of the plume, so that the concentration is intermittently zero over short periods whereas at other times the concentration is other than zero, albeit quite variable. This complex behaviour can be very important for many hazardous pollutants. Consider three examples:

(a) The pollutant may be inflammable within a band of concentrations, outside of which either there is insufficient material to maintain ignition or too little oxygen. Consideration of the mean concentration alone might suggest this dangerous band is restricted to a fairly short range downwind. Consideration of the distribution of concentrations, the fluctuations, would however indicate that inflammable concentrations could occur over a much greater range of downwind distance.

(b) The pollutant may be toxic (e.g. chlorine gas) and the effective toxicity may increase more rapidly than linearly with concentration c. For example, the toxicity of chlorine is believed to increase like $c^{2.75}$. Thus, whilst consideration of the mean concentration field might suggest it is fairly safe to enter the plume at a given location, in reality, because of the fluctuations, it would be highly dangerous since one breath of chlorine at the concentration of one of the peaks could be fatal. The non-linearity further emphasizes the danger.

(c) Some odours can only be perceived by the human nose above some threshold. The designers of an industrial plant that has some odorous pollutant as a waste product must take into account the likely fluctuations in concentration outside the boundaries

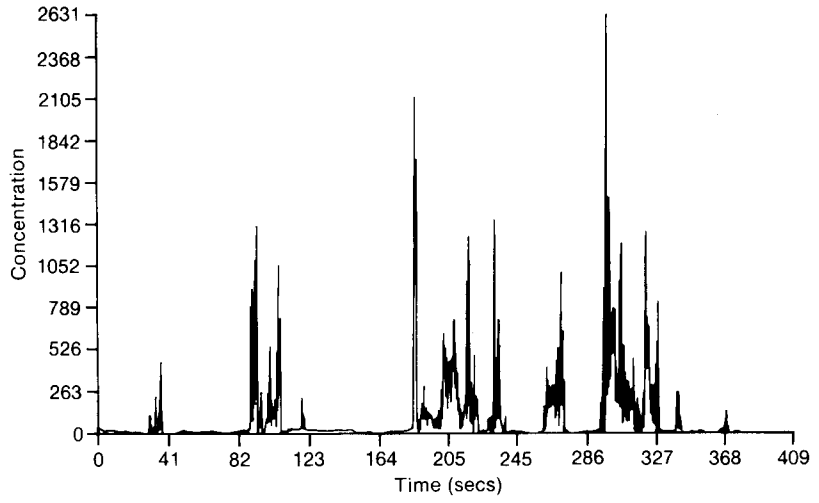

Figure 1. Example of a record of concentration at a point downwind from a point source showing the nature of the concentration fluctuations.

of the plant if they are to avoid a stream of complaints from the public. Rightly, they are not concerned whether the mean concentration can be smelt, but rather whether they can detect the peak concentrations.

Most progress has been made so far in specifying the statistics of the concentration fluctuations with time at a point. However, there is much interest in the spatial distribution of concentration fluctuations. For example, with an inflammable gas, if ignition occurs at some point in the plume where the concentration at the time is within the flammable range it is important to know what is the probability that the flame could travel back along zones of the plume within the range of flammability without any breaks back to the source, or to some location of particular concern (like a home). This is a very difficult problem, although Thomson (1990) has made progress in specifying the nature of spatial covariances of concentration.

2. Available research

It is only within the last 10 years or so that effective research has been directed at this problem, and only now that the beginnings of a practical scheme are emerging. This is the result of complex theory and experimental data. The scheme will no doubt be improved with time, but already it is able to give very useful guidance on the magnitude of the fluctuations and the probability of any concentration being realized at any one time at any downwind position. The background theory will not be given in any detail here. For further details see Sawford (1987), Sykes (1988), Thomson (1990) and Mylne and Mason (1991).

3. The plume and the basic concentration fluctuation parameters

Although the scheme is intended for use with plumes in the atmospheric boundary layer, it will assume homogeneous isotropic turbulence with an exponential Lagrangian velocity correlation function with finite time-scale τ_L. These assumptions are the easiest to study, and the results provide a useful test case for verifying and developing ideas. Moreover, in the atmosphere, several stages of the plume's development occur before the inhomogeneities become important. At large travel-times the inhomogeneities (or the non-stationariness) always become important so that the user must be wary of the results at long range. Initially we will also assume the source has sufficiently small dimensions that it can be treated as a point source.

If σ_1 is the standard deviation of single particles in the across-wind y direction then

$$\sigma_1^2 = 2A(\exp(-T) - 1 + T) \tag{1}$$

where $A = \sigma_v^2 \tau_L^2$ and $T = t/\tau_L$.

If $\frac{1}{2}\sigma_\Sigma^2$ is the variance of the y component of the centroid of a pair of particles taken about the centreline, then

$$\sigma_\Sigma^2 = 4A\left[\exp(-T) - \exp\left(-\frac{T}{2}\right) + \frac{T}{2} + \right.$$
$$\left. + \frac{1}{2}\left\{1 - \exp\left(-\frac{T}{2}\right)\right\}^2\right]. \tag{2}$$

If $2\sigma_\Delta^2$ is the variance of the y component of the separation of a pair of particles, then

$$\sigma_\Delta^2 = 4A\left[\exp\left(-\frac{T}{2}\right) - 1 + \right.$$
$$\left. + \frac{T}{2} - \frac{1}{2}\left\{1 - \exp\left(-\frac{T}{2}\right)\right\}^2\right]. \tag{3}$$

Equations 1–3 satisfy the identity

$$\sigma_\Delta^2 + \sigma_\Sigma^2 = 2\sigma_1^2. \tag{4}$$

The forms of these three variances are shown in Fig. 2.

Thomson's random walk studies have supported the following relationship between the concentration fluctuation and the mean concentration at any point on the downwind centreline:

$$\overline{c^2(0)} = \mu\overline{c(0)}^2\left(\frac{\sigma_1^4}{\sigma_\Sigma^2\sigma_\Delta^2}\right) \qquad (5)$$

where $\mu = 1 + 2\exp\left(-\frac{2\sigma_\Delta}{3\sqrt{A}}\right)$ and where $\overline{c(0)} = \frac{Q}{2\pi u\sigma_1^2}$.

From these relationships we can calculate $\mu\overline{c(0)}A/Q$ and $\sigma_c/\overline{c(0)}$ as functions of t/τ_L, where σ_c is the root-mean-square concentration fluctuation on the centreline given by

$$\sigma_c^2 = \overline{c^2} - \overline{c}^2. \qquad (6)$$

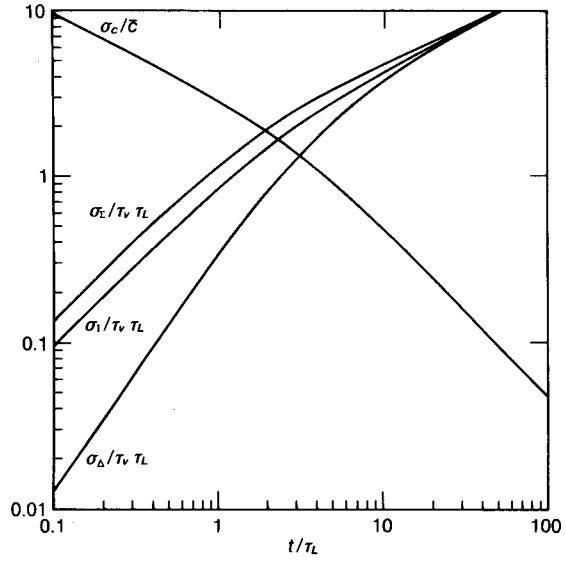

Figure 2. Forms of the three variances defined in the text with $T = t/\tau_L$.

4. The concentration probability density function

Observations made to date indicate that the probability of having a concentration c at any instant is given by the so-called clipped-normal probability density function (PDF)

$$p = \frac{1}{(2\pi)^{1/2}\sigma}\exp\left\{-\frac{1}{2}\left(\frac{c}{\sigma} - \gamma\right)^2\right\}$$

if $c > 0$, or

$$p = \frac{1}{2}\left\{1 - \mathrm{erf}\left(\frac{\gamma}{\sqrt{2}}\right)\right\}$$

if $c = 0$, indicating that there is usually a finite fraction of the time, called the intermittency, when the plume is off the centreline and $c = 0$ (note, not all papers define intermittency this way). A clipped-normal distribution is a Gaussian (or normal) distribution that is centred off the origin, and the part to the right of the origin stands, but the part to the left is integrated and represented by a δ-function of the same magnitude placed at the origin to represent the probability of having zero concentration. This distribution satisfies the requirement that ${}_0\int^\infty p(c)\mathrm{d}c = 1$. The two parameters σ and γ are determined from

$$\frac{\overline{c}}{\sigma} = \frac{\gamma}{2}\left\{1 + \mathrm{erf}\left(\frac{\gamma}{\sqrt{2}}\right)\right\} + \frac{1}{(2\pi)^{1/2}}\exp\left(-\frac{\gamma^2}{2}\right) \qquad (7)$$

$$\frac{\sigma_c^2 + \overline{c}^2}{\sigma^2} = \frac{1}{2}(1 + \gamma^2)\left\{1 + \mathrm{erf}\left(\frac{\gamma}{\sqrt{2}}\right)\right\} + \frac{\gamma}{(2\pi)^{1/2}}\exp\left(-\frac{\gamma^2}{2}\right) \qquad (8)$$

where

$$\mathrm{erf}(x) = \frac{2}{\sqrt{\pi}}\int_0^x \exp(-s^2)\mathrm{d}s.$$

Values of erf(x) are given in Table I.

The values of $\sigma/\overline{c}$ and γ are determined as functions of $\sigma_c/\overline{c}$, which in turn has already been determined as a function of T. Having thus found γ as a function of T, the magnitude of the intermittency I is obtained from the PDF:

$$I = \frac{1}{2}\left\{1 - \mathrm{erf}\left(\frac{\gamma}{\sqrt{2}}\right)\right\}. \qquad (9)$$

These various functions are plotted in Fig. 3. The variation of $\sigma_c/\overline{c}$ with T is like $T^{-1/2}$ for $T < 2$ and like T^{-1} for $T > 10$. This can in fact be seen most easily in Fig. 2.

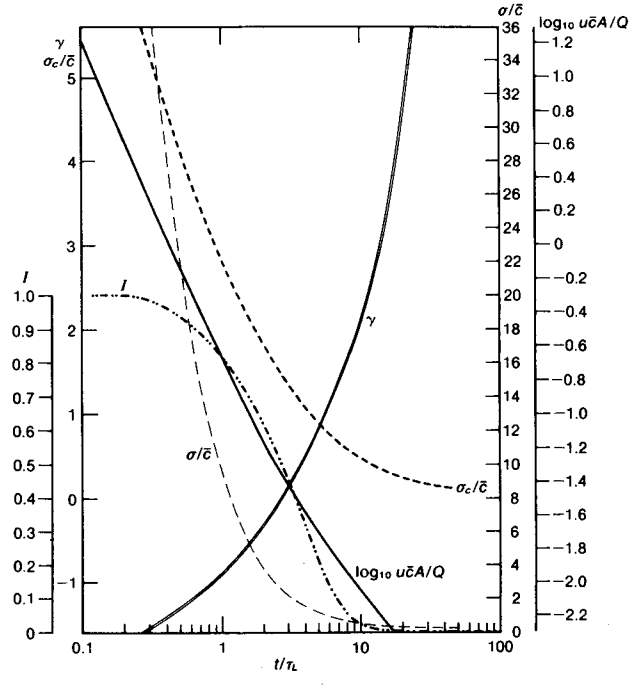

Figure 3. Variation of the concentration fluctuation parameters with travel time on the averaged plume centreline assuming a clipped-normal probability distribution function.

Table I. The error function erf (x) extracted from Jahnke and Emde (1945)

x		0	1	2	3	4	5	6	7	8	9	d
0.0	0.0	000	113	226	338	451	584	676	789	901	013	113
1	0.1	125	236	348	459	569	680	790	900	*009	*118	111
2	0.2	227	335	443	550	657	763	869	974	*079	183	106
3	0.3	286	389	491	593	694	794	893	992	*090	*187	100
4	0.4	284	380	475	569	662	755	847	937	*027	*117	93
5	0.5	205	292	379	465	549	633	716	798	897	959	94
6	0.6	039	117	194	270	346	420	494	566	638	708	74
7		778	847	914	981	*047	*112	*175	*238	*300	*361	65
8	0.7	421	480	530	595	651	707	761	814	867	918	56
9		969	*019	*068	*116	*163	*209	*254	*299	*342	*385	46
1.0	0.8	427	468	508	548	586	624	661	698	733	768	38
1		802	835	868	900	931	961	991	*020	*048	*076	30
2	0.9	103	130	155	181	205	229	252	275	297	319	24
3		340	361	381	400	419	438	456	473	490	507	19
4	0.95	23	39	54	69	83	97	*11	*24	*37	*49	14
5	0.96	61	73	84	95	*06	*16	*26	*36	*45	*55	10
6	0.97	63	72	80	88	96	*04	*11	*18	*25	*32	8
7	0.98	38	44	50	56	61	67	72	77	82	86	6
8		91	95	89	*03	*07	*11	*15	*18	*22	*25	4
9	0.99	28	31	34	37	39	42	44	47	49	51	3
2.0	0.995	32	52	72	91	*09	*26	*42	*58	*73	*88	17
1	0.997	02	15	28	41	53	64	75	85	95	*05	11
2	0.998	14	22	31	39	46	54	61	67	74	80	8
3		86	91	97	*02	*06	*11	*15	*20	*24	*28	5
4	0.999	31	35	38	41	44	47	50	52	55	57	3
5		59	61	63	65	67	69	71	72	74	75	2
6		76	78	79	80	81	82	83	84	85	86	1
7		87	87	88	89	89	90	91	91	92	92	1
8	0.9999	25	29	33	37	41	44	48	51	54	56	3
9		59	61	64	66	68	70	72	73	75	77	2

If we suppose that there is some threshold value of c above which detrimental consequences occur then the probability P that $c > c_*$ (where c_* is this threshold value) is given by

$$P = \frac{1}{2}\left[1 - \text{erf}\left\{\frac{1}{\sqrt{2}}\left(\frac{c_*}{\sigma} - \gamma\right)\right\}\right]. \qquad (10)$$

5. Example

An example may help to see how the scheme can be operated. Suppose $u = 6\ \text{m s}^{-1}$, $\tau_L = 6$ s, $\sigma_v = 0.5\ \text{m s}^{-1}$, the source strength $Q = 100\ \text{g s}^{-1}$ and the downwind distance $x = 120$ m. What is the probability that the concentration c exceeds 200 mg m^{-3} there?

From the given parameters, $A = 9$, $T = 3.333$ and $\mu A/Q = 0.54$. Therefore from equations (1), (2), (3), (5) and (6) or Figs 2 or 3:

(a) $\log_{10} 0.54\bar{c} = -1.474$. Therefore $\bar{c} = 62.2057$ mg m^{-3}.

(b) $\sigma_c/\bar{c} = 1.2431$. Therefore $\sigma_c = 77.35$ mg m^{-3}.

Using equations (7), (8) or (9) or Fig. 3 we infer

(c) $\gamma = 0.25106$,

(d) $\sigma/\bar{c} = 1.8623$. Therefore $\sigma = 115.84$ mg m^{-3}, where, if Fig. 3 is used, the values of the parameters are found for $T = 3.333$.

The intermittency then works out to be 0.4 and $P(c > c_*) = 7.28\%$.

6. Concentrations off the centreline

The profile of concentration is assumed to be normal in the crosswind direction with standard deviation σ_1:

$$\bar{c} = \frac{Q}{2\pi u \sigma_1^2} \exp\left(-\frac{y^2 + z^2}{2\sigma_1^2}\right). \qquad (11)$$

Thomson's random walk studies indicate that across the plume $\overline{c}^2$ behaves like

$$\overline{c^2} = \overline{c^2(0)}\ (\bar{c}/\overline{c(0)})^q \qquad (12)$$

where $q = 2\sigma_1^2/\sigma_\Sigma^2$. q is approximately 1 out to $T = 2$ and thereafter slowly increases asymptotically to 2. σ_c is then obtained from $\sigma_c^2 = \overline{c^2} - \overline{c}^2$. The other parameters can be found exactly as before on the centreline, with the caveat that the value of $P(c_*)$ should be the smaller of that found by the method just described, and that found by assuming that $P(c_*)$ is proportional to the 'mittency' m (to coin a new word meaning the opposite of intermittency I, i.e. $m = 1 - I$, the fraction of the time spent within the plume).

$$\frac{P(c_*(y))}{P(c_*(0))} = \frac{m(y)}{m(0)}. \qquad (13)$$

The value of m can either be found from the method described earlier for points on the centreline, or by $m(y)/m(0) = \overline{c(y)}/\overline{c(0)}$. The two estimates are somewhat different and, although the first method is more accurate, the second is more consistent with the suggested method of finding $P(c_*)$.

In our example consider a point 10 m off the centreline at $x = 120$ m. Using equation (11) we get $\overline{c(10)} = 19.2574$ mg m^{-3} and using equations (1), (2), (3), (6) and (12) $\sigma_1^2 = 42.6421$, $\sigma_\Delta^2 = 18.9569$, $\sigma_\Sigma^2 = 66.3274$, $q = 1.2858$ and $\overline{c^2(10)} = 2180.86$, $\sigma_c(10) = 42.5442$, and $\sigma_c(10)/\overline{c(10)} = 2.2092$.

Now we infer γ from equations (7) and (8) since we have $\sigma_c/\overline{c}$. Alternatively Fig. 3 can be used for the γ and the remaining parameters using an artificial value of $T = 1.49$ corresponding to $\sigma_c/\overline{c} = 2.2092$. Therefore $\gamma = -0.5739$. It follows from equations (7) to (9) that $\sigma = 109.45$, $I = 0.717$, and $P(c > 200) = 0.76\%$, almost one tenth of the value of P on the centreline. Note that the alternative way of estimating P would have given 2.25%, so taking the minimum estimate, the first value stands, although the degree of uncertainty is rather high at these very low values of P.

7. The effect of averaging time

The fluctuations typically have a much smaller time-scale than τ_L. Consequently the peak concentrations may only persist for a relatively short time. The effect of a pollutant, and in particular a toxic pollutant, may be governed by the average concentration in one breath which takes one or more seconds to draw into the lungs. It is expected, then, that the peak averaged concentrations may be significantly smaller than the instantaneous peak concentrations. Random walk simulations suggest that the time-scale τ_f for fluctuations at a point is given by

$$\tau_f = 0.43 \frac{\sigma_\Delta}{u}. \tag{14}$$

The effect of averaging over a time t_a is then to reduce the concentration variance according to the equation

$$\frac{\sigma_c^2(t_a)}{\sigma_c^2(0)} = 2\frac{\tau_L^2}{t_a^2}\left\{\exp\left(-\frac{t_a}{\tau_f}\right) - 1 + \frac{t_a}{\tau_f}\right\}. \tag{15}$$

In the example we have been following, at 120 m, let $t_a = 1$ s. Then $\sigma_\Delta = 4.354$ and $\tau_f = 0.29$. It follows that $\sigma_c(t_a) = 48.9$. From Fig. 3 we infer $\gamma = 1.0$ and $\sigma = 61$. Hence $P = 0.06\%$, which is clearly a very significant reduction as a result of time averaging.

Thomson has looked at the spatial correlation function for the concentration values. If

$$r = \frac{\overline{c(\mathbf{x})c(\mathbf{x}+\Delta)}}{\sigma_c^2}$$

then $r = 1$ at $\Delta = 0$, and it falls away like

$$1 - A\left(\frac{\Delta}{\sigma_\Delta}\right)^{2/3}$$

up to about $\Delta = \sigma_\Delta$, whereafter it behaves like $(\sigma_\Delta/\Delta)^{2/3}$ out to at least $\Delta = L$. This slow tail, which is only evident in the longitudinal direction (parallel to the mean wind), he ascribes to inertial meandering of the plume.

8. The effect of source size

The effect of source size is rather complex from a theoretical standpoint. In practice however, its main consequence is to reduce the concentration variance out to $T = 1$. This is expected because the finite size must broaden the instantaneous plume and thereby slow down the penetration of 'clean' air into the body of the plume, the process which is responsible for generating internal fluctuations in concentration. Referring back to the section on the concentration fluctuation parameters off the centreline, the finite size (denoted by σ_0) modifies both the formulae for q and $\overline{c^2(0)}$;

$$q = \frac{\sigma_1^2 + \sigma_0^2}{\sigma_\Sigma^2 + \sigma_0^2} \tag{16}$$

and

$$\overline{c^2(0)} = \mu\overline{c(0)}^2 \frac{(\sigma_1^2 + \sigma_0^2)^2}{(\sigma_\Sigma^2 + \sigma_0^2)(\sigma_\Delta^2 + \sigma_0^2)}. \tag{17}$$

The consequences are summarized in Fig. 4 where experimental data due to Fackrell and Robins (1982) are compared with Thomson's random walk modelling results. As can be seen in Fig. 4, the larger σ_0 is the smaller is the maximum variance and the further downwind it occurs. These points are further illustrated in Figs 5 and 6.

9. Real situations in the boundary layer

For a source near the ground the assumption of isotropic homogeneous turbulence does not appear very realistic. However, the high frequency turbulence responsible for generating the international spread of the instantaneous plume and its internal concentration fluctuations is virtually isotropic and homogeneous, especially in the earlier stages of the plume's growth. Broadly speaking then, we can assume the plume develops as predicted by isotropic theory until $\sigma_c/\overline{c}$ is about 1, after which it evolves in a self-similar manner; that is, it is as though t/τ_L becomes constant since, as the plume deepens, so the mean value of τ_L increases.

In very stable conditions, a difficulty arises in specifying the sometimes large meanders of the plume due to intermittent gravity-driven motions as pools of cooler air slide down into hollows and valleys. Likewise some difficulties occur in very unstable conditions due to the complexity of the buoyancy driven motions. Increased research interest is now focused on concentration behaviour in light-wind situations, whether in very unstable or very stable conditions.

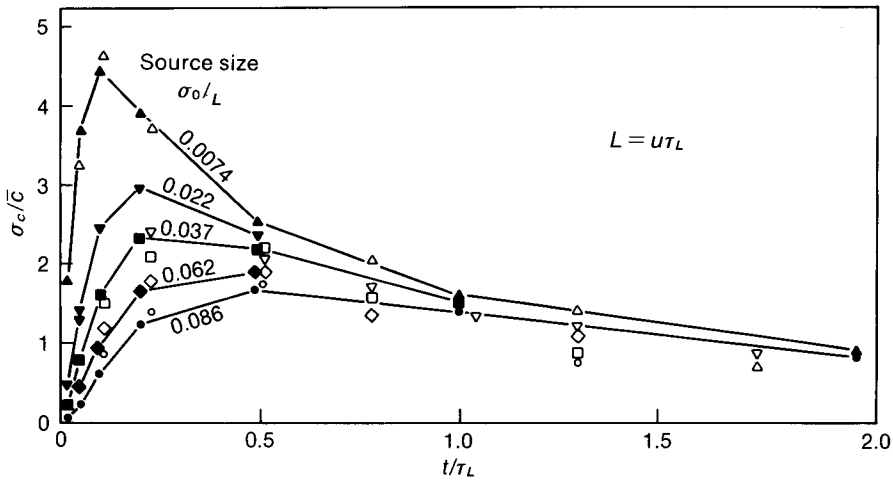

Figure 4. Variation of normalized concentration variance with travel time and with source size. A comparison of theory due to Thomson (1990) (solid symbols), and experimental data due to Fackrell and Robins (1982) (open symbols).

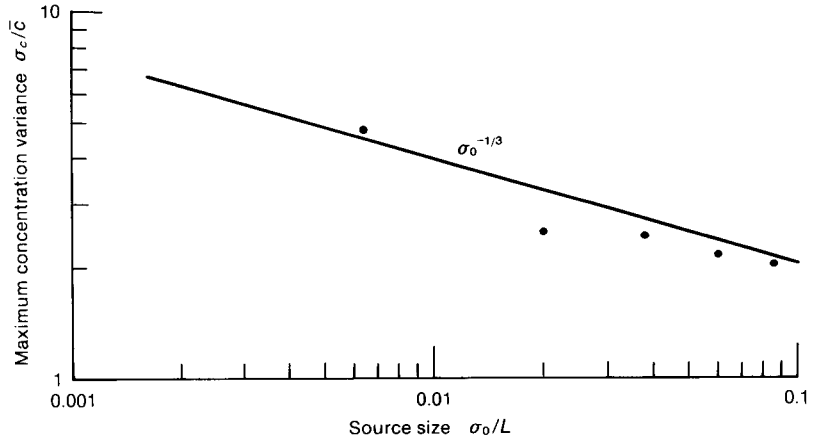

Figure 5. Variation of maximum concentration variance with source size, according to experimental data due to Fackrell and Robins (1982).

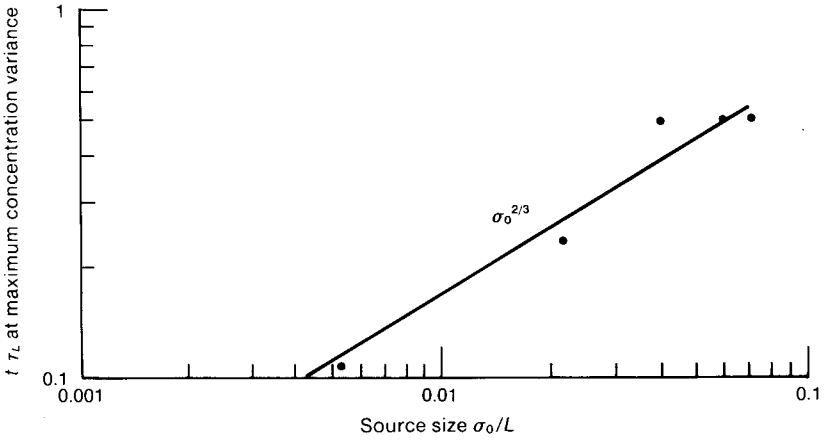

Figure 6. Variation with source size of the travel time at maximum concentration variance (Fackrell and Robins 1982).

10. Fluctuations in concentration at long range

So far we have considered the fluctuations in concentration within a plume from a continuous source out to a distance of perhaps 1 km. Fluctuation analysis also becomes very important at downwind distances much greater than this when the time over which the emission occurs is smaller than the travel time, or when the synoptic situation changes over a time that is smaller than the travel time. In both these situations it is probable that any receptor only experiences a small part of the possible range of fluctuations. The concentrations the receptor sees, and the risk these may imply, can only be described in statistical terms.

Classically, plumes of debris have always been considered in the same terms as plumes of smoke emanating from a factory chimney. It was recognized that such a plume contains a lot of structure (as we have already seen), blobs and wisps of high concentration surrounded by areas of lower or zero concentration. However, when the plume is averaged over many minutes, these irregularities are largely ironed out and a smoother distribution of concentration is achieved. The plume can then be described in terms of just a few simple parameters. Principal of these are (i) the position of the centroid, or centre of mass, of the plume material (considered as a function of distance downwind from the source), and (ii) the width of the plume (again a function of downwind distance), often expressed as the standard deviation of the concentration distribution about the centroid. In reality the second parameter may be two parameters — the horizontal width and the vertical depth.

Such a description has been used for plumes out to much greater distances than the short distances over which chimney plumes are normally visible. For example the plume from the aluminium smelter at Mt. Isa in Australia has been tracked by instrumented aircraft out to 1800 km in simple meteorological situations when the plume's character can still be described in terms of these few basic parameters (Carras and Williams 1988). They have analysed these measurements in terms of the way the width varies with distance (see Fig. 7).

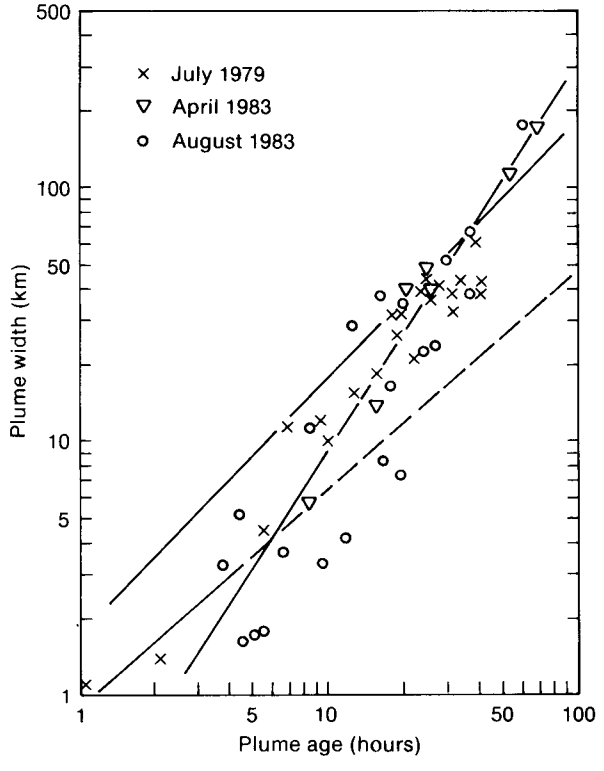

Figure 7. Log–log plot of the measured values of plume width (as a standard deviation) as a function of plume age at Mount Isa, Australia.

However, experience in the atmosphere, as well as modelling studies, suggest that such simple plume ideas are invalid in most meteorological situations after some 20 hours of travel because by that time the plume has grown so wide that synoptic-scale variations in the wind-field can gradually distort and deform the plume into shapes that cannot sensibly be described by the simple parameters described above. In the conditions outlined at the beginning of this section, it is as though we are forced to look at the complex structure of the plume in a similar way as we looked at the instantaneous structure of the plume at very short range in earlier sections of this paper.

This approach has been supported by our experiences with the radioactive-debris plume from the Chernobyl Reactor accident in late April and early May 1986. The resulting depositions, and the consequences they had on the safety of food and on wildlife stimulated many organizations and governments to review the models they had available at that time. Most, if not all of these, were found wanting and this resulted in new, widespread modelling activities. A brief description will now be given of one of these new models, that developed at the Meteorological Office.

11. The UK Nuclear Accident Model

The Meteorological Office has developed a sophisticated random-walk or Monte-Carlo model in order to simulate, in both forecast and hindcast modes, the transport, decay and deposition of radioactive debris emitted from any site in Europe. It is given the acronym NAME (The Nuclear Accident Modelling Exercise). A global version of the model capable of treating emissions from any site in the world will be developed shortly. The plume is simulated by releasing a large number of 'particles' at the source (at hourly intervals, reflecting the emission profile in time and space) and allowing them to be transported by 3-dimensional winds taken from the output of the Meteorological Office's weather forecasting models. When run in the hindcast mode, the 'actual' analysed winds are used from earlier forecast runs rather than forecast winds. A 10-day roll-over archive is used to store past winds for this purpose. A time-step of 15 minutes is used (an appropriate eddy turnover time in the convective boundary layer) and at each step a random perturbation is added to the horizontal displacements (and to the vertical displacements outside the boundary layer) to account for turbulent diffusion:

$$\mathbf{x}_{i+1} = \mathbf{x}_i + \mathbf{u}(\mathbf{x}_i)\Delta t + \mathbf{A}r$$

where Δt is the time-step, r is a random number from the standard normal (Gaussian) distribution and $\mathbf{A}$ is a coefficient chosen so that the implied turbulent energy remains quasi-constant in time. Within the boundary layer the particles are randomly reassigned in the vertical at the end of each time-step so that over a period

of time each particle will sample the mean wind at each level. Particles are released from different heights to allow for initial buoyant rise at the source.

The model is multi-level, with a realistically evolving boundary layer, inferred at each hour from the forecasting model output. As its height changes, so particles are entrained and detrained from the layer into the layer above.

A mass of pollutant or radioactivity is associated with each particle at the outset, and concentrations in air are calculated by counting the particles in each grid-volume weighted by the mass they each then carry. If the initial emissions are only coarsely known, comparison of the calculated concentrations can be compared with any field measurements to refine the emissions and the mass each particle carries.

The particle 'mass' is constantly being modified by radioactive decay, by chemical or physical transformations, by dry deposition and by wet deposition. The wet deposition in the model requires a good knowledge of the precipitation field, and this is obtained by inputting the results of a semi-independent programme which combines observations from surface rain-gauges, from weather radar (corrected for false inputs), from satellites and from the weather forecast model's output on rain.

In areas where weather radar output is available the resolution of the rainfall field is as good as 5 km. Even if the model's implied concentrations of pollution in the air contain some errors, at least such a highly resolved rainfall field will provide valuable information on where heavy depositions of pollution are likely to have occurred, and this is vital to agricultural monitoring teams in situations like Chernobyl. An example of the output of the model is given in Fig. 8. It confirms the distorted and convoluted nature of the plume.

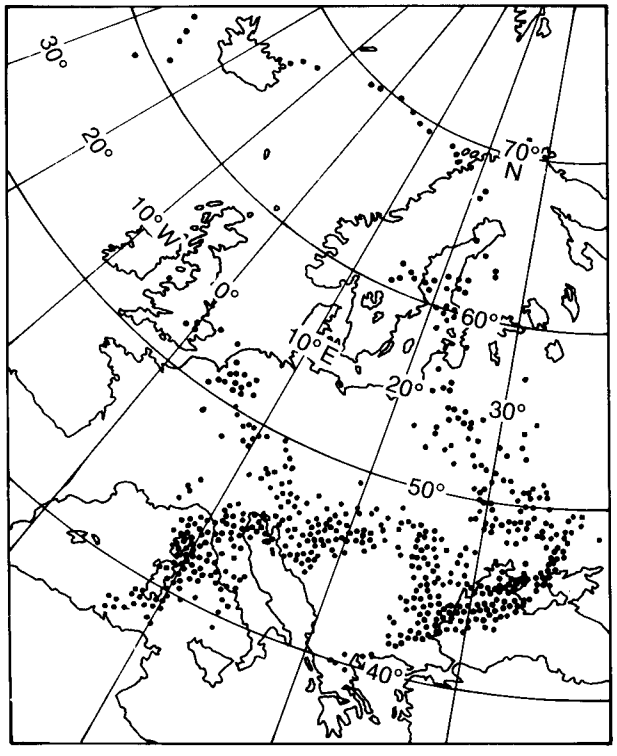

Figure 8. Simulation of the Chernobyl plume at midday on 2 May 1986 using the UK Nuclear Accident Model (NAME). In spite of the relatively few particles simulating the release the model does quite well in indicating the debris over southern Europe and over eastern England.

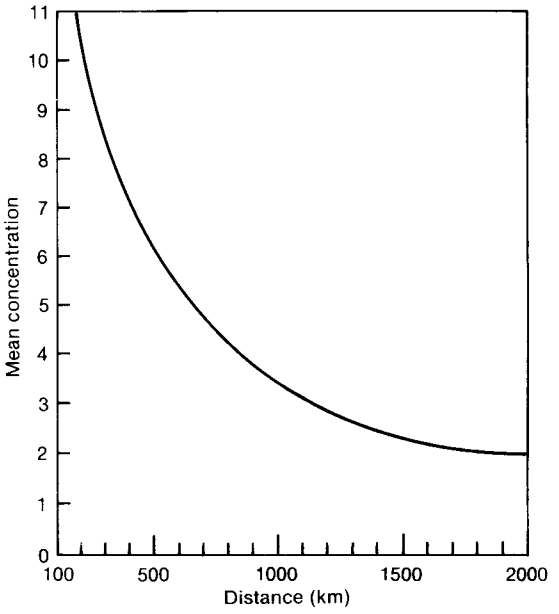

Figure 9. Variation of the mean concentration within plume material as a function of distance. The concentration is equated to the number of particles found in the grid-square (roughly 35 km square) when 200 particles are released per hour.

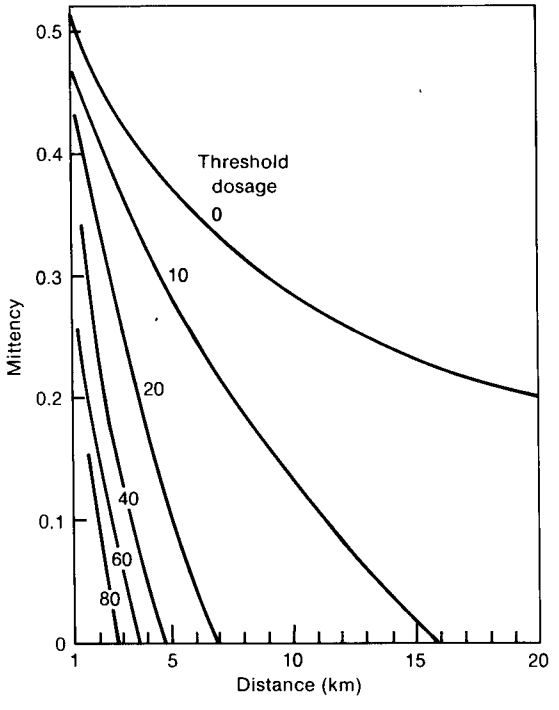

Figure 10. Variation of concentration mittency (fraction of time the concentration exceeded the given threshold) with distance for several specified threshold dosages. Units of dosage are related to the sum over time of the number of particles in a grid-square in each time-step.

12. Statistical description of a plume at long range

The NAME model has been run on several randomly selected occasions out to 5 days with a continuous release of particles from a specified source located at a gridpoint near the centre of the model area which lies in Cumbria. The plumes grow over these 5 days and show all the distorting features evident in Fig. 8. The following parameters have been determined for both concentrations in the atmosphere, for time-integrated concentrations (or dosages), and for depositions on the underlying surface:

(a) the mittency of the plume for specified threshold values, i.e. what fraction of the time the concentration exceeded the given threshold,

(b) the mean concentration or dosage or deposition at specified positions and at specified times after the start of the release, and

(c) the PDF of the 'observed' concentrations or dosages about their respective means.

This work is not yet finished, but it already shows a degree of order and meaningfulness in its results. For example the distributions in (c) above are very similar to those at short range discussed in earlier sections. It still has to be clarified as to whether the PDF is best represented by the clipped-normal PDF implied at short range, or whether a sample exponential distribution is better

$$p(c) = 1 - \exp\left(-\frac{c}{\bar{c}}\right).$$

Other examples of these preliminary results are shown in Figs 9 and 10.

Acknowledgements

I would like to thank three of my colleagues, Dr D.J. Thomson, Mr K.R. Mylne and Mr R.H. Maryon for their considerable help in the formulation of this paper. Much of the theory behind the method originates from Dr Thomson in the reference given below, and in other unpublished work. Invaluable experimental results supporting the theory come from the work of Mr Mylne. Mr Maryon and his small team has done the majority of the work on the Nuclear Accident Model.

References and bibliography

Carras, J.N. and Williams, D.J., 1988: Measurements of relative σ_y up to 1800 km from a single source. *Atmos Environ*, **22**, 1061–1069.

Fackrell, J.E. and Robins, A.G., 1982: Concentration fluctuations and fluxes in plumes from point sources in a turbulent boundary layer. *J Fluid Mech*, **117**, 1–26.

Jahnke, E. and Emde, F., 1945: Tables of functions with formulae and curves. New York, Dover Publications.

Mylne, K.R. and Mason, P.J., (1991): Concentration fluctuation measurements in a dispersing plume at a range of up to 1000 m. Submitted to *Q J R Meteorol Soc.*

Sawford, B.L., 1987: Conditional concentration statistics for surface plumes in the atmospheric boundary layer. *Boundary-Layer Meteorol*, **38**, 209–223.

Sykes, R.I., 1988: Concentration fluctuations in dispersing plumes. *In* Venkatram, A. and Wyngaard, J.C. (eds); Lectures on air pollution modeling. Boston, American Meteorological Society.

Thomson, D.J., 1990: A stochastic model for the motion of particle pairs in isotropic high-Reynolds-number turbulence, and its application to the problem of concentration variance. *J Fluid Mech*, **210**, 113–153.

Notes and news

Fourth Workshop on Operational Meteorology, Whistler, B.C. Canada, 15–18 September 1992

The workshop, sponsored by the Atmospheric Environment Service of Environment Canada and the Canadian Meteorological and Oceanographic Society, will have a principal theme of 'Forecasting in the Nineties'.

The Program Committee wishes to solicit papers on the following topics:

(a) The meteorological data explosion — the integration and effective use of information in an operational setting.

(b) Forecast techniques and conceptual models — their place in forecast decision making.

(c) Climate services — how can they be used effectively.

(d) Delivery — techniques and requirements to effectively deliver forecasts to the user.

The workshop format will consist of laboratory sessions, submitted papers, invited papers, panel discussions, poster sessions and demonstrations. A brief introduction of each poster session will be made during an appropriate oral session.

Titles and reviewers' abstracts of 400–800 words should be sent to

Neil McLennan
Chairman Program Committee
Atmospheric Environment Service
Suite 200, 1200 West 73rd Avenue
Vancouver B.C.
Canada V6P 6H9

Authors should indicate their preference for presenting their paper orally, in a laboratory or poster session, or as a demonstration. Preferences will be considered to the extent possible. Abstracts will be evaluated on their relevance to the theme as well as on quality. Papers not related to operational meteorology will not be accepted. The deadline for laboratory submissions is 1 October 1991, and for all others is 1 February 1992. Authors will be notified regarding the acceptance of their abstracts and instructions on the format of their papers by 1 November 1991 for laboratories and by 1 March 1992 for other sessions.

Complete camera-ready papers of not more than eight pages, including diagrams, must be received by the Program Chairman no later than 15 June 1992. A preprint volume will be prepared and distributed to all registered workshop attendees.

For additional information contact either Neil McLennan (Phone: 604-664-9073 Fax: 604-664-9066) or Gerard Neault (604-664-9052).

Reviews

The telemetry of hydrological data by satellite, by I.C. Strangeways. 209 mm × 295 mm, pp. v+60, *illus.* Wallingford, Institute of Hydrology, 1990. Price £7.00.

This short book, it is only 60 pages long, is a contribution to the Institute of Hydrology Report Series (No. 112). It is softback, and is intended to provide the basic information that a prospective user of satellite telemetry might need in setting up a communications system using facilities offered by both geostationary and polar-orbiting satellites. The author regards the information contained therein as a handbook intended as an introduction to satellite techniques and as an encouragement to use them. He is well placed to write such a document having been involved in developing automatic weather stations and using satellite telemetry for many years.

The information is contained in six chapters covering the Meteosat system, the practical evaluation of a satellite telemetry system, commercial equipment and operating costs, the international situation and conclusions. There are eleven references, of which five are to work reported by the author, and this is an indication that in reading this book one should bear in mind that it represents a rather personal view of satellite telemetry. In spite of this, it is extremely useful in that it sets down much material which is spread widely through a range of literature. The text is clear and easy to ready, and most of the diagrams are clear and concise, although some of the data listings have not reproduced well (for example fig. 3.6).

The emphasis throughout is on the Data Collection Platform (DCP) facility provided on the Meteosat series of satellites. The Argos polar-orbiting satellite communications system is mentioned, but there is no mention of commercial VSAT systems, the Meteosat Data Dissemination Mission (MDD) or the ESA CODE experiment based upon the Olympus satellite. Nevertheless the concentration on the systems most used by meteorologists and hydrologists serves to emphasize the practical nature of the book.

A strong argument in favour of using satellite communications is presented, based upon the falling costs of the equipment needed and ease of maintenance, although it is assumed that the costs of any such services in the future will remain free. It is argued that there are a significant number of benefits in using satellite telemetry and these are listed, although it is recognized that the proportion of these benefits with hydrological applications is not known. The reader is referred to 'an authoritative guide' as to the future of satellite telemetry in hydrology obtainable from ESA. It is a pity that this book was produced before the issue of WMO Report

TD No. 256 entitled '*Use of and requirements for satellite imagery and data transmission for hydrological purposes*' by T. Kinosita (WMO Tech. Reports to the Commission for Hydrology No. 24, 17 pp, 1990). This publication takes the form of a report on a questionnaire. It notes that out of 34 countries who responded 27 did not use satellites for the transmission of hydrological data from data collection platforms, whereas 16 countries said that they had plans to use satellites in this way as follows,

Satellite type:	geostationary	11
	polar orbiting	9
	communication	4.

This information has to be reconciled with that contained in the review publication, which notes on page 11 that in the 1990s it is expected that 5000 DCPs out of a total of 12 500 will be used for the collection of hydrological data. The implication is that most of the usage of DCPs for hydrology may be concentrated in a few countries. At the time the author wrote his book, only 400 stations were registered to use Meteosat and 1800 were registered with the US Geological Survey. This total of 2200 was expected to increase to 12 550. This expected increase is supported by the WMO survey, although the sixfold increase expected by ESA may be too optimistic and a three- or fourfold increase might be more realistic. The sentiment expressed by the author that 'anyone contemplating satellite telemetry for hydrology will probably use a geostationary satellite' (page 13) is not borne out by the WMO survey.

Whilst the majority of the information contained in this book is accurate, and there are useful descriptions of the Meteosat ground segment facilities and message dissemination procedures, there are some inaccuracies and omissions. For example, Eumetsat is not strictly funded by just the member countries of ESA but by the National Meteorological Services. There is no discussion of what causes system downtime, for example satellite decontamination exercises, eclipses, etc. Data distribution and charging policy issues are not discussed. Cost comparisons with UHF and microwave ground telemetry systems are not made recognizing that in the future the acquisition of sub-daily data may not be cost-effective using satellite systems if the service attracts a charge from the satellite operators.

Unfortunately the material contained in this manual will become out of date fairly quickly. For example, some of the information on Meteosat Second Generation is already out of date and the section on commercial equipment likewise. In spite of the limitations noted in this review, the author has assembled a lot of very useful information on satellite telemetry. This manual is an important source of practical data, and should therefore be essential reading for all those contemplating acquiring hydrological and meteorological data via satellites.

C.G. Collier

The hurricane, by R.A. Pielke. 184 mm × 252 mm, pp. xi+228, *illus.* London, New York, Routledge, 1990. Price £50.00. ISBN 0 41503 705 0.

The hurricane is one of meteorology's most fascinating and awesome phenomena, and its destructive force is seldom appreciated by those living out of the tropics. It is also an excellent example of many important meteorological processes at work — convection and the release of latent heat are essential components of this heat engine, as are the exchanges of sensible heat and moisture at the surface. Hurricane motion, so important to forecast accurately if lives are to be saved, is often irregular and depends not only on the large-scale steering flow in which the system is embedded, but also on its interaction with troughs and jets in middle latitudes. Any book devoted to the subject has to consider extratropical as well as tropical meteorology and has, therefore, plenty of ground to cover.

The author attempts to do just that in a non-mathematical framework which is aimed at the educated layman. The publisher's hand-out describes it as a 'well-illustrated and accessible book providing a state-of-the-art assessment of the climatology, forecasting and physical processes associated with tropical cyclones'. Well illustrated it certainly is, having some 190 pages of figures and diagrams. However, the choice of material is very strange, with over half the book taken up by maps of the tracks of every hurricane in the North Atlantic since 1871; of historical interest perhaps but barely the basis of a well-balanced survey of the subject. If it is to be heavily weighted towards the pictorial, which is not a bad idea for a subject like this, why not have more satellite pictures showing not just the textbook hurricane with an eye, but also the stages of development and the different structures that can occur? There are only three satellite pictures in the book, and all are of a large and fully mature system. The range of topics covered in the text is wide, but the explanation of the meteorology, being condensed into about 30 pages, is necessarily very sketchy. In fact the book gives the impression of being put together rather rapidly with insufficient thought given to clarity of presentation. To take just one example, the reader will be left wondering how the four pages devoted to diagrams showing the mean wind at 850 mb 'demonstrate clearly the validity' of criteria for hurricane development, in the absence of any further explanation. This only goes to show that writing at a level for the educated layman is really far harder than writing for the specialist; clarity is all important as is the ability to appreciate the reader's viewpoint in order to explain what it is that he doesn't understand. In this respect, I am afraid, the book fails.

C.D. Hall

Satellite photographs — 17 May 1991 at 0600 and 1300 UTC

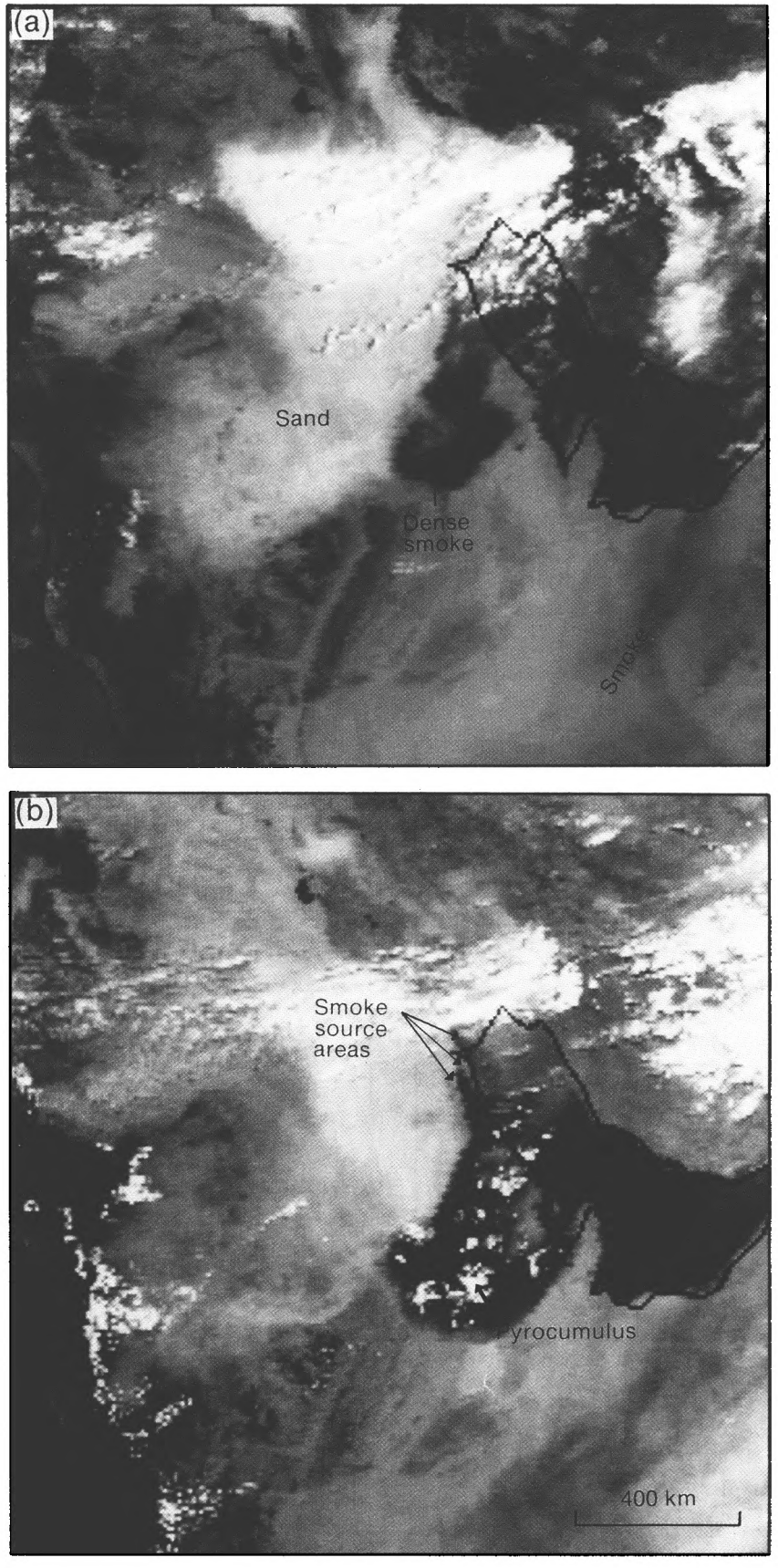

Figure 1. Meteosat visible images of the Persian Gulf area on 17 May 1991 at (a) 0600 UTC and (b) 1300 UTC.

Meteorological satellite imagery of the Persian Gulf area continues to show the effects of the many oil fires that are still burning in Kuwait. The smoke plumes have been seen to extend for many hundreds of kilometres and one example of this can be seen in the images shown here.

The two reprojected visible Meteosat images (Fig. 1) are products from the Meteorological Office's dedicated satellite-image processing system, Autosat-2. They show the type of imagery used within the Nowcasting Section of the Short-range Forecasting Research Division to monitor routinely the extent of the smoke over the Gulf region. This task was initiated in January this year, when smoke was first apparent in satellite imagery.

The plume shown (formed by the smoke from the 500 oil fires reported to be still burning in the area), extended southwards at a rate of 15 kn, consistent with the winds below 850 mb (5000 ft), as shown on the tephigram (Fig. 2).

In the 1300 UTC image (Fig. 1(b)), cumulus clouds can be seen within the smoke area. These have been termed 'pyrocumulus' and form typically during the day in this type of situation. One possible explanation for the formation of these clouds is that the upper layers of the smoke plume (having an albedo of 5–8%, as measured in recent field studies by the Meteorological Research Flight) absorb solar radiation, causing local heating of the surrounding air and hence strong ascent. In this situation, the unstable atmosphere allowed the developing clouds to penetrate high into the atmosphere, perhaps as high as 300 mb (30 000 ft), as illustrated on the tephigram and as suggested by their low brightness temperatures on the infra-red imagery (not shown here).

These clouds are unlikely to provide a mechanism for the transport of significant quantities of particles into the stratosphere. Firstly, precipitation from these clouds will have washed out the particles (typically between 0.1 and 10 μm) to the surface; secondly, the tropopause is very much higher than 300 mb.

The images show a light grey region covering a large area to the west of Kuwait. Its appearance and movement, combined with the 0600 UTC observations, (Fig. 3) indicate that it was a sandstorm, and was moving at a speed consistent with the observed near-surface winds.

The observations at 0600 UTC within the region covered by the image, reported generally very low visibility, even down to zero at some stations, indicating the extent and severity of the airborne sand and smoke.

G. Holpin and R. Bosworth

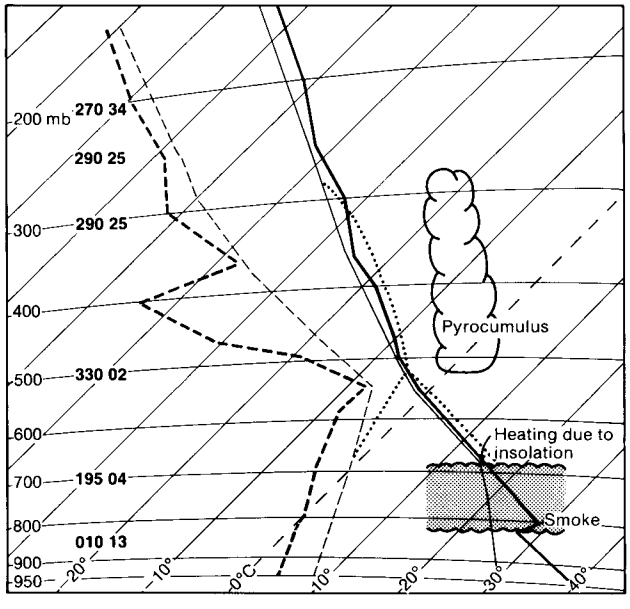

Figure 2. Tephigram for 17 May 1991 at 1200 UTC for King Khaled International Airport (location marked 'K' in Fig. 3), Riyadh, Saudi Arabia (thick lines) (not through plume). Also shown is a schematic showing typical plume depth, and a postulated ascent (thin lines) through the plume (using Kuwait surface data), constructed on the assumption that insolation causes the upper layers of the smoke to behave as if they were a surface, resulting in ascent (dotted line) and cloud formation.

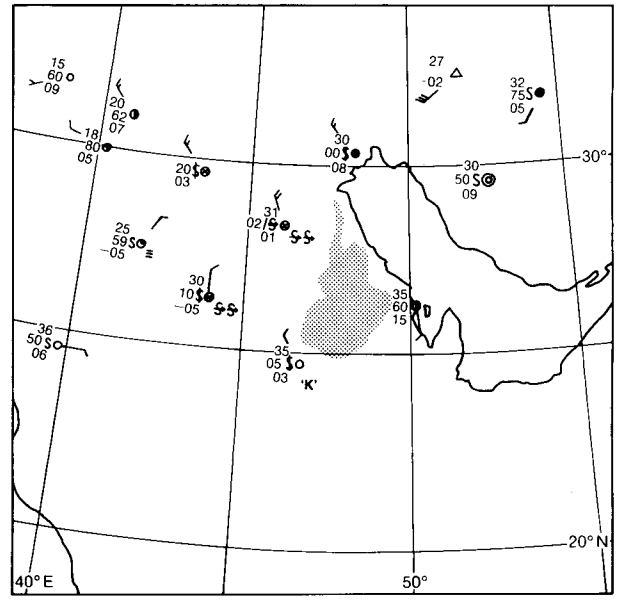

Figure 3. Middle East plotted surface observations on 17 May 1991 at 0600 UTC, with plume area shown stippled.

GUIDE TO AUTHORS

Content

Articles on all aspects of meteorology are welcomed, particularly those which describe results of research in applied meteorology or the development of practical forecasting techniques.

Preparation and submission of articles

Articles, which must be in English, should be typed, double-spaced with wide margins, on one side only of A4-size paper. Tables, references and figure captions should be typed separately. Spelling should conform to the preferred spelling in the *Concise Oxford Dictionary* (latest edition). Articles prepared on floppy disk (Compucorp or IBM-compatible) can be labour-saving, but only a print-out should be submitted in the first instance.

References should be made using the Harvard system (author/date) and full details should be given at the end of the text. If a document is unpublished, details must be given of the library where it may be seen. Documents which are not available to enquirers must not be referred to, except by 'personal communication'.

Tables should be numbered consecutively using roman numerals and provided with headings.

Mathematical notation should be written with extreme care. Particular care should be taken to differentiate between Greek letters and Roman letters for which they could be mistaken. Double subscripts and superscripts should be avoided, as they are difficult to typeset and read. Notation should be kept as simple as possible. Guidance is given in BS 1991: Part 1: 1976, and *Quantities, Units and Symbols* published by the Royal Society. SI units, or units approved by the World Meteorological Organization, should be used.

Articles for publication and all other communications for the Editor should be addressed to: The Chief Executive, Meteorological Office, London Road, Bracknell, Berkshire RG12 2SZ and marked 'For Meteorological Magazine'.

Illustrations

Diagrams must be drawn clearly, preferably in ink, and should not contain any unnecessary or irrelevant details. Explanatory text should not appear on the diagram itself but in the caption. Captions should be typed on a separate sheet of paper and should, as far as possible, explain the meanings of the diagrams without the reader having to refer to the text. The sequential numbering should correspond with the sequential referrals in the text.

Sharp monochrome photographs on glossy paper are preferred; colour prints are acceptable but the use of colour is at the Editor's discretion.

Copyright

Authors should identify the holder of the copyright for their work when they first submit contributions.

Free copies

Three free copies of the magazine (one for a book review) are provided for authors of articles published in it. Separate offprints for each article are not provided.

Contributions: It is requested that all communications to the Editor and books for review be addressed to the Chief Executive, Meteorological Office, London Road, Bracknell, Berkshire RG12 2SZ, and marked 'For *Meteorological Magazine*'. Contributors are asked to comply with the guidelines given in the *Guide to authors* which appears on the inside back cover. The responsibility for facts and opinions expressed in the signed articles and letters published in *Meteorological Magazine* rests with their respective authors.

Subscriptions: Annual subscription £33.00 including postage; individual copies £3.00 including postage. Applications for postal subscriptions should be made to HMSO, PO Box 276, London SW8 5DT; subscription enquiries 071–873 8499.

Back numbers: Full-size reprints of Vols 1–75 (1866–1940) are available from Johnson Reprint Co. Ltd, 24–28 Oval Road, London NW1 7DX. Complete volumes of *Meteorological Magazine* commencing with volume 54 are available on microfilm from University Microfilms International, 18 Bedford Row, London WC1R 4EJ. Information on microfiche issues is available from Kraus Microfiche, Rte 100, Milwood, NY 10546, USA.

July 1991

Edited by Corporate Communications Vol. 120
Editorial Board: R.J. Allam, R. Kershaw, W.H. Moores, P.R.S. Salter No. 1428

Contents

ISSN 0026–1149

Printed in the United Kingdom for HMSO
Dd 0291241 7/91 C13 503 12521

The Meteorological Magazine

August 1991

Quality of marine observations

HMSO

Met.O.998 Vol. 120 No. 1429

First published 1991

HMSO publications are available from:

HMSO Publications Centre
(Mail and telephone only)
PO Box 276, London, SW8 5DT
Telephone orders 071-873 9090
General enquiries 071-873 0011
(queuing system in operation for both numbers)

HMSO Bookshops
49 High Holborn, London, WC1V 6HB 071-873 0011 (counter service only)
258 Broad Street, Birmingham, B1 2HE 021-543 3740
Southey House, 33 Wine Street, Bristol, BS1 2BQ (0272) 264306
9–21 Princess Street, Manchester, M60 8AS 061-834 7201
80 Chichester Street, Belfast, BT1 4JY (0232) 238451
71 Lothian Road, Edinburgh, EH3 9AZ 031-228 4181

HMSO's Accredited Agents
(see Yellow Pages)

and through good booksellers

The Meteorological Magazine

August 1991
Vol. 120 No. 1429

551.5(26):551.509.5:53.088

The use of output from a numerical model to monitor the quality of marine surface observations

C.D. Hall, J. Ashcroft and J.D. Wright
Meteorological Office, Bracknell

Summary

To make optimum use of meteorological observations it is essential that regular monitoring is performed to identify those of poor quality. Output from numerical forecast models has proved to be very valuable for this purpose; short-period forecasts or background fields provide accurate global reference values against which observations may be compared. This paper presents some recent results of the monitoring of wind and pressure observations from ships and buoys using output from the UK operational global model.

1. Introduction

Great advances have been made in numerical modelling over the past two decades, and today we take for granted levels of accuracy in the forecasts of the basic meteorological parameters of mean-sea-level pressure, temperature and wind which were seldom achieved in the past. Central to the success of numerical weather prediction is the process of data assimilation by which the initial analyses or start fields are created. The methods of data assimilation ensure that the initial analysis, from which the numerical forecast is made, includes the information contained in meteorological observations, not just at one data time, but over perhaps a few days. Data assimilation is performed in a cyclical fashion — observations valid around a given analysis time are checked for quality before being merged with values from the numerical model to provide the starting analyses. A short-period forecast (usually 6 hours) is made from the analysis to create the starting point for the assimilation cycle at the next analysis time. The data assimilation method used in the UK operational models is described by Atkins and Woodage (1985), and details of more recent modifications are contained in Lorenc *et al.* (1991). Global analyses from such numerical systems achieve a realistic fit to all the data available, and moreover they inherit a realistic three-dimensional meteorological structure from the numerical model. As a consequence they show a high degree of accuracy, as do the short-term forecasts or background fields.

The success of numerical weather prediction depends critically on the quality of the observations used in the data assimilation. Quality-control checks are essential to weed out those observations too much in error to be of value, and many algorithms have been developed for this purpose — checks may be performed to identify incorrect message format, excess over climatological extremes, internal inconsistency, and inconsistency with neighbouring observations. Fields from a numerical system have a valuable role in quality control; they provide reliable reference values against which observations separated in space and time may be checked. Observation errors can be identified as long as they are not much smaller than the expected error of the field. However, the method has its limitations. Firstly, numerical models can at best only represent values on the coarse scale of their grid and will not be able to resolve much of the observed fine-scale structure of the atmosphere. Secondly, model fields are most accurate where there is a good coverage of observations and in

data-sparse areas they may contain substantial systematic and random errors.

At any one datum time two types of model field are available for assessing observation quality — an analysis and a background. The analysis represents the best fit to all observations passing the quality checks which are available up to that given time, and the background represents the best estimate of the observed values at the current time using only information contained in observations valid at earlier times. Because background values are generally independent of the current observations, they are found to be most suitable for studies of observation quality. Observation-minus-background differences (from now on referred to as O−B) are at the centre of many studies of data quality. Errors in both observations and background will contribute to the value of O−B, and the success of data monitoring depends on identifying those cases where the magnitude of O−B is too large to be due to background error alone.

Background values may be used in two quite different ways. Firstly, as part of an assessment of the quality of a set of observations valid at just one time. Such checks, often performed in real time, may be used as mentioned above to weed out those observations too erroneous for use in numerical data assimilation. The use of background values for this type of quality control, as it is performed for the operational forecasting models at Bracknell, is described by Bell and Dickinson (1987) and a description of more recent developments is contained in Lorenc and Hammon (1988). Secondly, they may be used to assess the quality of a sequence of observations from one source over a long period of time. For example, values of O−B for pressure observations from a ship with a given call-sign may be monitored over a period of a month or more to identify systematic departures from background values. In such a case the bias and standard deviation of O−B prove to be very valuable indicators of observation quality. This paper is concerned principally with the second monitoring method using period averages. The basic assumption lying behind this method is that the magnitude of the background errors, both systematic and random, averaged over a period of a month or more, varies only slowly in space. The assumption is generally valid in the free atmosphere and close to a homogeneous surface such as the open sea. On any one occasion, background errors may vary greatly within a small region, but the average over a month or more is found to vary little. In contrast, average observation errors may differ greatly between neighbouring stations or between national groupings of stations operating different types of instrument. Differences from background which are larger than the local average can therefore, in most cases, be attributed to larger than normal observation errors.

This paper describes some monitoring methods applied to surface observations of pressure and wind from marine sources — that is from ships, drifting buoys, and fixed buoys and platforms. Model fields are particularly suitable for the monitoring of observations of this type; they are at one level, and in the case of pressure relate to one of the basic model parameters. Moreover, the sea surface is relatively uniform and meteorological structure is less complex than over land where there is more fine-scale detail. Errors in marine observations may arise from a number of sources; the instrument may be malfunctioning or miscalibrated, figures may be mistaken while being transferred manually, or there may be corruption of data during transmission. A poorly sited anemometer can result in errors in the observations of wind. Errors can also arise in the pressure report if the adjustment to sea level is made incorrectly or not at all. In the case of a large ship, failure to allow for the changes in the barometer height due to changes in the ship's draught can lead to an error of perhaps 1 mb or greater. Some of these errors can be detected in real time by applying checks on the code format and the internal consistency of the report, but most information on quality can only be obtained by studying long sequences of observations from one ship or buoy.

Taking all marine surface observations together, the values of O−B have distinct characteristics. The vast majority of the observations show quite small departures from background and the distribution of O−B is nearly Gaussian with little or no bias. The errors in the background field probably contribute most to the values of O−B for these observations. There is, however, always a smaller group of observations departing much more from background for which observation error is the only reasonable explanation for the large values of O−B. Studies of the distribution of O−B and its variation at different points around the globe enable reasonably accurate estimates of background error to be made, and this provides the basis for the monitoring methods described here. Those ships or buoys for which, in a sufficiently large sample, the observed values of pressure or wind differ from the background by an amount greatly in excess of the estimate of background error, may be labelled as suspect with a high degree of confidence.

Recognizing the value of numerical fields for monitoring purposes, the WMO Commission for Basic Systems agreed in 1985 that there was a need for global NWP centres to co-ordinate their activities and ensure that feedback was provided to those responsible for making the observations. Since then a regular exchange of monitoring results has been established between a few active centres — the Meteorological Office, ECMWF, NMC Washington, and Tokyo. In 1988, three lead centres were nominated by WMO to produce lists of suspect stations at 6-monthly intervals for given data types, together with information on the nature of the error. Bracknell was allocated the role as lead centre for marine surface observations, ECMWF for radiosondes,

and Washington for satellite and aircraft data. Some of the monitoring work performed at ECMWF, mainly relating to radiosonde observations, has been described by Radford (1987). This paper covers some of the activities at the Meteorological Office, Bracknell in its role as a lead centre.

2. Monitoring results

2.1 Pressure

In a typical month about 110 000 surface reports from ships and buoys are received at Bracknell in time for use in the numerical forecasting system. The number of reports received from any one ship is very variable; there can be long gaps while it is in port or out of service, and while at sea some report rather infrequently. In any month about 4000 different ships each provide more than 20 reports, which is around the minimum number required for monitoring purposes. There are also about 170 moored buoys and platforms and 200 drifting buoys each providing at least 20 reports per month.

A histogram of O−B differences for all ship pressure observations in the period January–June 1990 is shown in Fig. 1(a), together with the Gaussian distribution with the same mean and standard deviation. Although almost all values fall within the range +5 to −5 mb, a small number of very large values, presumably resulting from erroneous observations, contribute to the large standard deviation of the population. Some of the largest differences from background are often due to coding errors in the 10 or 100s units and are easily detected by the automatic quality-control checks. The distribution of all those observations which fail these checks, and are therefore not used in the data assimilation, is broad and bimodal (Fig. 1(b)). The remaining 92% of the observations which pass the quality checks show a distribution of O−B which is very close to Gaussian (Fig. 1(c)); it has a mean of 0.0 mb and a standard deviation of 1.6 mb, and the principal contribution to the variance is assumed to be from background errors.

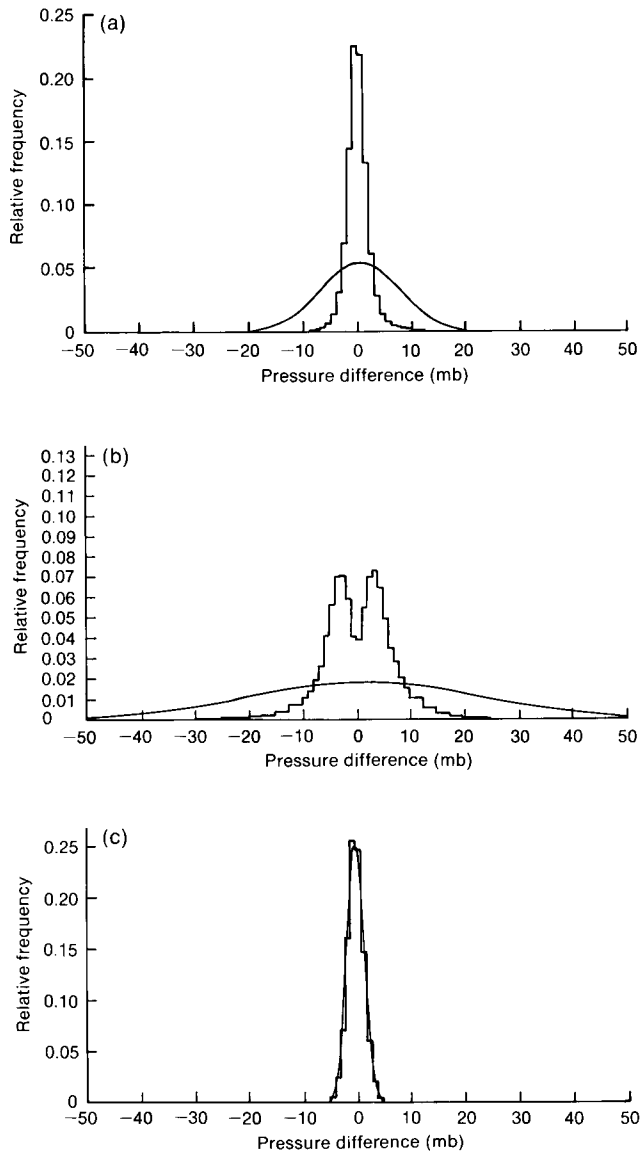

Figure 1. Histograms showing the distribution of O−B for pressure observations from ships for the period January–June 1990 for (a) all observations, (b) only observations failing quality checks, and (c) only observations passing quality checks. Gaussian distributions with the same mean and standard deviation are also plotted.

A global estimate of the background error, such as is provided in Fig. 1(c), will conceal large variations which may occur from place to place. Background values are likely to be most accurate in data-rich areas, such as in the North Sea or Mediterranean, or in areas such as the tropics where meteorological variability is low. In order to investigate the geographical distribution, values of O−B from observations which pass the quality-control checks have been calculated for 10° latitude–longitude boxes. The mean and standard deviation of O−B are plotted in Fig. 2 provided there are at least 10 observations available within a box. Observations of pressure from ships at all synoptic hours have been used over the 6-month period January–June 1990, and the number of reports in each 10° box, on which the calculations are based, is shown in Fig. 3. In almost all areas the magnitude of the mean is less than 1.0 mb, the exceptions being in the high latitudes of the southern hemisphere where only a small number of observations are available. In some boxes the statistics may be dependent on just one or two ships which have passed through the area in the period. Clearly a systematic bias in the observations from one of them will show a strong signal in the values shown; it is only in the data-rich regions of the main shipping lanes that there are enough observations from independent sources to smooth out such irregularities. The average standard deviation shows a great deal of variability with location; in the tropics the value lies between 1.0 and 1.5 mb, in northern latitudes between 1.5 and 2.0 mb, and in the Southern Ocean between 2.0 and 3.0 mb. The higher values reflect the effect of greater meteorological

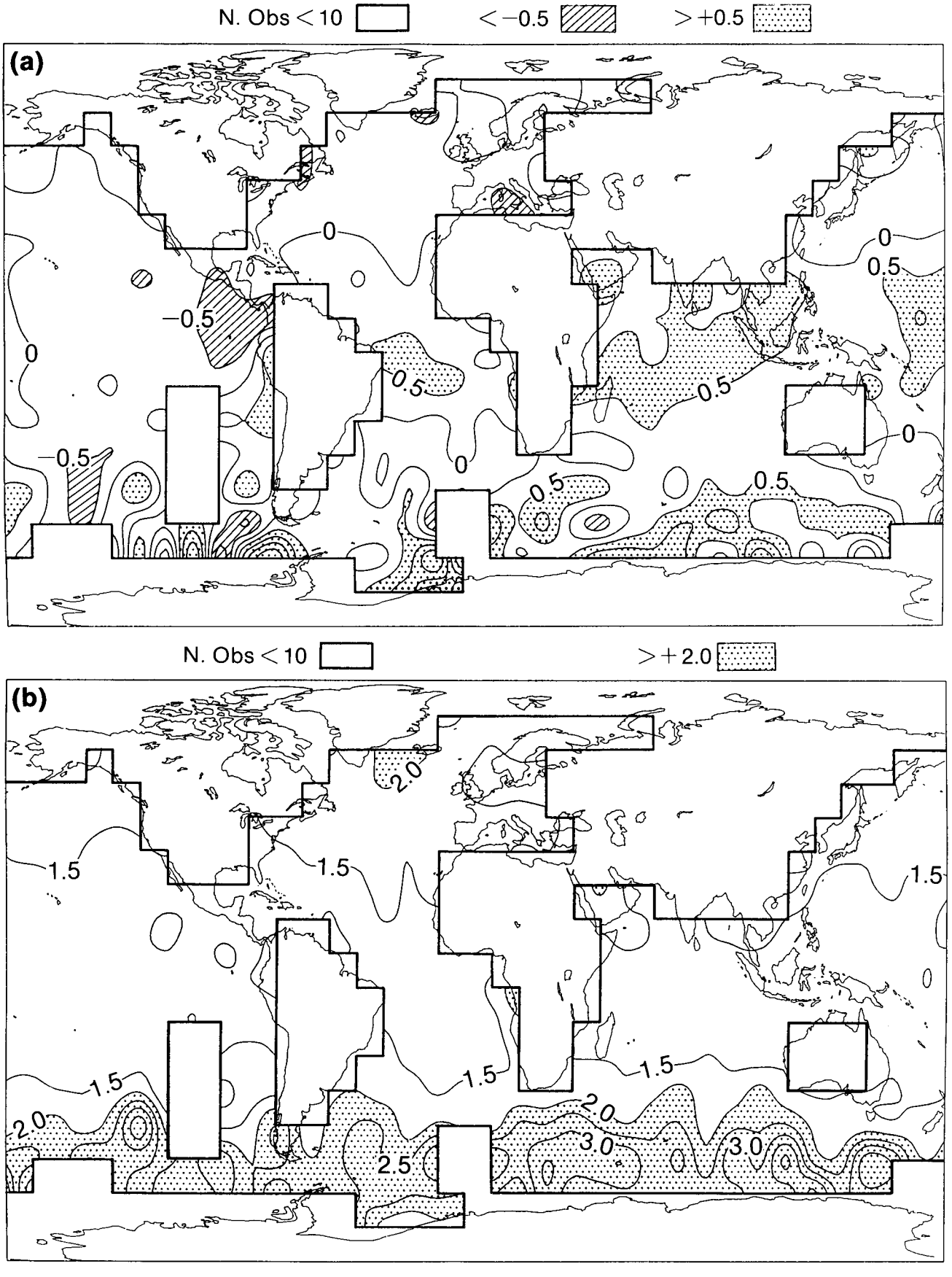

Figure 2. Average over the 6-month period January–June 1990 for (a) the mean, and (b) the standard deviation of O−B for pressure observations from ships which pass the quality-control checks. The contoured values are based on averages for 10° boxes where more than ten reports were available.

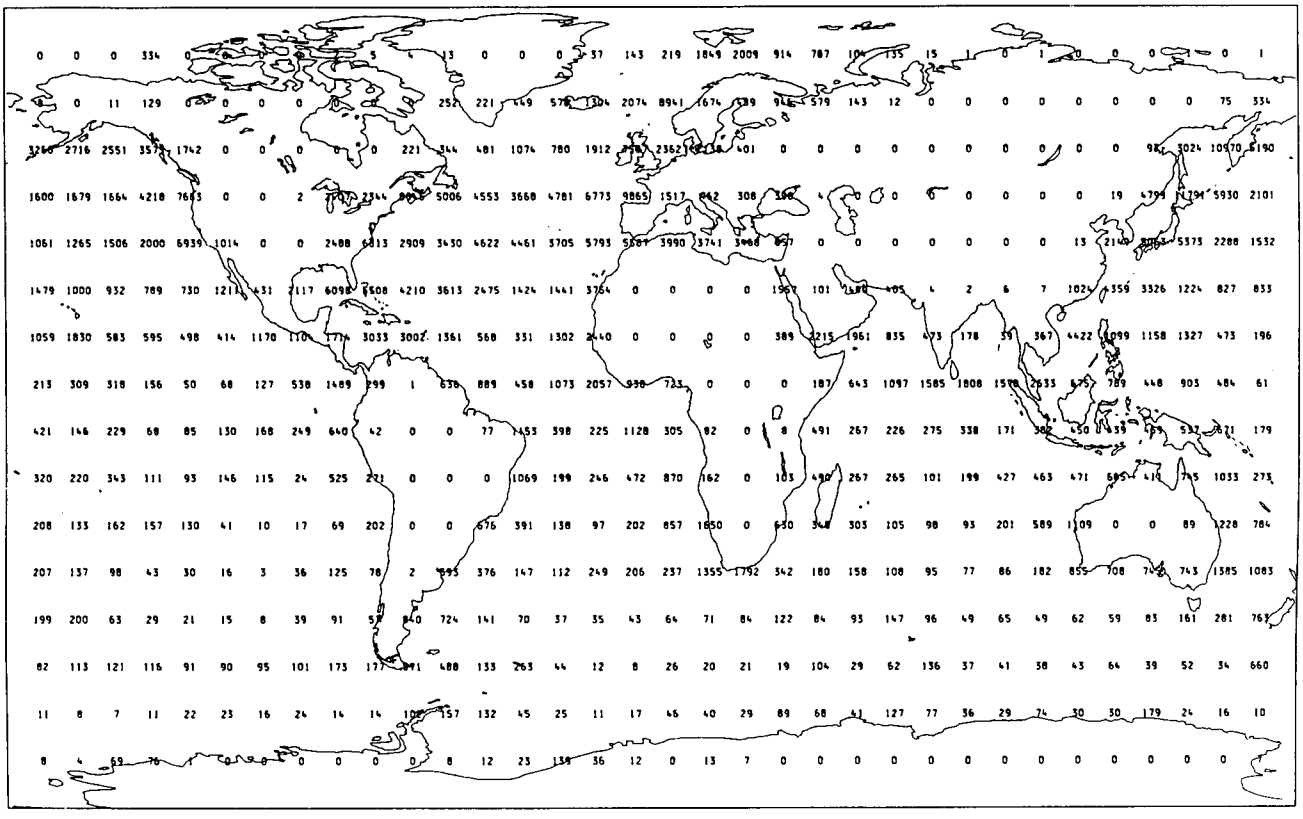

Figure 3. The number of ships within each 10° box in the period January–June 1990 used in Fig. 2.

variability and the higher background errors in areas where there are few observations.

The best way to display monitoring results for a given ship or buoy is in the form of a time sequence of values of O−B as in Fig. 4. The crosses represent the difference from background for each pressure observation from a ship operating in the North Sea and reporting regularly at each of the four main synoptic hours 00, 06, 12 and 18 UTC. The period covered is January–June 1990. The mean of the sample is +0.4 mb and the standard deviation 1.1 mb, which are close to the average for all reports from that area. The departures from background appear largely uncorrelated from one observation time to the next and can be attributed to random errors in the background values. It is noticeable that the scatter is larger in the first three months than it is in the last three, and this is almost certainly due to seasonal variability in the background errors; model forecast errors are larger in the winter than in the summer. There are four observations which differ substantially more from the background than the rest of the population: one value of O−B falls outside the plotting limits of the figure, and the magnitude of the others is close to 10 mb. The differences in the last three cases is no doubt due to an error of 10 being made while taking the pressure reading or while the figures were transcribed. This example is typical in that, for the great majority of ships, the values of O−B for pressure show a similar scatter about the zero axis, though few report quite as frequently.

Fig. 5 displays values of O−B for a ship on routes between Europe and the Caribbean, and the periods of 3 weeks or so spent in port account for the regular gaps in the sequence. In this case the observations of pressure show a bias with respect to background which remains at around +7 mb throughout the entire period. The standard deviation of the sample is 1.8 mb which is not much larger than average for the region in which the ship is operating. One likely reason for the errors is a miscalibration of the instrument. There are, however, two values of between +15 and +20 mb, deviating significantly from the rest of the sample, which seem to be in error for other reasons. Perhaps again a coding error of 10 mb has been made on these occasions. Instances of a bias in the observations of pressure from ships, which remains constant over long periods of time, are surprisingly common; regular monitoring at Bracknell shows that about 150 ships may be identified at any one time with a constant bias in excess of 2 mb in magnitude. In most cases, as in this example, the standard deviation is small. Where the bias is relatively small the cause of the error may be a failure to make a proper correction to sea level. On a large ship, the barometer may be at a height of perhaps 30 m, and the adjustment to give the value of pressure at mean sea level is about 3 mb depending on the temperature. Where the adjustment is made incorrectly, or not at all, an error will arise. A particular problem occurs where the height of the barometer changes due to changes in the draught of the ship; there will be errors of up to 1 mb or greater if this is not taken into account.

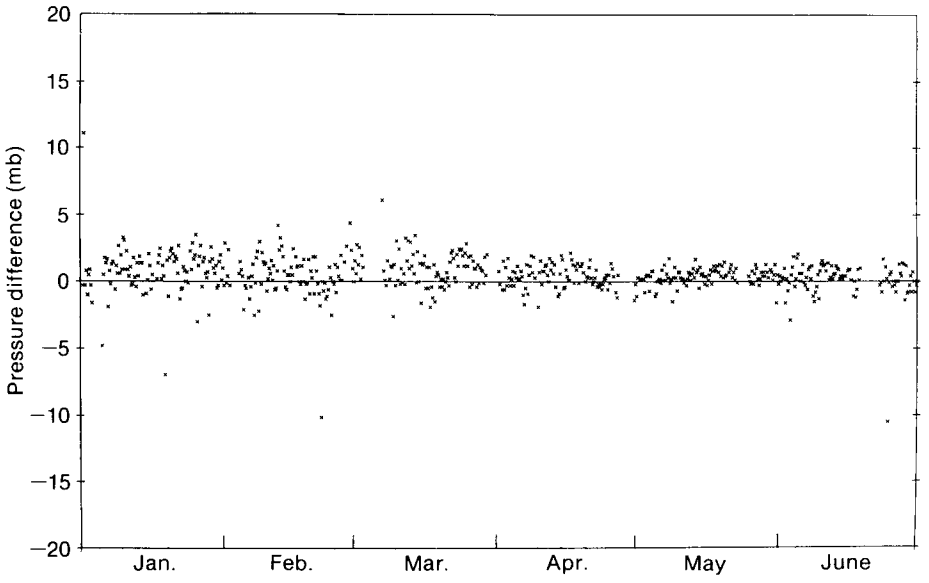

Figure 4. A time series of O−B for pressure observations from a ship in the North Sea for the period January–June 1990.

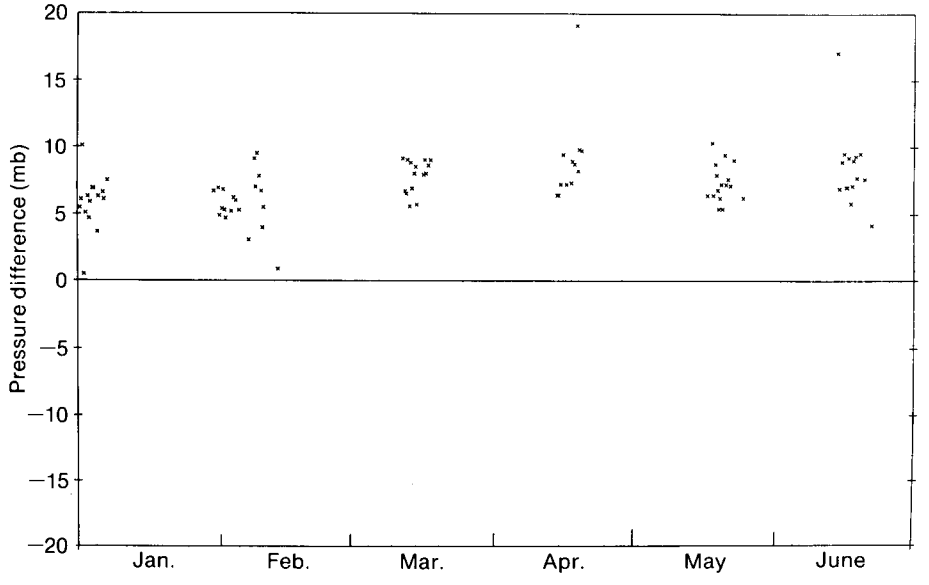

Figure 5. As for Fig. 4, but for a ship on routes between Europe and the Caribbean.

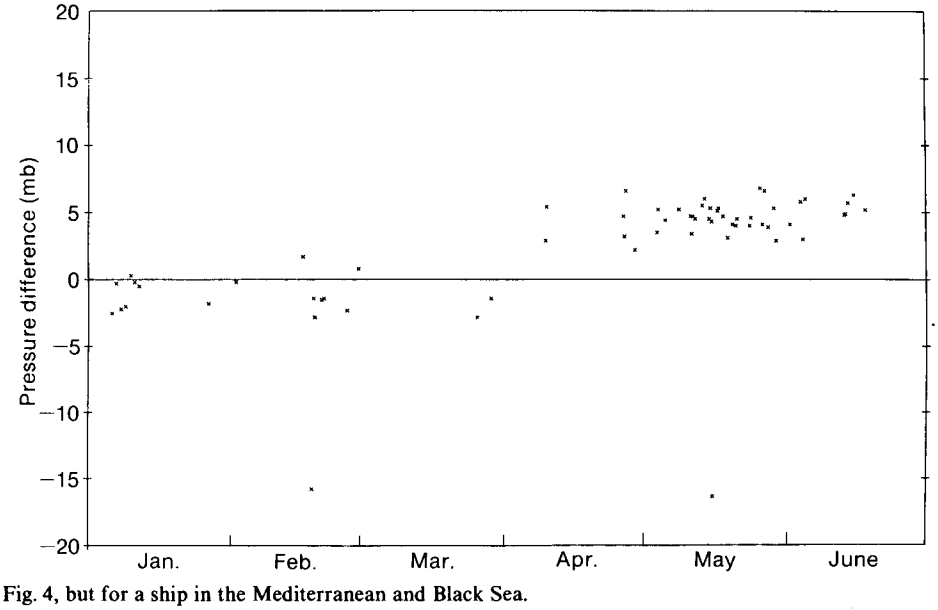

Figure 6. As for Fig. 4, but for a ship in the Mediterranean and Black Sea.

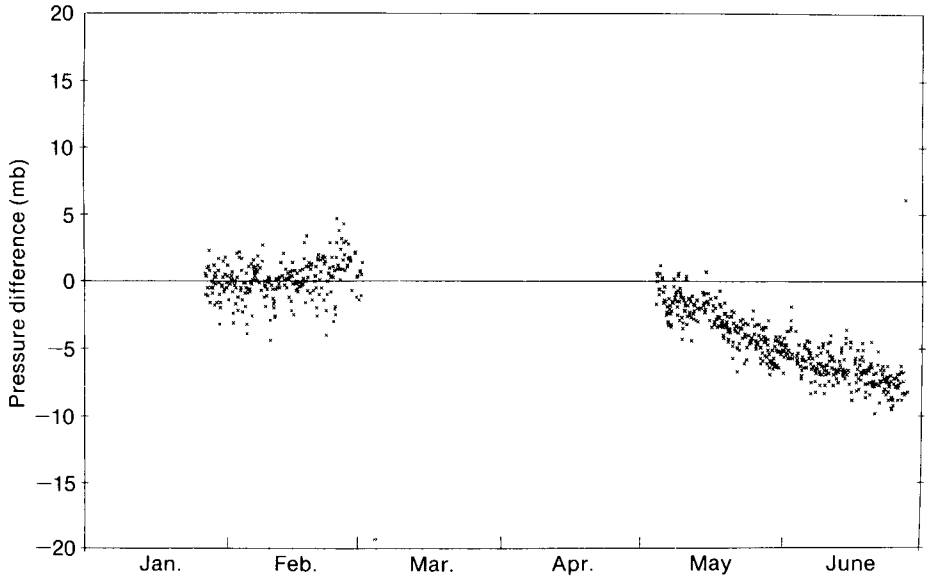

Figure 7. As for Fig. 4, but for a buoy in the Gulf of Mexico.

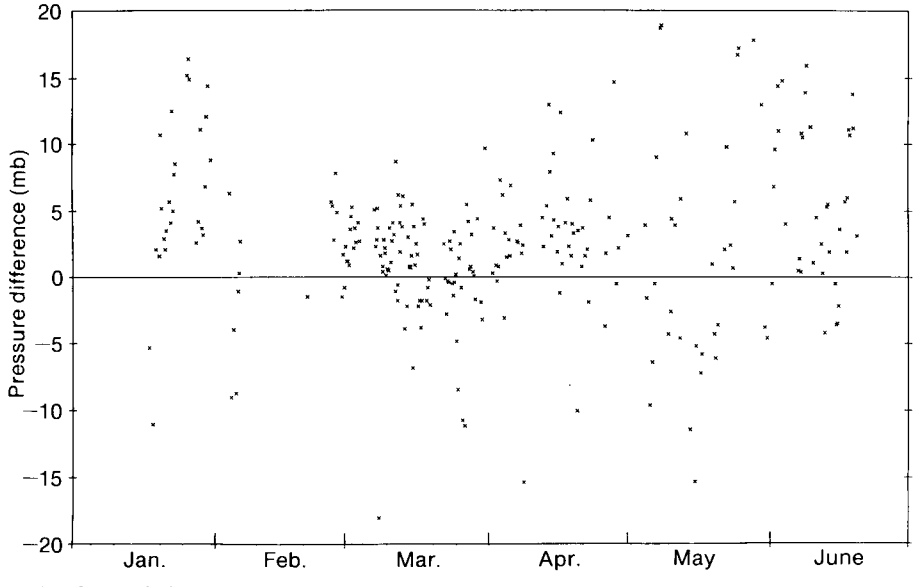

Figure 8. As for Fig. 4, but for a ship in the Southern Ocean.

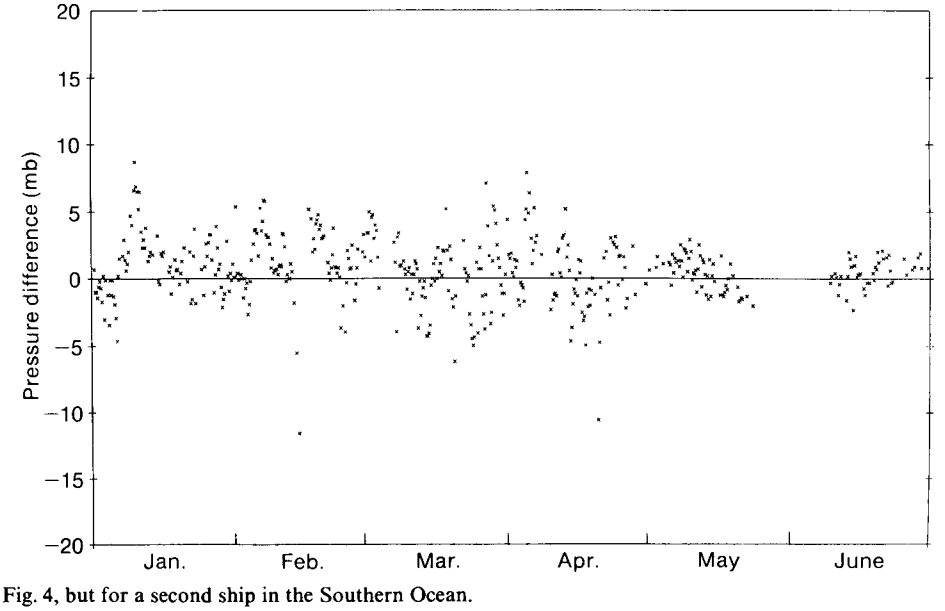

Figure 9. As for Fig. 4, but for a second ship in the Southern Ocean.

Time sequences of O−B will enable changes in the observation quality to be easily identified. Fig. 6 shows a case of a ship, operating in the Mediterranean and Black Sea, where a pressure bias developed suddenly; the observations seemed of good quality up to the beginning of April, but after that date all showed a bias of +5 mb. Again, two extreme values are evident where presumably there is a separate cause of the error. Most biases in pressure observations from ships seem to occur suddenly, as in this example, pointing perhaps to an occasion when the instrument became maladjusted or damaged, or the observation practice changed. In a few instances, particularly with the automatic instruments on a buoy, the bias grows gradually over a long period of time as the example in Fig. 7 shows. This drifting buoy is in the Gulf of Mexico and the bias increases in magnitude from near zero to −8 mb over a period of 2 months.

In all of the examples shown so far the errors have been systematic in that the standard deviation of O−B has been small at any one time. In a few cases the occurrence of large random errors may be very frequent as the example in Fig. 8 demonstrates; 65 of the 338 reports fall outside the plotting limits of this diagram, and those of magnitude less than 15 mb have a standard deviation of 5.0 mb. Occasionally the position of the ship in question appeared to be miscoded with east reported instead of west, or north instead of south, but this was not the major source of error. Over the 6 months it covered a wide area in the Southern Ocean off the Antarctic continent with excursions to New Zealand and South America. Model errors are known to be largest in these regions, and it is important to take into account the location of the ship before deciding what part of O−B may be attributed to observation error and what to background error. Fig. 2(b) shows that the standard deviation of O−B in the Southern Ocean is on average some 2 to 3 times larger than in the tropics, but it is nevertheless much less than found in this example. It certainly seems that the observations are highly unreliable, and this is confirmed by comparison with the time sequence of O−B pressure values shown in Fig. 9. In this case the observations came from a research ship which during January–March was at similar high latitudes of the southern hemisphere. The scatter of O−B is clearly much smaller and the standard deviation of 2.7 mb is very close to the average value for the region. From mid April to mid May the ship steered north across the tropical Atlantic to Europe and, after a spell in port, left for Arctic waters in June. The standard deviation of O−B in this second period is noticeably lower than in the first 3 months. It can be seen that the standard deviation of O−B for each part of the route taken by a ship is close to the average values shown in Fig. 2(b).

The mean (M) and standard deviation (S) of the differences from background are clearly very informative measures of observation quality:

$$M = \overline{(o-b)}, \quad S = \{\overline{(o-b)^2} - M^2\}^{1/2}$$

where o is the observed value; b the background value; and the mean, indicated by the overbar, is taken over a period of a month or more. However, as the last example shows, background errors may vary a great deal across the globe and ideally this should be taken into consideration as well. If t is the true value at the observation position, the true observation bias (TB) is given by

$$TB = \overline{(o-t)} = \overline{(o-b)} - \overline{(t-b)}.$$

Use can be made of the global statistics for each 10° box shown in Fig. 2: assume that the ship in question remains in one box where the mean O−B for all ships' observations passing the quality-control checks over a long period of time is m and the standard deviation s. In a large sample the mean observed value can be expected to be close to the mean of the true value, so a good approximation to $\overline{(t-b)}$ is m, and

$$TB = \overline{(o-b)} - m.$$

This represents quite a small correction to the estimate given by M as the local average m seldom exceeds 0.5 mb in magnitude. A normalized standard deviation NS may be defined by

$$NS = \{\overline{((o-b-m)^2 - TB^2)/s^2}\}^{1/2}$$

which takes a value of 1 if the standard deviation of O−B for the ship in question is equal to the past average for all the other ships in the box, and a value of 2 if it is twice as large, and so on. TB and NS have been calculated assuming that the ship remains in the same area so that m and s are fixed, but they can equally well be calculated allowing m and s to vary as the ship moves from one part of the globe to the other. Values of TB and NS calculated in this way are routinely monitored at Bracknell for all ships reporting regularly on the Global Telecommunication System (GTS).

Monitoring statistics are supplied each month to those responsible for the quality of observations exchanged on the GTS. The Marine Division at Bracknell is one such group receiving lists of ships for which the mean and standard deviation of O−B is much larger than average. They scan the lists for ships in the UK Voluntary Observing Fleet (VOF), and where a suspect case is found, the Port Met. Office network is alerted and a visit is made to the ship at the earliest opportunity. A recent example of the procedures in action concerns a support vessel, newly recruited to the UK VOF, stationed in the North Sea. Values of the standard deviation of O−B had been found to be very large and the Port Met. Officer visited the vessel to ensure that the observing staff understood how to read

the barometer and that the right corrections were being applied. However, the fault was finally found to be in the reporting of longitude which was coded as 20° E instead of 2° E. A time series of O—B pressure is shown in Fig. 10 for the relevant period. A sudden improvement in October 1990 followed the visit, marred only by a brief reversion to the erroneous practice for a week in December.

2.2 Wind

Observations of wind from ships and buoys can be monitored in a similar way to the observations of pressure. On the majority of ships, wind is measured using anemometers which may be fixed or hand-held. The reported speed will be dependent on the period over which the readings have been averaged, and the height of the instrument above mean sea level, both of which will vary a great deal from ship to ship. The wind flow is distorted by the structure of the ship, and factors affecting the wind measurement will include the siting of the anemometer, the size of the ship, and the bearing of the wind with respect to the alignment of the ship. It is common for the measurement to be taken visually from a dial, and a tendency to report gust values rather than time averages will lead to overestimation of the speed. Another cause of error in ship observations of wind may be a failure correctly to allow for the motion of the ship. The wind reports from other ships, such as those of the UK VOF, are based on visual estimates of the sea state and in these cases the factors outlined above do not apply.

For the monitoring results presented here the values of the background wind at the lowest model level (approximately at 25 m) have been used. Where ship winds are measured by an anemometer an apparent speed bias will be introduced into the values of O—B if its height is greatly different from 25 m. Another source of error is of course a systematic bias in the background values which is difficult to estimate independently of ship observations.

Histograms of O—B differences of wind speed are presented in Figs 11(a)–11(c) in the same way as in Figs 1(a)–1(c). As with observations of pressure, those wind observations which fail the quality-control checks show large differences from background, some in excess of 50 m s^{-1}, and as a result the standard deviation is large. The distribution of O—B wind speed for the remaining 96% of the observations is nearly Gaussian with a bias of +1.2 m s^{-1} relative to background and standard deviation of 3.3 m s^{-1}. The bias is about 15% of the mean observed speed. The difference between the height of the anemometer, where one is used for wind measurement, and the height at which the background is valid (25 m) has already been mentioned as a source of bias in O—B, but it alone seems unlikely to account for the magnitude of the bias found here. Rahmstorf (1989) demonstrated that routine wind reports prepared by ships' officers from reading the mast anemometer were higher than those measured by an anemometer sited on a long boom suspended from the side of the ship to minimize the effect of the ship superstructure. He found differences as large as 30% in moderate to strong winds.

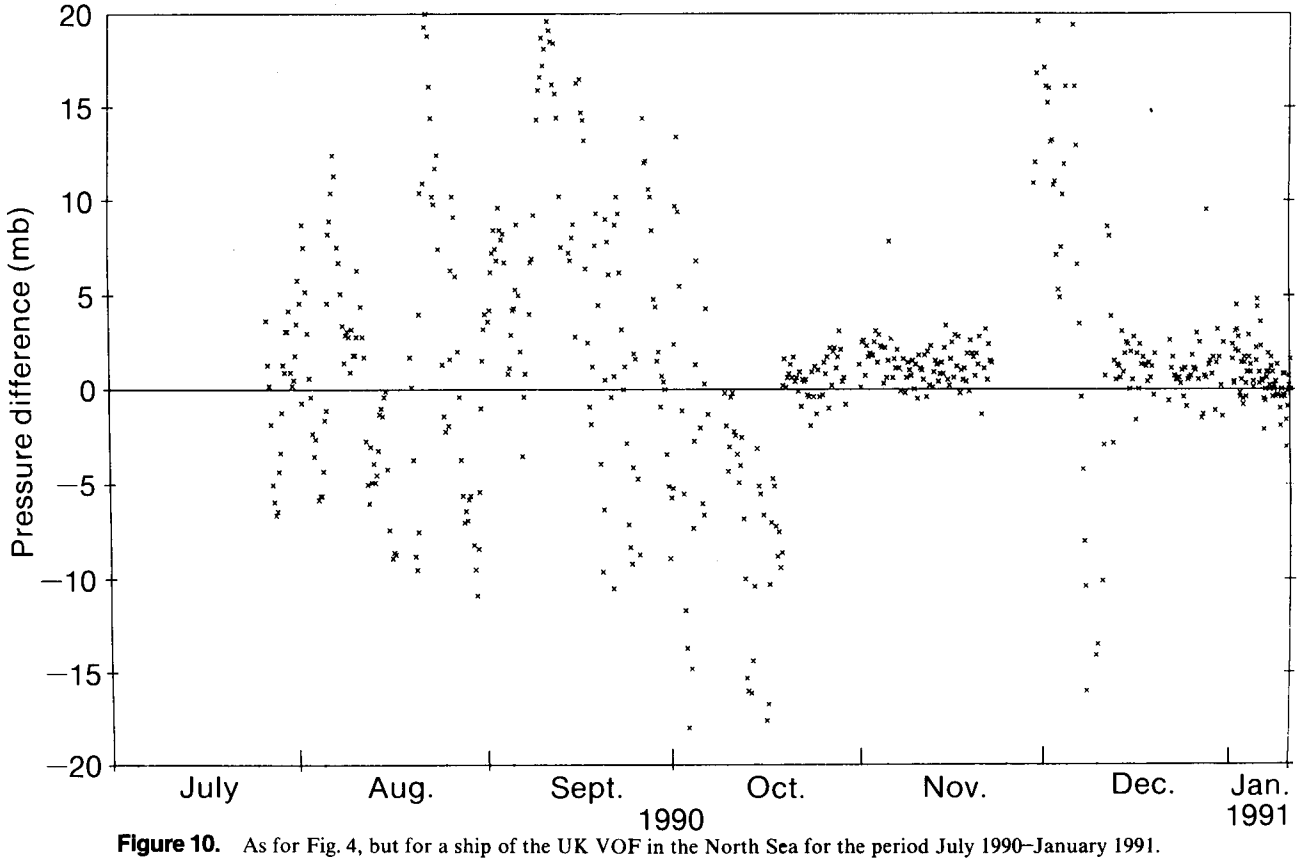

Figure 10. As for Fig. 4, but for a ship of the UK VOF in the North Sea for the period July 1990–January 1991.

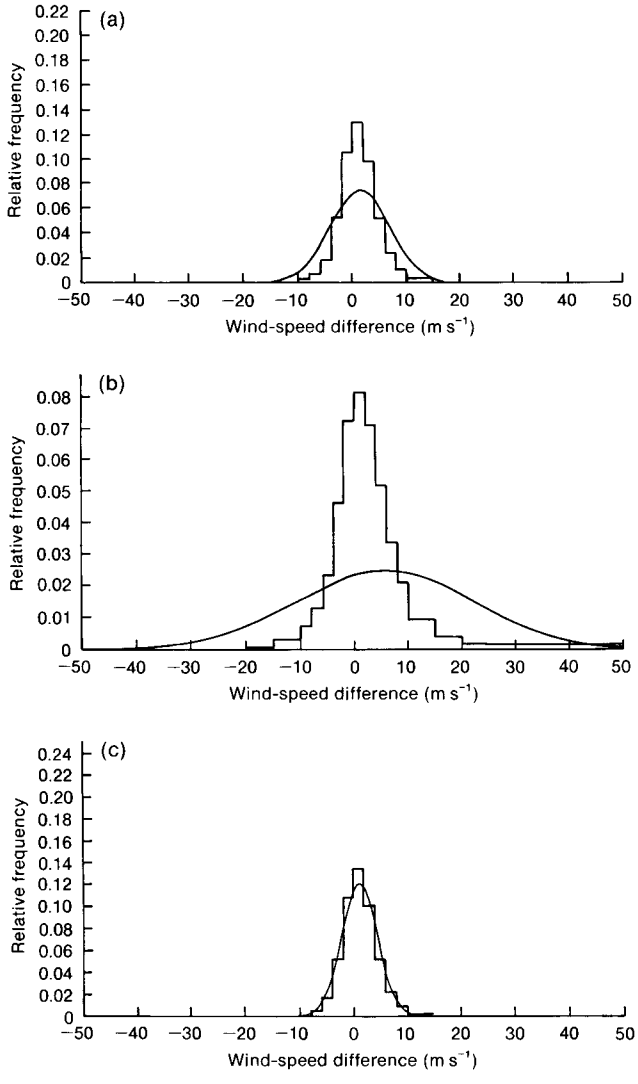

Figure 11. Histograms showing the distribution O—B for wind speed observations from ships for the period January–June 1990 for (a) all observations, (b) only observations failing quality checks, and (c) only observations passing quality checks. Gaussian distributions with the same mean and standard deviation are also plotted.

Other studies (e.g. Wilkerson (1986)), where comparisons have been made with observations from moored buoys, also show a positive speed bias in ship winds, and indicate that many are of suspect quality.

Ocean Weather Ship *Cumulus*, operating to the west or south-west of Britain at around longitude 20° W, provides a useful source of wind observations for reference. The ship is small and wind is measured by two anemometers, one on each side of the aft mast, at a height of 23 m above the sea surface. Values of O—B for the speed and direction over the period January–June 1990 are plotted in Figs 12(a) and 12(b). Values of direction have not been plotted if the speed is less than 5 m s^{-1}. The mean speed bias of −0.1 m s^{-1} is very small compared with the positive bias found from all ship observations taken together. Although not evident here because of the lack of reports, values of O—B for wind from many ships and buoys are smaller in the summer months, as they were for observations of pressure, reflecting the lower background errors.

Some ships show a speed bias considerably larger than average as Fig. 13 shows. In this case the ship was on routes in the Atlantic, Pacific and Indian Oceans during the 6-month period. After providing seemingly reliable observations for the first 4 months a bias of +10 m s^{-1} developed in May. In a similar way systematic differences between the observed and background wind directions are easily identified by inspection of a time series. Such problems can be found in observations from buoys and other automatic stations, and may be confidently attributed to observation error where they occur over the open ocean. Care must be taken if the observing position is close to the coast; the background values may be derived from land points in the model, and systematic errors of the numerical forecasts may be much larger than average, particularly if the land rises steeply to some coastal mountain peaks. An example of a direction error is shown in Fig. 14. The buoy in question is in the Arctic Ocean far from any land, and a constant bias of 130° is evident in the reported direction.

3. Concluding remarks

The examples presented above demonstrate the value of fields from a numerical forecasting system in the monitoring of the quality of meteorological observations. The numerical fields are particularly suitable as reference values; they are global in extent and are consistent both in space and time. On most occasions their accuracy is such that quite small observation errors may be detected. It is essential in all cases that the likely magnitude of the background error is quantified, and this is best done by reference to observations of known high quality.

The most important result obtained from the monitoring work performed at Bracknell is the identification of a large number of ships for which the observations of pressure appear to be of poor quality. In many cases there is a bias which remains constant for many months or even years; at any one time around 150 ships fall into this category. Apart from the bias, the observations from these ships appear to be of good quality. In addition there are in excess of 50 other ships where there are regular large errors in the pressure observations of a more random nature. The monitoring of observations of wind from ships shows that the reported speed is on average positively biased with respect to the background. The wind speed observed at weather ships, where the observing practices are known to be reliable, shows no such bias. Unlike the case of pressure, there are few ships reporting wind which stand out far enough from the average to be confidently labelled as suspect.

Monitoring serves no useful purpose unless it leads to improvements in the observing system. Recognizing this, WMO established lead centres for the monitoring of different types of observations, and since 1987

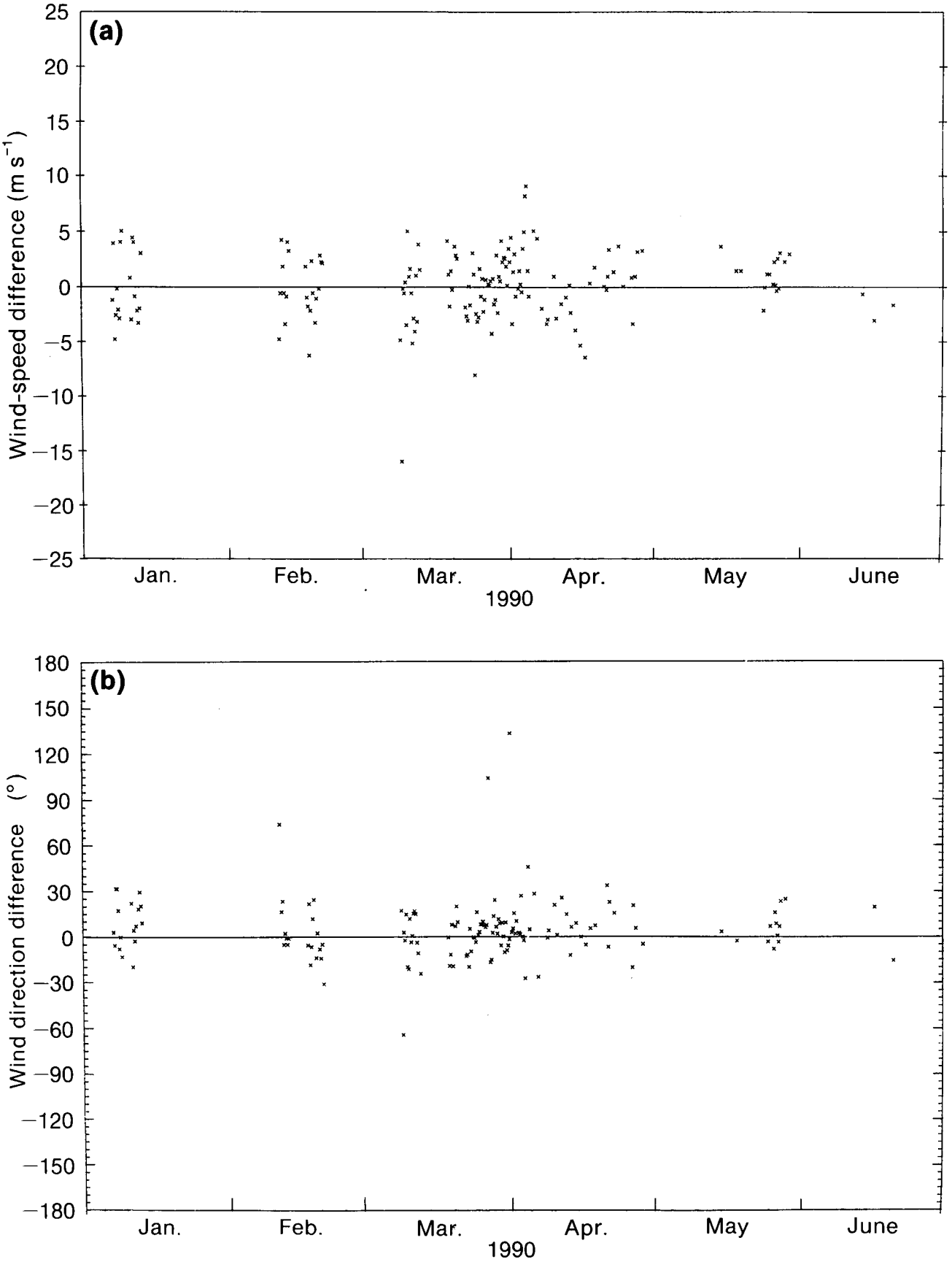

Figure 12. A time series of O−B for (a) wind speed, and (b) wind direction observations from Ocean Weather Ship *Cumulus* for the period January–June 1990.

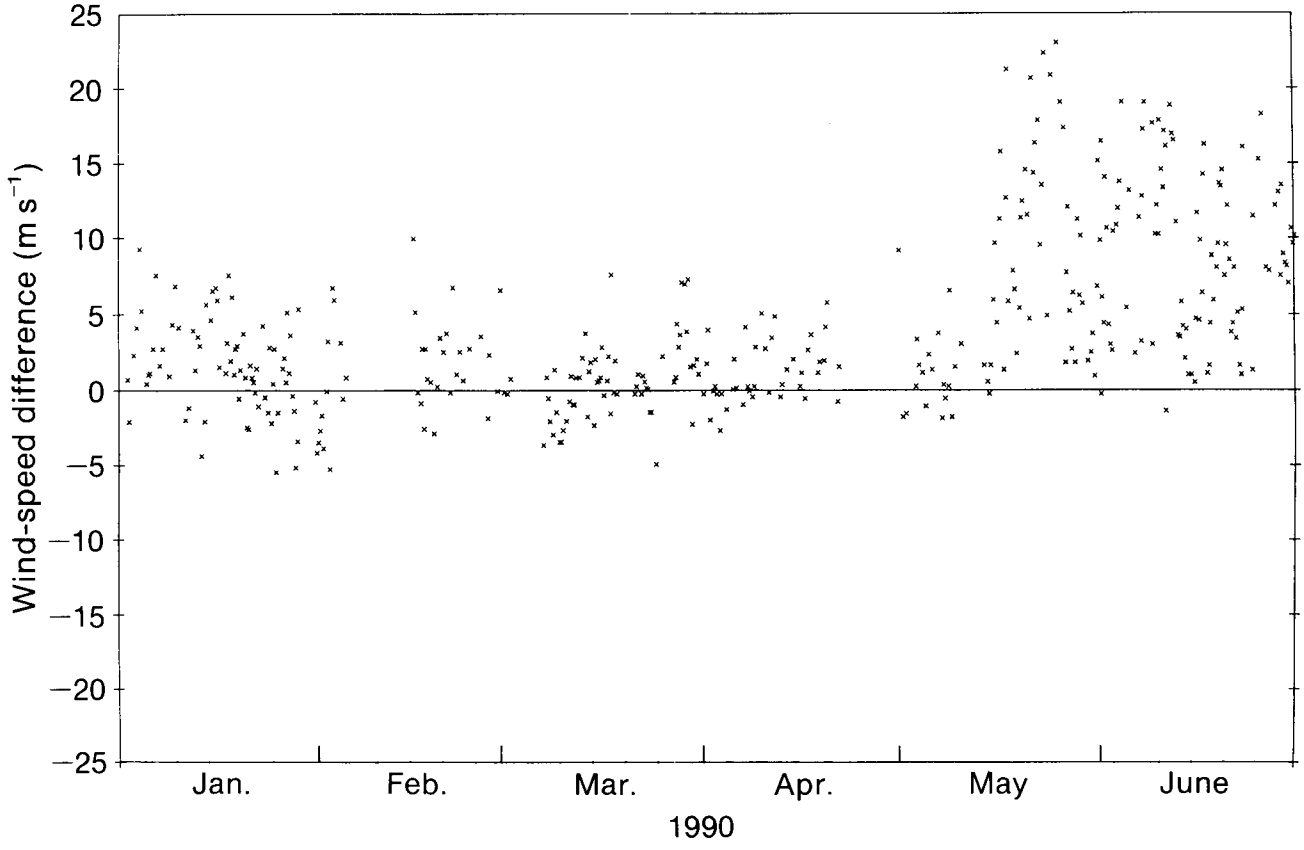

Figure 13. A time series of O−B wind speed observations from a ship on routes in the Atlantic, Pacific and Indian Oceans for the period January–June 1990.

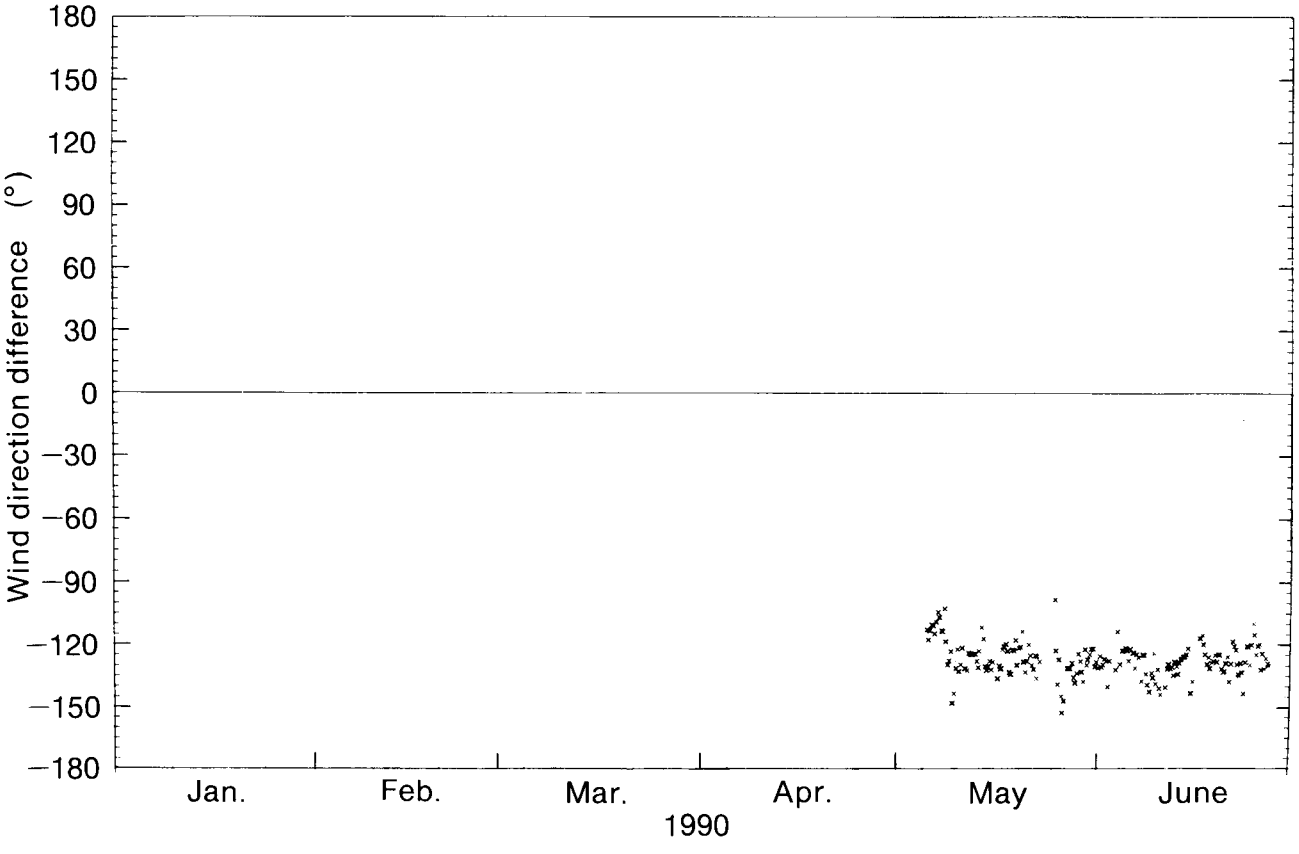

Figure 14. A time series of O−B wind direction observations from a buoy in the Arctic Ocean for the period January–June 1990.

Bracknell has been fulfilling its role as lead centre for marine surface data. Monthly monitoring statistics are routinely provided to some of the centres operating VOFs or ocean buoy systems. They are also exchanged with other numerical forecasting centres so that values from different models may be compared. Every 6 months a report is provided to WMO for distribution to members. As such feedback often operates slowly and is not always effective, changes have been made within the numerical forecasting system at Bracknell in order that optimal use is made of the observations. A correction is applied to observations of pressure from those ships and buoys for which a constant and long-standing bias can be identified. Other ships, where the quality of the observations seems low and a correction cannot be made, are eliminated from use within the forecast system. The correction and rejection lists are updated regularly each month to allow for changes in quality.

Successful feedback of results is an essential part of all monitoring procedures. It is important that those making the observations are provided with convincing information on why the observations are considered to be of poor quality and what the characteristics of the errors seem to be. It is only in this way that observation errors can be corrected and the full potential of the global observing system can be realised.

Acknowledgements

The authors would like to thank Captain R.C. Cameron of the Marine Branch for the information he supplied concerning the UK Voluntary Observing Fleet.

References

Atkins, M.J. and Woodage, M.J., 1985: Observations and data assimilation. *Meteorol Mag*, **114**, 227–233.

Bell, R.S. and Dickinson, A., 1987: The Meteorological Office operational numerical weather prediction system. *Sci Pap, Meteorol Off*, No. 41.

Lorenc, A.C., Bell, R.S. and Macpherson, B., 1991: The Meteorological Office analysis correction data assimilation scheme. *Q J R Meteorol Soc*, **117**, 59–89.

Lorenc, A.C. and Hammon, O., 1988: Objective quality control of observations using Bayesian methods. Theory, and a practical implementation. *Q J R Meteorol Soc*, **114**, 515–544.

Radford, A.M., 1987: ECMWF radiosonde monitoring results. Proceedings of ECMWF/WMO Workshop on Radiosonde data quality and monitoring, 95–114.

Rahmstorf, S., 1989: Improving the accuracy of wind speed observations from ships. *Deep-sea Res*, **36**, No. 8A, 1267–1276.

Wilkerson, J., 1986: Accuracy estimates of wind and wave observations from ships of opportunity in the WMO voluntary observing ship programme. European Space Agency Workshop on ERS-1 wind and wave calibration. Darmstadt, ESA, No. SP 262, 77–84.

Notes and news

Hydrological information

The International Association of Hydrological Sciences (IAHS) has submitted publicity material on the many titles published recently, e.g. *The physical basis of ice sheet modelling* and *Large scale effects of seasonal snow cover*.

Those interested in any hydrological subjects should apply to:

IAHS Press
Institute of Hydrology
Wallingford
Oxfordshire OX10 8BB
United Kingdom

or

Office of the Treasurer IAHS
2000 Florida Avenue NW
Washington, DC 20009
USA

Review

Pilots' weatherpack, by W.S. Pike, R. Reynolds and S.G. Cornford. 221 mm × 302 mm, pp. 24, *illus.* Reading, Royal Meteorological Society, 1991. About £3.50.

My impression of this weather pack is that it is a very clear and concise presentation bringing together examples of weather orientated aircraft accidents. The examples that have been studied emphasize how weather hazards are often encountered quite unexpectedly, irrespective of the time of year. With the upward trend of aircraft accidents, particularly amongst general aviation, this excellent information pack, when used for the training of pilots, serves a very useful purpose. It may also be useful in sixth-form Geography and Physics departments having a meteorology module in the syllabus.

The information emphasizes the important fact that a pilot must brief himself adequately to perform a safe flight and highlights the folly of flying on actual weather reports (METARs). Within the civil enclave, self briefing is the rule (AIC 30/1988) but a pilot can still talk to a forecaster at one of the three aviation centres (Bracknell, Manchester or Glasgow) for clarification purposes (AIC 30/1988) once the pilot has accessed some form of self-briefing data (AIRMET, F214/215 or WAFS charts).

Case 1: has been superbly illustrated with satellite pictures and highlights the impending dangers. Unfortunately FBUs (flight briefing units) do not have the benefit of satellite pictures. It should also be noted that the interpolation of satellite pictures, particularly IR (infrared) images, should be left to the 'professional' because wrong assumptions could be read into the analysis by the uneducated and inexperienced.

Case 2: highlights not only the foolishness of flying on actuals, and inadequate briefing, but also in not having sufficient training. A pilot may never know when he may be asked by ATC to descend, or climb, to a level which may be in cloud, to which an IFR (instrument flight rating) would be required.

Case 3: contains the message of avoiding flying near frontal zones because of the hazards.

Cases 4, 5 and 6: highlight the fact that air, in mass ascent, such as in a depression, or in well-developed areas of showers, or within organized bands of rain, can frequently result in the lowering of the main cloud base. This change in the cloud can invalidate a planned VFR flight.

Cases 7 and 8: highlight another important fact. When a cold easterly airstream becomes established, blowing out of Europe and across the United Kingdom, undercutting by the cold air forms some very strong inversions in the first few thousand feet. This has significant effects on air safety since engine performance is altered and also severe airframe ice may be experienced.

Although cases of airframe icing have been illustrated it must not be forgotten that carburettor icing is equally important on safe flying and so it is a pity that a case of carburettor icing has not been presented. However, the pack is well written and illustrated and is a good source of information to enlighten student pilots that the weather must not be taken for granted. Hopefully it will play its part in reducing aircraft accidents, and consequently save lives.

B.K. Lloyd

Books received

The listing of books under this heading does not preclude a review in the Meteorological Magazine at a later date.

Air traffic and the environment, edited by U. Schumann (Berlin, Heidelberg, New York, London, Paris, Tôkyo, Hong Kong, Springer-Verlag, 1990. DM 50.00) contains the proceedings of a German Aerospace Research Establishment (DLR) International Colloquium at Bonn in November 1990. The volume is the sixtieth in the series *Lecture notes in engineering* edited by C.A. Brebbia and S. Orszag. ISBN 3 540 53352 4.

Climate and development: climatic change and variability and the resulting social, economic and technological implications, edited by H.-J. Karpe, D. Otten and S.C. Trinidade (Berlin, Heidelberg, New York, London, Paris, Tokyo, Hong Kong, Barcelona, Springer-Verlag, 1990. DM 98.00) brings together interdisciplinary perceptions of the concerns about the subject which were voiced at the Hamburg Congress on Climate and Development. ISBN 3 540 51269 1.

Wave packets and their bifurcations in geophysical fluid dynamics, by H. Yang (Berlin, Heidelberg, New York, London, Paris, Tokyo, Hong Kong, Springer-Verlag, 1991. DM 78.00) is the first monograph on the subject. Some basic knowledge is included to make the book more readable to a wide range of researchers in allied areas. ISBN 0 387 97257 9, 3 540 97257 9.

Atmospheric particles and nuclei, by G. Götz, E. Mészáros and G. Vali (Budapest, Akadémiai Kiadó, 1991. £20.00) contains a presentation of the physical and chemical properties of aerosols. It is intended for students new to the subject, but also to be of use to research scientists. ISBN 963 05 5682 0.

Chemistry of atmospheres, second edition, by R.P. Wayne (Oxford, Clarendon Press, 1991. £45.00 (hardback), £19.50 (paperback)) lays the foundations for the study of the subject, on which rational decisions about environmental problems will need to be based. It is a 'necessary' second edition to incorporate recent developments. ISBN 019 855571 7, 019 855574 1.

Remote sensing in hydrology, by E.T. Engman and R.J. Gurney (London, Chapman and Hall, 1991.) is aimed at water resources scientists and managers. Each part of the hydrological cycle is detailed, and specific examples are used throughout. ISBN 0 412 24450 0.

The fragile environment, edited by L. Friday and R. Laskey (Cambridge University Press, 1991. £9.95, $15.95 (paperback)) explores the impact of the human species on its environment. The eight international contributors to this printing of the Darwin College Lectures address themselves to a broad readership. ISBN 0 521 42266 3, 0 521 36337 3.

Satellite photographs — 21 May 1991 at 0728 UTC

The main features of interest in the NOAA-10 AVHRR visible and infra-red (IR) images in Fig. 1 are the distinctive low- and high-level cloud patterns formed by horizontal and vertical wave motion, induced in the moist, stable, westerly airstream by the orography of Scotland and northern England. This airstream was on the northern flank of an anticyclone centred to the south-west of Ireland (Fig. 2).

Waves in the low- and middle-level cloud are most clearly seen on the visible image and have a wavelength of 5 km over north-east England (A), increasing to 10 km over central Scotland (B), and then to 15 km in much broader elements at (C) within the cloud band associated with the cold front. The westerly winds back a little just ahead of the front and this can be inferred by the different orientation of the waves at (C).

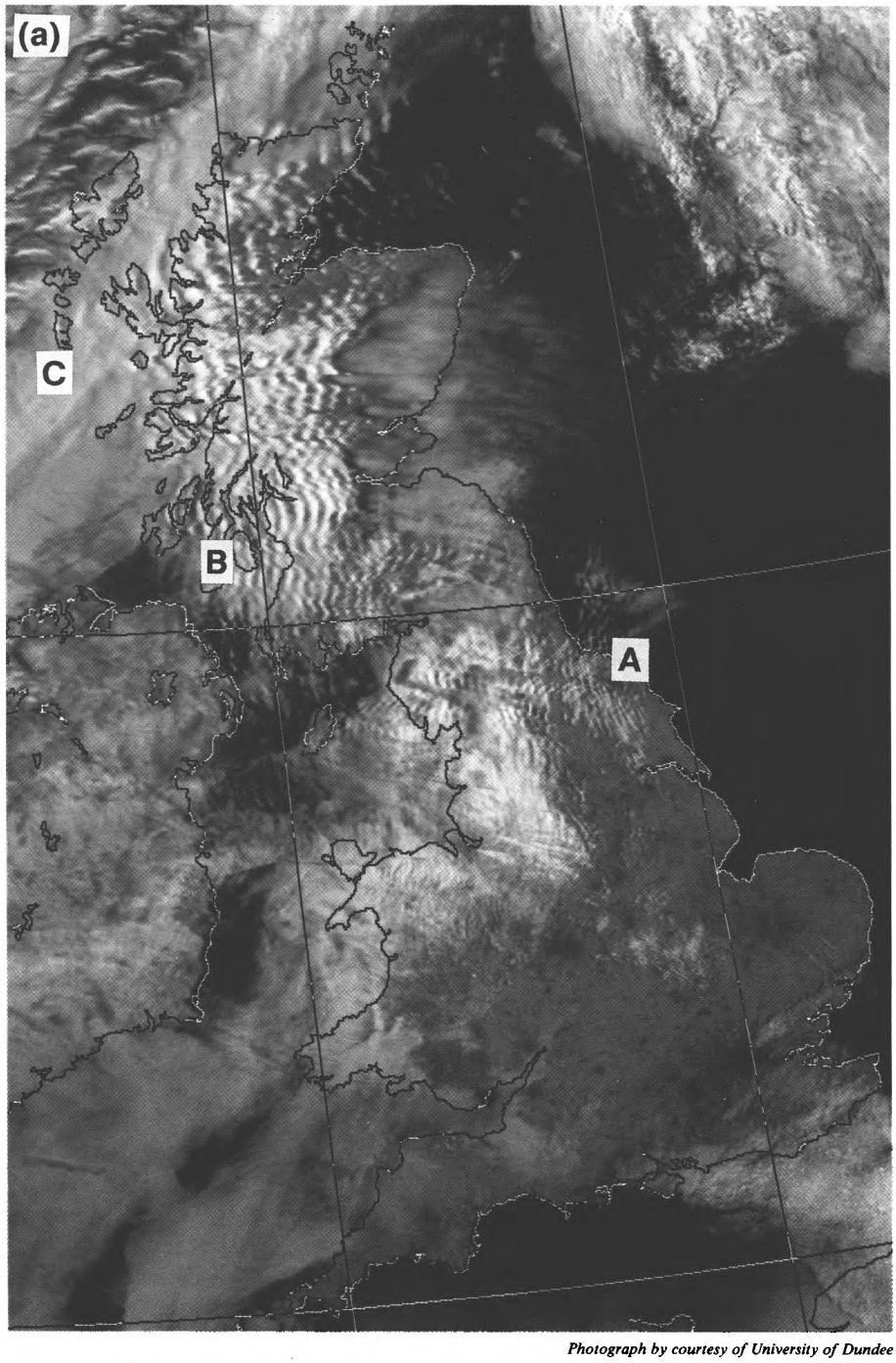

Photograph by courtesy of University of Dundee

Figure 1. NOAA-10 AVHRR images at 0728 UTC 21 May 1991 (a) visible, and (b) infra-red. The labelling A–D is referenced in the text.

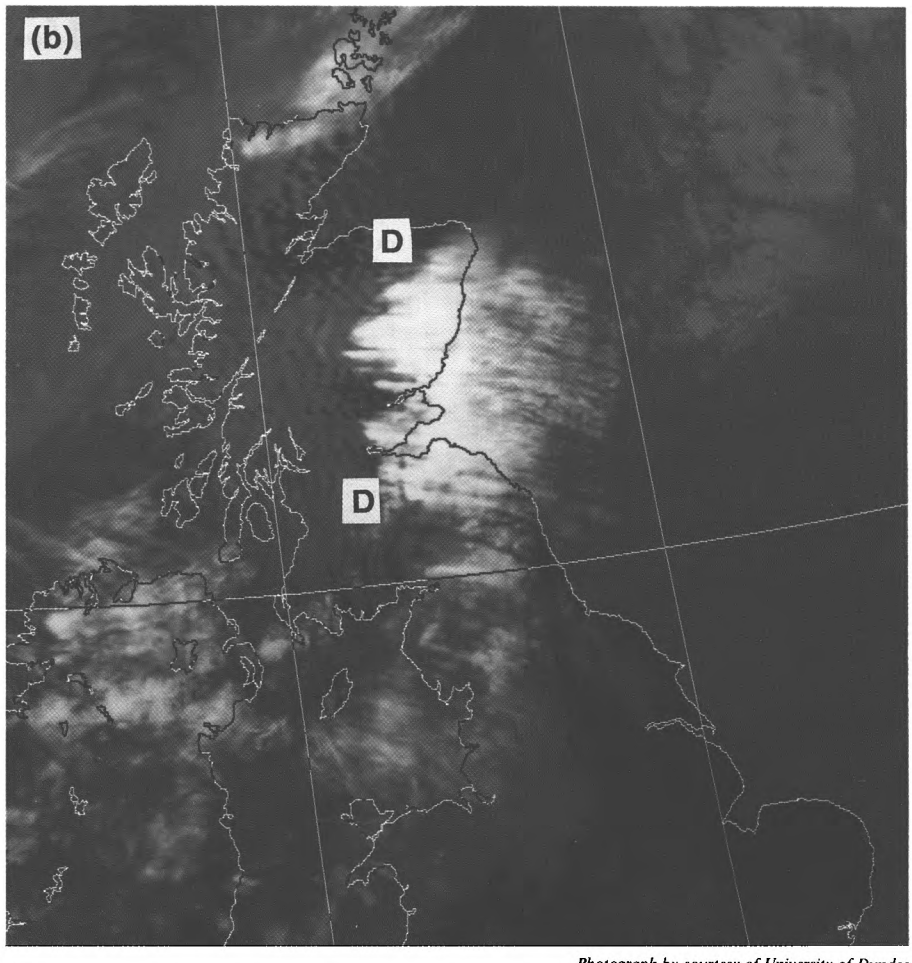

Photograph by courtesy of University of Dundee

Figure 1. Continued.

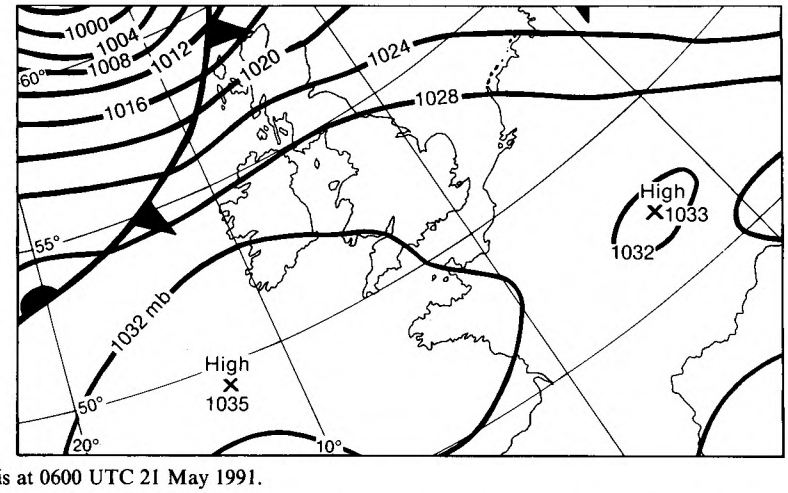

Figure 2. Surface analysis at 0600 UTC 21 May 1991.

On the IR image, these wave clouds are grey and therefore have relatively warm tops and the main feature is the area of orographic cirrus (D). The saw-toothed edge on the upwind side reflects the profile of the high ground. Comparison with the visible image shows the cloud to be relatively thin. Once formed in the vertically propagating waves, orographic cirrus can be very persistent and extend downstream in plumes for hundreds of kilometres. One factor that favours persistence is the fact that as air flows through upper-level waves, the level at which ice evaporates beyond the crest is lower than the condensation level upstream (see, for example, Scorer*). On static images it is often easy to confuse orographic and frontal cirrus, but movie-loops of images usually reveal clearly whether formation of the cloud is related to the high ground.

A.J. Waters and R. Bosworth

* Scorer, R.S.; *Cloud investigation by satellite.* Chichester, Ellis Horwood, 1986.

GUIDE TO AUTHORS

Content

Articles on all aspects of meteorology are welcomed, particularly those which describe results of research in applied meteorology or the development of practical forecasting techniques.

Preparation and submission of articles

Articles, which must be in English, should be typed, double-spaced with wide margins, on one side only of A4-size paper. Tables, references and figure captions should be typed separately. Spelling should conform to the preferred spelling in the *Concise Oxford Dictionary* (latest edition). Articles prepared on floppy disk (Compucorp or IBM-compatible) can be labour-saving, but only a print-out should be submitted in the first instance.

References should be made using the Harvard system (author/date) and full details should be given at the end of the text. If a document is unpublished, details must be given of the library where it may be seen. Documents which are not available to enquirers must not be referred to, except by 'personal communication'.

Tables should be numbered consecutively using roman numerals and provided with headings.

Mathematical notation should be written with extreme care. Particular care should be taken to differentiate between Greek letters and Roman letters for which they could be mistaken. Double subscripts and superscripts should be avoided, as they are difficult to typeset and read. Notation should be kept as simple as possible. Guidance is given in BS 1991: Part 1: 1976, and *Quantities, Units and Symbols* published by the Royal Society. SI units, or units approved by the World Meteorological Organization, should be used.

Articles for publication and all other communications for the Editor should be addressed to: The Chief Executive, Meteorological Office, London Road, Bracknell, Berkshire RG12 2SZ and marked 'For Meteorological Magazine'.

Illustrations

Diagrams must be drawn clearly, preferably in ink, and should not contain any unnecessary or irrelevant details. Explanatory text should not appear on the diagram itself but in the caption. Captions should be typed on a separate sheet of paper and should, as far as possible, explain the meanings of the diagrams without the reader having to refer to the text. The sequential numbering should correspond with the sequential referrals in the text.

Sharp monochrome photographs on glossy paper are preferred; colour prints are acceptable but the use of colour is at the Editor's discretion.

Copyright

Authors should identify the holder of the copyright for their work when they first submit contributions.

Free copies

Three free copies of the magazine (one for a book review) are provided for authors of articles published in it. Separate offprints for each article are not provided.

Contributions: It is requested that all communications to the Editor and books for review be addressed to the Chief Executive, Meteorological Office, London Road, Bracknell, Berkshire RG12 2SZ, and marked 'For *Meteorological Magazine*'. Contributors are asked to comply with the guidelines given in the *Guide to authors* which appears on the inside back cover. The responsibility for facts and opinions expressed in the signed articles and letters published in *Meteorological Magazine* rests with their respective authors.

Subscriptions: Annual subscription £33.00 including postage; individual copies £3.00 including postage. Applications for postal subscriptions should be made to HMSO, PO Box 276, London SW8 5DT; subscription enquiries 071–873 8499.

Back numbers: Full-size reprints of Vols 1–75 (1866–1940) are available from Johnson Reprint Co. Ltd, 24–28 Oval Road, London NW1 7DX. Complete volumes of *Meteorological Magazine* commencing with volume 54 are available on microfilm from University Microfilms International, 18 Bedford Row, London WC1R 4EJ. Information on microfiche issues is available from Kraus Microfiche, Rte 100, Milwood, NY 10546, USA.

August 1991

Edited by Corporate Communications
Editorial Board: R.J. Allam, R. Kershaw, W.H. Moores, P.R.S. Salter

Vol. 120
No. 1429

Contents

ISSN 0026–1149

Printed in the United Kingdom for HMSO
Dd 0291241 8/91 C13 503 12521

The Meteorological Magazine

September 1991

Climate change prediction
Dry spells of 1988–90

HMSO

Met.O.998 Vol. 120 No. 1430

First published 1991

HMSO publications are available from:

HMSO Publications Centre
(Mail and telephone only)
PO Box 276, London, SW8 5DT
Telephone orders 071-873 9090
General enquiries 071-873 0011
(queuing system in operation for both numbers)

HMSO Bookshops
49 High Holborn, London, WC1V 6HB 071-873 0011 (counter service only)
258 Broad Street, Birmingham, B1 2HE 021-643 3740
Southey House, 33 Wine Street, Bristol, BS1 2BQ (0272) 264306
9–21 Princess Street, Manchester, M60 8AS 061-834 7201
80 Chichester Street, Belfast, BT1 4JY (0232) 238451
71 Lothian Road, Edinburgh, EH3 9AZ 031-228 4181

HMSO's Accredited Agents
(see Yellow Pages)

and through good booksellers

3 8078 0010 2459 7

The Meteorological Magazine

September 1991
Vol. 120 No. 1430

551.583.1:551.513.1

Climate change prediction

J.F.B. Mitchell
Meteorological Office, Bracknell
Qing-cun Zeng
Chinese Academy of Sciences, Beijing, Peoples Republic of China

Summary

A brief description of climate processes is given. Numerical models are described and an assessment of their ability to simulate climate and climate change is given. Results from simulations with increased atmospheric CO_2 concentrations are given, including the temporal evolution of the warming, and estimates of the geographical distribution of changes. The main sources of uncertainty are listed, and possible shortcomings in current research programmes are identified.

1. Introduction

In order to predict changes in climate, one must first identify and understand the various components of the climate system. These include the atmosphere, the oceans, the cryosphere (land–ice and sea–ice), the biosphere and, over geological time-scales, the geosphere. The fundamental process driving climate is radiation. The climate system is heated by solar radiation, which is generally strongest in low latitudes, and cooled by long (thermal or infra-red) radiation to space, which is more uniformly distributed with latitude. The resulting temperature contrast between low and high latitudes drives atmospheric and oceanic motions which transport heat polewards and thus tend to reduce the equator-to-pole temperature gradient. The resulting circulations and their interactions with orography and the biosphere determine the earth's climate.

Changes in the radiative heating of the earth will produce changes in its climate. Changes in solar heating can arise from external factors such as variations in incident solar radiation due to changes in the earth's orbit, or in the earth's reflectivity, for example, due to addition of volcanic aerosols to the atmosphere, and to changes in the reflectivity of the surface such as that caused by deforestation. The long-wave cooling can be modified by changes in atmospheric composition, notably by changes in the concentration of greenhouse gases. Other non-radiative factors such as changes in orography can also affect climate, but these occur on geological time-scales, and so will not be considered further here. Note that changes in climate will themselves produce changes in the earth's radiation budget: these are known as radiative feedbacks and are discussed later in this section.

In this paper, we are primarily interested in predicting changes in climates over the next century or so, hence it may be possible to neglect changes in some of the more slowly varying components of the system. The atmosphere and land surface, including seasonal snow cover, adjust to changes in heating on time-scales of a year or less. The seasonal mixed layer of the ocean (typically up to 100 m deep) and sea ice respond over periods of up to a decade or so. The oceanic warm water sphere (down to the permanent thermocline, typically at half a kilometre) has a thermal response time of several decades, whereas the deep ocean, extending to several kilometres, has a time-scale of centuries to millenia. The major ice-sheets vary over millennia, so apart from the substantial contributions from changes in accumulation and

melting on sea level, they can be regarded as fixed in the present context.

In predicting climate change, it is generally assumed that for each specification of the factors affecting climate (solar heating, atmospheric conditions, orography), the earth's climate will move to a long-term steady state, known as the equilibrium climate, in which there is no net heating of the system. Note that this does not preclude considerable variability on interannual or even interdecadal time-scales, but there are no longer-term trends. If the factors affecting climate are changed (for example, by increasing the concentration of greenhouse gases), then the system will adjust slowly towards a new equilibrium state. The transition period is sometimes referred to as a 'transient' or 'time-dependent' climate change: the difference between the initial and final states is the 'equilibrium climate change'.

One possible method of predicting climate changes is to look for periods in the past when the factors affecting climate (solar parameters, greenhouse gas concentrations) were similar to those expected in the near future. One could then use reconstructions of the relevant past climates as a forecast for the future climate. Unfortunately, in the recent geological past, there are no close analogies to an increase in greenhouse gases, and so this method cannot provide reliable forecasts of climate over the next century or so.

The only alternative to the climate analogy approach is the use of physical-mathematical models of climate. Among such models, the most highly developed are general circulation models (GCMs). These are numerical models in which the equations of classical physics (including the laws of motion, and requirements for conservation of heat and mass) are solved in a 3-dimensional grid, with a horizontal spacing of 250–800 km, depending on the model concerned.

Many processes (for example, those associated with cloud or vertical mixing in the oceans) occur on much smaller scales than can be resolved by the model grid, and so are represented in a simplified or idealized way (parametrizations). These may be based on approximations of the underlying equations, data from observational studies or laboratory experiments, results from numerical experiments using a finer grid or, as a last resort, sensitivity experiments using the GCM itself. In a climate model, an atmospheric component (essentially the same as a weather prediction model) is coupled to a model of the oceans and sea ice, which may be equally complex.

Climate forecasts are derived in a different way from weather forecasts. A weather prediction model gives a description of the atmosphere's state up to 10 days or so ahead, starting from a detailed description of an initial state of the atmosphere at a given time. Such forecasts describe the movement and development of large weather systems, though they cannot represent very-small-scale phenomena, for example, individual shower clouds.

To make a climate forecast, the climate model is first run for a few (simulated) decades. The statistics of the model's output will be a description of the model's simulated climate which, if the model is a good one, will bear a close resemblance to the climate of the real atmosphere and ocean. The above exercise is then repeated with, for example, increased concentrations of the greenhouse gases in the model. The differences between the statistics of the two simulations (for example in mean temperature and interannual variability) provide an estimate of the accompanying climate change.

In this paper, reference will be made to atmospheric models run with prescribed sea-surface-temperature atmospheric models (referred to henceforth as AGCMs) coupled to an oceanic mixed layer, with or without allowance for ocean heat transport (A/MLMs) and atmospheric models coupled to full dynamical ocean models (CGCMs).

As alluded to above, changes in climate can lead to changes in the components of the earth's radiation budget which may be amplified (positive feedback) or reduced (negative feedback). The simulated strength of feedbacks (such as those due to cloud) vary from model to model. The relative strengths of the radiative feedbacks in different models have been analysed by substituting the globally averaged changes in the simple energy balance equation

$$\Delta T_s = \Delta Q/\lambda$$

where ΔQ is the applied radiative perturbation (W m^{-2}), ΔT_s is the equilibrium change in globally averaged surface temperature, and λ is the climate sensitivity parameter (W m^{-2} K^{-1}). For example, doubling CO_2 produces an increase of 4.4 W m^{-2} in the radiative heating of the troposphere and surface. If the system responded as a radiative black body, this would produce an equilibrium warming of 1.2 °C. Warming the atmosphere leads to an increase in atmospheric water content — water vapour is also a greenhouse gas — and estimates based on both observations (Raval and Ramanathan 1989) and models indicate that produces a positive feedback, increasing the warming to 1.7 °C.

Snow and sea ice reflect solar radiation back to space. The global warming associated with increases in greenhouse gases would reduce the aerial extent of snow and ice, increasing solar absorption, leading to a further increase in temperature. The magnitude of this feedback is generally much smaller than that due to water vapour, though estimates of the strength vary from model to model.

Clouds cool climate through reflecting solar radiation back to space, and warm climate through their greenhouse effect. In our present climate, it appears that the solar effect dominates. Any change in cloud amount, height or cloud radiative properties will alter the net effect of clouds on the earth's radiation budget.

Numerical studies suggest that doubling CO_2 amounts would lead to an equilibrium warming of 2–5 °C, much of the uncertainty being associated with uncertainties in the strength of cloud radiation feedbacks and associated processes (for example see Mitchell *et al.* (1989), Cess *et al.* (1989)).

Some scientists have suggested that the climate sensitivity is much smaller than indicated by models. A few, including Idso, and Newell and Dopplick considered the energy balance at the surface only or neglected the water vapour feedback (see Luther and Cess (1985) for references and a detailed explanation why such approaches are misleading). More recently, Lindzen (1990) and Ellsaesser (1989) have questioned the strength of the water vapour feedback in climate models. Lindzen argues that cumulus convection 'short circuits' much of the potential water vapour feedback by transporting heat from the boundary layer to the upper troposphere where it is more readily radiated to space. This process is undoubtedly represented in current general circulation models and provides, as expected, a strong negative feedback through changes in lapse rate (see, for example, Schlesinger and Mitchell (1987)). Lindzen and Ellsaesser also argue that as convection penetrates to higher levels in a warmer climate, the compensating subsidence will start from higher and therefore colder and drier levels. This would lead to a reduction in the absolute humidity in the upper troposphere in the descending branch of the Hadley circulation, and hence a 'local' negative water vapour feedback. Since Lindzen has yet not published the details of his argument, it is not possible to assess it quantitatively. Nevertheless, this mechanism is also included in current models (see, for example, Gregory and Rowntree (1990)). Indeed, on doubling CO_2 concentrations, the Meteorological Office high-resolution model produces decreases in absolute humidity in this region. It appears that other processes including the detrainment of warmer, moister air and lateral mixing of moistened air from the inner tropics and mid latitudes reduce the extent of the drying through deeper subsidence. The increased drying through subsidence appears to be responsible for the decreases in relative humidity in mid latitudes and the tropics which leads to the reduction in cloud in the upper troposphere and a strong positive cloud feedback found in many models (Mitchell and Ingram 1991). Thus, if models have exaggerated the positive water vapour feedback, it is also likely that they have *underestimated* the strength of the positive feedback associated with reductions in cloud amount. In summary, although tropical convection remains one of the major sources of uncertainty, it is unlikely that errors in the parametrization of convection lead to a gross overestimate of climate sensitivity (even removing the water vapour feedback *completely and globally* in a model with a sensitivity of 2.5 °C due to doubling CO_2 — the IPCC 'best guess' — would only reduce the equilibrium warming to about 1.4 °C).

2. Validation of numerical climate models

In this section, an attempt is made to answer the question 'To what extent should one believe results from climate models?' Firstly, the models are based on a firm physical basis with a minimum of adjustable parameters, as discussed in the previous section. Secondly, they show considerable skill in reproducing the large-scale features of current climate. Thirdly, they have been shown to be capable of reproducing many features of contemporary climate change, and some of the main features in more recent palaeoclimate. These last two points are expanded on below.

2.1 Simulation of present climate

The simplest way of validating a climate model is to prescribe present-day 'boundary conditions' and compare the long-term statistics of the resulting simulation with observational climatologies. This shows that AGCMs and A/MLMs have considerable skill in the portrayal of the large-scale distribution of pressure, temperature, wind and precipitation in both summer and winter, although this success is due in part to the constraints on sea surface temperature and sea ice. There has been a general reduction in the errors in more recent AGCMs as a result of increased horizontal resolution, improvements to the parametrization of convection, cloudiness and surface processes and the introduction of parametrizations of gravity-wave drag. For example, the three most recent simulations considered in the IPCC Working Group I Report (IPCC 1990) show a marked improvement in the simulation of the depth and position of the Antarctic circumpolar surface pressure trough (Fig. 1).

Changes in variability of climate are as important as changes in mean climate in the assessment of climate impacts. Hence, the ability of models to simulate the variability of current climate should also be assessed. The daily and interannual variability of temperature and precipitation have been examined but only to a limited extent. There is evidence that variability is overestimated in some models, especially in winter. The daily variability of sea level pressure can be well simulated, but the eddy kinetic energy in the upper troposphere (indication of the variability of the flow) tends to be underestimated. The level of interannual variability of global mean surface temperature in CGCMs (for example, Fig. 2) is comparable to that observed over similar time-scales if allowances is made for the estimated trend in the observed.

On regional scales, there are significant errors in all models. A validation of A/MLMs for five selected regions (typically 4×10^6 km^2) showed errors in area average surface temperature of 2–3 °C (IPCC 1990). This is small compared with the average seasonal range of temperature of 15 °C. Errors in mean precipitation for the same five regions ranged from 20–50% of the observed average. All the recent models reproduce the northern summer monsoon rainfall maximum over

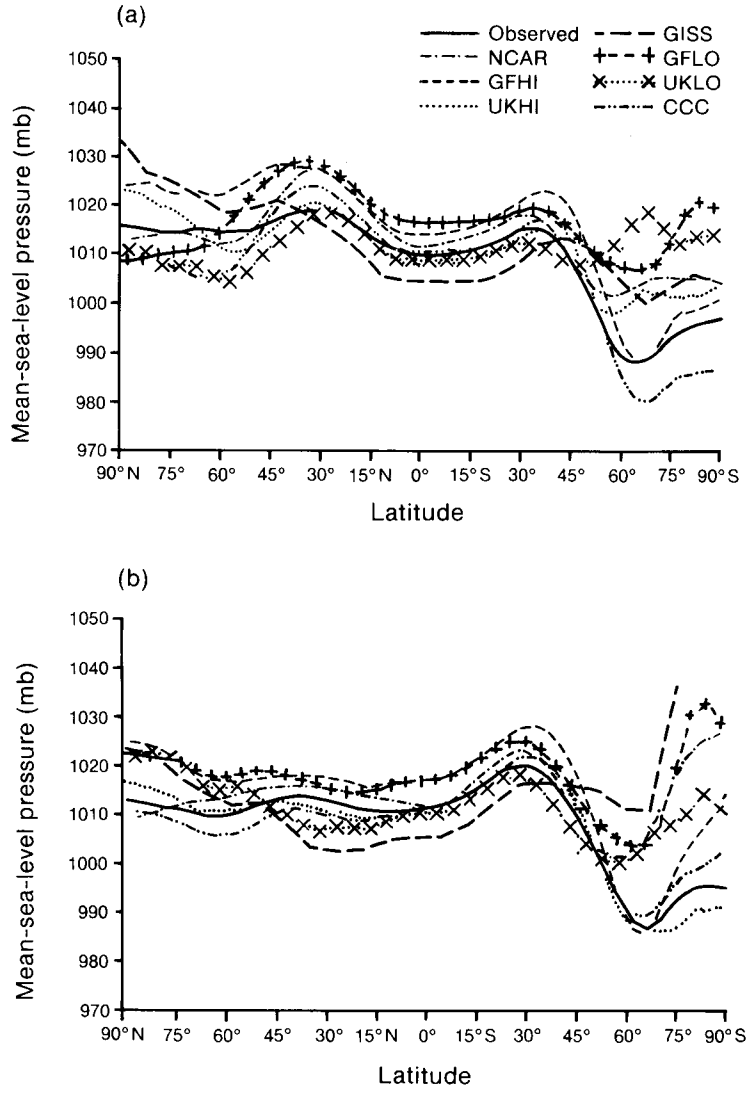

Figure 1. Zonally averaged mean-sea-level pressure (mb) observed (Schutz and Gates 1971, 1972) and modelled for (a) December, January and February, and (b) June, July and August using the following models: NCAR (National Center for Atmospheric Research) (15 spectral waves), GISS (Goddard Institute for Space Studies) (8° latitude × 10° longitude), GFLO (Geophysical Fluid Dynamics Laboratory) (15 spectral waves), UKLO (Meteorological Office) (5° × 7.5°), GFHI (Geophysical Fluid Dynamics Laboratory) (30 spectral waves), UKHI (Meteorological Office) (2.5° × 3.75°) and CCC (Canadian Climate Center) (32 spectral waves). The more recent high-resolution runs referred to in the text are GFHI, UKHI and CCC.

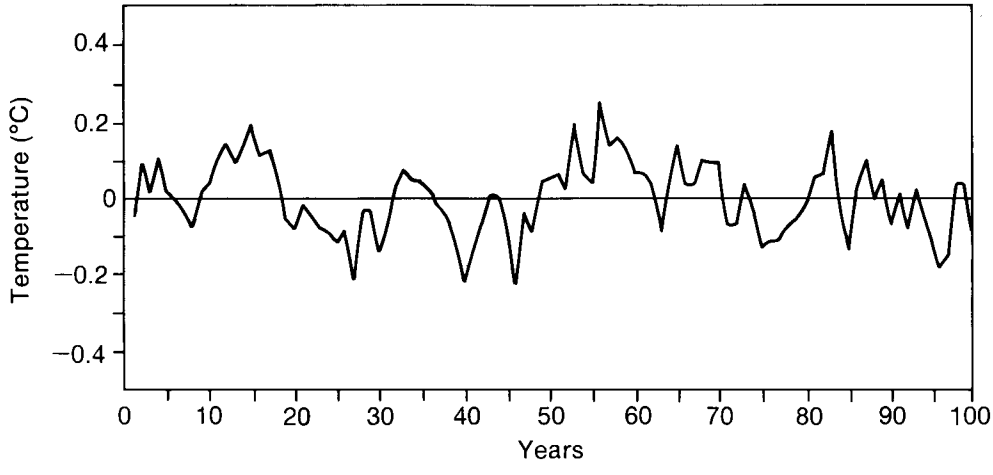

Figure 2. Temporal variation of the deviation of global mean surface air temperature (°C) of the Geophysical Fluid Dynamics Laboratory coupled ocean–atmosphere model from its long-term average (Manabe *et al.* 1991).

south-east Asia (Fig. 3), but in the example shown, the mean rainfall over south-east Asia is substantially less than observed as the simulated rain-band does not extend far enough to the north and east. Given the large errors in the simulation of present-day regional climate, confidence in the simulated changes in regional climate must be low.

Models of the oceanic circulation simulate many of the observed large-scale features of ocean climate, especially in low latitudes, although their solutions are sensitive to resolution and to the parametrization of sub-grid-scale processes such as mixing and convective overturning. It is particularly important that vertical mixing in the ocean is reproduced correctly as this determines the rate at which the ocean responds to increases in greenhouse gases. This can be validated to some extent by simulating the spread of passive tracers, such as that of tritium following the atomic bomb tests in the 1950s and 1960s. Current models are capable of reproducing the main features of the spread of passive tracers (for example, Fig. 4), though there may be errors in the detailed changes (for example, in Fig. 4(b), underestimating the strength of penetration near 30–50° N). In CGCMs, it has proved necessary to add empirical adjustments to the ocean surface fluxes in order to reduce errors in the simulated climate.

2.2 Simulation of contemporary climate change and recent palaeoclimate.

AGCMs have been used to simulate the atmospheric response to prescribed anomalies in sea surface temperature (SST), and have been notably successful in simulating the response to tropical SST anomalies. Large-scale positive SST anomalies occur in eastern tropical Pacific during the occurrence of El Niño, and models have simulated successfully the associated observed anomalies in precipitation and circulation (for example, Fennessy and Shukla (1988)). Other AGCMs have reproduced the relationship between large-scale SST distribution and summer rainfall in the Sahel (for example, Folland *et al.* (1989)).

A/MLMs have reproduced some of the large-scale features of the mid-Holocene climate, only the changes in the earth's orbital parameters being specified, and also the last glacial maximum, the distribution of land ice and the prevailing CO_2 concentration being the only prescribed changes (for example, COHMAP members (1988)).

2.3 Validation summary

The most recent models are able to simulate the large-scale features but not the regional-scale (400–2000 km) details of present climate. AGCMs reproduce the

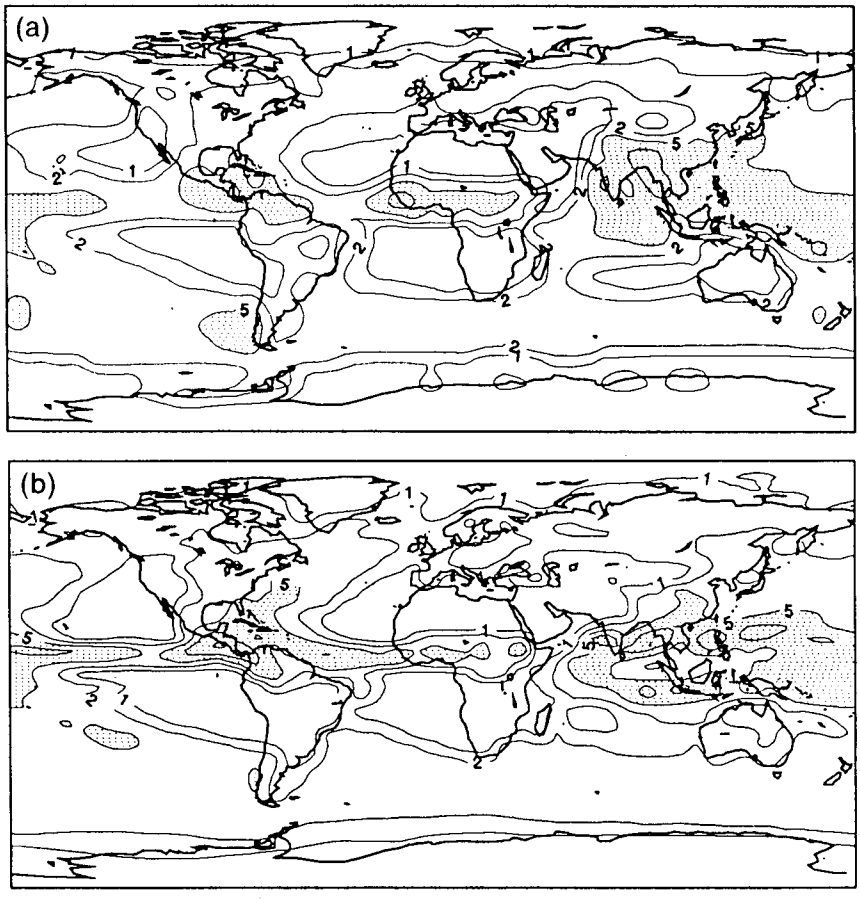

Figure 3. Preciptation (mm day^{-1}) for June, July and August, shown stippled where greater than 5 mm day^{-1}. (a) Observed (Jaeger 1976), and (b) simulated (Meteorological Office high-resolution model (2.5° × 3.75°)).

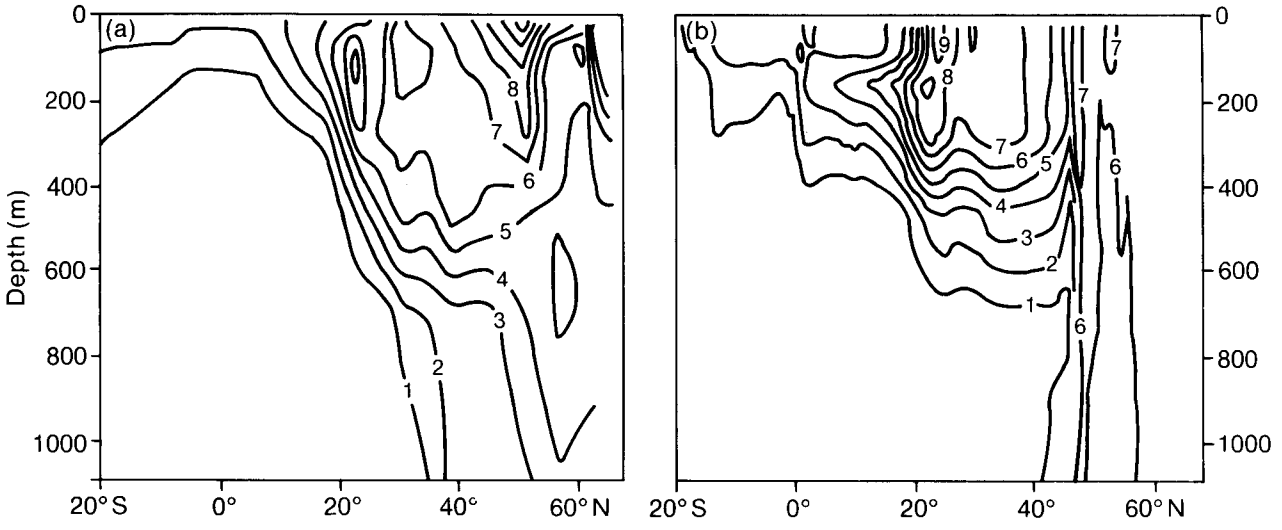

Figure 4. Tritium in the GEOSECS section in the western North Atlantic approximately 1 decade after major bomb tests. (a) GEOSECS observations, and (b) as predicted by a 12-level model in tritium units (Sarmiento 1983).

atmospheric response to contemporary SST anomalies, and A/MLMs are capable of reproducing the major changes in climate over the last 18 000 years provided certain boundary conditions (CO_2 concentrations, orbital parameters, major ice sheets) are prescribed. This, combined with the physical basis on which the models are developed, gives us some confidence in their ability to predict future changes in climate, particularly on larger scales. The least reliable aspects of models are their treatment of sub-grid-scale processes, and their ability to simulate variations in climate on a regional scale. Aspects of the simulation of present-day climate by CGCMs may be inadequate unless corrective measures, such as adjustments to the surface fluxes, are made.

3. Simulation of climate change

The simulation of climate change due to increases in greenhouse gases is now considered. Most of the understanding of greenhouse-gas-induced climate change is based on equilibrium experiments based on mixed-layer models. In the last year or so, several studies have been made of the time-dependent response to increases in greenhouse gases using CGCMs. However, results presented here will be based largely on the equilibrium experiments which have been analysed in much greater detail. Furthermore, the rates of increase in the time-dependent coupled experiments do not correspond to the IPCC scenarios of increases in greenhouse gases. Hence, in order to calculate the evolution of temperature resulting from the IPCC scenarios, we have used results from one-dimensional upwelling diffusion models calibrated using the more complex A/MLMs and CGCMs.

3.1 Equilibrium climate sensitivity

The equilibrium sensitivity of mixed-layer models to doubling CO_2 ranges from 2 to 5 °C. The range is due to uncertainties associated with sub-grid-scale parametrification, particularly those associated with cloud. Some of the more recent studies attempt to allow for changes in the microphysical properties of cloud — these more detailed, but not necessarily more accurate, models give an equilibrium sensitivity of 2–4 °C.

The observed change in temperature (1860–1990) seems to be consistent with an equilibrium warming of 1–3 °C, allowing as far as possible for natural variability and assuming other factors such as the effect of sulphate emissions on cloud albedo have not affected the warming due to increases in greenhouse gases. On the basis of modelling studies, the sensitivity of climate due to doubling CO_2 is most likely to lie between 1.5 and 4.5 °C, and, in view of the observational evidence, a 'best guess' of 2.5 °C was chosen to illustrate the IPCC scenarios.

3.2 Equilibrium and transient climate change

When the radiative heating of the earth–atmosphere system is changed by increases in greenhouse gases, the atmosphere will respond (by warming) immediately. The atmosphere is closely coupled to the oceans, so the oceans also have to be warmed; because of their thermal capacity this takes decades or centuries. This exchange of heat between the atmosphere and ocean will act to slow down the temperature rise forced by the greenhouse effect.

Consider the concentration of greenhouse gases in the atmosphere rising to a new level and remaining constant thereafter. The radiative forcing would also rise rapidly to a new level. This increased radiative forcing would cause the atmosphere and oceans to warm, and tend towards a new equilibrium temperature. Commitment to this equilibrium temperature rise would occur as soon as the greenhouse gas concentration had changed. But at any time before equilibrium is reached, the actual

temperature will only have risen by part of the equilibrium temperature change — known as the realized temperature change.

One CGCM (Manabe *et al.* 1991) predicts that, for the case of a steady increase in radiative forcing similar to that currently occurring, the realized temperature at any time is about 60–80% of the committed temperature. If the forcing was to be held constant, temperatures would continue to rise slowly, but it is not certain whether it would take decades or centuries for most of the remaining rise to equilibrium to occur.

3.3 Changes in global mean temperature based on the IPCC scenarios

The following results are derived from an upwelling-diffusing model, assuming that the temperature of surface water sinking in high latitudes does not change. The upwelling velocity is taken as 4 m yr^{-1} and the diffusivity as 0.63 $cm^2 s^{-1}$. The IPCC 'business-as-usual' scenario, in which effective CO_2 concentrations double over pre-industrial levels by 2020, gives a warming of 1.3–2.6 °C above pre-industrial levels at 2030, corresponding to a prescribed climate sensitivity of 1.5–4.5 °C (Fig. 5). The 'best guess' sensitivity gives a warming of 1.8 °C at the time of doubling, which is reduced to about 1.5 °C in the other scenarios (Fig. 6). Scenario B assumes an effective doubling of CO_2 by 2040, and scenario C by about 2050. Note that the changes in emission scenarios take some time to produce an effect — this is a result of the slowness with which both the gas concentrations and the oceans respond — much of the warming immediately after 1990 can be attributed to the system 'catching up' the effect of previous emissions.

3.4 Patterns of climatic change due to an effective doubling of CO_2

Only one AGCM has been used in both an equilibrium experiment coupled to a mixed-layer ocean, and in a long time-dependent experiment coupled to a deep ocean model (A CGCM, Stouffer *et al.* (1989)) (Fig. 7). The equilibrium sensitivity of this model to doubling CO_2 is 4 °C. In most regions heat is mixed down to the main thermocline, at about 500 m; and the surface temperature change at the time of doubling CO_2 in the time-dependent experiment (Fig. 7(b)) is similar to the equilibrium response (Fig. 7(a)), but reduced by 20–40% (Fig. 7(c)). The exceptions are round Antarctica, where there is little or no warming in the time-dependent experiment, and over the northern North Atlantic and north-western Europe, where the reduction is 40–60%. In these regions, a deep wind-driven circulation (circumpolar ocean) or deep convection (North Atlantic) mix heating down to several kilometres. The surface warming is greatest in high northern latitudes, and north of 30° S is generally greater over land than over the ocean at the same latitudes, as found in equilibrium experiments. The warming in northern high latitudes is generally greatest around the sea-ice margins in late autumn and early winter, and around the snow-line over the continents in spring. Over the low-latitude oceans and moist areas of the low-latitude continents, the warming is small relative to the global mean.

The changes in the hydrological cycle are qualitatively similar in these equilibrium and transient experiments. Hence, the remainder of this section is based on results from equilibrium experiments. Precipitation generally increases in high latitudes throughout the year and in mid latitudes in summer (Fig. 8). Precipitation generally increases in the tropics, these changes are accompanied by shifts in the main tropical rain-bands which vary from model to model, so there is little consistency in results for a particular region.

The warming produces an increase in global mean precipitation and evaporation. Enhanced precipitation increases soil moisture levels in high northern latitudes in winter. Most models produce a drying of the land surface over the northern mid-latitude continents in summer (for example, see Fig. 9) as a result of earlier snow melt, enhanced evaporation and, in some regions, reduced precipitation.

Predicted changes in the day-to-day variability of weather are uncertain. However, simulated episodes of high temperature become more frequent simply due to

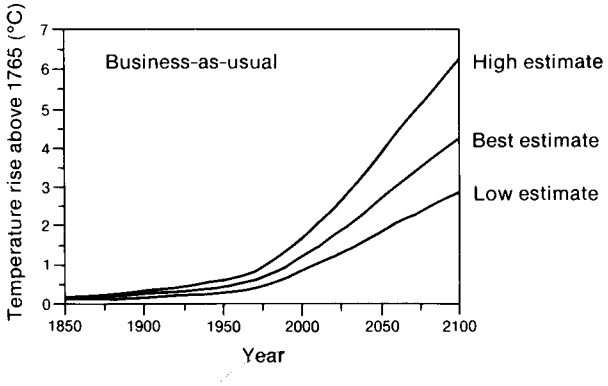

Figure 5. Evolution of global mean warming (above pre-industrial temperatures) assuming IPCC 'business-as-usual' scenario. The curves correspond to an equilibrium sensitivity to doubling CO_2 of 4.5, 2.5 and 1.5 °C, respectively (IPCC 1990).

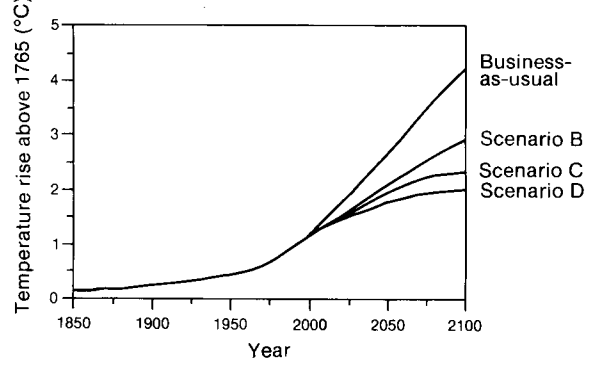

Figure 6. Evolution of global mean warming (above pre-industrial temperatures) assuming an equilibrium sensitivity to doubling CO_2 of 2.5 °C for the IPCC scenarios (IPCC 1990).

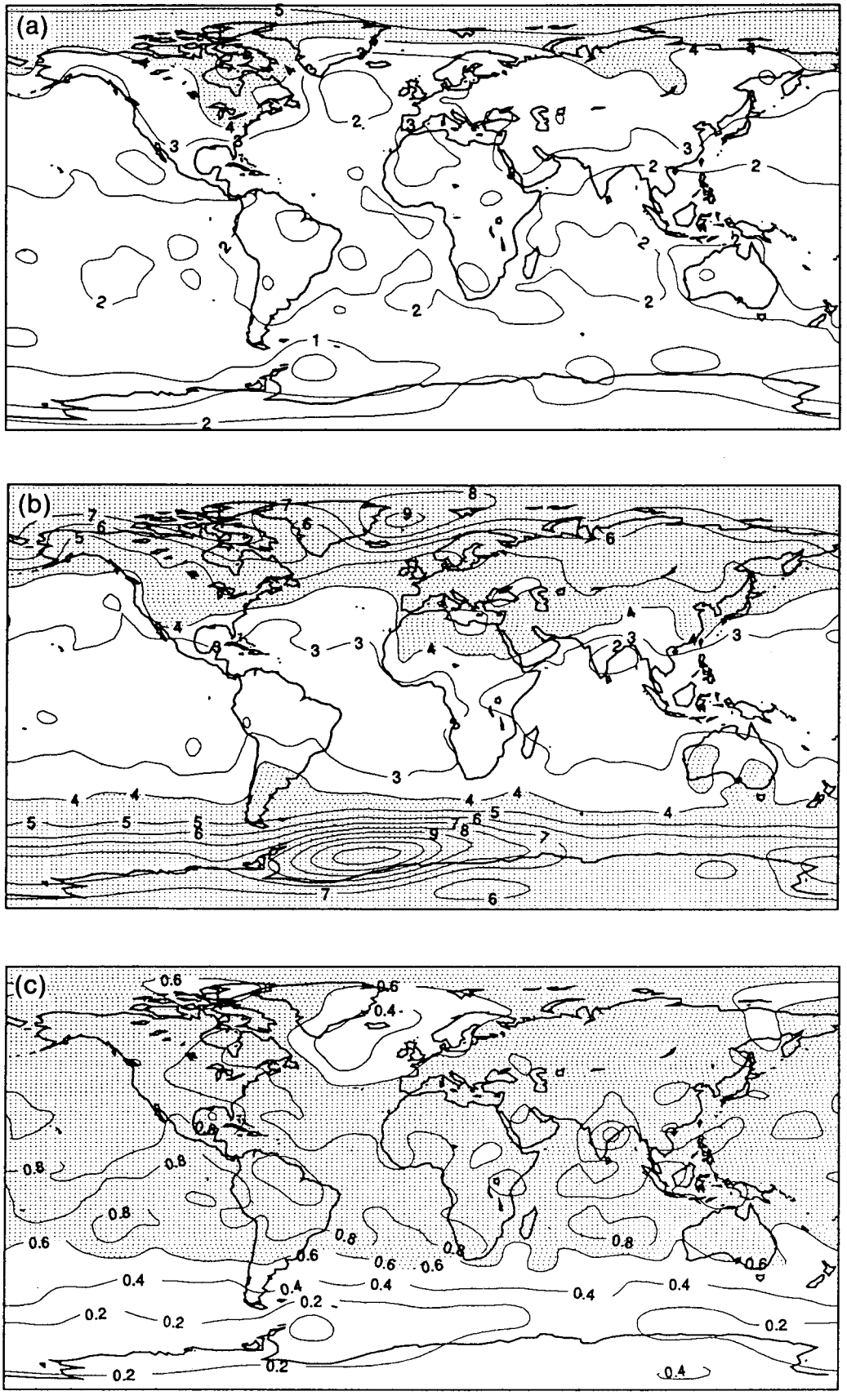

Figure 7. Geographical distribution of (a) time-dependent response of surface air temperature (°C) in the Geophysical Fluid Dynamics Laboratory coupled ocean–atmosphere model to a 1% per year increase of atmospheric CO_2. Shown is the difference between the 1% per year perturbation and the control run for the 60–80 year period when the CO_2 approximately doubles (Stouffer *et al.* 1989), (b) equilibrium response of surface air temperature (°C) in the atmosphere–mixed layer ocean model to a doubling of atmospheric CO_2 (Stouffer *et al.* 1989), and (c) ratio of time-dependent to equilibrium responses shown above (Manabe *et al.* 1991).

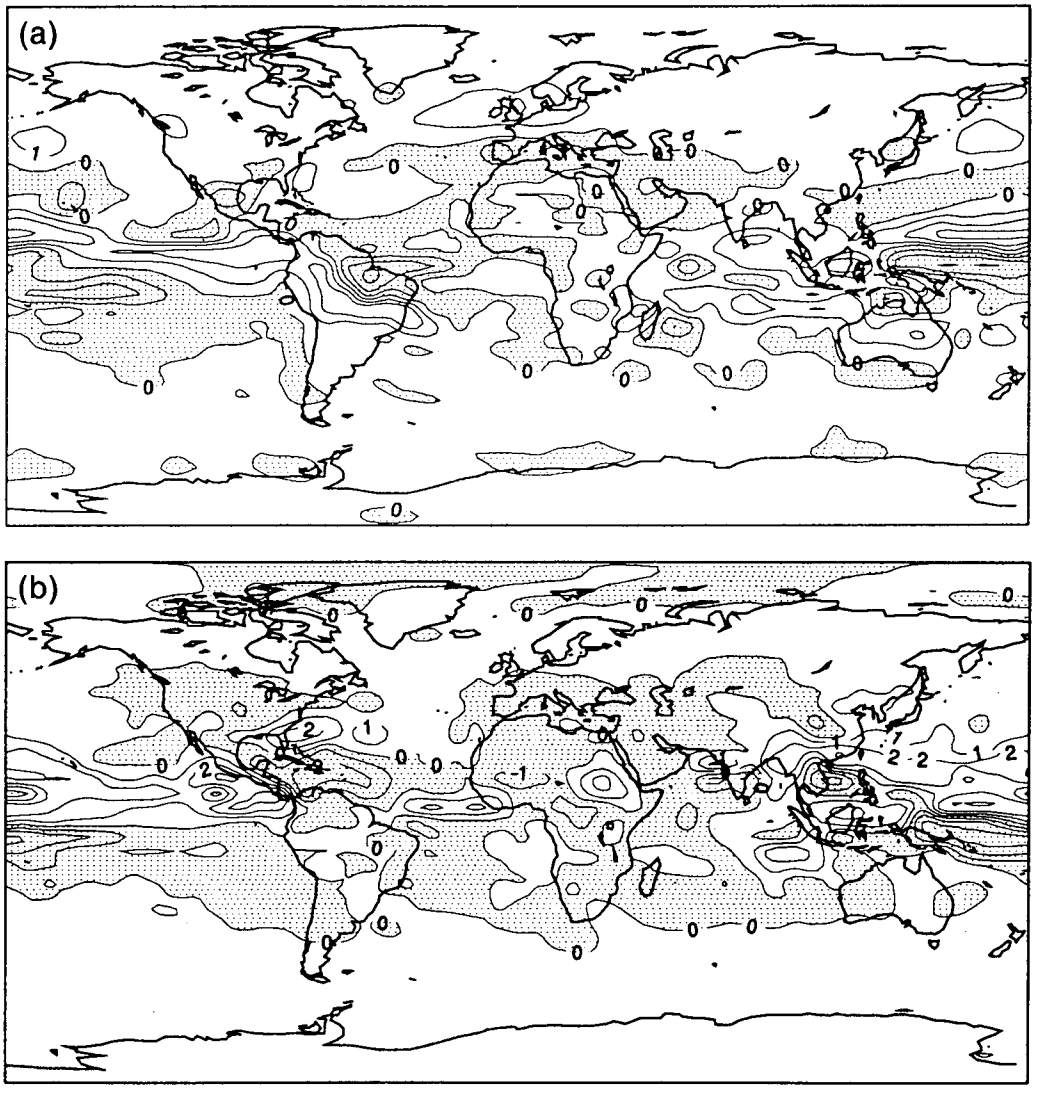

Figure 8. Simulated changes in precipitation-rate equilibrium following a doubling of atmospheric CO_2 concentrations in the Meteorological Office 2.5° × 3.75° resolution model (mm day^{-1}, contours at 0, ±1, +2 and +5 mm day^{-1}, with areas of decrease stippled) for (a) December, January and February, and (b) June, July and August.

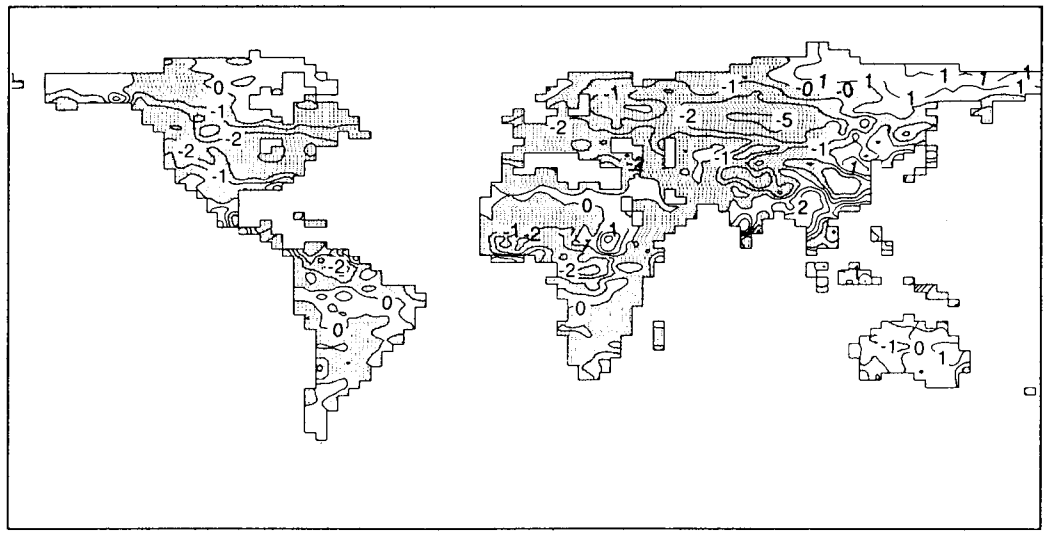

Figure 9. Simulated changes in soil moisture at equilibrium due to doubling atmospheric CO_2 in June, July and August. Contours at 1 cm intervals with areas of decrease stippled (Canadian Climate Center model with a horizontal resolution of 32 spectral waves (Boer (1990) personal communication).

the substantial increases in mean temperature. There is some evidence of an increase in convective precipitation. Numerical experiments show a reduction in mid-latitude storms, but as current models only resolve the larger disturbances, this does not rule out the possibility of smaller but more intense storms. An increase in the maximum intensity of tropical cyclones might be expected on theoretical grounds due to the increased availability of latent heat, but changes in the intensity of tropical disturbances simulated in different A/MLMs are inconsistent.

3.5 Estimating regional climate change: pre-industrial times to 2030 (IPCC 'business-as-usual' scenario)

The reader is reminded of the limited ability of current climate models to simulate regional climate change. In deriving the results below, the following assumptions have been made:

(a) The 'best guess' of the *magnitude* of the global mean equilibrium increase in surface temperature at 2030 is 1.8 °C (this is consistent with a climate sensitivity of 2.5 °C).

(b) The patterns of equilibrium and transient climate change are similar (this may be approximately true for the regions considered, but not for the high-latitude Southern Ocean, see Fig. 7).

(c) The regional changes in temperature, precipitation and soil moisture are proportional to the global mean changes in surface temperature (this will be approximately valid except in regions where the changes are associated with a shift in the position of steep gradients, for example where the snowline retreats, or on the edge of a rain-belt which is displaced).

Although it is hard to justify some of these assumptions on rigorous scientific grounds, the errors involved are substantially smaller than the uncertainties arising from the threefold range in climate sensitivity. The results below (IPCC 1990) are derived using equilibrium results from three high-resolution models (see caption to Fig. 1) and scaling them to give the appropriate change in global mean temperature. For a climate sensitivity of 1.5 °C the changes should be reduced by 30%, and for a climate sensitivity of 4.5 °C they should be increased by 50%. All the changes below are averages over the region — the range arises because of the use of different models.

3.5.1 Central North America (35–50° N, 85–105° W)

The warming ranges from 2 to 4 °C in winter and 2 to 3 °C in summer. Precipitation increases range from 0 to 15% in winter whereas there are decreases of 5–10% in summer. Soil moisture decreases in summer by 15–20%.

3.5.2 South-east Asia (5–30° N, 70–105° E)

The warming ranges from 1 to 2 °C throughout the year. Precipitation changes little in winter and generally increases throughout the region by 5–15% in summer. Summer soil moisture increases by 5–10%.

3.5.3 Sahel (10–20° N, 20° W–40° E)

The warming ranges from 1 to 2 °C. Area mean precipitation increases and area mean soil moisture decreases marginally in summer. However, there are areas of both increase and decrease in both parameters throughout the region which differ from model to model.

3.5.4 Southern Europe (35–50° N, 10° W–45° E)

The warming is about 2 °C in winter and ranges from 2 to 3 °C in summer. There is some indication of increased precipitation in winter, but summer precipitation decreases by 5–15%, and summer soil moisture by 15–25%.

3.5.5 Australia (10–45° S, 110–155° E)

The warming ranges from 1 to 2 °C in summer and is about 2 °C in winter. Summer precipitation increases by around 10%, but the models do not produce consistent estimates of the changes in soil moisture. The area averages hide large variations at the sub-continental level.

3.6 Simulation summary

Evidence from both modelling and observational studies suggest that the equilibrium global mean warming due to doubling atmospheric CO_2 is most likely to lie in the range 1.5–4.5 °C. Assuming an effective doubling of CO_2 by 2020 and an equilibrium sensitivity of 2.5 °C, simple models calibrated using the more complex GCMs predict a warming of just under 2 °C above pre-industrial levels by 2030. The warming is expected to be greatest over the higher northern latitudes in winter and least over the southern ocean throughout the year. Simulated precipitation increases in middle and high latitudes in winter, but soil moisture generally decreases in northern mid latitudes in summer. The magnitude of changes in precipitation is generally 0–15%. Little confidence can be placed in the variations in the changes on the regional scale (less than 2000 km).

4. Reducing uncertainties: current research programmes and their possible shortcomings

The assessment of recent results by IPCC gives an opportunity to review existing research programmes and to identify areas where further initiatives are required. The major sources of uncertainty in the simulation of climate change arise from:

(a) Lack of knowledge concerning the processes leading to the formation and dissipation of clouds, and determining their radiative properties. Furthermore, an improved understanding of the relevant microphysical processes needs to be matched with improved parametrization of these processes in large-

scale models of climate if the current uncertainties in climate sensitivity are to be reduced. This issue is addressed to some extent by the World Climate Research Programme (WCRP) through its Global Energy and Water Cycle Experiment (GEWEX) and the ongoing International Satellite Cloud Climatology Project, though it is not obvious, for example, that clouds and related processes are the top priority in GEWEX. Thus, it may be necessary to review widely spread programmes such as GEWEX to ensure that the major sources of uncertainty are given due priority.

(b) Lack of knowledge concerning the processes leading to the vertical mixing of heat into the deep ocean, particularly in high latitudes. The World Ocean Circulation Experiment (WOCE) of the WCRP was set up to describe the ocean circulation at all depths during a 5-year period (1990–1995). The area under consideration was belatedly extended to cover the high-latitude southern oceans and does not include the Norwegian Sea. In view of the apparent importance of high-latitude oceanic mixing in recent CGCM experiments, there may be a need for additional field experiments in high latitudes to supplement WOCE. The activities of the Joint Global Flux Study (part of the International Geosphere–Biosphere Programme of the International Council of Scientific Unions) is also relevant to the problem of ocean mixing.

(c) Lack of knowledge concerning the parametrization of tropical convection, which appears to be associated with an uncertainty of a factor of two in the magnitude of the sensitivity in the tropics. This is presumably addressed as part of GEWEX, but may need to be made more explicit.

(d) Lack of knowledge of land-surface processes and the interaction between climate and ecosystems. This gives rise to uncertainties in the simulations of important hydrological characteristics of the land surface such as soil wetness and evaporation. This is addressed explicitly in GEWEX and in the International Satellite Land Surface Climatology Programme.

Other factors which limit progress are insufficient computing power and lack of scientists with experience in the relevant topics. Note that in this paper we have assumed that changes in greenhouse gases are prescribed, and so additional uncertainties due to the effect of changes in climate on greenhouse gas concentrations are ignored.

Acknowledgements

This article appears in *Proceedings of the Second World Climate Conference* and is based on sections 3–6 of the Intergovernmental Panel on Climate Change Working Group I Report *Climate change — The IPCC scientific assessment*. The sections are: Processes and modelling (lead authors U. Cubasch and R.D. Cess); Validation of climate models (lead authors W.L. Gates, P.R. Rowntree and Q-C. Zeng; Equilibrium climate change (lead authors J.F.B. Mitchell, S. Manabe, T. Tokioka and V. Meleshko) and Time-dependent greenhouse-gas-induced climate change (lead authors F.P. Bretherton, K. Bryan and J.D. Woods). The reader is referred to the original report for further details of the findings presented above, and a full list of contributors to each section. The author is grateful to Howard Cattle, Peter Rowntree and an anonymous reviewer for useful comments on the text.

References

Cess, R.D., Potter, G.L., Blanchet, J.P., Boer, G.J., Ghan, S.J., Kiehl, J.T., Le Treut, H., Li, Z.-X., Liang, X.-Z., Mitchell, J.F.B., Morcrette, J.-J., Randall, D.A., Riches, M.R., Roeckner, E., Schlese, U., Slingo, A., Taylor, K.E., Washington, W.M., Wetherald, R.T. and Yagai, I., 1989: Interpretation of cloud-climate feedback as produced by 14 atmospheric general circulation models. *Science*, **245**, 513–516.

COHMAP members, 1988: Climatic changes of the last 18,000 years: observations and model simulations. *Science*, **241**, 1043–1052.

Ellsaesser, H.W., 1989: A different view of the climate effect of CO_2 updated. *Atmosphera*, **3**, 3–29.

Fennessy, M.J. and Shukla, J., 1988: Impact of the 1982–3 and 1986–7 Pacific SST anomalies on time mean prediction with the GLAS GCM. *In* Modelling the sensitivity and variation of the ocean–atmosphere system. Geneva, WMO TD-No. 254, WCRP-15.

Folland, C.K., Owen, J.A. and Maskell, K., 1989: Physical causes and predictability of variations in seasonal rainfall over sub-Saharan Africa. *In* Rango, A. (ed.), Remote sensing and large-scale global processes. Wallingford, IAHS publication No. 186.

Gregory, D. and Rowntree, P.R., 1990: A mass flux convection scheme with representation of cloud ensemble characteristics and stability-dependent closure. *Mon Weather Rev*, **118**, 1483–1506.

IPCC, 1990: Climate change — The IPCC scientific assessment. Cambridge University Press.

Jaeger, L., 1976: Monatskarten des Niederschlags für die ganze Erde. *Ber Deutscher Wetterdienst*, **18**, 1–38.

Lindzen, R.S., 1990: Some coolness concerning global warming. *Bull Am Meteorol Soc*, **71**, 288–299.

Luther, F.M. and Cess, R.D., 1985: Review of the recent carbon dioxide-climate controversy. *In* MacCracken, M.C. and Luther, F.M. (eds), Projecting the climate effects of increasing carbon dioxide. Washington DC, US Department of Energy.

Manabe, S., Stouffer, R.J., Spelman, M.J. and Bryan, K., (1991): Transient responses of a coupled ocean–atmosphere model to gradual changes of atmospheric CO_2. Part I. Annual mean response. To appear in *Journal of Climatology*.

Mitchell, J.F.B. and Ingram, W.J., (1991): On CO_2 and climate. Mechanisms of changes in cloud. Submitted to *Journal of Climatology*.

Mitchell, J.F.B., Senior, C.A. and Ingram, W.J., 1989: CO_2 and climate: a missing feedback? *Nature*, **341**, 132–134.

Raval, A. and Ramanathan, V., 1989: Observational determination of the greenhouse effect. *Nature*, **342**, 758–761.

Sarmiento, J.L., 1983: A simulation of bomb-tritium entry into the Atlantic Ocean. *J Phys Oceanogr*, **13**, 1924–1939.

Schlesinger, M.E. and Mitchell, J.F.B., 1987: Climate model simulations of the equilibrium climatic response to increased carbon dioxide. *Rev Geophys*, **25**, 760–798.

Schutz, C. and Gates, W.L., 1971: Global climatic data for surface, 800 mb, 400 mb: January. Santa Monica, Rand Corporation No. R-915-ARPA.

—, 1972: Global climatic data for surface, 800 mb, 400 mb: July. Santa Monica, Rand Corporation, No. R-1029-ARPA.

Stouffer, R.J. Manabe, S. and Bryan, K., 1989: Interhemispheric asymmetry in climate response to a gradual increase of atmospheric CO_2. *Nature*, **342**, 660–662.

551.577.38(420)

Were the dry spells of 1988–90 worse than those in 1975–76?

M.R. Woodley
Meteorological Office, Bracknell

Summary

Evidence is put forward to show that over England and Wales rainfall has been decreasing, with the greatest deficit in Northumbria. Compared with 1975–76, the recent dry spells are not so severe in terms of rainfall amount but are worse in terms of effective precipitation as shown by an examination of MORECS (Meteorological Office Rainfall and Evaporation Calculation System) data for an area on the border of Kent and East Sussex. In conjunction with rainfall levels generally there is some reason to believe that this may be typical of much of eastern and southern England.

1. Introduction

'After three of the driest years ever recorded, parts of Britain are facing a serious water shortage'. One might be forgiven for thinking those words applied to the last three years, but that was the introductory sentence of the June 1965 *Geographical Magazine*. Dr R.G. Allen (1965), then Director of the Water Research Association, wrote about the problems of water demand, irrigation and rainfall deficiencies, and the anxieties being expressed about the future. Since then many parts of the United Kingdom have experienced two major dry spells, one in the mid 1970s, and the other within the last 3 years. This paper compares, in general terms, the recent dry weather with that of the previous decade, together with a closer examination of the effect of the rainfall deficit for one small area of southern England.

2. Rainfall over England and Wales since 1970

The periods of dry weather which have affected virtually all of England and Wales in the last two to three years, have revived memories of the exceptional drought of 1975–76, catalogued in the *Atlas of Drought in Britain* (Institute of British Geographers 1979), and raised further anxieties about receding water levels. In the south and east of England especially, views were expressed in newspapers, and on radio and television, that any prolongation of the dry weather beyond the summer of 1990 may lead to severe water problems in 1991. Water authorities are very concerned about declining water levels in wells and aquifers, and in some cases groundwater levels are approaching, or falling below, the minimum historical levels (Institute of Hydrology 1990). The very warm and dry weather which prevailed for much of 1989, preceded by a drier than normal winter (which was also the warmest this century), led to hose-pipe bans during the summer. Fears of worse to come were somewhat ameliorated by the very wet winter of 1989/90 (the wettest since 1914), but the return of the warm and dry weather in 1990 wiped out most of the benefits of recharged groundwater levels, and there were reports of a continued hose-pipe ban in early 1991 in a few areas. Provisional totals for the winter of 1990/91 show the season's rainfall to have been just above normal, at 104% of the 1941–70 average.

Running means, calculated over a period of years, will give a smoothed guide to changes in rainfall amounts, but a more direct and immediate response to excess or shortfall in rainfall totals can be gauged by using cumulative differences from the average monthly values. Fig. 1 shows the accumulated differences, month by month, from the 1941–70 average for England and Wales. This has been used as the best available starting point since almost all the monthly values after 1970 have been based on the CARP (Comprehensive Areal Rainfall Program) technique devised by Shearman and Salter (1975). The graph quite clearly demonstrates the marked deficit which reached its lowest point in August 1976, together with a secondary minimum in the autumn of 1978. Through much of the next 10 years monthly rainfall totals were often above average but a further decline began in 1988.

The extent of the decrease in rainfall has varied across England and Wales, and the differences may be gauged by examining the areal rainfall for each of the water company regions in England and Wales. Fig. 2 shows the total rainfall from January 1971 to September 1990, expressed as a percentage of the 1941–70 average. Each region shows a deficit, and is most marked in Northumbria. The decline in rainfall amounts, if it is sustained or becomes more marked, could have serious consequences should the general demand for water continue to increase.

3. Comparison of recent rainfall totals with the 1970s

The drought of the 1970s reached its nadir in August 1976, for the following months of September and

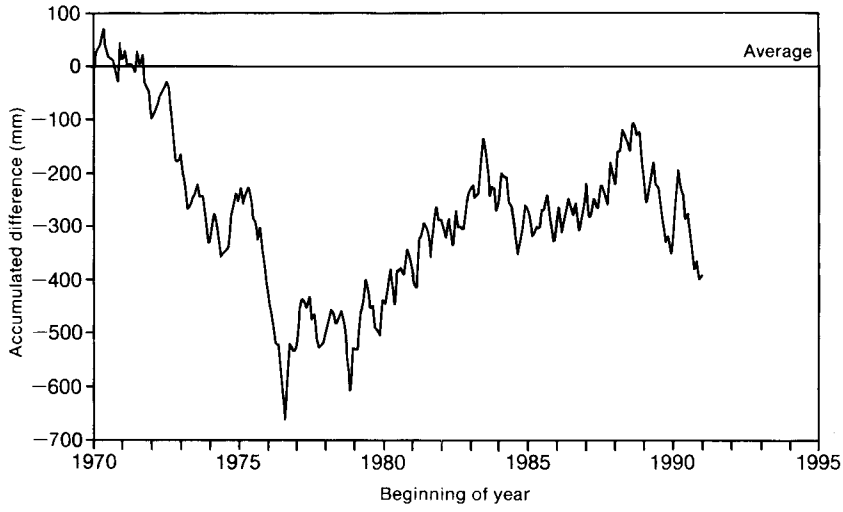

Figure 1. Cumulative differences from the 1941–70 average of monthly rainfall since 1970 over England and Wales. Values since September 1990 are still provisional.

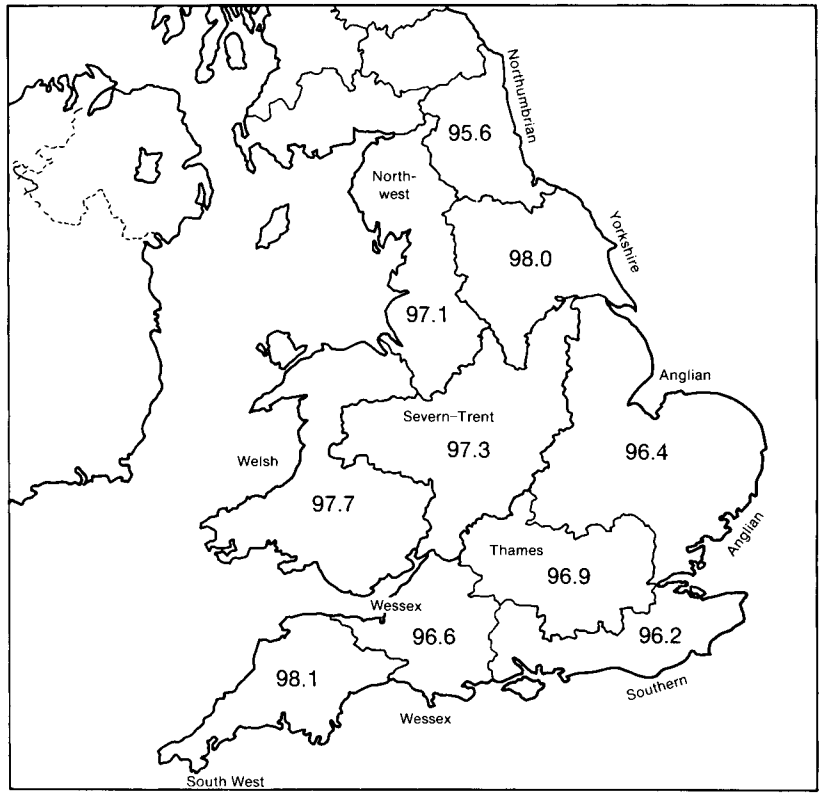

Figure 2. Percentage of the 1941–70 average rainfall over the water company regions from January 1971 to September 1990.

October were very wet, both receiving nearly twice the normal amount. Fig. 3 shows the percentage of 1941–70 rainfall over the period May 1975 to August 1976 (inclusive) together with the calculated return period, for a rainfall event specifically starting in May. It should be noted, however, that wet or dry spells can start in any month: thus there are 12 times as many opportunities and the return periods given in Figs 3–5 can be divided by 12 to give an approximate assessment of events starting at any time. In the more recent dry spell the equivalent period is from August 1988 to November 1989, inclusive: Fig. 4 shows the values for that 16-month span, and Fig. 5 values for the longer period of 26 months from August 1988 to September 1990. This last period includes the exceptionally wet winter of 1989/90.

4. The effect on ground moisture levels

The effect of a dry spell on both the available water content (AWC) for plants and crops, and general water supplies may be serious enough in the short term, but potentially disastrous if the drought is prolonged. The

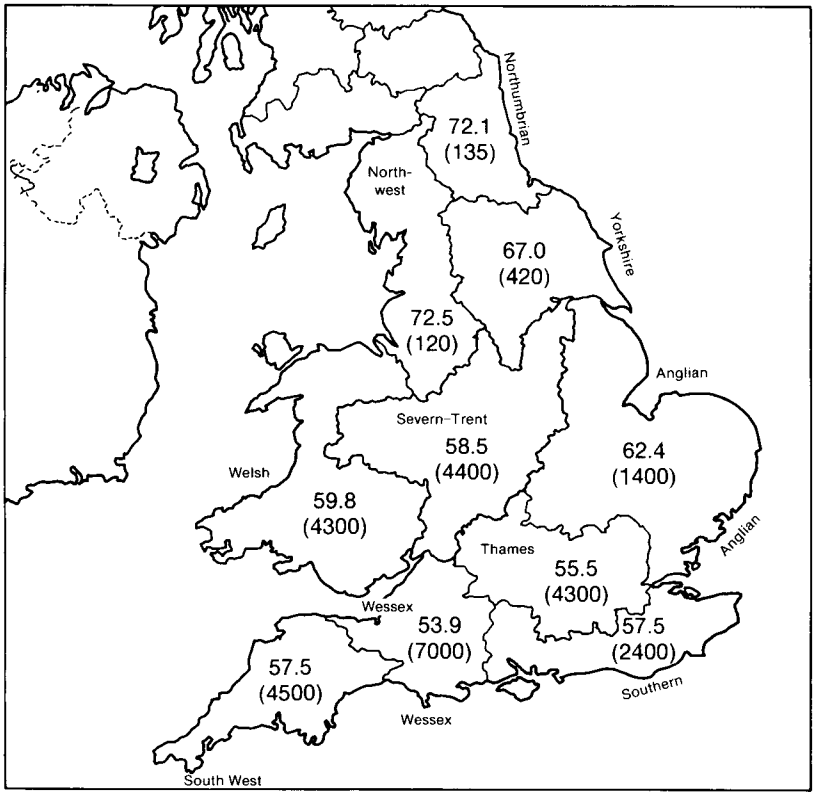

Figure 3. As Fig. 2 but for the period from May 1975 to August 1976. The associated return period in years is stated within the brackets.

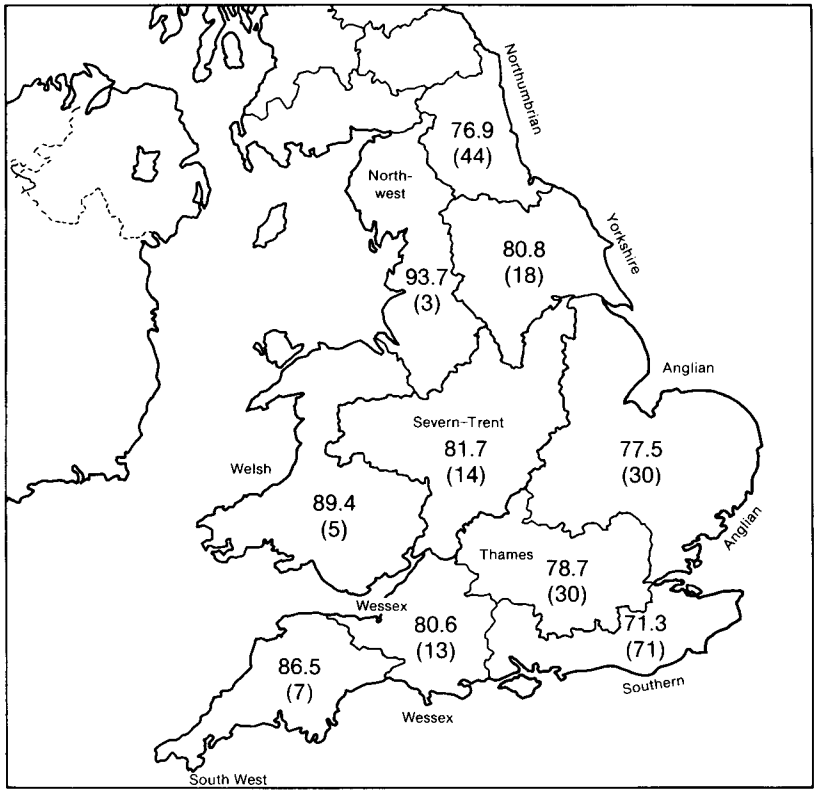

Figure 4. As Fig. 3 but for the period from August 1988 to November 1989.

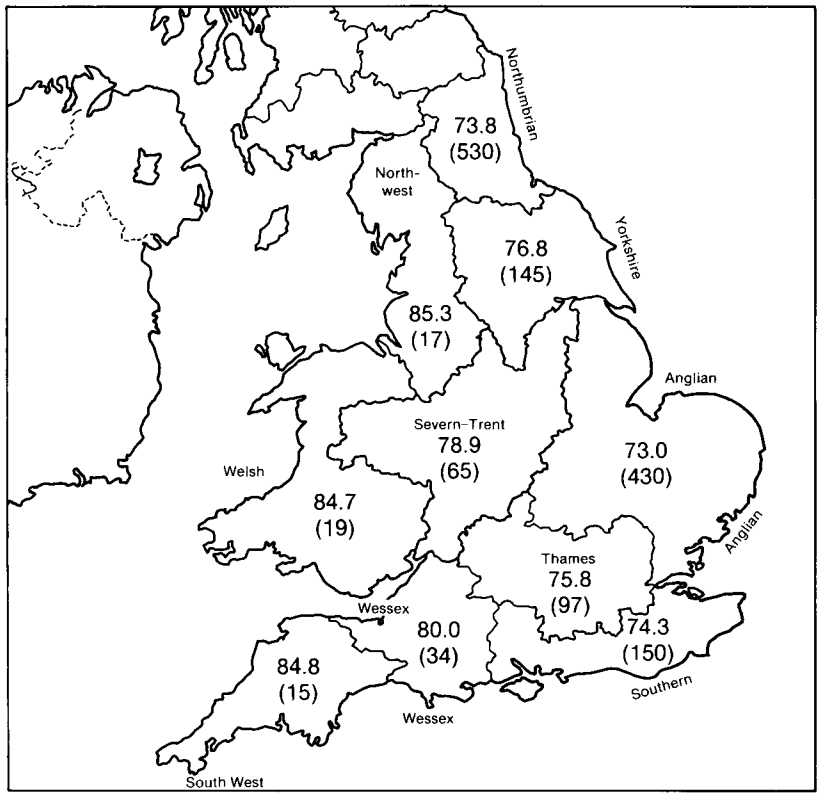

Figure 5. As Fig. 3 but for the period from August 1988 to September 1990.

dry periods during the 1970s, coupled at times with the exceptional warmth of 1975 and 1976 caused widespread concern. Since both 1989 and 1990 have shown similar characteristics, it is instructive to compare these years with those of 1975–76 in terms of effective precipitation and soil moisture deficits. A study covering the whole of England and Wales is outside the scope of this paper, but a comparison over a small area has been undertaken.

The MORECS (Meteorological Office Rainfall and Evaporation Calculation System) Bulletin has been designed to provide estimates of weekly and monthly values in the form of data within a grid of 40-kilometre squares. An account of the physical processes can be found in Hydrological Memorandum No. 45 (Thompson *et al.* 1981). The core of the scheme is a system which determines the evapotranspiration from various crop and land surfaces. It is broadly defined as a combining of the processes of evaporation from the surface of the earth and transpiration from vegetation, and can be calculated by taking into account a number of factors including sunshine, wind speed, temperature and vapour pressure as well as the state and height above ground of the crops. Once the values of these two processes have been assessed the soil moisture deficit (SMD) can be evaluated by the differences between the rainfall received and the evaporation; and the effective precipitation (EP) is the excess left after the ground has absorbed the precipitation, i.e. run-off from the ground into rivers, aquifers, etc.

The variables SMD and EP, together with the rainfall amount are important indicators of conditions for farmers, growers, hydrologists, and many others. They show when irrigation may be necessary (as SMD values become relatively large), and if regulatory measures by water companies are necessary when water levels in boreholes and aquifers fall below acceptable levels during long periods with negligible or no EP. In the summer months the amount of evapotranspiration from surfaces exceeds the average rainfall over much of Great Britain, so that the community is dependent on the land reaching its maximum water capacity in winter months, and reservoirs and underground water resources are replenished.

In the Southern water region the rainfall for the 6 months from August to January provides, on average, about 60% of the annual average (based on the 1941–70 average), and around one-third of the annual average rainfall occurs in the three months from November to January. This pattern appears to be repeated in the other water regions of England and Wales. The latter period is of great importance, for evapotranspiration and soil moisture deficit are at or close to the minimum, and the contribution by effective precipitation at its highest. A dry winter can lead to a serious water shortage if the following summer is dry, which indeed proved to be the case in 1988–89. Tables I–III, for grassland use, show the end of month values of rainfall, SMD and EP, together with the 1961–85 long-period average values, for MORECS grid square 173, which

Table I. Comparison of MORECS values (mm) for grid-square 173 — rainfall

Month	1961–85 average	SD	Rainfall 1975	1976	1988	1989	1990	1991
Jan.	73	34	142	19	186	27	107	90
Feb.	50	30	24	31	47	53	116	37
Mar.	61	31	108	18	87	69	4	38
Apr.	51	28	45	11	36	94	51	
May	58	24	79	23	48	2	8	
Jun.	57	32	15	9	14	57	58	
Jul.	47	21	23	42	79	33	11	
Aug.	57	29	28	10	42	29	36	
Sep.	73	51	144	127	47	29	34	
Oct.	71	49	45	141	73	75	126	
Nov.	83	43	82	145	34	39	74	
Dec.	82	34	39	84	17	126	61	

Notes:
SD = Standard deviation.
In the current MORECS model SMD for grass cannot exceed 125 mm.

Table II. Comparison of MORECS values (mm) for grid-square 173 — soil moisture deficit (for grass)

Month	1961–85 average	SD	Soil moisture deficit 1975	1976	1988	1989	1990	1991
Jan.	7	1	0	7	0	23	0	2
Feb.	2	2	5	1	9	1	4	0
Mar.	7	8	1	17	1	13	4	13
Apr.	20	18	23	60	18	4	50	
May	42	27	36	100	55	92	108	
Jun.	60	30	98	124	91	107	108	
Jul.	80	26	118	125	95	122	124	
Aug.	79	36	125	124	100	125	109	
Sep.	56	39	18	37	103	125	109	
Oct.	36	37	6	0	63	77	21	
Nov.	11	23	0	0	41	54	1	
Dec.	1	1	0	0	38	2	0	

Notes: as Table I

Table III. Comparison of MORECS values (mm) for grid-square 173 — effective precipitation (for grass)

Month	1961–85 average	SD	Soil moisture deficit 1975	1976	1988	1989	1990	1991
Jan.	62	32	124	9	170	0	89	76
Feb.	35	29	17	13	33	11	88	23
Mar.	35	27	79	0	39	41	0	16
Apr.	14	18	19	0	0	34	0	
May	7	11	20	0	0	0	0	
Jun.	5	14	0	0	0	0	0	
Jul.	0	0	0	0	0	0	0	
Aug.	0	>0	0	0	0	0	0	
Sep.	10	25	0	0	0	0	0	
Oct.	25	37	6	76	0	0	0	
Nov.	42	45	63	134	0	0	36	
Dec.	63	30	32	79	0	58	45	

Notes: as Table I

covers most of the Kent and East Sussex border area, for the years 1975–76 and 1988–91. In particular Table II shows that while the SMD levels were at or near the theoretical possible maximum of 125 millimetres in 1975, 1976, 1989 and 1990, the last of these years showed the longest period of deficit in excess of 100 millimetres. Table III reveals that the number of months with nil effective precipitation in 1988, 1989 and 1990 was greater than in either 1975 or 1976.

5. Conclusion.

Figs 1 and 2 show that rainfall has declined over England and Wales as a whole over the last 20 years. Comparison of the areal rainfall and the return periods (Figs 3–5) show that the dry spell of 1975–76 was quite exceptional, and neither the 16-month period in 1988–89 (Fig. 4) nor the 26-month period 1988–90 (Fig. 5) are anything like so severe. It is noticeable, however, that over the longer of the two time-spans, the return periods have become much greater, and notably so in Northumbria. From the point of view of Table III the effect of the 1988–90 dry spells, and particularly the long, dry period in 1990, appears to have had a greater effect on underground water reserves than in 1975–76. Two of the three winter months 1990/91 had below normal effective precipitation, and March 1991 was also less than average*. The water companies may have good reason to be concerned about future supplies in the face of these facts, especially as the 1990/91 winter rainfall for England and Wales as a whole is below normal.

* This article was written in the early spring of 1991. Since then there has been one very dry month (May) and one very wet month (June) over almost all of England and Wales. Both months were cooler than normal.

Thus it must be concluded that for at least one small area of England the precipitation contribution to water storage systems and aquifers is markedly less than normal and apparently less than in 1975–76. If this pattern has been repeated across much of southern and eastern England (as supported by Fig. 5), then the anxieties expressed by water and river authorities appear fully justified, and even Wales and western districts of England may have cause for concern. Though the provisional winter rainfall figure of 228 mm, for England and Wales, is 4% below the 1941–70 average, it is close enough to normal to warrant the need for above-average rainfall (and below-average evapotranspiration) in the following months if the situation is to be ameliorated.

Acknowledgements

Thanks are due to D. Hollis for computing the rainfall return periods, J. Fullwood for advice on aspects of the MORECS system, and Dr J. Brownscombe for helpful discussions about precipitation statistics as well as the calculations for Fig. 1.

References

Allen, R.G., 1965: Water in Britain. *Geogr Mag*, **38**, 89–101.

Institute of British Geographers, 1979: Atlas of drought in Britain 1975–76.

Institute of Hydrology, 1990: Hyrological summary for Great Britain September 1990. (Prepared for the Department of the Environment.)

Shearman, R.J. and Salter, P.M., 1975: An objective rainfall interpolation and mapping technique. *Hydrol Sci Bull*, **20**, 353–363.

Thompson, N., Barrie, I.A. and Ayles, M., 1981: The Meteorological Office Rainfall and Evaporation Calculation System MORECS. *Hydrol Mem Meterol Off*, No. 45.

Correspondence

Discussion on the review of *Pilot's weatherpack*

I am very grateful to have B.K. Lloyd's fair review of *Pilot's weatherpack* (*Meteorol Mag*, **120**, 149–150). Perhaps it should be made clear that the Case 1 analysis was principally the work of S.G. Cornford (now retired), whereas all subsequent accidents were investigated later by W.S. Pike, who appreciates the valid point made regarding inclusion of a case featuring carburettor icing. R. Reynolds kindly organized the pack's printing.

Aircraft piston-engine induction-system icing (commonly known as carburettor icing) is caused by internal cooling within the fuel system where a sudden drop in temperature (of up to 30 °C) occurs at the carburettor venturi, due to fuel vaporization and air expansion there. Although this is a gradual process which causes a progressive decline in engine power, it is often described to pilots as being 'stealthy', because sometimes the first sign of this mechanical problem developing is when the engine(s) stutter or fail completely in flight. Commonly, the pilot has overlooked sufficient remedial application of carburettor heat, available at the flick of a switch in most modern aircraft, but at the simultaneous cost of increased fuel consumption.

Accidents result if the ice cannot be melted before a forced landing has to be made. Damaging occurrences are also reported due to the inability of the engine(s) to develop sufficient power for a successful take-off to be achieved. Of the 10–15 incidents where carburettor icing is suspected each year, only half of these result in accident reports to the Air Accident Investigations Branch (AAIB) of the Department of Transport, and fatalities are, also, quite rare — occurring approximately once every three years on average.

Frequently, other factors are cited as contributing to an accident (e.g. airframe icing, fuel contamination, mechanical failure, etc.) and the AAIB Bulletin or Report will mention that 'conditions conducive to severe carburettor icing' were in existence. Often this is because the hard evidence rapidly disappears following an accident! Water found in a fuel system could be either pre-existing contamination or melted ice.

A more comprehensive guide to the various forms of carburettor icing can be found in the CAA's *Aeronautical Information Circular* (AIC No. 59/1990 (Pink 8)). Carburettor icing is more likely to occur with MOGAS fuel (because of its greater volatility and higher possible water content) than when AVGAS fuel is used. Also, some types of aircraft appear to be more prone than others.

Above all it should be mentioned that carburettor icing is not just a winter phenomenon, but it is even more likely to appear on warm days in conditions of high humidity. An interesting diagram in the abovementioned AICs (Fig. 1) relates the risk of carburettor icing to (1) engine power setting, (2) temperature, and (3) humidity/dew-point temperature. It is noticeable that at 'low descent-power' a serious risk of carburettor icing exists for ambient temperatures as high as 32 °C when combined with dew-point temperatures of between 16 and 20 °C. Probabilities of carburettor icing also increase whenever aircraft are operating in or near cloud, fog and precipitation.

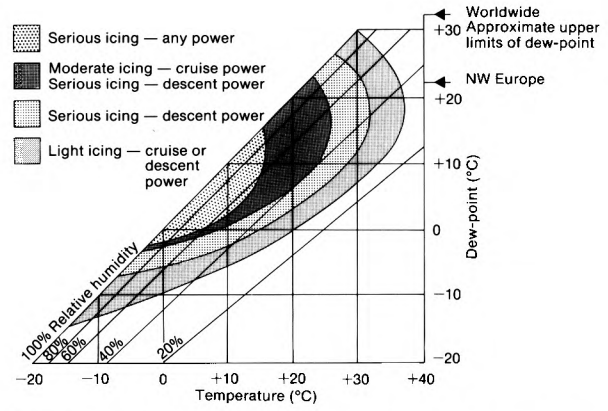

Figure 1. Carburettor icing in air free of cloud, fog or precipitation. The risk and rate of carburettor icing will be greatest when operating in cloud, fog and precipitation.

If we have the opportunity to revise the *Pilot's weatherpack* (now titled *Weather as a hazard*) to include an accident featuring carburettor icing in interesting or unusual circumstances, we will do so.

W.S. Pike

19 Inholmes Common
Woodlands St. Mary
Newbury
Berkshire RG16 7SX

Reply by B.K. Lloyd

Thank you for giving me the opportunity to reply to Mr W.S. Pike's letter.

I agree with all that Mr Pike has said, and to identify an incident totally attributable to carburettor icing would be difficult. However, I was particularly pleased with his final paragraph. An article featuring carburettor icing should be included if he were to have the opportunity to revise the *Pilot's weatherpack* (now titled *Weather as a hazard*).

May I point out that the AICs that he has quoted have now been reissued under AIC 59/1990 (Pink 8) dated 2 August. Another source of information is the *General aviation safety sense* series, particularly leaflet Nos 3a (winter flying) and 14 (piston engine icing) which may be of some use. These leaflets are prepared by the Safety Promotions Section and the Public Relations Department of the Civil Aviation Authority.

B.K. Lloyd

Civil Aviation Services
Central Forecasting Division
Meteorological Office
London Road
Bracknell
Berkshire RG12 2SZ

Review

Land surface evaporation: measurement and parameterization, edited by T.J. Schmugge, J.-C. André. 179 mm × 260 mm, pp. xv+424, *illus.* New York, Springer Verlag, 1991. Price Dm.168.00. ISBN 0 387 97359 1.

It is by now well known that the atmosphere responds to variations in its surface boundary conditions. Several model experiments in the last two decades have shown that this sensitivity occurs on a number of spatial scales, ranging from that of a mesoscale model grid-square of some hundred square kilometres to the general circulation grid-square size of several thousands of square kilometres. This book is the result of a workshop held in October 1988 in Banyuls and aims to present a review of land surface evaporation processes from both a modelling and measurement point of view. The combination of these two aspects in a single book make it stand out from other workshop proceedings. In effect, the title is slightly misleading as the various contributions deal not only with evaporation but cover many more aspects of the land surface energy and water balance. The book draws heavily on examples from the HAPEX-Mobilhy experiment which took place in an area of 100 km × 100 km in south-western France in 1986. The principal focus of this experiment was to measure the model hydrological and atmospheric fluxes on the scale of a general circulation grid-square.

The first chapters present the reader with a state-of-the-art review on the modelling of land surface processes in a variety of atmospheric models: global climate models, numerical weather prediction models and mesoscale models. They do not only describe the physical background of the parametrizations but also show how sensitive the models are to these parametrizations. In the case of climate modelling, examples are shown of the use of these models to predict the consequences of Amazonian deforestation. The two chapters on numerical weather prediction models and mesoscale models show how model results are critically dependent on the initialization of the land surface parametrizations. Unfortunately there is considerable overlap and repetition in the content of these chapters as all present in some detail the respective land surface parametrizations used in these models. A particularly relevant problem raised in these chapters is how the ultimate products of large-scale meteorological models, fluxes representative of areas of several hundreds of square **kilometres**, are to be tested. Current practice, and several examples of this are given in this book, is to test the one-dimensional representation against local flux data obtained over several hundreds of **metres**. Although this is an obvious necessary requirement for a parametrization scheme to be acceptable, it clearly is not a sufficient one. A dramatic illustration of this problem is given in the chapter on climate modelling where in one case the prediction of run-off agrees very well with observations and in the other case not at all. Why does the small-scale physics appear to work on the large scale in the first one, but not in the second?

The section on measurement describes in detail the various measurement techniques currently available to measure the various components of the energy balance. An important aspect of these chapters is that they cover a range of scales from micrometeorological measurements, using profile and eddy correlation methods, to flux measurements from aircraft, which integrate over several kilometres, to remote sensing measurements. The section provides insight into the effects of land surface variability on the structure of the surface layer and the use of aircraft to estimate fluxes over inhomogeneous or inaccessible terrain. Although aircraft have considerable potential in estimating area-averaged fluxes, it is pleasing to see the aircraft work described in a realistic way, so that future planning of large-scale field experiments can draw from the experiences of earlier experiments.

Overall the book presents a valuable overview of current knowledge of land surface processes and makes, through its reference to the HAPEX-Mobilhy experiment, a case for well planned large-scale international field experiments. Any researcher interested in hydrology and meteorology, from plot or catchment to continental or global scale, will not be disappointed by purchasing this well produced book.

A.J. Dolman

Books received

The listing of books under this heading does not preclude a review in the Meteorological Magazine at a later date.

The earth as transformed by human action, edited by B.L. Turner II, W.C. Clark, R.W. Kates, J.F. Richards, J.T. Mathews and W.B. Mayer (Cambridge University Press, 1991. £75.00) is the culmination of an undertaking involving the examination of the toll taken on the world by the human race while taking technical and social strides forward. The papers included are aimed at a broad audience. ISBN 0 521 36357 8.

Global environmental change, edited by R.W. Corell and P.A. Anderson (Berlin, Heidelberg, New York, London, Paris, Tokyo, Hong Kong, Springer-Verlag, 1991. DM 158.00) contains papers presented at a NATO workshop on the subject. The workshop's three central themes were the needs to: develop the global observation and monitoring systems, better understand basic Earth system processes and improve models of global change. ISBN 0 387 53128 9.

Satellite and radar photograph — 2 July 1991 at 1700 UTC

During the afternoon of 2 July 1991 a slow-moving front extended from the north-west tip of Denmark to eastern Spain (see Fig. 1). On the COST-73 (Co-operation in Science and Technology) image shown in Fig. 2 this front can be seen as a band of cloud and patchy rain; just east of the front there there is an area of heavy convective rain (marked A in Fig. 2) with intensities of over 30 mm h^{-1} in a few places, and a large area of medium and high cloud spreading north and east from it. This system formed shortly before 1500 UTC when several intense convective cells started to develop over southern Belgium in the warm air near a shallow wave on the front. The cells moved northwards and became organized into a band running inland from the coast; an area of high-level outflow cloud spread north-east from them over the next few hours. By 1700 UTC (Fig. 2) the cells had organized into a mesoscale convective system (MCS) with a band of convective rain over 100 km long, new developments spreading north from its north-western end, and with the anvil of medium- and high-level outflow cloud covering more than 25 000 km^2. To the north-east of the outflow cloud a small thunderstorm (marked B in Fig. 2) can be seen over The Netherlands with its own upper-level outflow cloud spreading away from it.

The MCS continued to expand and develop over the next few hours as it moved over the North Sea. The intensity of precipitation gradually decreased, but the area covered by it increased as lighter rain started to fall from the outflow cloud. By 2100 UTC the MCS had overtaken and engulfed the smaller thunderstorm (B in Fig. 2) and the combined area of medium- and high-level outflow cloud covered around 125 000 km^2. After this time the system started to shrink and become less organized, finally dissipating in the early hours of 3 July.

R.B.E. Lilley

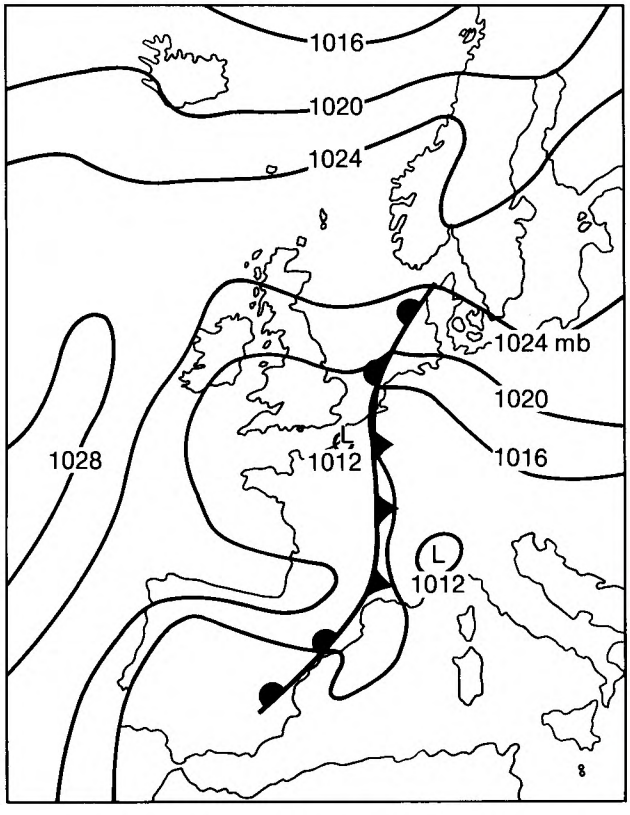

Figure 1. Surface analysis for 1800 UTC on 2 July 1991.

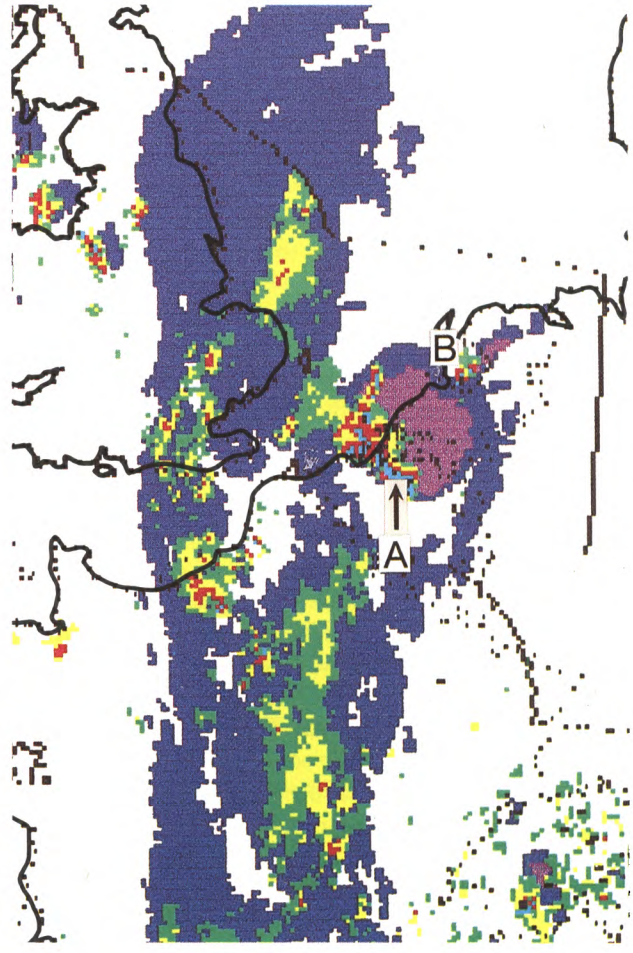

Figure 2. COST-73 European radar and satellite composite picture for 1700 UTC on 2 July 1991. Cloud is shown from the Meteosat infra-red data, with dark blue indicating cloud-top temperatures from −15 °C to −45 °C, and purple indicating tops colder than −45 °C. Rainfall rates (mm h^{-1}) shown are: green (0.3–1), yellow (1–3), red (3–10), light blue (10–30) and black (> 30). See text for explanation of lettering.

GUIDE TO AUTHORS

Content

Articles on all aspects of meteorology are welcomed, particularly those which describe results of research in applied meteorology or the development of practical forecasting techniques.

Preparation and submission of articles

Articles, which must be in English, should be typed, double-spaced with wide margins, on one side only of A4-size paper. Tables, references and figure captions should be typed separately. Spelling should conform to the preferred spelling in the *Concise Oxford Dictionary* (latest edition). Articles prepared on floppy disk (Compucorp or IBM-compatible) can be labour-saving, but only a print-out should be submitted in the first instance.

References should be made using the Harvard system (author/date) and full details should be given at the end of the text. If a document is unpublished, details must be given of the library where it may be seen. Documents which are not available to enquirers must not be referred to, except by 'personal communication'.

Tables should be numbered consecutively using roman numerals and provided with headings.

Mathematical notation should be written with extreme care. Particular care should be taken to differentiate between Greek letters and Roman letters for which they could be mistaken. Double subscripts and superscripts should be avoided, as they are difficult to typeset and read. Notation should be kept as simple as possible. Guidance is given in BS 1991: Part 1: 1976, and *Quantities, Units and Symbols* published by the Royal Society. SI units, or units approved by the World Meteorological Organization, should be used.

Articles for publication and all other communications for the Editor should be addressed to: The Chief Executive, Meteorological Office, London Road, Bracknell, Berkshire RG12 2SZ and marked 'For Meteorological Magazine'.

Illustrations

Diagrams must be drawn clearly, preferably in ink, and should not contain any unnecessary or irrelevant details. Explanatory text should not appear on the diagram itself but in the caption. Captions should be typed on a separate sheet of paper and should, as far as possible, explain the meanings of the diagrams without the reader having to refer to the text. The sequential numbering should correspond with the sequential referrals in the text.

Sharp monochrome photographs on glossy paper are preferred; colour prints are acceptable but the use of colour is at the Editor's discretion.

Copyright

Authors should identify the holder of the copyright for their work when they first submit contributions.

Free copies

Three free copies of the magazine (one for a book review) are provided for authors of articles published in it. Separate offprints for each article are not provided.

Contributions: It is requested that all communications to the Editor and books for review be addressed to the Chief Executive, Meteorological Office, London Road, Bracknell, Berkshire RG12 2SZ, and marked 'For *Meteorological Magazine*'. Contributors are asked to comply with the guidelines given in the *Guide to authors* which appears on the inside back cover. The responsibility for facts and opinions expressed in the signed articles and letters published in *Meteorological Magazine* rests with their respective authors.

Subscriptions: Annual subscription £33.00 including postage; individual copies £3.00 including postage. Applications for postal subscriptions should be made to HMSO, PO Box 276, London SW8 5DT; subscription enquiries 071–873 8499.

Back numbers: Full-size reprints of Vols 1–75 (1866–1940) are available from Johnson Reprint Co. Ltd, 24–28 Oval Road, London NW1 7DX. Complete volumes of *Meteorological Magazine* commencing with volume 54 are available on microfilm from University Microfilms International, 18 Bedford Row, London WC1R 4EJ. Information on microfiche issues is available from Kraus Microfiche, Rte 100, Milwood, NY 10546, USA.

September 1991

Edited by Corporate Communications Vol. 120
Editorial Board: R.J. Allam, R. Kershaw, W.H. Moores, P.R.S. Salter No. 1430

Contents

ISSN 0026–1149

Printed in the United Kingdom for HMSO
Dd 0291241 9/91 C13 503 12521

The Meteorological Magazine

October 1991

Deposition processes
Probabilities in weather forecasting
The autumn of 1990

HMSO

Met.O.998 Vol. 120 No. 1431

First published 1991

HMSO publications are available from:

HMSO Publications Centre
(Mail and telephone only)
PO Box 276, London, SW8 5DT
Telephone orders 071-873 9090
General enquiries 071-873 0011
(queuing system in operation for both numbers)

HMSO Bookshops
49 High Holborn, London, WC1V 6HB 071-873 0011 (counter service only)
258 Broad Street, Birmingham, B1 2HE 021-643 3740
Southey House, 33 Wine Street, Bristol, BS1 2BQ (0272) 264306
9–21 Princess Street, Manchester, M60 8AS 061-834 7201
80 Chichester Street, Belfast, BT1 4JY (0232) 238451
71 Lothian Road, Edinburgh, EH3 9AZ 031-228 4181

HMSO's Accredited Agents
(see Yellow Pages)

and through good booksellers

3 8078 0010 2455 5

The Meteorological Magazine

October 1991
Vol. 120 No. 1431

551.510.42

Deposition processes for airborne pollutants

F.B. Smith
Meteorological Office, Bracknell

Summary

This is an introductory account of how airborne pollution is ultimately lost from the atmosphere to the Earth's surface. It describes the three main processes: dry deposition, wet deposition and occult deposition, and how they may be measured or estimated. With the problem of 'acid rain' in mind, it assesses what fraction each process makes to the total sulphur deposition in the United Kingdom.

1. Wet deposition

Non-reactive gases are not readily removed from the atmosphere. With this exclusion, precipitation tends to be very efficient at removing most pollutants. Moderate rain will often remove more in one hour than dry deposition will over two or more days. Of course, rain is a very sporadic event. In the lowlands of England it rains only about 3–4% of the time, and even in wet areas like north-west Scotland it rains only some 8–10% of the time. However, as we shall see later, wet deposition is comparable in importance to dry deposition and in the United Kingdom is typically responsible for 70–80% of the total deposition of sulphate, for example.

Pollution is affected by precipitation to a degree which depends on its height in the atmosphere: if the pollution is within the stratosphere it is unaffected since precipitation does not occur there. A typical residence time for pollution within the stratosphere is about 1 year. If the pollution is within the 'free' troposphere (above the boundary layer) it may or may not be affected by any precipitation according to whether or not it is drawn into the cloud. Typical residence times in the free troposphere are thought to be of the order of 10–20 days. If, however, it is within the boundary layer it is subject to dry and wet deposition. A typical residence time for European pollution is 3–4 days.

Pollution comes in a variety of forms:

(a) As particles. One of the most important parameters here is the size of the particle. If it is above about 20 μm (where 1 μm is one thousandth part of a millimetre) then it has a significant fall velocity (see section 2). Smaller particles cannot rely on fallout unless over time they tend to stick together to form progressively larger particles which eventually have a significant fall velocity. This is fairly common and is the main loss route in very arid regions. In most areas, however, small particles are either lost in rain or are carried by turbulence to the ground where dry deposition can take place. The latter, however, tends to be very inefficient for sub-micron particles and they have to rely on wet deposition.

(b) As free gases. Reactive free gases may be adsorbed on to or into cloud droplets, raindrops or snowflakes at a rate which depends on relative gas vapour pressures in the air and in the droplets, sometimes on the pH of the droplets, on the surface area of the drops or flakes, and on how reactive they are.

(c) As captured gases. Gases can be adsorbed on to other particles which are in turn incorporated in to rain or snow. Even some very small particles can become attached to other larger particles of a different kind.

Particles can get into precipitation elements either (a) by being captured, that is, swept out, as the element falls through the air, or (b) by becoming the cloud

condensation nucleus for a developing cloud droplet which subsequently turns into a precipitation element by coalescence. This coalescence may take place simply by random turbulent collisions, or by differences in electrical charge. Particles can also get into cloud droplets as a result of so-called phoretic effects. These are processes by which very small particles and cloud droplets may be brought together by forces acting on the particles pushing them towards the droplet. These forces depend ultimately on the gradient or flux of, for example, temperature, water vapour, electrical charge, or radiation in the vicinity of the droplet. Finally, particles can enter droplets by Brownian capture: when the particles are sufficiently small ($\ll 0.1\ \mu$m) that they are moved by molecular bombardment and can collide with, and be captured by, larger cloud droplets.

Some particles are hydrophobic, that is they are repulsed by water. Obviously they are not good candidates to become cloud condensation nuclei. PCBs are good examples of hydrophobic particles. They can, however, become attached to hygroscopic particles which are particles that tend to attract and hold water molecules to themselves without necessarily dissolving in the resulting liquid water. When this happens, they can be more readily rained out.

Chemical changes can also affect a pollutant's ability to be wet deposited. One of the best known examples of this is the reactive gas, sulphur dioxide, which whilst it is to some extent absorbed directly into raindrops and reaches the ground as sulphur dioxide, can undergo oxidation to sulphate (which is a fine aerosol) either before or after being incorporated into rain. This increases the efficiency of the removal process. The oxidation rate depends not only on the availability of suitable oxidants (like ozone) but also on the relative humidity (or the amount of cloud, see Fig. 1).

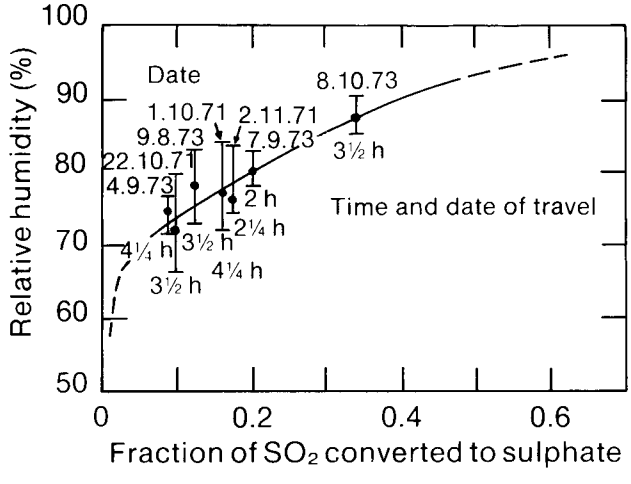

Figure 1. The inferred fraction of sulphur dioxide converted to sulphate as a function of relative humidity. Measurements were made along flight paths off the east coast of the United Kingdom. (Smith and Hunt (1978)).

1.1 Wash-out

From the above discussion, it is clear that pollutants may be removed from the air by precipitation both in cloud and below cloud. Removal in-cloud is generally called rain-out (even though the precipitation may be in the form of snow), whereas below-cloud removal is usually called wash-out. Rain-out is more efficient than wash-out if the concentration is the same in and below cloud.

Considering wash-out first, and following the discussion given by Lyons and Scott (1990) a falling droplet sweeps out an air volume, and its path will intersect that of some of the pollutant particles in this volume. This fraction of particles in the droplet's path is known as the target efficiency, T, and the fraction of these contacting particles that actually stick is the retention efficiency, r. Hence the actual collection efficiency E is

$$E = rT.$$

Very little is known of r and it is usually taken as 1 so that the wash-out coefficient, Λ, is given by

$$\Lambda = \int FTA d(D)$$

where D is the diameter of the falling drop, A is the cross-sectional area of the drop, and F is the number of drops in interval $d(D)$ per unit volume, times their fall-speed.

If the wash-out process occurs uniformly over the plume volume, then the concentration in the air decreases in time t due to wash-out alone according to

$$C_a(t) = C_a(0) \exp(-\Lambda t).$$

This method is, strictly speaking, only applicable to particles of a single size and to highly reactive gases which are irreversibly captured by the precipitation. Normally the method can only be applied in an empirical sense if a range of particle diameters is involved.

The resulting concentration in the rain may be expressed in terms of a related wash-out ratio ω:

$$C_r = \omega C_a$$

where C_r is the resulting concentration in the rain. If C_a and C_r are expressed in g m^{-3} then ω is usually of the order of 10^5. If, however, C_r is expressed in g l^{-1} then ω is of the order of 10^2. Note that ω depends on the total depth of the polluted column through which the rain falls. The values quoted refer to a depth of the order of 1000 m.

1.2 Wet deposition

The resulting wet deposition D_w is obtained by identifying the concentration in the rain in terms of g l^{-1} multiplied by the rainfall R in millimetres as the

deposition in terms of g m^{-2}.

$$D_w = C_r \times R = \omega C_a R.$$

The wash-out ratio can also be used to define a wet deposition velocity by analogy to the dry deposition velocity (see later).

$$v_w = \frac{dD_w}{dt} / C_a = \omega \frac{dR}{dt}$$

where t is here time, and the units of v_w are here in m s^{-1}. With light rain falling at a rate of 1 mm h^{-1} and a value of ω of 100, v_w is about 3 cm s^{-1}, which is of the order of a 1000 times greater than the corresponding dry deposition velocity.

Wash-out ratios for snow tend to be several-fold higher than for rain although R for snow is usually less than for rain due to the lower temperatures involved.

Λ is related to ω through the relation:

$$\Lambda = \frac{\omega}{h} \frac{dR}{dt}$$

where h is the depth of the polluted layer through which the rain is falling, R is in mm, and t, the time, is in seconds. Assuming $\omega = 100$, $h = 1000$ metres, then Λ is approximately $3 \times 10^{-5} R'$, where R' is the rainfall rate in mm h^{-1}. Jones (1983) suggests a value of Λ between 3×10^{-5} and 3×10^{-4}, consistent with our estimate when rain-out is artificially included and when we allow for heavier rainfall rates.

Note that we have assumed a linear relation between Λ and R. However, some theories and experimental evidence have pointed to a dependence:

$$\Lambda = aR'^{b}$$

where b is not 1 but lies in the range 0.7 to 0.9.

1.3 Rain-out

Rain-out is, as previously stated, generally even more efficient than wash-out if the pollution gets into the precipitating cloud. The relationships can be made exactly analogous to the relationships for wash-out. However ω is no longer a function of the depth through which the rain falls. Its magnitude is frequently 5–10 times greater than for wash-out. For reactive gases and hygroscopic particulates a value around 500 is typical. (The deposition of caesium-137 on the United Kingdom from the cloud of debris from the Chernobyl reactor accident implied a total ω of about 650 (Smith and Clark 1989).) The corresponding value of Λ is $1.5 \times 10^{-4} R'$, where R' is the rainfall rate in mm h^{-1}.

Note that if the equation for the deposition in terms of C_a and R uses mutually consistent units, so that R is given in metres, then $\omega = 5 \times 10^5$.

1.4 The measurement of wet deposition

By comparison with dry deposition, wet deposition is fairly easy to assess, although it certainly has its pitfalls. These pitfalls include:

(a) the difficulty of accurately measuring rainfall and snowfall,

(b) the variability of precipitation between sites separated by relatively short distances, especially in topographically complex terrain (like mountainous areas),

(c) with some pollutants the difficulty in sampling sufficient material to analyse,

(d) contamination or degradation of the collected rainwater before analysis takes place, and

(e) the additional effects of dry deposition whose representativeness in terms of deposition on surrounding natural surfaces is largely unquantified.

Generally it is best to use 'wet-only collectors' that are electrically controlled to open only when precipitation is falling, and the collected sample is kept at sufficiently low temperature to minimize degradation. It also helps to collect the samples at frequent intervals (e.g. daily) and analyse them as quickly as possible. Some research collectors can analyse the rainwater internally as soon as the amount in the collecting vessel reaches some prescribed amount. 'Bulk' collectors are open all the time and sacrifice some accuracy for the cheapness of the equipment. It is usually best with both types of collector to measure the absolute amount of rainfall with a properly exposed approved type of rain-gauge.

1.5 The seeder-feeder effect

In mountainous terrain a substantial proportion of the rainfall originates from the scavenging of cloud droplets in cloud capping the mountain tops, called 'feeder cloud', by rain falling from higher frontal cloud, called 'seeder cloud' (see Fig. 2 and Browning *et al.*

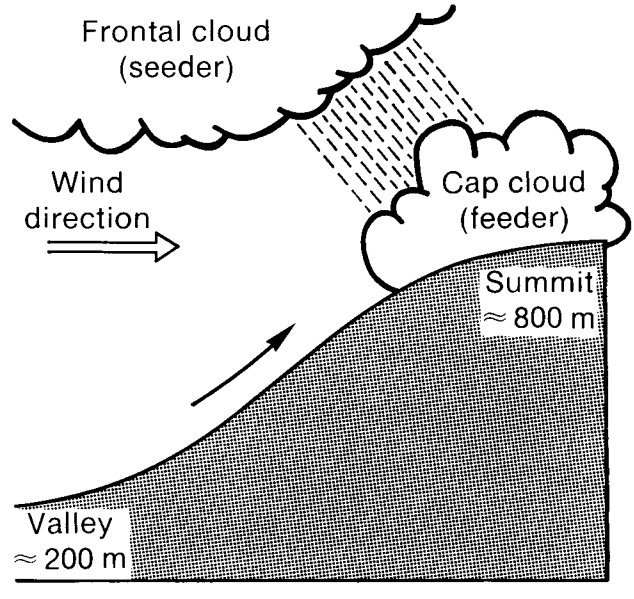

Figure 2. Seeder-feeder mechanism for enhanced rainfall concentrations of major ions in rain from Browning *et al.* (1974).

(1974)). The figure schematically shows the situation at Great Dun Fell which has been investigated by several research groups (see *Acid Deposition in the United Kingdom 1986–1988* Third Report of the UK Review Group on Acid Rain, Dept of the Environment, London). Two factors are important. The first is that the rainfall is enhanced by altitude. The enhancement depends on a number of factors including the details of the orography in the area. At Great Dun Fell the rainfall at the summit is roughly twice that at the upwind valley bottom. Fig. 3 shows a very broad-brush relationship between rainfall, normalized by an estimate of the equivalent mean-sea-level rainfall in the same area, as a function of the height of the mountain/hill tops. It should not be used as an exact relationship. It is simply inferred from comparing the average annual rainfall map for the United Kingdom with a physical map showing height contours. The second factor of importance is that since the feeder-cloud water often has concentrations of ions that are several-fold higher than those in the seeder-cloud, the concentrations of these ions in the rain reaching the ground over the hills is often much higher than in corresponding rain over lower ground. At Great Dun Fell the enhancement in concentration is about 2.5 so that the deposition, the product of concentration and rainfall, is enhanced five-fold at the summit. More generally, where simultaneous measurements have been made of orographic cloud and rain composition, the concentrations of major ions (like sulphate) in the cloud usually exceed those in rain by a factor ranging from 1.5 to 8.

The *Acid Deposition in the United Kingdom 1986–1988* Report, referred to above, has estimated the percentage enhancement of wet-deposited nitrate due to the seeder-feeder mechanism on a 20 km × 20 km grid. The seeder rainfall was estimated by linear interpolation between west coast rainfall and east coast rainfall. Actual rainfall in any grid square was inferred from the average annual rainfall map, and the excess over the inferred seeder rainfall was ascribed to the additional scavenging of feeder-cloud water whose concentrations of major ions were assumed to exceed those in seeder rain by a factor of two. Fig. 4 shows the results. It indicates that fairly substantial areas in the north and west may have 60% or more enhancement of nitrate deposition due to orographic effects.

Choularton in Choularton *et al.* (1988) and in his contribution to the report cited above has expressed these enhancements in terms of some of the parameters described earlier. He suggests that wherever the weather radar suggests that cloud is in contact with the surface (excluding radiation fogs) occult deposition (see later) can be modelled with an enhanced deposition velocity of 10 m s^{-1} for the pollutants believed to be within the

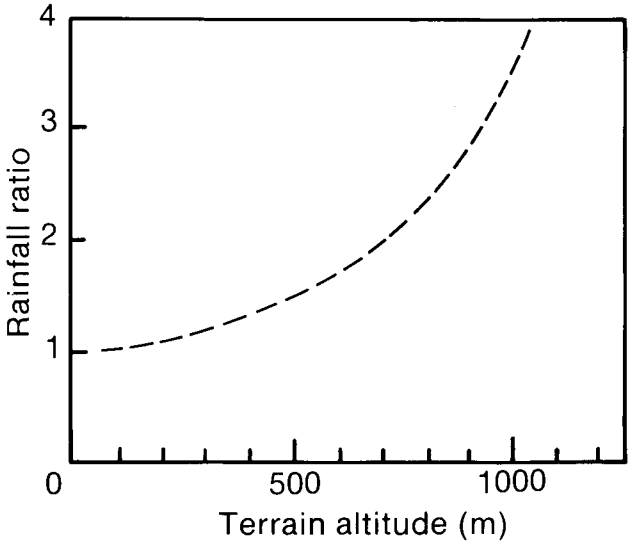

Figure 3. A rough guide to how rainfall, normalized by the equivalent sea-level rainfall in the same area, increases with terrain altitude.

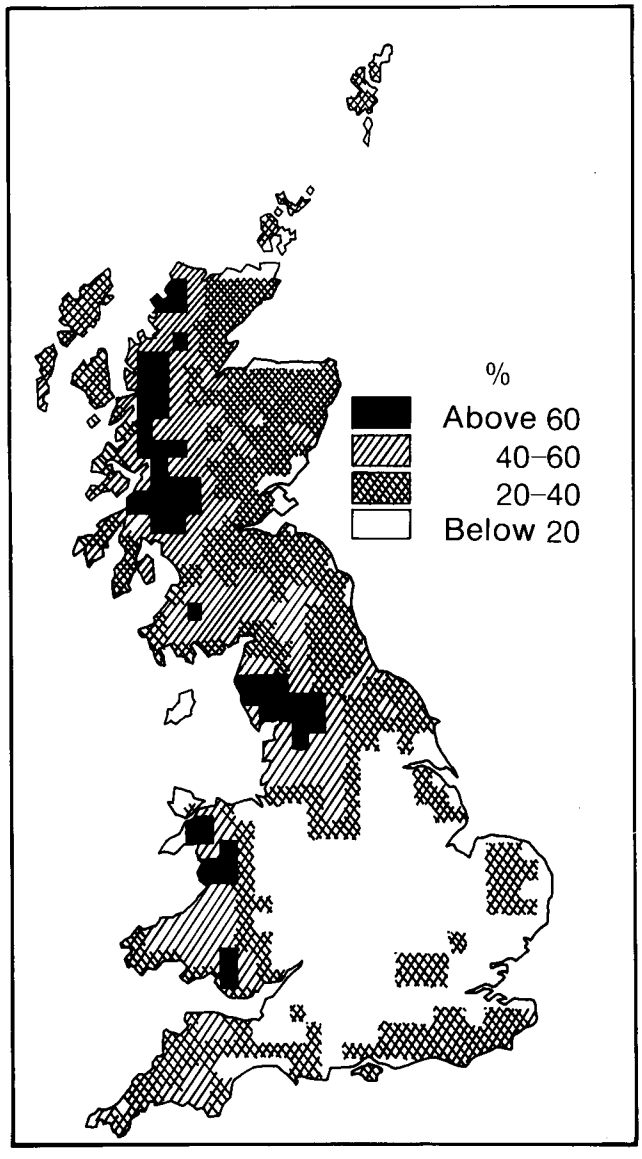

Figure 4. The estimated percentage enhancement in rainfall due to the seeder-feeder mechanism inferred by the method described in the text, due to Fowler *et al.* (1990).

cloud droplets, and that if the seeder-feeder mechanism is operative an enhanced scavenging coefficient should be used:

$$\Lambda = 3.4 \times 10^{-4} R'^{0.79}$$

where, again, R' is the rainfall rate in mm h^{-1}.

1.6 An important caveat

It should be stressed that this treatment of wet deposition has glossed over a great number of issues and complexities. Many of these are discussed by Slinn (1984).

2. Dry deposition

2.1 Introduction

The direct take-up of airborne gaseous or particulate material present in the lowest layers of the atmosphere to the surface or to vegetation by processes of absorption, impaction or sedimentation is called dry deposition, to distinguish it from deposition by precipitation, even though at times dew, cloud droplets or surface water may be involved.

Dry deposition on natural surfaces is very difficult to measure directly, certainly in any routine operational manner. Some alternative methods will be outlined later. The supposition is usually made that the rate of deposition, or flux, F, is proportional to the concentration in the air just above the surface at height z:

$$F = v_d C(z).$$

The coefficient v_d has the dimensions of a velocity and is therefore called the deposition velocity, and is a slowly varying function of height z. Normally it may be assumed that v_d is independent of the magnitude of $C(z)$ although it must depend on the physical and chemical characteristics of the species involved. Sometimes, however, the uptake of the species at the surface may be affected by how much of the species is already deposited. A good example of this is the reduction in the deposition rate of an acidic species on to a damp surface as the pH of the water film on the surface decreases as more of the species (and other acidic species) accumulate in the film.

If $C(z)$ is measured a metre or so above the ground then the stability of the air will influence how rapidly turbulent transfer can carry species down to the surface. In stable conditions, this transfer may become very slow as atmospheric turbulence is suppressed. The magnitude of $C(z)$ (for any specified emission rate) may also respond to changes in stability. Consequently v_d and $C(z)$ may both vary with stability in some systematic way. Consequently $\overline{v_d\, C(z)}$ averaged over a variety of stability conditions may be significantly different from $\overline{v_d}\ \overline{C(z)}$ (where the individual averaging is over the same ensemble of conditions). Similarly the ground may be both a potential source and sink of some species like ammonia (for example) and whether source or sink at any one time may depend on many factors likely to include the time of day, the time of year, temperature and other factors affecting relevant soil and vegetation processes. Here again v_d may take a range of possible values which correlate with $C(z)$.

In most real-life scenarios, surface conditions are not totally homogeneous so that v_d may change from point to point. The question of how to average v_d under these circumstances has not been entirely resolved, but a plausible suggestion is that v_d may be averaged in a way related to the way the surface roughness is averaged over heterogeneous terrain. If this is so then the average v_d is rather strongly influenced by a few 'hot-spots' of high-deposition rate and also might be a significant function of wind direction at any point.

2.2 Expression of deposition velocity in terms of resistance

Over horizontally uniform surfaces, the downward vertical flux may be expressed in terms of the eddy diffusivity $K(z)$:

$$F = K(z) \frac{dC}{dz}.$$

If F is virtually constant with height in the first 10 metres or so, then

$$C(z_2) - C(z_1) = \int_{z_1}^{z_2} \frac{F}{K(z)}\, dz \equiv F \int_{z_1}^{z_2} \frac{dz}{K(z)}$$

which is an analogous to Ohm's Law in electricity. The integral can therefore be compared to a resistance r. If $z_1 = 0$ and $C(0) = 0$, then

$$v_d^{-1} = \int_0^{z_2} \frac{dz}{K(z)} = r.$$

However, $K(z)$ is not defined in any simple way as $z \to 0$ corresponding to the actual physical surface. Consequently the resistance r is normally subdivided into an aerodynamic part plus parts appropriate to close to the surface:

$$r = \frac{1}{v_d} = r_a + r_b + r_s$$

where

r_a = the resistance to transport through the turbulent zone,

r_b = the resistance through the laminar sublayer very close to the physical surface,

r_s = surface resistance which will depend on one or more of surface moisture, pH, the reactivity of the species, the physical properties of the species and the status of the stomata on any vegetation.

By analogy with the flux of momentum

$$r_a = \frac{u(z)}{u_*^2} .$$

The sublayer resistance r_b has been expressed by Chamberlain (1960) as

$$r_b = \frac{1}{B u_*}$$

where B is a sublayer Stanton number. Chamberlain showed that B decreases slowly with increasing u_* but varies very little with surface roughness z_o. Typically $B \approx 0.125$ for gases.

The surface resistance is quite variable and the hardest of the three to estimate accurately. Rather typical values for a short grass field are as follows:

(a) wet conditions, $r_s \approx 0$,

(b) dry daytime conditions, $r_s \approx 50$–100, and

(c) dry night-time conditions, $r_s \approx 300$–1000.

Consequently semi-empirical values of v_d can be evaluated. For example, if $z_o = 0.1$ as it might be over growing wheat, and the stability is near neutral, then the values of v_d in Table I apply for a reactive gas.

The overall likely average of these numbers when averaged over a year are in reasonable accord with Fowler *et al.*'s (1991) estimate for the whole of the United Kingdom with all its different surfaces. His estimate for sulphur dioxide is 0.24 cm s^{-1}. Fowler divided the United Kingdom into 20 × 20 km grid squares and used up to five land-use categories in each square using a classification method developed at the UK Institute of Terrestrial Ecology. The atmospheric resistances ($r_a + r_b$) were calculated from the z_o of the vegetation and average wind speeds assuming a logarithmic wind profile in the surface boundary layer. For each vegetation type a seasonal pattern of leaf area was defined, and the physiological processes controlling gas uptake by stomata were modelled using 'big leaf' methods for a range of vegetative species. The resulting v_d show a marked diurnal and annual variation, as exampled by the variation over a pine forest as seen in Fig. 5. Fowler notes the pronounced effect of day length on stomatal opening and hence on the deposition velocity. The very small December increase in v_d is due also to the temperatures then being close to the threshold for stomatal opening. In midsummer the value of v_d dips slightly at midday due to typical water stress on the trees at that time.

Table I. Typical values of v_d over growing wheat when the wind speed and the concentration of the depositing reactive gas are measured at 10 metres in neutral stability conditions

Conditions	$U_{10} = 2$ m s^{-1}	$U_{10} = 8$ m s^{-1}
Wet	0.89 cm s^{-1}	3.56 cm s^{-1}
Day dry	0.53 cm s^{-1}	0.97 cm s^{-1}
Night dry	0.16 cm s^{-1}	0.19 cm s^{-1}

2.3 Dry deposition of particles

The deposition of particles to surfaces depends very much on their ability to cross the laminar sublayer. Large particles whose diameters exceed 10 μm are usually heavy enough to fall through by sedimentation or by the inertia of the particles. In contrast very small

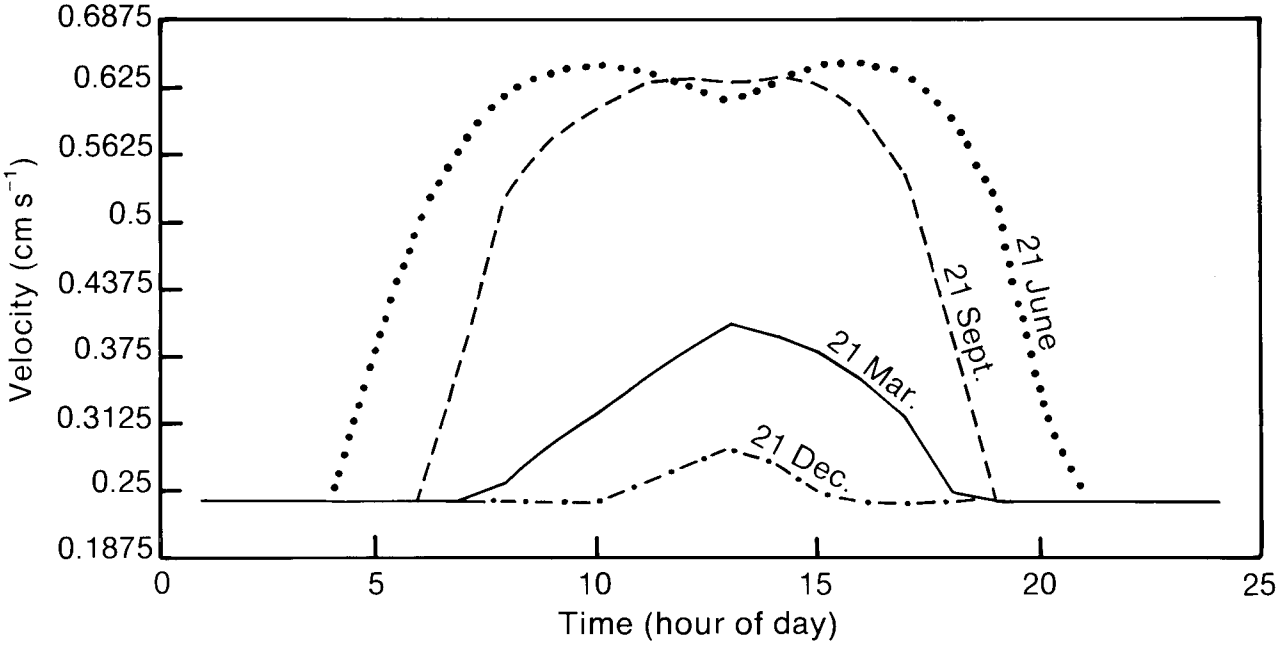

Figure 5. The diurnal cycle in the deposition velocity of sulphur dioxide gas to a UK forest at four different times of the year (Fowler *et al.* (1990)).

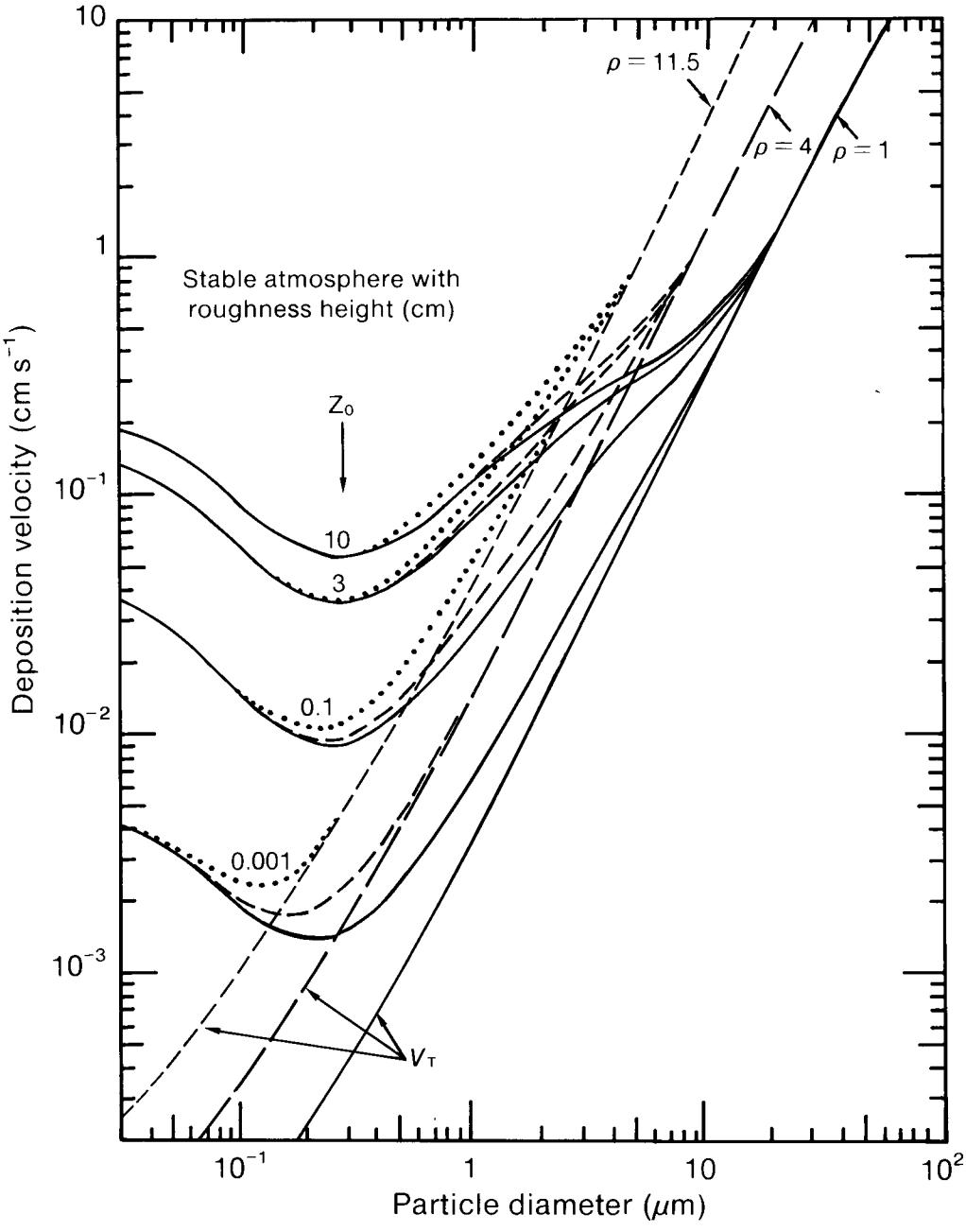

Figure 6. Extrapolation from correlations of wind-tunnel measured deposition velocities at a reference height of 1 m, for particles of density 1, 4 and 11.5 g cm^{-3} (after Sehmel (1980)). V_T represents the terminal settling velocity. The diagram comes from Nicholson (1988).

particles whose diameters are less than 0.1 μm are quite responsive to Brownian motions and can diffuse across the layer. Intermediate sized particles however tend to be too large to be affected by Brownian motions and too small to have sufficient inertia or weight to penetrate the layer. These sized particles therefore display minimum values of v_d within the range of diameter as can be seen in Fig. 6 which comes from a review paper by Nicholson (1988).

2.4 The measurement of estimation of dry deposition velocity

Various methods have been devised for estimating the dry deposition velocities of various species in various field conditions (see Hicks (1986) for a fuller description). On the whole it seems these methods tend to be more successful overall for gases than for particulates although the reasons for this are not fully understood. The different methods can be classified as follows: micrometeorological methods (profile methods and correlation methods), collection on to surrogate surfaces, collection on to natural surfaces, and budget techniques.

2.5 Profile method

This method depends on a direct analogy between the downward flux of the depositing species and the flux of heat and momentum. It uses the flux-gradient relationship

$$F = K(z)\frac{dC}{dz},$$

where $K(z)$ is inferred from the wind profile. In near-neutral conditions $K(z) \approx ku_*z$. This method, as well as the correlation method, involves collecting data over a period of time that is unlikely to exceed at most a few hours. These methods are therefore best suited to studying the effects of environmental conditions on deposition mechanisms. The profile method is only suitable for a limited range of species, mainly the more reactive gases, and is only recommended when other methods cannot be used. A typical error in v_d for a reactive gas, inferred from data collected over 30–60 minutes, is about 0.05 cm s^{-1}. At best it is difficult to measure the small gradients accurately, partly because of the wide range of time-scales involved in the concentration fluctuations. Moreover, it is advisable to use the same intrument to measure the concentrations at the different heights to avoid spurious gradients implied by different instruments with slightly different responses. It is also expedient to sample over a large range of heights within a layer that is nevertheless shallow enough to be contained within the so-called constant-stress layer. It is also important to make these measurements within a period of time when the meteorological conditions are not changing. Finally the site has to have a large uniform upwind fetch so that the profile is not affected by upwind variations in deposition rate and surface roughness and sensible heat flux.

It is not surprising that with all these caveats the method is prone to significant error. The method appears to work best for gases. Particles of a few μm in size are probably the largest that can have their v_d estimated by this approach.

2.6 Correlation methods

Eddy-correlation techniques require the simultaneous measurement of vertical velocity and concentration with sufficient time response over the range of frequencies in which the two are effectively correlated. Unfortunately while there are a number of instruments capable of measuring certain gaseous concentrations with adequate response, there are few instruments available for measuring particle concentrations on the right time-scale (thought to be about half a second). Electrical and optical sensors have been used, as have flame photometric detectors. The method depends on the identity $F = -\overline{wc}$.

It is necessary to eliminate any small residual mean vertical velocity due to a finite sampling period or due to the peculiar position of the site or due to a false alignment of the anemometer. Elimination can be realized by numerical or electronic filtration of the data before the mean product is calculated.

The eddy-correlation technique has provided the most consistent and controversial differences between field estimates of v_d and those estimated from theory and wind-tunnel studies. In particular, values found by the flame photometer detectors seem to be consistently an order of magnitude greater than those found from the latter methods. They also sometimes give unexpected upward fluxes at night, and the overall impression is that further study of this method is required before its findings can be trusted. Differences encountered with particles may be due in some cases to the presence of large particles, although this requires verification in actual field studies.

2.7 Surrogate surfaces

The use of surrogate surfaces appears to be successful although the results strictly only apply to those surrogate materials and not necessarily to natural surfaces in the same situation. Wet/dry bucket samplers are thought to work best for particles with a significant terminal velocity. Results for certain radionuclides appear to agree with known inputs and atmospheric concentration fields. Success with some of the acidic species is less certain because of the difficulty in totally eliminating contamination from wind-blown dust, from insects and from bird droppings. Surrogate collectors may also disturb the airflow and are not representative of the real surface of interest. For example, buckets have been found to over-collect particles with diameters much greater than 1 μm but under-collect sub-micron particles. Consequently it is very important to know the particle size spectrum and to be able to correct for these collection effects to some reasonable extent. Although surrogate surfaces seem best for larger particles, gases have also been collected on special filter-paper surfaces.

Overall the results from surrogate surfaces are comparable to those found by other reliable techniques.

2.8 Natural surfaces

Perhaps the most obvious method for particles is to use natural surfaces. Whilst leaves can be removed and the particles washed off and analysed, it is much harder to deal with creviced bark and some other natural materials. These surfaces are much less convenient in the sense it is harder to wash-off the particles for analysis, and they may be 'contaminated' by wet deposition. Another problem is that vegetation may take up the same species through their roots and these may be partially leached to the leaf surface and affect the results of analysis.

The estimates of v_d obtained from a limited number of samples may also be prone to error because of the wide variety of orientations and exposure of natural surfaces.

Measurements of deposition to snow have been frequently studied. The analysis is relatively easy and is representative of fairly uniform surfaces. Since the deposition rates depend on particle size, the greatest difficulty encountered here is to measure accurately the particle size spectrum in the air itself.

Overall the agreement between results from this method and those from theory and from wind-tunnel experiments is generally poor. In addition to the reasons

already postulated, the effect of the complicated flow pattern around trees and other vegetation could easily have a profound effect.

2.9 Budget methods

This method is perhaps applicable when concerned with transport over very long distances well in excess of 100 km and only when a broad average deposition velocity is required. Two approaches may be used. The first is to optimize the agreement between model predicted air concentrations (using an operational model like the EMEP (European Monitoring and Evaluation Programme) model for acid species over Europe) and observed daily-averaged concentrations measured at many monitoring stations across the region by adjusting the value of the deposition velocity in the model. For example the EMEP model allows for loss of the species from the boundary layer into the free troposphere above, only in a highly parametrized manner, and any systematic error would result in an erroneous v_d.

The second approach is to compare the total downwind flux of the species using an instrumented aircraft to fly at different levels across the plume with either the emission strength at the source or the total flux at some other distance separated sufficiently from the first to yield a measurable difference of flux. This has been done several times by the Meteorological Office and The UK Central Electricity Research Laboratories over the North Sea in which the flux of sulphur dioxide and sulphate originating from a large power station has been studied.

On a smaller scale the same principle can be applied although it is then often necessary to label the particle species, for example by using an isotope of the species which can be readily detected *in situ* by a Geiger counter, for example.

2.10 How important is dry deposition to the long-term total deposition?

On the whole, micron-sized and submicron-sized particles dry deposit relatively slowly with deposition velocities smaller than 0.1 cm s^{-1}. However many of them are rather efficiently washed out or rained out in precipitation. Under these circumstances dry deposition only contributes a rather small proportion of the total deposition in Europe. Reactive gases like sulphur dioxide dry deposit more readily. If we take Fowler's estimate of 0.24 cm s^{-1} for sulphur dioxide as valid, then in a location which has an annual average rainfall of, say, 800 mm and assuming the simple wet deposition law discussed in section 1.2:

$$\text{wet deposition} = D_w = \omega CR$$

where C is the average air concentration and R is the annual rainfall in millimetres, and w is a coefficient whose magnitude is around 500. If $C = 10\ \mu g\ m^{-3}$ then the annual dry deposition is about 0.76 g SO_2 m^{-2} and the wet deposition would be 2 g SO_2 m^{-2}, on the assumption that in rain the average concentration in the air is only about half the annual average since rain cleans the air so relatively quickly. Dry deposition would then constitute only about 32% of the total. Also since it typically rains only about 3–4% of the time this means that wet deposition is about 50–100 times more efficient than dry deposition when it is actually occurring.

2.11 Effect of dry deposition on long-range transport

Neglecting the spatial variations in the deposition velocity that must occur, the effect on the amount of material still airborne can be represented rather simply by a source-depletion method provided the value of v_d is not too high (i.e. comparable to the vertical turbulent velocities). In the simplest models of long-range transport the easiest way to allow for dry deposition is then by assuming that the pollutant is at all times vertically well-mixed within the boundary layer. The concentration in the air is then a function of the horizontal co-ordinates x and y. Integrating acrosswind $C = C(x)$. The variation with x is then given by:

$$\frac{\partial C}{\partial x} = \frac{1}{u}\frac{\partial C}{\partial t} = -\frac{1}{u}\frac{v_d C}{h'}$$

i.e.

$$C = C_o \exp\left(-\frac{v_d x}{uh}\right)$$

where h is the depth of the boundary layer. Typically $h = 600$ m, $u = 8$ m s^{-1} and, for sulphur, $v_d = 0.2$ cm s^{-1} so that the length-scale, L, is given by:

$$\text{dry deposition length} — L = \frac{uh}{v_d} = \frac{600 \times 8}{0.2 \times 10}\ \text{km},$$

i.e.

$$L = 2400\ \text{km}.$$

Since the flux F of the material to the ground is proportional to $v_d\, C(x)$, differentiating with respect to v_d and putting the result to zero, says that the rate of dry deposition is very insensitive to the exact value of the overall v_d at downwind distances between about 1000 km and 4000 km. The overall decrease in concentration with larger v_d virtually balances the larger v_d in the expression for the dry deposition within the range of distances.

3. Occult deposition

Sometimes cloud or fog is at ground level, particularly on hills in maritime climates. Pollutants within the boundary layer are advected up the hillside and become absorbed into cloud droplets as the moisture in the air condenses or may form the condensation nuclei on which the droplets grow. Soon after the condensation

level the droplets are often large enough so that as they blow across the vegetation they are deposited on to the foliage, carrying the pollutants with them. This form of deposition is called occult (or hidden) deposition because it is not easily assessed from standard meteorological data.

The capture of wind-driven cloud droplets by vegetation has been measured in several field experiments (Gallagher *et al.* 1988, Fowler *et al.* 1991). These experiments show that the process is efficient with equivalent deposition velocities of 1–4 cm s^{-1} over moorland and in excess of 10 cm s^{-1} over forests. Moreover, the relatively large concentration of major ions in cloud water (50–2000 μeq l^{-1}) increases the importance of this pathway in upland areas. Fowler *et al.* (1991) have estimated the average annual occult deposition rate over the United Kingdom. They did this as follows:

(a) The country was divided into 20 × 20 km grid squares.

(b) Cloud-base statistics were interpolated from meteorological records to each of the squares.

(c) Wind velocity data were also interpolated to the squares.

(d) A land-use database was used to infer the proportion of land within each square which is either forest, moorland, grassland or arable crop-land. The altitude of these areas was also obtained.

(e) The data from (d) were used to obtain average z_o, and hence v_d.

(f) Surface cloud was assumed to contain concentrations of major ions a factor of 2 larger than in normal rain, as measured in the UK air pollution 'secondary' network.

(g) Liquid water content of the cloud water was taken as 0.2 g m^{-3}.

Resulting implied occult depositions, averaged over each 20 × 20 km grid square, ranged from very small values in most lowland areas to in excess of 160 mgS m^{-2} a^{-1} for the sulphur ions in some of the mountainous areas of Scotland (in the Cairngorms) where normal dry deposition is only about 40 mgS m^{-2} a^{-1} and wet deposition is about 600 mgS m^{-2} a^{-1}.

Radiation fogs, which occur rather frequently in some maritime lowland areas in winter, contribute relatively little to the annual deposition of major ions because the wind speeds are normally very small under these conditions.

References

Browning, K.A., Hill, F.F. and Pardoe, C.W., 1974: Structure and mechanism of precipitation and the effect of orography in a winter-time warm sector. *Q J R Meteorol Soc*, **100**, 309–330.

Chamberlain, A.C., 1960: Aspects of the deposition of radioactive and other gases and particles. *Int J Air Pollut*, **3**, 63–88.

Choularton, T.W., Gay, M.J., Jones, A., Fowler, D., Cape, J.N. and Leith, I.D., 1988: The influence of altitude on wet deposition. Comparisons between field measurements at Great Dun Fell and predictions of a seeder-feeder model. *Atmos Environ*, **22**, 1363–1371.

Fowler, D., Morse, A.P., Gallagher, M.W., Choularton, T.W. and Dore, A., (1991): Measurements of cloud water deposition on vegetation using a lysimeter and a flux gradient technique. To appear in *Tellus*.

Gallagher, M.W., Choularton, T.W., Morse, A.P. and Fowler, D., 1988: Measurements of the size dependence of cloud droplet deposition at a hill site. *Q J R Meteorol Soc*, **114**, 1291–1303.

Hicks, B.B., 1986: Measuring dry deposition: a re-assessment of the state of the art. *Water, Air and Soil Pollut*, **30**, 75–90.

Jones, J.A., 1983: Fifth report of a working group on atmospheric dispersion. Chilton, Oxfordshire, National Radiological Protection Board.

Lyons, T. and Scott, W., 1990: Principles of air pollution meteorology. London, Belhaven Press.

Nicholson, K.W., 1988: The dry deposition of small particles: a review of experimental measurements. *Atmos Environ*, **22**, 2653–2666.

Sehmel, G.A., 1980: Particle and gas dry deposition review. *Atmos Environ*, **14**, 983–1011.

Slinn, W.G., 1984: Precipitation scavenging. *In* Randerson, D. (ed.); Atmospheric science and power production. US Dept of Energy, Technical Information Center.

Smith, F.B. and Clark, M.J., 1989: The transport and deposition of airborne debris from the Chernobyl nuclear power plant accident with special emphasis on the consequences to the United Kingdom. *Sci Pap, Meteorol Off*, No. 42.

Smith, F.B. and Hunt, R.D., 1978: Meteorological aspects of the transport of pollution over long distances. *Atmos Environ*, **12**, 461–478.

551.509.314:551.509.5

On the use of numerical probabilities in weather forecasting

R.M. Morris
Meteorological Office, Bracknell

Summary

A concept of risk assessment in weather forecasts expressed as numerical probabilities is considered from the point of view of the customer as well as that of the forecaster. For the customer the information quantifies the risk of specific events occurring or the risk of specific thresholds being exceeded, e.g. temperatures falling below 0 °C during defined periods of time. For the forecaster the concept is an intrinsic one because it allows him to express his forecasts in a language that is ideally suited to his perception of the evolution of a weather system on any occasion. For both customer and forecaster the concept has the immensely powerful attribute that it is amenable to objective evaluation thereby providing a measure of skill and an assessment of the forecaster's value to the customer.

1. Introduction

The notion that weather forecasting is an inexact science is (probably) properly understood by only a small number of enlightened people. Most interpret it to mean that forecasts cannot be relied upon for accuracy — defined in some way. What is not appreciated is the reason why the accuracy can vary and that it is possible for a forecaster to anticipate the likelihood of the forecast being within or outside the range of average accuracy as defined. The key word is 'accuracy' and the definition will almost certainly depend upon what is at stake. For example horticulturists are not too concerned if the temperature falls to +8 °C rather than +11 °C but they would be very concerned if it fell to 0 °C rather than +2 °C. Similarly offshore drillers are not too concerned whether the wind is 5 kn or 30 kn but if it reaches 65 kn rather than 55 kn they are very concerned because the risers are liable to break at such speeds. These examples reveal that the most important consideration for many users of weather forecasts is risk assessment in relation to specific thresholds, rather than categorical forecasts.

The use of probabilities in weather forecasting in the United Kingdom is extremely limited and, until recently, confined entirely to some commercial forecasts. The most extensive use is found in forecasting for aviation, for aerodromes as well as *en route* weather. On the face of it, it is surprising that greater use is not made of risk assessment forecasts by industry and commerce since the concept would appear most suitable for their needs. The main reason for this could be the lack of clear guidelines issued by the forecasters on how to interpret probability forecasts. For example a recent study in the USA, where probabilities are used in public forecasts disseminated on radio and television, showed that people were confused as to whether a 10% chance of rain meant that 10% of the area would have rain or whether there was a 1 in 10 chance of rain affecting anyone. (Despite this apparent ambiguity the public appear to prefer numerical values to words by a 2:1 majority.)

Then there is the tricky question of how the forecast is to be used to make commercial decisions; given a 30% chance of frost the horticulturist can weigh up the risk to his flowers in terms of cost to himself but he also needs to know something about the quality of the forecast service too. In other words is that 30% chance realistic, pessimistic or optimistic. Fortunately probability forecasts are very amenable to verification which helps in making these decisions.

Public interest in risk assessment attached to weather forecasts has increased in the United Kingdom, almost certainly as a consequence of the severe winter storms experienced in early 1990. National radio and television companies are now keen to issue forecasts in this format to the public. It is appropriate therefore to look at the concept of probability forecasting from the practical point of view of the forecaster and the user who has to interpret the information.

2. Qualitative forecasts

Descriptive weather forecasts are most widely used for issue to the public through Press, radio and television, Videotex and TIS (Telephone Information Services), etc. It is a very convenient way of describing weather conditions likely to affect an area over a period of time. Unfortunately, in achieving this objective there is a loss of precision in the forecast. Subjective interpretation by the user of the information is paramount and it is very difficult to verify the accuracy of the forecast. Risk may be mentioned in the forecast, e.g. 'perhaps later' but never quantified.

A descriptive forecast serves a very useful purpose as an overview of the weather situation or as a preamble to a more detailed site-specific forecast, but except in the most simplistic weather situations its utility is distinctly limited. The information content is scanty and the scope for misinterpretation of language is large.

3. Categorical forecasts

Quantitative forecasts of weather elements, e.g. wind, temperature, precipitation, cloud, etc. are issued widely to industry and commerce on a commercial basis. Wind and max./min. temperatures are also issued to the public. Values of the elements are necessarily for fixed sites and usually for fixed times. Interpolation problems are minimized by increasing the number of sites and decreasing the temporal spacing of forecasts at each site through the forecast period. These forecasts are precise and categorical and many commercial customers insert the figures into prediction models to help with their own decision-making.

To the forecaster, categorical values of weather elements represent the best estimate that the man–machine mix can provide. To the user, the information is unequivocal and unambiguous but, in making his own decisions, he still has to make some allowance for forecast error.

Assuming that reliable and accurate observations are available, categorical forecasts are easily verified. The most common parameters derived for this purpose are the mean error and the root-mean-square (r.m.s.) error. Both can be applied to scalar and vector fields. The mean error gives an indication of any bias and the r.m.s. error gives a measure of the spread of forecast values from the actual values obtained. Given a zero bias and normal distribution of data, the user may expect about 84% of all forecasts to lie within one r.m.s. error and 98% of all forecasts to lie within twice the r.m.s. error range of accuracy. Figs 1(a) and 1(b) illustrate typical r.m.s. error distributions with increasing forecast period for surface wind and surface temperature for specific locations. The error values are calculated from a large sample of data. Superimposed on each graph is a specific set of forecasts issued on one occasion for that location. The recipient of the forecast data can assess the implications of the range of error at each forecast time.

Consider Fig. 1(a); in fact the r.m.s. values plotted here are the mean for a cluster of six offshore platforms in the central and northern North Sea and indicate a steady increase of error as the forecast period increases. The forecast values are for one platform in the cluster with a peak wind speed of 30 m s^{-1} at T+96. If the Offshore Installation Manager (OIM) interprets this forecast sensibly he would deduce that a reasonable expectation is for the actual wind to lie in the range 25–35 m s^{-1} but he cannot ignore the possibility that the actual value will lie outside this range. The statistical accuracy can be presented in a slightly more revealing way by looking at the errors with respect to wind speed observed. Fig. 2 shows this for four bands of wind speed and not surprisingly the errors are rather greater for the higher speeds; note too that the mean errors show a small positive bias at low speeds and a definite negative bias at high speeds. The most practical use that the OIM can make of this information is to recognize that if a stormy spell of weather is expected then the forecasts are likely to underestimate the severity at some stage.

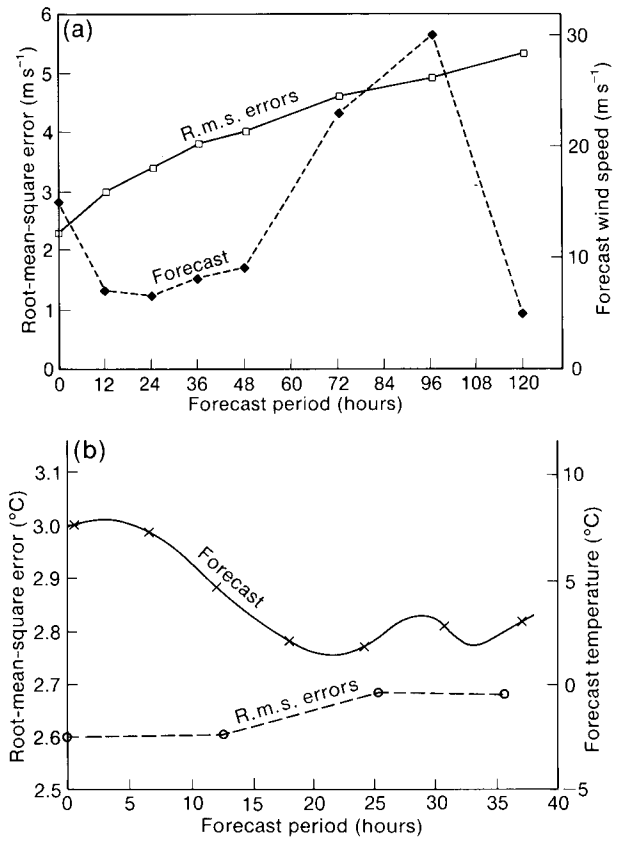

Figure 1. Typical root-mean-square errors with respect to forecast period, and a specific forecast of site values for (a) wind speed and (b) temperature.

4. Causes of variation in accuracy

Weather forecasts are largely based upon Numerical Weather Prediction (NWP) models nowadays, with the (human) forecaster having the role of fine-tuning the product and adding value to it. There are two fundamental reasons why NWP models do not yield perfect forecasts: firstly there is the limitation of the modelling itself, e.g. simulation of the complex processes of transferring heat, momentum and moisture through the atmospheric boundary layer, and secondly the starting conditions, from which the complex equations are integrated forward in time, are imperfectly specified. To put matters in perspective, modern NWP systems contain about one million points in the model global atmosphere at each of which equations are solved to produce forecast values of wind, temperatures, pressure and humidity — and yet the total number of data values available as starting conditions is one order of magnitude less than this. Thus there is a high degree of interpolation required at the start, more in some areas than others. To make matters worse the data contain errors too, and part of the analysis process is concerned with minimizing these errors — a task requiring a good deal of skill.

Despite these limitations, NWP global models consistently yield good guidance on the evolution of weather systems up to 5 days ahead, and occasionally up to 8–9 days depending on the stability of the weather situation. Most impressively the models can predict the

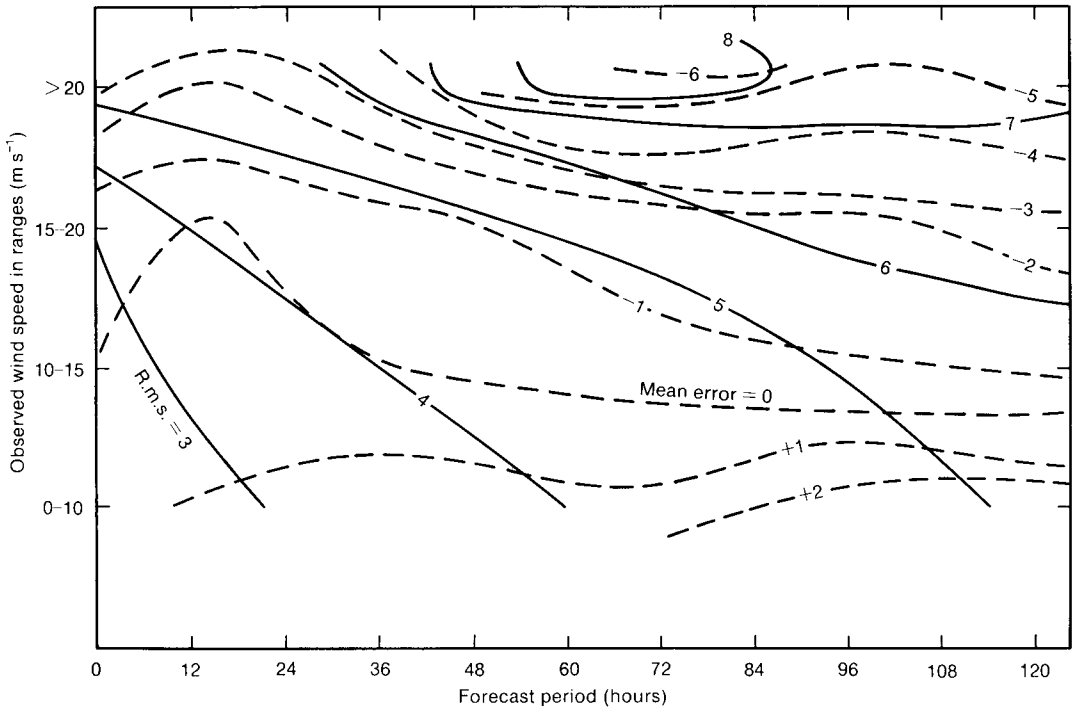

Figure 2. Errors and root-mean-square errors of wind speeds in ranges with respect to forecast period.

birth and growth to peak intensity of major depressions several days before the event. Finer-grid (but limited area) models are used to predict the evolution of sharp boundaries rather better, e.g. fronts with associated precipitation. The modelling of land topography depends upon the grid used and in order to produce realistic forecast values of weather variables for valleys, plains and mountain slopes, mesoscale models with spacing between points of only 10–15 km are used.

The above considerations lead to a broad categorization of error sources as follows:

(a) features poorly represented in the analysis,
(b) speed of development poorly simulated,
(c) speed of movement of a system too slow or too fast, and
(d) local topographical effects poorly represented.

Even small errors as defined above can lead to large inaccuracies when verification is applied to a fixed place at a fixed time. This is largely because the spatial variation of a weather element is not usually uniform; rather there are sharp gradients of wind, temperature and precipitation associated with fronts and troughs for example.

This knowledge may help the user to understand the uncertainties associated with his forecast but is there a way in which the forecaster can express this uncertainty which minimizes the range of error that the user has to allow for on a specific occasion?

5. Risk assessment — a value-adding process by the forecaster

A competent and efficient forecasting organization will have a thorough knowledge of the characteristics and formulation, and hence limitations, of the NWP models which support it. Thus systematic errors which occur in specific situations can be anticipated, e.g. a tendency to move fronts too quickly northwards in winter (say) or a tendency to underestimate the speed of development of intense depressions in certain geographical areas. By monitoring the NWP forecast and comparing with the analysis, deficiencies can be spotted early and consequences allowed for. Local forecasters develop expertise in noting how mesoscale topography can modify weather conditions in small localities. What all this means is that the forecaster can make a quantitative estimate of the likely error in a specific forecast which may be more or may be less than the average r.m.s. errors at a specific place.

It follows therefore that the forecaster could, in principle, issue modified error bands associated with each forecast, which the user may compare with the r.m.s. errors. He would then know whether to have more (or less) confidence in the forecast than usual. Unfortunately this would be a very laborious task for the forecaster but more importantly it would not necessarily help the user to make the right decisions.

To help the user interpret the (categorical) forecast it is necessary to know what values of a specific weather element are most important to him. Thus, in the example given of a forecast wind speed of 30 m s^{-1} at T+96, the crucial threshold for damage may be 35 m s^{-1} and since this figure is precisely one r.m.s. error range above the forecast then clearly it is a matter of assessing the risk. The uncertainty can be quantified by the forecaster from his consideration of all the aspects of the particular synoptic situation. If the forecaster is very confident that the wind will reach 30 m s^{-1} (perhaps with

some timing error) then the user will almost certainly decide not to risk damage and make alternative plans. On the other hand the synoptic situation may be quite volatile, e.g. different NWP models offering different solutions and solutions changing with succeeding initial conditions, and the forecaster's confidence in the 30 m s^{-1} value corresponding lower. On this basis the user may decide to delay making the decision until the situation is more certain.

It may be argued that consideration of uncertainty is best handled by direct dialogue between the forecaster and the user. This is probably true but there are two drawbacks; it may not always be possible to talk to the forecaster at short notice and, importantly, there is no objective means of evaluating the accuracy of the forecaster's advice. These difficulties can be minimized by the issue of a risk assessment table, constructed by the forecaster, which states the likelihood of a weather event occurring in a specified period. The risk is usually defined as a probability, with values ranging from 0 (no chance) to 1 (certain). Table I illustrates the concept in relation to wind speed threshold values at an offshore location. Although the scheme is best applied to specific sites for ease of verification, the principle can also be applied to areas on the assumption that a single occurrence of the event within the area implies a hit. Each user of the information should have his own thresholds to which the risk relates. On the face of it the user is now in possession of all the forecast information he needs to make his decisions — with one exception — how reliable is the forecast service? Should he make any allowance for shortcomings in the service?

One of the prime advantages of a forecast in numerical probability terms is its suitability to meaningful evaluation. There are several characteristics of forecasting performance that can be assessed:

(a) Bias — does the forecaster consistently overestimate or underestimate the risk?

(b) Accuracy — Brier scores can be calculated as a measure of accuracy.

(c) Skill — the Brier score may be compared with similar scores for climatology, persistence, NWP categorical and, of course, other forecasters.

Table I. Wind speed probability forecasts, for an oilfield, issued at 0900 UTC on 1 January 1990

Date	Period (UTC)	Wind speed (kn) probabilities >30	>45	>60
1st	1200–1800	0.4	0.1	0.0
	1800–2400	0.2	0.0	0.0
2nd	0001–0600	0.2	0.1	0.0
	0600–1200	0.6	0.5	0.3
	1200–2400	0.7	0.4	0.1
3rd	0001–1200	0.8	0.6	0.3
	1200–2400	0.7	0.4	0.2
4th	0001–1200	0.5	0.3	0.0

6. Bias — use of reliability diagrams

A lot of information about the forecaster performance can be derived from examination of the distribution of forecast probability against the observed relative frequency of occurrence of the event (summed over a number of forecast issues). Figs 3(a)–3(d) illustrate some examples. For the perfect forecaster who always issues probabilities of 0 or 1 and always succeeds there will only be two points on the graph. The realistic forecaster will use the full range of probabilities, and if he is perfectly calibrated all points will lie on the leading diagonal. In practice the forecaster is unlikely to be so good; Figs 3(c) and 3(d) show contrasting performance in the remote forecasting of rainfall (defined as wet or dry) and fog respectively for a specific location within a specified period. Apart from the curious over-optimism in use of P = 0.9 the forecasting of uncertainty in rainfall occurrence is quite reliable. By contrast there is clearly over-forecasting of fog which is perhaps not surprising in view of the patchy distribution of the element and the desire of the forecaster to cover his expectation in some way. (In this latter case one would expect the local forecaster to do better, given his superior knowledge of local climatology.) Reliability diagrams may be drawn up for any threshold, e.g. winds exceeding 35 m s^{-1}.

7. Skill — use of Brier scores

A probability forecast, e.g. Table I, can be verified by noting whether the event occurred or not and scored using the Brier scheme:

$$\text{score} = (V-P)^2$$

where P = forecast probability, and
V = 1 if event occurs, and
= 0 if event does not occur.

It can be seen that the best score is zero and the worst score is one.

The Brier score (BS) is objective and provides an evaluation measure that encourages forecasters to make forecasts that truly reflect their judgement, i.e. the forecaster cannot maximize his expected score by hedging. Taken in conjuction with the reliability curves, the Brier scores provide a useful quantitative measure of the quality of the forecaster's advice. Clearly one can compare the merits of different forecasting services from comparison of these parameters providing, of course, the same periods, thresholds and locations are used.

A measure of absolute accuracy is one characteristic, but skill may be quite another. In essence, skill is all about showing that the forecaster can give better advice to the user than if he simply relied upon climatology (clim) or persistence (pers) to estimate a future weather condition. This is a commercially important consideration; it is also extremely useful for the forecaster to know what he is up against! NWP and persistence forecasts are usually expressed in categorical terms, i.e.

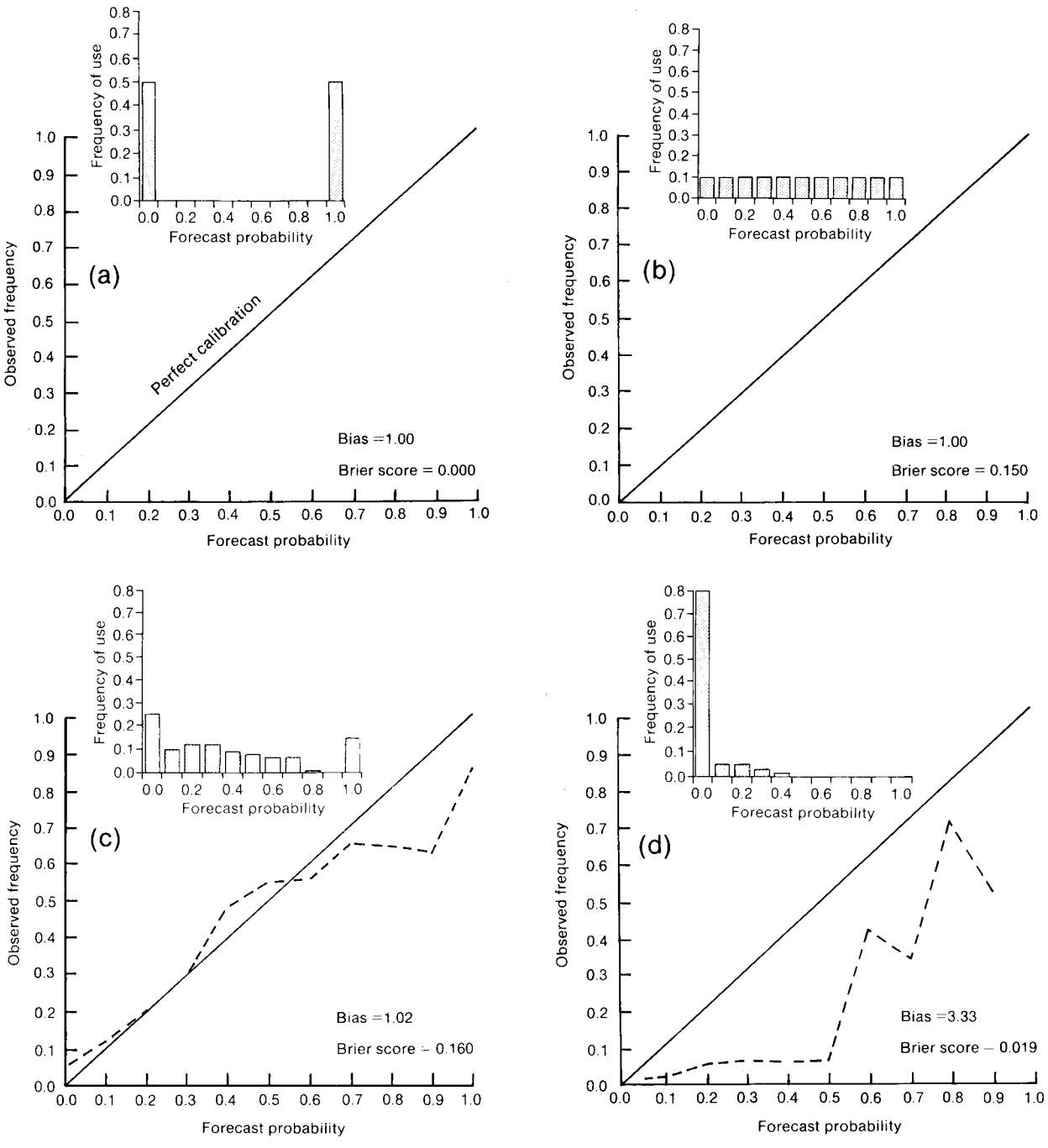

Figure 3. Forecast probabilities compared with observed frequencies for (a) perfect prognosis, (b) perfect reliability, (c) actual performance for rainfall over a period, and (d) as (c) but for fog. In each diagram a histogram of the frequency of use of the forecast probabilities is included.

probabilities of 0 or 1, in relation to specific thresholds, and can be scored accordingly. Forecasts based on climatology can be expressed in categorical or probabilistic terms, although the latter is not usually readily available. The skill is defined as follows:

$$\text{skill score} = \frac{\text{BS (clim/pers/NWP)} - \text{BS}}{\text{BS (clim/pers/NWP)}} \times 100.$$

It could be asserted that the case for probability forecasts rests on the demonstration of positive skill compared with the alternative means of expressing forecasts.

More detailed information on probability forecast evaluation is contained in the Appendix.

Acknowledgements

The assistance of John Norris whilst a chief forecaster in the Central Forecasting Office at Bracknell, who provided the calculations of Brier scores and the reliability diagrams, is gratefully acknowledged. Also thanks to Mrs Mai McGinnigle for help with the illustrations and finally the advice and encouragement from Professor Allan Murphy was much appreciated.

References and Bibliography

Brier, G.W., 1950: Verification of forecasts expressed in terms of probability. *Mon Weather Rev*, **78**, 1–3.

Murphy, A.H., 1973: A new vector partition of the probability score. *J Appl Meteorol*, **12**, 595–600.

Murphy, A.H. and Dann, H., 1984: Impacts of feedback and experience on the quality of subjective probability forecasts. *Mon Weather Rev*, **112**, 413–423.

Murphy, A.H. and Epstein, E.S., 1967: A note on probability forecasts and "hedging". *J Appl Meteorol*, **6**, 1002–1004.

Sanders, F., 1963: On subjective probability forecasting. *J Appl Meteorol*, **2**, 191–201.

—, 1967: The verification of probability forecasts. *J Appl Meteorol*, **6**, 756–761.

Winkler, R.L. and Murphy, A.H., 1968: "Good" probability assessors. *J Appl Meteorol*, **7**, 751–758.

Appendix

In assessment of probability forecasts, the attributes with which we are most concerned are bias, accuracy and skill.

Overall, bias may be defined as the ratio of the average forecast probability of an event to the corresponding observed relative frequency of occurrence of that event. This ratio is variously known as global bias, bias in-the-large, reliability in-the-large, or simply bias. The last-named is used here. The optimum bias value is unity. Values less than one are indicative of under-forecasting; values over one of over-forecasting.

A further aspect of bias is the correspondence between observed relative frequency and forecast probability for subsamples of the complete data set; notably, for each of the discrete probability values available to the forecaster — in the present case the 11 values 0, 0.1,.....0.9, 1.0. This quantity is known by the names bias in-the-small, reliability in-the-small or simply reliability.

The measure of accuracy used here is the Brier probability score (*PS*) (Brier 1950). Each of the parameters examined may be considered to be a nominal binary predictand, i.e. each probability forecast is considered to be a two-event situation in which the forecast event will or will not occur. For such predictands, the Brier score may be expressed as:

$$PS = \frac{1}{N} \sum_{i=1}^{N} (V_i - P_i)^2$$

where N is the total number of forecasts, P_i is the forecast probability in the ith case, and V_i is the verifying observation. V_i takes the value 1 if the event occurs and 0 if it does not. In this form, *PS* has a range from 0 (the best possible score) to 1.

The Brier score is a 'strictly proper' scoring rule, i.e. it is an evaluation measure that encourages forecasters to make the forecast corresponding with their judgement — the forecaster cannot minimize his expected score by hedging (Murphy and Epstein 1967, Winkler and Murphy 1968).

It has been shown by Murphy (1973) that provided the forecast probabilities possess only a finite number of distinct values, then the Brier score may be partitioned into three separate terms:

$$PS = UNC + REL - RES. \qquad \text{(A1)}$$

In this expression, *UNC* represents the uncertainty and is a measure of the variance of the observations; it does not depend in any way upon the forecasts. It is, in fact, the Brier score that would result if all the forecasts consisted of the (sample) climatological frequency. Values of the *UNC* range from a maximum of 0.25 when the event occurs on half the possible occasions to a minimum of zero when the event occurs always or not at all.

REL is the reliability mentioned earlier. It is the weighted mean squared difference between the forecasts and the corresponding observed relative frequencies over all the subsamples. Reliability may be represented qualitatively by a diagram in which relative frequency is plotted against the forecast probability for each of the specific probability values. In a reliability diagram the diagonal line from the origin represents perfect, or zero, reliability.

RES is the resolution term. This is the weighted mean squared difference between the observed relative frequency in the subsamples and the overall relative frequency. It takes values between 0.25 (the best) and 0. Sanders (1963) considers that resolution reflects a forecaster's ability to 'sort' occasions into subsets.

To demonstrate forecasting skill it is necessary to compare the achieved accuracy (represented here by the Brier score) with the score that would be produced by some reference procedure. The reference procedure used here is the (constant) forecast of the overall sample relative frequency (i.e. the sample climatological probability). This is in fact given directly by the uncertainty term *UNC*.

We may thus define a skill score *SS* as follows:

$$SS = \left(\frac{UNC - BS}{UNC}\right) \times 100.$$

Substituting from (A1), we get

$$SS = \left(\frac{RES - REL}{UNC}\right) \times 100.$$

SS can take values between 100 and minus infinity. Thus, the skill of the forecasts is positive if the magnitude of the resolution term exceeds that of the reliability term. A negative skill score indicates a result inferior to that obtained by a repeated use of a constant value based upon the sample climatology.

551.506.1(41-4)

The autumn of 1990 in the United Kingdom

G.P. Northcott
Meteorological Office, Bracknell

Summary

The autumn was warm and dry over much of England and Wales but close to average elsewhere, although some places around the Moray Firth and the Firth of Forth were unusually wet; it was generally sunny except over northern and eastern Scotland, northern and eastern England and East Anglia, where it was rather dull in places.

1. The autumn as a whole

Autumn temperatures were generally above normal over England and Wales and below or near normal over Scotland and Northern Ireland, ranging from 1.1 °C above normal at places in Cambridgeshire and Dorset to 0.6 °C below normal in the west of Northern Ireland. Autumn rainfall totals were generally below normal over England and Wales and above normal over Scotland and Northern Ireland, with amounts ranging from 169% at Dunbar, Lothian Region to 52% at Lyneham, Wiltshire. Sunshine was generally above average over the autumn period, except for northern and eastern Scotland, northern and eastern England and East Anglia, where amounts were near or just below average, and ranged from 128% at Rhoose, South Glamorgan to 67% at Cockle Park, Northumberland.

Information about the temperature, rainfall and sunshine during the period from September 1990 to November 1990 is given in Fig. 1 and Table I.

2. The individual months

September. Mean monthly temperatures were generally near or below normal, ranging from 2 °C below normal in western Scotland to 0.6 °C above normal in the Channel Islands. On the 28th the temperature fell to −1.4 °C at Hurn, Dorset, giving the coldest September night there in nearly 50 years of records. Monthly rainfall totals were well above normal in northern Scotland, the Western Isles, and parts of North Wales, but below normal elsewhere, with a large part of the Midlands and south-east England having less than half the normal rainfall, and ranged from 181% at Cape Wrath, Highland Region to 36% at Folkestone, Kent and in central London. Monthly sunshine amounts were below average over East Anglia and much of Scotland, apart from the Forth–Clyde valley; elsewhere amounts were near or above average, reaching nearly 140% in South Wales. In contrast north Norfolk was rather dull with only 76% of average sunshine.

After a hot start to the month cooler weather spread from the north-west by the 3rd, bringing some rain to most places, especially in the west and north. A somewhat settled spell between the 7th and 15th was followed by generally cooler and more changeable weather. During the night of the 18th/19th heavy rain and strong winds caused a landslip on the West

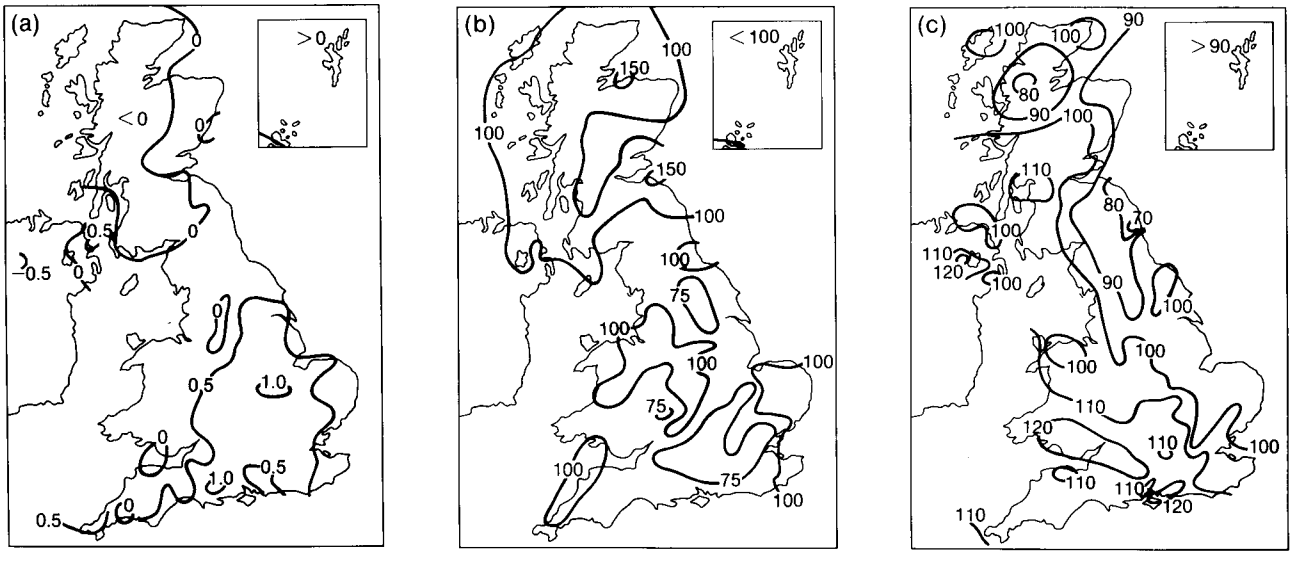

Figure 1. Values of (a) mean temperature difference (°C), (b) rainfall percentage and (c) sunshine percentage for autumn, 1990 (September–November) relative to 1951–80 averages.

Table I. District values for the period September–November 1990, relative to 1951–80 averages

District	Mean temperature (°C)	Rain-days	Rainfall	Sunshine
	Difference from average		Percentage of average	
Northern Scotland	0.0	−1	113	98
Eastern Scotland	+0.1	0	105	91
Eastern and north-east England	+0.4	0	86	89
East Anglia	+0.5	0	83	101
Midland counties	+0.6	−1	89	104
South-east and central southern England	+0.7	−1	77	114
Western Scotland	−0.1	−1	102	109
North-west England and North Wales	+0.2	−1	95	105
South-west England and South Wales	+0.4	0	87	120
Northern Ireland	+0.1	0	109	108
Scotland	0.0	−1	108	99
England and Wales	+0.5	0	87	105

Highest maximum: 26.4 °C in south-eastern and central southern England in September.
Lowest minimum: −5.9 °C in western Scotland in November.

Highland line from Fort William to Mallaig at Glenfinnan. Heavy showers on the 22nd/23rd in the south and west later became widespread over England and Wales with hail and thunder in places. It remained unsettled in most places for the rest of the month apart from a brief spell of fine weather on the 27th. Thunder was reported over Dorset during the evening of the 29th and for a time around London after noon on the 30th.

October. Mean monthly temperatures were above normal everywhere, ranging from near normal at Benbecula, Western Isles to nearly 2 °C above normal at Gatwick, West Sussex. The temperatures of 24.3 °C at Valley, Gwynedd and 22.3 °C at Kinloss, Grampian Region were the highest in their respective localities since 1959. The value of 11.8 °C in the register of Central England Temperatures indicates that October was the warmest for 12 years. Monthly rainfall amounts were above normal in many areas although some central and southern areas ended the month with less rainfall than normal. Amounts ranged from 219% at Edinburgh, Lothian Region to only 61% at Stansted, Essex. Sunshine amounts were about average over the whole of the United Kingdom, although some places were generally rather dull, and ranged from 130% over East Anglia to as little as 63% at Eskdalemuir, Dumfries and Galloway Region.

The weather was changeable over the month as a whole, being generally unsettled with one or two brighter interludes. The month was rather windy with strong to gale force winds on 8 days. In the south-east a thunderstorm on the 15th ended a very warm spell with a dramatic display of lightning reported at Colchester, Essex. Other thundery outbreaks occurred over South Wales on the 3rd, Scotland on the 16th, and mainly eastern areas of England and Wales between the 17th and 19th, and more widely spread between the 25th and 27th, sometimes accompanied by hail. During the 28th scattered thundery activity continued in southern England and South Wales, and isolated thunderstorms with hail occurred in the north-west; thunder was reported along the south coast on the 31st.

November. Mean monthly temperatures were generally about average and ranged from 0.7 °C below normal at Aspatria, Cumbria to 1.0 °C above normal at Gatwick, West Sussex. Apart from a few places in the east, mainly near the coasts, rainfall amounts were generally below normal and ranged from 30% of normal at Carlisle, Cumbria to more than 180% at Lowestoft, Suffolk. Sunshine amounts were generally above average in western and southern areas of the United Kingdom, but below average in central and eastern areas, ranging from 160% in west Cornwall to 71% around Blackpool and Manchester. Western Scotland was generally sunny in contrast to eastern areas where it was rather dull. At Paisley the sunshine total for the month was equal highest with that of 1947 in a record back to 1885, although at nearby Glasgow Airport the total was 5 hours short of the amount recorded in November 1947.

After a quiet beginning to the month the weather was unsettled between the 9th and 27th, with some rain, hail, thunder and even snow in places. Thunder was reported along the south coast on the 1st, in the Glasgow and Leeds areas on the 14th, over East Sussex on the 22nd, East Anglia on the 23rd, eastern Scotland, west Cornwall, and Kent on the 24th and Fife, the Thames Valley, eastern Kent and the Isle of Wight on the 25th, and was accompanied by hail over south-west England, South Wales and the Isle of Wight on the 21st and Cumbria and Lancashire on the 23rd. Hail was reported over North Wales on the 18th, the Isle of Man and Salisbury Plain on the 20th, Devon and Cornwall on the 23rd and northern and eastern Scotland and west Cornwall on the 25th.

Review

Remote sensing in hydrology, by E.T. Engman and R.J. Gurney. 160 mm × 240 mm, pp. xiv+225. *illus.* London, Chapman and Hall, 1991. ISBN 0 412 24450 0.

During the 1990s a number of satellite missions are planned which will provide data of great interest to hydrologists as well as meteorologists. It is timely therefore that two hydrologists should produce a book which demonstrates graphically how hydrology is expanding from the study of local or regional scales to consider the global hydrological cycle. In 11 chapters, totalling 255 pages, the reader is treated to careful descriptions, often quantitative, of the full range of hydrological subjects from basic measurements of precipitation, snow, evapotranspiration and soil moisture, through runoff and snowmelt modelling, ground water and water-quality measurements to water resources management and modelling.

This well-presented book is targetted at water resources scientists and managers, but it is likely to be of significant interest also to hydrometeorologists, and those involved in remote sensing and environmental monitoring who wish to find out more about the combined contribution of remote sensing and hydrology to their subject. We are told in chapter 1 that remote sensing offers a unique approach to studying hydrology across the disparate scales, and subsequent chapters demonstrate this. Each chapter follows roughly the same format: an introduction, general approach, measurement theory/details/examples, future applications and references.

There are some differences of emphasis and presentation between individual chapters. For example, in the description of the basic principles of remote sensing (chapter 2) there is no mathematics at all, yet in discussing snowmelt and runoff modelling there are many equations and detailed model flow charts. Similarly in some chapters we find excellent descriptions of the physics behind the measurements, a good example in chapter 7 being the description of what happens to the dielectric constant of soil as water is added to it. However in the chapter on precipitation there is no clear description of absorption and scattering processes underlying passive microwave techniques, nor the physics of ground-based radar measurement techniques.

Perhaps it is a little unfair to demand that a book on hydrology should contain such information, but at least there should be some pointers towards the source of further information. Also it would have been useful to include some comparison of techniques, particularly for measuring precipitation, and some discussion of measurement problems for various parameters. In general this book is uncritical. There is no mention also of the considerable work being undertaken to calibrate runoff models using radar data, or to use adaptive updating to cope with both measurement and forecast errors arising from the use of remotely sensed data. In addition there are a few inaccuracies which are no fault of the authors. These are due mainly to the rapid changes in plans for remotely sensing systems. For example, Table 11.1 defines the Tropical Rainfall Monitoring Mission (TRMM) incorrectly. The TRMM orbit will be at an inclination of 35°, the microwave radiometer has additional channels at 10 and 22 GHz, the radar will operate at a single frequency of 14 GHz and the launch will probably be in 1996.

Whilst these omissions and slight inaccuracies may irritate some readers, they should not be allowed to detract from the general high standard of the text. This reviewer found reading this book an enriching experience. There is no doubt that the authors are right in saying that only the microwave region of the electromagnetic spectrum offers the potential for truly quantitative measurements in many areas. Data from the ERS-1 SAR, SSM/I and TRMM present exciting opportunities for future work. Every hydrologist and hydrometeorologist should obtain this book, and read it cover to cover, as within is contained a wealth of information. This information will underpin large areas of hydrological science in the next decade. Increasingly, hydrologists will be called upon to contribute to better land surface parametrizations in global NWP models and GCMs using improved interpretation of remotely sensed data. In turn the model products and the remotely sensed data should significantly increase our understanding of continental-scale hydrological processes, and hence the impact of climate change on the hydrological cycle.

C.G. Collier

Books received

The listing of books under this heading does not preclude a review in the Meteorological Magazine at a later date.

Numerical adventures with geochemical cycles, by J.C.G. Walker (Oxford University Press, 1991. £30.00) contains a methodology for computational simulation of aspects of the earth's geochemical evolution. Programs which will execute on a personal computer are described. ISBN 0 19 504520 3.

Atmospheric data analysis, by R. Daley (Cambridge University Press, 1991. £55.00) outlines the physical and mathematical basis of all aspects of the subject, with the emphasis on theory. However, many practical considerations and examples are included, and it can be used as a textbook or reference book. ISBN 0 521 38215 7.

Satellite and radar photographs — 7 July 1991 at 0600 UTC

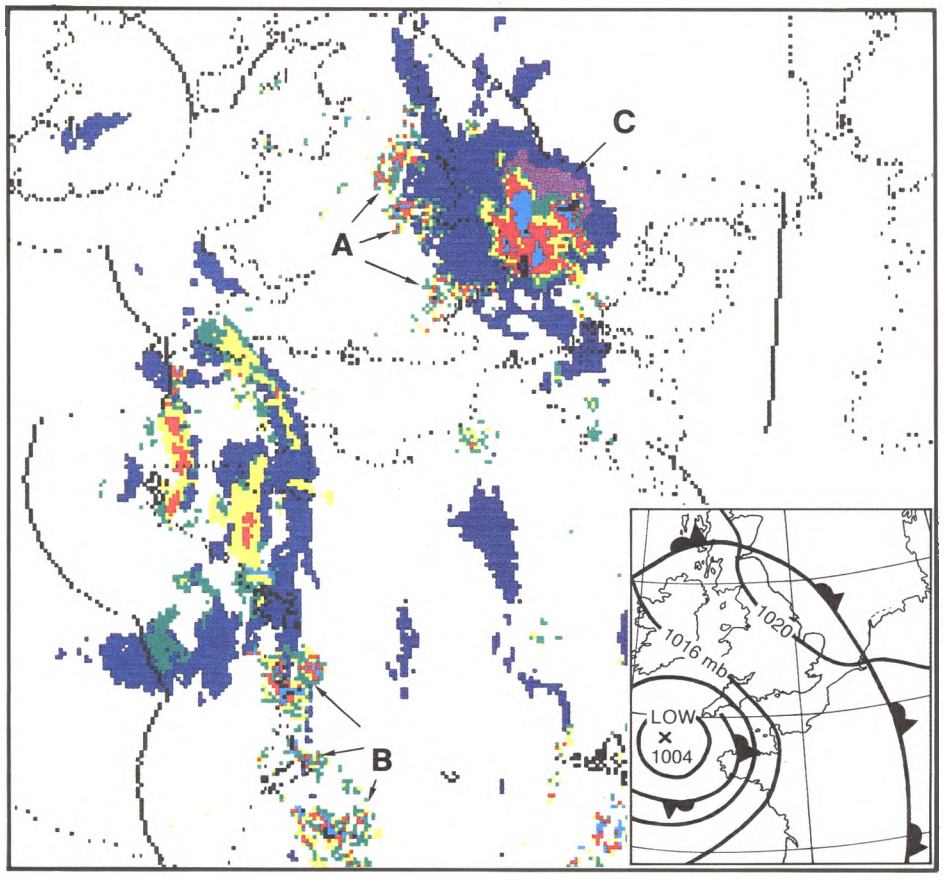

Figure 1. COST-73 satellite and radar image for 0600 UTC on 7 July 1991. Dark blue represents cloud tops with temperatures between −15 and −45 °C, and mauve <−45 °C. Rainfall intensities (mm h^{-1}) are shown as follows: green < 1, yellow 1–3, red 3–10, light blue 10–30, black > 30. Coastlines, national boundaries and the limits of radar coverage are shown in black. The surface analysis for that time is inset.

Composite satellite and radar images provide the analyst with vital information on the location and evolution of significant areas of cloud and precipitation, especially in otherwise data-sparse regions. Sometimes, however, the radar images can be misleading and apparently indicate rain in areas that are in fact dry or even cloud-free. An example is shown in Fig. 1 which was taken during a period when a warm south-easterly airstream covered the British Isles (see inset to Fig. 1). Areas of apparent heavy rain A, some collocated with the western portion of the cloud band in eastern England, are in fact returns from the ground — Anaprop. Surface reports showed these areas to be dry. Other examples can be seen in south-west France at B. Anaprop is caused by refraction of the radar beam by a low-level temperature inversion and hydrolapse (Fig. 2). Time-lapse sequences can help to discriminate these spurious echoes since they tend to remain stationary, whereas those associated with precipitation usually move. In the future, data from Doppler radars may provide a mechanism for removing these unwanted returns.

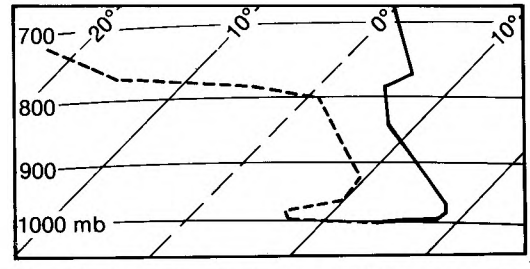

Figure 2. Tephigram for Crawley at 0000 UTC on 7 July 1991. The low-level temperature and humidity structure is representative of areas where spurious echoes have been identified at A in Fig. 1.

The large area of heavy rain at C, collocated with the area of cold cloud tops, is associated with a mesoscale convective system which developed over the southern North Sea and subsequently moved northwards. The evolution of a similar system over the near continent is shown in Lilley*.

A.J. Waters

* Lilley, R.B.E.; Satellite and radar photographs — 2 July 1991 at 1700 UTC. *Meteorol Mag*, **120**, 1991, 172.

GUIDE TO AUTHORS

Content

Articles on all aspects of meteorology are welcomed, particularly those which describe results of research in applied meteorology or the development of practical forecasting techniques.

Preparation and submission of articles

Articles, which must be in English, should be typed, double-spaced with wide margins, on one side only of A4-size paper. Tables, references and figure captions should be typed separately. Spelling should conform to the preferred spelling in the *Concise Oxford Dictionary* (latest edition). Articles prepared on floppy disk (Compucorp or IBM-compatible) can be labour-saving, but only a print-out should be submitted in the first instance.

References should be made using the Harvard system (author/date) and full details should be given at the end of the text. If a document is unpublished, details must be given of the library where it may be seen. Documents which are not available to enquirers must not be referred to, except by 'personal communication'.

Tables should be numbered consecutively using roman numerals and provided with headings.

Mathematical notation should be written with extreme care. Particular care should be taken to differentiate between Greek letters and Roman letters for which they could be mistaken. Double subscripts and superscripts should be avoided, as they are difficult to typeset and read. Notation should be kept as simple as possible. Guidance is given in BS 1991: Part 1: 1976, and *Quantities, Units and Symbols* published by the Royal Society. SI units, or units approved by the World Meteorological Organization, should be used.

Articles for publication and all other communications for the Editor should be addressed to: The Chief Executive, Meteorological Office, London Road, Bracknell, Berkshire RG12 2SZ and marked 'For Meteorological Magazine'.

Illustrations

Diagrams must be drawn clearly, preferably in ink, and should not contain any unnecessary or irrelevant details. Explanatory text should not appear on the diagram itself but in the caption. Captions should be typed on a separate sheet of paper and should, as far as possible, explain the meanings of the diagrams without the reader having to refer to the text. The sequential numbering should correspond with the sequential referrals in the text.

Sharp monochrome photographs on glossy paper are preferred; colour prints are acceptable but the use of colour is at the Editor's discretion.

Copyright

Authors should identify the holder of the copyright for their work when they first submit contributions.

Free copies

Three free copies of the magazine (one for a book review) are provided for authors of articles published in it. Separate offprints for each article are not provided.

Contributions: It is requested that all communications to the Editor and books for review be addressed to the Chief Executive, Meteorological Office, London Road, Bracknell, Berkshire RG12 2SZ, and marked 'For *Meteorological Magazine*'. Contributors are asked to comply with the guidelines given in the *Guide to authors* which appears on the inside back cover. The responsibility for facts and opinions expressed in the signed articles and letters published in *Meteorological Magazine* rests with their respective authors.

Subscriptions: Annual subscription £33.00 including postage; individual copies £3.00 including postage. Applications for postal subscriptions should be made to HMSO, PO Box 276, London SW8 5DT; subscription enquiries 071–873 8499.

Back numbers: Full-size reprints of Vols 1–75 (1866–1940) are available from Johnson Reprint Co. Ltd, 24–28 Oval Road, London NW1 7DX. Complete volumes of *Meteorological Magazine* commencing with volume 54 are available on microfilm from University Microfilms International, 18 Bedford Row, London WC1R 4EJ. Information on microfiche issues is available from Kraus Microfiche, Rte 100, Milwood, NY 10546, USA.

October 1991

Edited by Corporate Communications
Editorial Board: R.J. Allam, R. Kershaw, W.H. Moores, P.R.S. Salter

Vol. 120
No. 1431

Contents

ISSN 0026–1149

ISBN 0-11-728861-6

9 780117 288614

Printed in the United Kingdom for HMSO
Dd 0291241 10/91 C13 503 12521

FILE

The Meteorological Magazine

November 1991

Meteorological Office research
Assessment of model fluxes

HMSO

Met.O.998 Vol. 120 No. 1432

Table I. Links with other UK-based activities

Topic	Met. Office Division	Main collaborating organization	Special linking mechanism
Oceanography	E	University of Oxford Rennell Centre PML	Hooke Institute, CPP, UK WOCE
Cryosphere	E	BAS, SPRI	CPP
Upper atmosphere	E	Universities of Cambridge and Oxford	Hooke Institute, UGAMP
Atmospheric chemistry	E, P	Universities of Cambridge and Oxford	Hooke Institute, UGAMP
Mesoscale meteorology	P	Universities of Reading and Leeds	JCMM
Clouds and radiation	P	UMIST and University of Reading	CPP, JCMM
Hydrological and land processes including carbon cycle	E	IH	MITRE, TIGER
Space instrumentation	O	RAL	
Use of data in models	S	ECMWF	
Weather radar	S	RAL, UMIST, IH, Universities of Salford, Essex, Lancaster and Edinburgh	

This is only a partial tabulation — many more links are maintained through CASE studentships, Gassiot grants and informal collaboration.

KEY:

BAS	British Antarctic Survey
CASE	Co-operative Award in Science and Engineering
CPP	DoE — funded Climate Prediction Programme at the Hadley Centre
ECMWF	European Centre for Medium-range Weather Forecasts
IH	Institute of Hydrology
JCMM	Joint Centre for Mesoscale Meteorology
MITRE	Meteorological Office/Institute of Hydrology Terrestrial Model
PML	Plymouth Marine Laboratory
RAL	Rutherford Appleton Laboratory
SPRI	Scott Polar Research Institute
TIGER	Terrestrial Initiative on Global Environmental Research
UGAMP	UK Universities Global Atmospheric Modelling
UMIST	University of Manchester Institute of Science and Technology
WOCE	World Ocean Circulation Experiment

can be done without jeopardizing the core activities. Efforts are made to secure sponsorship from industry and contracts, for example from the Commission for the European Communities (CEC), to conduct research that supports the core activities.

3.2 Formulation of the Research Programme as a series of projects

The Research Programme is formulated as individual Projects, 32 of them at present (see Table II), each led by a Project Manager at Grade 7 (or above). Project proposals with resource requirements identified over a 3-year period are prepared or updated on a yearly basis by Project Managers each under the guidance of a Tasking Manager (generally the relevant Divisional Director) in the light of a series of discussions with key external and internal customers. The broad Research Programme is considered by the Meteorological Office Board of Management as part of the corporate planning procedure and is presented in detail to the Meteorological Research Sub-Committee in December each year.

2.2 Statement of Aims

The primary aim of the Meteorological Office Research Directorate is to support and develop the services provided by the Office by maintaining a sufficient base of scientific expertise to enable improvement of capabilities for observing, analysing and predicting the atmosphere and oceans.

2.3 The integrated nature of research and operations

A strength of the Office, and one of the ways it differs from most other National Meteorological Services, is the integrated management of its research and operations. This ensures that research carried out in-house is responsive to operational requirements (and vice versa) not only in the setting of objectives but also in the day-to-day interactions of the staff. The research contributes to a core capability that benefits the whole range of customers, both military and civil.

2.4 Quality research underpinning the Meteorological Office's reputation

The quality of research within the Meteorological Office has been a major factor in determining the high regard in which it is held nationally and internationally. Research of a high standard provides credibility and underpinning of the quality and competitive edge of its present and future services. It also provides an attractive framework for recruiting, training and retaining high-calibre staff for the Office as a whole.

2.5 Relationship between research conducted in-house and externally

Operational meteorological requirements continue to pose major scientific challenges and so the approach has to be one of quality science carried out within long-term programmes by scientists in close contact with the practical demands of operational forecasting and services. This is best achieved by in-house research, but the range of expertise required is such that there is considerable collaboration with other organizations (Table I). It is to our mutual advantage that meteorological research in universities and elsewhere is strengthened and that collaborative links are further developed. Contracted research is also carried out at the European Centre for Medium-range Weather Forecasts (ECMWF). The Office provides a focus for the national research effort related to observation and prediction of weather and climate. It is a national centre of excellence for research into weather and climate, and also for modelling of the oceans.

2.6 Importance of international collaboration in research

Meteorology has a strong tradition of international collaboration both operationally and in research. This is not only for the obvious reason that many atmospheric events take place on a global stage but also because the task of observing the atmosphere is a massive undertaking whether it be on a global scale or on the scale of individual clouds and weather systems. The Meteorological Office is therefore involved, in some cases as prime mover, in many collaborative research projects both bilaterally with scientists in other nations in Europe, and further afield, and also as part of major international programmes such as the World Climate Research Programme (WCRP). The C-130 aircraft of the Meteorological Research Flight (see section 5) is a key observational facility that provides a passport for participation in international field experiments.

2.7 High-calibre staff as the Meteorological Office's greatest asset

The collective expertise, understanding, flair and dedication of the staff is the Office's greatest asset. The highest priority for the Research Directorate is to continue to attract and retain research scientists of high calibre; this depends on the maintenance of a stable research programme whose science is not only useful but also recognized as being scientifically excellent. In order to carry out the kind of research that will enable the Office to remain at the forefront of the science it is necessary for career planning to give opportunities and incentives for innovative scientists and technical specialists to advance and acquire a reputation within specific areas of expertise.

3. Management of the Research Programme

3.1 Factors influencing the content of the Research Programme

The long-term strategic context of the Research Programme is determined by the Director of Research in the light of:

(a) the broad user requirements articulated by the Director of Operations and to a lesser extent by the Director of Commercial Services, and

(b) an understanding within the Research Divisions of the scientific opportunities.

Although specific efforts are made to inform end users about the Research Programme and in some cases to undertake special research for them, the major proportion of the research is carried out to create the Office's core capability, with the Director of Operations serving as the main proxy customer. The understanding and prediction of climate and pollution-related processes are treated separately as part of the Office's Public Meteorological Services (PMS); climate prediction research is also undertaken directly on behalf of the DoE as part of the Climate Prediction Programme (CPP). Although funded on a year-by-year basis, the CPP is seen by DoE as being a long-term programme. Opportunities are taken to make research products and expertise available for commercial exploitation when it

The Meteorological Magazine

November 1991
Vol. 120 No. 1432

551.5:06(b)

Strategic approach to research in the Meteorological Office

K.A. Browning,
Meteorological Office, Bracknell

Summary

The success of the Meteorological Office builds on the excellence of its research. This article describes the aims of the Research Programme, and its organization and management. It summarizes the motivation and key strengths of the Office's Research Division and it highlights growth areas for research during the 1990s.

1. Introduction

1.1 Nature and size of the Research Programme

The Director of Research is responsible for a broad programme of both research and development. There is no purely curiosity-driven research within the Programme but the nature of the Meteorological Office's operational requirements is such as to require fundamental as well as applied research. The Research Directorate is composed of three Divisions: Short-range Forecasting Research (S-Division), Extended-range Forecasting and Climate Research (E-Division) and Atmospheric Processes Research (P-Division). The main sources of funding are the Ministry of Defence (MOD) and Department of Environment (DoE). Eleven per cent of Office staff work in the Research Directorate. In addition the Director of Research has programme responsibility for Observational Instrumentation research carried out by a small team within the budget of the Director of Operations. A few other Operations staff also contribute to research projects. In return, some staff of the Research Directorate support the operational implementation of recently developed systems.

2. Strategic approach

2.1 What determines the size of the Research Programme?

Improvements in the quality, range, effectiveness and efficiency of meteorological services are required by the MOD, other government departments, the Civil Aviation Authority (CAA), industry and the general public. A key requirement is the development of weather forecasting products. Another is the maintenance of a broad and up-to-date knowledge base for provision of advice on meteorology and climate to government. Fulfilment of these requirements calls for a diversity of expertise and a wide range of research activities of a viable size. Factors taken into account in determining the overall size of the Research Programme are:

(a) the anticipated requirements over a 10-year time span,
(b) the amount of research conducted by other National Meteorological Services and the need to remain competitive with them, and
(c) the magnitude of the total turnover of the Meteorological Office.

First published 1991

HMSO publications are available from:

HMSO Publications Centre
(Mail and telephone only)
PO Box 276, London, SW8 5DT
Telephone orders 071-873 9090
General enquiries 071-873 0011
(queuing system in operation for both numbers)

HMSO Bookshops
49 High Holborn, London, WC1V 6HB 071-873 0011 (counter service only)
258 Broad Street, Birmingham, B1 2HE 021-643 3740
Southey House, 33 Wine Street, Bristol, BS1 2BQ (0272) 264306
9–21 Princess Street, Manchester, M60 8AS 061-834 7201
80 Chichester Street, Belfast, BT1 4JY (0232) 238451
71 Lothian Road, Edinburgh, EH3 9AZ 031-228 4181

HMSO's Accredited Agents
(see Yellow Pages)

and through good booksellers

3 8078 0010 2451 4

3.3 Control of the Research Programme and the role of serendipity

The Director of Research is responsible for the execution of the Research Programme. He is provided with regular summaries of resource out-turn by his Budget Manager and quarterly summaries of progress by his Tasking Managers. Research by its very nature rarely goes according to plan. Important though plans are they must not be used as a straitjacket. Serendipity has to be exploited. Hence the Director of Research will use his judgement to authorize departures from the plan or even new starts or premature termination of projects if he deems it necessary in the interests of the customers and/or the broader strategy. Where major departures from the plan are necessary he will seek the approval of the Meteorological Office Board at which he reports quarterly on progress against targets specified in the Research Programme. On a day-to-day basis the research is line-managed within Divisions in a manner that relates to particular expertise or skills and/or facilities. Some individual Research Projects, however, cut across skill areas and even across Divisions. Project Managers are responsible for horizontal co-ordination of these activities within agreed resource allocations laid down in the Research Programme.

3.4 Attribution of research costs to customers

Each Research Project is cost accounted. Attribution of costs is spelled out in the Summary Tables attached to each Research Programme document and is open for scrutiny during the various consultative stages. Attribution is between:

(a) Meteorological Office core,
(b) the research component of the Public Meteorological Services, and
(c) direct sponsorship by particular customers (DoE, CAA, Defence Services and Commercial Services).

The Director of Operations, as the customer for the core research, exploits the results to sustain and improve the quality of the services he is responsible for providing to the end customers, and he passes on an appropriate fraction of these research costs to his customers.

4. Evaluation of the Research Programme

4.1 The formal assessment of research

The Research Programme document, in addition to providing a description and justification of the work plan, gives costs and milestones. The Annual Research Progress Report prepared at the end of each financial year presents the corresponding out-turn and attainment of milestones in addition to summarizing the main achievements, publications completed, and deviations from plans. The excellence of the research is assessed by the Meteorological Research Sub-Committee. The chairman assigns an overall quality rating to projects in the light of the members' markings and after appropriate discussion. Tasking Managers may revise their programmes accordingly.

4.2 Other more telling indicators of the value and quality of research

The value of research, especially long-term research of the kind so important to the Meteorological Office, is not easily represented by quantitative measures such as the attainment of short-term targets. Rather, the true value of the research is evident from the overall improvement of forecast accuracy over a period of years; it is also evident from time to time when, for example, the Office receives the accolade of becoming a World Area Forecast Centre for Civil Aviation, or when its Chief Executive is asked to chair a Working Group of the Intergovernmental Panel on Climate Change, or in the joint establishment with the DoE of the Hadley Centre which brought with it the contract for the 'DoE Climate Prediction Programme'. Accordingly it is important to avoid becoming beguiled by the quantitative aspects of the short-term targets or, indeed, spending too much time in operating complex evaluation procedures, except in the larger development projects where more formal project management techniques are used.

4.3 Lessons to be learned from evaluating the Research Programme

Although the quantitative aspects of the evaluation procedure should not be carried too far, the discipline of this approach is nevertheless a valuable means not only of sharpening up the conduct and presentation of research but also of identifying problems at an early stage. The kind of lessons that might be learned can be illustrated by some of our earlier successes and failures. For example, the successful development and application of the weather radar network in the United Kingdom was a result of an effective in-house research effort, close collaboration with external partners and timely and effective technology transfer to operational implementation. The slow progress with a related programme can be attributed to the premature contracting out to industry of a still-evolving methodology. Other projects, by contrast, have suffered from being continued in-house for too long. These are the kinds of problem evaluation procedures should identify at an early stage.

5. Motivation of the research in the main Functional Areas

5.1 Short-range forecasting research (S-Division)

The motivation of S-Division is to develop numerical weather and ocean prediction systems (including data quality control and analysis procedures, and forecasting models) so as to satisfy the needs of the Office in providing weather and ocean forecasting services to its

Table II. Project titles in 1991/92

S-Division
- Representation of atmospheric dynamics in numerical models
- Ocean forecast modelling
- The processing, quality control and assimilation of observations (including satellite data) for NWP
- Observation assessment studies
- Improvements to the operational global and regional NWP system
- Very-short-range weather forecasting
- Development of satellite image products
- Interpretation of satellite image products
- Interpretation of satellite and radar images
- Improvements to the operational mesoscale prediction system

E-Division
- Analysis, modelling and theoretical studies of the dynamics and photochemistry of the middle atmosphere
- Development of methods of extended-range forecasting
- Seasonal to multi-decadel climate variability
- Simulation of climate and climate change
- Ocean and sea-ice modelling
- Basic dynamical processes in rotating fluids
- Climate prediction programme
- Intergovernmental Panel on Climate Change
- Development and testing of parametrizations of physical processes for NWP and climate models

P-Division
- Observational verification of mesoscale processes
- Improved parametrizations of mesoscale processes
- Improved description of radiative processes
- Improved description of clouds and their occurrence
- Observational verification of boundary-layer models
- Development of boundary-layer models
- Development of specific forecasting techniques
- Improved description of atmospheric dispersion
- Nuclear Accident Response Model
- Measuring and predicting atmospheric composition
- Tactical decision aids

O-Division
- Space instrument concept and design evaluation
- Interpretation of satellite instrument data

customers. Research is also carried out to meet the specialized forecasting needs of particular customers, such as the Armed Forces and the CAA. There are increasing demands from users for more area-specific predictions of local weather phenomena. These are derived from numerical models themselves or through diagnostic procedures and/or by using detailed observations from space and special networks of earth-based sensors. Short-range forecasting is concerned with timescales from hours to a few days. Medium-range forecasting research (4–10 days ahead) is contracted to ECMWF. Longer-range forecasting research is carried out in E-Division.

5.2 Extended-range forecasting and climate research (E-Division)

The motivation of E-Division, of which the Hadley Centre for Climate Prediction and Research forms the major part, is:

(a) to develop extended-range forecasting techniques for predicting the weather over periods from a week to a season,

(b) to develop and maintain an up-to-date knowledge base on the physics of climate and climate change enabling the Office to provide expert advice to Government,

(c) to develop the art of modelling the coupled climate system including atmosphere, oceans, ice and land surface so as to predict climate changes resulting from both natural and man-made effects to the end of the next century, and

(d) to develop and use observational databases to improve climate models, to understand climate fluctuations, and to detect climate change.

5.3 Atmospheric processes research (P-Division)

The motivation of P-Division is to provide expert background and guidance to ensure that the Office's services and products relating to both weather and climate benefit from advances within the wider meteorological community in the ability to represent and predict physical processes in the atmosphere. A range of strategic observational and theoretical studies is pursued to address key issues of relevance to the Office. In some cases the magnitude of the research tasks is such that participation in international programmes provides the most effective means to meet objectives.

5.4 Observational instrumentation research (O-Division)

The motivation of the research part of O-Division is to ensure that the satellite instrumentation employed, either directly by the Meteorological Office or indirectly by funding through, for example, space agencies, is cost-effective and soundly based on requirements. Advanced construction, calibration and validation work are undertaken to maintain a capability for ensuring that these requirements are met.

6. Key strengths

The Meteorological Office has over the years developed particular strengths that enable it to undertake research effectively. The strengths consist of a combination of specialized skills, facilities, infrastructure, etc. as follows:

6.1 Key strengths of the Meteorological Office as a whole

- The integrated management of research and operations.

- The numbers, quality and motivation of the staff.
- Very powerful computing facilities.
- A unified modelling facility (para. 6.1.1).
- Status as a Regional Telecommunications Hub of the World Meteorological Organization (WMO).
- Excellent training facilities.
- Responsibilities as the National Meteorological Service.
- National and international reputation and influence.

6.1.1 Attributes of the Meteorological Office Unified Model

— Atmospheric and Ocean Model with data assimilation options.
— Global and limited area configurations.
— Extensive range of parametrizations including explicit clouds.
— General purpose software system allowing easy exchange of modules.
— User interface allowing easy use by scientists.
— Extensive diagnostic system.

6.2 Key strengths in S-Division

- Expertise in numerical modelling and data assimilation and in the processing and interpretation of satellite and radar data.
- Computing facilities — the research makes extensive use of the Office's supercomputer and graphics workstations.
- An operational software suite developed to carry out quality control, analysis, forecasting, post-processing and diagnostic monitoring, using a variety of remote-sensing and *in situ* observations.
- Mesoscale forecasting facilities for detailed forecasting in the British Isles; there is a broad base of experience in the manipulation of satellite and radar imagery.

6.3 Key strengths in E-Division

- Expertise in numerical modelling and interpretation of climate data.
- Supercomputing facilities — climate modelling has been developed on the main Office supercomputer and this facility is now supplemented by a dedicated supercomputer funded by DoE with powerful front-end facilities, mass storage and workstations.
- A coupled model of the atmosphere, oceans, ice and land surface — this forms the basic tool for climate research and prediction.
- An archive of climate data — experience exists within the office for blending remotely sensed and *in situ* observations to provide a properly analysed and quality-controlled climate database for research.

6.4 Key strengths in P-Division

- Expertise in carrying out field experiments, and in interpreting small-scale models in terms of the physical processes that need to be represented in weather forecasting and climate models.
- Computing facilities — these allow for the use of numerical simulations of small-scale atmospheric motions to provide an overall description and understanding of processes that cannot be observed in their entirety.
- The instrumented C-130 research aircraft of the Meteorological Research Flight (para. 6.4.1) — data collected by this versatile aircraft at different levels within the troposphere underpin a large part of the research programme and provide a ticket for full participation in international collaborative projects.
- The Cardington balloon facility — this is a tethered balloon facility which carries instruments aloft for detailed study of parts of the atmosphere close to the ground.

6.4.1 The Meteorological Office Research Flight (MRF)

The MRF is composed of an aircraft facility and four scientific groups which use the aircraft for a wide programme of atmospheric research. The large capacity and long endurance (up to 11 hours) of the C-130 make it ideal for the task. It is flown by RAF aircrew permanently based at MRF. The current research activities are in the areas of:

— The investigation of mesoscale phenomena.
— The characteristics and microphysical properties of clouds.
— The radiative transfer through clouds and cloud-free air.
— The generation of tropospheric ozone from man-made pollutants.

Some of these activities are undertaken jointly with other organizations.

6.5 Key strengths in the research part of O-Division

- Expertise in the design and construction of satellite instrumentation and in the interpretation of the data for meteorological purposes.
- The C-130 aircraft provides a test bed for field calibration and evaluation of new space instruments.
- Development laboratories — access is available to laboratories and environmental test facilities both at the Meteorological Office and at RAE Farnborough.

7. Science growth points — opportunities and challenges for the Meteorological Office

7.1 The enabling technologies

The 1990s will be a decade of expanding opportunities brought about by technological advances:

(a) in computing, especially parallel computing and graphics workstations, and
(b) in automated observing systems, especially but not exclusively, space-borne systems.

The opportunities lie in the better forecasting of both weather and climate.

7.2 The need to improve numerical models

One of the outstanding challenges of the 1990s will be to improve the performance of the numerical models used to predict weather and climate. This will require much greater understanding of a variety of dynamical and physical processes in the atmosphere, and the interactions between them, and the ability to represent these processes faithfully in practical numerical models. It will also require increases in computer power, both to allow use of more sophisticated representations, and to allow the resolution of the models to be increased.

7.3 The need to understand and parametrize physical processes

A particular challenge will be to improve the representation (parametrization) of mesoscale and cloud-scale processes in numerical models. This will call for the Office to redouble its efforts in the area of process studies using a combination of field measurements with the C-130 aircraft and special cloud-scale numerical models. The World Climate Research Programme is paying particular attention to these issues within the Global Energy and Water Cycle Experiment (GEWEX) and some of the Meteorological Office research will be undertaken within the context of this international programme.

7.4 The need to improve the exploitation of data, especially from satellites

Satellites are playing an increasingly important role, not only in providing global data for weather forecasting and for climate monitoring, but also for research into the processes that need to be represented in weather and climate models. The scientific community has underestimated the magnitude of the task of using data from satellites. The Office will strengthen its efforts in this area through involvement with the development and evaluation of space instrumentation, through the development of techniques for blending space and other observations to provide optimal analyses, and through the exploitation of these data in weather forecasting and for climate research. Four-dimensional data assimilation will be a priority area for further research.

7.5 The Meteorological Office role in climate research and prediction both regionally and globally

The Meteorological Office has a leading role nationally in the increasingly prominent field of climate research and prediction. There will be great benefits to the nation, both economically and for policy formulation, in having a capability for predicting climate change due to both natural and man-made causes. It is government policy that this leadership shall also be exerted internationally through participation in appropriate international activities. This leadership will require a continuing programme of the highest scientific integrity and excellence.

7.6 The Meteorological Office role in the climate space segment

The Office is currently overseeing the national contribution to space programmes required for weather forecasting, through the European organization EUMETSAT and through bilateral arrangements with the USA. With the move towards a Global Climate Observing System, the Office will be well placed to play a similar role with regard to the new generation of operational space programmes for climate.

7.7 The increasing involvement of the Meteorological Office with the oceans

The close coupling of the oceans and the atmosphere is something that needs to be represented within numerical models whether they be required for predicting the state of the atmosphere or of the ocean. Increased effort into coupled atmosphere-ocean modelling and the use of appropriate observations will lead to important improvements in both long- and short-term prediction capability which in different ways will be of special interest to the DoE and the Navy. Collaboration with the Natural Environment Research Council (NERC) will be particularly appropriate in some aspects of the research.

7.8 The development of very-short-range weather forecasting methods

An aspect of weather forecasting that has great potential for improvement and commercial exploitation is very-short-range (0–12 hours) area-specific weather forecasting. This is the kind of forecasting that has to do with predicting extreme events. The Office has pioneered separately the development of very-fine-mesh forecasting models, and nowcasting techniques using imagery; these are key areas that will be brought together and developed for wider exploitation.

7.9 The bottom line

The above are all long-term research tasks. The operational success of the Meteorological Office has depended in the past, and will continue to depend, on stable long-term, broadly based, quality research. Although the Research Programme is driven by the requirements of customers (e.g. Director of Operations, Director of Commercial Services, Department of the Environment, etc.), it is important to ensure that, in meeting these demands, the ethos of long-term quality research is not compromised by over-commitment to

commercial opportunities giving short-term financial gain. To avoid this the Office's Research Programme will be supported and promoted in a way that enables it to be recognized for its quality and integrity and its prime-mover scientists will continue to be offered attractive career prospects within their speciality.

In summary:

— A lot of challenging meteorological research remains to be done over the coming decade.

— The Meteorological Office offers excellent resources and facilities as well as an exciting research environment in which to pursue this work.

— The tasks are enormous and they depend upon: a stable, long-term research programme, and close national and international co-operation.

551.509.313:551.551.8

An assessment of the surface fluxes from the Meteorological Office numerical weather prediction models. Part I: Momentum

J.O.S. Alves
Meteorological Office, Bracknell

Summary

The ocean and atmosphere interact by exchanging fluxes of momentum, heat and moisture across their boundary. Estimates of these fluxes come from operational numerical weather prediction models. An assessment of the surface momentum fluxes from such models is carried out using fluxes from the Meteorological Office's Fine and Coarse Mesh models, an ocean model of the North Atlantic is also used to assess the ocean response to the NWP fluxes and biases in them.

1. Introduction

The ocean and atmosphere exchange heat, momentum and fresh water across the ocean surface. Specification of these fluxes serves as a lower boundary condition for atmospheric models and an upper boundary condition for ocean models. The FOAM (Forecasting Ocean Atmosphere Model) group of the Meteorological Office (MO) is developing an ocean model to be used for forecasting studies. This model will require the specification of the surface fluxes, up to 6 days ahead of time, as its upper boundary condition. It has been suggested that, at least in the near future, the best estimates of the surface fluxes will come from NWP (Numerical Weather Prediction) models (Burridge and Gilchrist 1989). Further, they will be the only source of forecast surface fluxes. As a first stage in the development of FOAM an assessment of the surface fluxes from the current MO operational NWP models has been carried out. Results for the momemtum fluxes form the contents of this document.

Alves and Foreman (1989) integrated an ocean model using NWP fluxes and compared the results with those from a similar integration using climatological fluxes. The experiments were carried out for October 1988 and March 1989. They reported that the NWP forced integration developed the observed sea surface temperature (SST) anomalies reasonably well. The lack of a sufficiently accurate observed SST field prevented them from being able to assess the surface fluxes adequately.

There are three main errors that can occur in the surface fluxes from a NWP model. Firstly there is the forecast error. This depends on the ability of the model to represent the real atmospheric situation and to forecast it correctly. It depends on all the model formulations, observations used, data assimilation scheme and indeed on the quality of the fluxes. This topic will not be discussed further and such errors will be ignored as the main interest is in the calculation of the surface fluxes themselves. A second source of errors is the parametrization of the fluxes, for example, how a particular flux can be calculated from the model fields. As will be seen in later sections this is still not fully understood. Thirdly, the model parametrizes the surface

fluxes as functions of the basic model fields; wind, temperature and humidity. Inadequacies in their simulation would lead to errors in the fluxes.

To assess the quality of the surface fluxes an ocean model was used. The aim was to reveal any biases in the momentum fluxes and to quantify the sensitivity of the ocean model to these biases by comparing results from ocean model integrations using NWP momentum fluxes with similar integrations using climatological fluxes. Fluxes from the two MO operational models were compared, together with their parametrizations. A brief discussion of the parametrization of the fluxes in view of recent literature is also included.

A brief description of the operational NWP models used by the MO and a fuller description of how they parametrize the surface momentum fluxes is given in section 2. Section 3 describes the ocean model and the experiments carried out. Results for the momentum fluxes from the ocean model test, including a discussion of the flux parametrizations, are given in section 4. In section 5 a summary is presented and conclusions are drawn. Recommendations are made for future development.

2. The NWP models

2.1 The MO NWP models

The MO used two operational numerical weather prediction models, described by Bell and Dickinson (1987). The 'Coarse Mesh' (CM) model was global and used a latitude/longitude resolution of 1.875° × 1.5°. The 'Fine Mesh' (FM) model had twice the resolution of the CM, 0.9375° × 0.75°, and covered an area from 30° N to 80° N and from 80° W to 40° E. Output from the global CM model was used to supply boundary conditions for the limited-area FM model. Both models used sigma (σ) coordinates in the vertical (σ = ratio of pressure to surface pressure). Both models were run twice a day, at 00 UTC and 12 UTC. The CM model produced forecasts up to 6 days ahead and the FM model up to 36 hours ahead. Only the first 12 hours of each forecast were used in this study.

From each model, monthly mean fields consisting of the first 12 hours of each forecast were formed for the month of October 1989. The fields available from the NWP archives are shown in Table I indicated by a '✓' and those not available in the model archives are indicated by a 'X'. They will be discussed in later sections.

2.2 Parametrization of the surface processes.

The parametrization of the boundary-layer processes is described fully in Bell and Dickinson (1987). A brief summary and recent changes are outlined below. The surface wind stress $\tau = (\tau_x, \tau_y)$ is defined in terms of bulk aerodynamic formulae. For the CM model the bulk formulae take the explicit form

$$\tau_x = \rho C_D |\mathbf{v}| u_1 \quad (1)$$

$$\tau_y = \rho C_D |\mathbf{v}| v_1 \quad (2)$$

where C_D is the drag coefficient, $|\mathbf{v}| = (u_1^2 + v_1^2)^{1/2}$ and u_1 and v_1 are the first model-level horizontal wind components. In the FM model an implicit finite difference scheme (Kitchen 1986) is used for the turbulent fluxes in the boundary layer and the bulk aerodynamic formulae take the form

$$\tau_x = \rho C_D |\mathbf{v}| (\alpha u_1^{t+\Delta t} + (1-\alpha) u_1^{t}) \quad (3)$$

$$\tau_y = \rho C_D |\mathbf{v}| (\alpha v_1^{t+\Delta t} + (1-\alpha) v_1^{t}) \quad (4)$$

where $\alpha = 0.5$ and the superscripts t and $t+\Delta t$ refer to successive time-levels; Δt represents a time step.

The drag coefficient C_D depends on the surface roughness length z_o and the bulk Richardson number Ri_B. It is calculated using different empirical functions which depend on the stability of the boundary layer (see Bell and Dickinson 1987). Bell and Dickinson indicate that in the CM model z_o over the sea was a constant value of 10^{-4} m. For the FM model the surface roughness length z_o was a variable and was calculated using the Charnock formula (Charnock 1955)

$$z_o = M u_*^2 / g \quad (5)$$

where M is a constant (taken to be 0.019), u_* is the surface friction speed and g is the acceleration due to gravity.

In the FM and CM models the wind mixing energy (WME) is calculated from the wind stress every time-step using the formula

$$\mathrm{WME} = |\tau|^{3/2} / \rho_s^{1/2} \quad (6)$$

where $|\tau|$ is the magnitude of the wind stress and ρ_s is the density of the sea water (1025 kg m^{-3} in the forecast models). The archiving of the data from the forecast models involves compressing each field. The wind mixing energy was over-compressed and low values of the WME were effectively set to zero. For this reason no tests were carried out involving the NWP wind-mixing energy values.

Table I. Fields extracted from NWP archives. X = not available.

	FM	CM
Wind-mixing energy	X	X
Wind-stress components	✓	✓
σ, wind components	✓	X
10-metre wind components	✓	✓

3. Use of an ocean model to assess the surface fluxes

The ocean model used is based on that of Cox (1984) where a leap-frog differencing scheme is used to integrate the primitive equations. Approximations include that of Boussinesq, the hydrostatic assumption, a 'rigid lid' assumption and where the domain boundary crosses open ocean this boundary is assumed to be closed. The model uses regular latitude/longitude horizontal co-ordinates with a grid spacing of 1° throughout. In the vertical, depth coordinates are used with 17 vertical levels which are concentrated in the upper 200 metres. To allow tracers to diffuse along isopycnic surfaces a scheme, which solves the diffusion equation along isopycnics and then transforms back to model coordinates, is used and is based on that of Redi (1982). In the vertical, two mixing schemes are employed. Below the mixed layer the stability dependent scheme of Pacanowski and Philander (1981) parametrizes the eddy diffusivity in terms of the Richardson number, which itself depends on the static stability and vertical shear of the flow. In the mixed layer a scheme similar to that of Kraus and Turner (1967) is used. In this scheme convective mixing takes place when there is surface density increase through cooling or evaporation. After this, and where there is net surface heating, the mixing energy of the wind is used to overcome the stability of the upper layers and mix the more buoyant water downwards. A mixed layer depth is diagnosed as the depth to which mixing occurs.

Surface fluxes of momentum, non-penetrating heat, solar radiation and fresh water are used as the upper boundary conditions for ocean model integrations. Interaction between the ocean and the atmosphere is shown schematically in Fig. 1. Momentum flux is used by the ocean model to drive the Ekman drift currents and the long-term average wind stress drives the upper ocean circulation. Water near the surface is mixed downwards using the wind mixing energy. Heat is either input or removed from the ocean through the specification of the heat fluxes. The salt budget is modified at the surface by the freshwater flux.

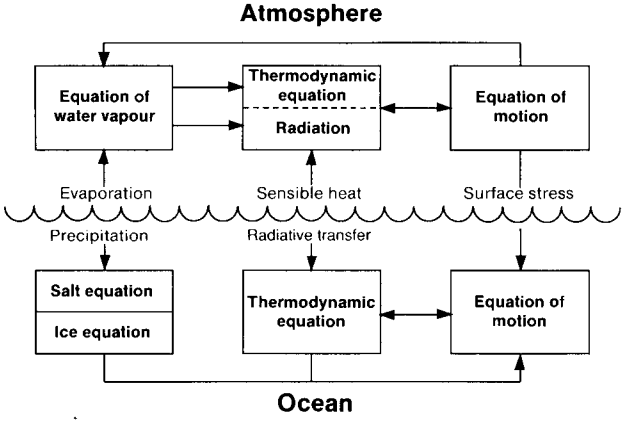

Figure 1. Schematic diagram of the interaction between the ocean and the atmosphere.

For the month of October 1989 forcing fields were extracted from the NWP archives for each forecast starting at 00 UTC and 12 UTC each day. The T+3, T+6, T+9, and T+12 forecasts from the FM model were used to form 3-hourly averaged forcing fields. For the CM model only the T+6 and the T+12 fields were available. The T+6 was copied and relabelled the T+3 and the T+12 was copied and relabelled the T+9, so forming a set of 3-hourly forcing fields. The fields extracted consisted of the surface wind stress components.

The ocean model's domain covers the North Atlantic from 30° S to 80° N. The region covered by the FM is contained within the domain of the ocean model. It is desirable to use the FM model's forcing fields where possible because of its improved physics and higher resolution. To achieve this the FM and CM fields were merged together so that the FM values were used within the FM domain and those of the CM outside the FM domain, with a smoothing applied at the FM boundary. The resulting fields will be from hereon referred to as the 'merged' fields.

The ocean model was started with salinity and temperature fields interpolated from the Levitus (1982) atlas for March. The currents were set to zero. It was integrated for 7 months using climatological forcing fields (wind stress and wind mixing energy — Hellerman and Rosenstein (1983), solar radiation, IR radiation, sensible heat, latent heat and evaporation — Esbensen and Kushnir (1981), and precipitation — Jaeger (1983)). Throughout the integration a relaxation of the surface temperature and salinity back to the Levitus climatology was employed, based on that of Haney (1971). The end product was the starting point for the experiments described below, it being a set of model fields valid for 1 October.

Relaxation of the surface temperature and salinity was switched off for the rest of the experiment. The ocean model was then integrated for one more month, October, still using the climatological fluxes. This formed the control run hereafter referred to as the 'climatological' run. This 1-month integration was repeated replacing the climatological momentum flux with the NWP one. In the following sections this will be referred to as the 'NWP' run or the 'operational' run. Monthly mean fields for temperature, salinity, currents, mixed layer depth and the forcing fields were obtained for each run and compared with the climatological control run. These will be discussed in the section to follow. For the purpose of comparison all fields presented have been linearly interpolated onto the ocean model's grid.

4. Momentum fluxes

4.1 Results

The monthly mean climatological wind stress (Hellerman and Rosenstein 1983) used to drive the climatologically forced ocean model is shown in Fig. 2 together with the monthly mean difference in the magnitude between the merged NWP wind stress and the climatological wind stress. The main areas of strong wind stress are those associated with the South-East Trades (wind stress magnitude exceeding 0.1 N m^{-2}), the North-East Trades (reaching over 0.075 N m^{-2}) and the mid-latitude westerlies of the North Atlantic (reaching over 0.15 N m^{-2}). The wind stress due to the South-East Trades from the NWP models is generally some 25% stronger than the corresponding climatological value (for example 0.025 W m^{-2} stronger where the climatological value is 0.1 N m^{-2}). Near the equator and the area of the North-East Trades, the NWP wind stresses are weaker. In the western equatorial Atlantic the NWP wind stress is some 0.025 W m^{-2} weaker in a region where the climatological wind stress is around 0.05 N m^{-2}, representing a 50% smaller value. In the North-East Trades differences of up to 0.025 N m^{-2} also occur although here this represents only about 30% of the climatological value. In the mid-latitude North Atlantic westerlies the NWP wind stresses have a much larger magnitude, 50% larger, than the climatology. Large departures of the NWP values from the climatology are expected in this region as it is associated with the North Atlantic storm track.

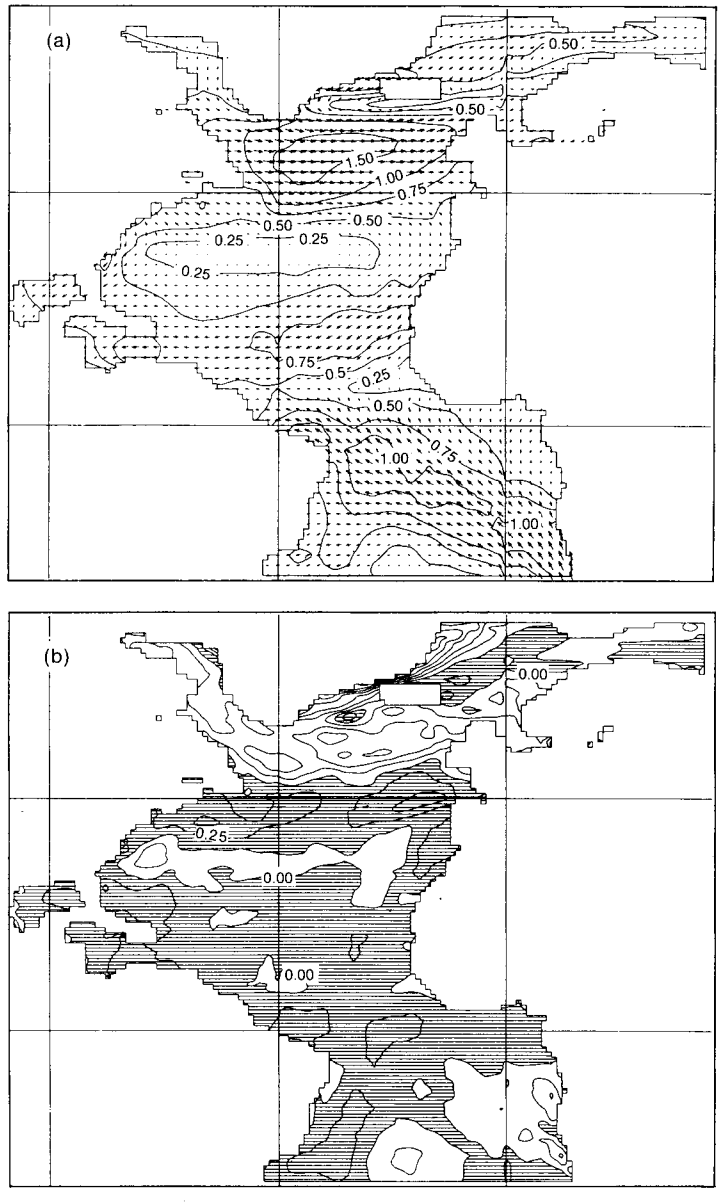

Figure 2. (a) Monthly mean climatological wind stress for October 1989; contours at 0.25, 0.5, 0.75, 1 and 1.5 (× 0.1) N m^{-2}, and (b) monthly mean difference between the NWP merged wind-stress magnitude and the climatology for October 1989; contours every 0.25 (× 0.1) N m^{-2}, and negative areas are shaded.

The monthly mean model top-layer current field produced by the climatology forced run is shown in Fig. 3. Strongest currents are those associated with the equatorial current system and the North Atlantic western boundary currents. In the mid-equatorial Atlantic the surface equatorial current has a magnitude of around 20 cm s^{-1} and intensifies towards the west to form a western boundary current when it approaches the Brazilian coast, where its magnitude increases to over 1 m s^{-1}. The surface Gulf Stream has its maximum strength of 20 cm s^{-1} off the coast of USA and separates from the coast near Cape Cod, further north than Cape Hatteras where it is normally observed to leave the coast (a deficiency common to ocean models).

Over short time-scales the wind stress produces near-surface Ekman drift currents superimposed on the main current system. Over longer time-scales (order of a month) the wind stress can affect the upper ocean current structure via the wind-stress curl. The mean monthly differences between the model top-layer currents from the two runs is shown in Fig. 4(a). In the equatorial region the differences in the wind stress between the two integrations of 0.025 N m^{-2} introduce appreciable differences in the surface currents. The equatorial current itself is weakened by the reduced wind stress, its magnitude being reduced by up to 10 cm s^{-1} (50%) in the mid-equatorial Atlantic and up to 20 cm s^{-1} (20%) in the more intense current off the Brazilian coast. For the Gulf Stream, differences of up to 5 cm s^{-1} (20%) occur. In the mid-latitude North Atlantic the large wind-stress anomaly produces relatively large surface current differences between the two runs which are comparable with the magnitude of the currents themselves.

The relatively large differences in the model top-layer current fields shown in Fig. 4(a) arise as a result of Ekman drift and are limited to the upper 20 metres or so of the ocean. Fig. 4(b) shows the difference in the two current fields at 35 metres (fourth model level). Outside the equatorial latitudes the difference between the two fields is negligible, whereas around the equator there are relatively large vector differences of up to 20 cm s^{-1} (50%). This difference extends to depths of over 100 metres and clearly indicates a change in the equatorial current system. It verifies the dependence of the equatorial currents on the relative long-term average wind stress forcing and it shows their sensitivity to changes in the mean wind stress over a period as short as one month.

The difference in the monthly mean SST produced by the two runs is shown in Fig. 5. Outside the equatorial region there is negligible difference except for areas of coastal upwelling. On the equator the modification to the upper ocean current field introduces a warming of up to 0.8 °C of the sea surface. Differences in the temperature structure between the two runs of up to 1 °C exists down to depths of over 100 metres (not shown). This change in the temperature structure leads to a corresponding change in the mixed layer depth which is generally reduced by a few tens of metres in some places (Fig. 6).

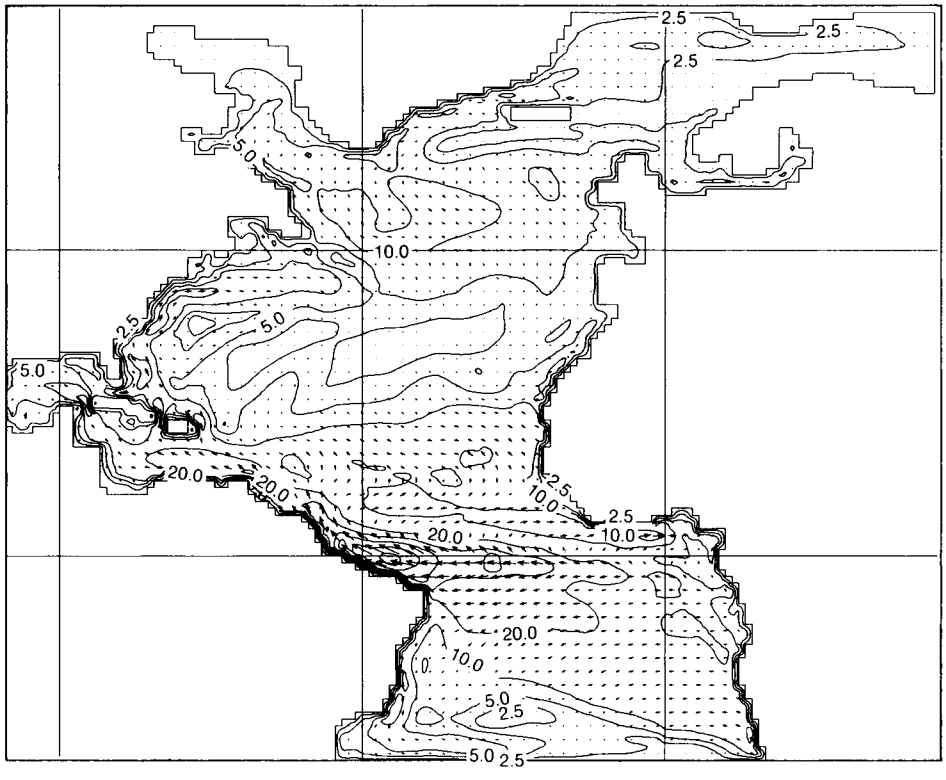

Figure 3. Monthly mean model top-layer current vector field produced by the climatological control run for October. Contours at 2.5, 5, 10, 20, 40, 60, 100 cm s^{-1}.

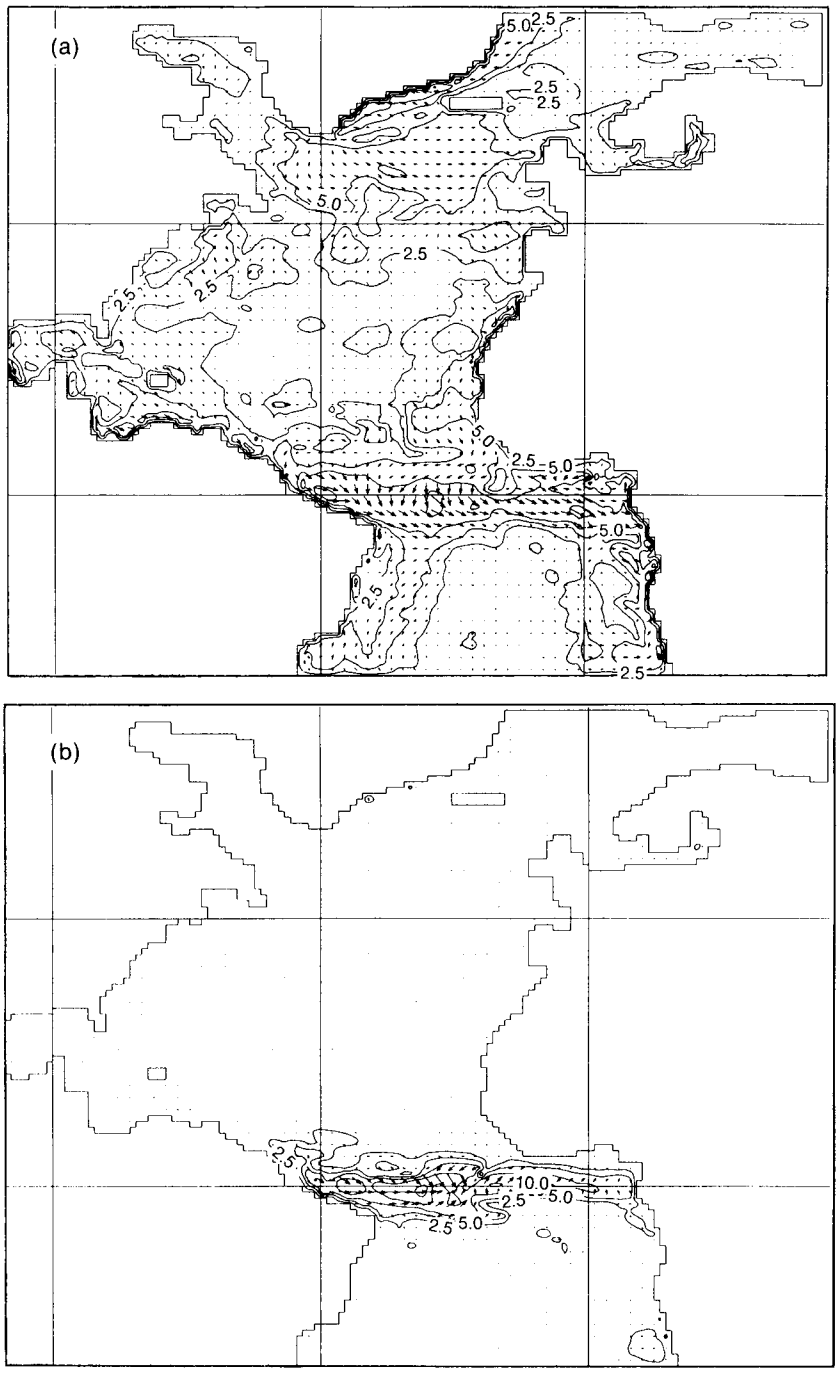

Figure 4. Monthly mean difference between the NWP momentum-forced run for October 1989 and the climatological run for (a) the model top-layer current, and (b) the 35-metre current. Contours at 2.5, 5, 10, 20 and 40 cm s^{-1}.

4.2 Discussion

Wind stress depends on the wind components and the drag coefficient, equations (1) and (2). Fig. 7 shows the 10-metre monthly mean wind from the CM model for October 1989. Actual sigma 1 wind was not available in the model archives and the 10-metre wind is used throughout this discussion instead. The strongest winds are the Trades and the mid-latitude westerlies. The mean wind speed in the CM model reaches over 6 m s^{-1} in the North-East Trades and over 8 m s^{-1} in the South-East Trades and the mid-latitude North Atlantic westerlies. Away from the coast (where interpolation errors may occur) differences of up to 0.75 m s^{-1} occur between the two models in an area where the CM wind is around 6 m s^{-1}, this corresponding to a difference of just over 10%. Ignoring the dependence of the drag coefficient on the wind speed in the FM model, the wind stress is proportional to the square of the wind speed (equations 1 and 2) and the wind mixing energy is proportional to the cube of the wind speed (equation 6). An uncertainty of 10% in the wind speed (a figure representative of the differences in Fig. 2) would therefore render uncertainties of 20% in the wind stress magnitude and 30% in the value of the wind mixing energy.

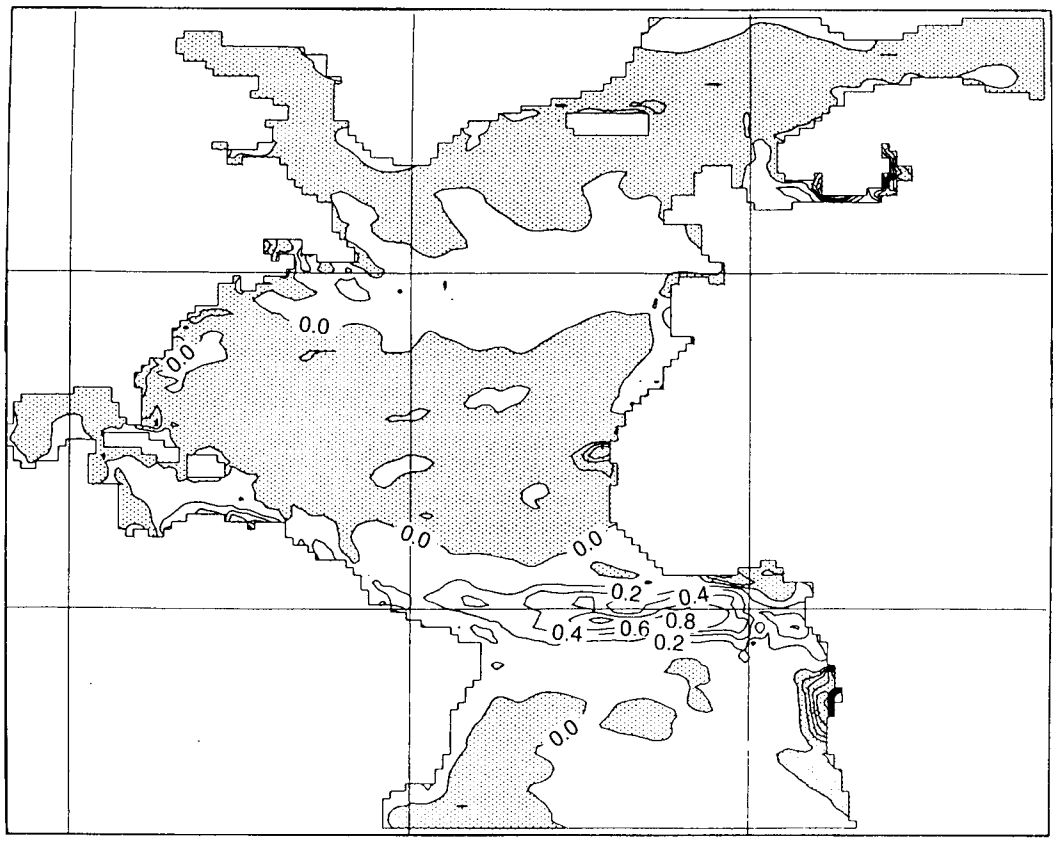

Figure 5. SST monthly mean difference between the NWP momentum-forced run and climatological control run for October 1989. Contours every 0.2 °C and negative areas are shaded.

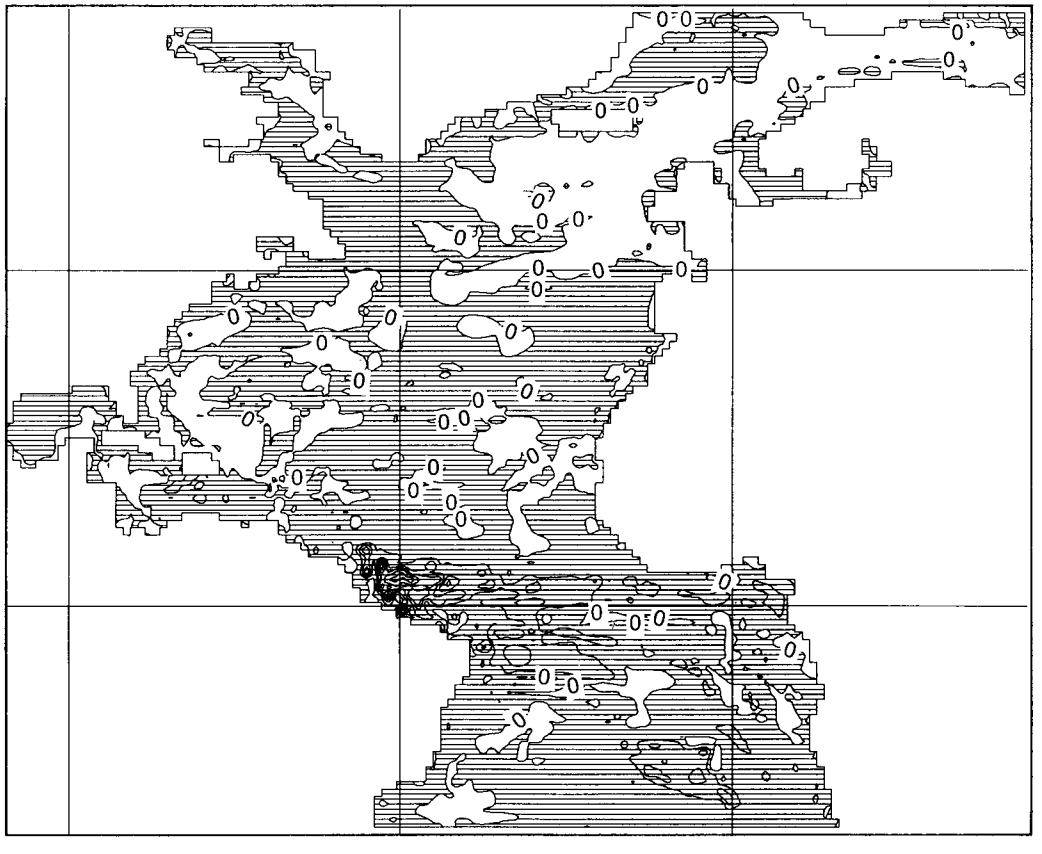

Figure 6. Mixed-layer depth monthly mean difference between the NWP momentum-forced run and the climatological control run for October 1989. Contours every 10 metres and negative areas are shaded.

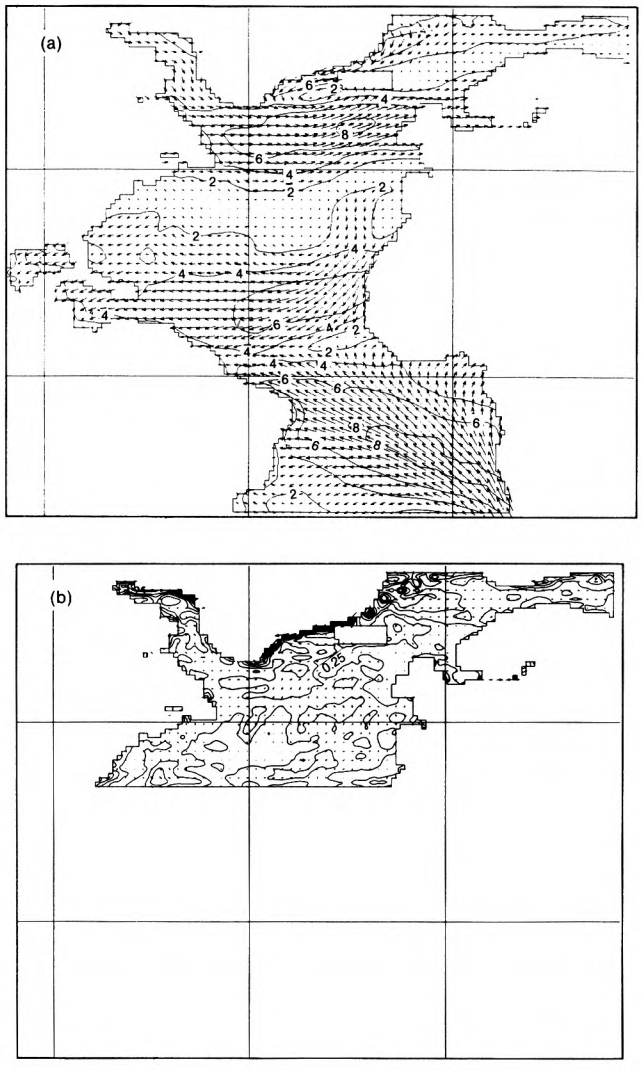

Figure 7. (a) CM model's monthly mean 10-metre wind vectors for October 1989; contours every 2 m s^{-1}, and (b) vector difference between the FM and CM models' monthly mean 10-metre winds for October 1989. Contours every 0.25 m s^{-1}.

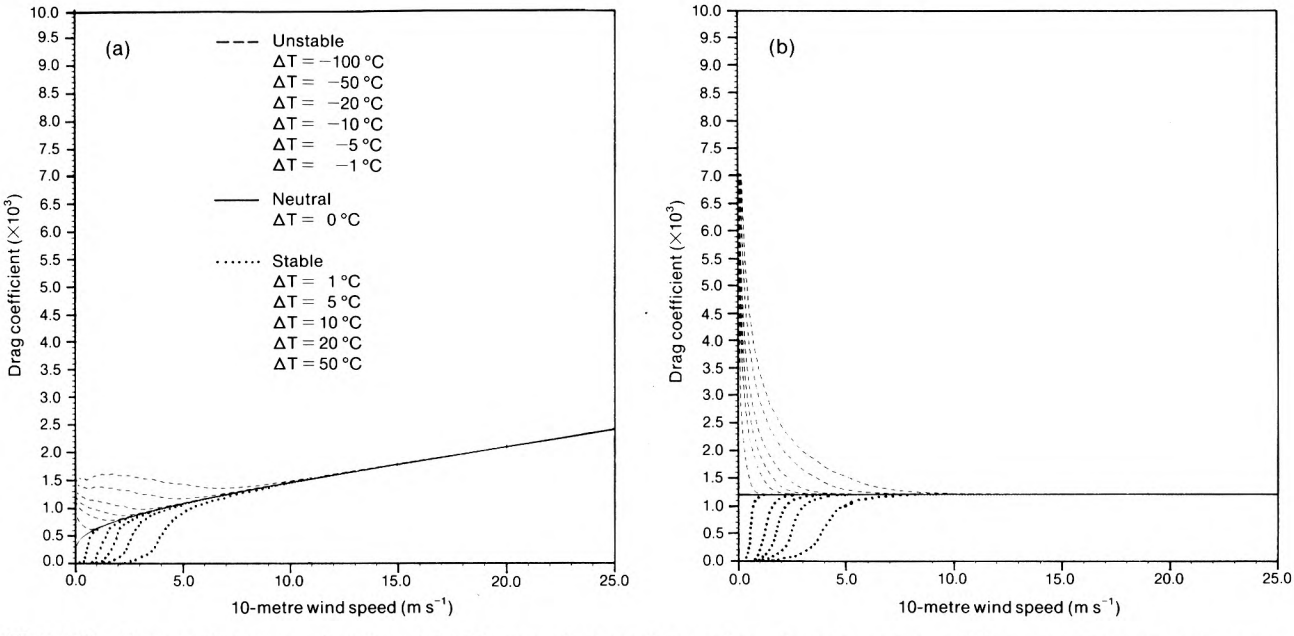

Figure 8. Drag coefficient as a function of the 10-metre wind speed for various air–sea temperature differences (ΔT) and zero humidity difference for (a) FM model, and (b) CM model.

Fig. 8 shows the drag coefficient at 10 metres for the FM and CM models as a function of the 10-metre wind for different stabilities (ΔT). The drag coefficients shown are those at 10-metres, although the model uses the drag coefficient at the first sigma level which is at about 30 metres above the ground. The reason for this is to allow for the easy comparison with other authors who use the 10-metre drag coefficient. For wind speeds greater than 6 m s^{-1} or so the different stability curves approach that of the neutral curve. The values of C_D from the two models agree well for wind speeds in the range 5 to 8 m s^{-1}. For wind speeds greater than 8 m s^{-1} the Charnock formula (5) in the FM model causes the drag coefficient to increase with wind speed whereas for the CM model the constant roughness length gives a constant neutral C_D. For a wind speed of 25 m s^{-1} the FM would use a value for C_D of 2.4×10^{-3}, twice that used by the CM model. It must be emphasized that although in Fig. 7(a) the mean wind speeds do not reach over 10 m s^{-1}, the field represents monthly mean values and the individual model time-step values may be much greater than this.

For wind speeds less than 5 m s^{-1} the stability dependence becomes important. The Charnock formula (5) in the FM model causes the surface roughness length to tend to zero quadratically with the wind speed. The neutral C_D line therefore decreases with wind speed and tends to zero. As an example, the value of C_D used by the FM model for a wind speed of 1 m s^{-1} is about 6×10^{-4}, half that used by the CM model. For stable conditions the difference between the two models' value of C_D is mainly due to the decrease in the neutral value in the FM model. Under slightly unstable conditions the value of C_D is very close to its neutral value and the difference between the two models is more or less due to the difference in the neutral value as a result of using the Charnock formula for the FM model. The differences between the two grow as stability and wind decrease. For conditions of free convection (Ri_B less than -100) the CM uses a value for C_D of around 1.5×10^{-3}, approximately four times larger than that used by the FM model. This is simply a consequence of using the Charnock formula for low wind speeds.

Parametrization of the drag coefficient has been reviewed by Garratt (1977). Later Blanc (1985) reviewed several empirical schemes used by different authors. His results for the neutral and slightly unstable drag coefficient are shown in Fig. 9. The variation between the schemes is large, for example the drag coefficient for a 10 m s^{-1} wind speed varies from 1.2×10^{-3} to 1.9×10^{-3}, a 50% difference. This indicates the difficulty in parametrizing the drag coefficient and the large

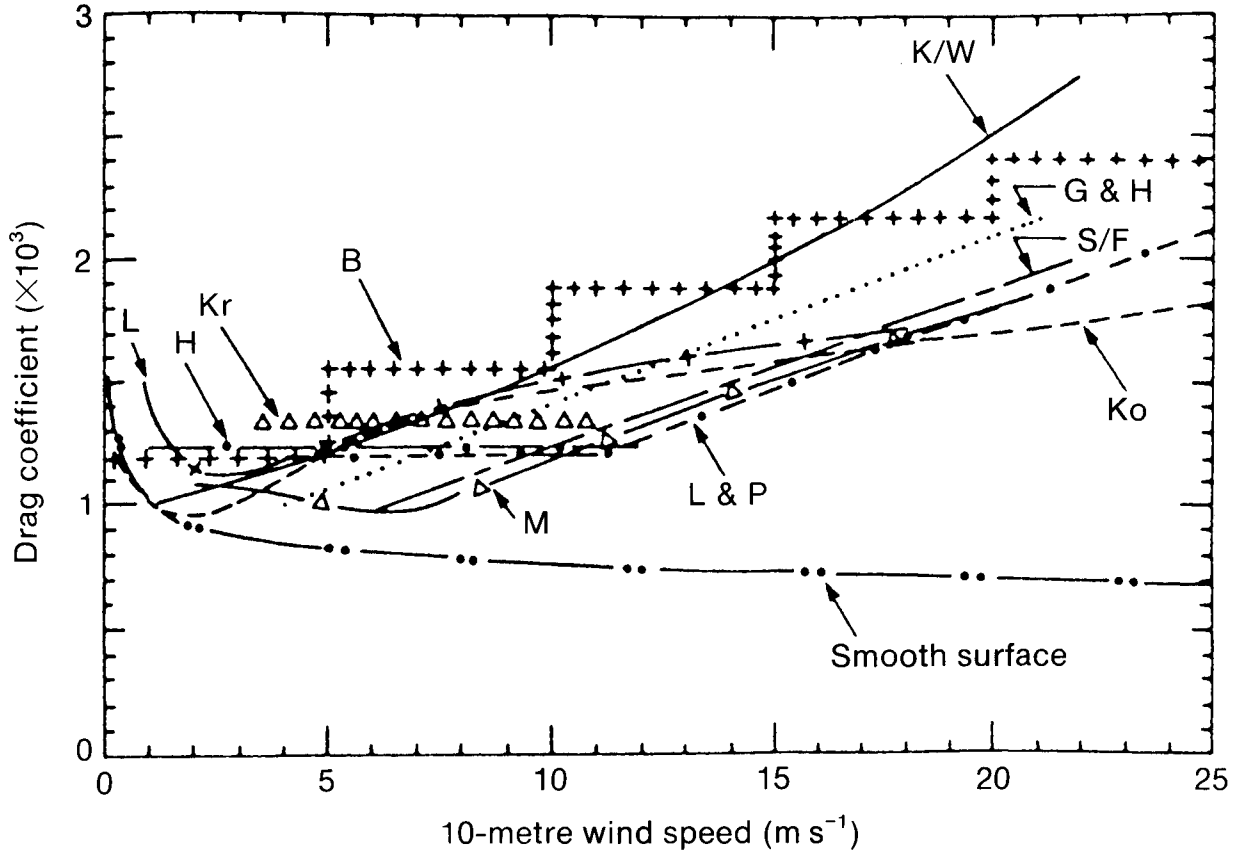

Figure 9. Drag coefficients for ten selected schemes and for a smooth surface under neutral or slightly unstable conditions as a function of the 10-metre wind speed (from Blanc 1985). Sources are: K/W = Kitaigorodskii *et. al.* (1973), Wu (1980); Ko = Kondo (1975); G & H = Garratt (1977), Garratt and Hyson (1975); B = Bunker (1976); Kr = Krügermeyer (1976); S/F = Smith (1980), Friehe and Schmitt (1976); H = Hasse *et. al.* (1978); L = Liu *et. al.* (1979); M = Masagutov (1981); L & P = Large and Pond (1981, 1982).

differences in the various empirical formulae. For all the empirical relations shown in Fig. 9 the neutral drag coefficient increases with wind speed for strong winds. The CM model has a constant C_D of 1.2×10^{-3} which deviates largely from those of Fig. 9 for wind speeds greater than 10 m s^{-1}. As an example, for a wind speed of 20 m s^{-1} the CM uses a value for C_D of 1.2×10^{-3} while the average of the schemes represented in Fig. 9 is 2×10^{-3}, i.e. 40% larger. For wind speeds less than 10 m s^{-1} the value used by the CM model is in good agreement with the other parametrizations. The use of the Charnock formula in the FM model produces a drag coefficient which increases with wind speed. For wind speeds greater than 5 m s^{-1}, the FM model's drag coefficient is in good agreement with that of the authors shown in Fig. 9. For low wind speeds, less than 5 m s^{-1}, the FM C_D decreases with wind speed, such is not the case with the other authors. As an example, the average value for C_D from Fig. 9 for a wind speed of 1 m s^{-1} is 1.1×10^{-3}, but the FM uses a value of 0.6×10^{-3}, a 45% underestimate. As regards the empirical relations of Fig. 9, the FM agrees well for large wind speeds but underestimates the value of C_D for light winds. On the other hand, the CM model agrees well for light winds but underestimates the value of C_D for strong winds.

Table II. Average neutral drag coefficient from various sources ($\times 10^3$). The letters refer to different parts of Fig. 10.

Source	Wind speed (m s^{-1}) 5	10	15	20	25
a_1	—	1.2	1.5	1.8	2.1
a_2	1.2	1.2	1.6	1.7	
b	—	1.2	1.6	1.9	2.2
c	1.0	1.3	1.7	2.2	—
d_1	1.2	1.2	1.4	1.8	—
d_2	1.2	1.2	1.5	1.8	—
Average	1.2	1.2	1.55	1.85	2.15
FM	1.0	1.4	1.8	2.1	2.4
CM	1.2	1.2	1.2	1.2	1.2

Fig. 10 shows several sets of observational measurements of the drag coefficient. For each of these plots and for wind speeds of 5, 10, 15, 20 and 25 m s^{-1} an average value was estimated and an overall average calculated as shown in Table II. The values from the FM and CM models are also shown.

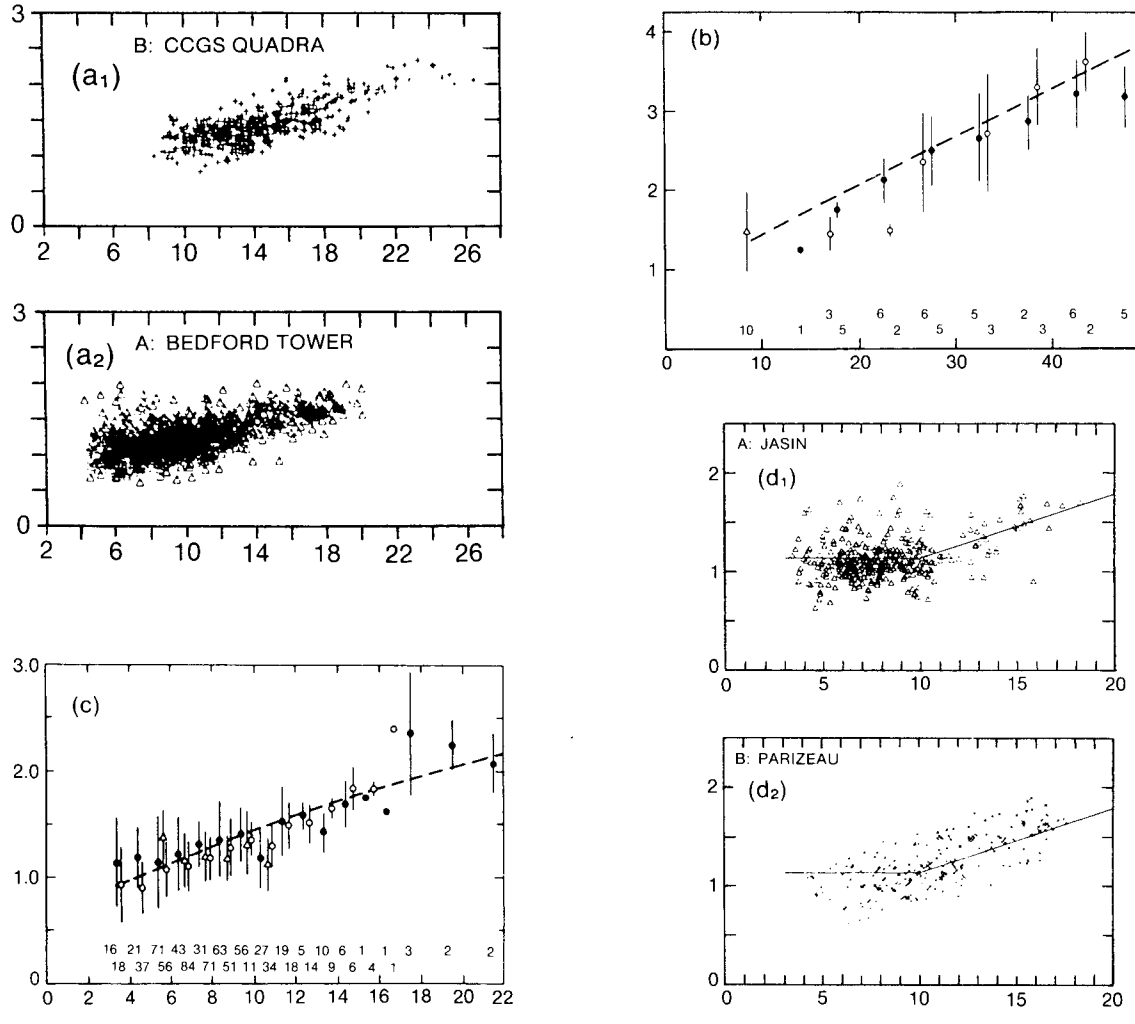

Figure 10. Experimental plots of the drag coefficient ($\times 10^3$) as a function of wind speed (m s^{-1}). (a) and (b) are from Large and Pond (1981), and (c) and (d) from Garratt (1977).

As already discussed the CM agrees well for wind speeds up to 10 m s^{-1} but badly for stronger winds. For light winds the FM model's C_D decreases with wind speed but this is not observed for C_D at a wind speed of 5 m s^{-1}. The table does however show that for the wind speeds of 10, 15, 20 and 25 m s^{-1} the use of the Charnock formula overestimates the drag coefficient by 10–15% when compared with the average observed values. However, it must be emphasized that the observed values have a large spread and that only the mean value has been considered in the above table.

Use of the Charnock formula to parametrize the surface roughness length has been discussed in detail by Hasse (1986). The failure of this formula to represent the roughness length for light winds, as seen from the FM drag coefficient, arises as a result of the flow becoming smooth and viscous effects coming into operation. Hasse (1986) suggests that for aerodynamically smooth flow the surface roughness should be proportional to the viscosity and inversely proportional to the friction velocity. This would imply that the drag coefficient would increase with decreasing wind speed for light winds. There is little *in situ* experimental evidence to support this except for laboratory experiments. For large wind speeds Hasse concludes that the Charnock formula is an attempt to represent a very complex interaction between the air, sea and waves in a simple formula.

Further development in the parametrization of the surface roughness length, and therefore the neutral drag coefficient, requires the consideration of the influence of the sea state on the atmospheric flow and vice versa. Geernaert (1987) indicates that there is evidence that the drag coefficient decreases with increasing wave fetch and/or increasing water column depth. He also suggests that the neutral drag coefficient exhibits a weak dependence on wind speed for open ocean conditions but exhibits a strong dependence for limited conditions of fetch and/or depth. Geernaert (1988) listed conditions for which wave-induced variations of the drag coefficient have been observed. There have been several attempts to parametrize the surface roughness using sea state parameters (for example Kitaigorodskii (1973), Hsu (1974), Huang and Long (1981), Byrne (1982), Donelan (1982), Geernaert *et al.* (1986), Toba and Koga (1986) and Toba *et al.* (1990)). Toba *et al.* (1990) found that in storm conditions the drag coefficient can be larger by a factor of two or three than the value predicted by the Charnock relation. Geernaert (1988) compared four wave-dependent parametrizations of the surface roughness, they being those of Kitaigorodskii (1973), Byrne (1982) and Donelan (1982), and a fourth which used a generalized version of the Charnock formula incorporating wave parameters. He concluded that the parametrization scheme of Kitaigorodskii (1973) best fitted the experimental data from near coastal locations. His results showed that the drag coefficient under strong winds increases with decreasing fetch and decreasing depth of water. Later, Janssen (1989) found there to be a strong dependence of the drag coefficient of air flow over sea waves on the wave age. For a young wind sea (small wave age) there was a strong coupling between wind and waves, whereas hardly any coupling was apparent for old wind sea. This dependence of the neutral drag coefficient on sea state explains some of the scatter in the observed values shown in Fig. 10, although a large proportion of the scatter is attributed to experimental uncertainties (Geernaert 1987).

For the new MO NWP 'unified model' the surface roughness will be initially parametrized using the Charnock formula but it will be constrained to remain at or above 10^{-4} metres. This leads to a neutral drag coefficient with the same values as that of the FM for strong winds, but having a minimum of 1.2×10^{-3} for light winds.

5. Summary and conclusion

The wind stress from the NWP models when compared with the climatological values showed large differences which were up to 50% of the climatological value. Over the tropical ocean, apart from limited areas within the Trade winds, the CM wind-stress magnitude was less than that of the climatology. In the west equatorial Atlantic the CM wind stress was up to 50% less than the climatology. These differences introduced anomalies in the surface current due to Ekman drift which are superimposed on the basin-scale circulations. The equatorial current system, which is driven by the longer term (order of one month) wind-stress curl, was reduced by up to 50% due to the lower magnitudes of the wind stress in the CM equatorial latitudes.

Comparison of the FM and CM 10-metre winds showed an uncertainty of 10% in the wind magnitude which leads to an uncertainty of 20% in the wind stress magnitude and 30% in the wind mixing energy. The wind mixing energy from the NWP models was not used in this study due to compressing problems while archiving the NWP model output.

Published values of the drag coefficient differ by over 50%. The average of the empirical results considered agree well with the FM and CM values for wind speeds in the range 5 to 8 m s^{-1}. For stronger winds the values of C_D were observed to increase with wind speed. The CM underestimates the values of C_D for strong winds as it uses a constant value. The FM uses the Charnock formula to parametrize the surface roughness length as a function of wind speed. Comparison with experimental results suggest that the FM overestimates the value of C_D by 10% to 15% for strong winds, although the experimental results showed a large scatter. For light winds the published values for the neutral C_D either

remained constant in good agreement with the CM value of 1.2×10^{-3} or increased slightly with decreasing wind speed. This was underestimated by the FM model which reduces the value of the neutral C_D to zero with the wind speed.

Geernaert (1988) suggested that the drag coefficient depends on the sea state and therefore on wave parameters such as fetch and water column depth. He concluded that the dependence of the neutral drag coefficient is less for the open ocean than for near coastal areas where the wave fetch is smaller and the water column depth is less deep. Janssen (1989) found that the drag coefficient additionally depended on wave age. Toba *et al.* (1990) stated that in storm conditions the drag coefficient can be up to two or three times larger than that when the Charnock formula is used.

A major factor in the determination of wind stress is now thought to be the influence of surface waves on the sea. Improvements to the simulation of wind stress are therefore most likely to arise from a parametrization of the drag coefficient which takes account of waves. The only satisfactory means of doing this is to couple a wave model to the atmosphere forecast model.

References

Alves, J.O.S. and Foreman. S.J., 1989: Use of operational NWP air-sea fluxes to drive an ocean model. *In.* Boer, G.J., 1989. Research activities in atmospheric and oceanic modelling. CAS/JSC Work. Group Numer. Exp. Report No. 13.

Bell, R.S. and Dickinson, A., 1987: The Meteorological Office operational numerical weather prediction system. *Sci Pap Meteorol Off*, No. 41.

Blanc, T.V., 1985: Variation of bulk-derived surface flux, stability and roughness results due to the use of different transfer coefficient schemes. *J Phys Oceanogr*, **15**, 650–669.

Bunker, A.F., 1976: Computations of surface energy flux and annual air–sea interaction cycles of the North Atlantic Ocean. *Mon Weather Rev*, **104**, 1122–1140.

Burridge, D. and Gilchrist, A., 1989: Estimates of surface fluxes from global operational numerical weather predictions. *Phil Trans R Soc Lond*, **A 329**, 303–315.

Byrne, H.M., 1982: The variation of the drag coefficient in the marine surface layer due to temporal and spacial variations in the wind and sea state. Ph.D. Dissertation, University of Washington.

Charnock, H., 1955: Wind stress on a water surface. *Q J R Meteorol Soc*, **81**, 639–640.

Cox, M.D., 1984: A primitive equation, three dimensional model of the ocean. GFDL Ocean Group Technical Report No. 1. Princeton, GFDL.

Donelan, M.A., 1982: The dependence of the aerodynamic drag coefficient on wave parameters. *In* First International Conference on Meteorology and Air-Sea Interaction in the Coastal Zone. Boston, American Meteorological Society.

Esbensen, S.K. and Kushnir, Y., 1981: The heat budget of the global oceans: An atlas based on estimates from surface marine observations. Report no. 29, Climate Research Institute, Oregon State University.

Friehe, C.A. and Schmitt, K.F., 1976: Parametrization of air–sea interface fluxes of sensible heat and moisture by the bulk aerodynamic formulas. *J Phys Oceanogr*, **6**, 801–809.

Garratt, J., 1977: Review of drag coefficients over oceans and continents. *Mon Weather Rev*, **105**, 915–929.

Garratt, J.R. and Hyson, P., 1975: Vertical fluxes of momentum, sensible heat and water vapour during the air mass transformation experiment (AMTEX) 1974. *J Meteorol Soc Japan*, **53**, 149–160.

Geernaert, G.L., 1987: On the importance of the drag coefficient in air–sea interactions. *Dyn Atmos Oceans*, **11**, 19–38.

—, 1988: Drag coefficient modelling for the near coastal zone. *Dyn Atmos Oceans*, **11**, 307–322.

Geernaert, G.L., Katsaros, K.B. and Richter, K., 1986: Variation of the drag coefficient and its dependence on sea state. *J Geophys Res*, **9**, 4762–4779.

Haney, R.L., 1971: Surface thermal boundary conditions for ocean circulation models. *J Phys Oceanogr*, **1**, 241–248.

Hasse, L., 1986: On Charnock's relation for the roughness at sea. *In* (eds) E.C. Monahan and G. MacNiocaill, Oceanic whitecaps and their role in air–sea exchange processes. Dordrocht, Reidel.

Hasse, L., Grünewald, M., Wucknitz, J., Dunckel, M. and Schriever, D., 1978: Profile derived turbulent fluxes in the surface layer under disturbed and undisturbed conditions during GATE. *'Meteor' Forschungsergeb*, **13**, 540–545.

Hellerman, S. and Rosenstein, M., 1983: Normal monthly wind stress over the ocean with error estimates. *J Phys Oceanogr*, **13**, 1093–1104.

Hsu, S.A., 1974: A dynamic roughness equation and its application to wind stress determination at the air-sea interface. *J Phys Oceanogr*, **4**, 116–120.

Huang, N. and Long, S., 1981: On the importance of significant slope in empirical wind studies. *J Phys Oceanogr*, **11**, 569–573.

Jaeger, L., 1983: Monthly and areal patterns in mean global precipitation. *In* (eds) A. Street-Perrott, A. Beran and R. Radcliffe, Variations in the global water budget. Dordrecht Reidel.

Janssen, P.A.E.M., 1989: Wave-induced stress and the drag of air flow over sea waves. *J Phys Oceanogr*, **19**, 745–754.

Kitaigorodskii, S.A., 1973: The physics of air–sea interactions. Translated from Russian by A. Baruch, Israel Program of Scientific Translations, Jerusalem.

Kitaigorodskii, S.A., Kuznetsov, O.A. and Panin, G.N., 1973: Coefficients of drag, sensible heat and evaporation in the atmosphere over the surface of the sea. Izv. Acad. Sci. USSR, *Atmos Ocean Phys*, **9**, 644–647 (English translation).

Kitchen, J.E., 1986: An implicit version of the operational model boundary layer routine. (Unpublished copy available in the National Meteorological Library, Bracknell.)

Kondo, J., 1975: Air–sea bulk transfer coefficients in diabatic conditions. *Boundary Layer Meteorol*, **9**, 91–112.

Kraus, E.B. and Turner, J.S., 1967: A one-dimensional model of the seasonal thermocline, II. The general theory and its consequences. *Tellus*, **19**, 98–105.

Krügermeyer, L., 1976: Vertical transports of momentum, sensible and latent heat from profiles at the tropical Atlantic during ATEX. *'Meteor' Forschungsergeb*, **11**, 51–77.

Large, W.G. and Pond, S., 1981: Open ocean momentum flux measurements in moderate to strong winds. *J Phys Oceanogr*, **11**, 324–336.

—, 1982: Sensible and latent heat flux measurements over the ocean. *J Phys Oceanogr*, **12**, 464–482.

Levitus, S., 1982: Climatological atlas of the world ocean. N.O.A.A. Prof. Paper No. 13.

Liu, W.T., Katsaros, K.B. and Businger, J.A., 1979: Bulk parametrizations of air–sea exchanges of heat and water vapor including the molecular constraints at the interface. *J Atmos Sci*, **36**, 1722–1735.

Masagutov, T.F., 1981: Calculations of vertical turbulent fluxes in the near-water atmospheric layer over the ocean in tropical latitudes. *Meteorol Gidrol*, **12**, 61–68.

Pacanowski, R.C. and Philander, S.G.H., 1981: Parametrization of vertical mixing in numerical models of tropical oceans. *J Phys Oceanogr*, **11**, 1443–1451.

Redi, M.H., 1982: Oceanic isopycnal mixing by coordinate rotation. *J Phys Oceanogr*, **12**, 1154–1158.

Smith, S.D., 1980: Wind stress and heat flux over the ocean in gale force winds. *J Phys Oceanogr*, **10**, 709–726.

Toba, Y. and Koga, M., 1986: A parameter describing overall conditions of wave breaking, whitecapping, sea-spray production and wind stress. *J Phys Oceanogr*, **19**, 745–754.

Toba, Y., Noriko, I., Kawamura, H., Ebuchi, N. and Jones, I.S.F., 1990: Wave dependence of sea-surface wind stress. *J Phys Oceanogr*, **20**, 705–721.

Wu, J., 1980: Wind-stress coefficients over the sea surface near neutral conditions — A revisit. *J Phys Oceanogr*, **10**, 727–740.

Satellite photographs — 27 June 1991 at 0805 UTC

The NOAA-10 infra-red image (Fig. 1) illustrates the pattern of sea surface temperature near the Strait of Gibraltar and the Alboran Basin. The image has been 'enhanced' so that the whole grey-scale range (from black to white) occurs within a few degrees Celsius (approximately 17–22 °C) — corresponding to the range of sea surface temperatures. The visible image taken at the same time (Fig. 2) indicates that only a few patches of cloud are present over the sea, and hence confirms that almost all the structure seen over the sea in the infra-red image is due to variation in the sea temperature.

The main feature is the region of cold water close to the Strait of Gibraltar. Daily inspection of infra-red images suggests it to be commonly observed, particularly during the summer months, although there are often significant day-to-day differences in its pattern. In the Alboran Basin, large anticyclonic gyres are normally present which sometimes draw in cold water from the Strait of Gibraltar.

The cold sea can have significant effects on the weather. For example, at Gibraltar, the highest incidence of sea fog occurs in August. A change of wind direction to an easterly bringing moisture-laden air from the Alboran Basin frequently results in either fog or very low cloud, whereas onshore winds at observing stations in the Alboran Basin away from the region of cold water do not lead to these conditions.

G.A. Monk

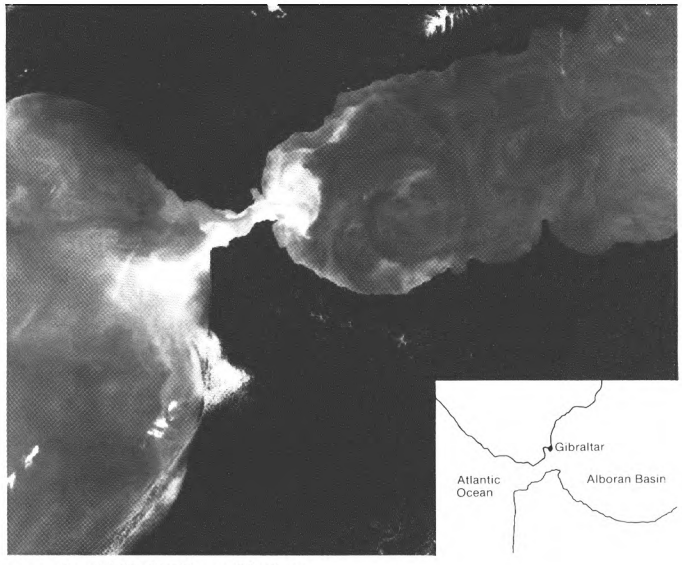

Figure 1. NOAA-10 infra-red image for 0805 UTC on 27 June 1991. The insert shows the places mentioned in the text.

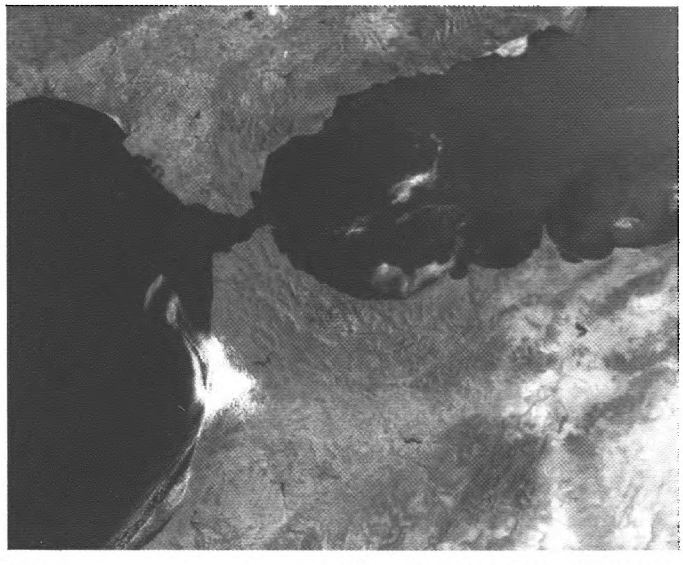

Figure 2. As Fig. 1 but visible image.

Photographs by courtesy of University of Dundee

GUIDE TO AUTHORS

Content

Articles on all aspects of meteorology are welcomed, particularly those which describe results of research in applied meteorology or the development of practical forecasting techniques.

Preparation and submission of articles

Articles, which must be in English, should be typed, double-spaced with wide margins, on one side only of A4-size paper. Tables, references and figure captions should be typed separately. Spelling should conform to the preferred spelling in the *Concise Oxford Dictionary* (latest edition). Articles prepared on floppy disk (Compucorp or IBM-compatible) can be labour-saving, but only a print-out should be submitted in the first instance.

References should be made using the Harvard system (author/date) and full details should be given at the end of the text. If a document is unpublished, details must be given of the library where it may be seen. Documents which are not available to enquirers must not be referred to, except by 'personal communication'.

Tables should be numbered consecutively using roman numerals and provided with headings.

Mathematical notation should be written with extreme care. Particular care should be taken to differentiate between Greek letters and Roman letters for which they could be mistaken. Double subscripts and superscripts should be avoided, as they are difficult to typeset and read. Notation should be kept as simple as possible. Guidance is given in BS 1991: Part 1: 1976, and *Quantities, Units and Symbols* published by the Royal Society. SI units, or units approved by the World Meteorological Organization, should be used.

Articles for publication and all other communications for the Editor should be addressed to: The Chief Executive, Meteorological Office, London Road, Bracknell, Berkshire RG12 2SZ and marked 'For Meteorological Magazine'.

Illustrations

Diagrams must be drawn clearly, preferably in ink, and should not contain any unnecessary or irrelevant details. Explanatory text should not appear on the diagram itself but in the caption. Captions should be typed on a separate sheet of paper and should, as far as possible, explain the meanings of the diagrams without the reader having to refer to the text. The sequential numbering should correspond with the sequential referrals in the text.

Sharp monochrome photographs on glossy paper are preferred; colour prints are acceptable but the use of colour is at the Editor's discretion.

Copyright

Authors should identify the holder of the copyright for their work when they first submit contributions.

Free copies

Three free copies of the magazine (one for a book review) are provided for authors of articles published in it. Separate offprints for each article are not provided.

Contributions: It is requested that all communications to the Editor and books for review be addressed to the Chief Executive, Meteorological Office, London Road, Bracknell, Berkshire RG12 2SZ, and marked 'For *Meteorological Magazine*'. Contributors are asked to comply with the guidelines given in the *Guide to authors* which appears on the inside back cover. The responsibility for facts and opinions expressed in the signed articles and letters published in *Meteorological Magazine* rests with their respective authors.

Subscriptions: Annual subscription £33.00 including postage; individual copies £3.00 including postage. Applications for postal subscriptions should be made to HMSO, PO Box 276, London SW8 5DT; subscription enquiries 071–873 8499.

Back numbers: Full-size reprints of Vols 1–75 (1866–1940) are available from Johnson Reprint Co. Ltd, 24–28 Oval Road, London NW1 7DX. Complete volumes of *Meteorological Magazine* commencing with volume 54 are available on microfilm from University Microfilms International, 18 Bedford Row, London WC1R 4EJ. Information on microfiche issues is available from Kraus Microfiche, Rte 100, Milwood, NY 10546, USA.

November 1991

Edited by Corporate Communications
Editorial Board: R.J. Allam, R. Kershaw, W.H. Moores, P.R.S. Salter

Vol. 120
No. 1432

Contents

ISSN 0026–1149

ISBN 0-11-728862-4

9 780117 288621

Printed in the United Kingdom for HMSO
Dd 0291241 11/91 C13 503 12521

The Meteorological Magazine

December 1991

Indian Ocean circulation model
Meteorological products for agriculture
July 1959 temperatures

HMSO

Met.O.998 Vol. 120 No. 1433

First published 1991

HMSO publications are available from:

HMSO Publications Centre
(Mail and telephone only)
PO Box 276, London, SW8 5DT
Telephone orders 071-873 9090
General enquiries 071-873 0011
(queuing system in operation for b

HMSO Bookshops
49 High Holborn, London, WC1V
258 Broad Street, Birmingham, B1
Southey House, 33 Wine Street, B
9–21 Princess Street, Manchester,
80 Chichester Street, Belfast, BT1
71 Lothian Road, Edinburgh, EH

HMSO's Accredited Agents
(see Yellow Pages)

and through good booksellers

The Meteorological Magazine

December 1991
Vol. 120 No. 1433

551.465(267)

An Ocean General Circulation Model of the Indian Ocean for hindcasting studies

D.J. Carrington
Meteorological Office, Bracknell

Summary

As part of the WMO TOGA (Tropical Oceans Global Atmosphere) programme, an Ocean General Circulation Model of the Indian Ocean has been developed at the Meteorological Office with the aim of being able to hindcast the upper-level circulation. In this paper the background to this project is outlined, including an overview of the important processes in tropical ocean dynamics and the main features of the Indian Ocean circulation. A description of the model is then given, and the model simulation of the climatological seasonal cycle currents in response to climatological wind stresses and heat fluxes is discussed. In a subsequent paper the response of the model to interannually varying forcing fields (a further step towards developing the hindcasting capability of the model) will be discussed.

1. Introduction

In the early 1980s, the World Climate Research Programme of the World Meteorological Organization inaugurated an international co-ordinated programme of research, called TOGA (Tropical Oceans Global Atmosphere) to run from 1985 to 1995. It is designed to investigate the interactions between the tropical oceans and the atmosphere with a view to furthering the understanding of this coupled system and ultimately to forecast its changes (WCRP 1985).

TOGA consists of two main streams of research: observational and modelling. The principal aim of the modelling programme is to produce a realistic fully coupled operational model of the tropical oceans and global atmosphere. The achievement of this objective is necessarily a step-by-step process — each of the tropical oceans is studied separately, and a hierarchy of models is used to explore the physical processes involved.

One of the contributions being made to this research by the Meteorological Office Unit at the Hooke Institute in Oxford is the development of an Ocean General Circulation Model (OGCM) of the Indian Ocean for hindcasting the upper-level circulation. In this paper a description of the model is given and an assessment made of its ability to simulate the climatological currents in the Indian Ocean in response to climatological forcing. In a subsequent paper the next step in developing the hindcasting capability of the model, namely the use of fields derived from operational Numerical Weather Prediction model analyses to force the model, will be discussed.

Before proceeding to the description of the model in section 3, an introduction to the subject of modelling the Indian Ocean is given in section 2. The important aspects of tropical ocean dynamics are outlined, leading to an overview of the Indian Ocean circulation; a summary of the modelling work relevant to this study is then given. This section provides the background for both this paper and the subsequent paper in which further results are presented.

2. Background to Indian Ocean modelling

2.1 Tropical ocean dynamics

Overviews of ocean circulation in the Tropics have been provided by Hastenrath (1985) and Knox and Anderson (1985). The principal driving force for surface

currents in the Tropics is the wind stress. Since the TOGA programme is concerned with tropical ocean to global atmosphere interaction, the currents which are of greatest interest are those which have the maximum impact on low latitude sea surface temperatures, namely the wind-driven surface currents of the tropical regions. The World Ocean Circulation Experiment (WOCE) will seek further understanding of the circulation in the global ocean, both in the surface layers and at depth.

The wind drives the ocean both directly and indirectly. Because of the Coriolis force the direct forcing results in Ekman drift, by which wind-driven currents flow to the right of the wind direction in the northern hemisphere and to the left in the southern hemisphere. In the Tropics, two differences with respect to circulation in higher latitudes arise. Firstly, the Coriolis parameter on the Equator is zero so that the current direction there tends to be directly downwind. Secondly, the reversal in direction of the Ekman drift relative to the wind direction across the Equator results in divergent flow away from the Equator if the wind is easterly, convergent if westerly; divergence leads to upwelling on the Equator, convergence to downwelling. The zero value of the Coriolis parameter on the Equator enables equatorial currents to be spun-up rapidly; for example, a zonal wind stress of 0.2 dyn cm^{-2} acting for 1 month over a depth of 50 m will produce a current speed of about 1 m s^{-1}.

The wind affects currents indirectly in two ways. Firstly, the curl of the wind stress produces vertical motion in the oceanic boundary layer (so-called 'Ekman pumping'); this leads to vertical displacement of the thermocline, resulting in horizontal density gradients which in turn produce geostrophic currents. Secondly, changes in the wind forcing can generate waves in the surface currents. These waves provide a key mechanism by which information can be transmitted rapidly within the tropical oceans. The equatorial region forms a wave-guide for zonally-propagating waves, enabling information to be carried across a tropical ocean far more rapidly than at mid latitudes. Rossby waves are the principal mode for westward-propagating waves and Kelvin and Yanai (mixed Rossby-gravity) waves for eastward-propagating disturbances.

Because the applied wind stress on an ocean is a time-variant property, wind-driven currents vary correspondingly. On the inter-seasonal time-scale, the wind patterns in the tropical Pacific and Atlantic remain fairly constant and nowhere are there large-scale seasonal reversals in wind direction. However, in many parts of the Indian Ocean the wind direction does reverse seasonally (see Fig. 1). This factor (together with the distinctly different geography of the Indian Ocean in comparison with that of the Pacific and Atlantic, the Indian Ocean having a northern land boundary at sub-tropical latitudes) results in the principal currents being significantly different from those in the other two oceans, especially in the equatorial and north Indian Ocean.

2.2 Indian Ocean circulation

2.2.1 Equatorial currents

During the winter monsoon (or North-east Monsoon), an eastward Equatorial Counter Current (ECC) lies between the two westward currents — the North Equatorial Current (NEC) and South Equatorial Current (SEC) — driven by the Trade Winds. In contrast to the Pacific and Atlantic, the ECC lies to the south of the Equator, at about 5°S; this is consistent with the applied wind field in Fig. 1(a).

During the summer monsoon (or South-west Monsoon), the NEC and ECC disappear and are replaced by a single eastward current, the South-west Monsoon Current (SMC). The boundary between the SMC and the SEC lies close to the Equator.

The transition periods between the monsoons tend to be characterized by a rather more variable current pattern; the SEC is the only main current which persists though all the seasons, though its latitudinal position varies. A strong (up to 1 m s^{-1}) eastward current, the Wyrtki Jet (Wyrtki 1973), has been observed (Knox 1976) to develop on the Equator during both transition periods as a result of strong westerly winds.

The principal sub-surface current is the Equatorial Undercurrent (EUC) which exhibits a strong semi-annual cycle. It is effectively wind forced, being created by the sub-surface longitudinal pressure gradients which result from the surface wind-driven flow. It flows westward during the transition periods between the monsoons and eastward the rest of the year. This is in contrast to the EUC in the Pacific and Atlantic which flows eastward thoughout the year in response to the sub-surface zonal density gradient along the Equator, formed mainly by the westward surface flow. In the Indian Ocean the behaviour of the EUC seems to be more complex and is not a simple function of the equatorial winds.

2.2.2 Western boundary

The western boundary current of the Indian Ocean is unique amongst the major western boundary currents of the world in that it exhibits complete reversal in direction in an annual cycle (with the exception of the boundary current in the western Pacific which also undergoes a seasonal reversal, though of smaller amplitude, in response to the reversal in the monsoon winds). During the North-east Monsoon, the surface current is southward along most of the length of Africa, including a strong cross-equatorial flow. Between about April and May the flow everywhere northward of about 10°S reverses direction; the cross-equatorial flow becomes northward and a major boundary current, the Somali Current, is generated. A component of the SEC turns northward to form the cross-equatorial flow, the remainder turning southward as during the North-east Monsoon.

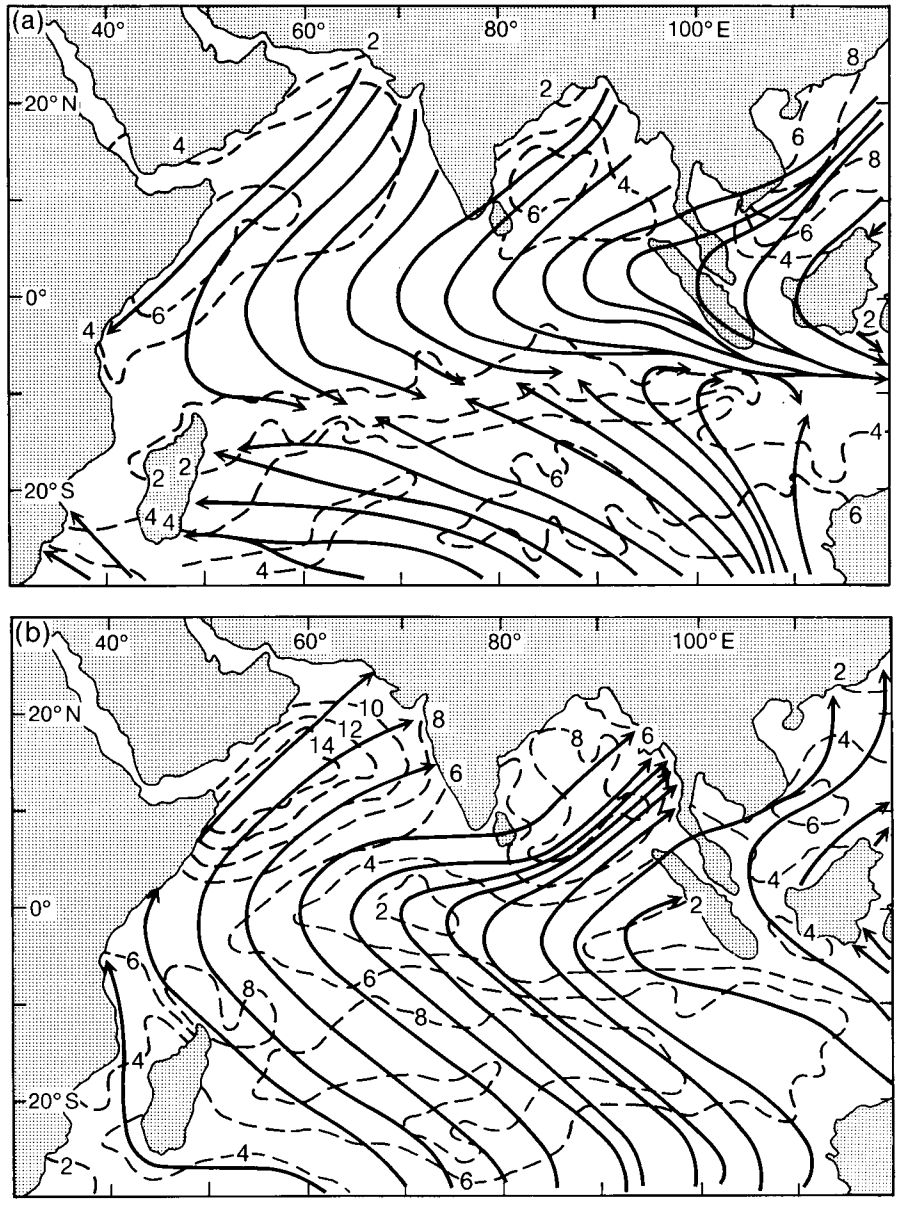

Figure 1. Surface wind field over the tropical Indian Ocean in (a) January and (b) July; streamlines, and isotachs (m s^{-1}). (From Hastenrath and Lamb, 1980).

In association with the Somali Current, a major recirculation pattern develops. The flow separates from the coast at approximately 9–10° N and forms a large gyre, the 'Great Whirl' (first recorded by Findlay (1866)). A second, smaller, recirculation pattern has also been detected offshore between about 10° N and 12° N, the 'Socotra Eddy'. These current systems appear to be a complex result of both remote and local forcing (Lighthill 1969, Leetmaa 1973) and may have a natural time-dependence rather than being a steady-state pattern (McCreary and Kundu 1988).

2.2.3 Interannual variability

It is well known that the monsoon winds, and the rainfall on the Indian sub-continent associated with the summer monsoon, vary from year to year. Far less is known about the interannual variability in the ocean currents which must result. Most of the earlier work carried out on the link between the Indian Ocean and the monsoon has concentrated on the sea surface temperatures (SSTs) in the Arabian Sea. Schott and Quadfasel (1982) observed large interannual differences in the currents in the Somali region during the onset of the South-west Monsoon, and there is a correlation between low SSTs in the Arabian Sea, a wet monsoon in India and a strong two-gyre system in the Somali region. The need for greater understanding of the interannual variability in the Indian Ocean as a whole has been stressed by Knox and Anderson (1985).

A model of the Indian Ocean which seems to simulate well the climatologically observed currents in response to forcing by climatological winds should provide a suitable tool for studying this interannual variability when forced by interannually varying winds.

2.3 Indian Ocean modelling

2.3.1 General

Lighthill (1969) was the first to try to model the wind-driven circulation of the Indian Ocean. Wunsch (1977) later investigated the response of a model to a seasonally varying wind-forcing. Climatological winds have subsequently been used as forcing in a hierarchy of model types; for example, Schott *et al.* (1988) used both a reduced-gravity model and a multi-layer model forced by the climatological winds of Hellerman and Rosenstein (1983). Many limited-area modelling studies have been carried out, with particular interest being paid to the Somali region; McCreary and Kundu (1988), for example, used an idealized wind stress pattern and a so-called 2½-layer model to produce a two-gyre system.

Only recently has much work been done using observed winds for forcing a model. Luther and O'Brien (1989) used the ship-wind data set of Cadet and Diehl (1984) to force a reduced-gravity model of the whole Indian Ocean. The simulated currents are qualitatively realistic; the two-gyre system is reproduced in some years and not in others, a feature of interannual variability which is in agreement with observations.

In order to simulate the temperature field accurately the thermodynamics as well as the dynamics of the model upper levels must be represented realistically and vertical heat transport must be included. Therefore the forcing by observed winds of a more complex model, which represents the 3-dimensional circulation, is required.

2.3.2 OGCMs

Bryan (1969) was the first to develop a general circulation model of the ocean (an OGCM), which was later adapted by Semtner (1974) and then by Cox (1984). The use of OGCMs has been explored extensively, including their response to observed forcing. Thus, Philander and Seigel (1985) clearly demonstrated the ability of such models to reproduce the observed variations of thermal and velocity structure of equatorial oceans in response to NWP model winds, and since then, study of the tropical Pacific Ocean using OGCMs forced by actual winds has become relatively well advanced. Leetmaa and Ji (1988) used wind stresses both from ship reports and from operational atmospheric analyses when assimilating hydrographic and thermal data and estimates of sea surface temperatures derived from satellite radiances and ship observations into the National Meteorological Centre's OGCM for operational hindcasting of the tropical Pacific. Harrison *et al.* (1989) have further indicated the sensitivity of a Pacific OGCM to the wind stress field used, and Merle and Morlière (1988) have outlined the progress made towards a similar operational model of the Atlantic.

Use of OGCMs of the Indian Ocean has, to date, been very limited. The Meteorological Office model described here is the first one to be used for hindcasting purposes.

3. The model

A 'primitive equation' ocean model is used. This takes the six so-called primitive equations of fluid motion — the x and y components of the momentum equation, the thermodynamic energy equation, the continuity equation, the hydrostatic approximation and the equation of state — and solves them numerically on a finite-difference grid. The numerical scheme is that given by Cox (1984) using the finite-differencing methods of Bryan (1969). The barotropic mode is excluded from the solution. It was thought reasonable to do this since the barotropic velocities in the upper levels (those of interest) are an order of magnitude smaller than the baroclinic velocities. This has the advantage of significantly relaxing the constraints on the time-step used; the time-step for the model grid used here (described below) is 72 minutes, whereas it would need to be about 2 minutes with the barotropic mode.

The complete model domain is from 27° N to 36° S and from 35° E to 125° E. An irregular horizontal grid is used, illustrated in Fig. 2. The maximum latitudinal grid-spacing is 1°; this reduces towards the Equator from 24° N and 24° S, according to a sine function, to be ⅓° within ±1° of the Equator. Longitudinal grid-spacing is 1½° east of 64° E, decreasing westward to be ½° everywhere west of 56° E. The important dynamics of the equatorial and western boundary regions can therefore be relatively well resolved. There are 16 levels in the vertical with a resolution of 10 m for the top 30 m. The model has a constant depth of 4000 m.

The vertical mixing scheme of Pacanowski and Philander (1981) is used, in which the vertical eddy viscosity and eddy diffusivity coefficients depend upon the local Richardson number. The horizontal eddy diffusion coefficient varies across the grid and is set to be proportional to the larger of the latitudinal and longitudinal local grid-spacing. It takes a minimum value of 2×10^7 cm^2 s^{-1}. The coefficients of diffusivity of heat and salinity are constant across the grid, set also at 2×10^7 cm^2 s^{-1}.

The model has closed boundaries except on the southern side. The coast of southern Africa is artificially forced to run due south down the 35° E meridian. The open boundary conditions applied on the southern boundary are designed to keep the vertical profiles of temperature and salinity close to climatology (the climatological fields used are those given by Levitus (1982)).

For these and other model details, including stability considerations, see Gordon (1985).

4. Seasonal-cycle experiment

An experiment was performed with the model in order to simulate the climatological seasonal cycle of currents in the Indian Ocean.

4.1 Experiment details

Climatological forcing fields were used. The applied heat flux is based on a Haney (1971) condition:

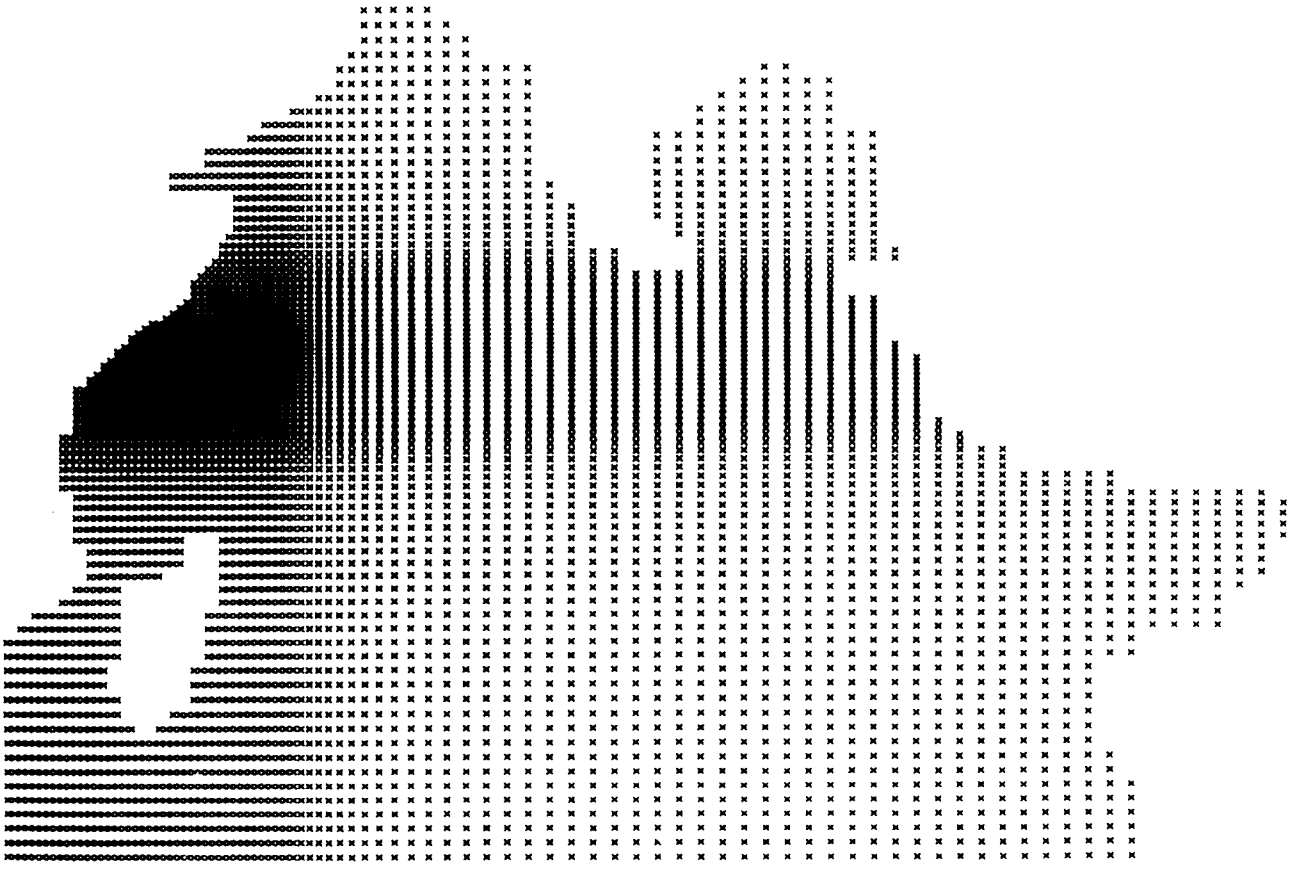

Figure 2. The Indian Ocean model horizontal grid.

$$Q = Q_C + \lambda_H (T - T_C)$$

where

Q = net heat flux
Q_C = climatological net heat flux
T = temperature at the 5 m level (the uppermost grid-point)
T_C = climatological SST
λ_H = Haney heat flux coefficient = -35 W m^{-2} K^{-1}.

There is therefore a negative feedback acting on the SST, pulling it towards climatology. Note that when $T = T_C$ the heat flux is equal to the climatological value. The net surface heat flux climatology is taken from Esbensen and Kushnir (1981) and the SST climatology is from the Meteorological Office (Bottomley *et al.* 1990).

The salinity flux is of similar form and depends on the net difference between precipitation (P) and evaporation (E).

$$P - E = (P_C - E_C) + \lambda_S (S - S_C)$$

where

S = the salinity at the uppermost grid point
λ_S = 2 mm(day)$^{-1}$ (ppt)$^{-1}$.

The value of the coefficient, λ_S, is chosen so that relaxation back to the Levitus (1982) climatology occurs on the same time-scale as that of temperature; model experiments have shown that this is necessary for the temperature and salinity fields to evolve in a consistent manner, but there is no specific physical justification for it. The precipitation and evaporation climatologies are taken from Jaegar (1976) and Esbensen and Kushnir (1981) respectively.

For both the heat and salinity fluxes, the magnitude of the feedback term ($\lambda_H(T - T_C)$ and $\lambda_S(S - S_C)$ respectively) indicates the amount of deviation of the model fluxes from the prescribed climatological surface fluxes and is the size of the 'anomalous' flux of heat and fresh water consequently added to or subtracted from the model. These anomalous flux fields may be used as a model diagnostic and will be discussed further in section 4.2.

The applied climatological wind stress is the monthly mean fields given by Hellerman and Rosenstein (1983), who calculated the data on a 2° grid from over 100 years' surface wind observations.

The starting fields used for the experiment were the climatological temperature and salinity fields for September derived from observations by Levitus (1982) and zero velocities. The model was run for just over three years. After a two-year spin-up period, by which time the model had settled to the applied fluxes to a

depth of 200–300 m, the final year (November–October) was taken to represent the seasonal cycle.

4.2 Model results

4.2.1 Currents

The model simulation of the seasonal cycle is compared with estimates of current climatology from observations. The current climatologies used are those given by Hastenrath (1985) (taken from Düing (1970)), Knox and Anderson (1985) (taken from Deutsches Hydrographisches Institut (1960)) and an analysis by Rao *et al.* (1989) of the ship-drift data set produced by Cutler and Swallow (1984); the observed surface currents for January and July taken from Rao *et al.* are illustrated in Fig. 3.

The aim of the present study is to simulate the wind-driven circulation and SSTs. The focus of attention is therefore on the upper-level currents, the currents at the uppermost velocity grid-point (5 m) being used for this purpose. Monthly mean currents are presented; this facilitates easy comparison with data from other sources. Because the model SSTs are strongly influenced by the SST climatology used in the heat flux parametrization scheme, they will not be discussed here.

The principal features of the Indian Ocean circulation are well reproduced by the model in response to forcing by seasonally varying climatological winds. Fig. 4 shows the simulated surface currents for three months — January, July and May.

The equatorial surface currents compare well with observations. In January, the NEC, extending to just south of the Equator, and the strong ECC can be seen in Fig. 4(a). Maximum current velocities are realistic: in excess of 60 cm s^{-1} for the NEC, around 40 cm s^{-1} for the ECC, and 20–30 cm s^{-1} for the SEC. The latitudinal positions of these currents are also consistent with observations. In July (see Fig. 4(b)), the maximum

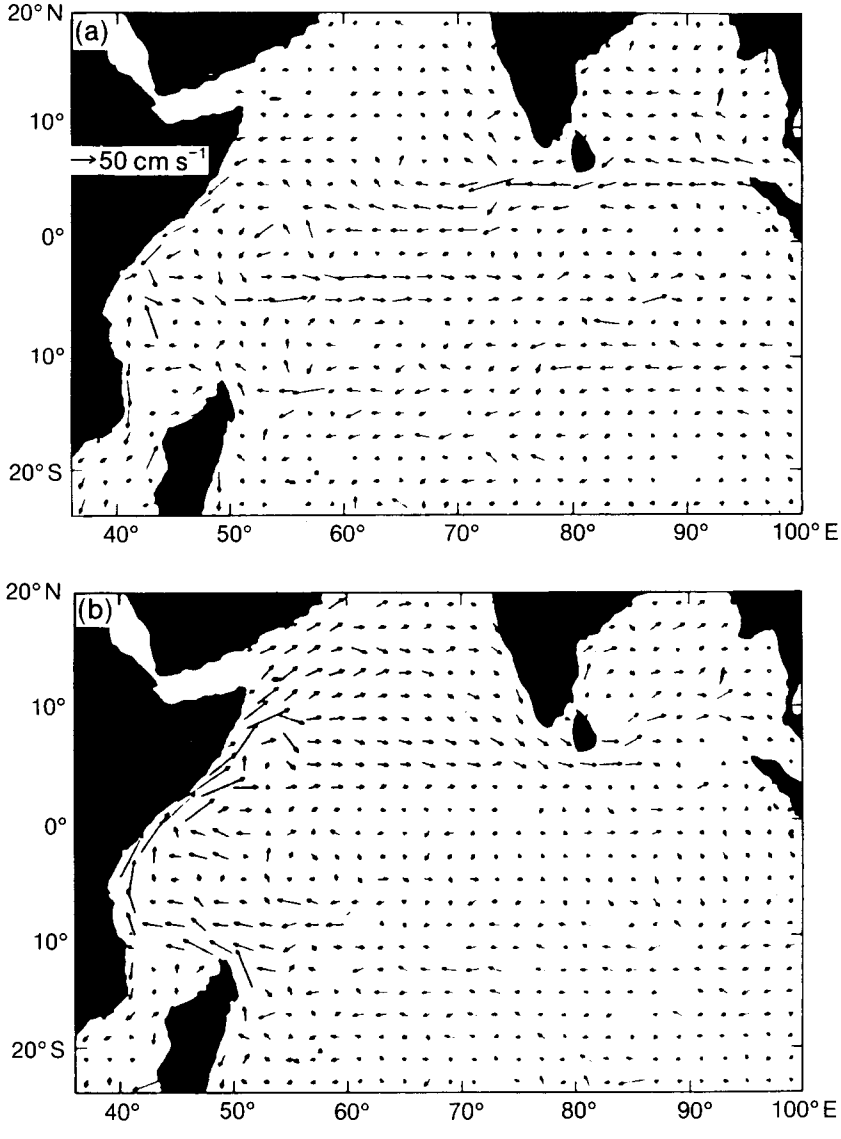

Figure 3. Observed mean monthly ship-drift currents for (a) January and (b) July from analysis by Rao *et al.* (1989) of ship-drift climatology of Cutler and Swallow (1984).

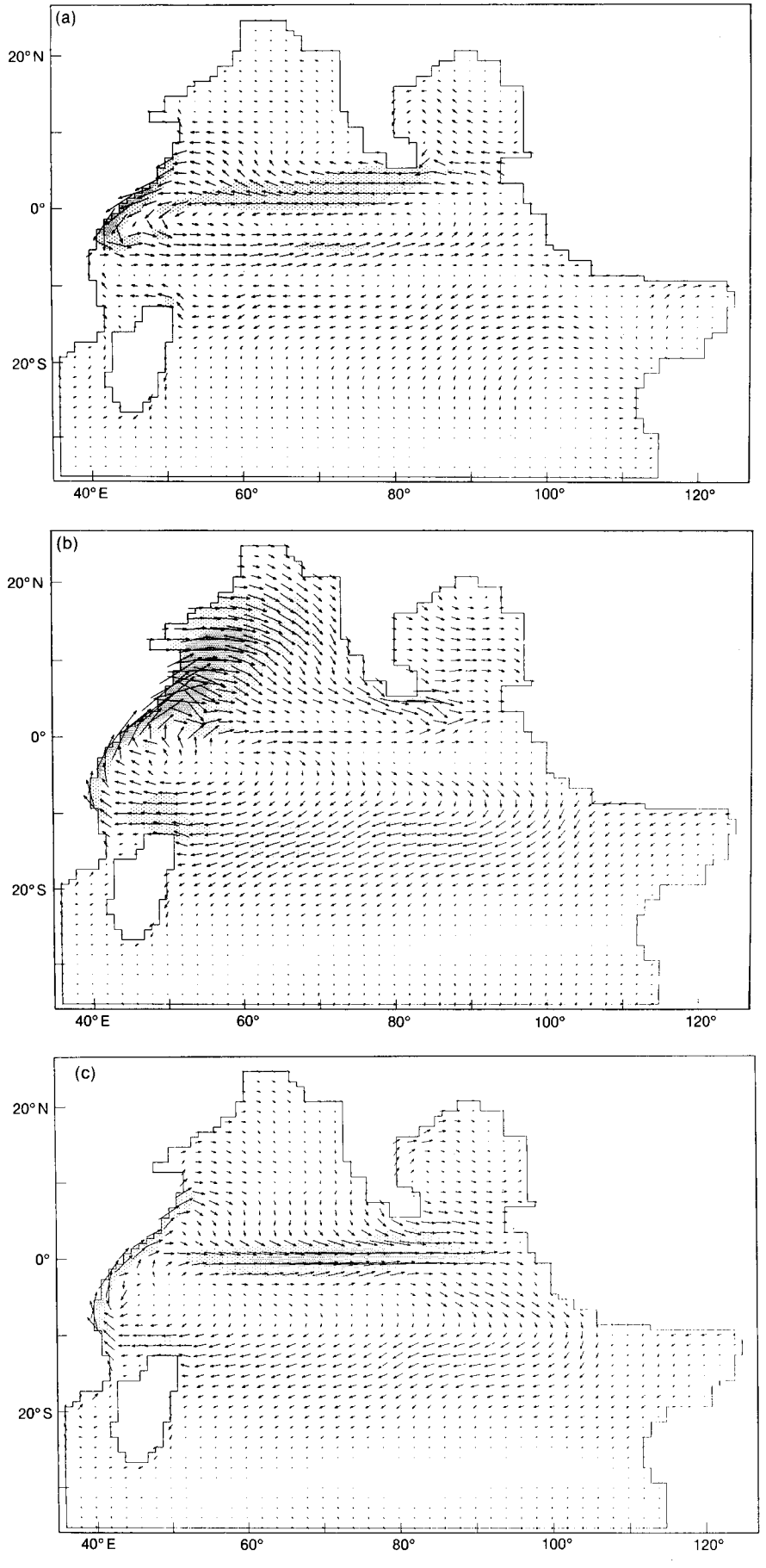

Figure 4. Model seasonal cycle — 5 m currents for (a) January, (b) July and (c) May. Light shading 40–80 cm s^{-1}, heavy shading > 80 cm s^{-1}.

velocity in the SMC of over 80 cm s^{-1} is perhaps too strong, but the weaker flow in the SEC, situated well to the south of the Equator at around 10°S, is well simulated. In both May and September the Wyrtki Jet reaches a maximum velocity of 100 cm s^{-1} (see Fig. 4(c)) which compares well with observations.

In the region of the Somali Current, the seasonal reversal in direction of the flow along the western equatorial boundary is reproduced. Northward flow from where the SEC meets the African coast, across the Equator and into the Somali Current can be seen in Fig. 4(b); a velocity maximum in the Somali Current in excess of 100 cm s^{-1} is reasonable. However, two weaknesses in the circulation are that the recirculation associated with the 'Great Whirl' is obscured in the uppermost model levels (see below), and the model fails to reproduce the Socotra Eddy at all, possibly because the island of Socotra is not represented and the model resolution is lower at that latitude and longitude.

The tendency of the model to obscure the Great Whirl in the upper levels highlights a general model weakness, namely that the Ekman component of the simulated surface currents is too strong. In the case of the Somali Current, where the wind stress is towards the north-east, the Ekman current is in an eastward direction; the recirculation, which involves westward flow, is not reproduced. At lower model levels, however, the gyre is simulated; this is illustrated in Fig. 5 which shows the currents at 35 m for July. The problem seems to be related to the way in which the downward transfer of momentum from the wind stress is parametrized in the model, but it is not well understood and attempts to eliminate the problem by using other methods to apply the wind stress have been unsuccessful.

In a qualitative sense the principal aspects of the sub-surface currents in the equatorial region are well reproduced, though lack of data makes quantitative comparison difficult. Fig. 6 shows a depth–time plot of zonal velocity at 73° E on the Equator. There is a marked semi-annual cycle in the ECC, as would be expected.

The model simulation of the currents in the deep ocean is not reliable for three reasons. Firstly, there is no barotropic component to the flow, so the deep currents in the model must balance the baroclinic velocities in the upper levels, which, in general, is unrealistic. Secondly, the model spin-up time for the deep ocean is far greater

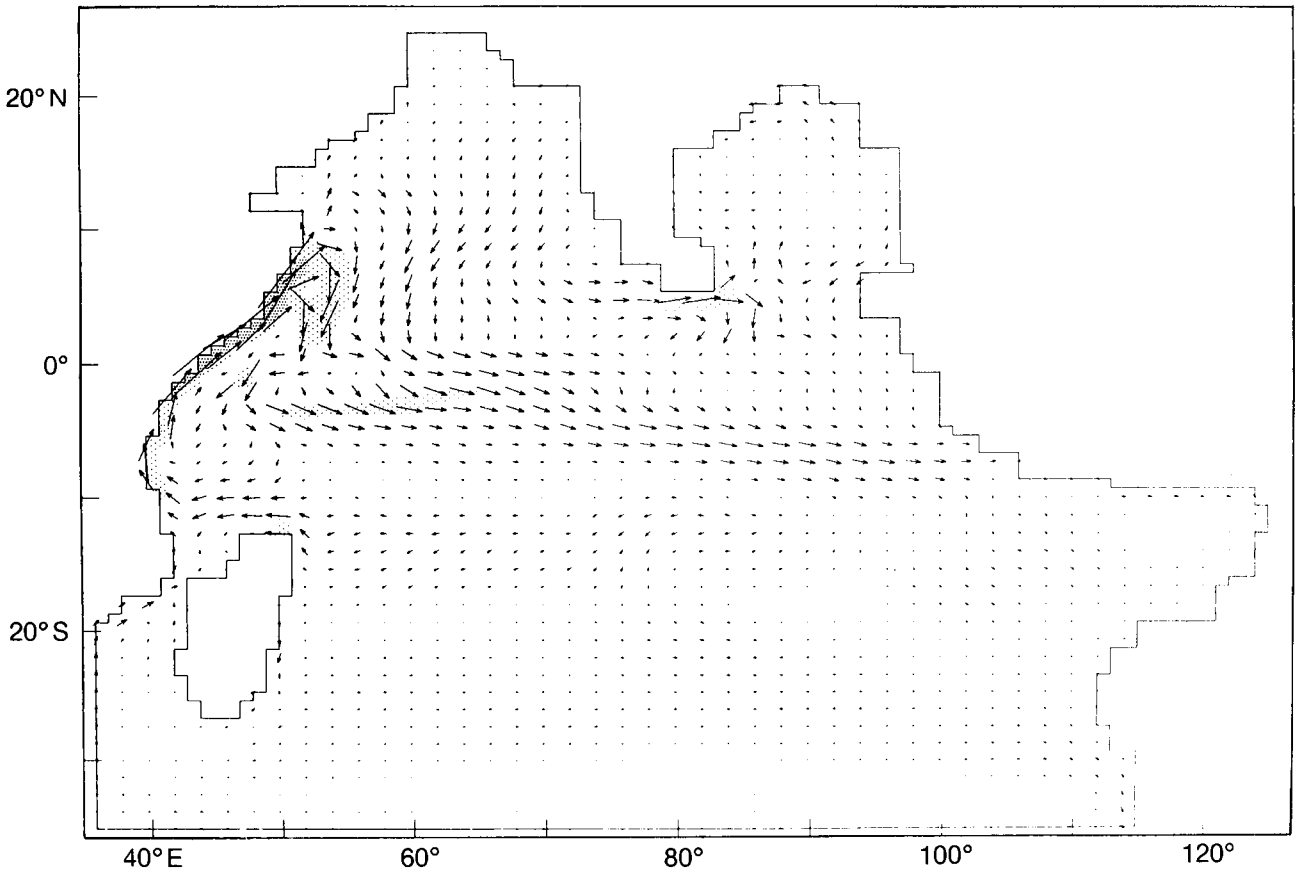

Figure 5. Model seasonal cycle — 35 m currents for July. Shading as in Fig. 4.

than that for the upper layer and so the density distribution will not have reached equilibrium. Thirdly, the model ocean has a flat bottom and does not represent bottom topography. No analysis will therefore be made of the deep currents.

4.2.2 Anomalous heat and water fluxes

The fields of anomalous fluxes of heat and fresh water are indicators, as described above, of the deviation of the model from the prescribed surface climatological fluxes. This deviation can result from inaccuracies in one or all of the following quantities: the climatological fluxes of heat and fresh water; the climatological SST and surface salinity fields to which the model surface fields are being forced; and the model simulation of surface temperature and salinity.

The anomalous heat flux over most of the model domain is found to be generally in the range 0 to -35 W m^{-2}, which is equivalent to the SST being too warm by 0 to 1 °C. These anomalies are as likely to be a result of inaccuracies in the climatological fields as in the model simulations. The only instances of large anomalous heat fluxes (of magnitude much greater than 35 W m^{-2}) are in areas of strong upwelling, where the model SSTs are significantly cooler than the climatological SSTs; this is illustrated in Fig. 7 which shows the anomalous heat flux for July in which the upwelling along the Somali coast during the South-west Monsoon may be

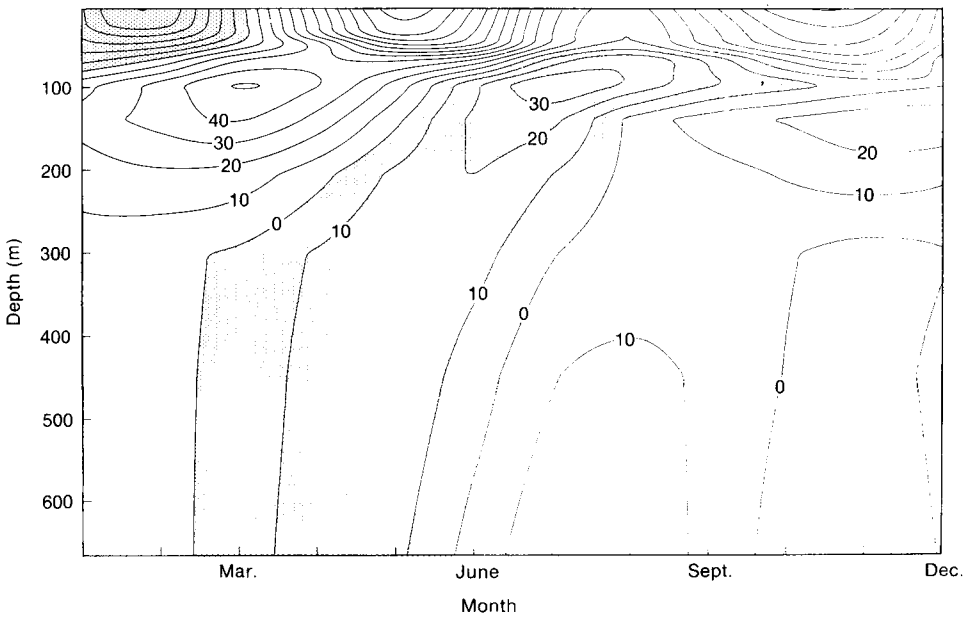

Figure 6. Model seasonal cycle — depth–time plot of zonal velocity (cm s^{-1}) at 73° E on the Equator (westward values shaded).

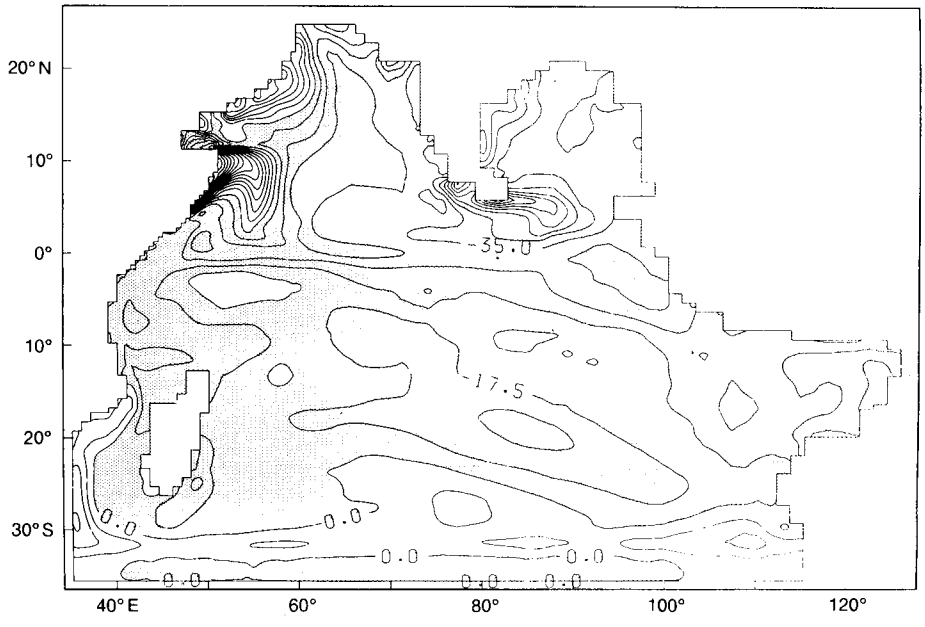

Figure 7. Model seasonal cycle — anomalous heat flux (W m^{-2}) for July. Positive values correspond to downward heat flux. Contour interval 17.5 W m^{-2} and negative values shaded.

clearly seen. The main reason for the large anomalous fluxes here is that the climatological fields do not resolve the coastal upwelling regions.

The anomalous water flux principally indicates inconsistencies between the flux of precipitation-minus-evaporation ($P-E$) and the climatological surface salinity field. This is most apparent in the Bay of Bengal since the land surface runoff associated with the Ganges River is not included in the ($P-E$) climatology; Fig. 8 shows the anomalous water flux for July.

5. Conclusions

An Ocean General Circulation Model of the Indian Ocean has been developed with a view to being able to hindcast the upper-level circulation.

When forced by climatological winds and heat fluxes the model reproduces well the seasonal cycle of the principal surface currents, the only major weakness being in the Somali region. This ability of the model to simulate successfully the seasonal cycle gives confidence in its suitability as a tool for proceeding to an investigation of the interannual variability in the currents in the Indian Ocean in response to actual winds and heat fluxes. For this purpose forcing fields derived from the operational Numerical Weather Prediction model analyses of the Meteorological Office and the European Centre will be used. This will be discussed in a subsequent paper.

Acknowledgements

I would like to thank Dr R. Corry, Dr D.L.T. Anderson and Dr C. Gordon for their contributions to the work described in this paper.

References

Bottomley, M., Folland, C.K., Hsuing, J., Newel, E. and Parker, D.E., 1990: Global Ocean Surface Temperature Atlas (GOSTA). A joint project of the Meteorological Office and Dept. of Earth, Atmospheric and Planetary Sciences, Masachusetts Institute of Technology.

Bryan, K., 1969: A numerical method for the study of the circulation of the world ocean. *J Comput Phys*, **4**, 347–376.

Cadet, D.L. and Diehl, B.C., 1984: Inter-annual variability of surface fields over the Indian Ocean in recent decades. *Mon Weather Rev*, **112**, 1921–1935.

Cox, M.D., 1984: A primitive equation, 3-dimensional model of the ocean. GFDL Ocean Group Technical Report No. 1, GFDL/NOAA, Princeton, N.J.

Cutler, A.N. and Swallow, J.C., 1984: Surface currents of the Indian Ocean (to 25°S, 100°E): compiled from historical data archived by the Meteorological Office, Bracknell, UK. I.O.S., Wormley, UK, Report No. 187.

Deutsches Hydrographisches Institut, 1960: Monatskarten für den Indischen Ocean, Publ. No. 2422.

Düing, W., 1970: The monsoon regime of the Indian Ocean. International Indian Ocean Experiment, Oceanographic Monograph No. 1. Honolulu, University Press of Hawaii.

Esbensen, S.K. and Kushnir, Y., 1981: The heat budget of the global ocean: An atlas based on estimates from surface marine observations. Report No. 29, Climate Research Institute, Oregon State University, Corvallis.

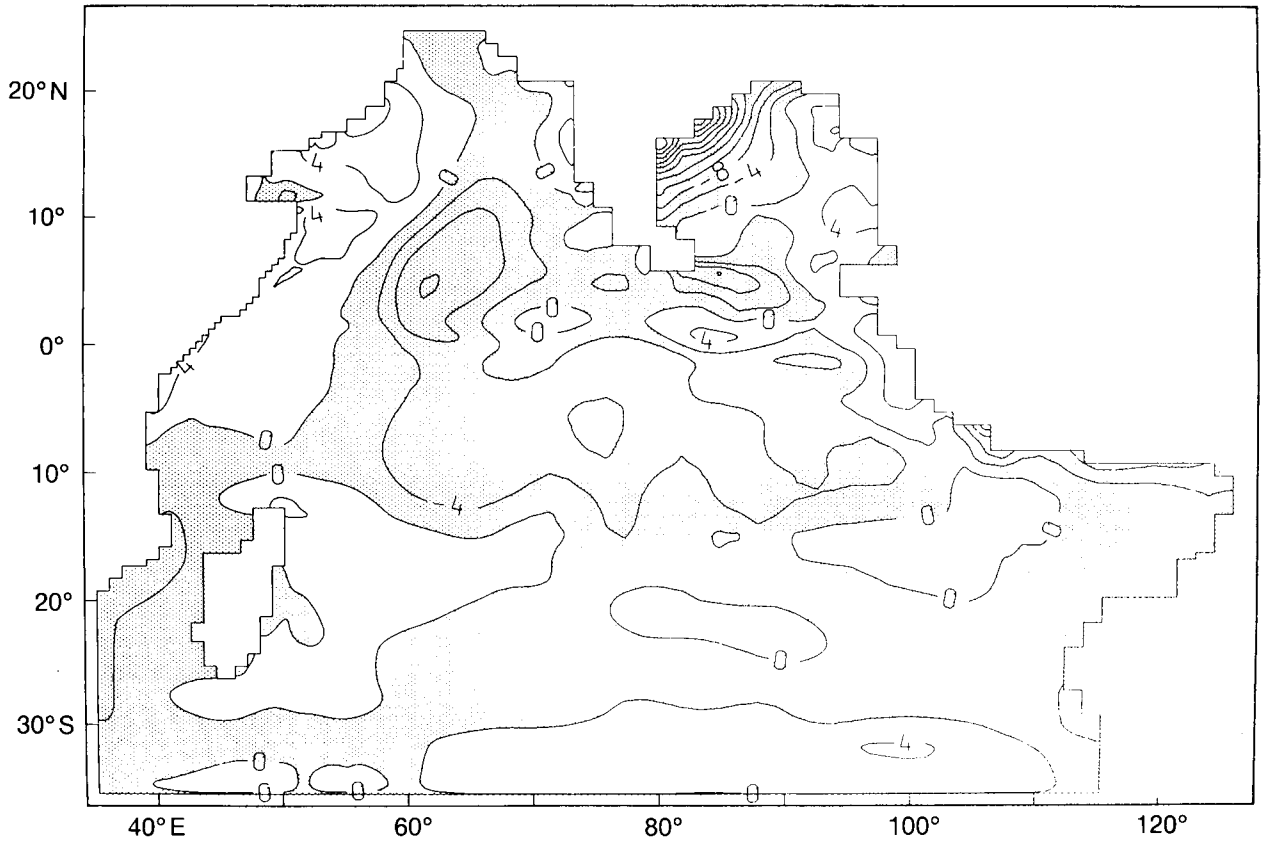

Figure 8. Model seasonal cycle — anomalous fresh water flux (mm(day)$^{-1}$) for July. Negative values correspond to downward fresh water flux. Contour interval 4 mm(day)$^{-1}$ and negative values shaded.

Findlay, A.G., 1866: A directory for the navigation of the Indian Ocean. London, Richard Holmes Laurie.
Gordon, C., 1985: The tropical Pacific version of Cox's ocean model on the Met. Office Cyber 205. Unpublished.
Haney, R.L., 1971: Surface thermal boundary conditions for ocean models. *J Phys Oceanogr*, **1**, 241–248.
Harrison, D.E., Kessler, W.S. and Giese, B.S., 1989: Ocean circulation model hindcasts of the 1982–83 El Niño: thermal variability along the ship-of-opportunity tracks. *J Phys Oceanogr*, **19**, 397–418.
Hastenrath, S., 1985: Ocean circulation. *In* Climate and circulation of the tropics. Dordrecht, Reidel.
Hastenrath, S. and Lamb, P.J., 1980: On the heat budget of hydrosphere and atmosphere in the Indian Ocean. *J Phys Oceanogr*, **10**, 694–708.
Hellerman, S. and Rosenstein, M., 1983: Normal monthly wind stress over the world ocean with error estimates. *J Phys Oceanogr*, **13**, 1093–1104.
Jaegar, L., 1976: Monthly maps of precipitation for the whole world ocean. Offenbach, Deutscher Wetterdienst, Ber. 18, Nr. 139.
Knox, R.A., 1976: On a long series of measurements of Indian Ocean equatorial currents near Addu Atoll. *Deep Sea Res*, **23**, 211–221.
Knox, R.A. and Anderson, D.L.T., 1985: Recent advances in the study of low-latitude ocean circulation. *Prog Oceanogr*, **14**, 259–317.
Leetmaa, A., 1973: The response of the Somali Current at 2°S to the South-west monsoon of 1971. *Deep Sea Res*, **20**, 397–400.
Leetmaa, A. and Ji, M., 1988: Operational hindcasting of the tropical Pacific. *Dyn Atmos Oceans*, **13**, 465–490.
Levitus, S., 1982: Climatological atlas of the world ocean. Washington, NOAA Prof. Paper No. 13.
Lighthill, M.J., 1969: Dynamic response of the Indian Ocean to onset of the South-west monsoon. *Phil Trans R Soc London*, **A265**, 45–92.
Luther, M.E. and O'Brien, J.J., 1989: Modelling the variability in the Somali Current. *In* Nihoul, J.C.J. and Jamart, B.M. (eds); Mesoscale/Synoptic coherent structures in geophysical turbulence, Amsterdam, Elsevier.
McCreary, J.P., Jun and Kundu, P.K., 1988: A numerical investigation of the Somali Current during the South-west Monsoon. *J Mar Res*, **46**, 25–58.
Merle, J. and Morlière, A., 1988: Toward an operational 3-dimensional simulation of the tropical Atlantic Ocean. *Geophys Res Let*, **15**, 653–656.
Pacanowski, R.C. and Philander, S.G.H., 1981: Parametrization of vertical mixing in numerical models of tropical oceans. *J Phys Oceanogr*, **11**, 1443–1451.
Philander, S.G.H. and Seigel, A.D., 1985: Simulation of El Niño of 1982–1983. *In* Nihoul, J.C.J. (ed); Coupled ocean–atmosphere models. Amsterdam, Elsevier.
Rao, R.R., Molinari, R.L. and Festa, J.F., 1989: Evolution of the climatological near-surface thermal structure of the tropical Indian Ocean. 1. Description of mean monthly mixed layer depth, and sea surface temperature, surface current, and surface meteorological fields. *J Geophys Res*, **94C**, 10,801–10,815.
Schott, F., Fieux, M., Kindle, J., Swallow, J. and Zantopp, R., 1988: The boundary currents east and north of Madagascar, 2, direct measurements and model comparisons. *J Geophys Res*, **93C**, 4963–4974.
Schott, F. and Quadfasel, D.R., 1982: Variability of the Somali current system during the onset of the South-west Monsoon, 1979. *J Phys Oceanogr*, **12**, 1343–1357.
Semtner, A.J., 1974: An oceanic general circulation model with bottom topography. Numerical Simulation of Weather and Climate, Tech. Report No. 9, Department of Meteorology, UCLA.
WCRP, 1985: Scientific plan for the tropical ocean and global atmosphere programme. WCRP publications series No. 3, September 1985. Geneva, WMO/TD No. 64.
Wunsch, C., 1977: Response of an equatorial ocean to a periodic monsoon. *J Phys Oceanogr*, **7**, 497–511.
Wyrtki, K., 1973: An equatorial jet in the Indian Ocean. *Science*, **181**, 262–264.

551.586:631:65:06

Products and services offered to the agricultural industry by the Meteorological Office*

J.R. Starr
Meteorological Office, Bracknell

Summary

The planning and development of meteorological products and services to the agricultural industry is presented in the light of the emerging commercialism within both the Ministry of Agriculture's Advisory Service and the Meteorological Office itself. Products and services are discussed in terms of 'customer benefits' and 'profitability'; several cost-benefit studies are presented, drawn from both livestock and cropping sectors. While benefits can be large it is noted that the farming community is only likely to benefit if it takes a long-term view of the subscription services. Market research, and market and costings information systems are seen as vital in the search for profitable markets in the agricultural (and other) sectors.

1. Introduction

Most agricultural operations are weather-sensitive; the Meteorological Office has, for many years, had a programme of research and development aimed at providing timely operational weather information services to the agricultural industry.

These services have been targeted at three groups:

(a) the agrochemical industry,

(b) the Agricultural Development & Advisory Service (ADAS) of the Ministry of Agriculture, Fisheries and Food (MAFF), and

(c) the individual farmer or co-operative of farmers.

A close liaison developed with ADAS such that, by 1983, small groups of agricultural meteorologists were attached to each of the five ADAS Regions in England and Wales. Through this link the farming community was served directly, often by on-farm visits (although farmers continued to use forecasts issued by Weather Centres through the usual channels of TV, radio, the Telephone Information Service and, for a time, through the Viewdata system 'Prestel').

There was always a recognition of the need to be accountable for Met. Office resources and some cost-benefit studies were attempted (e.g. the value in carrying out a 'frost survey' of a locality before attempting to establish a frost-sensitive horticultural crop (Rumney 1986)).

2. Commercial pressures

It was in 1987 that ADAS was encouraged, by Government policy, to adopt a firm commercial stance, which resulted in an emphasis on tactical (rather than strategic) revenue-earning services. In response to cuts in funding, the ADAS agro-met. presence was reduced to one 3-man unit based in the West Midlands.

A positive response to these ADAS cuts in funding, however, has been to increase the 'interface' within ADAS, colleges, universities, agrochemical companies, contractors, co-operatives, consultants, with the farming press and overseas international units. These contacts have increased industry awareness of the presence of agricultural meteorology and have resulted in significant increases in revenue; CEC (Commission of the European Communities) contracts have also been sought (e.g. Hough 1990).

In April 1990, the Met. Office was granted 'Agency Status' by its parent ministry, which implied greater flexibility in the allocation of financial and manpower resources, and the setting of realistic (but strict) revenue targets.

In recent years, therefore, it has become vital for the Agricultural Sector to demonstrate that it is an important and cost-effective component of both ADAS and the Met. Office Commercial Services.

3. Services to the customer

3.1 Business plans

Thus it has been that, in anticipation of this commercialism within ADAS and the Met. Office, Agricultural Business Plans have been developed. The stated Aim of the Agricultural Market Sector is 'to lead the productive application of meteorology to agriculture, particularly but not exclusively in the UK'.

The mechanism through which that Aim is realized requires five key components:

(a) an effective interface with the agricultural industry,

(b) an active and relevant R & D programme,

(c) a portfolio of services which cater for industry needs and which are commercially viable,

* This article formed the basis of a lecture by the author at the first colloquium on 'Les Applications de la Météorologie et leurs Intérêts Economiques' organized by Météo-France at Salines Royales d'Arc-et-Senans (Franche-Comté Region) 22–26 April 1991.

Met.O.998

THE METEOROLOGICAL MAGAZINE

1991 *Volume 120*

Published for the Meteorological Office by HMSO

INDEX

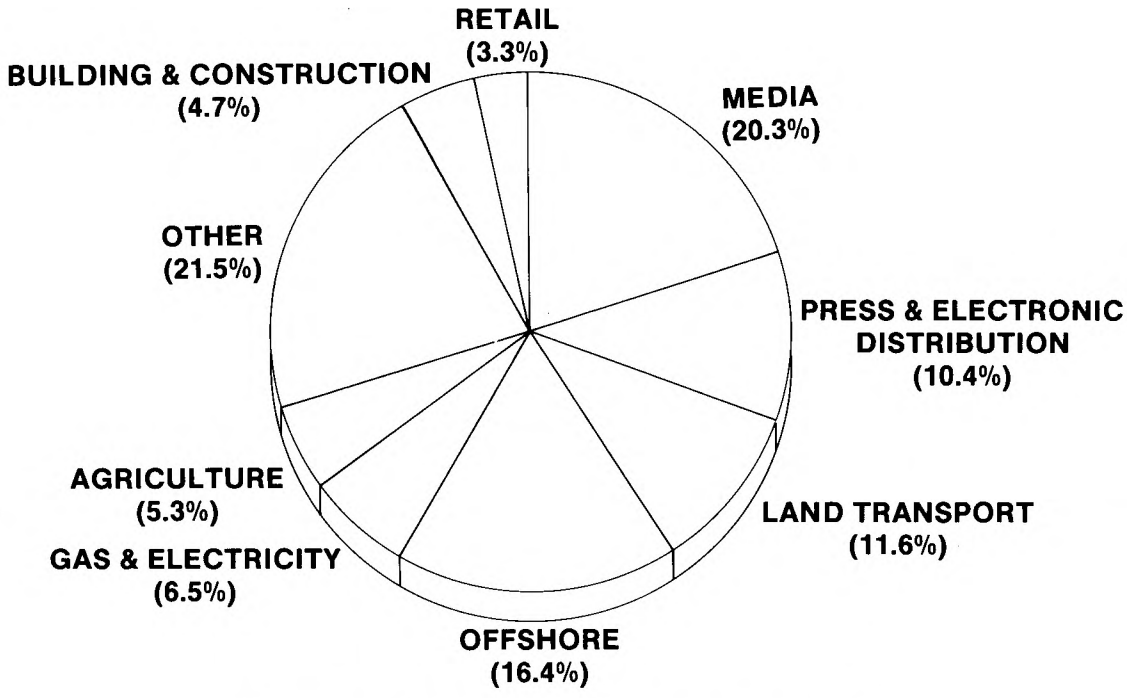

Figure 1. Major Markets — the Agricultural Sector share 1989/90.

(d) an appropriate and sustainable mix of staff skills and numbers, and
(e) a rational and up-to-date strategy.

In 1989/90 the Agricultural Market Sector contributed 5.3% of the total £12 million revenue from Commerce and Industry (Fig.1). By 1995/96 it is planned to increase this revenue to £19M in real terms with at least a proportional rise in the contribution from Agriculture (Fig. 2).

3.2 Costs

While the need for commercially viable services has been appreciated for many years, attention has been focused on revenue alone, rather than the revenue in relation to the true costs of the service. These include not only the direct costs of production including staff time, distribution, etc. but also hidden 'core' costs incurred by every National Meteorological Service such as those inherent in maintaining and developing the observational network.

To identify these true costs for every Market Sector, a Financial and Management Information System (FAMIS) is coming on-line.

Contributions towards 'core costs' amount to 'profit'; the Met. Office is now aiming to market services that result in profitability rather than simply 'revenue'.

3.3 Benefits

The challenge of pricing Services at an acceptable level in the face of strong competition and with these considerable overheads has led the Meteorological Office to produce detailed Marketing Plans in which the Benefits of its Services to the customer are emphasized.

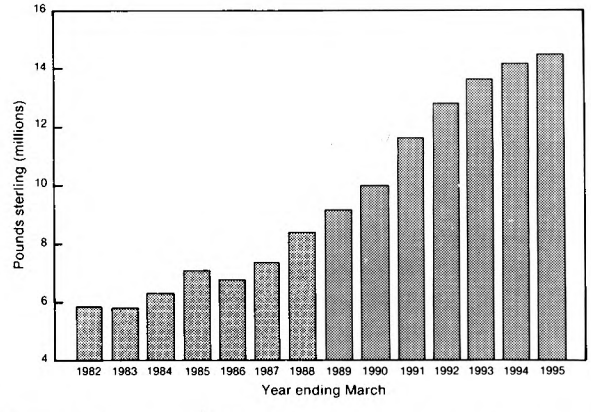

Figure 2. Commercial Service Revenues — actual to 1989, projected to 1995.

These are seen as:

- cost savings
- safety
- improved commercial advantage (competitive edge)
- improved planning
- improved decision-making

The 'brand' name of 'The Met. Office', equated with quality, excellence and reliability, is seen as synonymous with these Benefits.

3.4 Products and Services

Products, then, are being developed, after detailed market research, that are market-led with Customer Benefits as the arbiter. At the same time, developments in Information Technology have meant that high-quality products, tailored to customer needs, can be

delivered so as to allow the customer to take timely action.

A list of Products and Services developed for the Agricultural Industry is given in the Appendix.

To serve the individual farmer, co-operatives and the agrochemical industry, a Market Sector Manager operates from a Weather Centre developing tailored operational services with a substantial forecasting element for targeted customers.

Of crucial importance is the establishing and care of 'Key Clients' by the Market Sector Manager.

4. Costing the benefits

Market research indicates that customers perceive agrometeorological products and services as bringing qualitative benefits, for example as aids to management decisions, but that they have difficulty, even in a controlled trial, in quantifying these benefits. There follow some examples of where it has been possible to do this.

4.1 Foot-and-mouth disease

A numerical model to predict the spread of foot-and-mouth disease is described by Gloster (1983). The disease is not endemic in the United Kingdom; outbreaks are rare, but when they do occur the government maintains a slaughter and compensation policy. During the major epidemic of 1967/68 over 400 000 animals were destroyed and £27M paid in compensation. Estimates of total cost have reached up to £150M (1967/68 prices). Clearly, outbreaks have imposed a severe financial strain on the livestock industry in the United Kingdom.

When an outbreak occurred in cattle on the Isle of Wight in 1983 model output, in the form of daily inhaled virus dosage for cattle within a 10 km radius of the source, was used by the MAFF as an aid to: targeting the risk area for secondary outbreaks, recognizing the relative importance of the airborne route for disease spread, defining areas beyond which markets could continue, etc. In the event, the model indicated meteorological conditions not to be conducive for spread of the virus beyond the island and indeed no secondary outbreaks occurred.

The minimal cost (the order of £100 000) incurred during the outbreak confirmed to MAFF the value of meteorological input in rationalizing the targeting of scarce veterinary resources. The model has now become an integral feature of the guidance resources available to the MAFF epidemiological control team and is also in use in other countries.

4.2 Lamb wind-chill

Starr (1981) reports on trials of a lamb wind-chill forecast trial in southern England. Critical values of a 24-hour wind-chill index likely to result in losses in young lambs were deduced after extensive field trials over several seasons. The forecast trials were run with the co-operation of a number of Berkshire farmers who daily telephoned in to a Weather Centre to be briefed on the forecast chill-factor; particularly important was the 12-hour night-time factor. Farmers saw the benefit in aiding management decisions as to whether to put out the lambs (which were born in-house) or to extend their stay for an extra period under cover.

Thus a severe wind-chill forecast on 21 March 1981 was responded to by a co-operating farmer by retaining all his lambs 'in-house'; 43 lambs died overnight on a neighbouring farm! Under more moderate conditions single and twin lambs might be put out and, for a low index, the triplets — the more sheltered fields being allocated to these weakling stock.

Lamb losses are significant even in lowland Great Britain (about 5%) so benefits of such a service are clear; however the number of farmers taking up the service has been low even though the price represents the market value of only 3 or 4 fat lambs!

4.3 T-Sums*

Daly (1986) reports on an upland grazing trial to evaluate the profitability of an early lamb enterprise, utilizing grass grown according to the T-Sum 200 method.

Nitrogen was applied to two halves of an upland field in Wales at either the date of T-Sum 200 or in late April (usual for the farm). A second dose was applied about 2½ months later. Welsh halfbred ewes and lambs were stocked at 19 ewes and 30 lambs per hectare from May until September and weighed at monthly intervals.

Lamb liveweight produced came to 757 kg ha^{-1} when grassland was fertilized at T-200 and 621 kg ha^{-1} when fertilized later. The T-200 early June fertilizer also gave a more even pattern of grass growth than the late April/mid-July application.

The net output of lamb per hectare after deducting initial weights at the start of the trial was £718 ha^{-1} from the T-200 half and £612 ha^{-1} from the later fertilized half, leading to an overall estimated gross margin of £238 ha^{-1} and £192 ha^{-1} respectively.

4.4 Cutworm

Cost-benefit estimates were made prior to the introduction of an operational cutworm treatment programme for ADAS.

Taking crop area as 170 400 ha, potential loss in high-risk years as £1.098M and corresponding cost of spray treatments as £0.468M, then cost before introduction of the model is estimated as:

* Studies in Holland and elsewhere have demonstrated that the optimum response of grass to spring nitrogen occurs when the nitrogen is applied as soon as the average daily temperatures, summed from 1 January (ignoring negative values), reach 200 (°C).

High-risk year:	
Crop loss	£1.098M
if 25% of sprays effective	£0.823M
cost of spray	£0.468M
net loss to industry	£1.291M
Low-risk year:	
Only 5% of potential loss at risk and this is saved by treatments. Net loss is spray cost − value of crop saved	£0.468M − £0.055M = £0.413M
Average cost (mean of low/high figures)	= £0.852M

After introduction of the model:

High-risk year:	
Crop loss is only	£0.110M
If 90% of sprays effective spray cost	£0.468M
net loss	£0.578M
Low-risk year:	
Ability to identify the situation saves 90% of sprays	£0.047M
5% still at risk of which 10% not effectively treated	£0.001M
net loss	£0.048M
Average cost	= £0.313M

Costs to ADAS:	
including staff field-intelligence travel	£8 400
Agromet. support at Met. Office costs to ADAS	£1 500
3-day forecasts from a Weather Centre	£2 600
Total cost to ADAS for cutworm service	= £12 500

This contrasts with a potential saving to the industry of £0.54M.

4.5 Forecasts especially designed (tailored) for arable farmers

A market trial was establish with Loddon Farmers, an arable farmer's co-operative in north-east Norfolk (Marketing Solutions 1989). In market research undertaken beforehand, weather information needs were established and a trial forecast service matched as nearly as possible to the identified needs:

(a) Detailed forecasts comprising rainfall, wind speed and direction, sunshine, temperature, sea-breezes, relative humidity and 2-, 3- and 4/5-day outlooks, plus seasonally extra elements such as Smith Period and potential evaporation figures. Forecasts were issued at 0600 with updates at 1200 and 1830.

(b) The forecast was localized to north-east Norfolk, with coastal corrections for the benefit of farmers near the coast. It was competitively priced for the trial at £100.

(c) The service was exclusive to Loddon Farmers of whom 22 initially took up the service. It was delivered by a recorded telephone message on an ex-directory number.

The trial ran for the 6 months May–October 1988. During the trial selected farmers were interviewed and all were interviewed at the end of the trial, the interviews concentrating on the perceived (observed) benefits. The farmers were frequent and regular users of the service; average calls per day varied from 12.8 to 18.7, maximum use being during the harvest and in May when spray applications were frequent. Fifty-four per cent of the calls were in the morning.

Perceived benefits were:

(a) easier planning and decision making; especially useful was the 4/5-day forecast,

(b) greater accuracy and confidence in activities, enabling the day's activities to be 'fine-tuned',

(c) time and cost savings, e.g. overtime planning; less spray wastage; less time on jobs which would have been spoilt due to inclement weather,

(d) convenience of access to forecast, and

(e) other specific benefits mentioned: potential evaporation and soil moisture information for irrigation guidance; Smith Periods as guide to requirement as to when to spay against potato blight; grain-drying need indicated by relative humidity.

All the trialists expressed satisfaction with the service, most spoke of the qualitative benefits (Miller 1990). The service had become integrated into their daily management decisions with the result that few farmers were able to point categorically to savings specifically due to weather information.

Despite this, example of cost savings were quoted by two of the group:

(a) A saving of £9 ha^{-1} in sprays was identified as a consequence of being able to spray with a cheaper spray at the right time. If 40 hectares are sprayed in a day the saving is £360; with 150 farmers making a similar saving on at least one day a year the saving amounts to £54 000.

(b) Cutting a hay crop just before rain can result in losses of £2 000 to £3 000 due to spoilage. One farmer was sure that, through the service, he had avoided such a loss. Thus a co-operative of 100 farmers could save up to £300 000 by cutting only when dry weather is forecast.

The trial allowed re-evaluation of the product, for example inclusion of dew formation and sunshine intensity information, and the proposal of pricing options.

Savings for farmers taking a repayment service are likely to be marginal in the short term compared with

using freely available forecasts or even local knowledge, as noted by Grant (1990). Those who are prepared to go through a learning curve of how best to apply forecast information and use confidence probabilities are the ones likely to achieve long-term benefits.

5. Summary

The commercial culture of the Meteorological Office demands market-led services and products which bring customer-benefits and are profitable. To achieve the correct marketing mix requires careful attention to market research, study of market penetration and being prepared to abandon lines that, however popular, are not profitable.

In developing new agrometeorological products and services there is a need to react to changing farming and ADAS policy, and to capitalize on the current demands for environmental protection, strategies for climate change and the increasing market opportunities overseas (where collaborative agreements with other National Meteorological Services are being sought).

The market among horticultural and farming co-operatives and the agrochemical industry has great potential while the 'Futures' market is a relatively untapped source of revenue.

Market research and the building of a marketing information system by the Meteorological Office Marketing Department will be vital aids to exploring and quantifying the many opportunities in the Agricultural Sector while promotion, marketing and close attention to 'key clients' will continue to be important aspects of the workload of the Market Sector Manager and the Meteorological Office ADAS Unit.

6. Acknowledgements

I am grateful to M. Lee, J. Cochrane, J. Gloster, M. Hough, and B. Callander for supplying examples of cost-benefits and to F. Hayes and M. Nicholls for discussions on the manuscript.

References and bibliography

Daly, M., 1986: T-Sum upland grazing trial. UKF Unpublished Report.

Gloster, J., 1983: Forecasting the airborne spread of foot-and-mouth disease and Newcastle disease. *Philos Trans R Soc London*, **B302**, 535–541.

Grant, M.A., 1990: Operating a semi-commercial meteorological service. Proceedings of the Technical Conference on Economic and Social Benefits of Meteorological and Hydrological Services. Geneva, WMO. Report No. 733.

Hough, M., 1990: Agrometeorological aspects of crops in the UK and Ireland. CEC Joint Research Centre, Catalogue No. CD-NA-13039-EN-C.

Keane, T, Harsmar, P.-O. and Jung, E., 1987: Economic benefits of agrometeorological services. Report No. 27, Commission for Agricultural Meteorology. Geneva, WMO.

Marketing Solutions, 1989: The Met. Office support in the provision of services to the agricultural market — final report.

Miller, I.S., 1990: Benefits of accurate weather forecasting to farmers. *Weather*, **45**, 400–403.

Rumney, R., 1986: A cost/benefit analysis of a spring frost survey. *Agric Mem, Meteorol Off*, No. 1072.

Starr, J.R., 1981: Weather and lamb mortality in a commercial lowland sheep flock. *Agric Meteorol*, **24**, 237–252.

Appendix

Meteorological Products and Services for Agriculture and Forestry (extract from the Meteorological Office's *Commercial Product and Services Manual*, 1991)

Most small businesses will have greatest in the Direct Access Forecaster Service, the Warning Service and Weatherfax. On a very irregular basis they may also express an interest in the Work Days, Growing Days, Irrigation Planning, Climate Suitability and Windbreaks services. Larger companies will express interest in various combinations of products, to make a package. Weatherbase, Work Days, Weather Sensitivity Analysis, Soil Moisture Information and forecast services should always be brought to the attention of large companies, distributors, merchants and manufacturers. Other services should be mentioned as appropriate, examples are:

Heat-Stress Warning — Pig and chicken farmers
Frost Warnings — Fruit growers/Nurseries
Odour-Plume Analysis — Housed livestock
Lamb Wind-Chill — Lowland sheep farmers
Irrigation Planning — Irrigation enquiries
Dedicated services — Co-operatives

A.1. Data Services relevant to feasibility assessment, design, planning or monitoring of a project

World Weather — For different reasons, large growers and importers/exporters of fruit, vegetables and grain need to know what the weather is currently doing abroad and what it will do in the near future.

Weatherbase — Summary data tailored to the needs of the agricultural community — daily, weekly or monthly reports from UK Weather Stations for a variety of crop monitoring purposes.

A.2. Analyses and Consultancies relevant to feasibility assessment, design or planning of a project

Work Days — defines how often a weather dependent task can be done, e.g. crop spraying, autumn cultivations.

Growing Days — relates crop growth to weather to assess the length of growing season for an area, or the time of year (is it longer or shorter than usual?).

Weather Sensitivity Analysis — helps to identify if and/or by how much an activity or demand for produce is weather dependent, e.g. when do consumers switch over to buying salad foods in significant quantities?

Irrigation Planning — an assessment of how much

water can be used in an average, wet or dry season. An objective basis for equipment purchase and licence application. Various rotations can be assessed. The program is designed for UK conditions but limited overseas use (mainly near Continent) is possible.

Climate Suitability — a detailed appraisal to provide the objective basis to answering the question will a crop grow well in a particular location? — United Kingdom and overseas.

Wind-breaks — based on an analysis of wind data, the optimum orientation of a wind-break to protect crops, livestock or buildings can be advised. Wind-breaks can also reduce heat loss. The resultant shading, and light loss can also be assessed.

Depending upon what needs to be protected, protection may only be needed at certain times of the year, e.g. winter for a glasshouse or spring for a delicate crop. In such instances the overall prevailing wind direction may not dictate the best position for the wind-breaks.

Grass Growth — how well is the grass growing in a particular locality compared with average. Useful in forecasting seasonal yields. The program is not sufficiently accurate to model grass-growth in absolute terms but it provides useful information for comparing yields between months and years.

Soil Moisture Information — information can be provided in regular weekly reports for 40 km × 40 km areas for a variety of soil types and crops; the MORECS model. Plus detailed long-period assessments for investigational work and use in Weather Sensitivity Analyses. There is a range of three soil types and over ten crop types.

Accumulated Temperatures — a parameter that is indicative of crop growth and development. Effective day degrees, a similar parameter, can also be calculated.

Return Periods — for a range of meteorological parameters it is possible to provide an indication of how often important extremes will occur, for use in assessing appropriate design tolerances.

Crop, Pest and Disease Indices — the weather conditions liable to encourage a range of pests and diseases have been correlated with outbreaks and indices established. Mostly based on recent past weather but some estimate of future risk can be made particularly if the relationship is temperature dependent.

Odour-Plume Analysis — an assessment of the environmental effects of farm odours given off by housed livestock. It includes information on preferred directions of plume drift on days when odours are likely to remain concentrated at low levels.

Statistics — averages, variability and extremes can be derived from vast archives, the analysis of frost occurrence being a particular case.

Some of the above analyses can be based on overseas data.

A.3. Consultancy-type forecasts

Farmers and growers, as individuals, can be provided with a direct-access forecast service where contact is directly with an experienced forecaster, when required, via an ex-directory telephone contact. The period of the forecast is usually the next 24 hours with outlook up to 5 days ahead.

Forecasts can be provided to agricultural advisory services (government or private) for up to 4 or 5 days ahead as an integral part of their crop and livestock advisory bulletins.

An indication of future trend is possible out to 9 days ahead.

Lamb wind-chill — a customized service aimed at reducing the risk of lamb mortality particularly within first 48 hours of birth and especially if multiple birth. Useful management information for farmers who can take action to protect new-born lowland lambs.

Weather — numerical information sent as a routine (daily) service direct to the customer. Forecast for 5 days ahead and delivered by 7 a.m.

Services to farming co-operatives — dedicated recorded-message forecasting service for co-operatives and associations.

T-Sums — an aid to optimum application of spring nitrogen on grass.

A.4. Warnings of weather events

The customer is contacted by the Met. Office when significant (usually adverse) weather of specific interest is expected. Some examples are:

Heat stress in intensive poultry and pig units at high temperatures and low wind speeds.
Strong winds causing structural or crop damage.
Heavy rain liable to cause flooding.
Housing and transporting livestock before snow.
Implementing contingency heating plans prior to very low temperatures.
Frost on orchards, soft fruit and nursery stock.
Protection of crops against damage by hail.
Dry spells for hay and silage making.

Once the critical values are forecast to occur a warning is telephoned or faxed to the recipient, perhaps several days in advance, with daily update until an event has occurred or the danger is passed.

551.524.36(425)

A reassessment of the highest temperature during July 1959

G.P. Northcott
Meteorological Office, Bracknell

Summary

A recent reference to the highest temperature measured in July 1959 has led to a re-examination and reassessment of the previously published value.

1. Introduction

In a recent article in *Weather* (Brugge 1991) the published highest monthly maximum for July 1959, 96 °F (35.5 °C) at Gunby, Lincolnshire, was referred to. Recent examination of the maximum temperatures for July 1959 suggest that the value of 96 °F was perhaps excessive for that location and height particularly when compared to the surrounding stations and notably that at Cottesmore, then Rutland, now Leicestershire, about 4 miles (6 km) to the south and at a similar height above mean sea level (AMSL).

2. Station details

Gunby climate station was situated on the Lincolnshire Wolds, National Grid Reference (NGR) SK 899218, at a height of 440 feet (134 m) AMSL and was open from January to October 1959, after which it ceased to be a climate station, but became a rainfall station, which it remained for three further years.

Some description of the actual site of Gunby is of interest. A photograph of the site shows the screen standing in a field of growing cereal, with no enclosure fence, but with the area immediately surrounding the screen trampled. An inspection was carried out in July 1958, when it was noted that the original screen had single louvres, and the stand was a somewhat unsteady pedestal. However, by early November 1958 the screen had been replaced by a Stevenson screen and the pedestal had been replaced by a stand; there is no indication of an enclosure fence having been erected.

Cottesmore, also situated on the Wolds, NGR SK 909154, at a height of 450 feet (137 m) AMSL, had been a climatological station some years previously, but in 1959 was a synoptic 5-day-week station only and was closed over the weekend. Thus no readings were taken on the Sunday. However, the maximum temperature read at 06 UTC on the Monday morning was the maximum for the weekend. On 6 July 1959 at 06 UTC the maximum was read at Cottesmore as 89 °F (31.7 °C) and the observer noted in the register that the entries for rain and maximum referred to those values for the previous day (Sunday, 5 July).

3. Synoptic situation on 5 July 1959

In the *Monthly Weather Report* for July 1959 (Meteorological Office 1959) the following description is given of the weather over the first week;

> 'Weak fronts in a moist south-westerly airsteam gave cloudy weather with some slight occasional rain in most districts during the first three days of the month. Meanwhile an anticyclone had been moving eastwards from the Bay of Biscay and as pressure rose over Germany on the 4th, wind over the British Isles became light but mainly southerly and weather sunny and warm generally except in northern Scotland. many places recorded between 14 and 15 hours of sunshine and temperature rose into the eighties in most districts and reached 88 °F at Cromer. On the 5th thunderstorms, associated with an eastward moving weakening upper trough, broke out in western districts and moved slowly across the country reaching south Yorkshire and Lincolnshire during the afternoon. In many midland and eastern districts the 5th was the warmest day of the year, so far, with afternoon temperatures exceeding 90 °F; Gunby recorded 96 °F and Cromer 94 °F.'

The hourly plotted chart for 16 UTC on 5 July (Fig. 1) has a front drawn along a line from just west of the Isles of Scilly to Anglesey to Carlisle and across to the Moray Firth, and a thermal low pressure area, with a central pressure value of 1012.6 mb near Wittering. A large area of Sferics plotted across the top of the shallow low pressure area confirming the thundery outbreaks in 'south Yorkshire and Lincolnshire during the afternoon'.

4. Re-examination of highest temperatures

A map was plotted of the maximum temperatures in southern and eastern England on 5 July 1959 (Fig. 2) using the values published in Table III of the *Monthly Weather Report* (Meteorological Office 1959). Those maxima that occurred on other days did not generally exceed the values on this, the hottest day of the month. The 90 °F isotherm bends a little around Cottesmore

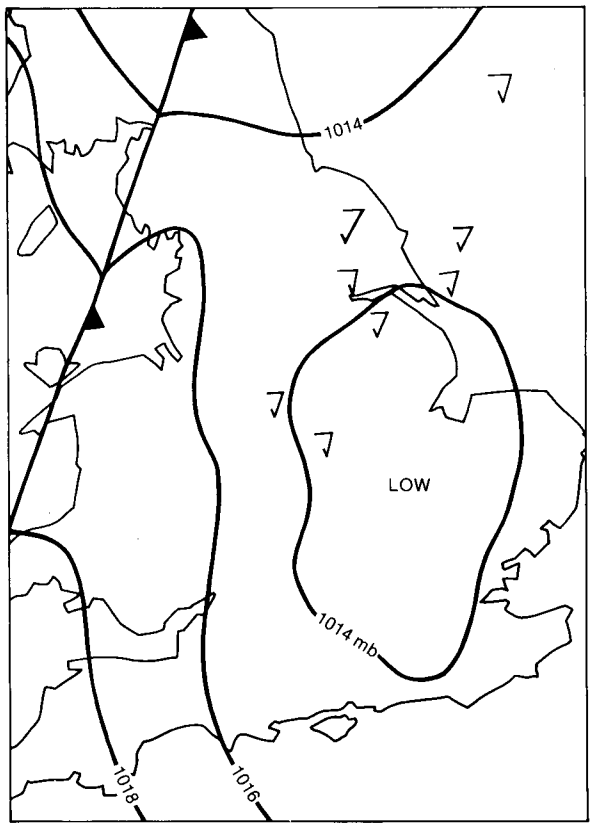

Figure 1. Surface chart for 16 UTC on 5 July 1959, with sferics added.

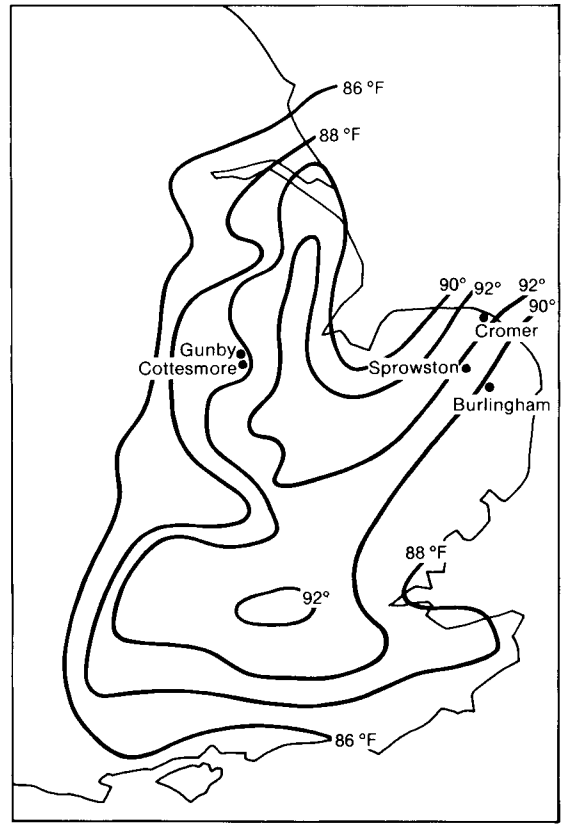

Figure 2. Map of maximum temperatures in southern and eastern England on 5 July 1959.

with its 89 ° F, having passed very close to Gunby, and suggesting that the highest temperature during the day should have been about 90 ° F.

An examination of the archived evidence shows that the observer at Gunby measured 81 ° F at 09 UTC on the 5th, and on the following morning his reading of the maximum thermometer gave him 96 ° F for the previous day. The entry on the return is absolutely clear and the 9 and 6 are quite distinct, with no possibility of confusion with say a zero. However, when read the values are entered into a Climatological Register to make up the observation before it is transcribed on to a Metform 3208 (Monthly Climatological Return). It is possible that an error was made in reading the maximum, or that the maximum temperature was correctly read, but wrongly transcribed on to the Metform 3208 because of problems of legibility at the earlier stage. The earliest 'original' stage kept in the National Meteorological Archives is the Metform 3208. Climatological Registers are not deposited within the Archives.

The maximum temperature on the 5th at Gunby was accepted as the highest temperature for July 1959 only and not as general record-breaker; it is difficult to obtain precise details of the thinking of the Quality Control staff of the period, but the *Observers' Handbook* (Meteorological Office 1956, 1969), referring to gross errors in temperature states 'One of the commonest of such gross errors is the misreading of the thermometer by 5 or 10 whole degrees ...'. However, there is no evidence that the value recorded on the Metform 3208 was other than that read on the instrument. No evidence has come to light to suggest that the value of 96 ° F on 5 July 1959 has previously been queried, let alone investigated. However, it is not the highest value for July in the literature.

5. July extremes

The extreme for July was 38.1 °C, recorded in a Glaisher stand at Tonbridge on the 22nd in 1868, but this value was amended to 35.9 °C recorded in a Stevenson screen at Cheltenham on 3 July 1976, following the discovery that the temperature in a Glaisher stand is generally higher than the temperature in a Stevenson screen (Laing 1977). The extremes given for East Anglia and Lincolnshire in *Climatological Memorandum 133* (Meteorological Office 1984: revised 1989) are 36.1 °C at Halstead, Essex on 19 August 1932 and 35.6 °C at Cambridge Botanic Garden on 9 August 1911 and 19 August 1932 as well as 35.6 °C at Earl's Colne and Norwich on 19 August 1932.

6. The reassessment and statement

The differences in the maxima and minima at Gunby were compared with those for Cottesmore and Wittering over the 2-month period of June and July 1959, and a similar exercise was carried out to compare Cromer with two nearby stations, Sprowston (NGR TG 251123) and Burlingham (NGR TG 373101). For this purpose the

relevant maximum and minimum temperatures were extracted from the Daily Registers for Cottesmore and Wittering. For the other stations examined in this way copies were taken of the relevant Metform 3208 returns for June and July 1959. These data were passed to the Observation Provision Branch of the Meteorological Office for examination by their networks section, who produced the statement reassessing the Gunby value and checking the rather high value read at Cromer on that day.

The full statement on the 'highest daily maximum temperature during July 1959' made by the networks section is as follows:

'Gunby (situated on the Lincolnshire Wolds) reported a maximum temperature of 96 °F on 5 July 1959. This value was recorded as the highest monthly maximum for July 1959, but appears to be unreasonably high in comparison with neighbouring stations:

Station	Altitude (m)	Max. Temp. (°F)
Gunby	134	96
Cottesmore	138	89
Wittering	80	91

Maximum temperatures at Gunby were compared with those from Cottesmore and Wittering for the period from 15 June to 20 July 1959. Values were generally similar except on three days:

Station	Altitude (m)	Maximum temperature (°F) 22 June	1 July	5 July
Gunby	134	88	69	96
Cottesmore	138	77	74	89
Wittering	80	79	75	91

There would seem to be little reason why temperatures should differ by these amounts and allowing for the fact that Gunby was only open from January to October 1959 it would therefore be unsafe to accept the value on 5 July as the highest maximum temperature for the month.

The values at Gunby on 22 June, 1 July and 5 July should therefore be changed to 77 °F, 74 °F and 91 °F respectively.

The next highest value was 94 °F, reported at three stations: Westminster (London), Boxworth (Cambridgeshire) and Cromer (Norfolk). The values at the first two stations agree well with those of their neighbouring stations. The value at Cromer seems a little high in comparison with its neighbours:

Station	Altitude (m)	Max. Temp. (°F)
Cromer	54	94
Sprowston	28	89
Burlingham	27	87

A study of maximum temperature values from 15 June to 20 July 1959 showed that Cromer was usually 0–10 °F colder than Sprowston or Burlingham but on some occasions was a few degrees warmer. This is as might be expected for a station close to the North Sea. On 5 July the wind during the early afternoon was from the south-south-east and with the hills to the south of Cromer rising to between 200 and 250 feet a value of 94 °F can be accepted even though a little dubious. There is insufficient evidence to declare that the value of 94 °F is wrong, especially 31 years after the event.'

7. Corrective action

As a result of the reassessment of the values for the month of July 1959 it was clear that the 5th remained the hottest day, but that the information about the corrected highest value should be brought to a wide readership. The following correction appears in the December 1990 and the Summary issues of the *Monthly Weather Report* (Meteorological Office 1991):

'Vol. 76 No. 7, **Temperature**

A recent re-examination of the high temperatures in July 1959 show that it is unsafe to accept the value of 96 °F (35.5 °C) recorded on the 5th at Gunby, Lincolnshire, as the highest of the month. The Metform 3208 in the Archives for Gunby for July 1959 has been annotated accordingly. The next highest value was 94 °F (34.5 °C), reported at three stations: Westminster (London), Boxworth (Cambridgeshire) and Cromer (Norfolk). The value at the first two agree well with their neighbouring stations; the value at Cromer, although it seems a little high, is acceptable...'

Acknowledgements

Thanks are due to Philip Eden whose letter, now published in *Weather*, (October 1991) started the investigation, to Mick Wood, the Archivist for making available the returns and to Eddie Spackman of the Observation Provision Branch for his advice and for a statement based on comparison of the available data.

References

Brugge, R., 1991: The record-breaking heatwave of 1–4 August 1990 over England and Wales. *Weather*, **46**.

Eden, P., 1991: Gunby, Lincs., Putting the Record Straight; Letter in: *Weather*, **46**, 330–331.

Laing, J., 1977: Maximum summer temperatures recorded in Glaisher stands and Stevenson screens. *Meteorol Mag*, **106**, 220–228.

Meteorological Office, 1956: *Observer's Handbook*, 2nd ed., p. 13. London, HMSO.

—, 1959: *Monthly Weather Report*, July 1959, **76**, No. 7, London, HMSO.

—, 1960: *Monthly Weather Report*, Summary 1959, **76**, No. 13. London, HMSO.

—, 1969, *Observer's Handbook*, 3rd ed., p. 12. London, HMSO.

—, 1991: *Monthly Weather Report*, December 1990, **107**, No. 12, p. 291. London, HMSO.

—, 1984, revised 1989: *Climatological Memo Meteorol Off* No. 133, p. 15. London, HMSO.

Notes and news

The Professor Dr Vilho Vaisala Award

Malcolm Kitchen of the Meteorological Office was presented with the prestigious Professor Dr Vilho Vaisala Award by the President of the World Meteorological Organization (WMO), Mr Zou Jingmeng, at the Met. Office HQ at Bracknell on 16 September 1991.

Malcolm helped to organize the WMO Radiosonde Comparison held at the Office's experimental site at Beaufort Park near Bracknell in 1984. The award came for his definitive report comparing the performance of the upper-air stations of the Global Observing Network. If his recommendations are adopted they will lead to a substantial improvement in compatibility of the different instruments and systems used around the world. He acted as the WMO's Commission for Instruments and Methods of Observation Rapporteur on Radiosonde Compatibility from 1985 to 1989.

Before 1984 Malcolm had worked in the Office's Cloud Physics section and the Meteorological Research Flight. He has also been responsible for the operational trials of the ATD lightning detection system. His present interests are in developments to the combined radar and satellite short-period rainfall measuring and forecasting system FRONTIERS.

In presenting the Award, which consists of a diploma and a cheque for US$1,000, Mr Zou, who is also the Administrator of the State Meteorological Administration of China, said:

> 'Mr Kitchen has provided an important contribution to the standardization of upper-air measurements. The presentation of the Vaisala Award to Mr Kitchen is a well-earned recognition of his work for the meteorological community, to which I should like to add the appreciation of WMO for his valuable contribution to meteorological operations and research.'

Reviews

Climate and development: Climate change and variability and the resulting social, economic and technological implications, edited by H.-J. Karpe, D. Otten, S.C. Trinidade. 154 mm × 234 mm, pp. xiv+477, *illus.* Berlin, Heidelberg, New York, London, Paris, Tokyo, Hong Kong, Springer-Verlag, 1990. Price DM. 98.00. ISBN 3 540 51269 1.

This book consists of papers presented at the Hamburg Congress on Climate and Development in November 1988. The Congress was interdisciplinary and attracted 40 contributors from 13 countries, though most delegates were from Germany and the USA. There are 9 introductory addresses, mostly of little interest, 11 scientific contributions, 9 which focus in turn on the concerns of industry, non-governmental organizations (NGOs) and developing countries, and 5 on international programmes in this area. The Congress agreed two statements: a three-page Manifesto and a two-page Action Plan.

It is understandable that a book should emerge from such a conference, though it is a pity that the editors felt they had to include all the material to hand. Beyond the ephemeral material there are some useful summaries of current evidence and predictions of global warming, and the different emphases of the various groups are of some interest. Inevitably there are conflicts in the conclusions reached by the scientists who contributed and these will not be easy to resolve for most readers.

Klaus Hasselmann of the Max-Planck-Institut für Meteorologie in Hamburg provides an excellent well-illustrated 12 000-word summary of the state of the art in climate forecasting. A later contribution by Wilfred Bach goes over too much of the same ground, though he does introduce the distinction between transient and equilibrium response. There is also an interesting paper by Gundolf Kohlmaier on the place of land biosphere changes in the atmospheric CO_2 budget. Given the unbalanced state of current global carbon models, this is an important area deserving further analysis and research and this is one of the most original papers here.

The Russian contribution by Budyko and Sedunov has the title *Anthropogenic Climate Changes*. It runs to over 5000 words, but is rather repetitive and not always easy to read. It has value as a review of Russian research in English, though most of the figures have inadequate captions. The authors seem inclined to regard warming as an improvement on the current Russian winter, a welcome aided by their happy assumption that precipitation will increase whilst they seem to set aside the fact that evapotranspiration will also be greater. The all-important oceans are represented by a single paper which gets no further than describing the various international programmes such as WOCE and TOGA.

Ian (here rendered as Ivan) Burton from Canada puts forward the aim of a rapid reduction in CO_2 output (of over 20% in all developed countries by 2005), a target which few others accept and most regard as impracticable. But even this Canadian target is not enough for the NGO group which asks for a reduction in emissions of at least 30% by 2000 and 60% by 2015, surely pie in the CO_2 sky! It is disconcerting to discover how other actors on the global-change stage can reinterpret these messages. Thus a German author from the coal industry manages to delay CO_2 doubling for 200–300 years, partly on the assumption that there will be major and continuing changes in the efficiency with which we produce our energy from fossil fuel. However, he also manages to improve his scenario by describing doubling in terms of CO_2 alone, neglecting the role of methane, nitrous oxide and the CFCs which contribute, as CO_2 equivalent, to produce the IPCC date of *circa* 2030 for doubling.

The Action Plan put forward at the Congress fully accepts the reality of future global warming and envisages relatively strong international responses in due course. However, there is no agreed target, emphasizing the long way future international negotiations have to go. One of the introductory statements is well worth study in this regard, a perceptive political comment by a member of the German *Bundestag*. His core point is that the threat of future global warming essentially adds a further strong reason why we need to take up such challenges as under-development and resource depletion, yet makes them even more difficult to solve constructively and effectively.

The socio-economic aspects also addressed by the Congress are represented by a number of shorter papers. There are some useful ideas in a rather selective survey of energy options by Roger Revelle and David Burns. The one UK contribution rehearses Martin Parry's views of the impact on agriculture, necessarily limited by the inability to say anything reliable about future precipitation. Michael Glantz of NCAR writes on climatic variability, climatic change and development in sub-Saharan Africa, but the paper says little that is new. Uncertainties over future water balance abound, yet it is not until page 405 that we find J. Nemec of FAO considering the effect of higher E on the future P-E equation.

The last substantial paper is a 7000-word essay by Thomas Potter and Lars Olsson of the World Climate Programme of WMO. It is an overview of international developments, trends and views, which describes what has been done and discusses why progress remains rather slow. It concludes that the fundamental 'renewable natural resources' on which all others depend are climate and water and the goal of any development must be to leave these as 'substantial natural resources'. That summarizes succinctly the aim of most of the authors of this book, but they cannot agree on how to bring it about.

K.M. Clayton

Global environmental change, edited by R.W. Corell and P.A. Anderson. 169 mm × 247 mm, pp. xiv+264, *illus.* Berlin, Heidelberg, New York, London, Paris, Tokyo, Hong Kong, Springer-Verlag, 1991. Price DM158.00. ISBN 0 387 531289.

Autonomous Robotic Warfare? Acoustic Submarine Interception? Thus might one speculate upon encountering the acronyms 'ARW' or 'ASI' in the context of NATO. In fact, they stand for Advanced Research Workshop and Advanced Study Institute, and for those who have not been directly involved in NATO scientific programmes it may come as a surprise to find that they refer to NATO's programme of environmental rather than defence or weapons research.

Global environmental change is the report of a conference designed to assist NATO plan its environmental research programme; in designing this particular 5-year programme of ARWs and ASIs the programme arthitects wished to ensure that the NATO programme was consistent with, and complementary to, existing internationally-organized endeavours. The programme also aims specifically to promote interdisciplinary collaboration. Both of these are laudable aspirations and the conference, which is primarily a review of questions rather than answers, seems to me to represent real progress towards achieving them. The full background to the conference is explained at length in the Preface and in the two chapters of Part 1.

Part 2 surveys the landscape of international activity related to the global environment. For those who don't know your JGOFS from your GEWEX, or — shame on you — thought that a TOGA was something you wore, then prepare to receive your education here. It is unusual, and therefore doubly valuable, to find almost all the major programmes described in the pages of one document. The scientific goals of the individual programmes are described in greater detail in Part 5.

Part 3, probably the most readable, deals with the state of some of the scientific disciplines concerned with the environment, covering hydrology, ecology, biogeochemical modelling (particularly carbon cycle), climate observations and the human dimensions of environmental change. In this latter chapter, the author masked much good material by fulfilling the physical scientist's caricature of social science. Attempting to cover too broad a canvas, he alternated between truisms and imponderables and indulged in unhelpful grandiloquence — why did it have to be 'substantive priorities' rather than plain 'priorities'?

But this was my only real complaint, for the authors of the rest of Part 3 generally made a good job of outlining the status of their discipline and, in the spirit of the workshop, of acknowledging where appropriate its limitations, whether of physical scale ('Ecologists have not until recently concerned themselves with global issues') or of cross-disciplinary collaboration ('hydrology ..(needs).. a willingness to simultaneously consider non-water fluxes').

The chapter on climate observations seems to be more of an excuse for the author to advance his objections to the conclusions of the IPCC Scientific Assessment (that global temperature has increased by 0.5 °C over the last century) than an objective review, but it makes interesting reading.

Part 4 completes the tour of the science with a review of modelling and data needs. The chapter on 'Earth system and astronomical climate modeling' almost attempts too much in covering all length- and time-scales, but in the end settles, somewhat arbitrarily it seems to this reader, on simulation of the last glacial-interglacial cycle.

Overall the book is an excellent, though volatile,

contemporary reference document (it will be obsolete in 3–5 years). Although there is no index, the information is clearly presented and the quality of production is high.

B.A. Callander

Chemistry of atmospheres (second edition), by R.P. Wayne. 154 mm × 234 mm, pp. xiii+447, *illus.* Oxford, Clarendon Press, 1991. Price £45.00 (hardback), £19.50 (paperback). ISBN 0 19 855571 7, 0 19 855574 1.

This is a revised edition of a book first published in 1985 and has a number of features reflecting the changes in our understanding of atmospheric chemistry since that time. Most important of these is the discovery of the Antarctic ozone hole, which has now been fairly well explained by the scientific community and a clear and accurate account is given by Dr Wayne. There has also been additional material added on extra-terrestrial atmospheres and the book includes a brief summary of the recent IPCC document on climate change. Although these changes are very welcome there are large parts of the book which have undergone little revision despite some possibly substantial changes in our understanding. To avoid these doubts regarding some of the details it would probably have been more useful to the reader if appropriate references had been placed within the text. As it is, many new references are included in the list at the end of each chapter but one is left wondering whether these are properly represented by the comments in the text.

The book starts at a rather basic level, leading the reader gently into the subject. This is on the whole accurate and well written, although I was confused by the remark on p. 21 that 'no geologic evidence exists for large fluctuations of CO_2 in the past'. Once the more advanced material gets under way, Dr Wayne's sometimes over-florid style occasionally gets the better of him such as in the section on models of atmospheric chemistry where we learn (p. 112) that some 'inspired guesswork' is required in the formulation of family models. This section is perhaps a little outdated since the wider availability of supercomputers has meant that the old one-dimensional models have become largely supplanted by two-dimensional models, with an increase in the use of three-dimensional models. The chapter on stratospheric chemistry is generally well presented and clear. Some of the material has not been revised since the early edition. One example of this is the table on p. 138 showing the relative contributions of the various catalytic cycles in destroying ozone. The table is taken from a 1981 compilation when not all the reservoir species were properly established nor their reaction rates known very accurately. Thus one is left wondering whether 1990 reaction rates might provide a different quantitative picture. Nonetheless the essential points are effectively made in that the processes are nonlinear. A number of reactions are also isolated as being 'important' without proper justification, in my view. The chapter on tropospheric chemistry is extensive. This is a subject of great complexity and Dr Wayne is not entirely successful in clarifying all the relevant processes. The remainder of the book gives a good introduction to the ionosphere and planetary atmospheres, subjects which have been much less extensively investigated. Again there has been a modest amount of new material added from the first edition but the author can perhaps be excused due to lack of space in a book of this size. The final chapter describes the evolution of atmospheres. This might be considered more the domain of astronomy but contains a small part on climate change on the earth.

On the whole I have only minor criticisms of a book that is generally clear, well written and covers a wide ground. Further, the physical processes relevant to particular phenomena are generally well explained. The changes from the first edition are relatively minor so those in possession of the first edition probably wouldn't wish to buy the new edition. For others, whether students in the subject or researchers of longer standing, the book is definitely recommended.

J. Austin

Books received

The listing of books under this heading does not preclude a review in the Meteorological Magazine at a later date.

Impact of climatic variability and change on river flow regimes in the UK, by N.W. Arnell, R.P.C. Brown and N.S. Reynard (Wallingford, Institute of Hydrology, 1990. £12.00) examines the recent past variability of river flow regimes and considers the possible consequences of future climate change. Conclusions are drawn on both investigations, and future research needs are identified. ISBN 0 948540 26 5.

Prediction and regulation of air pollution, by M.E. Berlyand (Dordrecht, Boston, London, Kluwer Academic Publishers, 1991. Dfl.175.00, $108.00, £61.00) presents the scientific and methodological foundations of the subject. Practical recommendations for their implementation in a variety of scenarios are also included. ISBN 0 7923 1000 4.

Historic storms of the North Sea, British Isles and Northwest Europe, by H.H. Lamb and K. Fryendahl (Cambridge University Press, 1991. £55.00, $95.00) discusses all the wind storms with serious effects since the Middle Ages. The lead author founded the Climate Research Unit at the University of East Anglia and has been embroiled with the subject for several decades. ISBN 0 521 37522 3.

Satellite photographs — 22 October 1991 at 0428 UTC

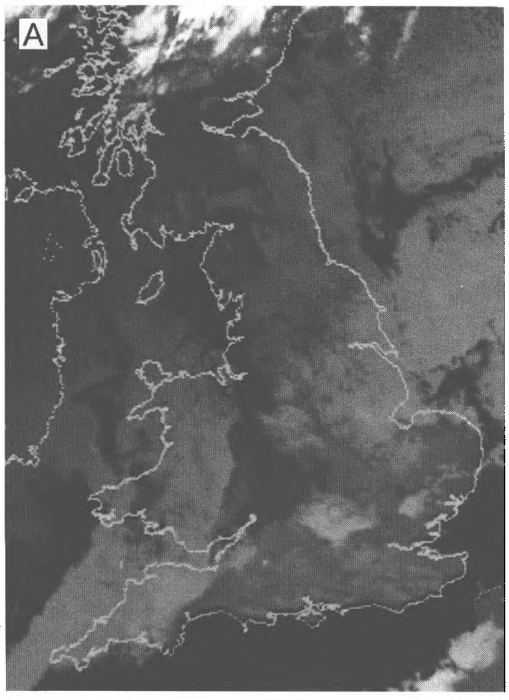

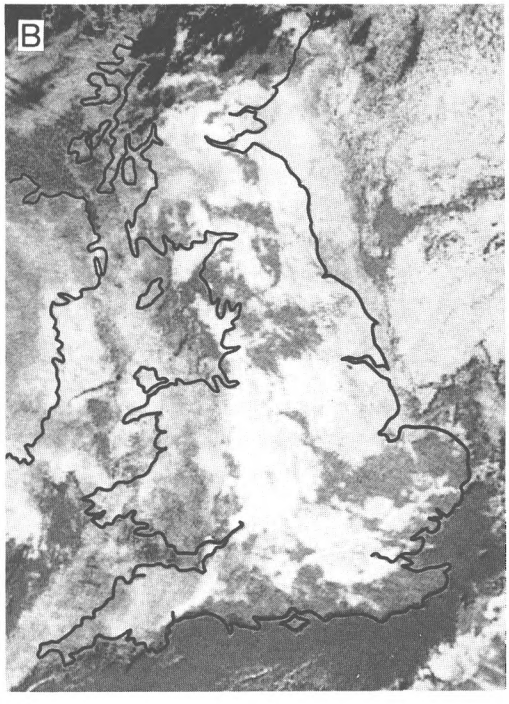

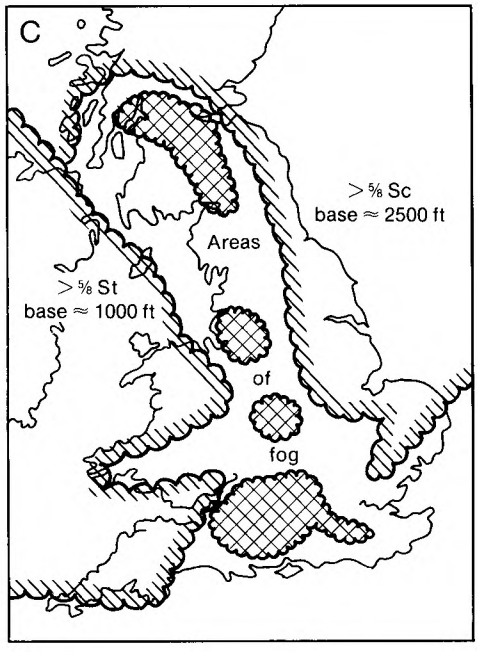

During the day, fog is easily detectable from its bright appearance in the visible and its comparatively warm brightness temperatures. At night, this method is no longer, of course, possible. Conventional infrared images alone are not sufficient; fog often has the same brightness temperature and texture as the underlying surface.

Images intended to show the distribution at night can, however, be produced from two channels (i.e. different wavelengths) of the imaging instrument on the NOAA series of polar orbiting satellites. It turns out that fog/low cloud emits radiation less efficiently at one wavelength than at the other. Land and sea surfaces emit with approximately the same efficiency.

Fog will, therefore, have a different apparent temperature in the two channels, whereas land and sea will have the same. Thus, the difference in the apparent temperatures is indicative of the presence of fog. Images are generated routinely on Autosat-2 from this temperature difference.

Image A shows the UK area at about 0428 UTC on 22 October 1991 in the infrared: the dark areas are relatively warm; the light areas cool.

Image B shows the temperature difference between the two infrared channels. The white areas are where fog and low cloud is present. The black areas (in the north and to the west of Cornwall) are due to cirrus cloud.

'C' shows a simplified representation of the distribution of fog and clouds derived from the observations at 0500 UTC.

The position of the low stratus in the west corresponds to the light grey signature in image B, and the relatively warm cloud tops shown in image A. The stratocumulus in the east and in south-west Britain is also light grey in image B, but image A shows that the cloud tops are relatively cool.

The fog over central Britain correlates well with areas that are both dark (and hence, relatively warm) in image A and bright (and hence, with a relatively large inter-channel temperature difference) in image B. The marked differences between the two images over central England shows the value of the inter-channel temperature difference in determining the position of the fog.

R.J. Allam and G. Holpin

GUIDE TO AUTHORS

Content

Articles on all aspects of meteorology are welcomed, particularly those which describe results of research in applied meteorology or the development of practical forecasting techniques.

Preparation and submission of articles

Articles, which must be in English, should be typed, double-spaced with wide margins, on one side only of A4-size paper. Tables, references and figure captions should be typed separately. Spelling should conform to the preferred spelling in the *Concise Oxford Dictionary* (latest edition). Articles prepared on floppy disk (Compucorp or IBM-compatible) can be labour-saving, but only a print-out should be submitted in the first instance.

References should be made using the Harvard system (author/date) and full details should be given at the end of the text. If a document is unpublished, details must be given of the library where it may be seen. Documents which are not available to enquirers must not be referred to, except by 'personal communication'.

Tables should be numbered consecutively using roman numerals and provided with headings.

Mathematical notation should be written with extreme care. Particular care should be taken to differentiate between Greek letters and Roman letters for which they could be mistaken. Double subscripts and superscripts should be avoided, as they are difficult to typeset and read. Notation should be kept as simple as possible. Guidance is given in BS 1991: Part 1: 1976, and *Quantities, Units and Symbols* published by the Royal Society. SI units, or units approved by the World Meteorological Organization, should be used.

Articles for publication and all other communications for the Editor should be addressed to: The Chief Executive, Meteorological Office, London Road, Bracknell, Berkshire RG12 2SZ and marked 'For Meteorological Magazine'.

Illustrations

Diagrams must be drawn clearly, preferably in ink, and should not contain any unnecessary or irrelevant details. Explanatory text should not appear on the diagram itself but in the caption. Captions should be typed on a separate sheet of paper and should, as far as possible, explain the meanings of the diagrams without the reader having to refer to the text. The sequential numbering should correspond with the sequential referrals in the text.

Sharp monochrome photographs on glossy paper are preferred; colour prints are acceptable but the use of colour is at the Editor's discretion.

Copyright

Authors should identify the holder of the copyright for their work when they first submit contributions.

Free copies

Three free copies of the magazine (one for a book review) are provided for authors of articles published in it. Separate offprints for each article are not provided.

Contributions: It is requested that all communications to the Editor and books for review be addressed to the Chief Executive, Meteorological Office, London Road, Bracknell, Berkshire RG12 2SZ, and marked 'For *Meteorological Magazine*'. Contributors are asked to comply with the guidelines given in the *Guide to authors* which appears on the inside back cover. The responsibility for facts and opinions expressed in the signed articles and letters published in *Meteorological Magazine* rests with their respective authors.

Subscriptions: Annual subscription £33.00 including postage; individual copies £3.00 including postage. Applications for postal subscriptions should be made to HMSO, PO Box 276, London SW8 5DT; subscription enquiries 071–873 8499.

Back numbers: Full-size reprints of Vols 1–75 (1866–1940) are available from Johnson Reprint Co. Ltd, 24–28 Oval Road, London NW1 7DX. Complete volumes of *Meteorological Magazine* commencing with volume 54 are available on microfilm from University Microfilms International, 18 Bedford Row, London WC1R 4EJ. Information on microfiche issues is available from Kraus Microfiche, Rte 100, Milwood, NY 10546, USA.

December 1991

Edited by Corporate Communications
Editorial Board: R.J. Allam, R. Kershaw, W.H. Moores, P.R.S. Salter

Vol. 120
No. 1433

Contents

ISSN 0026–1149

ISBN 0-11-728863-2

9 780117 288638

Printed in the United Kingdom for HMSO
Dd 0291241 12/91 C13 503 12521